PB86-225059

Proceedings: 1985 Joint Symposium on Stationary Combustion NOx Control Volume 2. Industrial Processes Fundamental Studies, and Slagging Combustors

Acurex Corp., Mountain View, CA

Prepared for

Environmental Protection Agency
Research Triangle Park, NC

Jul 86

U.S. Department of Commerce
National Technical Information Service
NTIS

PB86-225059

EPA/600/9-86/021b
July 1986

PROCEEDINGS:
1985 JOINT SYMPOSIUM ON STATIONARY COMBUSTION NO_X CONTROL
Volume 2. Industrial Processes, Fundamental Studies, and Slagging Combustors

S. Peralo

Acurex Corporation
555 Clyde Avenue
Mountain View, California 94039

EPA Contract 68-02-3695
EPRI Research Project 2154-5

EPA Project Officer:
Michael C. Osborne

Air and Energy Engineering
Research Laboratory
U.S. Environmental Protection Agency
Research Triangle Park, NC 27711

EPRI Project Manager:
D. Eskinazi

Air Quality Control Program
Electric Power Research Institute
3412 Hillview Avenue
Palo Alto, CA 94303

AIR AND ENERGY ENGINEERING RESEARCH LABORATORY
OFFICE OF RESEARCH AND DEVELOPMENT
U.S. ENVIRONMENTAL PROTECTION AGENCY
RESEARCH TRIANGLE PARK, NC 27711

REPRODUCED BY
NATIONAL TECHNICAL
INFORMATION SERVICE
U.S. DEPARTMENT OF COMMERCE
SPRINGFIELD, VA. 22161

TECHNICAL REPORT DATA
(Please read Instructions on the reverse before completing)

1. REPORT NO. EPA/600/9-86/021b

2.

3. RECIPIENT'S ACCESSION NO. PB86 225059/AS

4. TITLE AND SUBTITLE
Proceedings: 1985 Symposium on Stationary Combustion NOx Control, Volume 2. Industrial Processes, Fundamental Studies, and Slagging Combustors

5. REPORT DATE
July 1986

6. PERFORMING ORGANIZATION CODE

7. AUTHOR(S)
S. Peralo, Coordinator

8. PERFORMING ORGANIZATION REPORT NO.
EPRI CS-4360

9. PERFORMING ORGANIZATION NAME AND ADDRESS
Acurex Corporation
555 Clyde Avenue
Mountain View, California 94039

10. PROGRAM ELEMENT NO.

11. CONTRACT/GRANT NO.
68-02-3695

12. SPONSORING AGENCY NAME AND ADDRESS
EPA, Office of Research and Development*
Air and Energy Engineering Research Laboratory
Research Triangle Park, NC 27711

13. TYPE OF REPORT AND PERIOD COVERED
Proceedings; May 1985

14. SPONSORING AGENCY CODE
EPA/600/13

15. SUPPLEMENTARY NOTES AEERL project officer is Michael C. Osborne, MD-63, 919/541-4113. (*) Cosponsor is EPRI, 3412 Hillview Ave., Palo Alto, CA 94303; project officer is D. Eskinazi.

16. ABSTRACT The two-volume proceedings document the more than 60 papers, describing recent advances in NOx control technology, that were presented at the 1985 Joint Symposium on Stationary Combustion NOx Control, May 6-9, 1985, in Boston, MA. The papers covered the following topics: the status and history of international NOx regulation, recent pilot- and full-scale technological developments relating to combustion modifications and flue gas treatment, boiler manufacturer updates on recent commercial technologies for NOx emissions control, fundamental combustion research, industrial applications, and advanced power plant concepts. There was also a summary session on the status of furnace sorbent injection for SO2 control. The two volumes are entitled Utility Boiler Applications; and Industrial Processes, Fundamental Studies, and Slagging Combustors.

17. KEY WORDS AND DOCUMENT ANALYSIS

a. DESCRIPTORS		b. IDENTIFIERS/OPEN ENDED TERMS	c. COSATI Field/Group	
Air Pollution	Furnaces	Air Pollution Control	13B	
Nitrogen Oxides	Sorbents	Stationary Sources	07B	11G
Combustion Control	Sulfur Oxides	Combustion Modification	21B	
Flue Gases	Slagging	Sorbent Injection		13H
Boilers			13A	
Electric Power Plants			10B	

18. DISTRIBUTION STATEMENT
Release to Public

19. SECURITY CLASS *(This Report)*
Unclassified

20. SECURITY CLASS *(This page)*
Unclassified

21. NO. OF PAGES

22. PRICE

EPA Form 2220-1 (9-73)

NOTICE

This document has been reviewed in accordance with U.S. Environmental Protection Agency policy and approved for publication. Mention of trade names or commercial products does not constitute endorsement or recommendation for use.

PREFACE

The 1985 Joint Symposium on Stationary Combustion NO_x Control was held May 6-9 in Boston, Massachusetts. This was the third symposium on NO_x control jointly sponsored by EPA and EPRI; the first was in Denver in 1980 and the second in Dallas in 1982. The symposium is a consolidation of EPRI's previous NO_x Control Technology Seminars and EPA's Symposia on Stationary Source Combustion. The objective of the symposium is to give attendees the opportunity to exchange information on the latest advances in combustion technology and flue gas treatment processes for stationary sources. Such an exchange of information contributes significantly to the development of cost-effective and reliable NO_x ignition control systems.

Over 60 papers were presented during the 4-day meeting which was attended by representatives of 13 nations. Topics ranged from full-scale applications of combustion modifications and flue gas treatment to fundamental combustion research. The speakers represented a variety of international organizations including electric utility companies, boiler and other related equipment manufacturers, research and development groups, and regulatory agencies.

Cochairmen of the symposium were David Eskinazi of EPRI and Michael C. Osborne of EPA. The keynote address was delivered by Robert C. Carr, Department Director of Environmental Control Systems of EPRI's Coal Combustion Systems Division and EPA's Carl R. Gerber, Director of the Office of Environmental Engineering and Technology, Office of Research and Development. The welcoming address was given by C. Bruce Damrell, Vice President, Engineering and Distribution of Boston Edison Company. The symposium proceedings has been published in two volumes:

- Volume 1: Utility Boiler Applications
  - Session I: Introduction
  - Session II: Manufacturer's Update of Commercially Available Technology
  - Session III: Low-NO_x Combustion Development
  - Session IV: Development and Application of Fuel Staging (Reburning)
  - Session V: Full-Scale Boiler Application
  - Session VII: Advanced Power Plants
  - Session VIIIa: Flue Gas Treatment
- Volume 2: Industrial Processes, Fundamental Studies, and Slagging Combustors
  - Session VIa: Externally Staged Combustors (Slagging Combustors)
  - Session VIb: Fundamental Combustion Studies
  - Session VIIIb: Stationary Engines and Industrial Process Systems
  - Session IXa: Overview of Furnace Sorbent Injection SO_2 Control
  - Session IXb: Fuel and Combustion Modifications for Commercial/Industrial Boilers

CONTENTS

VOLUME 1
UTILITY BOILER APPLICATIONS

(Volume 2 Table of Contents starts on page vi)

Paper Page

SESSION I: INTRODUCTION
Chairman, Michael Osborne, EPA

"Introductory Remarks," R. Carr. 1-1

"Opening Remarks," C. Gerber 2-1

1-1 "An Overview of the International NO_x Control Regulations," P. Dacey 3-1

1-2 "Legal Instruments and the State of Technology for Reducing NO_x Emissions in the Federal Republic of Germany," H. Keinhorst . . . 4-1

1-3 "Utility Perspective on Low NO_x Control," D. Mormile 5-1

1-4 "Role of NO_x Emissions in Acid Rain," J. Chang 6-1

1-5 "Boreal Montane Ecosystem Decline in Central Europe and the Eastern United States: Potential Role of Anthropogenic Pollution With Emphasis on Nitrogen Compounds," R. Bruck. 7-1

SESSION II: MANUFACTURER'S UPDATE OF COMMERCIALLY AVAILABLE TECHNOLOGY
Chairman, George Offen, EPRI

2-1 "Utility Steam Generators NO_x Control Update -- 1985," A. Larue, M. Acree, and P. Cioffi. 8-1

2-2 "1985 Update on NO_x Emission Control Technology at Combustion Engineering," R. Collette 9-1

2-3 "Current Developments in Low-NO_x Combustion Systems," R. Lisauskas, and C. McHale. 10-1

2-4 "Industrial and Utility Boiler NO_x Control," J. Vatsky and E. Schindler 11-1

SESSION III (PART 1): LOW-NO_x COMBUSTION DEVELOPEMENT
Chairman, Michael McElroy, EPRI

3-1 "Experimental Investigation of Retrofit Low-NO_x Combustion Systems," R. Lisauskas, R. Snodgrass, S. Johnson, and D. Eskinazi. 12-1

CONTENTS

Paper | Page

3-2 "Low-NO_x Coal Firing System Demonstration Results on a Tangentially Fired Boiler," A. Kokkinos, R. Lewis, and D. Lachapelle. 13-1

SESSION III (PART 2): LOW-NO_x COMBUSTION DEVELOPMENT
Chairman, David Eskinazi, EPRI

3-3 "Air Flow Modeling of a 750 MW Gas and Oil-Fired Boiler," G. Gilbert and D. Teixeira. 14-1

3-4 "Laboratory Flow Model Studies to Improve Overfire Air Mixing," R. Thompson, D. Eskinazi, A. Afonso, G. Gilbert, R. Yang, and C. McHale 15-1

3-5 "Status of EPDC's NO_x Control Technology," K. Fujiyama 16-1

3-6 "Development of Low NO_x Cell Burners for Retrofit Applications," A. Larue and L. Rodgers. 17-1

3-7 "Development of the Low-NO_x Burner for the Pulverized-Coal-Fired In-Furnace NO_x Reduction System," T. Narita, Y. Arikawa, T. Nawata, F. Koda, T. Masai, S. Morita, and K. Ohtsuka 18-1

3-8 "Fire-side Corrosion in Low-NO_x Combustion Systems," S. Chou, P. Daniels, L. Rodgers, G. Theus, and D. Eskinazi. 19-1

3-9 "Extrapolation of Burner Performance from Single Burner Tests to Field Operation," R. Lisauskas, D. Itse, and C. Masser. 20-1

SESSION IV: DEVELOPMENT AND APPLICATION OF FUEL STAGING (REBURNING)
Chairman, Robert Hall, EPA

4-1 "Pilot Scale Evaluation of NO_x Control from Pulverized Coal Combustion by Reburning," B. Overmoe, J. McCarthy, S. Chen, R. Seeker, G. Silcox, and D. Pershing. 21-1

4-2 "The Effect of Fuel Nitrogen in Reburning Application to a Firetube Package Boiler," J. Mulholland and R. Hall 22-1

4-3 "Screening and Optimization of In-Furnace-NO_x-Reduction Processes for Refinery Process Heat Applications," R. Yang, F. Garcia, and S Hunter 23-1

4-4 "Evaluation of In-Furnace NO_x Reduction," S. Miyamae, H. Ikebe, K. Makino, K. Suzuki, and J. Mogi 24-1

CONTENTS

Paper | Page

4-5 "Three-Stage Pulverized Coal Combustion System for In-Furnace NO_x Reduction," N. Okigami, Y. Sekiguchi, Y. Miura, K. Sasaki, and R. Tamaru 25-1

4-6 "Application of Reburning for NO_x Control in Cogeneration," R. Brown 26-1

SESSION V: FULL-SCALE BOILER APPLICATION
Chairman, Charles Allen, Arizona Public Service Co.

5-1 "Guidelines for Retrofit Low-NO_x Combustion Control," R. Thompson and M. McElroy 27-1

5-2 "Evaluation of Long-Term NO_x Reduction on Pulverized Coal-Fired Steam Generators," S. Hunter and V. Roman. 28-1

5-3 "Application of a Pulverized-Coal-Fired Low-NO_x PM Burner for Steam Generators," T. Namiki 29-1

5-4 "Field Evaluation of the Distributed Mixing Burner," B. Folsom, A. Abele, and J. Reese 30-1

5-5 "Design and Development of a Retrofit Low NO_x Burner," I. Stuart-Sheppard, W. Summons, and J. Arnott. 31-1

5-6 "Application of the MACT In-Furnace NO_x Removal Process Coupled with a Low-NO_x SGR Burner," N. Murakami 32-1

5-7 "Long Term Corrosion and Emission Studies of Combustion Modification Effects at Coal-Fired Utility Boilers," P. Natanson, R. Vaccaro, J. Ferraro, and D. Lachapelle. 33-1

SESSION VII: ADVANCED POWER PLANTS
Chairman, Donald Teixeira, Pacific Gas and Electric Co.

7-1 "NO_x Control and Atmospheric Fluidized-Bed Combustors," E. Petrill, W. Howe, T. Derbidge, and R. Divilio 34-1

7-2 "The Cool Water Project Clean Power From Coal," R. Wolk and N. Holt. 35-1

CONTENTS

Paper | Page

SESSION VIIIa: FLUE GAS TREATMENT
Chairman, Edward Cichanowicz, EPRI

8a-1 "Operating Experiences on Southern California Edison's 107.5 MW Selective Catalytic Reduction DeNO$_x$ System," H. Kerry and A. Weir, Jr. 36-1

8a-2 "Reduction of NO$_x$ Emissions for Brown Coal Combustion Systems in the Federal Republic of Germany," K. Hein, J. Konig, and V. Hoppe 37-1

8a-3 "Introduction of IHI-Denitrification System for Coal Fired Steam Generator," H. Aoki, T. Suzuki, and R. Ishimoto 38-1

8a-4 "Thermal DeNO$_x$ Technology Update," B. Hurst 39-1

8a-5 "Application of DeNO$_x$ Technologies in the Federal Republic of Germany and Europe," O. Rentz and W. Heer 40-1

8a-6 "Operating Experience on SCR System for Steam Generators," K. Suyama 41-1

8a-7 "Economics of NO$_x$, SO$_2$, and Ash Control Systems for Coal-Fired Utility Power Plants," D. Maxwell, L. Humphries, and D. Mobley 42-1

VOLUME 2
INDUSTRIAL PROCESSES, FUNDAMENTAL STUDIES, AND SLAGGING COMBUSTORS

SESSION VIa: EXTERNALLY STAGED COMBUSTORS (SLAGGING COMBUSTORS)
Chairman, Craig Derbidge, EPRI

6a-1 "Development of a Low NO$_x$/SO$_x$ Burner," O. Dykema. 43-1

6a-2 "NO$_x$ Control in an Air Cooled Cyclone Coal Combustor," B. Zauderer and K. Fujimura 44-1

6a-3 "Coal-Fired Precombustors for Simultaneous NO$_x$, SO$_x$, and Particulate Control," G. England, J. La Fond, and R. Payne. 45-1

CONTENTS

Paper | Page

SESSION VIb: FUNDAMENTAL COMBUSTION STUDIES
Chairman, Jon Haebig, EPA

6b-1 "Mechanisms Governing the Destruction of Nitrogen Species During Staged Coal Combustion," J. Wendt, K. Dannecker 46-1

6b-2 "Oxidation and Pyrolysis of Fuel Nitrogen in a Lignite -- Both as Received and After Ammonium Ion-Exchange," L. Timothy, J. Beer, and A. Sarofim 47-1

6b-3 "Reduction of NO_x Emissions from Natural Gas Flames by Fuel Staging," J. Beer 48-1

6b-4 "NO_x Prediction for Practical Pulverized Coal Reactors," L. Smoot, S. Hill, and P. Smith 49-1

6b-5 "Optimized Low-NO_x Pulverized Coal Combustion by Zone Control," K. Okazaki and K. Ohtake 50-1

SESSION VIIIb: STATIONARY ENGINES AND INDUSTRIAL PROCESS SYSTEMS
Chairman, Joseph McSorley, EPA

8b-1 "Utilization of Methanol as Fuel for a Gas Turbine Cogeneration Plant," D. Shore, G. Shiomoto, and G. Bemis 51-1

8b-2 "Development and Field Demonstration of a Low-NO_x Burner for TEOR Steamers," G. England, Y. Kwan, and R. Payne 52-1

8b-3 "Heavy Oil Low-NO_x Burner Application to an Oil Field Steamer -- Emission Measurements," H. Mason 53-1

8b-4 "Reduction of Nitric Oxide Emissions on a Full-Scale Cement Kiln Using Primary Air Vitiation," S. Hunter and R. Benson 54-1

8b-5 "NO_x Control for Glass-Melting Tanks," D. Fleming and R. Kurzynske. 55-1

8b-6 "Diesel Engine NO_x Control with SCR," J. Wasser and R. Perry. 56-1

8b-7 "Environmental Assessment of Catalytic Reduction on Natural Gas-Fired Engines," C. Castaldini 57-1

CONTENTS

Paper Page

SESSION IXa: OVERVIEW OF FURNACE SORBENT INJECTION SO_2 CONTROL
Chairman, Robert Hangebrauck, EPA

9a-1 "Review of International Development Activities for Furnace Sorbent Injection," D. Giovanni 58-1

9a-2 "Technical Status of EPA's LIMB Program," G. Martin and J. Abbott 59-1

9a-3 "EPRI's Research Program on Furnace Sorbent Injection," M. McElroy M. McElroy. 60-1

SESSION IXb: FUEL AND COMBUSTION MODIFICATIONS FOR COMMERCIAL/ INDUSTRIAL BOILERS
Chairman, John Wasser, EPA

9b-1 "Combustion Modification Techniques for Coal-Fired Stoker Boilers," G. Quartucy, H. Buening, and R. Yang. 61-1

9b-2 "Emissions Assessment of Coal-Water-Slurry-Fired Industrial Boilers," L. Waterland, R. DeRosier, D. Van Buren, and H. Mason 62-1

9b-3 "Development of Low-NO_x Combustion for Industrial Application," T. Suzuki, K. Morimoto, K. Ohtani, R. Odawara, T. Kohno, Y. Matsuda, and M. Suyari 63-1

9b-4 "Emissions Assessment of Cofiring Coal and Waste Plastic in a Commercial Boiler," L. Waterland, R. DeRosier, H. Lips, and H. Mason. 64-1

9b-5 "A Low-NO_x Burner for Gas-Fired Firetube Boilers," J. Kesslring and W. Krill. 65-1

APPENDIX A -- LIST OF ATTENDEES A-1

Session VIa: Externally Staged Combustors (Slagging Combustors)

Chairman, Craig Derbidge, EPRI

DEVELOPMENT OF A LOW NO_x/SO_x BURNER

by O. W. Dykema
Rocketdyne Division
Rockwell International
6633 Canoga Avenue
Canoga Park, California 91304

ABSTRACT

For more than 5 years, Rockwell International has been developing a unique burner capable of simultaneous control of both SO_2 and NO_x, and removal of sufficient of the fly ash to allow retrofit of gas and oil-fired boilers to coal with minimal derating. Underlying process theory was largely verified in a 20 GJ/hr (17 MBtu/hr) pulverized coal-fired burner and further development at a utility pilot-scale level (26 GJ/hr 25 MBtu/hr) is nearing completion. Full-scale burner demonstration (106 GJ/hr 100 MBtu/hr) is scheduled to start in the late spring of 1985.

KEY WORDS

SO_x, NO_x, Combustion, Boilers, Coal, Oil, Oil/Coal Retrofit

1.0 INTRODUCTION

For more than a decade, it has been suspected that SO_x and NO_x air pollution emissions might be more effectively controlled at their source (during initial combustion) than by cleaning the final products out of the bulk flue gases. Not only would there be less gas volume involved, and thus higher concentrations of the offending chemical species, but the high temperatures of combustion provide much faster reactions, thereby facilitating conversion of the offending species to the desired ones. Thus, it has long been suspected that SO_x and NO_x control in combustion could provide adequate air pollution control at quite reasonable cost.

In the conversion of a boiler designed for low-sulfur gas or oil fuels to pulverized coal (PC) firing, it is clear that SO_x and NO_x emissions will increase drastically unless advanced control techniques are implemented. For example, current U.S. New Source Performance Standards (NSPS), recognizing the state of the art in air pollution control technology in the late 1970s, allow SO_x emissions from new coal-fired boilers to be as much as 50% higher than those from new oil- or gas-fired boilers, and NO_x emissions can be more than 100% higher. Several other problems are introduced by such a conversion, however, which must also be addressed to make the conversion feasible. Three of these are: (1) the furnace volume is too small for the slower burning PC, (2) there is a drastic increase in the quantities of slag/fly ash generated by PC combustion, and (3) there is a significant mismatch between the new combustion gas temperature profile through the boiler and the existing heat-absorbing surfaces.

A boiler designed for gas or oil fuels is normally sized for heat release rates of the order of 260-520 kJ/s-m^3 (25-50,000 Btu/h-ft^3) while those designed for PC fuel are sized for heat release rates of the order of 160-230 kJ/s-m^3 (15-22,000 Btu/h-ft^3). Clearly, PC combustion cannot be efficiently accomplished within the gas/oil-designed boiler unless the PC heat release rate is greatly increased or additional PC combustion volume is added.

Slag and fly ash generated by gas and oil combustion are negligible compared to that generated by PC combustion. Boilers designed for gas and oil firing normally cannot accept molten slag on the furnace walls or in the furnace bottom. Furthermore, the furnace and convective section bulk gas flow areas and the spacing between convective tubes in the gas stream are smaller in gas- and oil-designed boilers. It was not intended that the bulk gases in these boilers would contain large concentrations of highly erosive/corrosive coal fly ash. Accelerated tube fouling, erosion, and corrosion are generally anticipated unless some change is made to prevent introduction of slag and at least a major fraction of coal fly ash.

Finally, an additional significant, but not so obvious, problem introduced by the substitution of PC fuels in boilers designed for gas and oil firing results from the mismatch between the new combustion gas characteristics and the surface area available to absorb heat. The volume of flue gases generated per unit of heat input, adiabatic flame temperatures, and combustion gas emissivities can all be significantly different from those for which the boiler was designed, regardless of how the coal is burned. Rockwell employs a comprehensive thermodynamic model of the boiler to adjust burner design characteristics such that the effects of this mismatch are minimized and boiler rating is maintained at maximum levels.

For more than 5 years, the Energy Systems Group of Rockwell International has been developing a burner which uniquely addresses all of the problems introduced by the conversion of boilers designed for gas and oil fuels to PC firing. Initially, the Rockwell development goal was to provide low-cost air pollution control by simultaneously controlling SO_x and NO_x within the combustion process. During that development program, however, it became apparent that the resulting low NO_x/SO_x burner also possessed characteristics which could resolve the special, major problems introduced in the gas/oil-to-coal conversion and make that conversion feasible. Accordingly, development of a hot gas slag/fly ash separator was added to the burner development program. The Rockwell burner currently under development, therefore, is most appropriate to the gas/oil-to-coal conversion case. In various other forms and modifications, it is also expected to offer major advantages in new and retrofitted boilers designed for coal, for a wide range of industrial and commercial applications, and with a wide range of solid and liquid fuels.

The burner is of the slagging type. Combustion is initiated within the burner, external to the boiler. SO_x emissions are controlled by capturing fuel sulfur as solid calcium-sulfur compounds for later removal within the burner, in the separator, and/or in a conventional downstream baghouse or precipitator. NO_x and the precursors of NO_x are converted to harmless molecular nitrogen. The burner is operated with gas/ash temperatures well above the ash fusion temperature. A simple, inertia-type separator within the burner removes slag and a major fraction of the (molten) fly ash, with slag tapped out of the burner external to the boiler. The combustion gases entering the boiler will then: (1) contain little SO_x and NO_x, (2) be partially combusted, (3) contain no slag and little fly ash (and that only in the very fine particle sizes), and (4) will be only slightly cooler than peak adiabatic flame temperatures. In applications to boilers designed for coal firing, the slag/fly ash separator is not necessary.

Rockwell believes that theoretical solutions have been found and experimentally verified for all of the separate subprocesses necessary to develop a practical burner providing all of these functions. The development program is now proceeding to integrate and optimize all of these subprocesses and to demonstrate a practical, workable burner.

2.0 BACKGROUND

Rockwell initiated this program in 1979 when in-house analytical studies indicated that, under certain combustion conditions, it is theoretically possible to reduce to zero both SO_x and NO_x emissions from fossil fuel combustion. Since this control would largely be accomplished during combustion in the burner it seemed likely that this ultimate SO_x and NO_x emissions control could be accomplished at low cost as well. Thus, the technical objective seemed exciting and it appeared that commercialization was also feasible and attractive.

Before committing to the long and expensive program necessary to implement the theoretical concepts in a practical, commercially successful product, however, a brief experimental program was necessary to validate the concepts. Pulverized coal was fired at the 5-MJ/s (17-M BTU/h) level in a combustor made up from hardware available at Rockwell from previous programs. Neither the hardware nor the range of testing were comprehensive. The objective was simply to demonstrate that at least in one reasonably large scale, prototypical burner, the theoretically predicted zero SO_x and NO_x emissions could be approached.

Test results with both eastern and western coals showed that when the burner was operated under conditions where 100% SO_2 capture was analytically predicted, 90-97% of the fuel sulfur was captured, as solid calcium-sulfur compounds. In addition, once captured, essentially all of this sulfur was retained in the solid form through a downstream, more oxidizing stage of combustion. When the burner was operated under conditions where poor sulfur capture was analytically predicted, sulfur capture ranging from just a few percent to as high as 50% was measured. Calcium, in the form of lime, was added to the high-sulfur eastern coal (Illinois No. 6 with 3.5% sulfur) to capture the sulfur. The alkaline low-sulfur western coal (Kaiparowits with 0.4% sulfur) inherently contained sufficient calcium, and none was added to that coal. Although that test facility did not include a final boiler section where combustion would be completed, these data were considered reasonably sound verification of the theoretical concepts for SO_x emission control in combustion.

Throughout the verification test program, with both eastern and western coals, test results repeatedly showed essentially full conversion of fuel-bound nitrogen to harmless molecular nitrogen. On several occasions, operating under test conditions where zero concentrations of NO_x (and its precursors HCN and NH_3) were theoretically predicted, NO_x (and HCN and NH_3) levels were too low to be measured with the available instrumentation (less than about 7 ppm). Overall averages of 15-20 ppm were measured. Again, when the burner was operated under conditions where poor NO_x control was analytically predicted, NO_x (and HCN/NH_3) levels greater than 500 ppm were measured.

Without a final boiler combustion stage, the question of subsequent generation of NO_x, by the thermal mechanism in the boiler, could not be evaluated. Not only is realistic testing of this type expensive (essentially requires a boiler), this phase of NO_x control was not a part of the NO_x control concept under verification. In any case, control of thermal NO_x formation during combustion within a boiler is a well studied and proven technique (for example, with fuel-rich initial combustion followed by overfire air).

A simple slag/fly ash separator was also designed and tested in the verification burner. The purpose of this separator is to remove sufficient amounts of the fuel ash to allow the retrofit of a boiler designed for gas or oil fuels to coal while minimizing boiler derating. Tests showed total removal within the burner/separator of 80% of the coal ash. The separator is not a part of the SO_x/NO_x control concept and is not considered necessary with a boiler designed to handle the ash from combustion of coal fuels.

In general, then, the results of this early test program were considered sufficient verification of the exciting possibilities of the analytical predictions to justify proceeding in further research and development. At the conclusion of the SO_x/NO_x and slag/fly ash separator testing, a more prototypical, utility pilot-scale test facility and burner (7 MJ/s or 25 MBtu/h) was built. Further testing with the verification burner included coal-oil mixtures, coal-water mixtures, high-sulfur residual oil, and shale oil. Pulverized coal testing, however, was shifted to the pilot-scale facility.

3.0 PILOT-SCALE PROGRAM

The pilot-scale Low NO_x/SO_x Burner (LNSB) program was initiated in 1982. The overall objective of that program is to supply all of the empirical information necessary to design, with reasonable understanding and confidence, a 29-MJ/s (100 MBtu/h) LNSB for subsequent demonstration on a full-scale, operating utility boiler. As such, the program includes a number of tasks necessary to develop or optimize certain aspects of this burner design (for example, refractory materials). The main line of effort is the pilot-scale test program.

The pilot-scale program is supported and guided by a utility consortium. Current members are Houston Power and Light Company, Niagara Mohawk Power Corporation, Southern California Edison Company, TransAlta Utilities Corporation (Calgary, Canada), and Wisconsin Public Service Corporation. The Canadian Electric Association also participates, through TransAlta. The program is run by a steering committee composed of representatives of the participating utilities. While Rockwell chairs this committee and has veto power in issues effecting budget, Rockwell has no vote in operational matters.

3.1 PILOT-SCALE TEST FACILITY

A schematic diagram of the pilot-scale test facility is shown in Figure 1. Coal and limestone, when required, are mixed, introduced together into a coal pulverizer, and pulverized to 70%-200 mesh. The pulverized fuel is then pneumatically transported to the coal silo shown in the figure. Approximately 8 h of fuel can be charged into this silo. During test, the coal is metered out of the run silo onto a weighbelt feeder, where the flow rate is measured and controlled. The coal is picked up from the weighbelt feeder and is pneumatically conveyed into the first stage of the burner using about 1.3% of the total combustion air as the transport medium.

Burner combustion air is driven by a forced draft (FD) fan. It first passes through a concentric-tube air preheater and then through an indirect, gas-fired heater. The combustion air temperature entering the burner is maintained at about 620°K (650°F). Final combustion (overfire) air is driven by a separate fan and is not heated. Fly ash-containing flue gases pass through the air preheater into a baghouse. An ID fan can be used to balance pressures in the burner.

The cost of purchasing and installing a real boiler for the final combustion and heat transfer stage was considered prohibitive. Instead, an attempt was made to simulate the boiler gas time-temperature and heat transfer profiles of a boiler using: (1) about 15 ft of bare steel ducting, externally cooled with water sprays and (2) a commercial fire-tube waste heat boiler. The bare steel ducting section was intended to simulate the radiant section of a boiler, with heat transfer occurring to a large extent by radiation to the cold walls. The flue gases spend about 0.7 s in this section, with the gas temperature falling from about 1800°K (2800°F) to about 1400°K (2100°F) at the entrance to the waste heat boiler. The waste heat boiler was intended to simulate the convective back pass of a boiler. The flue gases cool in this boiler to about 480°K (400°F) at the boiler exit. The bare steel ducting contains two sharp 90° turns intended to remove some of the larger fly ash particles during testing without the slag/fly ash separator.

This boiler simulation has proven to be much less than desired. When the separator is not installed, fly ash entering this simulated boiler section still contains about 10% of the carbon. Fly ash impinging on the cold walls of the bare steel ducting, particularly in the first 90° turn, is rapidly quenched. Gas analyses down the length of the bare steel ducting suggest other unusual quenching and reactions. In addition, the bare steel ducting represents a large radiation heat sink that drastically cools the downstream side of the slag/fly ash separator and the approaches to the slag tap. Although data are measured and recorded throughout the bare steel ducting and waste heat boiler sections, the meaning of much of that data is not clear. Burner performance data are considered truly representative only up to the point where the flue gases enter the bare steel ducting section and, perhaps at the simulated boiler exit.

The burner part of the test facility consists of refractory-lined, cylindrical ducting, about 20 ft long and 36 in. in outside diameter. The burner is divided into a number of short spool pieces to provide hardware flexibility. Combustion air can be injected (staged) at several locations along the burner length. Access ports are located about every 2 ft along the burner length through which gas samples and gas temperature measurements can be taken. As presently configured, the first stage is about 12 ft long and the second stage, containing the slag/fly ash separator, is about 10 ft long.

3.2 INSTRUMENTATION

Gas compositions vary considerably along the length of the burner and through the simulated boiler. The gases are the products of combustion of air-fuel mixtures varying from very fuel-rich to air-rich, and contain particulate matter that may still be reactive. A considerable development program was necessary to assure: (1) gas sample integrity through the sampling system; (2) accurate on-line and backup gas analyses; and (3) sampling and analysis system verifications.

Gas samples, still containing some particulate, are withdrawn at a number of locations throughout the burner and simulated boiler. A particulate filter is located at each probe. Both the probe and the filter are cooled with hot water (about 360K or 190°F) to prevent moisture condensation. Sample lines to the instrument shack are all heat traced. Figure 2 shows the gas sampling and analysis train.

Gas samples are routinely analyzed for CO, CO_2, O_2, N_2, and H_2 using the following instruments:

CO/CO_2	Horiba PIR-2000 Infrared Gas Analyzer
O_2	Beckman O_2 Analyzer Model 755
N_2	Gas Chromatograph, Honeywell/Spectra Physics
H_2	Gas Chromatograph, Hewlett-Packard 5840A

N_2 and H_2 are measured primarily to provide redundant data with which the internal consistency and compatibility of all gas concentrations can be checked.

NO_x concentrations are measured by a Thermal Electron Model 10 Chemiluminescent $NO/NO_2/NO_x$ Analyzer. This instrument includes a reactor to convert all nitrogenous species, such as HCN and NH_3 to NO_x. The assumption is made that any HCN and NH_3 in the products of fuel-rich combustion will be converted to NO_x in the final, excess air combustion and, therefore, HCN and NH_3 are routinely converted to and reported as NO_x. Early, more detailed measurements showed significant concentrations of these species in the fuel-rich section of the burner.

Concentrations of gaseous sulfur compounds in the products of fuel-rich combustion, containing reactive, calcium-bearing particulates, were the most difficult to measure. When sampling in the simulated boiler section, with excess air, the gas sample is simply valved through a Teledyne Series 600 Photometric Analyzer, measuring SO_2. When sampling the fuel-rich products, the sample is first valved through a high temperature furnace, with a measured quantity of excess air. Reactions in the furnace not only convert all sulfur species to SO_2 but also convert partially reacted hydrocarbons (which can interfere with the SO_2 measurement) to CO_2. On-line measurement of sulfur concentrations are backed up by simultaneously bubbling a measured gas sample through two NaOH sulfur traps. The resulting wet sample is subsequently analyzed for sulfur in the laboratory using conventional wet chemistry methods.

In addition, a check on the integrity and accuracy of the entire sampling and measurement system is periodically obtained. A calibration gas containing known concentrations of SO_2 and He is introduced into the sampling train immediately at the exit of the gas sample probe during the test. The measured increase in SO_2 during calibration must correspond to the excess introduced with the calibration gas.

The flow rate of pulverized coal into the burner is measured in three ways: (1) a weighbelt feeder measures (and controls) the rate of flow out of the coal storage silo and integrates this flow rate over the entire test, to coal exhaustion; (2) the total quantities of coal and limestone loaded into the silo for the test are measured and can be used as a check on the integrated total recorded by the weighbelt feeder; and (3) analyses of CO_2 and O_2 in the simulated boiler exit, under excess air conditions, together with measured air flow rates, provide a further check on instantaneous coal flow rates. Air flow rates are measured with Annubar instruments, calibrated by helium tracer techniques.

In addition, gas temperatures are measured at several locations throughout the burner and simulated boiler using shielded thermocouples and dual-beam pyrometers.

3.3 PILOT-SCALE DEVELOPMENT STATUS

There are six major areas in the LNSB wherein certain high levels of performance must be simultaneously achieved for the theoretical promise to be fulfilled in a practical, commercial burner: (1) a major fraction of the fuel sulfur must be captured under fuel-rich combustion conditions in a solid calcium-sulfur form, (2) the sulfur so captured must be retained in the solid form through subsequent oxidizing stages of combustion, (3) fuel nitrogen must be converted under fuel-rich combustion conditions to harmless molecular nitrogen, (4) little or no thermal NO_x must be formed in the boiler when the final overfire air is added, (5) a major fraction of the slag/fly ash from coal combustion must be separated from the combustion gases and hence removed from the burner before the gases enter the boiler, and (6) fuel carbon must be almost totally oxidized. Separation of fly ash from the hot gases is not necessary when the burner is applied to a boiler capable of handling the fly ash.

There are no rigidly defined LNSB program goals in each of these areas. The LNSB can be extremely useful in many applications even if some goals are exceeded and some are not. For example, most regulations today require extremely tight control of SO_2 emissions but rather simple control of NO_x emissions (acid rain legislation may change this). Informal program goals are: (1) sulfur capture exceeding the U.S. New Source Performance Standards (NSPS) or, with some of the very low sulfur coals, less than 86 ng-SO_2/J (0.2 lb SO_2/MBtu) SO_2 emissions; (2) sufficient retention of the captured sulfur to achieve the goals of (1) at the boiler exit; (3) conversion of over 95% of the fuel-bound nitrogen to gaseous molecular nitrogen (representing in most cases less than about 100 parts per million [ppm] NO_x remaining); (4) sufficiently little formation of NO_x in the final combustion to achieve less than 100 ppm NO_x at the boiler exit; (5) steady-state removal of about 80% of the coal ash, with the remaining fly ash in particle sizes less than 10 micrometers (μm); and (6) better than 99% total carbon burnout. As an overall goal, all of these six detailed goals should be achieved simultaneously (except for fly ash separation when not required).

Most of the pilot-scale testing to date (114 h) has been conducted without the fly ash separator. Design and fabrication of the separator and slag tap proceeded in parallel with initial burner testing. The separator/tap was only recently installed, and only three tests have been conducted since installation. The most representative examples, then, of the status of pilotscale demonstrated simultaneous performance in all six areas of interest is the data derived from the last few tests. Two of these tests, using Black Mesa and Whitewood coals, were conducted just before the slag separator was installed. The last test, using Spring Creek coal, is the most representative because the slag separator/tap was installed.

Table 1 shows the as-fired coal analyses. Black Mesa is a low-sulfur western U.S. bituminous coal. Whitewood coal, from a mine near Edmonton, Alberta, Canada, is the coal that will be used in the first full-scale burner demonstration program at that location. Whitewood is unusual for the very low sulfur, high moisture and ash, and the very high calcium content in the coal ash. Whitewood has an inherent calcium-sulfur mole ratio of 3.9, so no calcium was added to this coal. Spring Creek is a low-sulfur Montana coal with particularly high sodium content (8% of the ash) and low ash fusion temperatures. The Spring Creek test was conducted largely under conditions most favorable for slag separator/tap operation (high stoichiometries and temperatures), but some data were obtained as well under better conditions for SO_2 and NO_x control.

3.3.1 Sulfur Capture

Spring Creek is a very low-sulfur coal (0.2%). It seems clear that, as the sulfur content of a fuel approaches zero, the possible fractional sulfur capture will also approach zero but the remaining SO_2 emissions out the stack (the bottom line), nevertheless, should also approach zero.

Figure 3 shows SO_2 emissions data measured in tests of the three coals shown in Table 1. These data show the informal goal of 86 ng-SO_2/J (0.2 lb-SO_2/MBtu) SO_2 emissions was very nearly met with both Spring Creek and Whitewood coals; but the emissions from Black Mesa coal were somewhat higher. Figure 4 shows these same results expressed as percent sulfur capture. Here it is seen that the sulfur capture with both Black Mesa and Whitewood coals met the goal of 70% capture but that with Spring Creek coal did not. This data suggests, therefore, that if the sulfur content of a coal is sufficiently high, goals expressed as percent capture should easily be met.

It is fully expected, however, that percentage sulfur capture firing coals with less than 0.2% sulfur (if such could be found) would decrease to zero as the sulfur content of the coal decreases to zero. Under current Canadian regulations, this would present no problem because the regulation is stated in terms of SO_2 emissions. It is considered highly unlikely, however, that the U.S. NSPS regulation of 70% reduction can be met with a coal containing less than about 0.25% sulfur. It is likely that the percentage sulfur capture with Whitewood coal would be in the 50-60% range were it not for the heavy excess of calcium (3.9 calcium-sulfur mole ratio) in that coal.

High-sulfur eastern coals have not yet been adequately tested in the pilot-scale burner. As soon as satisfactory slag separator/tap operation is established, however, three such coals are scheduled for testing, including a Nova Scotia (Prince Mines) coal with 4.7% sulfur. If the sulfur capture data shown in Figure 4 do indeed describe a trend with coal sulfur content, there should be no problem achieving 90% sulfur capture with coals containing more than about 1-2% sulfur.

3.3.2 Sulfur Retention

The data presented in Figures 3 and 4 show not only sulfur capture within the burner, but retention of that captured sulfur through the final stage of combustion in the simulated boiler. The circles in Figures 3 and 4 represent SO_2 concentrations and sulfur capture in the combustion gases and particulates as they leave the burner and enter the simulated boiler before the final combustion air is added. The squares represent conditions within the waste heat boiler (simulated boiler exit) where gas temperatures are down to about 530°K (500°F). A slag separator/tap was not installed for the tests of Black Mesa and Whitewood coals, so a major fraction of the fly ash passed through the final combustion stage. Even in the Spring Creek test, 25-30% of the coal ash passed through final combustion.

Figures 3 and 4 show that SO_2 emissions and sulfur capture, within the scatter of the data, were not discernibly different at the boiler exit than they were at the burner exit. In fact, with Whitewood and Black Mesa coals, it might be argued that SO_2 emissions are lower, and the related sulfur capture higher, at the simulated boiler exit than they were at the burner exit. This means, of course, that sulfur captured in the solid calcium-sulfur form in the Rockwell LNSB remains in this form through the simulated boiler and into the baghouse.

A complete and accurate sulfur mass balance on the whole facility, to verify data from gas analyses, has not yet been obtained. This is largely because of the way in which the burner is shut down (air cooled for several hours). Without a slag separator installed, a steady-state ash balance cannot be achieved. Such balances will be routinely obtained after the separator/tap achieves stable, steady operation. Preliminary analyses of slag and fly ash from various locations within the burner, in the simulated boiler, and in the baghouse suggest high sulfur capture and retention in the burner slag and larger fly ash particles and less in the fly ash which reaches the baghouse.

The bottom line in SO_2 control, however, is the gaseous SO_2 emissions out the stack. Figure 3 shows that the LNSB goal in this regard is one-third of that currently allowed by Canadian regulation, and that goal was very nearly met with both Whitewood (a Canadian coal) and Spring Creek. Even the SO_2 emissions out the stack with Black Mesa coal were about one-half of the Canadian regulation.

3.3.3 NO_x Control

Figure 5 shows a summary of NO_x control performance with the three coals shown in Table 1. It is well known, from all testing under this program as well as in the literature, that minimum NO_x levels are achieved in combustion at stoichiometric ratios around 0.6. Although the data shown in Figure 5 are limited, the familiar "U-shaped" curve is indicated, by the burner exit data (circles). The major differences in the NO_x data shown in Figure 5 (burner exit) compared to other data in the literature, however, are: (1) the very low level of the minimum (about 50 ppm) and (2) the broad range of stoichiometry over which very low levels are achieved (less than 100 ppm over the range of about 0.5 to about 0.75.

Figure 5 also shows the informal LNSB goal of about 100 ppm relative to the U.S. NSPS. The LNSB goal represents reductions of about 80% from current U.S. NSPS. Such low NO_x levels have been demonstrated routinely throughout the LNSB program. In addition, there appears to be little interest in major reductions in NO_x emissions. As a result of the lack of interest, and of the ease with which very low NO_x levels have been achieved in the LNSB, very little effort has been devoted to further NO_x reductions beyond those levels shown in Figure 5.

3.3.4 NO_x Generation in the Boiler

At the same location within the burner where the low NO_x levels were measured (the circles in Figure 5), measurements also show carbon burnout in the 85-95% range. This degree of carbon burnout assures that essentially all of the fuel-bound nitrogen has been gasified. If all of this fuel-bound nitrogen were converted to NO_x, emission levels of over 2000 ppm would result. The fact that less than 100 ppm NO_x was measured indicates that essentially all of the fuel-bound nitrogen has been converted to harmless molecular nitrogen by the time the combustion gases leave the burner.

The combustion gases leaving the burner and entering the boiler, however, are still the products of fuel-rich combustion and are still very hot (just a few hundred degrees (K) less than adiabatic). The remaining excess air must be added to these gases to complete combustion of the carbon monoxide, hydrogen, and remaining unburned carbon (char). If this final stage of combustion is not properly controlled, a significant amount of new NO_x can be generated in the boiler. This is true regardless of how the initial combustion was achieved. The potential for significant NO_x generation in the boiler, then, is very real.

Figure 5 shows indications of the growth of NO_x in the simulated boiler. NO_x concentrations (corrected for dilution to a level of excess air which would show 3% oxygen) are shown in Figure 5 both at the burner exit (circles) and at the simulated boiler exit (squares). For direct comparison, the boiler exit NO_x

data are plotted in Figure 5 at the stoichiometric ratio at the burner exit. The degree of NO_x growth in the simulated boiler, therefore, can be seen by comparing the circles and squares at the same burner stoichiometric ratio.

These data indicate some cases where there was growth of NO_x in the simulated boiler (averaging 70 ppm) but also some data showing that NO_x concentrations were actually further reduced (an average of 97 ppm) in passing through the final stage of combustion. In no case was the NO_x growth sufficiently large to change the observation that final NO_x emission levels out the stack are well below current NO_x regulations. Such low levels are even below U.S. NSPS for natural gas and oil fuels (86 and 130 ng-NO_2/J or 0.2 and 0.3 lb NO_2 MBtu, respectively).

Because very low NO_x levels have consistently been achieved throughout the Rockwell LNSB program and because little interest has been expressed (except in Japan, California, and in large cities) in stringent NO_x regulation, little effort has been made to further reduce NO_x emission levels from levels such as shown in Figure 5. It appears quite feasible to reduce NO_x levels in the burner well below the 50 ppm shown. In addition, data suggest that final excess air is currently introduced into the fuel-rich gases from the burner too soon, while the gases are still too hot. Moving this final air injection point further downstream is expected to assure minimal generation of new NO_x in the simulated boiler.

3.3.5 Slag/Fly Ash Separation

Slag/fly ash separation is achieved in the Rockwell LNSB using a series of tubes, oriented vertically and normal to the hot gas flow, much like a slag screen. Some of the coal ash accumulates on the walls upstream of the separator and flows into the bottom of the separator where it can be removed from the burner via the slag tap. In addition, the vertical tubes remove molten fly ash from the hot gas stream. This fly ash impinges on the separator tubes and flows down the tubes and out the slag tap. The LNSB goal for total coal ash removal by both mechanisms is 80%. In earlier testing, during the concept verification test series, 80% removal was demonstrated. In that testing, no slag tap was used; the slag simply accumulated in a well below the separator.

The slag separator and slag tap have only recently been installed in the pilot-scale burner, and testing has just begun. The separator posts are water cooled and are constructed of steel with steel studs on the external surface, with refractory packed around the tubes and studs. The thickness of refractory and the water cooling are designed to maintain the external surface of the refractory below the fusion temperature of the coal ash. During initial testing, the molten fly ash freezes on and sticks to the refractory, coating it with a layer or skull of solid slag. Eventually, the slag skull becomes sufficiently thick and insulating that the slag surface temperature exceeds the ash fusion temperature. Subsequent molten fly ash impinging on the posts remains molten and runs down the posts and out the slag tap. It is this continually renewed layer of slag that resists erosion from the hot, fly ash-laden environment. A so-called "burn-in" period is necessary with a new separator, therefore, to establish the desired slag coating on all separator surfaces.

In the first two tests with the separator, with Black Mesa coal, build up of the desired slag layer was not complete. There were some early indications of excessive solid slag buildup near the bottom of the separator posts. It was for this reason that the third (and latest) test involved Spring Creek coal, which has the lowest ash fluid temperature (1390°K or 2045°F) in the available inventory. In addition, this test was conducted for the most part with very high stoichiometries in the burner to maximize the gas temperature in the separator.

Figure 6 shows a picture of the separator after the last test, looking downstream at the first row of separator posts. The requisite slag layer has been established over about 90% of the post surfaces. A very nearly steady-state gas pressure drop through the separator of less than 1 in. of water was measured. The figure also shows, however, a region at the bottom of the posts where the slag froze and built up to about 5 in. deep. The causes of this buildup are considered known. Appropriate hardware changes have been made, and it is expected that the next test will demonstrate resolution of this problem. To date, there has not been sufficient test time to fully "burn in" the separator and to establish steady flow of slag out the slag tap as well. In line with industry experience, it is expected that some problems will have to be resolved before steady-state slag flow through the tap is achieved.

In the last test, with average separator "burn-in" nearly (but not quite) complete, about 75% removal of the slag/fly ash by the burner/separator was measured.

3.3.6 Carbon Burnout

Finally, simultaneously with SO_x and NO_x control and slag/fly ash separation, a high level of carbon burnout must be achieved, at least by the boiler exit. Figure 7 shows carbon burnout data derived from gas analyses and baghouse ash analyses in the test of the Spring Creek coal.

Using analyses of combustion gases, carbon that appears as carbon monoxide or dioxide is considered "burned out," while the remainder, regardless of its form or location, is considered "not burned out." Carbon burnout is determined from slag and baghouse ash using ash as the tracer.

Figure 7 shows varying degrees of carbon burnout within the burner depending on the burner stoichiometries at the time and the location of gas sampling. At the burner exit, carbon burnout varies over the range of about 83-93%, generally measuring around 90%. The remaining 10% or so of unburned carbon is intended to be burned out in the boiler. It is particularly here that the boiler radiant section simulation in the Rockwell test facility (a length of bare steel ducting externally cooled with water sprays) may cause extraneous, difficult-to-interpret problems. The bare steel ducting includes two sharp 90° turns intended to remove some of the fly ash when the fly ash separator is not installed. Fly ash does, in fact, impinge on the cold, bare steel ducting in these turns and may cause rapid quenching of a significant portion of the desired remaining carbon burnout. While the trend of carbon burnout from gas sample data continues to rise as the gases progress down the burner and the simulated boiler, there is some indication that the carbon burnout limits, and actually appears to decrease in the steel ducting and waste heat boiler. Analyses of carbon remaining in slag removed from the burner and from the baghouse show only 0.12 and 0.10% of the carbon (better than 99.8% carbon burnout), respectively. Carbon monoxide and unburned hydrocarbons in the gases at the boiler exit were too low to be measured (i.e., all gaseous carbon present as carbon dioxide).

Table 2 shows a summary of the disposition of total carbon and ash for the Spring Creek test, based on slag/ash analyses. Steady-state flow of slag out the slag tap was not achieved in that test (or any other test to date), so the entire test must be considered transient conditions. Further, it was not possible to directly measure the total quantity of slag built up in the burner and separator over the duration of the test, so that quantity could only be determined by difference. Until steady-state slag accumulation and flow out of the slag tap is established, accurate carbon and sulfur balances are not possible. Nevertheless, the data in Table 2 show an estimated average disposition of coal ash and carbon over the period of the test.

4.0 REMAINING LNSB PROGRAM

The pilot-scale development program is nearing completion. Barring excessive problems in achieving steady-state slag separator and slag tap operation, that program is now expected to be completed by mid-summer of 1985. Sufficient performance is considered to have been already demonstrated in all other areas to justify moving on to the next stage of development of a commercial burner, full-scale demonstration on an operating utility boiler, at least with a low-sulfur western coal. The goal of 90% SO_2 control with a high-sulfur eastern coal has not yet been demonstrated, but pilot-scale testing of such coals is scheduled for the spring of 1985.

The full-scale demonstration program being planned will be conducted at the Wabamun Plant of TransAlta Utilities Corporation near Edmonton, Canada, and will use the Whitewood low-sulfur subbituminous coal. The technical plan and schedule for that program were discussed in a previous paper (Reference 1). Due to technical, financial, and organizational difficulties in the pilot-scale program, the start of the Wabamun demonstration program has been delayed more than a year from initial estimates. It is now scheduled to start in July or August 1985.

Total cost of the Wabamun program is currently estimated at $9.9 million (Canadian). About one-half of the funding is expected from the Alberta Office of Coal Research and Technology (OCRT), with the other half expected from a consortium of Canadian and U.S. utilities and Rockwell. Provisional funding commitments have been made by the Alberta OCRT and by more than one-half of the necessary utilities. At least two additional supporting utilities (Canadian and/or U.S.) are required.

Following the Wabamun program (complete in 1988), there remain requirements for further full-scale demonstrations, including at least one utilizing high-sulfur eastern coal, conversion of a boiler designed for gas and/or oil fuels to coal, conversion of a coal-fired boiler to LNSBs (to demonstrate improved SO_x and NO_x control wthout a separator installed), and conversion of special types of coal-fired boilers such as cyclone or arch-fired types.

5.0 CONCLUSIONS

Since the 1979 inception of the theoretical concepts for strong but low-cost control of SO_x and NO_x emissions in combustion, the Rockwell LNSB has been subjected to a wide range of testing with a wide range of coals, oil, shale oil, a coal-oil mixture, and coal-water mixtures. No data has been generated in any of this testing that might be construed to suggest that the theoretical predictions are not true or that they are fundamentally unattainable. The promise of SO_x and NO_x emission control to virtually zero levels, at costs 10-20% of competing technologies, remains as true today as ever. At least in a few cases, better than 95% SO_x reduction and zero NO_x emissions have been demonstrated. In a prototypical, pilot-scale burner with low-sulfur western coals, better than 70% SO_2 reduction, NO_x emissions less than 100 ppm, slag/fly ash removal over 70%, and carbon burnout over 99% have been simultaneously demonstrated. At least one case each of the better than 95% and 70% SO_2 reduction demonstrations were achieved using only the calcium inherent in those coals with nothing at all added to the coals. The very low NO_x levels in all cases are achieved at virtually no additional operating cost.

The LNSB program is proceeding in the process of development and larger and more complete demonstrations leading toward qualified, commercial burners for a wide range of applications in the 1988-1990 period.

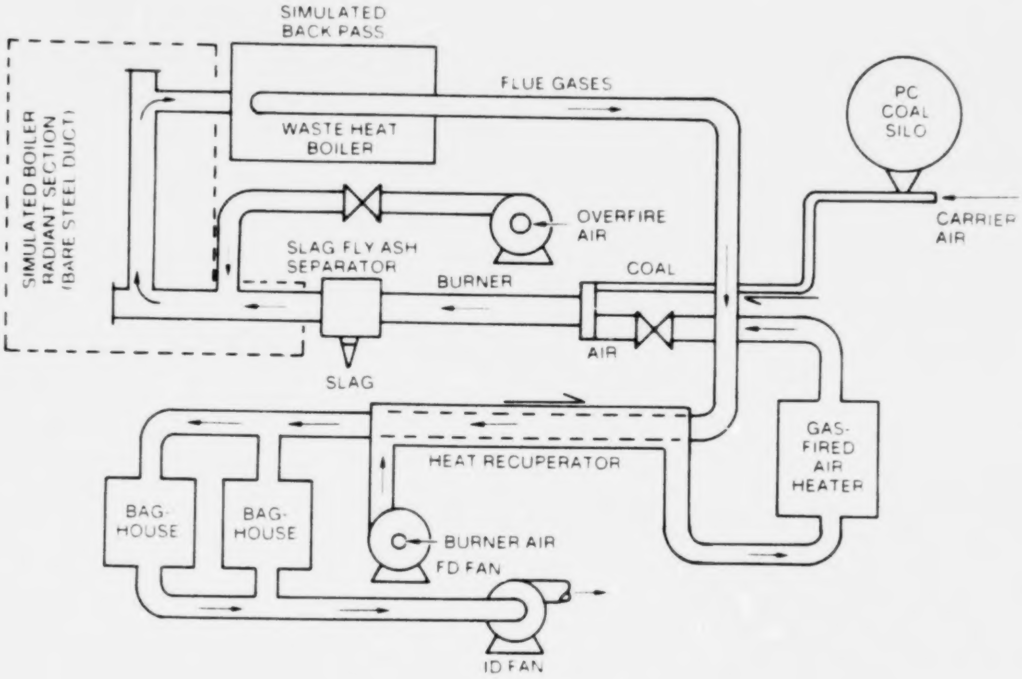
SIMULATED BACK PASS
FLUE GASES
PC COAL SILO
WASTE HEAT BOILER
SIMULATED BOILER RADIANT SECTION (BARE STEEL DUCT)
OVERFIRE AIR
CARRIER AIR
SLAG FLY ASH SEPARATOR
BURNER
COAL
AIR
SLAG
GAS-FIRED AIR HEATER
HEAT RECUPERATOR
BAG-HOUSE
BAG-HOUSE
BURNER AIR
FD FAN
ID FAN

Figure 1. Rockwell Pilot-Scale Test Facility

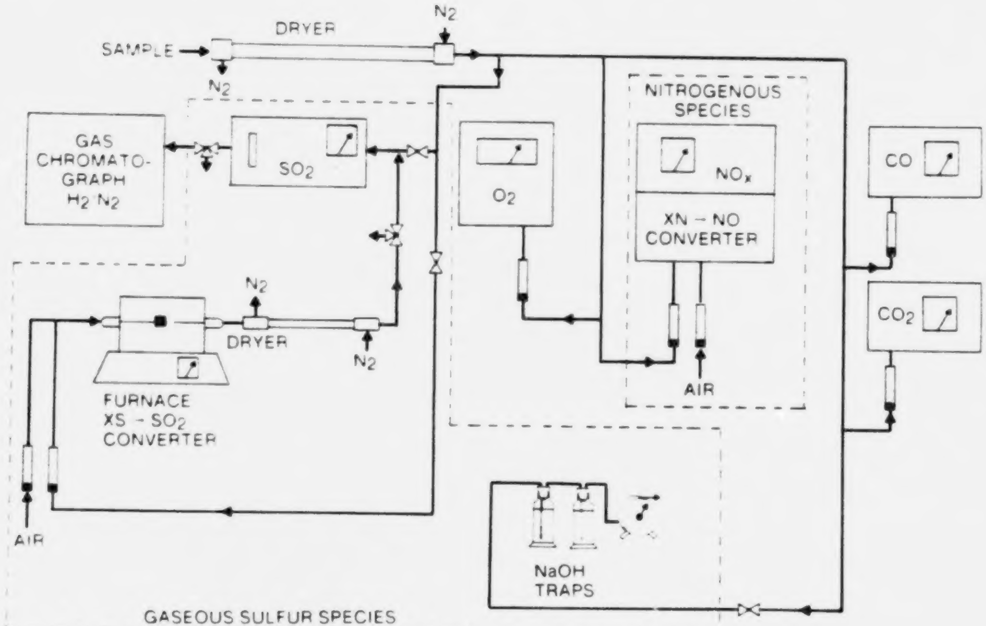
SAMPLE
DRYER
N2
N2
NITROGENOUS SPECIES
GAS CHROMATOGRAPH H2 N2
SO2
O2
NOx
XN → NO CONVERTER
CO
CO2
N2
DRYER
N2
FURNACE XS → SO2 CONVERTER
AIR
AIR
NaOH TRAPS
GASEOUS SULFUR SPECIES

Figure 2. Gas Sample Analysis System

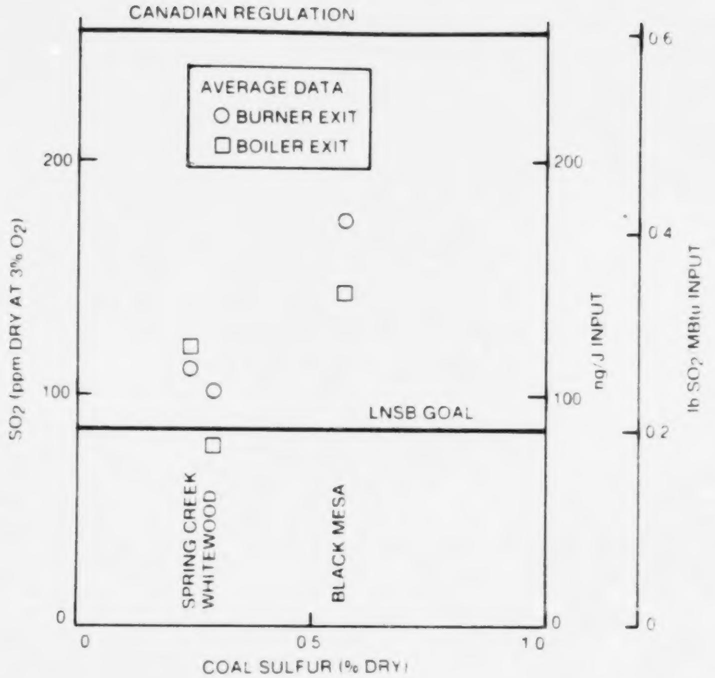

Figure 3. SO_2 Emissions, Low Sulfur Coals

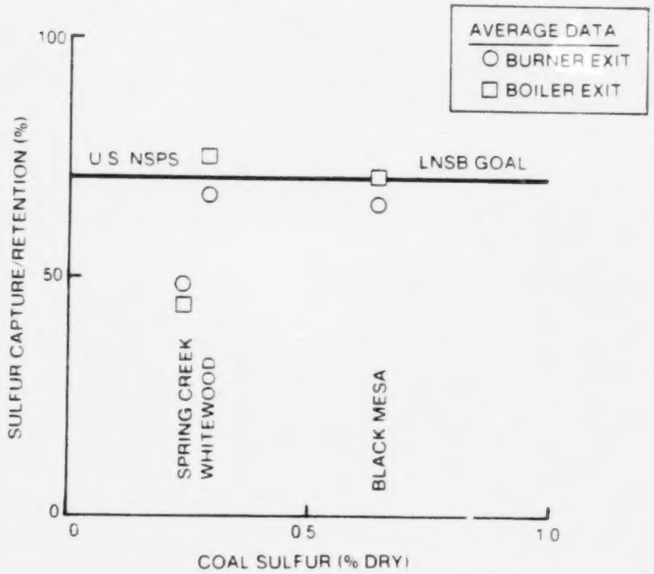

Figure 4. Sulfur Capture/Retention
Low Sulfur Coals

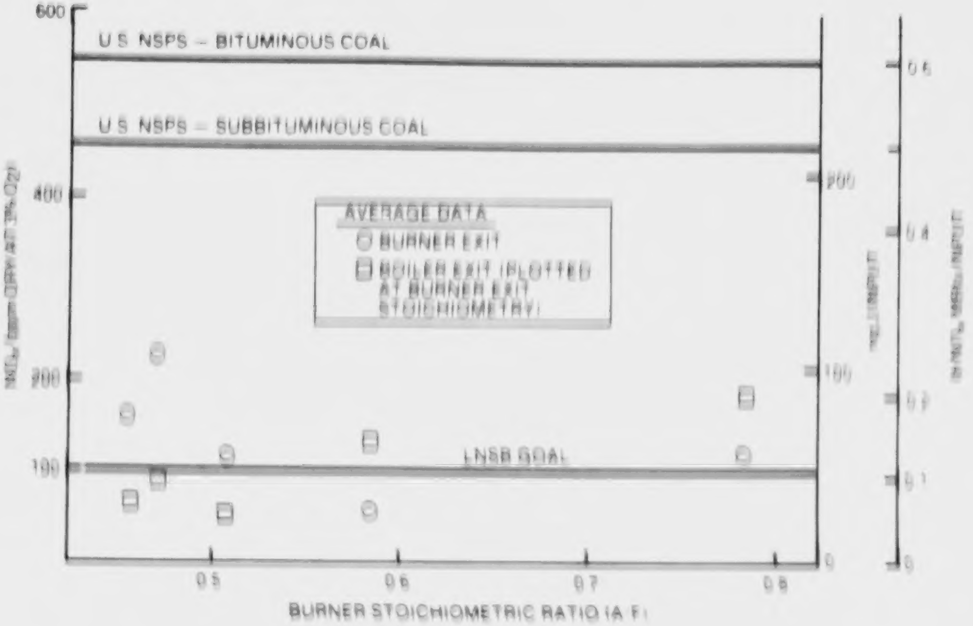

Figure 5. NO_x Control Black Mesa/Spring Creek/Whitewood

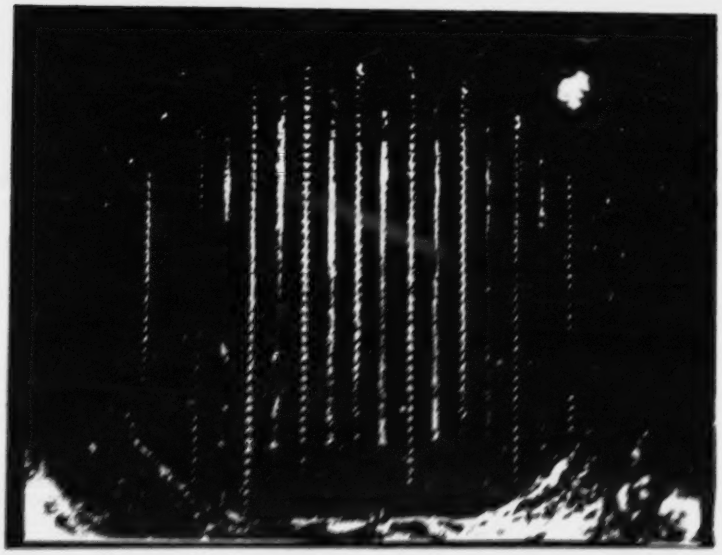

Figure 6. View Looking Downstream into the Pilot-Scale Slag/Fly Ash Separator

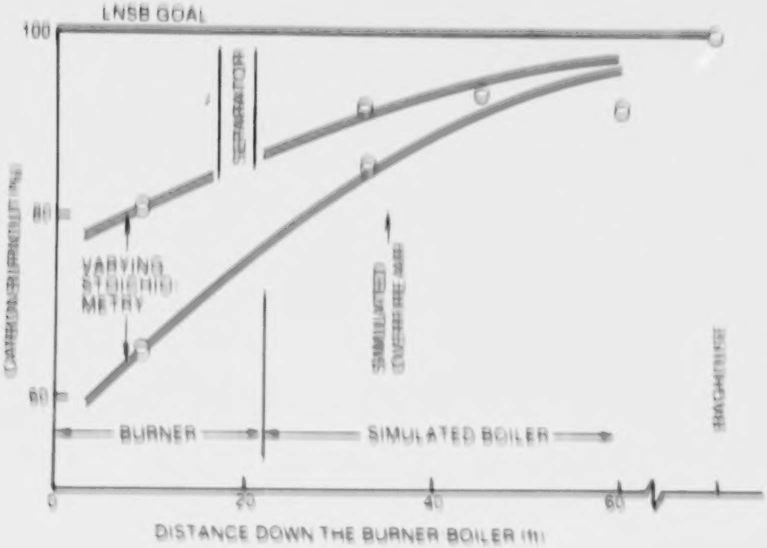

Figure 7. Carbon Burnout Spring Creek Coal

Table 1

COAL ANALYSES

	WEIGHT (%)		
	BLACK MESA	SPRING CREEK	WHITEWOOD
ULTIMATE ANALYSES, AS-FIRED			
CARBON	64.23	60.55	55.88
HYDROGEN	4.67	4.25	3.47
NITROGEN	1.14	0.88	0.78
SULFUR	0.53	0.21	0.97
OXYGEN	13.08	15.08	14.40
ASH	8.02	3.44	13.27
MOISTURE	5.00	14.20	8.00
LIMESTONE*	3.33	1.39	3.23
	100.00	100.00	100.00
HEATING VALUE, AS-FIRED			
MJ/kg	26.4	24.3	21.8
Btu/lb	11,340	10,460	9,360
Ca/S MOLE RATIO			
AS-RECEIVED	0.80	1.77	3.83
AS-FIRED	2.01	2.12	3.83
ASH FLUID TEMPERATURE (REDUCING)			
°K	1,725	1,390	1,675
°F	2,650	2,045	2,555

*BECAUSE OF THE IMPORTANCE OF THE CALCIUM CONTENT OF THE COAL, CALCIUM IS LISTED SEPARATELY AS LIMESTONE. CaO IN THE ASH ANALYSIS IS REMOVED FROM THE ASH CATEGORY, COMBINED WITH APPROPRIATE CARBON AND OXYGEN (REMOVED FROM THESE CATEGORIES) AND, WITH ANY ADDED LIMESTONE, THE TOTAL IS LISTED SEPARATELY

Table 2

ASH/CARBON DISPOSITION - SPRING CREEK COAL

LOCATION	ASH [kg (lb)]	PERCENT OF TOTAL ASH	CARBON/ ASH RATIO	CARBON [kg (lb)]	PERCENT OF TOTAL CARBON
INPUT	265 (585)	100	14.4	3798 (8375)	100
BURNED	0	0	—	3790 (8357)*	99.8
RETAINED IN BURNER/ SEPARATOR	200 (440)*	75	0.023	4.5 (10)	0.1
RETAINED IN BAGHOUSE	65 (144)	25	0.059	2.6 (6)	0.1

*BY DIFFERENCE

NO_x CONTROL IN AN AIR COOLED CYCLONE COAL COMBUSTOR

B.Zauderer,Coal Tech Corp.,P.O.,Box 154, Merion,PA 19066*
K.S.Fujimura,Southern California Edison Company,P.o.Box 800,Rosemead,CA 91770

ABSTRACT

This paper reports on the analysis of experiments on NO_x control in a 1 MMBTU/hr, staged, air cooled, cyclone combustor. The combustor exhausted into two ceramic lined vessels, which simulated the radiant furnace section of a boiler. Final combustion air was introduced between the two vessels, at a point where the cyclone combustion gas exhaust had cooled from 3000°F to about 2200°F. The stoichiometric ratio (SR) of the combustor was varied from 0.6 to 1.15. About a factor of three NO_x reduction, to less than 100 ppm,was obtained at a SR of 0.65,based on the coal and air feed rates to the cyclone combustor. The NO_x results are consistent with other experiments in a water cooled cyclone combustor and in conventional pulverized coal flames, which show that the minimum emission of the three primary fuel bound nitrogen compounds occur at about this SR. It is shown that the placement of the tertiary air injection in the simulated furnace was consistent with kinetic rate predictions for optimum NO_x reduction in staged combustion. The application of this NO_x control technique to commercial scale utility boilers is briefly described. Also, a brief description is given of experiments in which significant reductions in the SO_x emissions were observed,as a result of limestone injection in this cooled combustor.

INTRODUCTION

The most economic and lowest risk approach to the conversion of oil fired boilers to coal is one in which maximum utilization of the existing boiler capacity is used and in which the number of boiler sub-systems needed to burn the coal in an environmentally acceptable manner is minimized. To be economically advantageous, the conversion equipment must be financed by the oil-coal price differential and in the current period of high of real capital costs, coal combustion with additional environmental control at the stack can lengthen the required payback period and increase the risk of coal conversion. Consequently, since the early 1970's extensive research efforts have been focussed on combined combustion and environmental control, with one of the primary areas of emphasis being methods of simultaneously reducing sulfur and nitrogen oxides emissions during the coal combustion process. As a result of research in the past decade on the cyclone coal combustor, it appears that this device has the potential for providing such a low cost coal conversion technology. While the cyclone coal combustor has been in commercial use for decades, its mode of operation has generally required excess air operation in the combustion chamber. This produced high NO_x emissions. However, research on advanced cyclone combustors in recent years has led to the discovery of means for significantly reducing these environmental emissions from the combustor.

---

*-D.B.Bender,C.S.Cook,E.F.Fleming,S.A.Omori,and D.Rogers, participated in the 1 MMBTU/hr combustor experiments reported in this paper-See Acknowledgements.

In this paper, results of pilot scale research on a cyclone combustor, one of whose novel features is the use of air cooling, will be presented. The focus of the paper will be on the description and interpretation of experiments designed to reduce the nitrogen oxide emissions during staged combustion. The cyclone combustor was operated under fuel rich conditions. The combustion gas (at a temperature of about 3000°F) exhausted through a pair of internally, ceramic lined vessels, which were used to simulate the radiant section of a steam boiler. Following combustion gas cooldown in the first tank to about 2200°F, additional air was introduced to complete combustion in the second vessel, resulting in a gas exhaust of about 1500°F. The NO_x level measured at the stack decreased from 300 ppm at excess air conditions to below 100 ppm at a stoichiometric ratio, based on the fuel and air feed rate to the first stage,of 0.65. To date, the results of these experiments,which were performed in 1980-1, [See Acknowledgements], have only been presented in summary form (1,2). In addition, a number of critical issues related to these experiments have only been clarified in the past few years,in work performed, partly at Coal Tech. Among these issues were: The determination of the most probably cause for the poor carbon conversion in the combustor; and the proper description of the fuel bound and thermal nitrogen conversion process in the combustor and simulated radiant furnace. Detailed information on the experiments is contained in two unpublished reports (3,4).

Since the feasibility of retrofit of an oil fired boiler to coal with this combustor is dependent on NO_x control, the relationship NO_x control to a boiler retrofit will be briefly discussed. More details on this matter have been reported elsewhere (2).

In addition, the 1 MMBTU/hr air cooled combustor was,to the best of our knowledge, the first cyclone unit in which significant sulfur reduction by the injection of limestone into the combustor,was observed. The probable mechanisms responsible for this non-equilibrium sulfur capture process were identified subsequent to the completion of the experiments, and they were reported elsewhere,in summary form (1,2) and in more detail (5,6). The sulfur capture analysis and experiments will be briefly noted in this paper because it is an integral part of the environmental control process in the combustor.

THE AIR COOLED CYCLONE COAL COMBUSTOR

Background

The cyclone combustor is a high temperature (3000+°F) device in which a high velocity swirling gas is used to burn crushed or pulverized coal. The ash is separated from the coal in liquid form on the cyclone walls from which it flows by gravity forces toward a port located at the downstream end of the device. The cyclone combustor has a long commercial history as an ash removal device. In the U.S. (7) it was used to burn low ash melting temperature coals in a crushed form [50%-40 mesh], to save on pulverization power . In Germany, it was used (8,9) to burn low rank,very high ash coals in coarsely pulverized form [60%-100 mesh]. In both devices the secondary combustion air was injected tangentially along most of the entire top length of the combustor to provide relatively high excess air combustion conditions. As a result,both combustors produced very high NO_x emissions.

The combustors were built in size ranges of 100 to 700 MMBTU/hr. The German cyclones, which used a coarse pulverized coal instead of the crushed coal of the U.S. units, are more relevant to modern concepts. The German units produced up to 85%

slag retention. Recent analysis,of the wall burning process in these commercial scale cyclones (1,6,10),showed that these cyclones were not completely wall burning devices,as was apparently assumed (7-9). Instead a major fraction of the coal particle combustion must take place after re-entrainment of the coal particles,subsequent to their initial impact on the slag layer covering the inner combustor wall, by the tangential,swirling air flow. Therefore, the combustion process in these units is similar to that in the advanced units of present interest, and the scaling relationships used in the prior cyclone have some applicability to the advanced combustors.

The present advanced slagging and/or cyclone,coal combustors under study for boiler conversions are derived in large part from R&D on their applications to magnetohydrodynamic (MHD) power generation (e.g. 11,12). Two parallel and essentially independent research efforts were involved. One consisted of the development of a pressurized combustor for powering the combustion gas driven,MHD generator. Various configurations were studied. However, the one that is currently under development in the US is a horizontal cyclone (12) which is somewhat similar in concept to the earlier commercial units, with water cooled walls, and sidewall secondary air injection. This combustor uses a more conventionally pulverized coal (e.g. 70%-200 mesh), which is injected axially,using dense phase transport, at the closed end of the cyclone.

The air cooled,cyclone combustor concept,which was used for the experiments reported in this paper, is derived in part from a separate MHD related application as a heat source for a 3000°F,ceramic regenerative heat exchanger (11). Both an atmospheric and a pressurized (4 atm.) combustors were designed and tested,at the 1 MMBTU/hr scale. The interest in the cyclone for this application was motivated by the requirement for high slag retention in the combustor to prevent plugging the narrow heat exchanger passages with slag. The cyclone combustor was air cooled because it was hypothesized that it would result in improved slag retention (<90%).

EXPERIMENTAL PROCEDURE

Description of the 1 MMBTU/hour Air Cooled Cyclone Coal Combustor

Figure 1 is a sketch of the 1 MMBTU/hr,air cooled horizontal cyclone coal combustor (11, 13). An oil gun,located at the center of the closed end of the unit,was used to pre-heat the ceramic-lined combustor wall and to start coal combustion. Pulverized coal (37% to 70%-200 mesh), transported by primary air at about 160°F,was injected toward the wall through tubes,located in an annular region enclosing the central oil gun. Secondary air (SA),injected through swirl vanes located between the coal injection ports and the central oil gun, was used to adjust the overall combustor stoichiometry from 0.5 to 1.15.The ceramic liner was cooled by the SA and maintained at a temperature high enough, (2200-2500°F), to keep the slag in a liquid, free flowing state. The liner was encased in a metal shell, with the cooling air passing through external axial grooves. The SA tangential injection velocity of several 100 ft/sec plus the use of fine coal pulverization allowed the combustion of much of the coal particles in suspension near the cyclone wall. This improved slag retention, and values in excess of 90% were reported (11) in Illinois No.6 coal, with coal,pulverized from 50% to 70%-200 mesh, in excess air. With coarser coal sizes,(37% to 45%-200 mesh),and under fuel rich operation, incomplete carbon conversion was obtained (80-90%), and the slag rejection decreased significantly (13).

The NO_x control experiments were performed with this coarser coal particle size distribution. The great sensitivity of fuel rich carbon conversion was not appreciated at the time of the experiments. The motivation for using the coarser particle sizes was due to evidence from prior cyclone combustor experiments ⟨e.g.14⟩, which showed that high slag retention required coarse coal particles. In our subsequent analysis of the coal particle combustion in the 1 MMBTU/hr combustor ⟨6⟩,we demonstrated that the incomplete carbon conversion could be explained in large part by the use of the coarse coal particle size in this small combustor ⟨5,6,10⟩. This coal particle size also resulted in the carryover considerable unburned char into slag tap which made accurate measurements of the slag retention impossible ⟨13⟩.

Description of the Facility Used to Simulate the Radiant Furnace Section of a Boiler

There are two sources of NO_x in coal combustion, namely fuel bound nitrogen ⟨FBN⟩, and molecular nitrogen ⟨N_2⟩ in the combustion air. The planning ⟨3⟩ of the NO_x control experiments in the 1 MMBTU/hr combustor was based on previously reported observations ⟨e.g. 15,16⟩ that fuel rich combustion resulted in the reduction of NO_x from FBN. In addition, it was known from these references, as well as from MHD combustion systems ⟨e.g. 17⟩, that staged combustion, with a fuel rich, first stage followed by gas cooling of about 0.5 to 1 second duration, prior to the introduction of the final combustion air would result in significant overall total NO_x reduction.

Therefore, the experiments were planned to simulate a radiant furnace section of a boiler,fired with a fuel rich,cyclone combustor,a shown schematically in figure 2. The left side of the figure shows the location of the fuel rich combustors ⟨in this case,cyclones⟩, at the bottom of the radiant furnace. After a gas cooldown of about 800-1000°F in section (a) of the furnace, the final ⟨tertiary⟩ combustion air is introduced at location (m), which increases the temperature to below 3000°F, and further gas cooling occurs until a temperature of 2000°F or less is reached in the convective boiler passages.

The right side of figure 2 shows the experimental simulation of the boiler used in the experiments.This is shown in more detail in figure 3. The 1 MMBTU/hr cyclone combustor is located at the top left side of sketch. The upper furnace region (a) [see figure 2] is simulated by a steel vessel (A), internally lined with ceramic, and with an inner diameter of 14" and an active length of 10 feet. Final combustion air is introduced at the bottom of the duct [point (M)]. Gas mixing takes place in the expansion duct ⟨at the bottom of the two figures ⟩,and final combustion proceeds in the other ceramic lined vessel (B), whose inner diameter is also 14" and its working length is 10 feet. As will be shown in the results, the gas conditions and temperatures are in the range required for the furnace simulation.

Diagnostics.

The proper interpretation of the NO_x control experiments required very extensive diagnostics. The gas temperatures were measured with thirteen type B (Pt-6% Rh vs Pt-30% Rh) thermocouples located along the entire flow train, beginning at the insulating duct, downstream of the cyclone combustor exit ⟨see figure 2⟩ and extending to the exhaust of the second ceramic lined vessel. In addition,to calibrate the thermocouples, two suction pyrometers were placed at the top of the first heat exchanger duct and at the exit of the second duct. The temperature at the exit of the cyclone combustor was computed from a heat balance.

Three gas sampling probes,located at the suction pyrometer positions, and at the bottom of the first heat exchanger vessel, were used to measure the concentration of H_2,CH_4,CO,CO_2,O_2,N_2,SO_2,and H_2O⟨appx.⟩. The measurement instruments were a Beckman NDIR and a Carle Analytical Gas Chromatograph. A NO_x diagnostic probe was located at the exit of the second ceramic lined vessel, i.e. at the stack, where the temperature was about 1500°F.

Particulates were measured at the stack,by EPA Method 5, using a RAC "Staksamplr". However, this measurement proved to be of limited utility because the main interest was to determine the particle carryover out of the cyclone combustor stage. With the long and changing gas path in the system, as well as the continuing combustion taking place in the heat exchanger vessels, one cannot deduce, the first stage particle exhaust from a measurement at the stack.

Test Matrix

The combustor was operated with a total thermal input of 1 MMBTU/hr ± 5%. NO$_x$ control tests were performed with No.6 oil only, a 1/1/ and a 1/3 mixture of No.6 oil and Kaiparowits coal, and Kaiparowits coal only (Table 1). The oil was injected separately through the central oil gun (figure 1). The secondary and final combustion air preheat was 800°F and 630°F respectively. Some variation of air preheat was used but the results were not conclusive. The most important variable was the stoichiometric ratio of the first stage cyclone combustor which was varied from 0.7 to 1.1,based on fuel and air feed rates. A total of four separate test series were performed, with a total test cycle ,including heat up and cooldown of the facility,of several days. A test point was generally held for two hours. A total six separate stoichiometric operating points were obtained with coal only operation.

TEST RESULTS

Verification of the Facility's Thermal Simulation of the Furnace Region of a Boiler

A most important result was the verification that the facility produced the desired thermal simulation of the radiant section of the boiler,as shown in figure 2. The verification results are shown in figures 4 and 5,for two tests, using only coal as a fuel, at a SR' of 1.1 and 0.7 in the first stage. The use of a (') symbol on the SR is to show that the values are based on the flow rates of fuel and air to the first stage, rather than the measured O_2 at the stack. For example at a SR' of 0.65 based on the flow rates, the measured SR of the combustor was 0.78,based on the O_2 measurement at the stack. This difference was attributed to incomplete carbon conversion in the first stage. As will be shown below,SR' should be used in the data analysis. We will return to this point below.

One notes that at a SR' of 1.1, (figure 4) the gas temperature reaches the desired 2000°F range at the bottom of the first heat exchanger (MHX). This occurs after 1 second. This is the desired time interval and temperature location for tertiary air injection. At SR' of 0.7 in the first stage, where the gas flow time is somewhat longer due to the lower initial flow rate, the addition of tertiary air increase the temperature to about 2600+°F , which [illegible] below the temperature where thermal NO$_x$ becomes significant. Thus,we conclude that the facility did simulate a radiant furnace.

Carbon Conversion in the Cyclone Combustor

The first stage stoichiometry was obtained by two methods. One was based on the measured O_2 concentration in the stack, and the other was based on the flow rates of fuel and air. Based on a gas chromatographic (GC) analysis of the combustion products of the first stage, it was determined that the carbon conversion was in the 80-90% range. Table 2 shows the gas composition results for two fuel rich experiments. For the coal only case, Table 2 shows that 17% of the carbon-char is not not consumed in the cyclone combustor. In all the fuel rich experiments, the carbon conversion in the first stage was about 85% with a scatter of ±5%, biased toward the minus side. With mixed fuels, the carbon conversion was 88-89%, and at SR' of 1.1, it approached 100%.

Based on a post test examination of the flow train and a chemical analysis of the slag (3,4), it was concluded that most of the unburnt char was deposited in the sections immediately downstream of the cyclone combustor exit. While no char was found in the slag during these tests, in a subsequent test series (13) under fuel rich conditions, considerable char was found in the slag. In addition, the CO measurement at the stack yielded values in the 10 ppm range for all tests, which indicated complete carbon conversion in the second stage. Therefore, one can conclude that the unburnt carbon deposited in the wall region immediately downstream of the cyclone combustor. The temperatures prevailing in this fuel rich region are lower than in the cyclone. Also, wall burning is inefficient, even in a slagging cyclone combustor (10). Therefore, one can conclude that the char deposited immediately downstream of the combustor exhaust did not all burn coincidentally with the exhaust gases from the combustor. This phenomena is unique to the facility. Since in the data analysis, one is interested in the first stage stoichiometry based on the actual coal and air feed rates to the first stage, this value, labelled SR', rather than the one based on the measured O_2 value at the stack (SR), was used in evaluating the data.

In the discussion of these tests results, we will show that the poor carbon conversion was due to the use of a too coarse coal particle size for this combustor. However, for Kaiparowits coal, the poor carbon conversion does not affect the relationship of NO_x emissions to first stage stoichiometry. The reason for this is that Kaiparowits coal contains almost its entire sulfur in organic form. This was confirmed in the present tests. For first stage operation at SR'>1, the SO_2 level measured at the stack with the NDIR analyzer was 425 ppm @ 11% excess air (or 406 ppm @ 3% O_2). At SR'=0.7, SO_2 was 338 ppm, without final combustion, and 425 ppm with final combustion in the furnace simulation section. The latter result is attributed to the initial formation of H_2S, which is converted to SO_2 only with complete combustion. In any case, the results agrees with the assumption of complete conversion of the fuel sulfur 0.42% to SO_2, despite the fact that the carbon conversion was incomplete.

Based on studies of the form nitrogen evolution from coal particle combustion (18), one can reasonably conclude that a similar organic/inorganic ratio applies to the fuel bound nitrogen. Therefore, despite the incomplete char gasification in the first stage, both the sulfur and nitrogen will evolve during the devolatilization process of the Kaiparowits coal. However, this conclusion does not apply to coals with high inorganic sulfur or nitrogen, and one must therefore ascertain in each case if these compounds have evolved from the coal particles.

NO_x Test Results

Figure 6 shows a summary of all the NO_x data obtained at the stack, corrected for 11% excess air, over a range of SR from 0.65 to 1.3. Figure 7 shows the Test Series IV coal only and coal/oil fired NO_x results, corrected for 3% O_2 as a function of SR'. [We re-emphasize that SR is based on O_2 measured at the stack, and SR' is based on fuel/air feed rates, and the latter is the proper one to use in the analysis of the test results.] Due to the lower fuel bound nitrogen in the oil (0.17%) vs the coal (1.24%), the NO_x reduction in oil firing is less than in coal firing.

The important result is shown in figure 7, where one notes that the minimum NO_x levelof less than 100 ppm, is at SR' of 0.65. This relationship of NO_x reduction to first stage combustor stoichiometry has been widely observed by others in conventional pulverized coal burners ⟨e.g.19, 20⟩. The latter two references also show that the NO_x minimum at SR' of 0.6 to 0.7 is due to the minimum in the concentration of the three primary species, NO,HCN,NH_3 released by the FBN in the fuel rich,first stage.

DISCUSSION OF THE NO_x CONTROL TESTS IN THE 1 MMBTU/HR COMBUSTOR

Carbon Conversion in the First Stage

The carbon conversion in the experiments averaged about 85%. We analyzed this problem in a series of studies on the combustion processes in a cyclone combustor ⟨5,-6,10⟩, which were recently summarized ⟨1⟩. We should note that the summary paper contains an error in the char gasification rate, which has been corrected ⟨6⟩. Due to the importance of this matter to the interpretation of the present NO_x results, we briefly discuss the char gasification problem as it relates to the 1 MMBTU/hr combustor.

In the first place,we note that present NO_x control experiments were performed with a coarse coal particle size distribution, ranging from 37 to 45%-200 mesh ⟨13⟩. This was due in part to a change in the coal preparation method, and due to a desire to improve the slag retention by using coarser coal particle sizes. Since the point of maximum reduction of NO_x occurs at SR' of 0.65-7, we analyzed the combustion of a typical coal particle size distribution ⟨40%200 mesh⟩ used in the present NO_x tests and at SR'=0.7.

Our analysis of this combustor's performance ⟨5⟩ showed that all coal particles greater 44 microns ⟨about 2/3 of the coal weight⟩,impacted the slag layer prior to any extensive devolatilization. Although complete devolatilization is fairly rapid on the slag covered wall, we showed that gasification of char on the wall, which is very inefficient ,can account for only about 10% of the total. Thus char gasification must take place by re-entrainment of the particles by the high velocity gas stream.

Subsequent to devolatilization,char particles are very porous, with internal surface areas in the 100's m^2/gm range. Char gasification takes place by kinetic reactions with O_2,CO_2 and H_2O. The latter two reactions are much slower than the char-oxygen reaction. At SR' of 0.7 in Kaiparowits coal, the latter two reactions account about one-half of the total char gasified. In addition, for particles greater than 10 microns in diameter, the gas diffusion resistance into the pores drastically reduces the gasification rate.

To calculate the diffusion effect on the char gasification rate for various size particles, we used the "pore tree" diffusion theory of Simons ⟨21⟩. The kinetic rates given by Simons for char-O_2 ⟨22⟩, and those given by Bush for ⟨0.17%⟩ vs the coal ⟨1.24%⟩, the NO_x reduction in oil firing is less than in coal firing.

The results of the char gasification calculations are shown in Table 3. The interesting result in Table 3, Part 1, is that particles 100 microns, or greater, cannot be gasified with oxygen in a single gas transit time of 100 m.sec. This is mainly due to the depletion of the oxygen molecules at SR' of 0.7, which results in a factor of 6 reduction in the gasification rate during the final 25% of the char gasification by the oxygen. In fact,during this time, the combined reaction rate due to H_2O & CO_2 at the same temperature is about 50% of the oxygen rate, due to the high partial pressure of the former (0.247 atm.) compared to the low value of the latter, (0.0085 atm.)

Another interesting result in Table 3,Part 2 is that the CO_2 & H_2O reactions,-(which were computed on the basis of their combined partial pressures), are effective only in gasifying char particles below about 44 microns during the 100 m.sec. gas plug flow transit time. In fact even after 300 m.sec.,the computed carbon conversion (shown in Table 3,Part 3B, is only 71%, compared to a measured value in the 85% range in the present experiments.

On the other hand,if we compute the carbon conversion on the basis of total kinetically controlled reactions acting on the internal pore structure, we obtain an 85% carbon conversion in 100 m. sec., as shown in Table 3,Part 3B. However, rather than attributing the observed carbon conversion to complete kinetic control, a more probable explanation for the measured carbon conversion is that the particles break up during the gasification process, which increases the effective area available for gasification. We reached a similar conclusion in our analysis of the combustion process in the large commercial cyclones (6). In any case,it is concluded that the poor carbon conversion in the 1 MMBTU/hr cyclone combustor was due the use of a too coarse coal particle size distribution.

NO_x Control Results

Comparison with Other NO_x Control Tests in a Cyclone Combustor.

The explanation for the occurrence of the maximum NO_x reduction at SR' of 0.65 was given in the previous section. Similar NO_x control experimental results were reported in 1983 (24). In that case,a 10 MMBTU/hr water cooled,cyclone combustor was used as the first combustion stage. Tests were conducted with Wyoming,Utah,and Montana coals. No details were given on the location of the final air combustion air injection point, so that it is not possible to determine the relaxation time between first stage exhaust and second stage air injection. It appears from the graphical data (24) that the minimum NO_x for all coals was at a stoichiometric ratio of 0.7, which is near the present minimum of 0.65 based on SR' (i.e.feed rates). With Utah coal, this minimum point corresponded to a 260 ppm NO_x (@ 3% O_2) level, or a factor of 2 reduction from the value at SR of about unity. It was also concluded on the basis of post test inspection of downstream components, slag analysis, and stack particle probe sampling,that the carbon conversion was greater than 99.5%, which would imply SR=SR'. In more recently reported tests in this facility (25), with a different coal,the minimum NO_x level of 350 ppm occurred at SR=0.75, which represented a 30% NO_x reduction from SR of 0.9. Both these levels are considerably higher than the present results, and the percentage reduction are considerably less.

It should be noted that Kaiparowits coal is also a Utah coal. Thus an explanation of the higher NO_x levels,and the later shift in the NO_x minimum to higher SR, cannot be given without further experimental details. In general,one can conclude that the results are consistent with the present results.

Evaluation of the Present NO_x Results, and Application to Large Boilers.

In this section, we will focus on the boiler simulation aspects of the present NO_x control results,with the objective of applying the results to a practical boiler application. An example would be the use of the cyclone combustor in a conversion of an oil fired boiler to coal. Superficially, the results of the present experiments suggest that to achieve large NO_x reductions requires about a 1.5

second relaxation time (see figure 5) prior to final combustion air injection. We studied the retrofit of a 125 MWe boiler with a series of 150 MMBTU/hr cyclone coal combustors (2,26). In this boiler, the average "plug" flow upward gas velocity in the radiant section of the boiler is about 35 feet. Since space limitations on the furnace wall dictate that the eight combustors be placed on at least two elevations (see figure 8), the vertical separation between the two combustor levels must be less than one-half of the 53 feet deduced on the basis of the present experimental results. It is thus of considerable interest to determine the chemical effects that dictate the temporal separation between the two combustor stages, in order to determine if a closer spacing is feasible. The results of the following discussion, will show that considerably closer spacing between the stages is possible, while still achieving high NO_x reductions.

NO_x Formation in a Staged Combustor-Thermal NO_x.

As noted previously, there are two sources of NO_x. One is derived from fuel bound nitrogen (FBN), and the other from molecular nitrogen (N_2) in the combustion air. FBN conversion to NO_x is relatively insensitive to temperature, while N_2 is very temperature dependent, and it is the primary source of thermal NO_x. Thermal NO_x is controlled by the Zeldovitch mechanism, which at high temperature is dominated by the reaction (27)

$$N_2 + O == NO + N \qquad (1)$$

For the Kaiparowits coal, which is a low sulfur western bituminous coal, whose properties are given in Table 1, thermal NO_x only becomes significant at 3000°F temperatures. Using equation (1), we estimated (26) that for combustion of Kaiparowits coal at 15% excess air, the equilibrium, thermal NO_x level increases from about 200 ppm at 2000°F to about 2000 ppm at 3000°F. However, the rate of formation of thermal NO_x is a strong function of temperature. To obtain a simple upper bound for the rate of formation we used equation (2) from reference 33,

$$k_{no} = 7.6*10^{13}*\exp(-75{,}500/1.9872*T, {}^{o}K);\text{mols/cc-sec} \qquad (2)$$

from which we computed the following rates of formation of thermal NO/sec

2996°F	NO rate= 100 ppm/sec
3140°F	NO rate= 394 ppm/sec
3500°F	NO rate=8143 ppm/sec

From this one can conclude that by limiting the combustion temperature above 3000°F (at excess air conditions), to periods of under 1 second will limit the thermal NO_x formation to less than 100 ppm. This result applies to the section in the boiler's radiant furnace, immediately downstream of the final combustion air injection location.

NO_x Formation in a Staged Combustor-Fuel Bound NO_x.

In the fuel rich first stage combustor, only FBN compounds are of importance. Assuming that all the FBN were converted to NO, one obtains for Kaiparowits coal, an equilibrium, fuel derived NO concentration at 10% excess air of 2550 (daf). This clearly dominates the total NO level, if thermal NO is suppressed. As noted in discussion on char gasification, we concluded that almost all the FBN in Kaiparowits coal is organic in nature, and that it will be released in the first stage, cyclone combustor, even if the char gasification is incomplete. The three major species produced in the first stage are HCN, NH_3, and NO. In references 19 and 20 it is reported that the formation of the three species is at minimum at a SR' between 0.6 and 0.7. The key to the control of FBN produced NO_x, is to convert the above three gas molecules to N_2 prior to the introduction of the final combustion air, otherwise they will convert to NO_x.

Since no data on the relative concentrations of these three species was obtained in the present experiments, we used two published papers {20,29}, on this subject in which their relative concentration was measured for a Utah coal, (Kaiparowits coal is also from Utah), as a function of SR. Table 4 shows the relative levels of HCN,-NO,NH_3 as a function of SR of 0.5 and 0.7 from these studies {20,29}. The primary difference between the two results is in the relative NO and HCN values at SR of 0.7.

To calculate the conversion of HCN,NO,and NH_3 to N_2 in the fuel rich zone, prior to the introduction of the final combustion air, we used recently reported kinetic rates {31} on the destruction of these three species. They are

$$d[HCN]/dT=-5.5*10^{17}*\exp(-83,300/RT)*C*[HCN]*[H_2O]/[H_2]^{.5} \qquad (3)$$

$$d[NO]/dt=-2.2*10^{16}*\exp(-54,400/RT)*C*[NO]*[NH_3]/[H_2]^{.5} \qquad (4)$$

$$d[NH_3]/dt=d[NO]/dt=-d[HCN]/dt \qquad (5)$$

where the rates are in moles/cc-sec., [ ] is the species mol fractions, C is the total mol concentration in mols/cc, R is the gas constant, R is the gas constant in cal/mol-°K, and T is in °K. We assumed that all the FBN in the Kaiparowits coal had been converted to these three species, and the initial relative concentrations of the three species were equal to those reported in reference 29. Table 5 shows the estimated time for the reduction of the HCN and NO by a factor of ten at a SR of 0.7. For simplicity, we assumed that the H_2O,H_2,and NH_3 concentrations remained constant in the temperature range of interest, namely, 2000-3180°F. From Table 5 one notes that HCN and NO are reduced by a factor of 10 in less to 10 milliseconds to a little over 100 milliseconds, in the temperature range of 3180-2500°F, respectively. This compares with a gas flow residence time of 113 m.s. in the 1 MMBTU/hr combustor at SR of 0.7. We conclude that on the basis of FBN chemistry, the final combustion air could have been introduced at the exit of the first stage combustor.

However, at SR of 0.7, the first stage exhaust gases contain about 1/3 of the chemical energy in the fuel. Thus, the addition of final combustion air at this point will increase the final combustion temperature considerably above 3000°F, which will produce high thermal NO_x levels, as can be deduced from the results presented at the beginning of this sub-section. Therefore, the primary reason for the need to cool the first stage exhaust gases prior to final combustion is to limit the final combustion temperature to below 3000°F.

As a result the location of the final combustion air inlet, which will produce the minimum NO_x at the stack, is a function of the specific boiler thermal configuration. However, it should be noted that this final combustion air must be introduced at a point where the combustion air is above 2000°F, as was the case in the present experiments. Below this temperature, the CO combustion kinetics are too slow to permit complete CO combustion in a reasonable furnace dimension {26}.

SO_x REDUCTION WITH LIMESTONE INJECTION IN THE 1 MMBTU/HR CYCLONE COMBUSTOR

To show the potential of this combustor as a environmental control device, we briefly report on an experiment which was performed in the 1 MMBTU/hr air cooled cyclone combustor, in which limestone was injected adjacent to the coal ports (13). Since the combustor operates at temperatures in the 3000°F range, it was not known a priori if any effect would be observed. As a result a high Ca/S ratio of 9 was used. 25-35% reductions in the SO_2 emissions were measured (13) with the Kaiparowits coal. The lower number applies to a SR of 1.1, and the higher number to SR of 0.65-0.75. The reacted limestone mixed with the slag and was removed with it.

Subsequently (5,6), a theoretical explanation was uncovered which could account for the sulfur capture results. This explanation is based on a model in which the sulfur capture takes place during the period of calcination of the particle, where its temperature is in a range (1800°F) which is favorable to the capture of sulfur. The most optimistic sulfur capture rate is obtained by assuming that the entire internal pore area of the calcined CaO particle reacts at the kinetic rate for the CaO-SO_2 reaction. A dispersed phase kinetic rate of about 0.006 gm of SO_2/cm^2 sec-atm, deduced from reference 30 was used in a calculation to verify the experimentally observed sulfur reduction. For the maximum sulfur capture of 35% measured at SR of 0.7,and a suspended particle transit time equal to the gas transit time (about 100 milliseconds) in the 1 MMBTU/hr combustor, it was found that an internal particles pore area of only 18 m^2/gm, is required to obtain the observed sulfur capture. This pore area is about one-third of the maximum values reported for the high heating rates existing in a cyclone combustor (28). It was concluded that a high CaO porosity and a kinetically controlled CaO-SO_2 reaction acting on an entrained, calcining CaO particle could explain the observed sulfur capture in the 1 MMBTU/hr cyclone combustor. Further details are contained in elsewhere (1,2, 5,6).

CONCLUSIONS

A series of experiments on NO_x control was performed in a 1 MMBTU/hr, staged, air cooled, cyclone combustor. The combustor exhausted into two ceramic lined vessels, which simulated the radiant furnace section of a boiler. Final combustion air was introduced between the two vessels, at a point where the cyclone combustion gas exhaust had cooled from about 3000°F to about 2200°F.Temperature measurements along the gas path showed that good simulation of the radiant furnace region of a boiler was obtained.The final combustion air was introduced after a gas cooling time of 1 to 1.5 seconds.

The NO_x emissions decreased with decreasing SR', from SR' of 1.15 to SR' of 0.65, after which they increased again. It was shown that this minimum corresponds to the minimum in the three species HCN,NO,NH_3 which are emitted from the fuel bound nitrogen in the coal in the fuel rich,first stage. It was also shown that thermal NO_x was not a significant contributing factor to the total measured NO_x because the peak gas temperatures at excess air conditions were always below 3000°F. About a factor of three NO_x reduction, to less than 100 ppm,was obtained at an actual SR' of 0.65.

The combustor operated at a carbon conversion level of only 80-90%, which was shown to be a result of using too coarse (37% to 45%-200 mesh), coal particle size distributions in the test. It was shown that the observed carbon conversion qualitatively agreed with the results obtained in a model which included kinetic and pore diffusion effects in the gasification of a coal char particle suspended in the gas stream,under fuel rich conditions. However, pore diffusion effects appeared to overestimate the particle gasification time, even if it was assumed that the particles are entrained for periods of time which are several times greater than the simple plug flow gas transit time. It was hypothesized that particle breakup during the gasification process may account for the more rapid combustion rate at particle sizes which are initially large enough for the combustion to be diffusion controlled.

Despite the incomplete carbon conversion,it is concluded on the basis of Kaiparowits' coal properties and sulfur conversion measurements, that all the fuel bound nitrogen was released in the first combustion stage, i.e. the cyclone. As a result,- the NO_x data is properly presented by a SR value which is based on the coal and air feed rates, rather than one based on the O_2 level measured at the stack.

The present NO_x results are in general agreement with other experiments in a water cooled cyclone combustor and in conventional pulverized coal flames, which show that the minimum emission of the three primary fuel bound nitrogen compounds occur at SR in the range of 0.7. However, insufficient information is contained in the other cyclone combustor experimental results to compare with the present furnace simulation data.

A qualitative analysis of the kinetics of thermal and fuel bound NO_x formation and destruction was performed. The results showed that keeping the combustion temperature,under excess air conditions,above 3000°F for periods under one second, should control the thermal NO_x emissions in a furnace operated with a fuel rich cyclone combustor as a first stage. In addition, it was shown that the destruction of the fuel bound nitrogen species released under fuel rich conditions is sufficiently rapid above 2500°F, that only a fraction of the 1 to 1.5 second temporal separation between the two combustor stages,used in the present experiments, is necessary for high NO_x reductions in a large boiler. This is of considerable importance because a 1 to 1.5 second separation time is too long for effective placement of the cyclone combustors on a utility scale boiler. The actual separation depends on the final combustion temperature attained after CO and H_2 combustion, which is a function of the furnace configuration used. CO combustion kinetics are not a factor, provided the final combustion air is introduced when the combustion gases are above 2000°F.

Finally, a brief description was given of the results of an analysis of experiments on SO_x control,with limestone injection,in the air cooled combustor. It was stated that the observed SO_x reduction was consistent with a non-equilibrium sulfur capture process in the combustor.Full details are given elsewhere.

ACKNOWLEDGEMENTS

The NO_x control experiments,which are reported here were performed in 1980-1, under sponsorship of the Southern California Edison Company, using a 1 MMBTU/hr cyclone coal combustion facility leased from the Department of Energy and located at the General Electric Company in King of Prussia,PA. The authors,as well as the individuals identified on the bottom of the first page,namely,D.B. Bender,C.S.Cook,E.F. Fleming,S.A.Omori,and D.Rogers, participated in these experiments at the General Electric Company. The sulfur control experiments were also performed there under sponsorship of the Department of Energy. Most of the analyses presented in this paper was performed at Coal Tech with partial support from the Southern California Edison Company, and the Pennsylvania Science and Engineering Foundation.

REFERENCES

1. B.Zauderer & V.Tilli,"Appl.of an Air Cooled Cyclone Coal Combustor to Oil Fired Boiler Conversion",Proc.1st Pittsburgh Coal Conf., U.of Pittsburg,9/17/84,p.761
2. B.Zauderer, V.Tilli,K.S.Fujimura,& J.Griswold,"Appl.of an Air Cooled Cyclone Coal Combustor to Oil Fired Boiler Conversion & Environmental Control in Coal Fired Boilers", Proc.Coal Tech.'84,Houston,Industrial Presentations, 11/13/84,V.4,p.193
3. E.Fleming,et.al.,"Coal-Oil Mixed Mode Two Stage Combustor Tests for NO_x Control", Southern Cal.Edison (SCE) Rpt.No. 80-RD-135,Jan.1981
4. E.Fleming,et.al.,"Coal-Oil Mixed Mode Two Stage Combustor Tests for NO_x Con-

trol", Southern Cal.Edison (SCE) Rpt.No. 81-RD-28,May 1981
5. B.Zauderer,"Sulfur Capture with Limestone Injection in Cyclone Combustion Flow", Merion,PA: Coal Tech Corp. NSF Grant No.CPE-8260265,April 15,1983
6. B.Zauderer,E.Fleming & D.Simpson,"Res.on Combustion & Environmental Control in Cyclone Coal Combustor", Harrisburg,PA: Penns.Science & Engineering Foundation,9/84
7. Steam,New York: Babcock & Wilcox Co.,Ch.10 (1978 ed.)
8. H.Seidl,"Development & Practice of Cyclone Firing in Germany", Proc. Jt. Conf. on Combustion, ASME-I.Mech.Eng.,MIT,Cambridge,Mass June 1955,p92
9. H.Seidl,"The Horizontal Cyclone" B.C.U.R.A.Gazette,No.36,1962
10. B.Zauderer,"Anal.Inves.of Sulfur Capture & Slag Rejection in Cyclone Coal Combustors",Merion,PA: Coal Tech Corp,DOE Contr.DE-AC22-82PC50050,Jan. 1983
11. C.S.Cook,et.al.,"Renerative Air Cooled Cyclone Coal Combustor",Proc.Coal Tech'79,Houston,TX: Industrial Presentations,Nov.1979,Vol.2, p.113
12. J.A.Hardgrove,"MHD Coal Combustor Dev.Res.",9th Ener.Tech.Conf.,Wash.,3/82
13. C.S.Cook,C.H.Marston,E.Fleming,D.Bender,V.Tilli,B.Zauderer,et.al., "Evaluation of Closed Cycle MHD Power",King Of Prussia,PA: General Electric Co., DOE Contr.Rpt. No-.DE-AC01-78- ET10818, Nov, 1981
14. H.R.Hoy,et.al.,"Invest. Cyclone Coal Combustor",J.Inst.Fuel,Oct.'58,p.429
15. J.J.Marshall and A.P.Selker,"The Role of Tangential Firing & Fuel Prop. in Attaining Low NO_x Oper. for Coalfired Steam Gen.",2nd EPRI NO_x Control Tech.Seminar,Denver,CO,Nov.1978
16. S.Michelfelder,et.al.,Ijmuiden,Netherlands,Int.Flame Res.Inst.Doc.No.K20/a/ 90, Apr.1977
17. M.Petrick and B.YA.Shumyatsky,Editors,Open Cycle MHD Electrical Power Generation,Argonne,IL,Arg.Nat.Lab.,1978,Ch.5
18. J.H.Pohl & A.D.Sarofim,"Devolatilization & Oxidation of Coal N_2",16th Int. Symp.on Combustion,Pittsburgh,PA,Combustion Institute, p.491,(1977)
19. D.P.Ress,et.al.,"NO Formation in a Lab. Pulverized Coal Combustor", 18th Int.-Symp.on Combustion,Pittsburgh,PA,Combustion Institute,p.1305,(1981)
20. Y.H.Song,et.al.,"Conversion of Fixed N_2 in Rich Combustion" Proc.18th Int. Symp.on Combustion,Pittsburgh,PA,Combustion Institute, p.53,(1981)
21. G.A.Simons,"The Role of Pore Structure in Coal Pyrolysis & Gasification", Prog.Energy & Comb.Sci.,Vol.9,p269,(1983)
22. P.F.Lewis & G.A.Simons,"Char Gasification,Pt.II,Oxidation Re-sults",Comb. Sci. Tech.Vol.20,P117,(1979)
23. T.W.Bush,et.al.,"Gasification of Coal Char w.CO_2 & Steam at 1200-1899°C". Phillips Petroleum Res.Rpt. (1978)
24. J.C.Stansell,et.al,"TRW's Slagging Combustor System Progress" ,in Proc. Coal Tech'83,Houston,TX:Indust.Pres.,Nov.1983,
25. J.Kuenzly,"Adv.Slagging Combustion System",PETC Combustion Projects Review,-Pittsburgh,PA,Aug.27,1984
26. B.Zauderer,et.al.,"Appl.of Cyclone Coal Combustors to Oil Fired Boilers", South.Cal.Ed.Rpt.No.SCE-RD- 83-141,Nov. 83,Vol.3
27. L.D.Smoot and D.T.Pratt,Pulverized Coal Combustion & Gasification, New York: Plenum Press,1979
28. R.H.Borgwardt,et.al.,"IERL-RTP Res.on Sulfur Capture in LIMB", Proc. Jt. Symp. Stat.NO_x Control ,EPRI CS-3182,V.1,p.25-1,7/83
29. S.L.Chen,et.al."Fate of Coal N_2 During Combustion",Proc.Joint Symp. on Stationary NO_x Control,IERL-RTP-1086,Vol.VI.,p.154,Oct.1980
30. R.W.Coutant,et.al.""SO_2 Pickup by Limestone & Dolomite Particles in Flue Gas", J.Eng.Power,(1970),p113
31. J.W.Glass and J.O.L.Wendt,"Mech.Governing the Destruction of Nitrogeneous Species During Fuel Rich Combustion of Pulverized Coal", Proc.19th Int. Symp.on Combustion,Pittsburgh,PA:Combustion Institute, p.1243,(1982)
32. J.T.Kelly,et.al.,"Low NO_x Coal Fired Sys.",Proc.18th Int.Symp.Comb., Pittsburgh,PA:Combustion Institute,p.1275, (1981)
33. A.J.Sistino,"Anal. & exp.Studies of NO_x Kinetics in MHD",Argonne,Il: Argonne Nat.Lab. Report-ANL/MHD-80-17

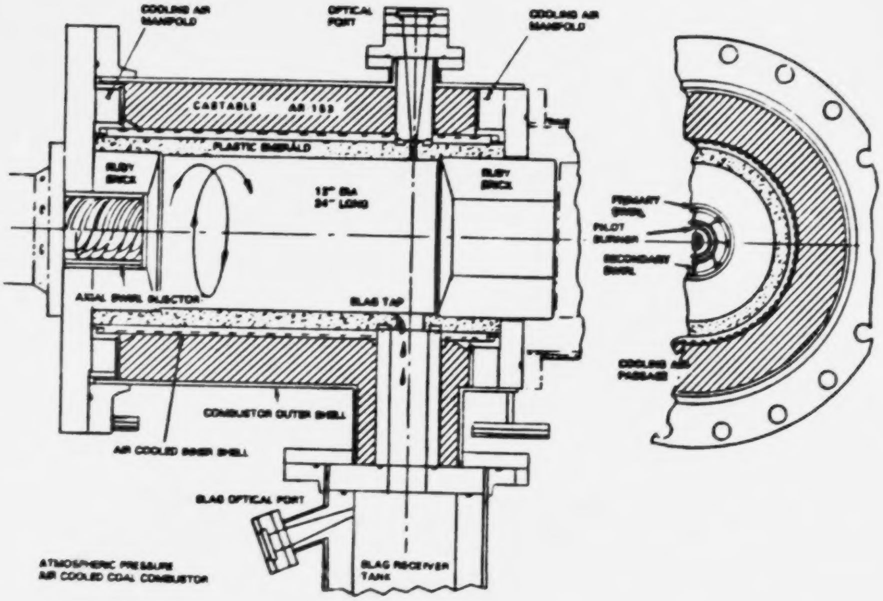
COOLING AIR MANIFOLD
OPTICAL PORT
COOLING AIR MANIFOLD
CASTABLE AR 153
PLASTIC EMERALD
RUBY BRICK
12" DIA
24" LONG
RUBY BRICK
PRIMARY SWIRL
PILOT BURNER
SECONDARY SWIRL
AXIAL SWIRL INJECTOR
SLAG TAP
COOLING AIR PASSAGE
COMBUSTOR OUTER SHELL
AIR COOLED INNER SHELL
SLAG OPTICAL PORT
ATMOSPHERIC PRESSURE
AIR COOLED COAL COMBUSTOR
SLAG RECEIVER TANK

Figure 1. Schematic of the 1 MMBTU/Hr Air Cooled Cyclone Coal Combustor

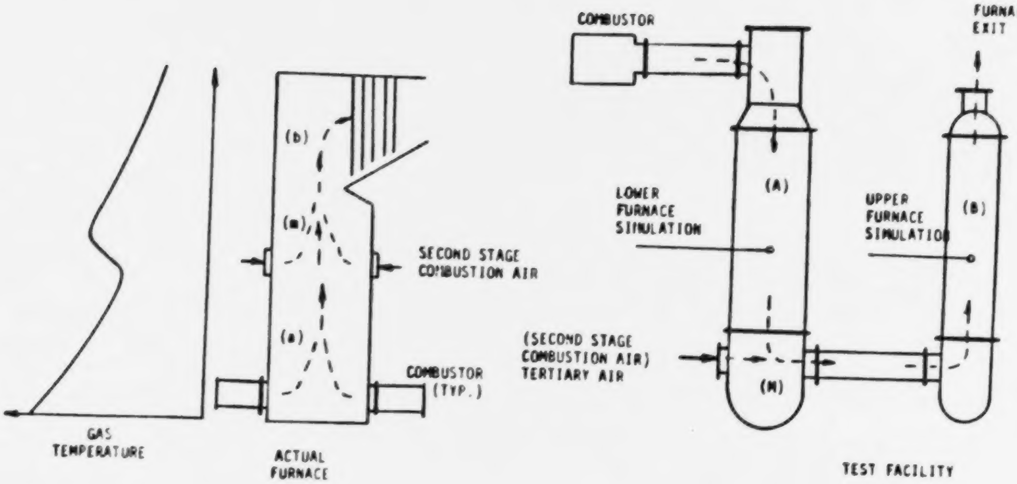
COMBUSTOR
FURNACE EXIT
(b)
(m)
(a)
SECOND STAGE COMBUSTION AIR
COMBUSTOR (TYP.)
GAS TEMPERATURE
ACTUAL FURNACE
(A)
LOWER FURNACE SIMULATION
UPPER FURNACE SIMULATION
(B)
(SECOND STAGE COMBUSTION AIR) TERTIARY AIR
(M)
TEST FACILITY

Figure 2. Radiant Furnace Simulation (Right Drawing) of a Cyclone Combustor Firing into a Radiant Furnace Section of a Boiler (Left Drawing)

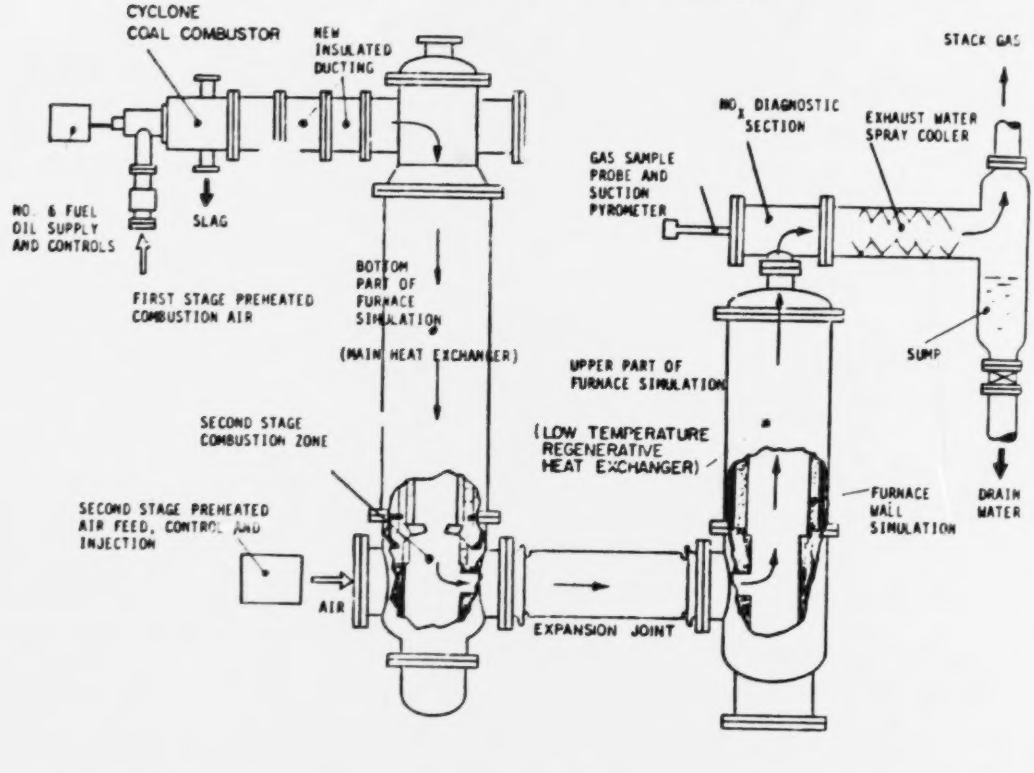
CYCLONE COAL COMBUSTOR
NEW INSULATED DUCTING
STACK GAS
NO_x DIAGNOSTIC SECTION
EXHAUST WATER SPRAY COOLER
GAS SAMPLE PROBE AND SUCTION PYROMETER
NO. 6 FUEL OIL SUPPLY AND CONTROLS
SLAG
FIRST STAGE PREHEATED COMBUSTION AIR
BOTTOM PART OF FURNACE SIMULATION
(MAIN HEAT EXCHANGER)
UPPER PART OF FURNACE SIMULATION
SUMP
SECOND STAGE COMBUSTION ZONE
(LOW TEMPERATURE REGENERATIVE HEAT EXCHANGER)
FURNACE WALL SIMULATION
DRAIN WATER
SECOND STAGE PREHEATED AIR FEED, CONTROL AND INJECTION
AIR
EXPANSION JOINT

Figure 3. Modified Combustor-Heat Exchanger Facility for Furnace Simulation

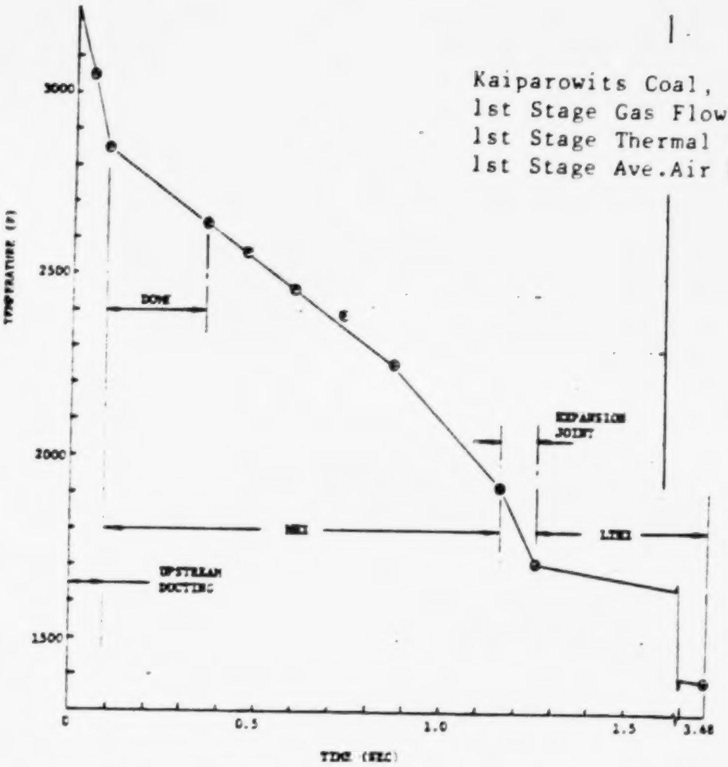

Kaiparowits Coal, SR'= 1.1
1st Stage Gas Flow Rate= 834 PPH
1st Stage Thermal Input= 1.06 MMBTU/HR
1st Stage Ave.Air Preheat=711 °F

Figure 4. Gas Temperature Profile vs Flow Time in Furnace Simulator

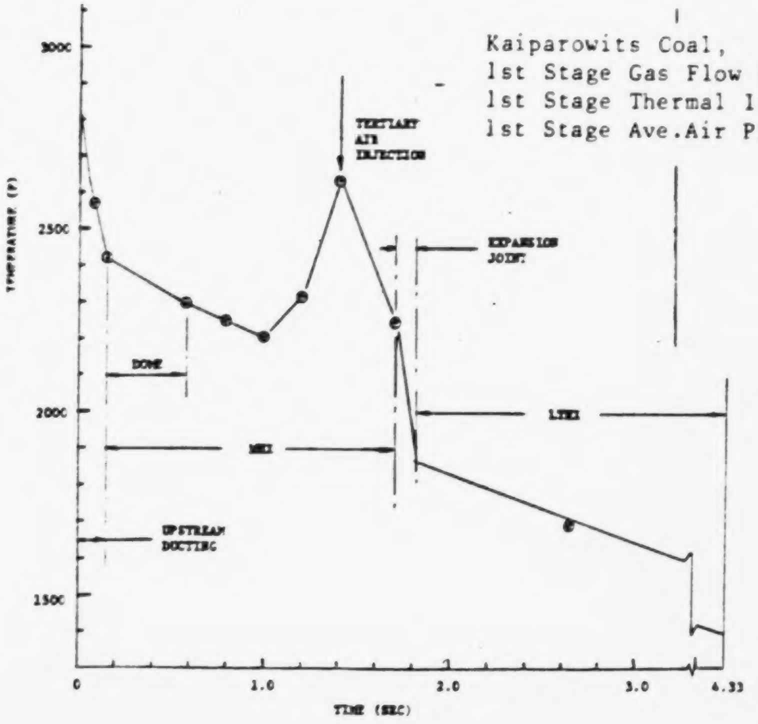

Kaiparowits Coal, SR'= 0.7
1st Stage Gas Flow Rate= 549 PPH
1st Stage Thermal Input= 0.95 MMBTU/HR
1st Stage Ave.Air Preheat=733 °F

Figure 5. Gas Temperature Profile vs Flow Time in Furnace Simulator

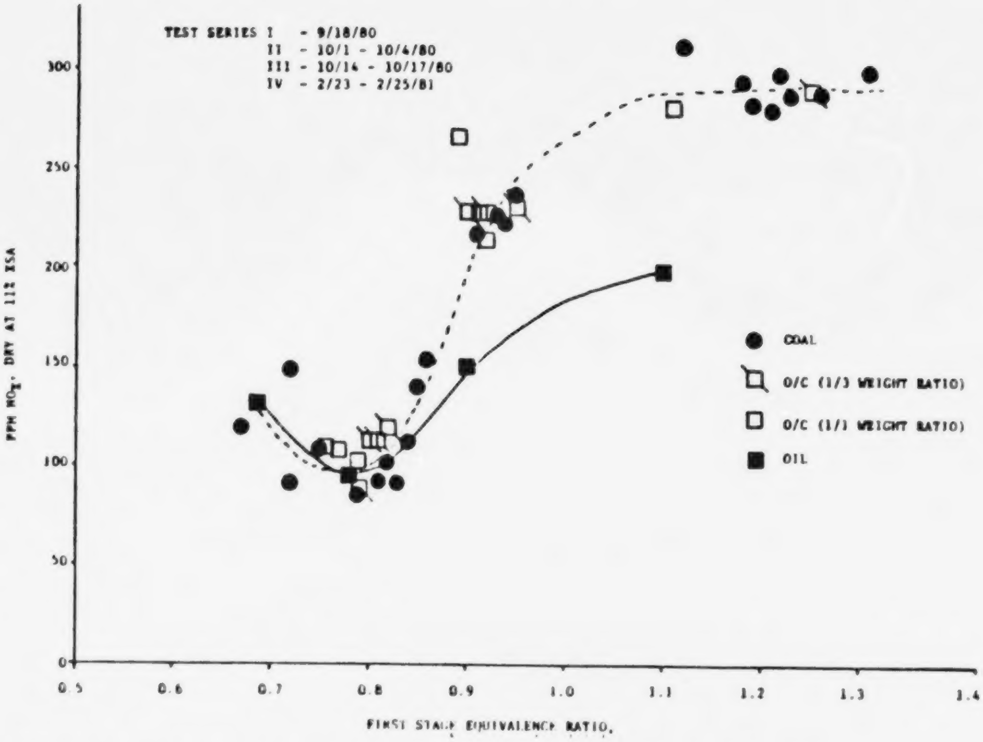

Figure 6. Series I-IV NO_2 Output Data (at 11% Excess Air) for Coal; Oil/Coal; Oil vs First Stage Stoichiometric Ratio; SR-(O_2 Derived)

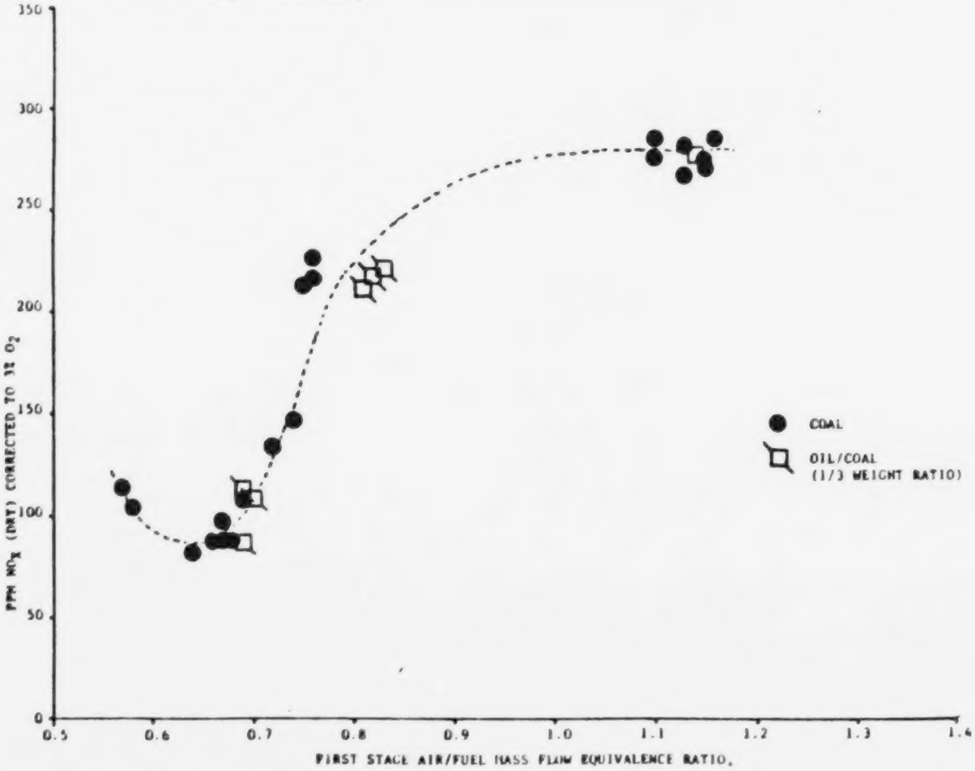

Figure 7. Series IV NO_x Output Data for Coal & Oil/Coal vs First Stage Air/Fuel Stoichiometric Ratio, SR'

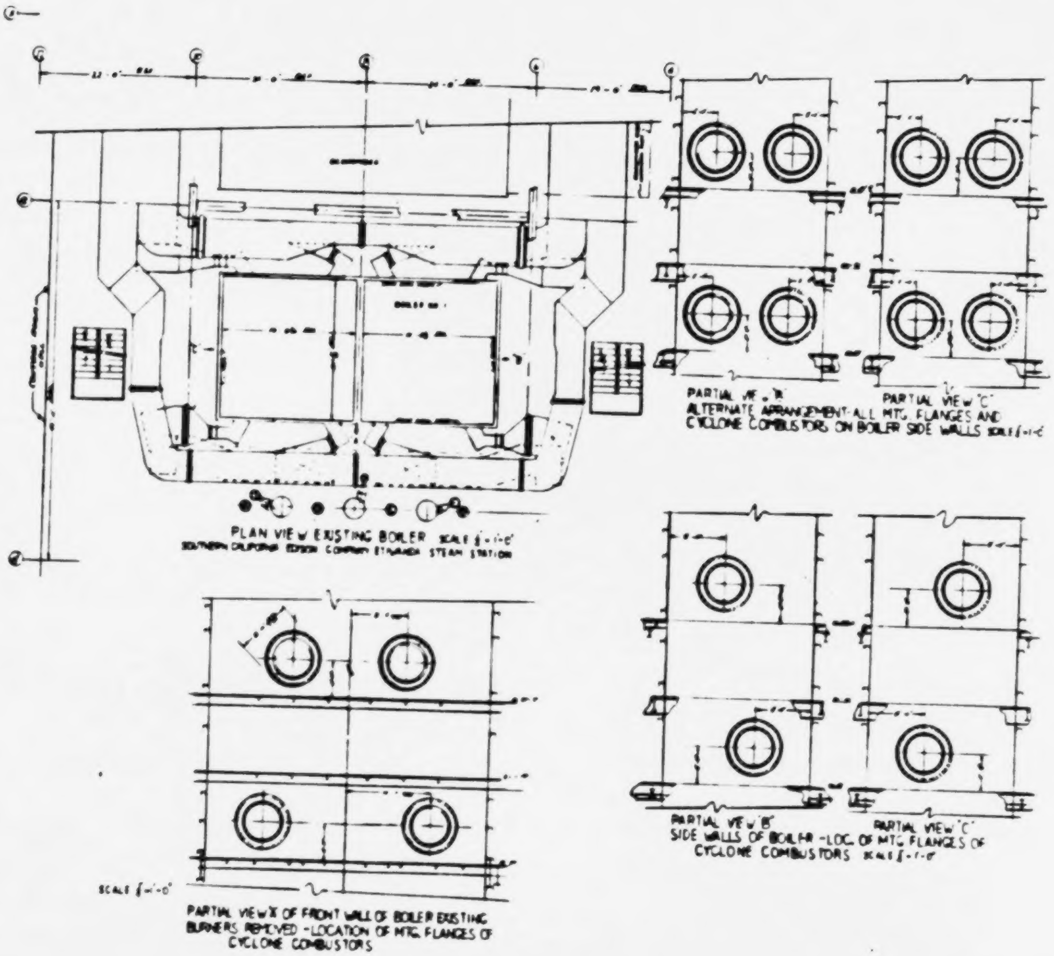
PLAN VIEW EXISTING BOILER SCALE ⅛"=1'-0"
SOUTHERN CALIFORNIA EDISON COMPANY ETIWANDA STEAM STATION
PARTIAL VIEW "A"
PARTIAL VIEW "C"
ALTERNATE ARRANGEMENT-ALL MTG. FLANGES AND CYCLONE COMBUSTORS ON BOILER SIDE WALLS SCALE ⅛"=1'-0"
PARTIAL VIEW "B"
PARTIAL VIEW "C"
SIDE WALLS OF BOILER -LOC. OF MTG. FLANGES OF CYCLONE COMBUSTORS SCALE ⅛"=1'-0"
SCALE ⅛"=1'-0"
PARTIAL VIEW "A" OF FRONT WALL OF BOILER EXISTING BURNERS REMOVED -LOCATION OF MTG. FLANGES OF CYCLONE COMBUSTORS

Figure 8. Two Concepts for Attaching Eight 150 MMBTU/Hr Cyclone Combustors to a 125 MWe Tangentially Fired Boiler

Table 1

KAIPAROWITS COAL PROPERTIES - AS RECEIVED

HHV-(Btu/lb) 11260

Proximate Analysis		Ultimate Analysis	
Moisture	9.7%	Moisture	9.7%
Ash	7.4%	Ash	7.4%
Volatile Matter	40.3%	Sulfur	0.42%
Fixed Carbon	42.6%	Carbon	64.22%
Sulfur	0.42%	Hydrogen	4.52%
		Nitrogen	1.24%
		Chlorine	0.01%
		Oxygen	12.49%

Table 2

FIRST STAGE COMBUSTION PRODUCTS[a]

	Coal SR'=0.69$\pm$0.02	%DRY[b]	Coal/Oil (3/1) SR'+0.70$\pm$0.01
H_2	1.0		1.8
CO_2	12.6		9.8
N_2	77.5		77.3
CO	8.9		11.1
Char[c]	17$\pm$1		11

a. SR'=1st Stage stoichiometric ratio based on measured fuel & air mass flow. Gas composition from GC.

b. Normalized to 100%,% char calculated from measured gas composition,SR', and C atom conservation

c. Given in weight % of coal-carbon input

TABLE 3. CHAR GASIFICATION TIMES FOR 1 MMBTU/hr CYCLONE @ SR=0.7

-Kaiparowits coal, SR=0.70; Second.Air=1000°F; 10% Heat Loss
-48.6% of char is gasified by CHAR-O_2 Reaction
-51.4% of char is gasified by CHAR-CO_2/H_2O Reaction
-% COAL; % CARBON CONV.= consumption, including VM & all the Char
-Wt%=% of total coal weight at stated particle size.

1. CHAR-O_2 REACTION TIME-DIFFUSION CONTROLLED-[MILLISECONDS]

D_p	Wt.%	T=0%	100%	300
20	20%	100%	2%	0%
44	17%	100%	17%	8%
74	30%	100%	28%	18%
100	25%	100%	48%	35%
150	8%	100%	62%	51%
TOTAL		100%	29%	20%

2. CHAR-CO_2/H_2O REACTION-DIFFUSION CONTROLLED-[MILLISECONDS]

D_p	Wt.%	T=0%	100%	300
20	20%	100%	69%	33%
44	17%	100%	83%	58%
74	30%	100%	90%	72%
100	25%	100%	92%	78%
150	8%	100%	95%	85%
TOTAL		100%	85%	64%

3.COMBINED EFFECT OF DEVOLATILIZATION AND ALL CHAR REACTIONS

3A. DIFFUSION CONTROLLED

% COAL CONSUMED	0%	70%	78%
% CARBON CONVERSION	0%	61%	71%

3B. KINETICALLY CONTROLLED

% COAL CONSUMED	0%	88%	98%
% CARBON CONVERSION	0%	85%	97%

Table 4

RELATIVE CONCENTRATION OF HCN, NO, NH_3 IN UTAH COALS

	FROM REF.29		FROM REF.20	
	SR=0.5	SR=0.7	SR=0.5	SR=0.7
NO	0.10	0.40	0.22	0.70
HCN	0.55	0.40	0.45	0.18
NH_3	0.35	0.20	0.33	0.12
TOTAL	1.00	1.00	1.00	1.00

TABLE 5.TIME TO REDUCE HCN,NO CONCENTRATION BY FACTOR OF TEN

Kaiparowits Coal,Stoichiometric Ratio=0.7

	$T_{GAS}=3180^{\circ}F$	$T_{GAS}=2500^{\circ}F$	$T_{GAS}=2000^{\circ}F$
HCN	0.001 sec.	0.136 sec.	23.9 sec
NO	0.003 sec.	0.070 sec.	2.0 sec.

COAL-FIRED PRECOMBUSTORS FOR SIMULTANEOUS NO_x, SO_x, AND PARTICULATE CONTROL

G. C. England
J. F. La Fond
R. Payne
Energy and Environmental Research Corporation
18 Mason
Irvine, California 92718

INTRODUCTION

A major obstacle to the conversion of gas- and oil-fired equipment to coal is the high cost of controlling emission of particulate matter and acid rain precursors (NO_x, SO_x). The presence of mineral matter in the coal and relatively long burning time required also complicates conversion. The ash formed during combustion of coal can deposit on heat transfer surfaces reducing efficiency and causing corrosion and erosion. The volume of gas- and oil-fired furnaces typically does not provide sufficient residence time at high temperature to completely burn the solid coal particles. Substantial derating of unit capacity may be required in order to minimize these potential drawbacks. Coal fired precombustor devices offer the potential for simultaneous removal of ash and reduction of NO_x/SO_x emissions at the burner prior to the boiler or heater furnace. This could reduce or eliminate derating and other ash-related problems, as well as reduce requirements for exhaust gas cleanup. The successful development of such devices would facilitate conversion to coal in the U.S., easing the burden of imported fuel supplies.

This paper presents background information related to the control of ash, SO_x and NO_x in precombustors. In addition, this paper describes results of tests in a small pilot scale precombustor conducted under EPA contract number 68-02-3130. This program is intended to establish the potential and compatability of requirements for simultaneous control of all criteria pollutants.

BACKGROUND

Ash Rejection

The presence of mineral matter in coal presents a wide variety of operational and environmental problems when fired in boiler and furnace systems, including: generation of fly ash; fouling and slagging of furnace walls and heat transfer surfaces; tube erosion; accelerated tube corrosion from condensation of vaporized minerals and potential interference with sulfur removal techniques.

Many precombustor concepts include removal of mineral matter contained in the coal as a molten slag during the combustion process. There are two primary types of ash rejection systems: 1) those which rely on centrifugal separation of the ash from the gases by introduction of a strong cyclonic flow field, and 2) those which use inertial separation of the particles from the gases by the use of slag baffles or screens. Figure 1 illustrates the configuration of conventional cyclone combustor designs. This kind of system has a long history and its limitations are fairly well understood. Recently, research effort on conventional cyclone combustors has focused on improving control of the coal combustion environment by altering the fuel injection technique, the coal size distribution, and the extent of combustion air preheating (1-3).

Another type of ash rejection system being developed at EER (4,5) is illustrated in Figure 2 and is known as the Vortex Containment Combustor (VCC). This kind of combustor is distinct from the system illustrated in Figure 1 since the coal particles remain centrifugally separated from the gas flow in an active zone until they are consumed. The smaller ash particles travel inward where they are collected on the walls of the system and removed as molten slag. Ash rejection efficiency as high as 95 percent has been demonstrated on a bench scale experimental system, whereas in commercial cyclone systems ash rejection efficiency is typically 80 to 85 percent. Inertial separation of the ash particles using baffles or screens has been investigated (6) as an alternative to cyclone systems. The use of this type of system could allow greater variability in the flow field generated upstream of the slag baffle without affecting slag rejection efficiency.

Since it appears that systems capable of 80 to 95 percent slag rejection efficiency are nearing commercial potential, the main challenge in design of these systems appears to be in establishing conditions which simultaneously maximize ash rejection, minimize NO_x formation and maximize SO_2 capture by the injection of sorbents. Particle trajectories, residence times and the presence of a molten slag layer are expected to have a substantial impact on these processes.

SO_x Control

The reduction of SO_2 emissions is the most challenging and least understood problem facing the development of a precombustor system capable of simultaneous NO_x/SO_x and ash control. Recently, much attention has been given to the injection of calcium based sorbents (limestone and dolomite) in or near the active combustion zone in order to reduce SO_2 emissions. When powdered limestone ($CaCO_3$) is injected into a high temperature environment, calcination takes place in which CO_2 is driven from the particles leaving reactive lime (CaO). Under fuel lean conditions CaO can react with SO_2 and O_2 to form calcium sulfate ($CaSO_4$) while under fuel rich conditions CaO and H_2S or COS can react to form calcium sulfide (CaS). The process is very sensitive to the reactivity of the sorbent which is a function of its specific surface area. Sorbent reactivity appears to be related to both the rate at which the sorbent is heated during calcination and the peak temperature which the sorbent experiences prior to reaction with the gaseous sulfur species (7-9).

Kinetics of the fuel lean reaction are fairly well understood and have been experimentally verified. However, relatively little work has been devoted to the study of fuel rich reactions which promote CaS formation. Borgwardt and coworkers (10) have investigated the kinetics of CaS formation but only under ideal conditions and at relatively low temperatures. Equilibrium calculations show that at low stoichiometric ratios and low temperatures a substantial amount of CaS can be formed. Figure 3 shows equilibrium calculations for an Illinois coal with and without added calcium. The temperature at each stoichiometric ratio was selected to be representative of temperatures in the experimental precombustor described later in this paper. When no calcium is added the figure shows that most of the sulfur exists as either H_2S, COS or S_2 at stoichiometric ratios below 0.7. At higher stoichiometric ratios SO_2 is thermodynamically favored. When calcium is added most of the H_2S and S_2 is replaced by CaS suggesting that very high retention of the initial coal sulfur as solid calcium sulfide should be possible. Figure 4 shows the effect of stoichiometry and temperature on equilibrium solid calcium-sulfur compounds for a Pittsburgh coal. Under fuel rich conditions CaS formation is favored. CaS is thermodynamically stable even at fairly high combustion temperatures. Under fuel lean conditions (which include the early combustion conditions of an overall rich coal flame) $CaSO_4$ is the favored species; however, above approximately 1300°C, $CaSO_4$ is not thermodynamically stable. The figure also illustrates that the stability of either solid sulfur species is low at conditions slightly below stoichiometric. This poses a problem in the design of practical staged combustion systems since the fuel rich products must eventually be made fuel lean in order to burn out all of the fuel. A precombustor system which removes the solid sulfur species prior to the addition of the second stage burnout air therefore shows promise of achieving very high sulfur removal, providing good carbon burnout and evolution of fuel sulfur can be achieved under the same conditions.

Although equilibrium calculations look favorable for the control of sulfur under fuel rich conditions the kinetics of sulfur evolution, sulfide formation, and sulfate decomposition complicate the analysis. Figure 5 shows sulfur species measurements made in a pilot scale test furnace burning Indiana coal. Under the fuel rich conditions which favor CaS formation a large fraction of the fuel sulfur remains bound in the coal char. This slow evolution of the fuel bound sulfur and the generation of high reactivity sorbents remain major obstacles to the capture of sulfur under fuel rich conditions.

The state and composition of the molten slag layer may also influence the efficiency of sulfur removal in a precombustor system. Additives such as calcium can affect slag fluidity as well as its capacity to retain sulfur. For example, Figure 6 shows a ternary diagram of the $CaO-Al_2O_3-SiO_2$ melt system (11). For a typical slagging coal ash (Illinois No. 6), the addition of CaO decreases the liquidus temperature significantly up to a calcium to sulfur ratio of about one. When the Ca/S ratio is increased above about 1.2 to 1.5 a dramatic rise in liquidus temperature occurs (see Figure 7). Note that this diagram is for a pure mixture and the presence of other components in the ash such as Fe_2O_3 can also reduce the liquidus temperature significantly. One benefit of this effect is that the addition of calcium oxide in the correct amounts can lead to increased fluidity of the molten slag layer and facilitate easy removal.

Slags formed by the mixing of coal ash with additives can produce liquid layers which are highly soluble to sulfur (12-14). The ultimate capacity of the slag mixture to hold sulfur may be an important mechanism in the overall sulfur capture process. Mass transfer limitations appear to inhibit direct gas phase sulfur absorption into the slag layer, but the formation of solid compounds containing sulfur (CaS in particular) in the free stream could greatly accelerate the slag capture process. In fact, if this form of sulfur transfer is extensive there is potential that sulfur in the slag layer could reach superequilibrium concentrations. In this case, the rate of sulfur regeneration and slag residence time would be critical controlling parameters.

NO_x Control

NO_x emissions from coal combustion arise from two sources, thermal NO and fuel NO. NO formed from molecular nitrogen (thermal NO) is dependent primarily on peak flame temperature and can be reduced by methods which lower the peak flame temperature such as flue gas recirculation. These methods are only partially effective with nitrogen containing fuels. NO formation from nitrogen in the fuel (fuel NO) is very sensitive to reactant stoichiometry and can be significantly reduced by initially burning the coal under fuel rich conditions. Staged combustion therefore involves creating a fuel rich zone to promote formation of molecular nitrogen from the nitrogen species (HCN, NH_3 and NO) which are evolved as the fuel decomposes, followed by a fuel lean zone optimized for minimum thermal NO formation while completing burnout of the fuel.

Equilibrium calculations for fixed nitrogen species resulting from combustion of CH_4 containing one percent nitrogen as NH_3 (Figure 8) show that NO levels below one ppm are theoretically possible even for high nitrogen fuels and that under fuel-rich conditions lower equilibrium levels are favored at higher temperatures. The conversion of fuel N to molecular nitrogen is kinetically limited, however, as illustrated by the model calculations shown in Figure 9. The concentration of total fixed nitrogen species (TFN = HCN + NO + NH_3) is shown versus time for three isothermal temperatures. These results were calculated for combustion of CH_4 with 1 percent HCN in the fuel at a stoichiometric ratio of 0.75. TFN decays sharply within the first 0.1 seconds, and then continues to decay at a much slower rate. The rate of decay, and hence the TFN level achieved, is enhanced by increasing temperature. The calculation indicates a requirement for long residence times and high-temperatures under fuel-rich conditions in order to achieve TFN levels below 100 ppm. This suggests NO_x could be effectively controlled by the following method:

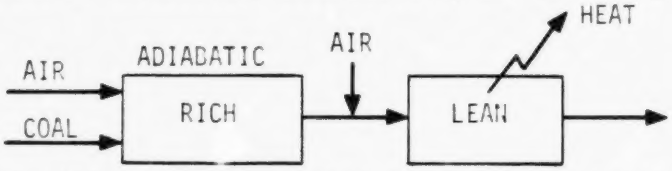

England, et al. (15,16) demonstrated that this approach was effective in reducing NO_x to levels below 100 ppm (corrected to 0 percent O_2) for liquid fuels with nitrogen content on the order of one percent.

The effectiveness of staged combustion of coal is complicated by the slow burnout of the char remaining after the initial release of volatile matter. Under fuel-rich conditions, char burnout is very slow (on the order of seconds) at normal combustion temperatures, and a significant fraction of the fuel nitrogen can remain in the char (char N). The char N cannot be converted to molecular nitrogen in the fuel-rich stage unless it is driven off the solid, and it can be partially converted to NO_x if it is burned out in the fuel lean second stage. Thus higher first stage temperatures should reduce NO from coal combustion because it accelerates the rate of TFN decay and reduces the amount of char N. Pilot-scale data (Figure 10) confirm that higher first-stage temperature produces lower NO_x emissions with coal combustion also (17).

Johnson et al. (18) and Chen et al. (19) observed a decrease in exhaust NO_x emissions when fuel rich zone temperature was decreased in systems which have significant first stage heat loss. Chen observed that when heat extraction was added to the rich zone of a bench-scale tunnel furnace, TFN concentration at the rich zone exit increased but exhaust NO_x (after complete burnout) decreased (see Figure 11). They deduced that this was a result of decreasing the second stage

NO_x Control

NO_x emissions from coal combustion arise from two sources, thermal NO and fuel NO. NO formed from molecular nitrogen (thermal NO) is dependent primarily on peak flame temperature and can be reduced by methods which lower the peak flame temperature such as flue gas recirculation. These methods are only partially effective with nitrogen containing fuels. NO formation from nitrogen in the fuel (fuel NO) is very sensitive to reactant stoichiometry and can be significantly reduced by initially burning the coal under fuel rich conditions. Staged combustion therefore involves creating a fuel rich zone to promote formation of molecular nitrogen from the nitrogen species (HCN, NH_3 and NO) which are evolved as the fuel decomposes, followed by a fuel lean zone optimized for minimum thermal NO formation while completing burnout of the fuel.

Equilibrium calculations for fixed nitrogen species resulting from combustion of CH_4 containing one percent nitrogen as NH_3 (Figure 8) show that NO levels below one ppm are theoretically possible even for high nitrogen fuels and that under fuel-rich conditions lower equilibrium levels are favored at higher temperatures. The conversion of fuel N to molecular nitrogen is kinetically limited, however, as illustrated by the model calculations shown in Figure 9. The concentration of total fixed nitrogen species (TFN = HCN + NO + NH_3) is shown versus time for three isothermal temperatures. These results were calculated for combustion of CH_4 with 1 percent HCN in the fuel at a stoichiometric ratio of 0.75. TFN decays sharply within the first 0.1 seconds, and then continues to decay at a much slower rate. The rate of decay, and hence the TFN level achieved, is enhanced by increasing temperature. The calculation indicates a requirement for long residence times and high-temperatures under fuel-rich conditions in order to achieve TFN levels below 100 ppm. This suggests NO_x could be effectively controlled by the following method:

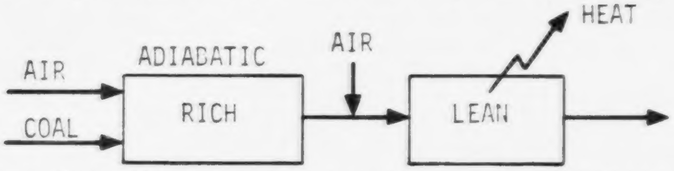

England, et al. (15,16) demonstrated that this approach was effective in reducing NO_x to levels below 100 ppm (corrected to 0 percent O_2) for liquid fuels with nitrogen content on the order of one percent.

The effectiveness of staged combustion of coal is complicated by the slow burnout of the char remaining after the initial release of volatile matter. Under fuel-rich conditions, char burnout is very slow (on the order of seconds) at normal combustion temperatures, and a significant fraction of the fuel nitrogen can remain in the char (char N). The char N cannot be converted to molecular nitrogen in the fuel-rich stage unless it is driven off the solid, and it can be partially converted to NO_x if it is burned out in the fuel lean second stage. Thus higher first stage temperatures should reduce NO from coal combustion because it accelerates the rate of TFN decay and reduces the amount of char N. Pilot-scale data (Figure 10) confirm that higher first-stage temperature produces lower NO_x emissions with coal combustion also (17).

Johnson et al. (18) and Chen et al. (19) observed a decrease in exhaust NO_x emissions when fuel rich zone temperature was decreased in systems which have significant first stage heat loss. Chen observed that when heat extraction was added to the rich zone of a bench-scale tunnel furnace, TFN concentration at the rich zone exit increased but exhaust NO_x (after complete burnout) decreased (see Figure 11). They deduced that this was a result of decreasing the second stage flame temperature sufficiently so that second-stage NO was reduced by NH_i compounds, similar to the "de-NO_x" mechanism of Lyon (20). This suggests that another approach to controlling NO_x in the precombustor may be:

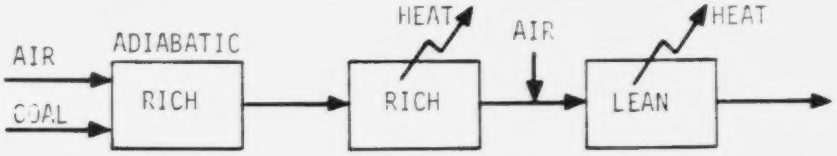

In this approach, the fuel rich zone is initially adiabatic in order to achieve maximum char burnout within the given residence time. Then some heat removal takes place in order to reduce the second stage flame temperature into the window where NO-NH_i reactions are favorable. Combustion air is added to the fuel rich combustion products with heat extraction in order to achieve complete burnout of the fuel while limiting peak flame temperatures.

Another approach to NO_x control is to destroy the NO which is formed during fuel lean combustion by the addition of a small fraction of fuel and air downstream from the main combustion zone:

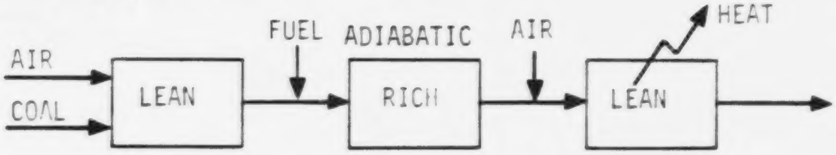

This is the basis of the reburning process (21) which has recently shown promise as an effective NO_x control method for large utility boilers and other fired equipment (21,22). The addition of fuel after the main fuel-lean combustion zone creates a fuel rich zone where hydrocarbon radicals can react with NO formed in the fuel lean stage through reactions such as

$$\begin{aligned} NO + CH &\longrightarrow N + CHO \\ &\longrightarrow HCN + O \end{aligned}$$

The fixed nitrogen compounds formed as a result are then partially converted to NO and N_2 in the final lean burnout stage, thereby achieving a reduction in NO_x from the initial level. Figure 12 shows the results of reburning applied to the VCC advanced cyclone concept under development at EER (4). Coal was initially burned under fuel-lean conditions (defined by SR_1) in the VCC achieving essentially 100 percent solid carbon burnout. Fuel was then added to the exhaust gases to make the stoichiometry slightly fuel rich followed by addition of more air to complete burnout. The figure shows that NO_x reduction of greater than 50 percent is possible using this technique.

EXPERIMENTAL

A series of pilot scale screening tests were conducted at 0.3 MW_t (1×10^6 Btu/hr) in the firetube test furnace shown in Figure 13. The test furnace itself is a horizontal cylinder 60 cm (24 in) inside diameter by approximately 3.2 m (10.5 ft) in length. The furnace is calorimetrically cooled with Dowtherm coolant circulated through the walls of each furnace section and through a convective heat exchanger. Combustion air can be preheated to 340°C (650°F) using an indirect fired air heater and can be metered to several separately controlled streams. Pulverized coal is fed using a scale-mounted screw feeder and hopper assembly, and is transported pneumatically to the burner. Coal feed rate is determined gravimetrically. Sorbents used for sulfur capture experiments were fed and metered similarly. Natural gas was fed from the local main gas line and was metered using a calibrated rotameter. Dopant gases (H_2S, SO_2) were fed from pressurized cylinders and metered with calibrated rotameters.

The experimental precombustor is illustrated in Figure 14. The walls of the precombustor were constructed from castable high temperature and insulating refractories poured into a steel shell. Provision for sampling within the precombustor was included at several stations along its length. Coal and primary air were injected axially at one end of the prechamber and combustion products exit at the other end. Coal was injected through a axial coal nozzle with a swirl vane spreader located at the tip. Primary air passed through fixed swirl vanes (45° angle) prior to entering the precombustor. Provision for injection of primary air, fuel and/or sorbent through tangential ports was also included.

The diameter of the precombustor was reduced at the exit providing a mean gas velocity of approximately 9 meters per second (at $SR_1 = 0.6$). A slag tap was located upstream of the "choke" to collect the molten slag and other particulate matter. Second stage air could be injected at the exit either through radial ports normal to the gas flow for rapid mixing, or through ports oriented parallel to the gas flow for more gradual mixing. The results shown in this paper were obtained with secondary air injected through the parallel ports and with coaxial coal/primary air injection along the axis of the precombustor.

Measurements

Exhaust gas species including O_2, CO_2, CO, NO_x and SO_2 were monitored continuously during the tests. Samples for all species except SO_2 were extracted using a water cooled probe and the sample was dried prior to transport to the analyzers. The accurate measurement of SO_2 is difficult in sample streams laden with sorbents, since reactions between SO_2 and sorbent can take place within the sample probe. A phase discrimination probe similar to that used by Case et al. (23) was used to separate the gas sample from the particle laden stream for measurement of SO_2. The sample stream is dried in a permeation tube dryer and then delivered to the SO_2 analyzer.

Solid samples were collected with a nitrogen quench probe and subsequently analyzed for composition. The nitrogen quench probe minimizes reaction between the sulfur and calcium in the probe by dilution of the sample with nitrogen at the tip of the probe. The sample was subsequently collected on filter paper at the end of the probe and analyzed for carbon, hydrogen, nitrogen and oxygen using a Perkin and Elmer 240B elemental analyzer. Sulfur content was measured using a LECO SC32 sulfur analyzer. Calcium content was determined by titration techniques. Solid samples were collected non-isokinetically.

Temperature measurements were made in the precombustor and firetube using type S thermocouples in a standard suction pyrometer.

Fuels

Natural gas doped with either H_2S or SO_2 and Illinois No. 6 coal were used for these tests. An analysis of the Illinois No. 6 coal is given in Table 1. The sorbent used for the results shown in this paper was limestone (Vicron 45-3).

RESULTS

Figure 15 shows NO_x emissions obtained with the Illinois coal and natural gas. Overall stoichiometric ratio was 1.2. With Illinois coal, NO_x emissions reached a minimum at SR_1 (first-stage stoichiometric ratio) approximately equal to 0.7. This minimum in NO formation as a function of stoichiometric ratio is due to a trade off between increasing formation of HCN and NH_3 species and decreasing NO formation as SR_1 is decreased. The minimum NO_x level firing Illinois coal was about 90 ppm (corrected to zero percent O_2). Measured NO_x concentrations when firing natural gas show minimum NO_x emissions below 30 ppm indicating that thermal NO_x formation is very low in this system. The difference in emissions between gas and coal can be attributed to conversion of fuel nitrogen to NO_x, and suggests that net fuel nitrogen conversion to NO_x is low.

NO_x emissions results are in approximate agreement with trends observed in pilot scale and bench scale experiments. This suggests that the conditions in the precombustor are nearly optimized for staged combustion when operated at SR_1 of approximately 0.7. The experimental system used here closely resembles the pilot scale precombustor successfully used to develop a low NO_x burner system for heavy oils (24). This concept could be directly applied to non-cyclonic systems which utilize inertial ash separation techniques (such as slag screens or baffles) rather than inducement of cyclonic flow. In cyclonic flow systems, considerable back mixing within the prechamber takes place which can significantly alter the distribution of residence time and radical species within the precombustor. There is some evidence (1) that NO_x emissions performance may be comparable in cyclonic and axial flow systems; however, the importance of the large difference in mixing between cyclonic and plug-flow systems has not yet been established.

Figure 16 illustrates results obtained with $CaCO_3$ sorbent injection into the primary air stream at calcium to sulfur molar ratio of two. Sulfur capture is shown for doped natural gas and for Illinois coal at similar first stage stoichiometric ratios. Overall sulfur capture based on exhaust SO_2 concentration methods with and without sorbent injection showed that modest overall SO_2 reduction was achieved with both natural gas (22 percent) and with coal (30 percent). There are a number of potential reasons for the improved overall sulfur capture when burning coal rather than doped natural gas, including: temperature effect in both the rich and lean stages on rich sulfur capture, sulfur regeneration, and lean sulfur capture; enhancement of sulfur capture due to mineral matter or solid carbon interaction with the sorbent; and additional uptake of sulfur in the slag layer. The difference in temperature distributions for coal versus natural gas firing is the most plausible explanation for the slightly improved sulfur capture, but several factors could be influencing the overall performance simultaneously.

Sulfur capture occurring solely in the first stage was calculated based on analysis of solid samples collected at the exit of the fuel rich zone. When firing coal, high carbon content of the samples suggested that much of the sulfur was present as unevolved sulfur in the char rather than as sulfur captured by calcium. Examination of the samples using scanning electron microscope and x-ray diffraction techniques supported this conclusion. Assuming that the coal sulfur evolves at the same rate as the coal nitrogen (25) the fraction of char sulfur was estimated in order to determine sulfur captured as CaS or as $CaSO_4$.

Calculated sulfur capture based on the solid analyses are presented in Figure 16 as shaded bars. Calcium utilization is on the order of 35 percent in the fuel rich zone for both coal and H_2S doped natural gas which would result in about 70 percent sulfur capture at a calcium to sulfur ratio of two. This level of sulfur capture is much higher than the overall capture observed in the exhaust. When the CaS formed in the fuel rich zone passes through the lean second stage flame, gaseous sulfur may be partially regenerated (or completely regenerated and partially recaptured) reducing the net sulfur capture to much lower levels. Temperature measurements made along the axis of the prechamber and furnace (Figure 17) suggest that peak temperature in the second stage flame exceeds 1300°C where $CaSO_4$ is no longer thermodynamically stable. The kinetics of gaseous sulfur regeneration from solids under fuel rich or fuel lean conditions are not well known. However, from these data it would appear that regeneration in the second stage flame is substantial and quite rapid. The implication of these results is that the solid sulfur species should be rejected prior to the second stage in order to minimize gaseous sulfur regeneration and loss of sulfur capture in the second stage. In practice this may be difficult to achieve while maintaining complete carbon utilization.

CONCLUSIONS

The simultaneous control of SO_x, NO_x and ash emissions in a coal fired fuel rich precombustor requires optimization of the controlling mechanisms for each process. While NO_x emissions below 100 ppm are possible when firing coal some tradeoffs appear to be necessary. Those conditions which maximize sulfur removal may not minimize NO_x emissions or particulate rejection. Complete evolution of the fuel sulfur is difficult to achieve under fuel rich conditions within reasonable residence time and temperature. If the char burnout is completed under fuel lean conditions it is likely that the sulfur contained in the char will be oxidized to SO_2. Significant sulfur capture appears to be possible under fuel rich conditions; however, if the sulfur which is captured as CaS or $CaSO_4$ is not removed prior to the second stage, gaseous sulfur will be regenerated and overall sulfur capture reduced.

Several key information gaps in the area of sulfur removal exist which currently limit the capability of the precombustor designer to specify a design which can achieve all emissions goals simultaneously. At present a design of precombustor systems involves a great deal of empiricism. Some of the key areas where further information is needed are:

- details of the evolution of sulfur from the coal and the distribution of gaseous and solid sulfur species;
- the extent and mechanisms of sulfur capture in the molten slag layer;
- the kinetics of sulfur capture under fuel rich conditions at temperatures representative of practical precombustion systems;
- the kinetics of gaseous sulfur regeneration under fuel rich and fuel lean conditions;
- the influence of sorbent type and fuel characteristics on calcium utilization under fuel rich conditions;
- the influence of sorbent additives.

Future effort on this program will attempt to address these areas.

DISCLAIMER

"Although the research described in this article has been funded wholly or in part by the United States Environmental Protection Agency, under contract No. 68-02-3130 to Energy and Environmental Research Corp., it has not been subjected to the agency's required peer and policy review and therefore does not necessarily reflect the views of the Agency and no official endorsement should be inferred."

REFERENCES

1. Kuenzly, J., Advanced Slagging Coal Combustion System: Phase 1, DOE-PETC Combustion Contractors Meeting, DOE Contract DE-AC22-84PC60422 (1984).
2. Cook, C. S., J. Hnat, S. Omori and B. Zauderer, A Regeneratively Air Cooled Cyclone Coal Combustor for Utility Boiler Application, 2nd International Coal Utilization Conference and Exhibition (1979).
3. Zauderer, B., and V. Tilli, Application of an Air Cooled Coal Combustor to Oil Fired Boiler Conversions. Proceedings, 1st Annual Pittsburgh Coal Conference, pp. 761-780 (1984).
4. Unpublished Data, EPA Contract 68-02-3633 (1983).
5. Unpublished Data, DOE Contract DE-AC22-83PC60420 (1984).
6. Dykema, O. W., SO_x and NO_x Control in Combustion, Coal Tech '83, Houston (1983).
7. Unpublished Data, EPA Contract 68-02-4208 (1985).
8. Unpublished Data, DOE Contract DE-AC22-84PC70771 (1985).
9. Bortz, S. and G. Flament, Recent IFRF Fundamental and Pilot Scale Studies on the Direct Sorbent Injection Process, 1st Joint Symposium on Dry SO_2 and Simultaneous SO_2/NO_x Control Technologies, San Diego (1984).
10. Borgwardt, R. H., Roache, N. F., Bruce, K. R., Surface Area of Calcium Oxide and Kinetics of Calcium Sulfide formation. Environmental Progress, Vol. 3, No. 2, pp. 129-135 (1984).
11. Levin, E. M., C. R. Robbins and H. F. McMurdie, Phase Diagrams For Ceramists, American Ceramic Society, Columbus, Ohio, Fourth printing (1979).
12. DeYoung, D. H., Sulfur Solubility in Slags for Cyclone Coal Combustors, Fuel Chemistry Division, Vol. 29, No. 4, ACS Meeting, Philadelphia, pp. 117-128 (1984).
13. Fincham, D. J. B. and F. D. Richardson, The Behavior of Sulfur in Silicate and Aluminate Melts, Proceedings Royal Society Series A223, pp. 40-62 (1954).
14. Carter, P. T. and T. G. Macfarlane, Thermodynamics of Slag Systems, Journal of the Iron and Steel Institute, Vol. 185, pp. 54-62 (1957).

15. England, G. C., M. P. Heap, D. W. Pershing, R. K. Nihart, and G. B. Martin, Mechanisms of NO_x Formation and Control: Alternate and Petroleum-Derived Liquid Fuels, Eighteenth Symposium (International) on Combustion, The Combustion Institute, Pittsburgh, PA (1980).

16. England, G. C., The Establishment of Design Criteria for Optimum Burners for Application to Heavy Fuel Fired Package Boilers, Final Report Volume II-Pilot Scale Tests, EPA Contract 68-02-3125, Available NTIS, Springfield, VA (1984).

17. Case, P. L., unpublished data, EPA Contract 68-02-3921 (1983).

18. Johnson, S. A., P. L. Cioffi, T. M. Sommer, and M. W. McElroy, The Primary Combustion Furnace System, An Advanced Low NO_x Concept for Pulverized Coal Combustion, Proceedings of Second NO_x Control Technology Seminar, Electric Power Research Institute, Palo Alto, CA (1979).

19. Chen, S. L., M. P. Heap, D. W. Pershing and G. G. Martin, Influence of Coal Composition on the Fate of Volatile and Char Nitrogen During Combustion. Nineteenth Symposium (International) on Combustion, The Combustion Institute, Pittsburgh, Pennsylvania (1982).

20. Lyon, R. K., Method for the Reduction of the Concentration of NO in Combustion Effluents Using Ammonia, U.S. Patent No. 3,900,554 (1975).

21. Chen, S. L., W. D. Clark, M. P. Heap, D. W. Pershing and W. R. Seeker, NO_x Reduction by Reburning with Gas and Coal - Bench Scale Studies Proceedings of the Joint Symposium on Stationary Combustion NO_x Control, Dallas, Texas (1982).

22. Takahashi, Y., et al., Development of Mitsubishi "MACT" In-Furnace NO_x Removal Process. Presented at U.S.-Japan NO_x Information Exchange, Tokyo, Japan, May 25-30 (1981).

23. Case, P. L., L. Ho, M. P. Heap, R. Payne and D. W. Pershing, Development of Criteria for Extension of Applicability of Low-Emission, High-Efficiency Coal Burners: Final Report, EPA Contract 68-02-2667 (1984).

24. England, G. C., Y. Kwan, R. Payne "Evaluation and Demonstration of Low-NO_x Burner Systems for TEOR Steam Generators: Final Report - Field Evaluation of Commercial Prototype Burner," EPA Contract 68-02-3692, available NTIS, Springfield, VA (1985).

25. Payne, R. unpublished data, IFRF (1980).

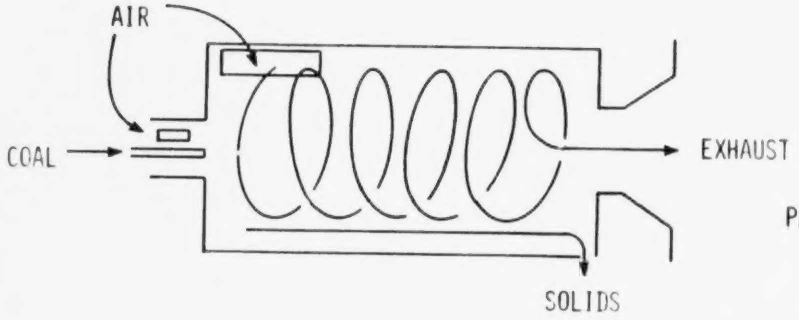
AIR
COAL
EXHAUST
SOLIDS

Figure 1. Common cyclonic precombustor configuration.

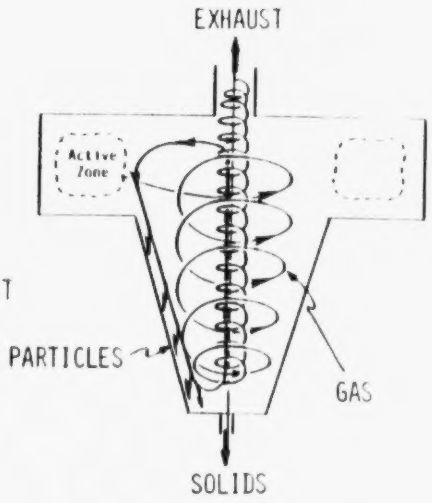
EXHAUST
Active Zone
PARTICLES
GAS
SOLIDS

Figure 2. EER's Vortex Containment Combustor.

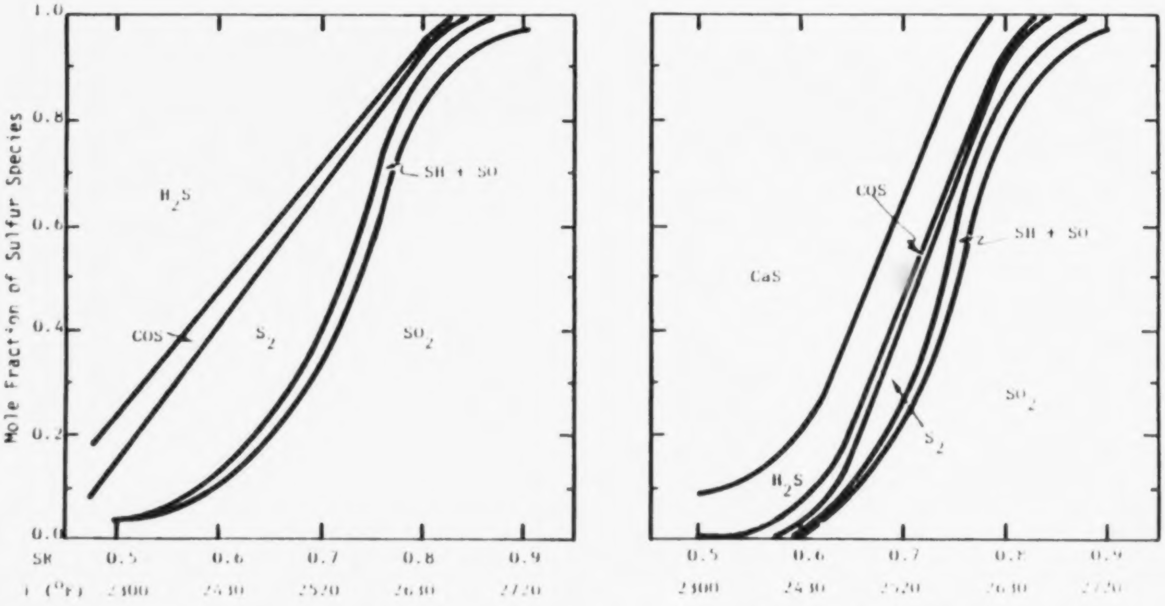

a) Illinois Coal

b) Illinois Coal with $CaCO_3$ Addition

Figure 3. Equilibrium sulfur speciation for Illinois coal without and with calcium addition ($^{Ca}/_{S} = 2$).

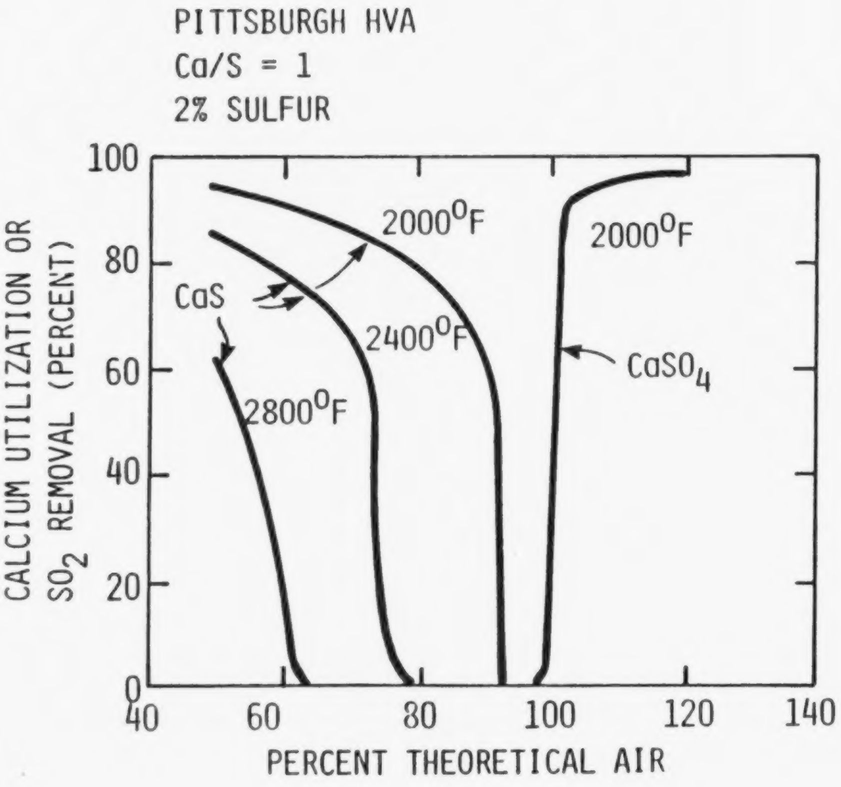

Figure 4. Equilibrium stability of solid calcium-sulfur compounds.

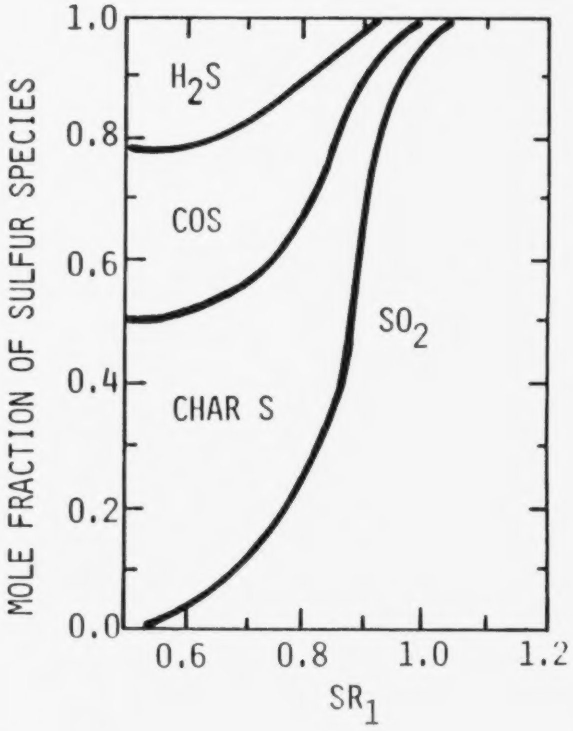

Figure 5. Measured sulfur speciation burning Indiana coal in a 1 x 10^6 Btu/hr furnace.

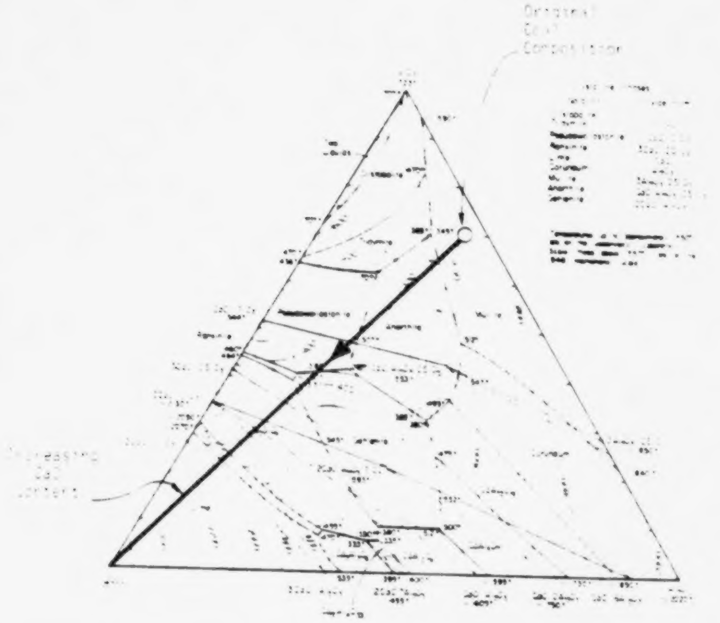
Original
Coal
Composition
Increasing
CaO
content

Figure 6. Ternary diagram for $CaO-Al_2O_3-SiO_2$ melts showing increasing CaO content; temperature in °C.

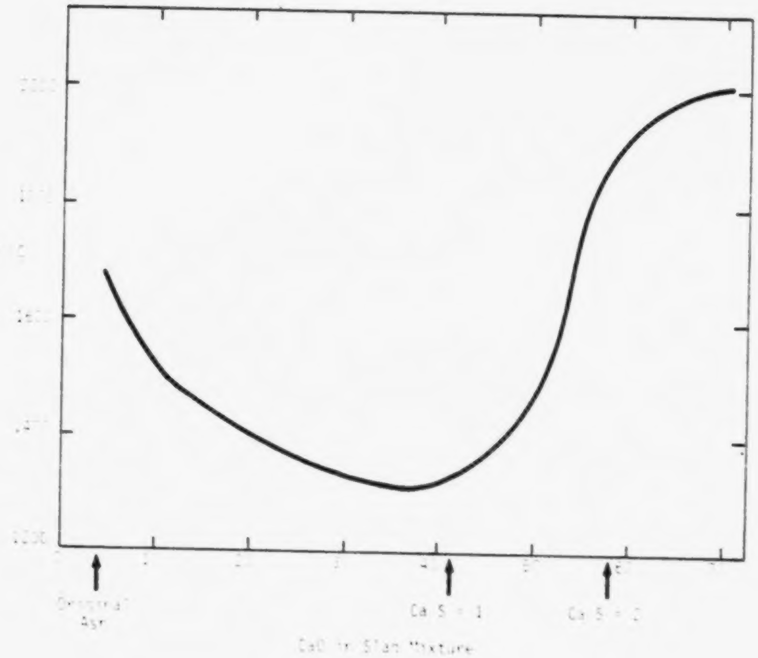

Figure 7. Liquidus temperature for pure $CaO-Al_2O_3-SiO_2$ melts which simulate an Illinois coal ash with increased CaO addition.

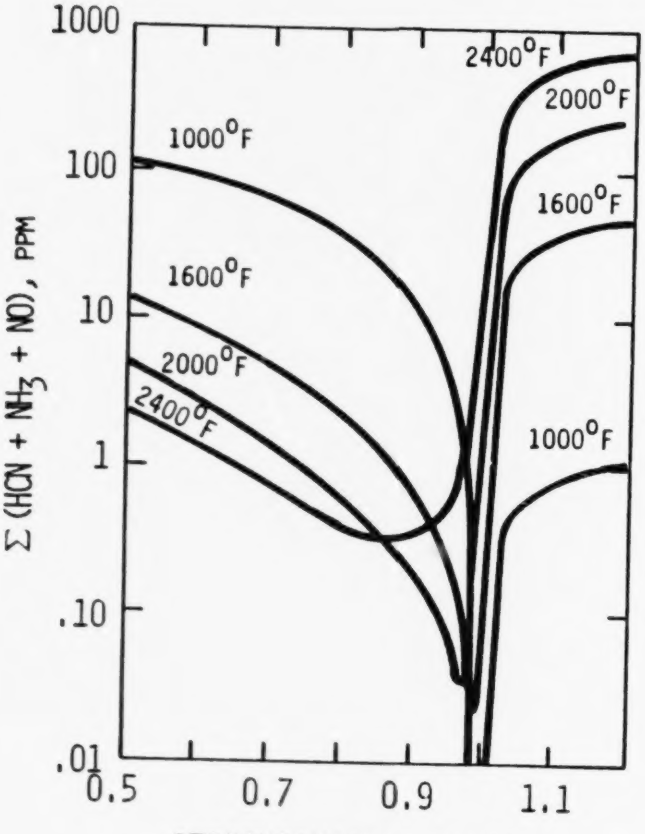

Figure 8. Effect of temperature on equilibrium total fixed nitrogen levels.

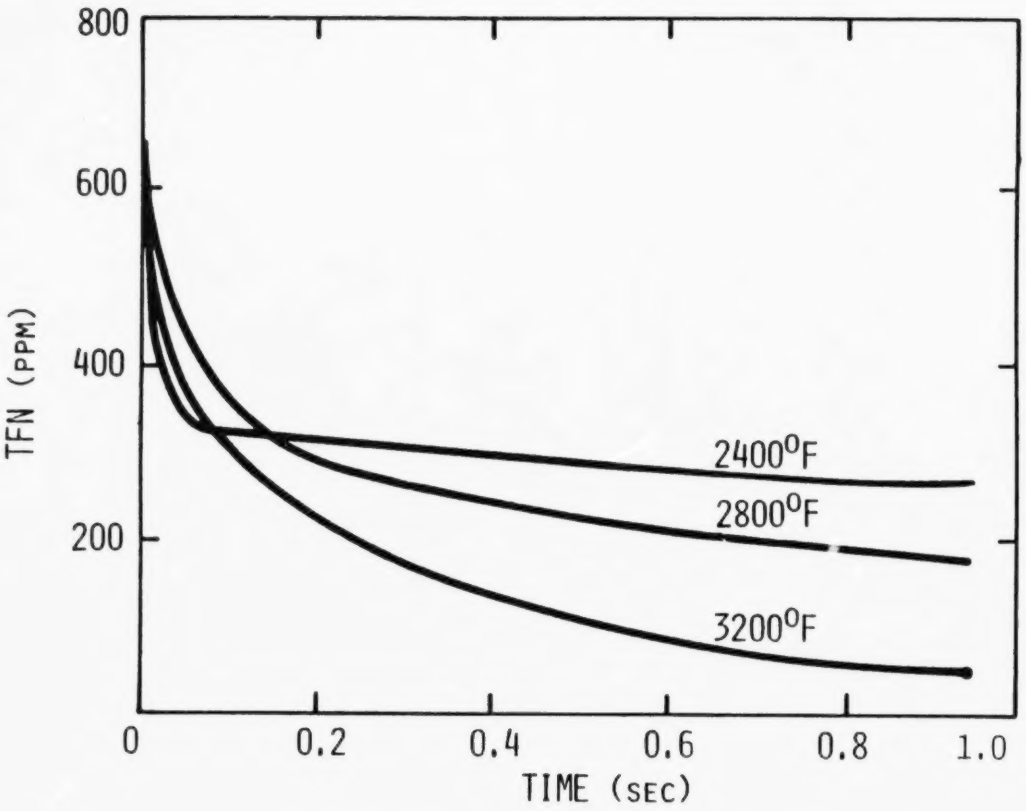

Figure 9. Calculated total fixed nitrogen (TFN) decay as a function of temperature (CH_4, SR = 0.75, 1% HCN in fuel).

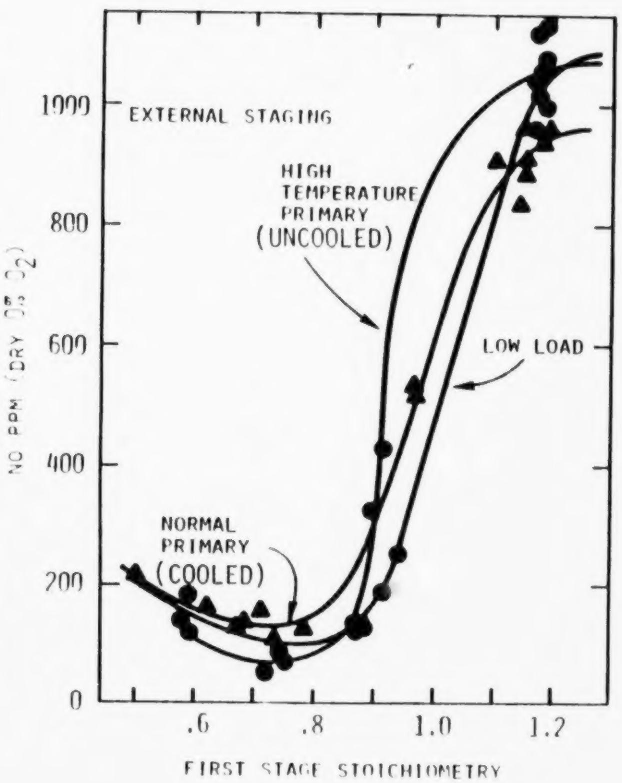

Figure 10. NO_x emissions from pilot-scale (0.3 MW_t) furnace firing Utah coal - effect of rich-zone heat extraction (17).

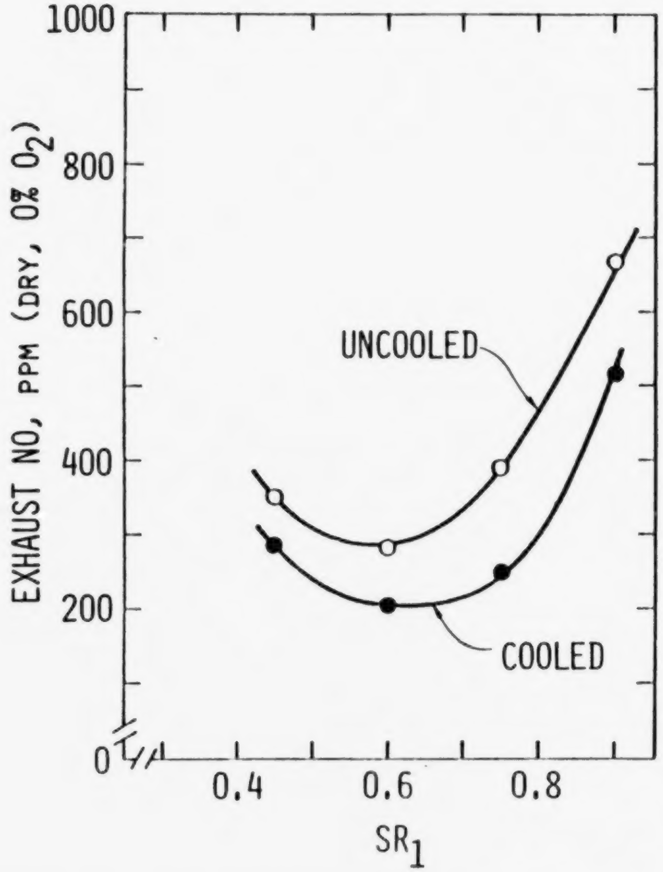

Figure 11. NO_x emissions from bench-scale (21 Kw_t) furnace firing Canadian coal-effect of rich zone heat extraction (19).

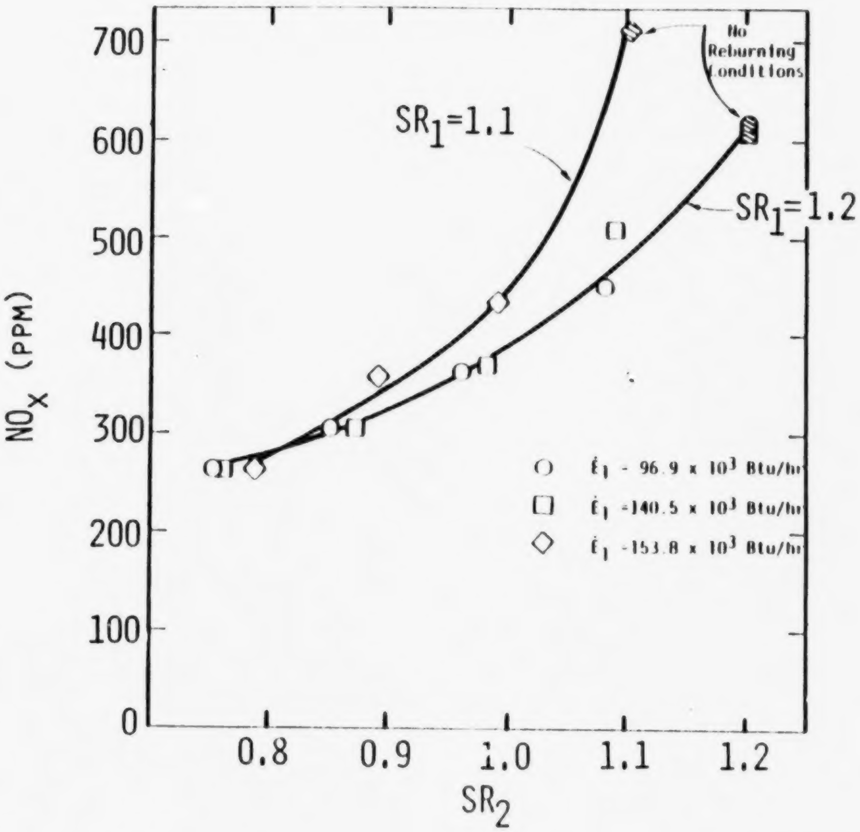

Figure 12. NO_x reduction achieved with reburning applied to the exhaust of an advanced cyclone precombustor (4).

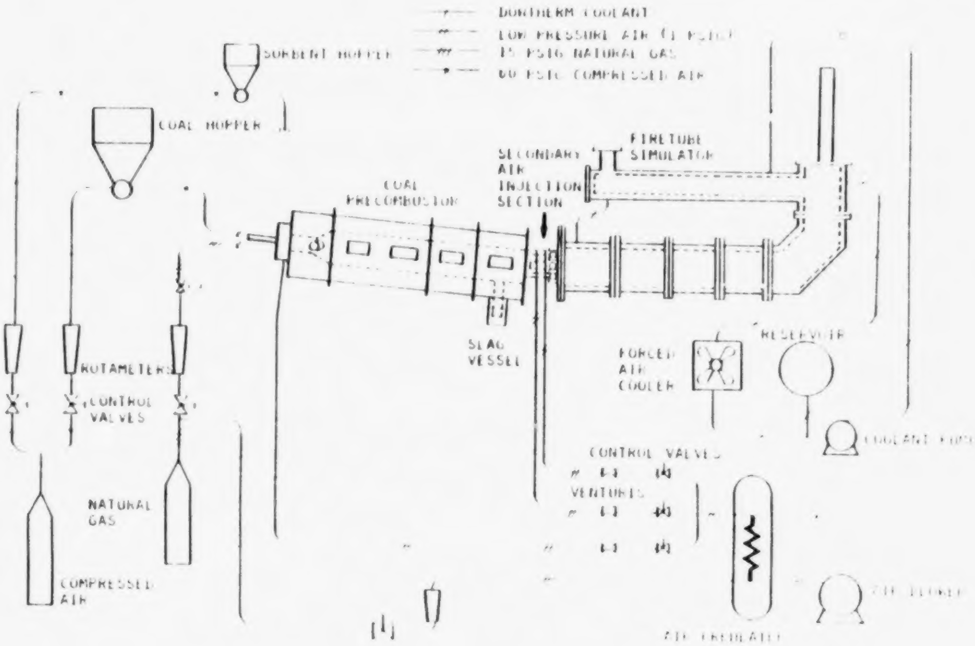
DOWTHERM COOLANT
LOW PRESSURE AIR (1 PSIG)
15 PSIG NATURAL GAS
60 PSIG COMPRESSED AIR
SORBENT HOPPER
COAL HOPPER
COAL PRECOMBUSTOR
SECONDARY AIR INJECTION SECTION
FIRETUBE SIMULATOR
SLAG VESSEL
ROTAMETERS
CONTROL VALVES
NATURAL GAS
COMPRESSED AIR
FORCED AIR COOLER
RESERVOIR
COOLANT PUMP
CONTROL VALVES
VENTURIS
AIR PREHEATER
AIR BLOWER

Figure 13. Coal-fired precombustor - firetube furnace facility.

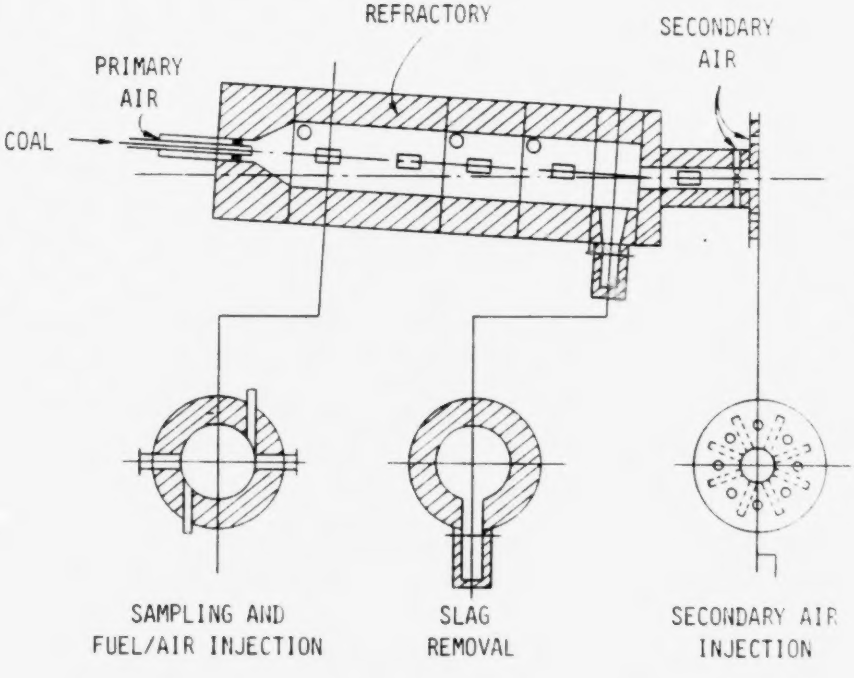
REFRACTORY
SECONDARY AIR
PRIMARY AIR
COAL
SAMPLING AND FUEL/AIR INJECTION
SLAG REMOVAL
SECONDARY AIR INJECTION

Figure 14. Detail of experimental coal-fired precombustor.

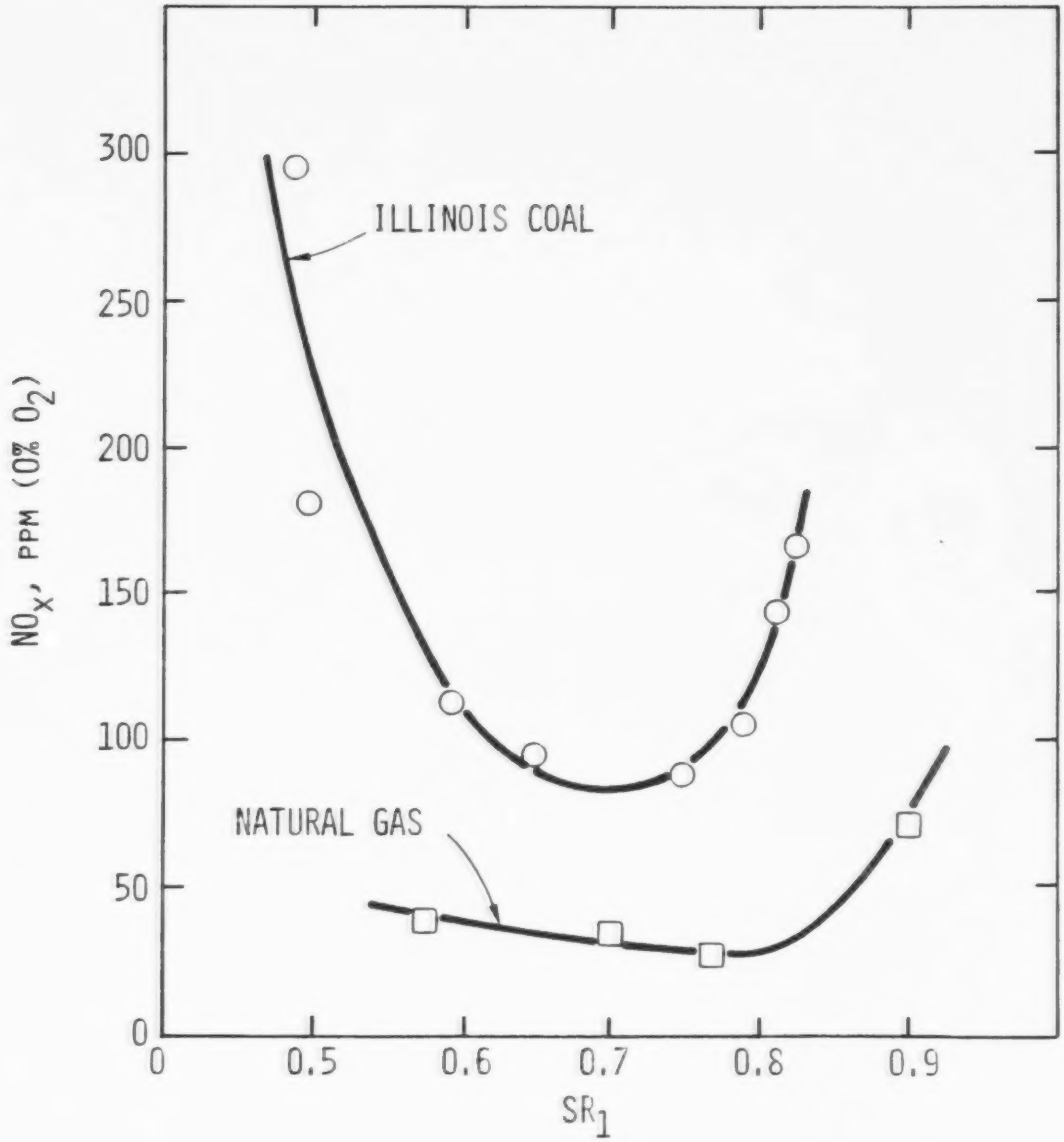

Figure 15. NO$_x$ emissions from Illinois coal and natural gas.

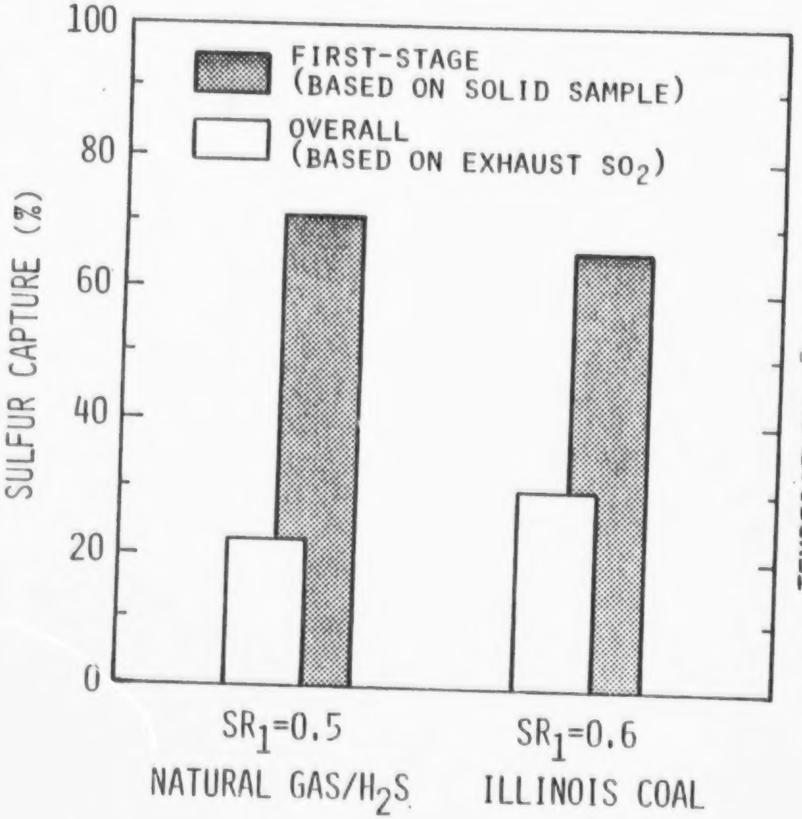

Figure 16. Overall sulfur capture in the exhaust compared to capture in the fuel-rich precombustor. Vicron 45-3 at Ca/S = 2.

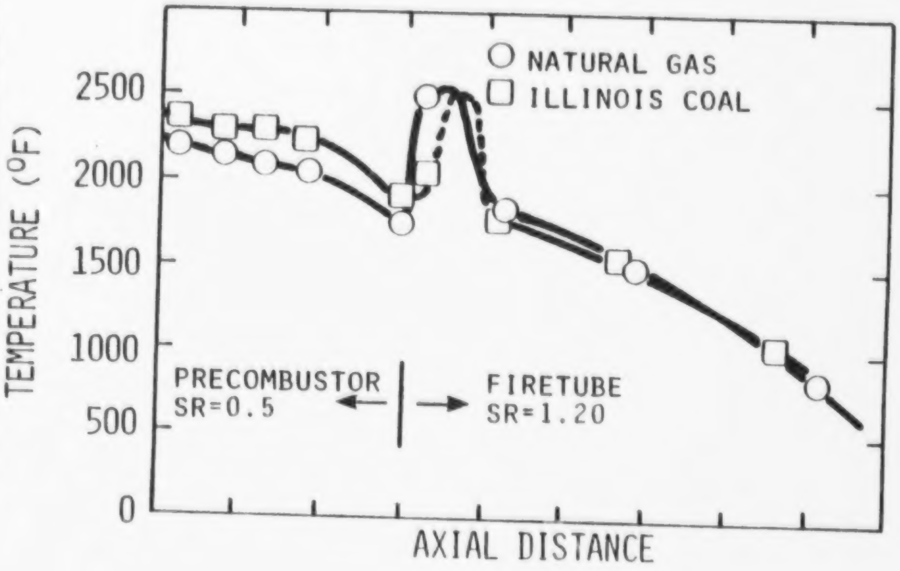

Figure 17. Temperature profile in the precombustor and in the furnace.

Table 1

ANALYSIS OF ILLINOIS #6 COAL

Proximate (%)		
Moisture		5.43
Ash		10.11
Volatile		35.41
Fixed C		49.05
Higher heating Value		10991 Btu/lb
Ultimate (%)		
Moisture		5.43
Carbon		63.03
Hydrogen		4.25
Nitrogen		1.12
Sulfur		3.13
Ash		10.11
Oxygen (by difference)		12.93
Elemental Ash (% Wt)		
SiO_2		49.39
Al_2O_3		17.97
TiO_2		0.64
Fe_2O_3		19.92
CaO		3.06
MgO		1.07
Na_2O		0.95
K_2O		2.10
P_2O_5		0.28
SO_3		4.16
Ash Fusion Temperatures (°F)	**Oxidizing Atmosphere**	**Reducing Atmosphere**
Initial	2310	1991
Softening	2404	2047
Hemispherical	2502	2270
Fluid	2530	2450

Session VIb: Fundamental Combustion Studies

Chairman, Jon Haebig, EPA

MECHANISMS GOVERNING THE DESTRUCTION OF NITROGEN SPECIES DURING STAGED COAL COMBUSTION

J.O.L. Wendt and K.M. Dannecker
Department of Chemical Engineering
University of Arizona
Tucson, Arizona 85721

ABSTRACT

Effects of coal composition on fuel nitrogen mechanisms during fuel rich combustion of pulverized coal were experimentally investigated in a 2 kg/hr down fired combustor. Although there is some variation from coal to coal, the data support the hypothesis that N_2 formation, NH_3 formation and destruction, and NO destruction follow the Fenimore mechanism. HCN destruction is also consistent with Fenimore, although there appears to be a source causing HCN formation.

INTRODUCTION

Mechanisms governing the fate of fuel nitrogen during pulverized coal combustion have been investigated by a number of researchers both in the U.S. and abroad. This paper contributes to an understanding of some of the kinetic limitations encountered in achieving extremely low levels of NO_x emissions through staged combustion.

In staged combustion, one can view the process as occurring in three different combustion zones, namely: (a) the short time scale phenomena regime (100 ms) in which pyrolysis, ignition and some oxidation occur; (b) the post flame, fuel rich zone (1-2s) in which nitrogenous species may be destroyed to form N_2 and (c) the leaning out zone at the staging point. This paper focuses on the second zone, namely in the post flame under fuel rich conditions. It is concerned neither with events occurring at short time scales during pyrolysis nor with events occurring at the leaning out zone where second stage air is added. HCN, NH_3, NO and char nitrogen enter this second zone. The volatile nitrogenous species are destroyed and the total fuel nitrogen leaving this zone depends largely on mechanisms of destruction of HCN, NH_3 and NO.

Previous work (Glass and Wendt, 1982) has shown for a Utah Bituminous coal that (a) char/NO reactions were not dominant, and (b) subsequent devolatilization of nitrogen from the coal residue in this zone was negligible. Furthermore, that work lent strong support to the hypothesis that the Fenimore (1976, 1979) mechanisms was the critical one in destroying the volatile nitrogenous species.

The Fenimore mechanism, which was originally developed from gas flame data, results in the following global rate expression determining the volatile nitrogenous species profiles:

$$-\frac{d}{dt} y_{HCN} = k_1' C_T y_{HCN} y_{H_2O}/y_{H_2}^{1/2} \qquad (1)$$

$$-\frac{d}{dt} y_{NO} = k_2' C_T y_{NO} y_{NH_3}/y_{H_2}^{1/2} \qquad (2)$$

$$\frac{d}{dt} y_{NH_3} = -\frac{d}{dt} y_{HCN} + \frac{d}{dt} y_{NO} \qquad (3)$$

Even though there may be an additional mechanism forming HCN, its destruction rate and the NH_3 formation rate can still be described by reaction (1). Thus, utilizing (3), one obtains:

$$k_1' = \frac{y_{H_2}^{1/2}}{C_T y_{HCN} y_{H_2O}} \left[\frac{d}{dt} (y_{NH_3} - y_{NO})\right] \qquad (4)$$

$$k_2' = -\frac{y_{H_2}^{1/2}}{C_T y_{NO} y_{NH_3}} \left[\frac{d}{dt} y_{NO}\right] \qquad (5)$$

The purpose of this research was to determine whether this Fenimore mechanism, which was shown by Glass and Wendt (1982) to be valid for one coal over a limited range, was, in fact, valid for a variety of coals over a wider temperature range. Previous data (Chen et al., 1982a,b) have indicated that lignites yield substantially higher NH_3 levels at the exit of the second zone than do bituminous coals. It remained to be seen whether Equation (4) and (5) yielded similar values for k_1' and k_2' for the wide range of H_2, NO, HCN and NH_3 levels likely to be encountered. Indeed, NO can be varied by adding it to the inlet mixture, thus simulating, to an extent, the process of reburning (Wendt et al., 1973), and it was not clear whether the Fenimore mechanism were valid under those conditions.

EXPERIMENTAL COMBUSTOR AND ANALYSIS TRAIN

The facilities utilized have been described by Glass (1981) and Glass and Wendt (1982). Essentially, they consist of a 2 kg/h, 15 cm ID downflow combustor with a "premixed" burner to allow self-sustaining combustion to occur in a plugflow mode. The apparatus has some of the salient features of practical combustion devices in that it simulates characteristics times and temperatures in the combustion zone, but is sufficiently well-defined aerodynamically to allow the extraction of time-resolved species profiles and thus the determination of pertinent mechanisms. Samples were withdrawn at various axial positions (ports) along the combustor, utilizing a water-cooled, water-quenched probe. A gas chromatograph was used to measure H_2 accurately (Argon being the carrier gas) and NP detectors and specific ion and gas electrodes measured the HCN content in the gas and the CN^- and NH_3 content in the quench-water respectively. Moisture content in the post flame gases were calculated from a hydrogen balance and so results are reported on a wet basis. Residence times are calculated from measurements of local temperature and molar composition. However, because the internal diameter of the combustor varied somewhat due to slag deposition, there is some error in this analysis.

The compositions of the coals investigated are shown in Table 1. The six coals consisted of two bituminous coals and four lignites, three of which were generically similar but different in moisture content and composition.

EXPERIMENTAL RESULTS

In this paper we shall present experimental species profiles for the Utah bituminous coal as being representative of high grade steam coals and for the Beulah Low Sodium Lignite #2 as being generically representative of low-grade coals. The other four coals exhibited profiles falling into either of the two categories above.

Utah Bituminous Coal

SR = 0.8. Figure 1 shows the time-resolved profiles for major species and gas temperature for two separate runs at SR = 0.8. The solid lines represent values that best satisfy both the hydrogen and oxygen element balances. Oxygen is consumed rapidly and H_2 rises to approximately 2%. The H_2O concentration was calculated from the hydrogen element balance. Temperatures, corrected for radiation from the thermocouple, ranged from 1960 K to 1500 K over 1 second. Figure 2 depicts the nitrogenous species measured. NO decays from 1000 ppm to 380 ppm in 1 second while HCN and NH_3 rise to small levels of less than 20 ppm.

SR = 0.6. At the more fuel rich stoichiometry of SR = 0.6, temperatures are lower and hydrogen concentrations are significantly higher, as shown in Figure 3. The nitrogenous species profiles at this stoichiometric ratio, shown in Figure 4, indicate levels of HCN significantly higher than those of NH_3, while NO decays rapidly from 800 ppm to levels significantly below those of the other nitrogenous species.

Effect of NO Addition. Experiments were conducted to determine how the proposed mechanism depended on inlet NO concentrations. This relates somewhat to the process of reburning, in which NO is destroyed by secondary fuel addition. Results are shown in Figures 5 and 6 for SR = 0.8 and 0.6. The addition of NO had little effect on the NH_3 concentrations, but HCN values were raised slightly. In these experiments the measured temperatures were significantly lower than those for the previous runs at SR = 0.8 and 0.6. The destruction rate of NO appears to be approximately first order in NO, which is consistent with the Fenimore mechanism only if NH_2 is constant.

Beulah Low Sodium Lignite #2

SR = 0.8. Major species for the lignite are shown in Figure 7. As before, temperature is corrected for thermocouple radiation, and CO_2, CO and H_2 were measured, but corrected for moisture. H_2O was calculated from the hydrogen balance, and is very high, due to the high initial coal moisture content.

Nitrogenous species are shown in Figure 8, where NH_3 levels are higher than for the Utah coal and are significantly higher than those of HCN.

SR = 0.6. At the lower stoichioimetric ratio results for major species are predictable, as shown in Figure 9. However, nitrogenous species, as shown in Figure 10, show levels of NH_3 much higher than those of HCN and NO, which are in contrast to the Utah bituminous coal results shown in Figure 4, but which are consistent with the data of Chen et al. (1982a,b).

DATA ANALYSIS

From the proceeding data, it is clear that H_2, H_2O, NO, NH_3 and HCN profiles vary markedly with coal and stoichiometric ratio. The purpose of this research was to determine if these variations could be correlated with the Fenimore mechanism as exhibited by Equations 4 and 5 for k_1' and k_2' respectively.

Figure 11 shows all the data for the Utah Bituminous coal (6 runs) at both stoichiometric ratios SR = 0.8 and SR = 0.8 with and without NO addition (reburning). The data are correlated in terms of $\log_{10} k_1'$ and $\log_{10} k_2'$ versus 1/T where k_1' and k_2' are given by Equations (4) and (5). There are some discrepancies at higher temperatures, but on the whole, the data correlate well, even though the nitrogenous species profiles varied dramatically. Figure 12 compares these data with the previous results of Glass and Wendt (1982). There seem to be discrepancies in k_2', but the data for k_1' agree reasonably well.

Figures 13 through 17 show similar data correlations for the W. Kentucky bituminous, the Texas Lignite, the Beulah Low Sodium Lignite #1, the Beulah Low Sodium Lignite #2 (which corresponds to the species profiles in Figure 7 through 10) and the Beulah High Sodium coals. In each case the data correlate well for both stoichiometric ratios. Only in the Beulah High Sodium case are there serious discrepancies at SR = 0.8.

Figure 18 shows a composite of correlation lines for k_1' and k_2' obtained for all coals. There is good agreement from coal to coal for k_2' but only fair agreement for k_1'. It is not clear whether the discrepancies in k_1' are really far outside the scatter in the data to inaccuracies in obtaining experimental gradients in this system. For engineering purposes, we think that, at present, a common value of k_1' can be used for all coals.

The model does not predict the HCN profiles, although it is consistent with the HCN data. Some mechanism forming HCN is important, especially when the HCN levels are low. Thus, we conclude that the Fenimore mechanism is reasonably accurate for NO destruction and NH_3 formation and destruction under fuel rich pulverized coal combustion conditions.

ACKNOWLEDGEMENTS

This work was supported in part by the U.S. Department of Energy under Contract DE-AC22-84PC70771, administered by the Pittsburgh Energy Technology Center.

REFERENCES

1. Chen, S.L., M.P. Heap, D.W. Pershing, and G.B. Martin, *Nineteenth Symposium (International) on Combustion*, p.1271, The Combustion Institute, Pittsburgh, Pennsylvania (1982a).

2. Chen, S.L., M.P. Heap, D.W. Pershing, and G.B. Martin, *Fuel*, *61*, 1218 (1982b).

3. Fenimore, C.P., *Combustion & Flame*, *26*, (1976).

4. Fenimore, C.P., *Seventeenth Symposium (International) on Combustion*, p.661, The Combustion Institute (1979).

5. Glass, J.W., "Fuel Nitrogen Conversion During the Fuel Rich Combustion of Pulverized Coal and Char", Ph.D. Dissertation, University of Arizona, available from University Microfilms, Ann Arbor, Michigan (1981).

6. Glass, J.W. and J.O.L. Wendt, *Nineteenth Symposium (International) on Combustion*, p.1243, The Combustion Institute, Pittsburgh, Pennsylvania (1982).

7. Wendt, J.O.L., C.V. Sternling and M.A. Matovich, *Fourteenth Symposium (International) on Combustion*, p.881, The Combustion Institute, Pittsburgh, Pennsylvania (1973).

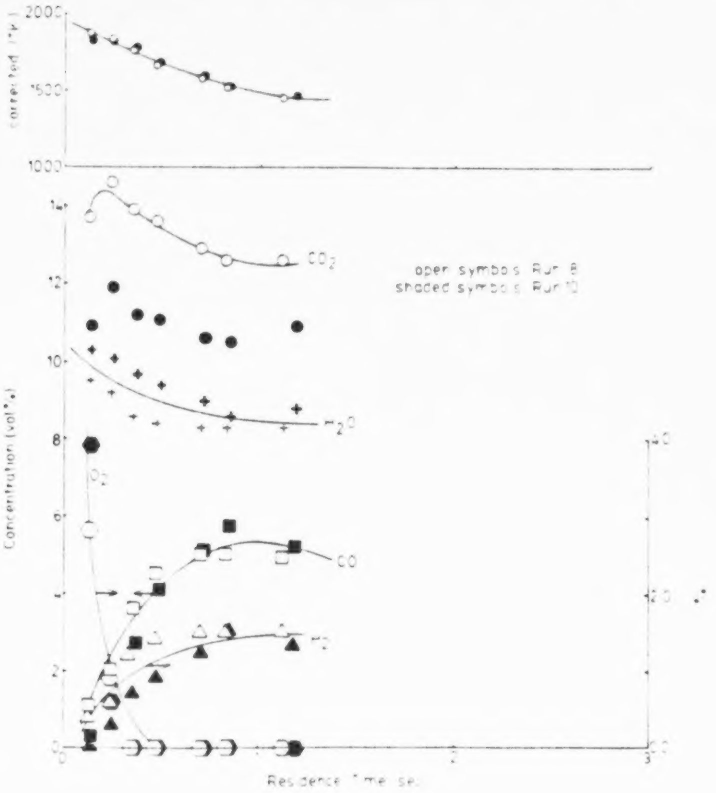

Figure 1. Utah Bituminous: SR = 0.8, Temperature and Major Species Profiles.

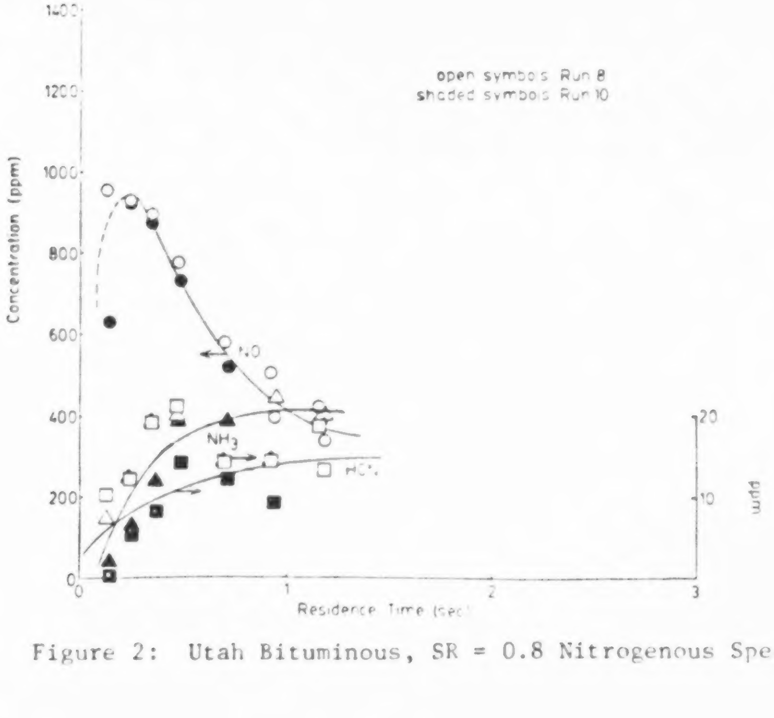

Figure 2: Utah Bituminous, SR = 0.8 Nitrogenous Species.

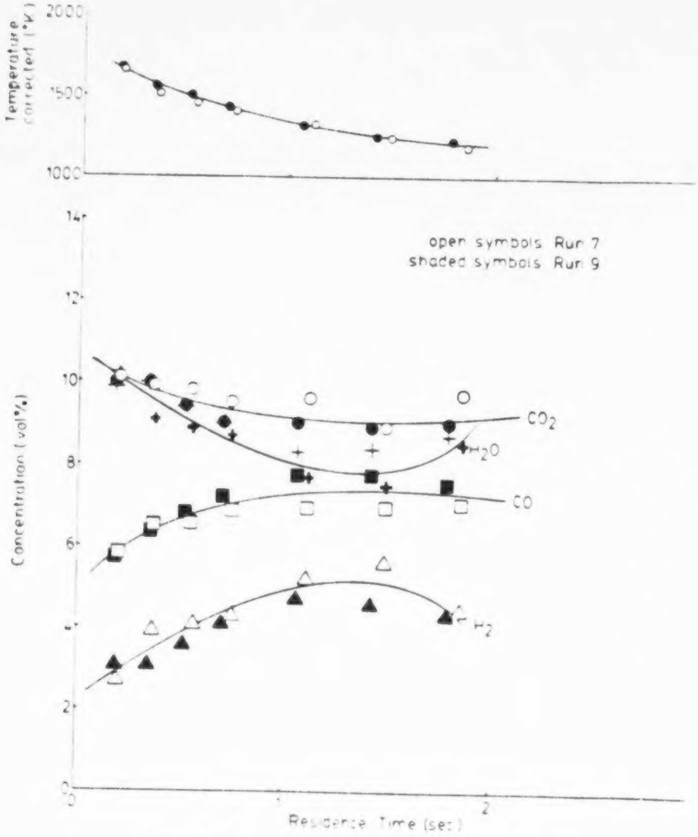

Figure 3. Utah Bituminous: SR = 0.6, Major Species and Temperature Profiles.

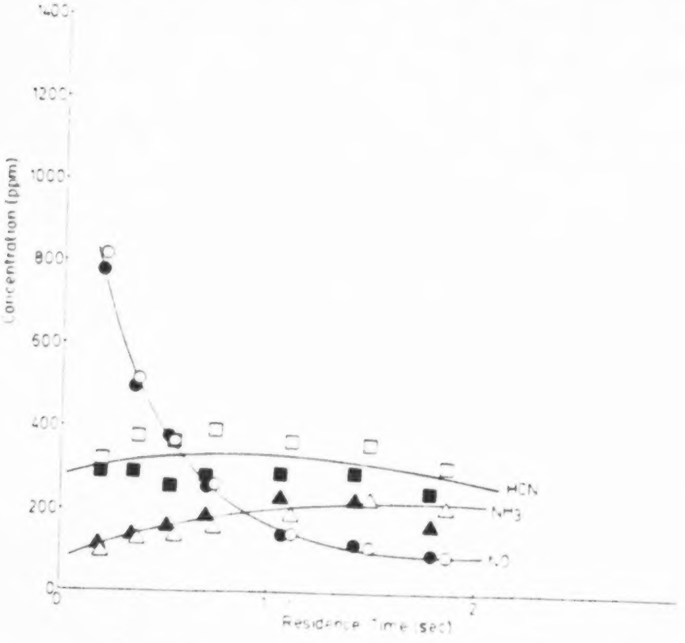

Figure 4. Utah Bituminous: SR = 0.6. Nitrogenous Species, Open Symbols: Run 7, Shaded Symbols: Run 9

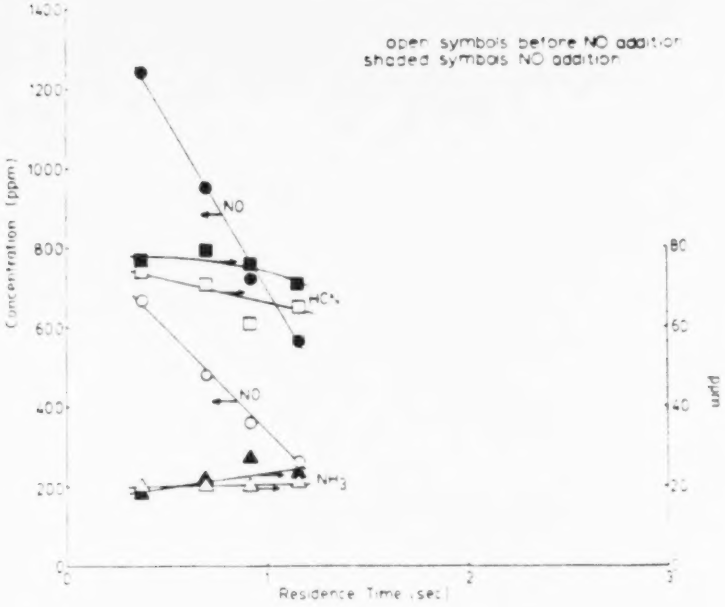

Figure 5. Effect of NO Addition on Nitrogenous Species. Utah Bituminous: SR = 0.8.

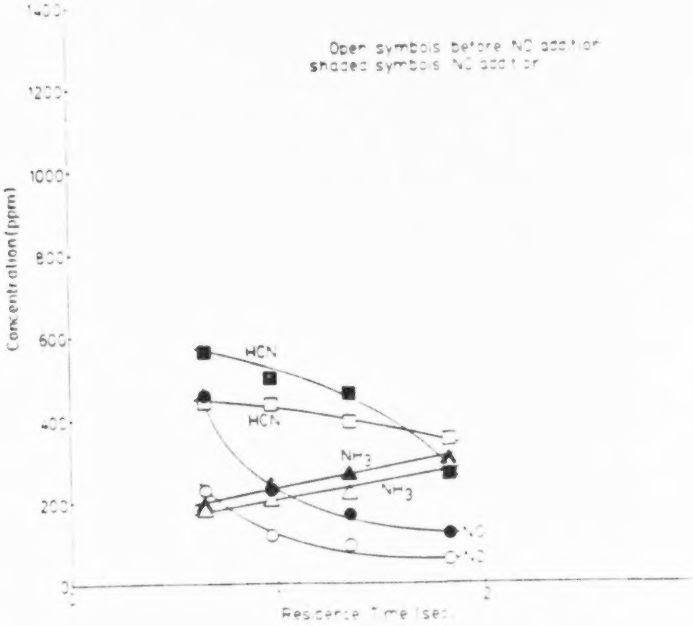

Figure 6. Effect of NO Addition on Nitrogenous Species. Utah Bituminous: SR = 0.6.

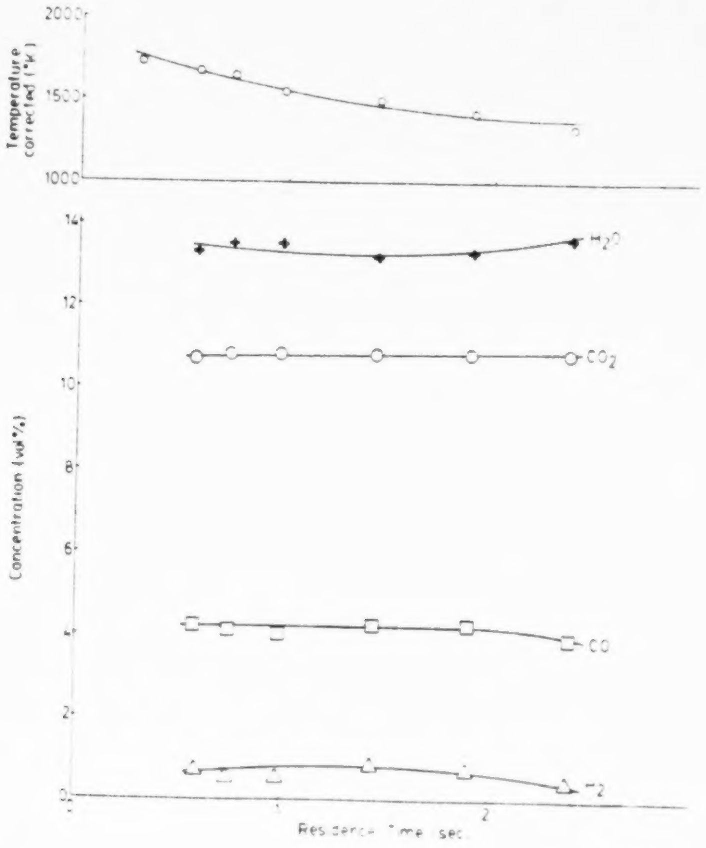

Figure 7. Beulah Low Sodium Lignite #2: SR = 0.82, Temperature and Major Species.

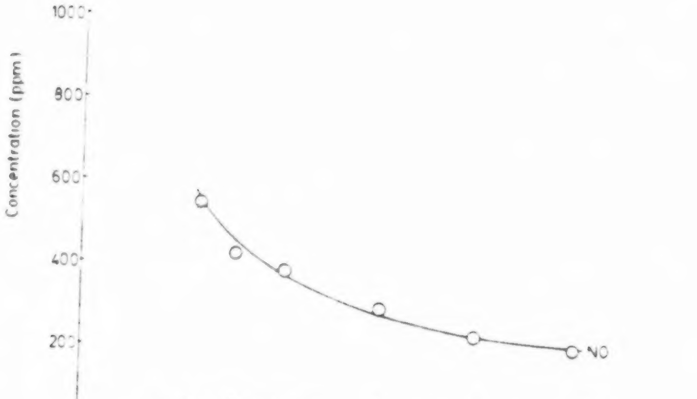

Figure 8. Beulah Low Sodium Lignite #2: SR = 0.82, Nitrogenous Species.

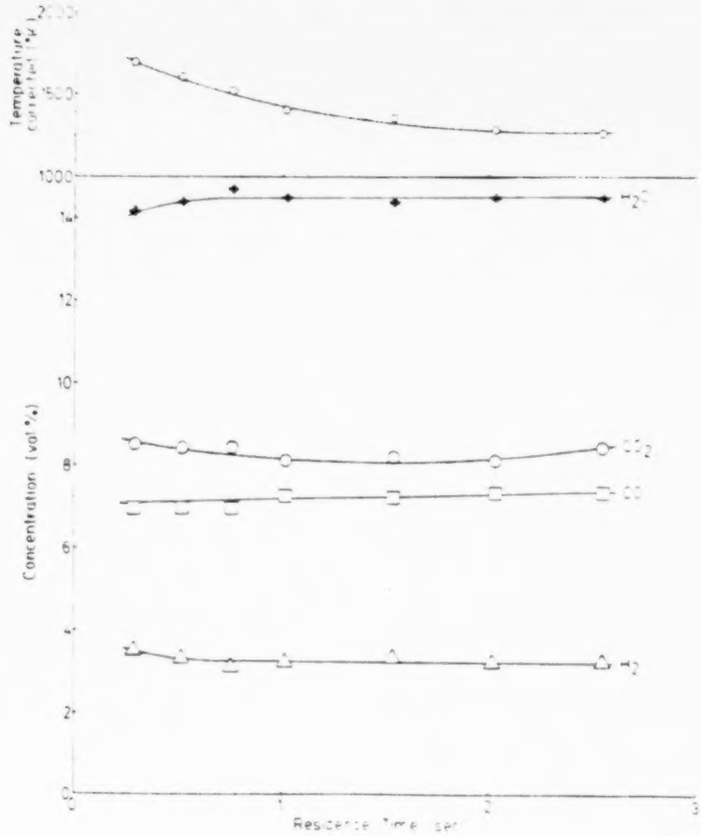

Figure 9. Beulah Low Sodium Lignite #2: SR = 0.62. Temperature and Major Species.

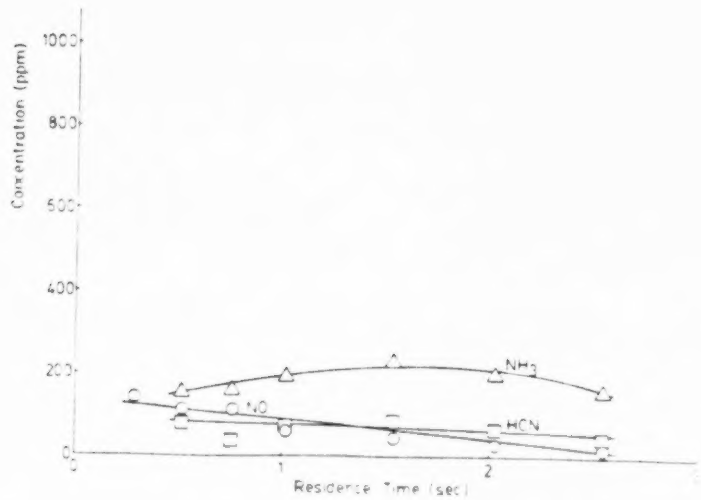

Figure 10. Beulah Low Sodium Lignite #2: SR = 0.62, Nitrogeneous Species.

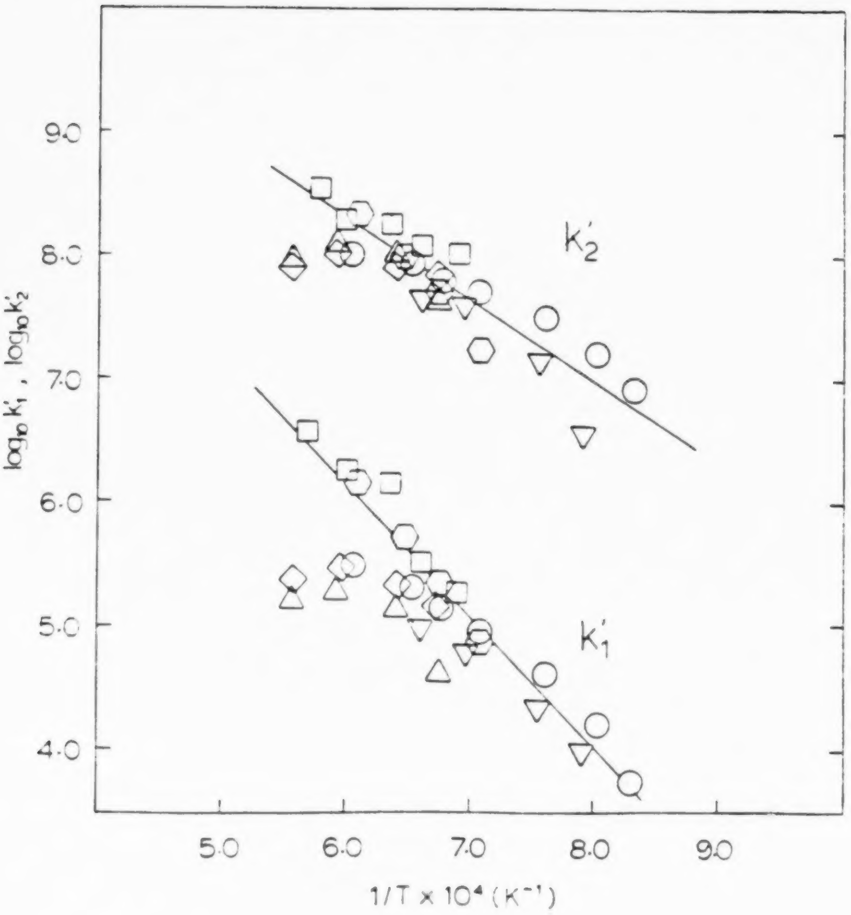

Figure 11. Reaction Rate Coefficient for Utah Bituminous

○ Runs 7 and 9, SR = 0.6 □ Runs 8 and 10, SR = 0.8
▽ Run 11, SR = 0.6, w/NO ◇ Run 12, SR = 0.8 w/NO
△ Run 12, SR = 0.8, w/o NO ⬡ Run 6, SR = 0.8

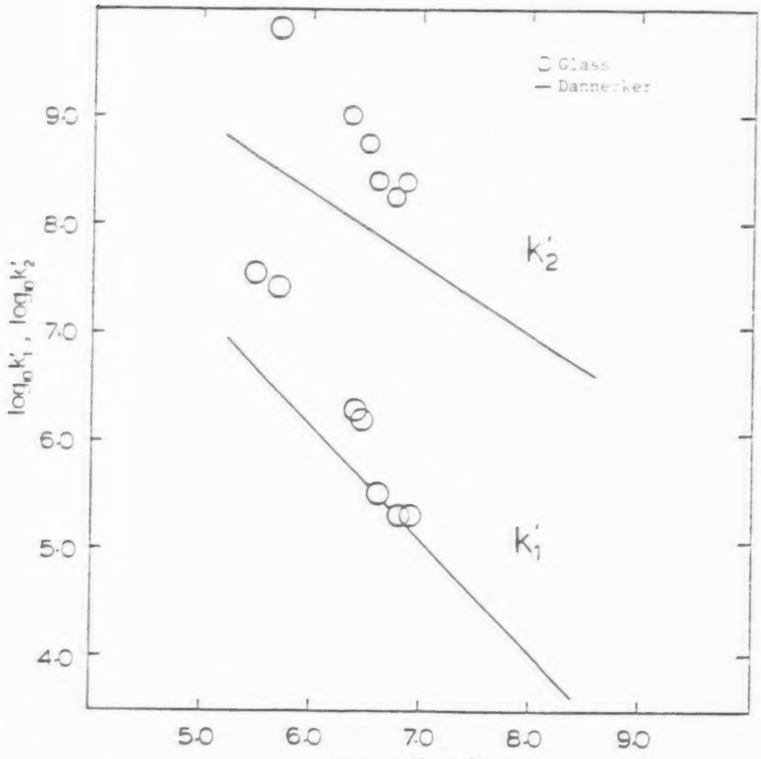

Figure 12. Comparison of Glass and Dannecker, Homogeneous Rate Constants, Utah Bituminous.

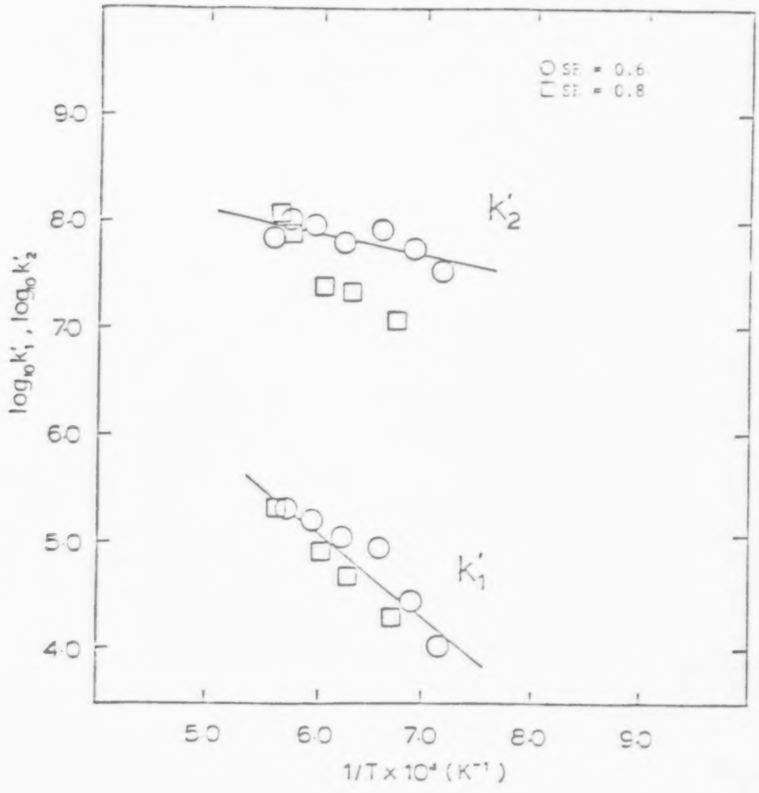

Figure 13. Homogeneous Rate Constants, Western Kentucky Bituminous.

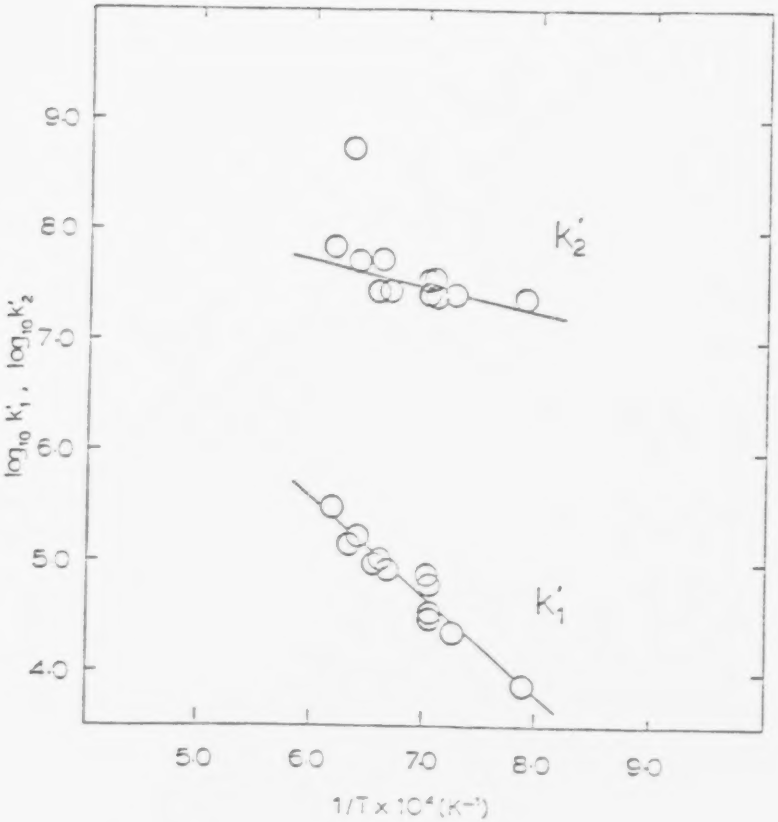

Figure 14. Homogeneous Rate Constants, Texas Lignite.

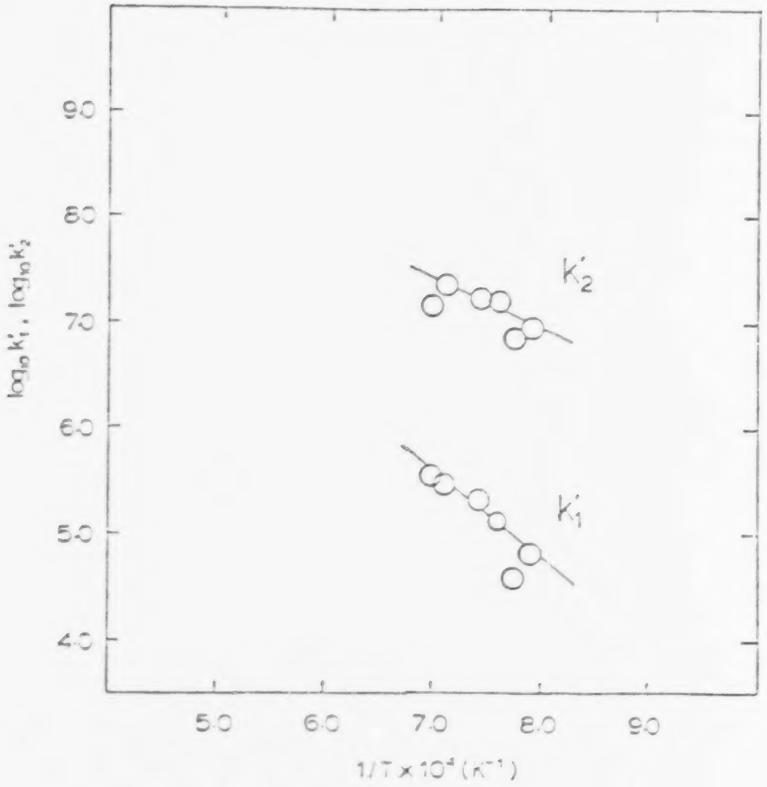

Figure 15. Homogeneous Rate Constants, Beulah Lignite Low Sodium #1.

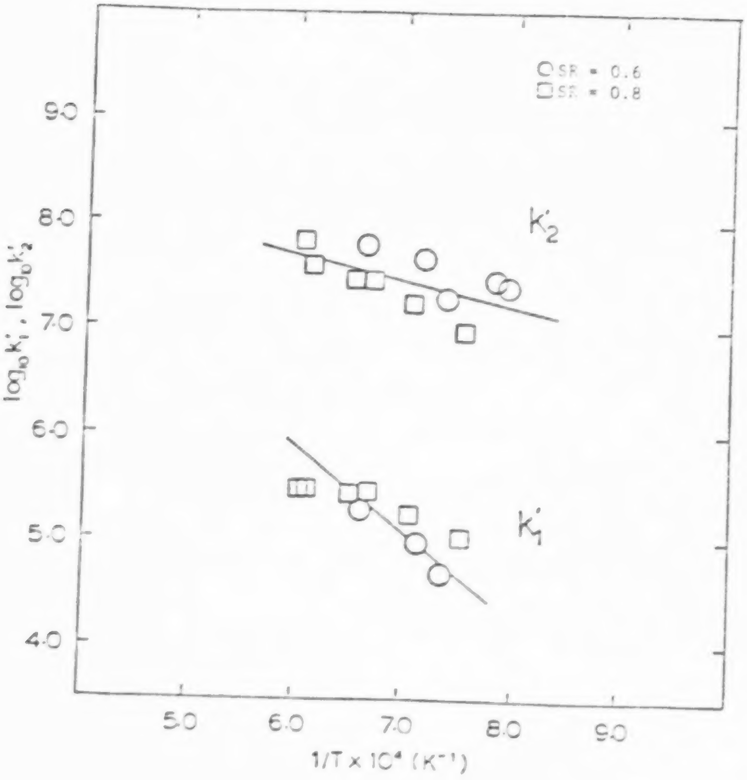

Figure 16. Homogeneous Rate Constants, Beulah Lignite Low Sodium #2.

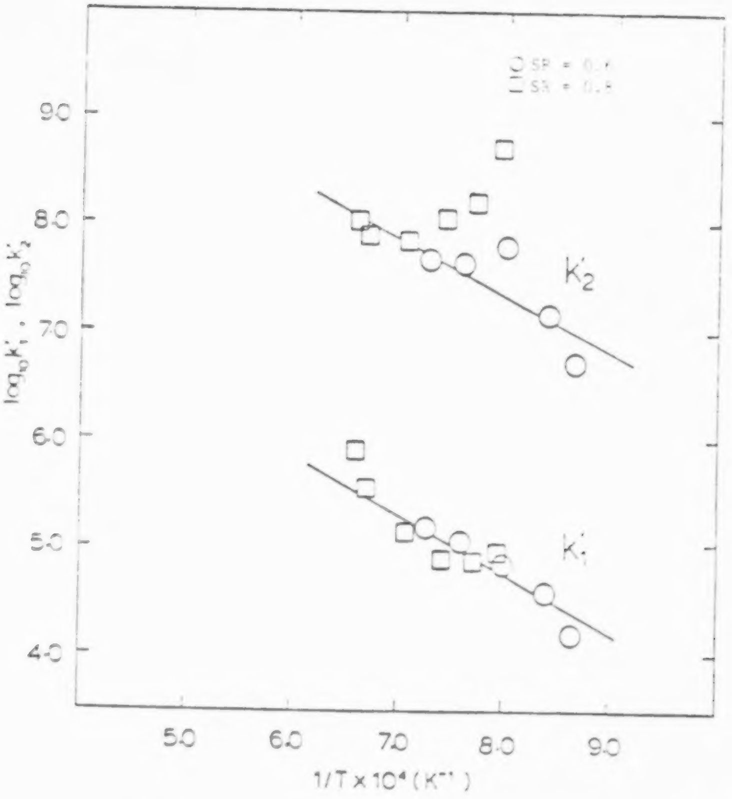

Figure 17. Homogeneous Rate Constants, Beulah Lignite High Sodium.

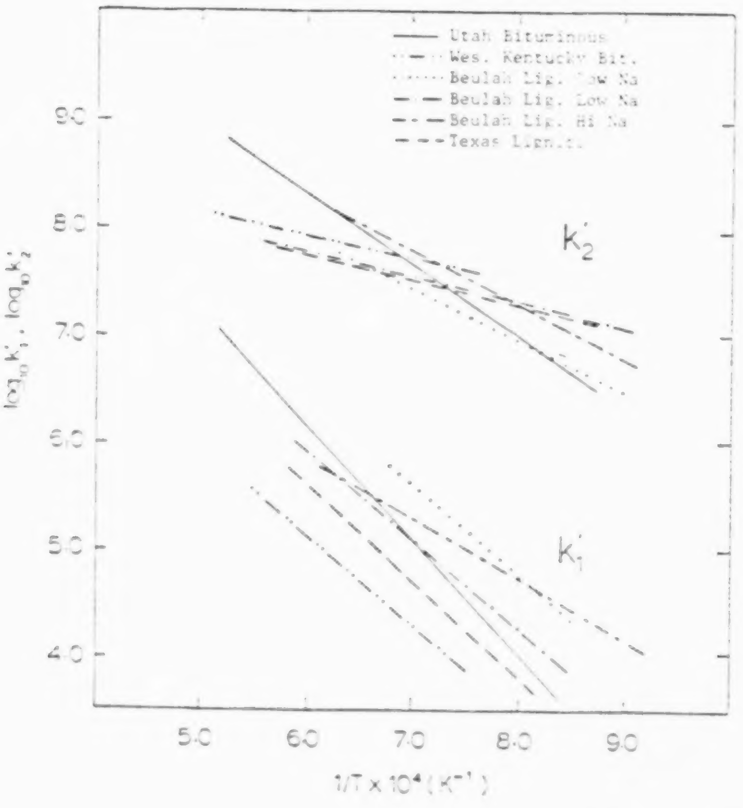

Figure 18. Homogeneous Rate Constants, Composite of All Coals.

Table 1

FUEL COMPOSITIONS

PROXIMATE ANALYSIS

	Volatile Matter	Fixed Carbon	Moisture	Ash
Utah Bituminous	39.2	47.4	4.5	8.9
Western Kentucky Bituminous	41.8	46.9	3.0	8.6
Texas Lignite	34.5	30.2	14.0	21.3
Beulah Lignite Low Na #1	38.3	35.3	13.1	13.3
Beulah Lignite Low Na #2	37.1	37.1	17.8	8.0
Beulah Lignite High Na	36.3	33.9	22.5	7.3

ULTIMATE ANALYSIS (dry, ash included basis)

	Carbon	Hydrogen	Nitrogen	Sulfur	Oxygen
Utah Bituminous.	70.87	5.11	1.64	1.03	12.08
Western Kentucky Bituminous	73.22	4.55	0.82	3.00	12.53
Texas Lignite	54.60	3.60	0.85	3.39	16.21
Beulah Lignite Low Na #1	62.34	3.07	0.92	3.48	16.90
Beulah Lignite Low Na #2	57.79	3.95	0.91	2.07	25.57
Beulah Lignite High Na	59.80	3.90	1.08	1.02	24.75

OXIDATION AND PYROLYSIS OF FUEL NITROGEN IN A LIGNITE -- BOTH AS RECEIVED AND AFTER AMMONIUM ION-EXCHANGE

L.D. Timothy, J.M. Beer, and A.F. Sarofim
Department of Chemical Engineering
Massachusetts Institute of Technology
Cambridge, Massachusetts 02139

ABSTRACT

The dependence of the conversion of the organically bound nitrogen in coal to nitric oxide on the volatility and amount of fuel nitrogen was studied by the pyrolysis and oxidation of a low rank Montana coal both as received and after ion-exchange with ammonium acetate. The nitrogen content of the coal was increased on treatment from 1.11 percent to 2.34 percent by weight (dry). Nitrogen retentions by the chars obtained during pyrolysis of both the raw and treated coals were measured over a temperature range of 550 to 1650 K. The added nitrogen was more volatile being released completely by 1400 K compared to 60% release of the nitrogen in the untreated coal at 1400 K. Conversion of the nitrogen to nitric oxide for combustion in different oxygen concentrations was found to vary from 35 to 55 percent, with the lower nitrogen content untreated coal having slightly higher conversion efficiencies than the treated coal.

INTRODUCTION

The oxidation of organically-bound nitrogen in fossil fuels is known to be a major source of nitrogen oxides emitted by stationary sources. During the past decade major progress has been made in developing both an understanding of the processes governing the conversion of fuel-bound nitrogen to nitrogen oxides and strategies for reducing NO_x emission primarily by the staging of air addition. Much of the early work was based on studies with gaseous and liquid fuels in which the nitrogen content could be varied by the addition of nitrogen-containing dopants such as ammonia for gaseous systems and pyrodine and quinoline for liquid systems. The conversion of the fuel nitrogen to nitric oxide is known to proceed through the gas phase reactions in which the fuel bound nitrogen is converted to N, NH, and NH_2 which in turn are either oxidized to NO or react with NO to form N_2. Although uncertainty exists with the rate constants of certain of the elementary steps in the fuel nitrogen reaction scheme, the mechanisms based on the early studies by Fenimore (1) and Haynes (2) are fairly well established and can explain many of the observed trends in fuel nitrogen conversion to nitric oxide.

For coals the problem is more complicated since an additional step is involved requiring the release of the nitrogen bound in the coal to the gas phase. As a consequence, changes in the conversion efficiency to nitric oxide of nitrogen bound in the coal is influenced by both the rate of release of the nitrogen to the gas-phase and the gas-phase reactions. The most extensive study of the influence of coal composition on the fate of volatile and char nitrogen during combustion is that by Chen et al (3) in which fifty coals from North America, Europe, and Asia were burned in a 21 KW refractory-lined tunnel furnace. The nitrogen content of the coals ranged from 0.68 to 2.46 percent by weight (daf). The emissions of nitric oxide, however, were found,for a given set of operating conditions, not to be governed by fuel nitrogen content alone. For example a Savage and a Beulah lignite, both with a nitrogen content of 1.05 % by weight (daf), gave NO emissions which differed by more than 60%. The coal dependent parameters which were found to best correlate the experimental results were the total nitrogen content, the nitrogen volatility as measured by the nitrogen released under a modified ASTM pyrolysis test, and the amount of HCN produced in a pyrolysis experiment.

The study by Chen et al (3) provides an empirical correlation of NO_x emissions with coal pyrolysis studies. Other studies have also recognized the importance of coal nitrogen devolatilization NO_x emissions and the dependence of nitrogen release during pyrolysis on coal type. Pohl and Sarofim (4), and Song et al (5) have shown that nitric oxide formation could be attributed to the sum of the contributions of the oxidation of the nitrogen in the volatiles and the nitrogen in the char, and showed that the volatile contribution increased with increased combustion (and therefore pyrolysis) temperature. Blair et al (6) and Freihaut et al (7) found that a major fraction of the nitrogen was released with the coal tars. The kinetics of the nitrogen release, however, is complicated. The initial volatiles are nitrogen free and then the nitrogen release appears to follow a complex time dependence which has been fitted by assuming that part of the nitrogen is loosely bound and the remainder tightly bound (8, 9). These observations, however, have not been related to the structural form of the nitrogen in the coal.

It is difficult to exactly describe the state of organic nitrogen in coal but it is believed to be mainly in aromatic structures (10). The release of nitrogen with the tars supports this view. The nitrogen retained by the char must be related to the competition between the reactions of the moieties in the coal structure which can decompose to form volatile tar and condensation reactions leading eventually to char formation. In the present study the use of ion-exchange to add nitrogen in the form of ammonium ions provided an opportunity to increase the fraction of the nitrogen in coal that would be devolatilized during pyrolysis, and to therefore systematically determine the effect of changes in the distribution of volatile and non-volatile nitrogen on NO_x formation. The coal selected for study contained a high concentration of alkaline earth metals present as cations on the carboxylic acid groups in the coal structure. The presence of most of the calcium and magnesium in the ion-exchangeable form was determined by float sink techniques (11), microscopy (11), and ion-exchange.

EXPERIMENTAL

Experiments were conducted with a Montana lignite with the composition given in Table 1. The coal was first ground and classified to obtain a size fraction of 110 µm. Half of the coal was then washed repeatedly in a 1 M ammonium acetate solution. The elemental composition of the coal was determined before and after ion-exchange. The analyses were carried out by the Huffman Laboratories, Wheat Ridge, CO.

The treated and untreated coals were then pyrolyzed in a crucible maintained in a furnace long enough to approach an asymptotic weight. Elemental analyzes were obtained on the residual char.

The treated and untreated coals were then burned in a laminar flow furnace in oxygen-helium mixtures with oxygen concentrations ranging from 5 to 100 percent. The gas flow was sufficiently high that the oxygen concentration remained essentially constant during reaction (the flow rate was approximately 40 times stoichiometric). The furnace temperature was maintained at 1250 K. The NO and NO_2 in the exhaust gases was measured with a Thermo Electron Chemiluminescent NO_x Analyzer, Model 14E.

RESULTS

The analyses of the Montana lignite after ion-exchange is shown in Table 2. The most notable differences in the composition of the treated and untreated coal are the increase of the nitrogen content, and the decrease in the calcium and magnesium contents. The nitrogen concentration more than doubled. If two ammonium ions replaced each calcium and each magnesium ion the increase in nitrogen due to ion exchange would be (28/40) x 1.11 = 0.78 for calcium and (28/24) x 0.43 = 0.50 for magnesium. For this coal, the increase in nitrogen is primarily a result of the replacement of the calcium ions and secondarily the replacement of the magnesium. The observed increase in nitrogen (1.23%) is slightly less than the sum (1.28%) of the calculated contributions but within the limits of uncertainty in the analyses.

The weight losses during pyrolysis and the compositions of the residual chars are presented in Table 3. The retention of the nitrogen in the char normalized with the nitrogen content of the untreated coal are plotted as a function of pyrolysis temperature in Fig. 1. It can be seen that approximately half of the added nitrogen is evolved by 700 K whereas only 20% of the nitrogen in the original coal is evolved at 700 K. At the ASTM temperature (1123 K), the nitrogen content of the treated coal is only slightly higher than that for the untreated, and the nitrogen content of the treated and untreated coals are indistinguishable above 1400 K.

The conversion of the fuel nitrogen of the treated and untreated coals is shown as a function of the oxygen content of the furnace atmosphere in Fig. 2. The fractional conversion to NO of the nitrogen in the lower nitrogen-content untreated coal is slightly higher than that for the treated coal. The nitrogen conversion efficiency is higher for the lowest O_2 concentration studied, falls to a minimum at 80% oxygen and then increases slightly.

DISCUSSION OF RESULTS

The study has demonstrated the potential for modifying the nitrogen content and volatility by the use of ion-exchange with ammonium salts. The experiments were conducted with a low-rank coal which has a natural high exchange capacity. The method, however, may be extended to other coals by the use of mild oxidation to provide ion-exchange sites.

The conversion of fuel nitrogen to nitric oxide has been shown by Chen et al (3) and others to be dependent on the fuel nitrogen volatility. In an unstaged combustor it is preferable to release the fuel nitrogen late in a regime where the oxygen content is low. For unstaged combustion, it is therefore preferable to have a low content of volatile nitrogen, as indeed has been found to be the case experimentally (3). By similar reasoning, for a staged combustor it is preferable to have the volatiles released in the fuel-rich first stage and to therefore have a high fraction of the nitrogen evolved with the volatiles.

The results in Ref. 3 showed that the nitrogen distribution in an ASTM proximate analysis test provided a reasonable measure of fuel nitrogen volatility for purposes of correlating NO_x emissions. The use of ammonium exchange can be useful in testing this criterion. For the coal used in this study the fractional retention of nitrogen at the ASTM temperature fell from about 0.6 for the untreated coal to 0.3 for the treated. This increase in volatile nitrogen for the untreated coal would be expected to yield higher conversion efficiencies. In this case the increase in conversion with increased fuel nitrogen volatility nearly compensated for the expected decrease in fuel nitrogen conversion with increasing fuel nitrogen content.

The effect of oxygen concentration on the fuel nitrogen conversion in this study is dominated by the increase in combustion temperature with oxygen concentration. The higher the oxygen content, the higher the temperature, and the faster the fuel nitrogen release. The decrease in fuel nitrogen conversion with increasing oxygen may be therefore partly a consequence of the increased local concentration of fuel nitrogen species during rapid pyrolysis.

It should be noted, in closing, that the ion-exchange of calcium and magnesium with ammonium may have some secondary effects. It is known that calcium catalyzes tar cracking to light gases and char oxidation kinetics. The treated coals, because of their low calcium contents, are therefore expected to have higher tar yields and longer burning times in addition to having higher NO_x emissions.

ACKNOWLEDGMENTS

This research was supported under EPA Contract No. CR-80-88484801. The authors wish to acknowledge Jeff L. Collett, Jr.'s assistance in obtaining the pyrolysis data and Dr. A. Korosi's suggestion for augmenting the nitrogen content of coal by ion-exchange.

REFERENCES

1. C.P. Fenimore. Combustion and Flame, Vol. 19, 1972, p. 289.
2. B.S. Haynes. Combustion and Flame, Vol 28, 1977, p. 113.
3. S.L. Chen, M.P. Heap, D.W. Pershing, and G.B. Martin. Nineteenth Symposium (International) on Combustion. The Combustion Institute, Pittsburgh, PA, 1983, p. 1271.
4. J.H. Pohl and A.F. Sarofim. Sixteenth Symposium (International) on Combustion. The Combustion Institute, Pittsburgh, PA, 1977, p. 491.
5. Y.H. Song, J.H. Pohl, J.M. Beér, and A.F. Sarofim. Combust. Sci. and Technol., Vol. 28, 1982, p. 31.
6. D.W. Blair, W. Bartok, and J.O.L. Wendt. Sixteenth Symposium (International) on Combustion. The Combustion Institute, Pittsburgh, PA, 1977, p. 475.
7. J.D. Freihaut, M.F. Zabielski, and D.J. Seery. Nineteenth Symposium (International) on Combustion. The Combustion Institute, Pittsburgh, PA, 1983, p. 1159.
8. Y.H. Song, J.M. Beér, and A.F. Sarofim. Combust. Sci. and Technol., Vol. 28, 1982, p. 177.
9. P.R. Solomon and M.B. Colket. Fuel, Vol 75, 1978, p. 749.
10. A.E. Beet. Fuel, Vol. 19, 1940, p. 170.
11. R.J. Quann. Sc.D. Thesis in Chemical Engineering. Massachusetts Institute of Technology. 1982.

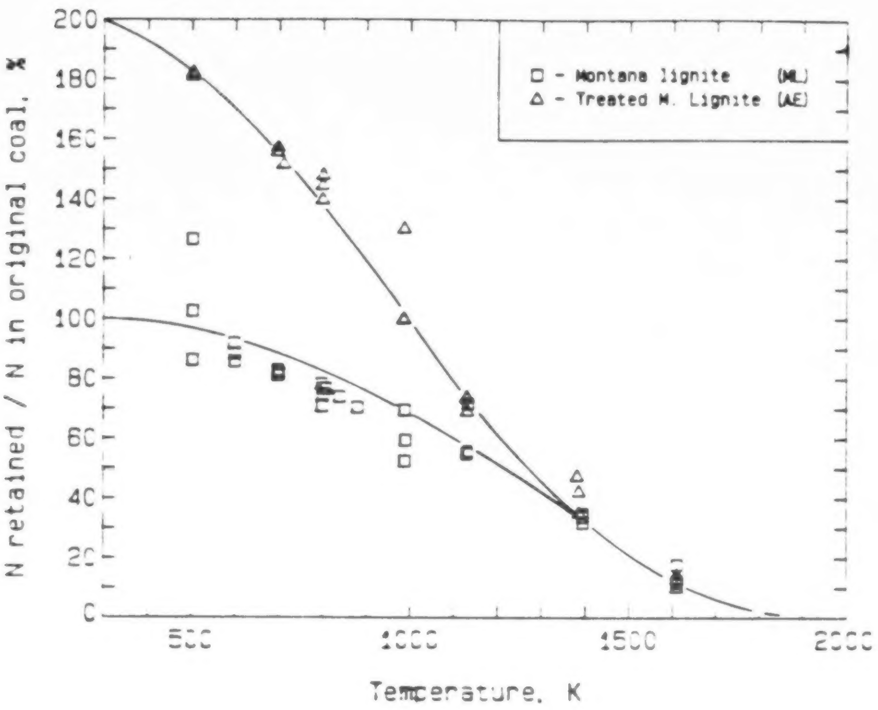

FIGURE 1. NITROGEN RETENTION CRUCIBLE EXPERIMENTS

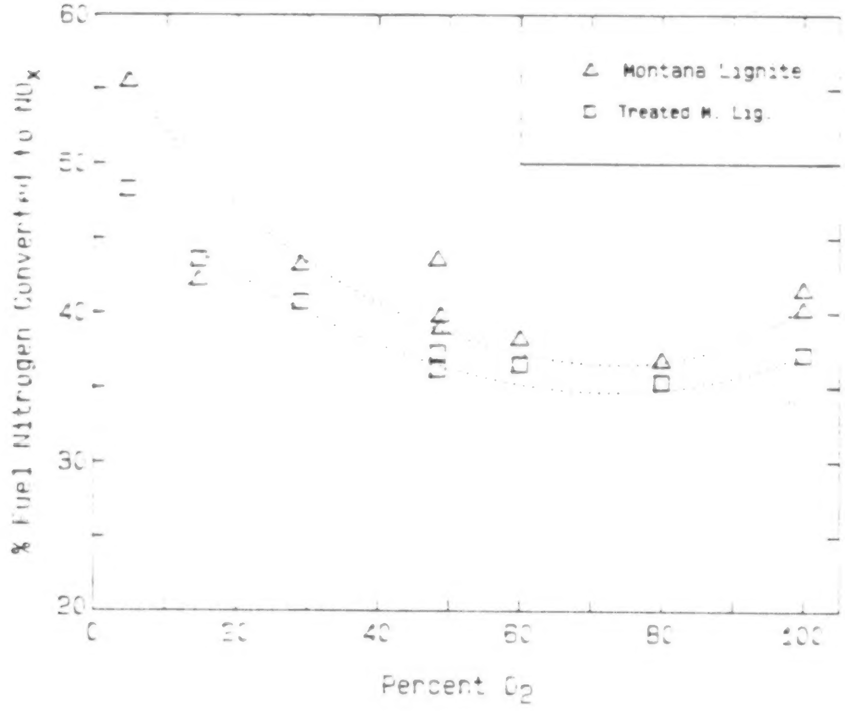

FIGURE 2. NO$_x$ CONVERSION EFFICIENCY

Table 1

ANALYSIS OF MONTANA LIGNITE

Proximate Analysis (%, as received)	
Moisture	8.17
Ash	8.81
Volatile Matter	49.58
Fixed Carbon	50.51
Ultimate Analysis (%, dry)	
C	61.89
H	3.98
N	1.11
S	0.60
Ash	8.09
O (measured)	23.54
Ash Analysis (%, coal)	
Al	0.39
Ca	1.29
Mg	0.46
Si	0.82

Table 2

ANALYSIS OF MONTANA LIGNITE

Proximate Analysis (%, as received)	
Moisture	3.37
Ash	2.53
Volatile Matter	----
Fixed Carbon	----

Ultimate Analysis (%, dry)	
C	66.60
H	4.02
N	2.34
S	0.40
Ash	2.44
O (measured)	23.57

Ash Analysis (%, coal)	
Al	0.38
Ca	0.18
Mg	0.03
Si	0.42

Table 3

PYROLYSIS RESULTS FOR RAW Ca AND TREATED MONTANA LIGNITE

Montana Lignite

Pyrolysis			% Retention of Elements		
Temp., K	Time, min.	% Wt. loss (dry)	N	C	H
503	960	5.84	105.11	95.68	93.94
698	120	25.07	82.12	81.01	60.51
798	45	31.63	74.71	78.17	47.06
988	30	37.77	60.53	77.49	23.66
1134	20	41.88	60.80	74.85	11.49
1394	15	44.08	33.42	76.22	5.01
1610	15	45.78	13.85	76.96	3.22

Ion-Exchanged Montana Lignite

Pyrolysis			% Retention of Elements		
Temp., K	Time, min.	% Wt. loss (dry)	N	C	H
503	960	8.05	86.32	90.07	95.23
711	120	28.46	73.57	78.91	55.30
800	45	34.08	64.25	75.45	47.17
987	30	41.91	49.87	74.94	26.50
1130	20	42.68	34.29	76.33	11.60
1381	15	45.01	19.74	75.96	5.83
1610	15	46.15	5.98	77.66	2.01

6b-3

REDUCTION OF NO_x EMISSION FROM NATURAL GAS FLAMES BY STAGED FUEL INJECTION

by

W.F. Farmayan, M. Toqan, Tae-U Yu, J.D. Teare and J.M. Beér

Department of Chemical Engineering and Energy Laboratory
Massachusetts Institute of Technology

Research Sponsored by the Southern California Edison Company

1985 Joint Symposium on Stationary Combustion NO_x Control

Boston, May 6-9, 1985

Introduction

Staged combustion has been demonstrated as an effective method for reducing nitrogen oxides emission. (Barnhart and Diehl, 1960., Radak et al., 1983) Under staged combustion conditions locally fuel rich zones develop in the flame in which fuel bound nitrogen species (FBN) react with NO to produce molecular nitrogen. A schematic of the pathways of FBN conversion and its interaction with NO is represented in Fig. 1. The degree to which the FBN conversion to N_2 is successful is determined by the thermodynamics of the system (temperature, pressure and chemical composition of the gas mixture), and the rates of the reactions in the fuel rich flame zone (Haynes 1975, Bowman 1975, Sarofim et al. 1978, Levy et al. 1978, Taylor 1984). In practical combustion systems the reactions of FBN and NO may be kinetically constrained and provision of sufficient residence time in the fuel rich zone is therefore essential for high conversion to N_2 (Farmayan, 1980, Beér et al. 1980 and 1982). The nitrogenous compounds in the fuel rich flame zones may have different origins: they may be pyrolysis products of nitrogen bearing fuels formed by the fixation of atmospheric nitrogen by hydrocarbon fragments early in the flame (Fenimore 1971), or be the result of reactions due to the secondary injection of hydrocarbons into the NO containing fuel lean burned gas. In this latter system of staged fuel injection, NO reacts with hydrocarbon fragments such as CH_2 to produce HCN and NH_i ($i = 3,2,1$) compounds in a flame zone which is turned fuel rich by the addition of the secondary fuel. The formed FBN is then partially reduced to N_2 following the pathway shown in Fig. 1. This method of NO reduction by fuel staging has been the subject of several patents (John Zink Co. 1973, Myerson 1975, Mitshubishi Heavy Industries 1981). Wendt et al. (1972) who in that pioneering work studied NO reduction by secondary fuel injection in a laboratory flat flame introduced the term "Reburning" for this method of NO abatement. Myerson (1974) using a ceramic laboratory scale flow reactor demonstrated extensive reduction of nitric oxide in combustion effluents by the addition of hydrocarbon mixtures in the temperature range of 1200 to 1700 K requiring residence times ranging from 50 to several hundreds of milliseconds. They confirmed that the principal product of the reaction was N_2 with HCN as the secondary product. Clark et al (1982) used pulverized coal as secondary fuel in a laboratory scale experiment and found that even a nitrogen bearing fuel like coal can be used as a "Reburn" fuel effectively as long as the primary NO concentration was high.

Practical applications to utility boilers have been reported by Mitshubishi Heavy Industries. Their system of over fire fuel and air was offered under the trade name of MACT and was reported to be capable of reducing NO emission by 50%. (Sakai et al. 1981, Takahashi et al. 1981 and 1982.) The Hitachi Zosen Co. has developed a special burner which achieves low NO_x emission by staged fuel injection (1981). The effectiveness of a combustion process termed "In-Furnace Control of NO Formation" (ICNF) developed and patented by the Southern California Edison Co. was investigated in conjunction with KVB Inc.. The ICNF process in which two discrete combustion stages are formed by secondary fuel injection was demonstrated in two full size utility boilers (45 MW and 175 MW). The primary fuel was oil or gas with gas as secondary fuel. In each case the ICNF process was reported to provide NO reduction in excess of what was obtainable from conventional combustion process modifications. (Radak et al. 1982).

In this paper, results obtained in an ongoing research program under the sponsorship of the Southern California Edison Co. at MIT on NO reduction by secondary fuel injection are reported. While the program includes experiments with both liquid and gaseous fuels and their combinations the following discussion is restricted to natural gas flames; both the primary and secondary fuel in these studies was natural gas. Experiments with fuel and air staging were carried out in the pilot plant size MIT Combustion Research Facility under well controlled conditions of mixing and heat extraction along the flame. The experiments were guided by mathematical modeling of the reactions involved in the reduction of NO emission from the flame.

2. Experimental

The experiments were carried out using the 1.2 m x 1.2 m x 4.5 m test section of the MIT Combustion Research Facility (CRF). The CRF is a pilot scale combustion tunnel equipped with a single, variable-swirl burner of up to 3 MW_{th} multi-fuel firing capability, variable heat extraction along the flame, and designed to permit detailed investigation of industrial type turbulent diffusion flames. A description of the CRF has been given elsewhere (Beér et al., 1981).

In-flame measurements were made of the spatial distributions of time average values of gas temperature and stable species concentrations (CO, CO_2, O_2, NO_x) using suction pyrometers and water-cooled gas probes respectively.

2.1 Experimental Input and Operating Conditions

The fuel used in these experiments was natural gas. The details of the input and operating conditions of the various experimental runs performed are given in Table (1).

Table 1

Reduction of NO_x from Natural Gas Flames by Staged Fuel Interaction (2nd Year)

Major Input Conditions and NOx Emission Levels

Flame No.	1	2	3	4	5	6	7	8	9
Flame Type	L-R-L	L-R-L	L-R-L	L-R-L	L-R-L	L-R-L	L-R-L	L-R-L	L-R-L
Input, Main Burner, MW	1	1	1	1	1	1	1	1	1
Input, Second. Fuel, MW	0.5	0.5	0.5	0.5	0.5	0.5	0.5	0.5	0.5
Burner Fuel Equivalence* Ratio:									
ϕ_1	0.85	0.85	0.85	0.85	0.85	0.85	0.85	0.85	0.85
ϕ_2	1.5	1.5	1.5	1.5	1.5	1.5	1.5	1.5	1.5
ϕ_3	0.95	0.95	0.95	0.95	0.95	0.95	0.95	0.95	0.95
ϕ_4	-	-	-	-	-	-	-	-	-
Air Preheat, °C	263	263	263	265	265	267	267	267	267
Swirl No., 5	1.8	1.8	1.8	1.8	1.8	1.8	1.8	1.8	1.8
Excess Air, Overall, %	5	5	5	5	5	5	5	5	5
Second. Air Inject. Pt., m	2.59	2.59	2.59	2.59	2.59	2.59	2.59	2.59	2.59
Tertiary Air Inject. Pt., m	-	-							
Second. Fuel Inject. Pt., m	1.68	1.68	1.68	1.98	1.98	1.98	2.29	2.29	2.29
Second. Air Injection Mode	T, Count	T, Count	T, Count	T, Count	T, Count	T, Count	T, Count	T, Count	T, Count
Second. Fuel Injection Mode	R, 8°	T, CO, 8°	T, Count, 8°	R, 0°	T, CO, 8°	T, Count, 8°	R, 0°	T, Co, 8°	t, Count, 8°
Final Stage NO_x, ppm as measured	64	65	65	69	69	69	98	98	105
Final Stage NO_x, ppm @ 3% O_2	61	62	62	66	66	66	93	93	100
Final Stage Temp. °C									
@ 4.42 m									
@ 5.95 m									

L-R-L Flames; 1 MW_{th} main burner input, 0.5 mw_{th} Second Fuel Input, effects of second fuel injection position, and angle

*The burner fuel equivalence ratios quoted in this table, and throughout the report, are based upon inputs of fuel and air and do not necessarily reflect actual local fuel equivalence ratios which of course are highly dependent upon flame flow pattern and mixing.

Table 1 (Continued)

Flame No.	10	11	12	13	14	15	16	17	18
Flame Type	R-L	R-L-L	R-L-L	R-L-R-L	R-L-R-L	R-L-R-L	R-L-R-L	R-L	R-L
Input, Main Burner, MW	1	1	1	1	1	1	1	0.6	0.6
Input, Second. Fuel, MW	-	0.2	0.35	0.35	0.35	0.35	0.35	-	-
Burner Fuel Equivalence* Ratio:									
ϕ_1	1.3	1.3	1.3	1.3	1.3	1.3	1.3	1.2	1.3
ϕ_2	0.95	0.81	0.71	0.79	0.79	0.79	0.79	0.95	0.95
ϕ_3	-	0.95	0.95	1.06	1.06	1.06	1.06	-	-
ϕ_4	-	-	-	0.95	0.95	0.95	0.95	-	-
Air Preheat, °C	244	244	246	244	245	244	244	240	240
Swirl No., S	1.8	1.8	1.8	1.8	1.8	1.8	1.8	1.8	1.8
Excess Air, Overall, %	5	5	5	5	5	5	5	5	5
Second. Air Inject. Pt., m	2.59	2.59	2.59	2.59	2.59	2.59	2.59	2.59	2.59
Tertiary Air Inject. Pt., m				4.42	4.42	4.42	4.42	-	-
Second. Fuel Inject. Pt., m	-	3.20	3.20	3.20	3.81	3.81	3.81	-	-
Second. Air Injection Mode	T, Count	T, Count	T, Count	T, Count	T, Count	T, Count	T, Count	T, Count	T, Count
Second. Fuel Injection Mode	-	R, 0°	R, 0°	R, 0°	R, 0°	T, CO, 8°	T, Count, 8°	-	-
Final Stage NO_x, ppm as measured	47	55	59	63	60	60	60	25	25
Final Stage NO_x, ppm @ 3% O_2	45	52	56	60	57	57	57	24	24
Final Stage Temp. °C		1457	1485	-	-	-	-		
@ 4.42 m								1240	1240
@ 5.95 m		-	-	1360	1386	-	1370		
	R-L Flame, 1 MW_{th} main burner input	R-L-L Flames effect of amount of second fuel admixing			R-L-R-L Flames, 1 MW_{th} main burner input, 0.35 MW_{th} second fuel input (limited by by tertiary air availability) effects of second fuel injection position and angle				R-L Flames; 0.6 MW_{th} burner input, of ϕ_1

Table 1 (Continued)

Flame No.	19	20	21	22	23	24	25	26	27	28
Flame Type	R-L	R-L	R-L	R-L	L-R-L	L-R-L	L-R-L	L-R-L	L-R-L	L-R-L
Input, Main Burner, MW	0.6	0.75	0.9	1.1	0.6	0.6	0.6	0.6	0.6	0.6
Input, Second. Fuel, MW	-	-	-	-	0.5	0.3	0.15	0.3	0.5	0.15
Burner Fuel Equivalence* Ratio:										
ϕ_1	1.5	1.3	1.3	1.3	0.88	0.88	0.88	0.88	0.88	0.88
ϕ_2	0.95	0.95	0.95	0.95	1.6	1.3	1.1	1.3	1.6	1.1
ϕ_3	-	-	-	-	0.95	0.95	0.95	0.95	0.95	0.95
ϕ_4	-	-	-	-						
Air Preheat, °C	238	249	250	250	252	249	249	246	249	251
Swirl No., S	1.8	1.8	1.8	1.8	1.8	1.8	1.8	1.8	1.8	1.8
Excess Air, Overall, %	5	5	5	5	5	5	5	5	5	5
Second. Air Inject. Pt., m	2.59	2.59	2.59	2.59	2.59	2.59	2.59	2.59	2.59	2.59
Tertiary Air Inject. Pt., m	-	-	-	-	-	-	-	-	-	-
Second. Fuel Inject. Pt., m	-	-	-	-	1.98	1.98	1.98	1.68	1.68	1.59
Second. Air Injection Mode	T, Count	T, Count	T, Count	T, Count	T, Count	T, Count	T, Count	T, Count	T, Count	T, Count
Second. Fuel Injection Mode	-	-	-	-	T, CO, 8°	T, CO, 8°	T, CO, 8°	T, CO, 8°	T, CO, 8°	T, CO, 8°
Final Stage NO_x, ppm as measured @ 4.8 m	37	29	35	43	45	38	50	33	50	39
Final Stage NO_x, ppm @ 3% O_2 (@ 4.8m)	35	28	33	41	43	36	48	31	48	37
Final Stage Temp. °C										
@ 4.42 m	1248	1285	1335	1375	1368	1310	1240	1296	1376	1249
@ 5.95 m										

R-L Flames;
effect of thermal
input

L-R-L Flames; 0.6 MW_{th} main
burner input varying
second fuel input,
effect of reburn
zone ϕ, secondary
fuel injection position

Table 1 (Continued)

Flame No.	29	30	31	32	33	34	35
Flame Type	R-L-LL	R-L-R-L	R-L-R-L	R-L-R-L	R-L-R-L	L	L
Input, Main Burner, MW	0.6	0.6	0.6	0.6	0.6	0.6	1.0
Input, Second. Fuel, MW	0.05	0.15	0.3	0.4	0.4	-	-
Burner Fuel Equivalence* Ratio:							
ϕ_1	1.3	1.3	1.3	1.3	1.3	0.95	0.95
ϕ_2	0.88	0.88	0.88	0.88	0.88	-	-
ϕ_3	0.95	1.1	1.3	1.3	1.47	-	-
ϕ_4		0.95	0.95	0.95	0.95	-	-
Air Preheat, °C	238	242	240	240	241	254	252
Swirl No., S	1.8	1.8	1.8	1.8	1.8	1.8	1.8
Excess Air, Overall, %	5	5	5	5	5	5	5
Second. Air Inject. Pt., m	2.59	2.59	2.59	2.59	2.59	-	-
Tertiary Air Inject. Pt., m	-	4.42	4.42	4.42	4.42	-	-
Second. Fuel Inject. Pt., m	3.81	3.81	3.81	3.81	3.81	-	-
Second. Air Injection Mode	T, Count	T, Count	T, Count	T, Count	T, Count	-	-
Second. Fuel Injection Mode	T,Count,8°	T,Count,8°	T,Count,8°	T,Count,8°	T,Count,8°	-	-
Final Stage NO_x, ppm as measured	24	25	26	32	32	87	150
Final Stage NO_x, ppm @ 3% O_2	23	24	25	30	30	83	143
Final Stage Temp. °C							
@ 4.42 m	1183	1220	1254	1295	1295	1183	1295
@ 5.95 m						-	-

R-L-R-L Flames
0.6 MW_{th} main burner input, varying second fuel input; effect of reburn ϕ_b, secondary fuel thermal input.

L Flames
0.6 and 1 MW_{th} input with 250°C air preheat

Table 1 (Continued)

Flame No.	36	37	38	39	40	41	42	43	44	45	46
Flame Type	R-L	R-L	R-L	R-L	R-L	R-L	L	L	R-L	R-L	R-L-R-L
Input, Main Burner, MW	0.6	0.6	0.6	0.6	0.6	0.6	0.6	1.0	0.6	1.0	0.6
Input, Second. Fuel, MW	-	-	-	-	-	-	-	-	-	-	0.3
Burner Fuel Equivalence* Ratio:											
ϕ_1	1.2	1.4	1.3	1.4	1.2	1.3	0.95	0.95	1.3	1.3	1.3
ϕ_2	0.95	0.95	0.95	0.95	0.95	0.95	-	-	0.95	0.95	0.87
ϕ_3	-	-	-	-	-	-	-	-	-	-	1.3
ϕ_4	-	-	-	-	-	-	-	-	-	-	0.95
Air Preheat, °C	216	216	213	248	246	246	46	46	46	46	46
Swirl No., S	1.8	1.8	1.8	1.8	1.8	1.8	1.8	1.8	1.8	1.8	1.8
Excess Air, Overall, %	5	5	5	5	5	5	5	5	5	5	5
Second. Air Inject. Pt., m	4.42	4.42	4.42	3.20	3.20	3.20	-	-	3.20	3.20	2.59
Tertiary Air Inject. Pt., m	-	-	-	-	-	-	-	-	-	-	4.42
Second. Fuel Inject. Pt., m	-	-	-	-	-	-	-	-	-	-	3.81
Second. Air Injection Mode	Cent-R	Cent-R	Cent-R	Cent-R	Cent-R	Cent-R	-	-	Cent-R	Cent-R	T, Count
Second. Fuel Injection Mode	-	-	-	-	-	-	-	-	-	-	T,Count,8°
Final Stage NO_x, ppm as measured	22	28	24	28	24	23	43	62	18	22	22
Final Stage NO_x, ppm @ 3% O_2	21	27	23	27	23	22	41	59	17	21	21
Final Stage Temp. °C											
@ 4.42 m	-	-	-	-	-	1164	1112	1231	1141	1248	-
@ 5.95 m	-	-	1103	1082	1082	1070	-	-	1044	1152	1183

R-L Flames, 0.6 MW_{th} input,
Using centerline compressed air
injector (identical to that
used for tertiary air) for secondary
air effect of secondary air injector
position

L, R-L, R-L-R-L Flames
without air preheat

3. Computer Modelling Studies

Thermodynamic and chemical kinetic computer calculations were carried out to evaluate the effects of major combustion process parameters on bound nitrogen species concentrations in natural gas flames. The calculations were intended to guide the choice of experimental parameters and aid in the interpretation of the experimental data.

3.1 Chemical Equilibrium Calculations

The thermodynamic calculations were carried out using a NASA computer code (Svehla and McBride, 1973) and were aimed at evaluating the effects of temperature and stoichiometry (fuel equivalence ratio) on the equilibrium concentrations of bound nitrogen species in methane-air combustion gases. Species considered in the equilibrium mixtures are listed in Table 2 and results of the calculations for $T = 1400$ K - 2300 K and $\phi = 0.8 - 2.9$ are shown in Fig. 2. Generally the thermodynamic considerations show that a minimum in the total of the bound nitrogen species occurs under fuel-rich conditions and that the minimum shifts to higher values of fuel equivalence ratio as the temperature of the combustion mixture increases. Also the value of the minimum increases with increasing temperature.

The results in Fig. 2 show the lower limit in total bound nitrogen species achievable for a given condition of temperature and stoichiometry (and pressure). Although the thermodynamics provide information on the direction in which the state of NO reduction moves in staged combustion processes, the chemical kinetics of bound nitrogen species transformations play an important role in determining the degree to which equilibrium conditions can be approached. In practical combustion systems, when "low NO_x" burners are used, the residence times in the fuel rich zone may represent a constraint; the equilibrium values shown in Fig. 2 may not be

Table 2

Chemical Equilibrium Calculations of Bound Nitrogen Species Concentrations in Combustion Mixtures

Species Considered in System

AR
CH_2O
CN_2
C_2H_2
C_2O
C_5
HCN
HNO_3
H_2O
NH_2
N_2
N_3
C(s)
CH_3
CO
C_2H_4
C_3
$C_6H_6(g)$
HCO
HO_2

H_2O_2
NH_3
N_2H_4
O
C
CH_4
CO_2
C_2H_6
C_3O_2
C_8H_{18}
HNCO
H_2
N
NO
N_2O
OH
CH
CN
C_2
C_2N

C_3H_8
CH_3OH
HNO
$H_2O(s)$
NCO
NO_2
N_2O_4
O_2
CH_2
CHN
C_2N
C_2N_2
C_4
H
HNO_2
$H_2O(1)$
NH
NO_3
N_2O_5
O_3

reached, and actual values are dependent upon the kinetics of the chemical as well as mixing-processes in the system.

3.2 Chemical Kinetic Calculations

A more realistic evaluation of bound nitrogen species behavior in a kinetically constrained system as encountered in real furnaces, were carried out with a general purpose computer code (Chemkin, Sandia laboratories, 1980). The code uses a very detailed reaction set incorporated into a simple plug flow model. The reaction set was developed by Taylor (1984) and comprises over 100 elementary reactions. A methane combustion mechanism, and hydrocarbon fragment/bound nitrogen species interactions are included in the reaction set. The chemical kinetic calculations were used to evaluate the effects of temperature, fuel-air stoichiometry and residence time on the determined bound nitrogen species concentrations.

3.3 Results of Computations

Results of the calculations are shown in Fig. 3-5; the individual cases considered are the following:

> Single stage, fuel-lean (Fig 3): effect of temperature in the final fuel-lean stage (see section 3.3.1)
>
> fuel equivalence ratio: 0.95
> temperature: 1700 K, 2000 K
>
> Two stage, rich-lean (Fig 3): effect of temperature in the final fuel-lean stage (see section 3.3.2)
>
> fuel equivalence ratio, first stage: 1.3
> temperature, first stage: 2000 K
>
> fuel equivalence ratio, second stage: 0.95
> temperature, second stage: 1700 K, 2000 K
>
> Two stage lean-less lean and first two stages of a three stage system lean-rich-lean (Fig. 4): effect of reburn zone stoichiometry and temperature (see section 3.3.3)
>
> fuel equivalence ratio, first stage: 0.8
> temperature, first stage: 2000 K

fuel equivalence ratio, "reburn" stage: 0.95, 1.3
temperature, "reburn" stage: 1700 K, 2000 K

First three stages of a four stage system, rich-lean-rich-lean (Fig. 5): effect of the reburn stage stoichiometry, temperature entering NO concentration (see section 3.3.4)

fuel equivalence ratio, first stage: 1.3
temperature, first stage: 1700 K, 2000 K

fuel equivalence ratio, second state: 0.8
temperature, second stage: 2000 K, 1700 K

fuel equivalence ratio, "reburn" stage: 0.95, 1.3, 1.6, 1.9
temperature, "reburn" stage: 1700 K, 2000 K

3.3.1 Single Stage Fuel-lean and Two Stage Rich-lean (Secondary Air Injection only) Combustion Systems (Fig. 3)

It can be seen in Fig. 3 that temperature is the overriding parameter affecting NO formation in fuel-lean combustion. NO concentrations increase by about three orders of magnitude with an increase in temperature from 1700 K to 2000 K; the increase can be explained in terms of thermal NO formation, i.e., Zeldovich kinetics. In the case of staged rich-lean combustion, the sum of the bound nitrogen species is greatly reduced under fuel-rich conditions (Fig. 3). With sufficient heat extraction (to reduce the temperature of the combustion mixture) the low concentrations of bound nitrogen species leaving the fuel rich stage can be maintained in the fuel-lean stage. If the temperature is allowed to rise unduely (i.e., above 1800 K) upon addition of secondary air, the thermal NO formation rates rise dramatically, offsetting the benefits gained by operating initially in a fuel rich mode.

3.3.2 Two Stage Lean-Less Lean (Secondary Fuel Addition Only (Fig. 4)

Negligible reduction in NO was achieved by the Lean Less Lean configuration with secondary fuel injection only. (See Fig. 4: fuel equiv. ratio, 1st. st. = 0.8, temp., 1st. st. = 2000 K, fuel equiv. ratio, 2nd.

st. = 0.95, temp., 2nd. st. = 1700 K, 2000 K). The calculations indicate that a fuel-rich zone is required for a significant reduction in NO emissions; this was also seen in the experiments.

3.3.3 Three Stage Lean-Rich-Lean (Secondary Fuel followed by Secondary Air (Fig. 4).

In Fig. 4 results are also shown for calculations carried out on the first two stages of a three stage Lean-Rich-Lean configuration. The intent was to examine the effect of temperature for a fuel-rich reburn zone. There is a noticeable destruction of NO under fuel-rich conditions (reburn fuel equivalence ratio: 1.3) and relatively high temperature (2000 K). As the temperature is reduced, e.g., to 1700 K the destruction rates become negligible, indicating that the high temperature for the reburn zone is quite necessary. It might be added that (as shown in the previous figure) the low bound nitrogen species concentrations leaving the reburn stage can be maintained with sufficient cooling of the final fuel-lean burnout stage.

3.3.4 Four Stage Rich-Lean-Rich-Lean: Secondary Air followed by Secondary Fuel followed by Tertiary Air (Fig. 5).

Early in the MIT program there was some speculation as to whether or not further reductions in NO emission could be achieved by following a rich-lean combustion sequence with another set of rich-lean stages. Calculations for the first three stages of a four stage Rich-Lean-Rich-Lean system are shown in Fig. 5. The third stage of the system consists of the reburn stage in which secondary fuel has been added. In Fig. 5 the effect of the reburn zone temperature is illustrated. As discussed before, for there to be appreciable NO destruction rates, relatively high temperatures must be attained in the reburn zone; considering a residence time constraint of less than a half second the calculations indicate an optimum temperature of about 2000 K - 2200 K. At temperatures in excess of this value the advantage gained by more rapid kinetics begins to be offset by equilibrium considerations, i.e., even under fuel rich conditions, the equilibrium bound nitrogen species concentrations are becoming undesireably high. The value of the optimum gas temperature may, however, be somewhat lower in turbulent diffusion flames than given by the model calculations. The effect of the temperaturue upon FBC conversion rates is via its effect upon free radial concentrations. It can be expected that due to their generation in the reaction zones between rich and lean eddies the free radical concentrations will be higher in the turbulent diffusion flames and therefore a lower temperature suffices for reaching optimum conditions for the "Reburn" stage.

From Fig. 5 it becomes clear that the reburn effect becomes minimal for low NO concentration values entering the reburn stage. This is simply a result of the approach of the bound nitrogen species concentrations towards the lower limit as set by equilibrium. Consequently, improvement in terms of NO emission, on an optimized rich-lean configuration, by following with a second rich-lean sequence can be expected to be negligible. This conclusion was also supported by the results of our experiments.

4. Experimental Results

The experimentation was carried out with the following general objectives:

(1) Separate the effects of temperature, individual stage stoichiometry (particularly the reburn stage) and individual stage residence time on NO_x emission.

(2) Explore in more detail flow pattern and mixing effects on NO_x formation. For this aspect of the experimentation, furnace side injectors were fabricated which permitted the injection of the secondary fuel transversely across the primary burner flow both in a "cross-fire" (radial) and "corner-fire" (Tangential) mode (Fig 6).

Input conditions for each of the experimental flames considered are detailed in Table 1 along with the corresponding exhaust NO_x emission levels. Schematics of the various CRF staging configurations corresponding to the individual flames listed in Table 1 are shown in Fig. 7.

The effects of a number of staged flame input conditions on NO_x were examined in Flames 1-46; the measurements consisted of exit gas composition (NO_x, CO, CO_2, and O_2) and temperature only. The flames may be grouped as follows according to the class of flame and parameter(s) or effect(s) being studied.

(1) Overall fuel-lean (L) flames; baselines, effects of air preheat, fuel input (Flames 34, 35, 42, 43).

(2) Lean-rich-lean (L-R-L) flames; 1 MWth main burner input, 0.5 MWth secondary fuel input; effect of secondary fuel admixing: side wall injection position and injector nozzle angle (flames 1-9).

(3) L-R-L flames; 0.6 MWth main burner input; effect of reduced overall thermal input (also increased residence time), reburn zone stoichiometry, and secondary fuel injection position (Flames 23-28).

(4) Rich-lean (R-L) flames; baseline experiments for comparison with flames with reburn fuel addition; effect of overall thermal input (Flames 10, 20-22).

(5) R-L flames; effect of fuel-rich zone stoichiometry (Flames 17-19).

(6) R-L flames; effect of reduced air preheat (Flames 44 and 45).

(7) R-L flames; 0.65 MWth input; using centerline compressed air injector for secondary air; this is identical to the tertiary air injector used for the rich-lean-rich-lean flames (Flames 36-41).

(8) Rich-lean-less lean (R-L-LL) flames; secondary air followed by secondary fuel; effect of amount of secondary air and secondary fuel admixing (i.e., fuel-lean zone quenching effect by secondary air and effect of secondary fuel thermal input) (Flames 11 and 13).

(9) Rich-lean-rich-lean (R-L-R-L) flames; effects of main burner (primary fuel) input, secondary fuel input and reburn zone stoichiometry, secondary fuel injection position and injector angle, and air preheat (flames 13-16, 30-33, 46).

5. Discussion

5.1 Temperature Versus Stoichiometric Effects, Comparisons of Staging Configurations

One of the major thrusts of the experimental effort was to clearly differentiate between temperature and stoichiometric effects upon overall NO_x emission.

In considering the problem of differentiating temperature and stoichiometric effects on NO emissions, particularly when the various staging configurations are compared, it would of course be desirable to maintain as similar a temperature history in the furnace for each case as could be possible. However, the temperature history for each case could not be identical. Two parameters were identified as having gross effects upon the average temperature of the combustion mixture which merited close examination and control when the various staging strategies were studied. These included the total thermal input (chemical and sensible heat, fuel and air, all primary secondary, etc. streams) and furnace heat sink configurations (heat extraction).

For these tests the heat sink configuration was maintained constant, i.e., the furnace was restricted to a single overall length and consisted of refractory lined water cooled sections up to and including the cylindrical end section. With this type of heat sink configuration and with a constant total inside furnace area, effects of variations in heat extraction from the combustion mixture for a given thermal input from one staging configuration to the next could be minimized, although not entirely eliminated.

The effect of fuel thermal input on NO_x emission was determined by varying this parameter from 0.6 MW to 1.35 MW.

The overall thermal input could be varied in a number of ways depending upon amount of overall fuel injection, air preheat and combinations there of achieved by the various combinations of primary, secondary, etc. fuel and air streams.

The effect of thermal input on NO_x emission is best illustrated by the curve shown in Figure 8. The experimental values shown in this figure are for flames with several staging configurations (R-L, R-R-L, L-R-L, R-L-R-L). The only common input conditions among these flames are the air preheat temperature (T_{air} ~$250^{\circ}C$), the swirl number ($S = 1.8$) and the existence of at least one fuel rich stage with a ϕ of 1.3 prevailing in that zone. From Figure 8 it seems that the NO_x emission level is proportional to the square of the thermal input value. It can be seen that at low values of thermal input the NO_x concentration approaches an assymptotic value of 20 ppm. On the other hand, it increases rapidly at high values of thermal input.

The equation that best describes this behavior is given below.

Concentration of NO_x emitted =

$$105.96863 - 313.2534\ T + 365.314\ T^2 - 118.48\ 66\ 3T^3\ \text{(ppm)} \qquad \text{E.1}$$

where T ≡ Thermal input

A high peak flame temperature (close to or greater than 1800 K) results in significant formation rate of NO. As the thermal input is increased the flame peak temperature increases and this temperature hike results in the formation of larger amounts of NO.

It is of special interest to compare the R-L-R-L and R-L flames obtained with approximately the same overall input and combustion chamber heat sink configuration. Flames 45 (R-L) and 46 (R-L-R-L) are two flames representative of these two staging configurations which are the most similar (of the flames investigated) in their temperature history. The NO_x emission exhibited by these two flames is essentially identical (NO_x concentration ~21 ppm). This implies that the R-L configuration can achieve the same low emission values of NO as the R-L-R-L arrangement.

The effect of fuel rich stage equivalence ratio upon NO_x emission was obtained for several staging configurations (RL-R-L, R-L-LL, L-R-L, R-L,L) where the total thermal input was maintained between 0.6 to 0.75 MW. The results of this study are shown in Figure 9.

It can be seen that as the fuel equivalence ratio of the richest stage is increased while maintaining the total fuel equivalence ratio at 0.95, NO_x emission level decreases. The minimum value of NO_x concentration is achieved between a ϕ of 1.2 and 1.3. Figure 9 shows that all staging configurations achieve the same low NO_x concentration as long as there exists a fuel rich stage with a ϕ of 1.25 along the path of the flame.

5.2 Effect of Secondary Air and Secondary Fuel Admixing (R-L-LL Flames, No. 11-12)

Successful application of the staging concept requires that the reduction in concentration of the total bound nitrogen species achieved in the fuel-rich regions be preserved in the fuel-lean. This in turn requires that the temperature in the fuel-lean regions be controlled below values at which the Zeldovich NO formation rates are appreciable (1800 K). It was thought that the low bound nitrogen species concentrations leaving the primary zone of a R-L-LL configuration could be better preserved by addition of more secondary air, or in other words, with increased quenching of the primary zone reaction mixture. This sequence followed by addition of more secondary fuel, it was thought, could possibly result in even further reductions in NO via the hydrocarbon fragments produced in the secondary fuel addition zone. A comparison of the NO emissions of Flames 17 and 29 shows however, that this was not borne out. Apparently the effect of choosing the staging configuration R-L-LL instead of the R-L configuration did not result in further reduction in the NO_x concentration ($NO_x \sim 23$ ppm).

5.3 Secondary Fuel Injection Mode

Mode of secondary fuel injection was considered to be a principal variable in the reburn staging systems under investigation. The overall NOx emission is likely to be sensitively affected by variations in the patterns of local stoichiometry and temperature in the flame especially in the fuel-rich NO destruction regions. It is thought, for example, that for a given average input stoichiometry, a broadening of the range of local fuel equivalence ratios encountered in the reburn region of the furnace could possibly have a beneficial effect on the overall NO_x emission. In practical terms, the formation of a highly fuel-rich core or fireball surrounded by a less fuel-rich outer annulus along the furnace walls (in the reburn region) represents such a broadening of the fuel equivalence ratio distribution.

A number of flames were investigated, of the L-R-L and R-L-R-L staging configurations, for which the side wall secondary fuel injector nozzle angles were varied. The cases considered were (Fig. 6): (1) horizontally opposed or radial mode, (2), tangential mode 8 degree nozzle offset from the central axis, fuel co-swirled with the main burner flow, and (3) tangential mode, 8 degree offset, counter swirled. The particular flames investigated included No. 1-9, and 14-16, and are detailed with respect to input conditions in Table 1.

The effect of these varying modes of secondary fuel injection (at a given secondary fuel injection position) for both the L-R-L and R-L-R-L cases was negligible. The results tend to indicate that the impact of the gas jets on the overall flow field was relatively small, and that the gas was rapidly dispersed and combusted in the passing combustion mixture regardless of injection mode.

6. Conclusions

Fuel staging is shown both theoretically and experimentally to provide significant reductions in NO_x emission from natural gas flames. The NO emission level was reduced from 155 ppm for the base case of single stage lean combustion, to 38 ppm (3% O_2) for a case of staged fuel injection, (Rich-Lean-Rich-Lean) in a 1 MW thermal input flame with 250°C air preheat. Still lower values down to 17 ppm were found when the combustion air was not preheated ($T_{air} = 20^{\circ}C$).

Both modeling and experiments showed the peak flame temperature and the fuel equivalence ratio in the most strongly fuel rich stage (in the case of multiple fuel staging) to have the overwhelming effects upon the exit NO concentrations.

When the initial (first stage) NO concentrations are low, as in the case of a non nitrogen bearing fuel such as natural gas, fuel staging is less effective, and reduction in NO emissions obtained by fuel staging can be explained simply on the basis of staged combustion with reduced lean stage temperatures without reference to the "Reburn" reactions. Indeed, both modeling and experimental studies show that the R-L (air staging) and R-L-R-L (fuel and air staging) configurations result in similar NO emissions.

The pronounced reductions of NO emissions obtained by the use of staged fuel injection are encouraging. It is felt, however, that because of the specially favorable conditions for controlling mixing and temperature history in the MIT Combustion Research Facility, conditions which can not be achieved equally in large boiler furnaces, results of the present study should be used primarily as a guide regarding the trend of NO emission levels as they are affected by the parameters of this study, rather than as an indication of absolute levels of NO_x emission attainable in large boiler furnaces.

Acknowledgements

Final support from the Southern California Edison Company is gratefully acknowledged. Special thanks to Mr. L.J. Radak for the valuable discussions on the paper. Also we are greatly indebted to Professor A.F. Sarofim and B.R. Taylor for allowing us to use the detailed kinetic mechanism of NO_x formation they have developed. Significant contributions to the experimental research were made by the CRF technical staff, Don Bash, William Mason and Mark James.

7. References

Barnhart, D.C. and Diehl, E.K.: J. Air Pollution Control Assoc., 10 397 (1960).

Beér, J.M., Jacques, M.T., Farmayan, W.F., and Taylor, B.R., Eighteenth Symposium (International) on Combustion pp. 101-110. The Combustion Institute, Pittsburgh, 1980.

Beér, J.M., M.T. Jacques, W.F. Farmayan, A.K. Gupta, S. Hanson, and W.C. Rovesti "Reduction of NO_x and Solid Emissions by Staged Combustion of Coal Liquid Fuels." Nineteenth Symposium on Coal Liquid, Haifi, Israel, Aug. 1983.

Beér, J.M., Jacques, M.T., and Farmayan, W.F., "Control of NO_x by Combustion Process Modifications" (MIT-EL-81-001), Department of Chemical Engineering and Energy Laboratory Electric Utility Program, Massachusetts Institute of Technology (April 1981)

Bowman, C.T., Progress in Energy and Combustion Science 1975. Vol. 1 pp. 33-45. Pergamon Press. Oxford, New York.

Clark, W.D., Chen, S.L., S.B. Greene, W.R. Seeker, and M.P. Heap, "Reburning with Pulverized Coal for NO_x Control", Presented at Western States Section of The Combustion Institute Spring Meeting, University of Utah, April 5-6, 1982.

Farmayan, W.F., M.Sc. Thesis, "The Control of Nitrogen Oxides Emission by Staged Combustion," Department of Chemical Engineering, Massachusetts Institute of Technology, Cambridge, MA, April 1980.

Fenimore, C.P., "The Formation of Nitric Oxide from Fuel Nitrogen in Ethylene Flames" Combustion and Flame, 19, 289 (1972).

Fenimore, C.P., Thirteenth Symposium (International) on Combustion. The Combustion Institute, 1971, p. 373.

Haynes, B.S., The Formation and Behavior of Nitrogen Species in Fuel Rich Hydrocarbon Flames", Ph.D. Thesis, School of Chemical Engineering, University of New South Wales, Australia, December (1975).

Hitachi Zosen Company. Ultra Low-NO_x Burner - Two-Stage Fuel Feed Combustion. Presented at U.S.-Japan NO_x Information Exchange, Tokyo, 1981.

Kee, R.J., Miller, J.A. and Jefferson, T.H., "CHEMKIN: A General-Purpose Problem-Independent, Transportable, Fortran Chemical Kinetics Code Package", Sandia Laboratories, New Mexico, Doc. No. SAND 80-8003, 1980.

Levy, J.M. Longwell, J.P., and Sarofim, A.F. MIT Energy Laboratory Report on Fuel Nitrogen Conversion Mechanisms (1978).

Levy, J.M., Taylor, B.R. Longwell, J.P. and Sarofim, A.F., "C1 and C2 Chemistry, Rich Mixtures Lean-Air Flame", The Nineteenth Symposium on Combustion. The Combustion Institute, Pittsburgh, PA p. 167, 1982.

Myerson, A., Method for Removing the Oxides of Nitrogen as Air Contaminants. U.S. Patent 3,867,507, Exxon Research and Engineering Company, 1975.

Radak, L.J., Weir, Jr., Morton, B.G. and Mansour, M.N.: "In-Furnace Control of NO Formation in Gas and Oil-Fired Utility Boilers." EPA Symposium on Stationary NO_x Control, Dallas, TX. 1982.

Sakai, M., et al. Mitsubishi "MACT" In-Furnace NO_x Removal Process for Steam Generator. Presented at U.S.-Japan NO_x Information Exchange, Tokyo, 1981.

Sarofim, A.F., Pohl, J.H., and Taylor, B.R., "Strategies for Controlling Nitrogen Oxide Emissions During Combustion of Nitrogen Bearing Fuels," AIChE Symposium Series No. 175, 74, 67, (1973).

Svehla, R.A., and McBride, B.J., Fortran IV Program for Calculations of Thermo-Dynamics and Transport Properties of Complex Systems, NASA Space TN-D7056, Lewis Research Center, 1973

Takahashi, Y., et al. Development of Mitsubishi "MACT" In-Furnace NO_x Removal Process. Presented at U.S.-Japan NO_x Information Exchange, Tokyo, 1981.

Takahashi, Y., et al. Development of "MACT" In-Furnace NO_x Removal Process for Utility Steam Generators. Presented at 44th Annual Meeting of American Power Conference, 1982.

Taylor, B.R., "Reactions of Nitrogen Species In Fuel-Rich Flames", Sc.D., Department of Chemical Engineering, M.I.T., 1984.

Wendt, J.O.L., Sternling, C.V., and Matovich, M.A. Fourteenth Symposium (International) on Combustion. The Combustion Institute, 1973. pp 897.

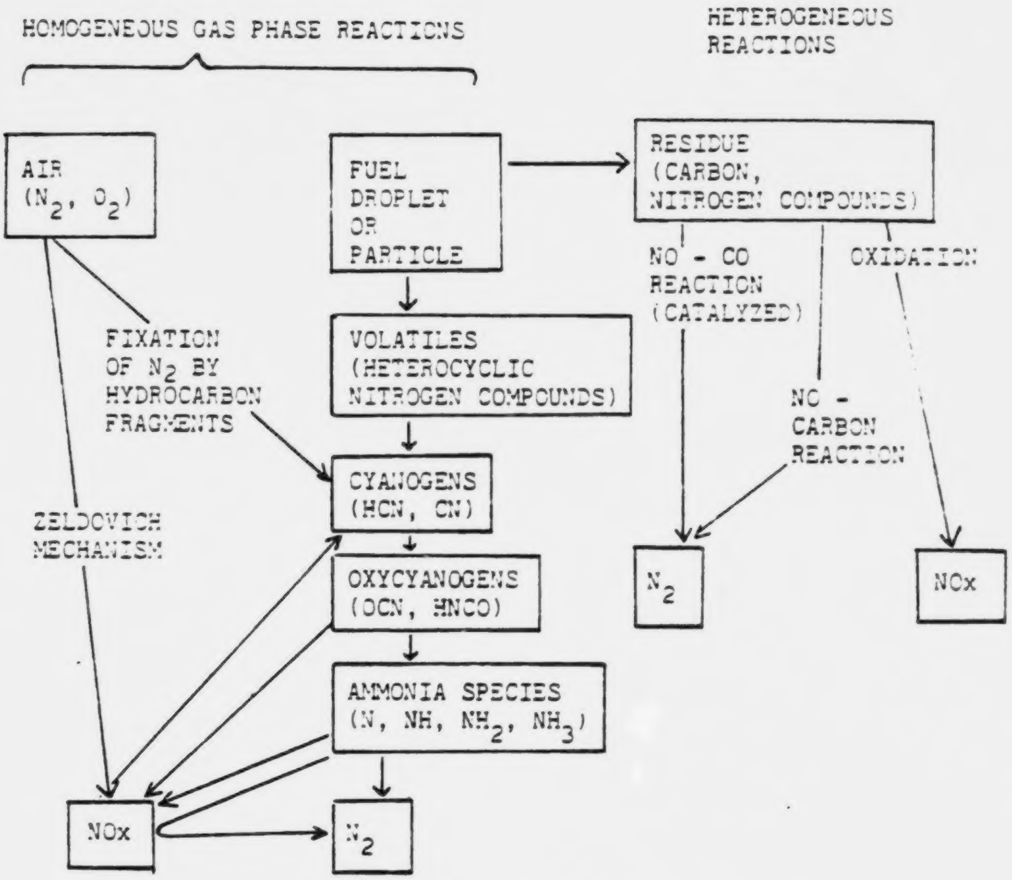

HOMOGENEOUS GAS PHASE REACTIONS
HETEROGENEOUS REACTIONS
AIR (N_2, O_2)
FUEL DROPLET OR PARTICLE
RESIDUE (CARBON, NITROGEN COMPOUNDS)
NO - CO REACTION (CATALYZED)
OXIDATION
VOLATILES (HETEROCYCLIC NITROGEN COMPOUNDS)
FIXATION OF N_2 BY HYDROCARBON FRAGMENTS
NO - CARBON REACTION
CYANOGENS (HCN, CN)
ZELDOVICH MECHANISM
N_2
NOx
OXYCYANOGENS (OCN, HNCO)
AMMONIA SPECIES (N, NH, NH_2, NH_3)
NOx
N_2

Figure 1. MECHANISTIC PATHWAYS OF NITROGEN OXIDES FORMATION IN FOSSIL FUEL COMBUSTION

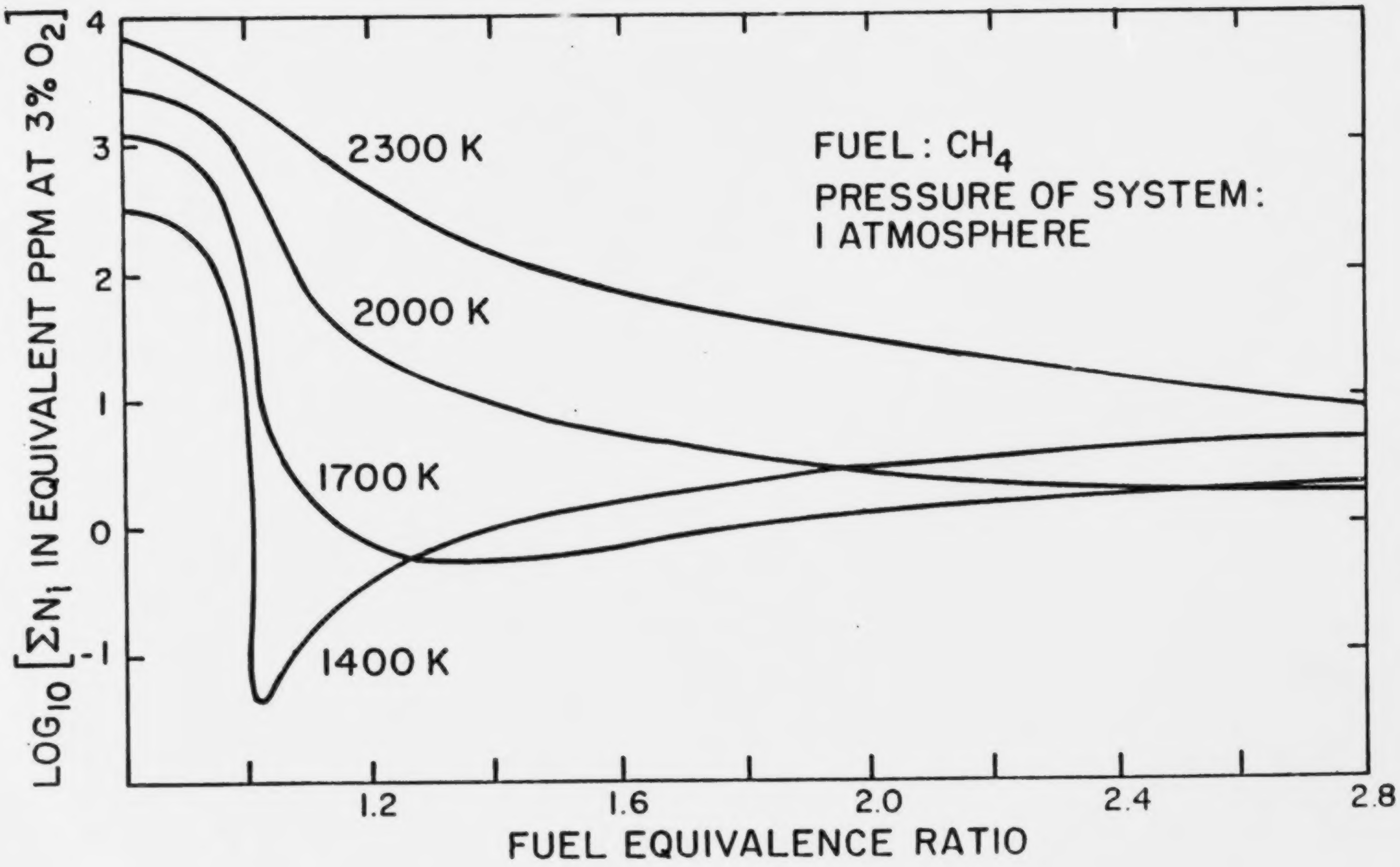

Figure 2. The Effect of Fuel Equivalence Ratio and Temperature on the Equilibrium Concentration of Total Bound Nitrogen Species

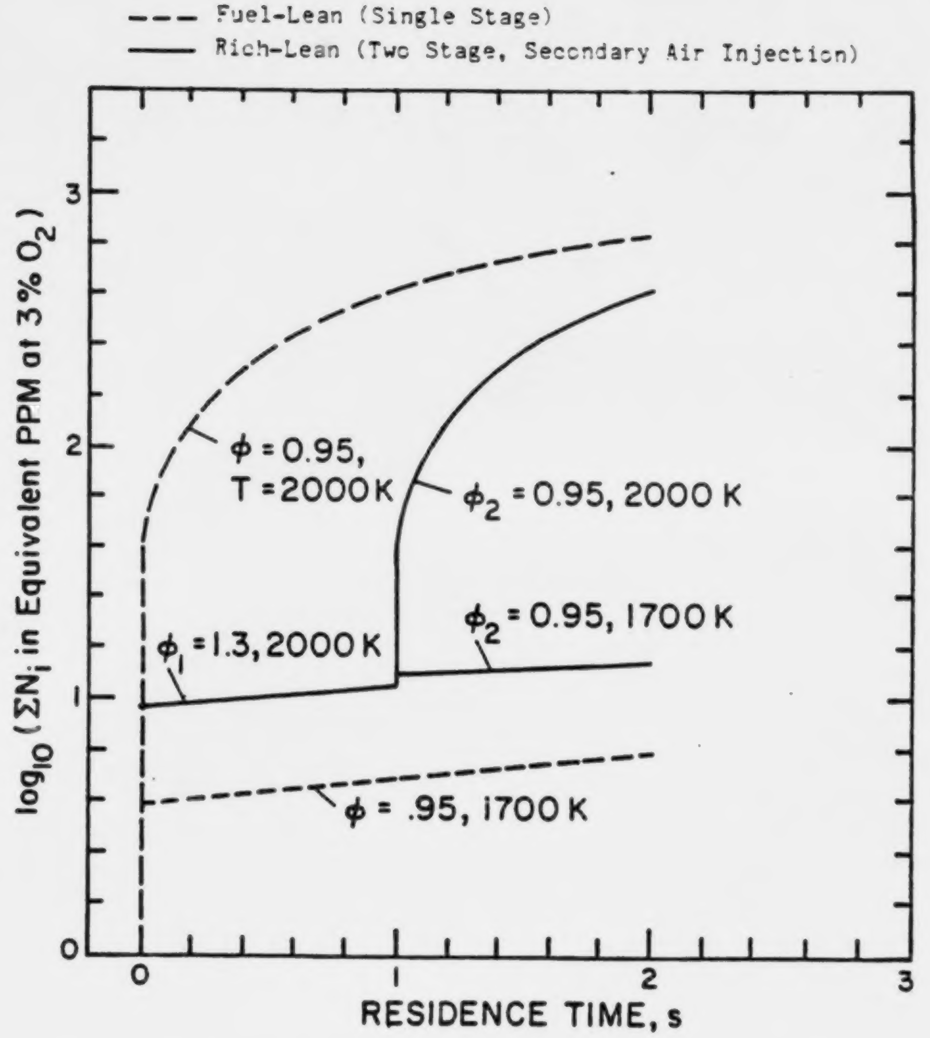

Figure 3. The Effect of Combustion Air Staging and Final flame Temperature on the Concentrations of Total Bound Nitrogen species as determined by Plug Flow Modeling Calculations (Fuel: methane).

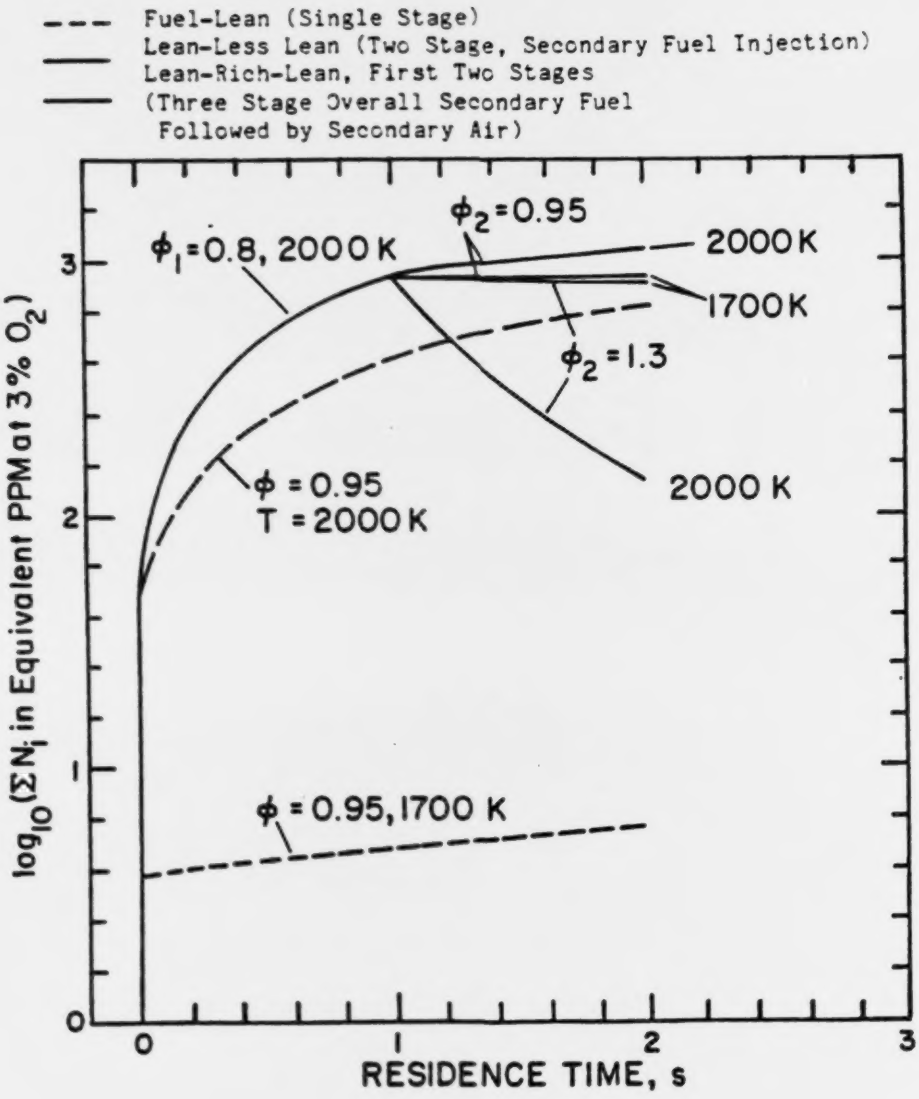

Figure 4. The Effect of fuel Staging, Reburn Zone Stoichiometry and Temperature on the Concentrations of Total Bound Nitrogen Species as Determined by Plug flow Modeling Calculations (Fuel: methane)

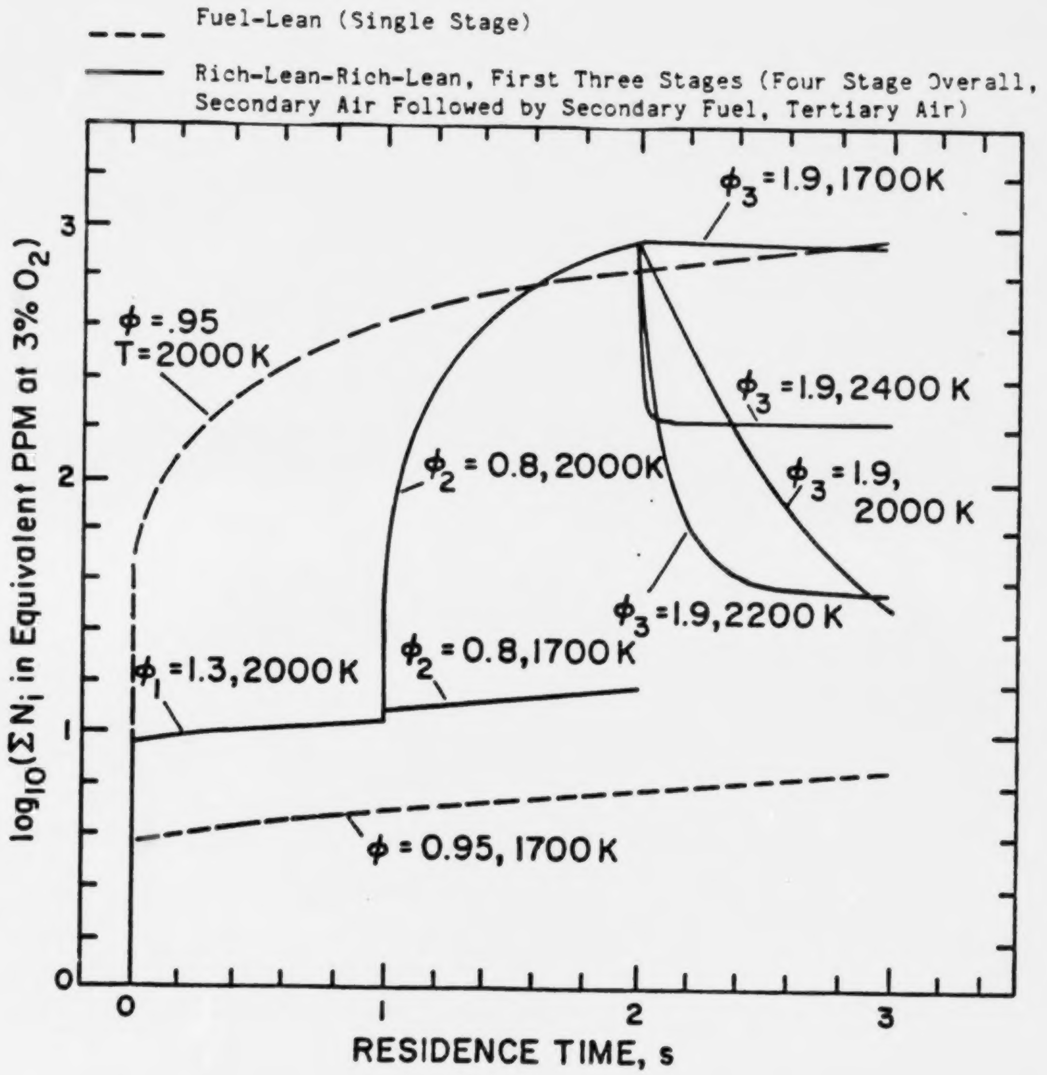

Figure 5. The Effect of Combined Air and Fuel (Multiple) Staging of Reburn Zone Temperature on the Concentrations of Total Bound Nitrogen Species as Determined by Plug Flow Modeling Calculations (Fuel: methane)

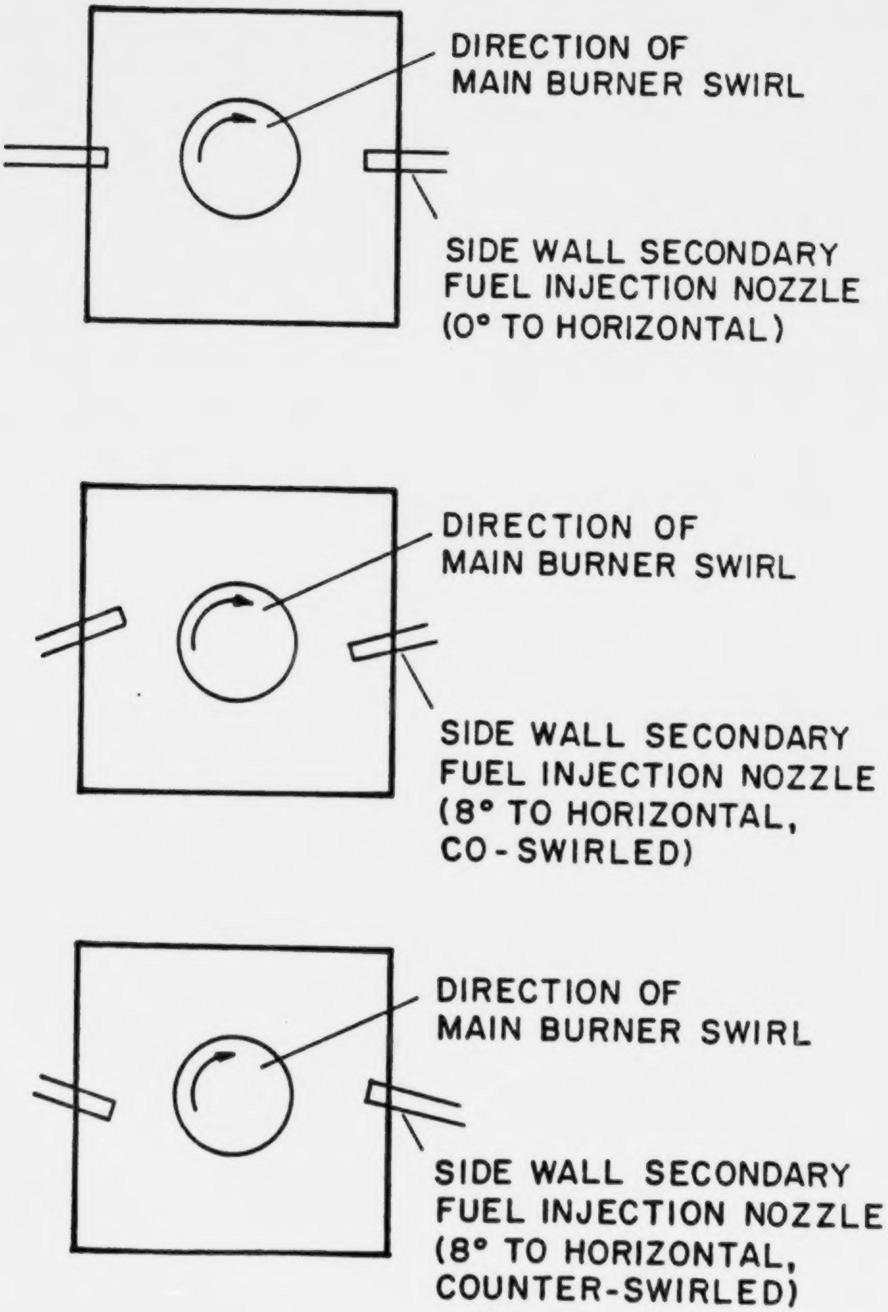
DIRECTION OF MAIN BURNER SWIRL
SIDE WALL SECONDARY FUEL INJECTION NOZZLE (0° TO HORIZONTAL)
DIRECTION OF MAIN BURNER SWIRL
SIDE WALL SECONDARY FUEL INJECTION NOZZLE (8° TO HORIZONTAL, CO-SWIRLED)
DIRECTION OF MAIN BURNER SWIRL
SIDE WALL SECONDARY FUEL INJECTION NOZZLE (8° TO HORIZONTAL, COUNTER-SWIRLED)

Figure 6. Modes of Side Wall Secondary Fuel Injection

(1)

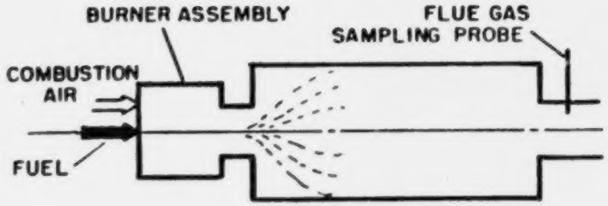
BURNER ASSEMBLY
FLUE GAS SAMPLING PROBE
COMBUSTION AIR
FUEL

(2)

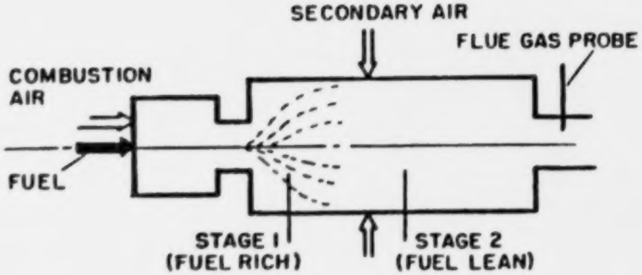
SECONDARY AIR
FLUE GAS PROBE
COMBUSTION AIR
FUEL
STAGE I (FUEL RICH)
STAGE 2 (FUEL LEAN)

(3)

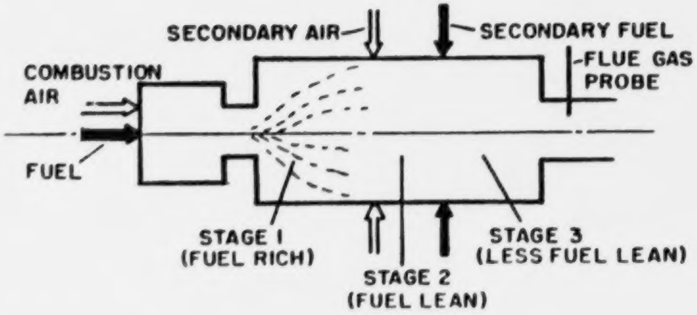
SECONDARY AIR
SECONDARY FUEL
FLUE GAS PROBE
COMBUSTION AIR
FUEL
STAGE I (FUEL RICH)
STAGE 2 (FUEL LEAN)
STAGE 3 (LESS FUEL LEAN)

(4)

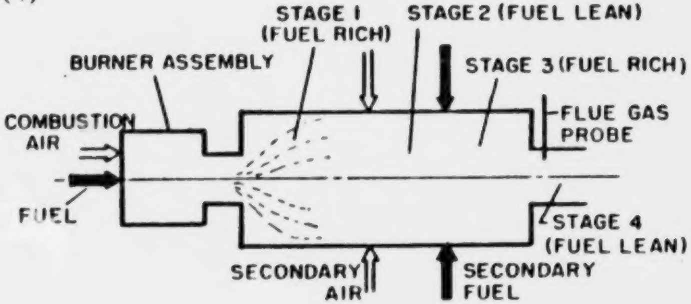
STAGE I (FUEL RICH)
STAGE 2 (FUEL LEAN)
BURNER ASSEMBLY
STAGE 3 (FUEL RICH)
COMBUSTION AIR
FLUE GAS PROBE
FUEL
STAGE 4 (FUEL LEAN)
SECONDARY AIR
SECONDARY FUEL

(5)

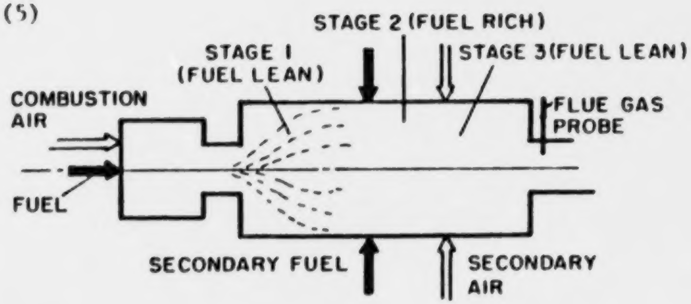
STAGE 2 (FUEL RICH)
STAGE I (FUEL LEAN)
STAGE 3 (FUEL LEAN)
COMBUSTION AIR
FLUE GAS PROBE
FUEL
SECONDARY FUEL
SECONDARY AIR

Figure 7. Schematic of Fuel and Combustion Air Staging in the MIT-CRF

(1) Lean Case (L)

(2) Rich-Lean Case (R-L)

(3) Rich-Lean-Less Lean Case (R-L-LL)

(4) Rich-Lean-Rich-Lean Case (R-L-R-L)

(5) Lean-Rich-Lean Case (L-R-L)

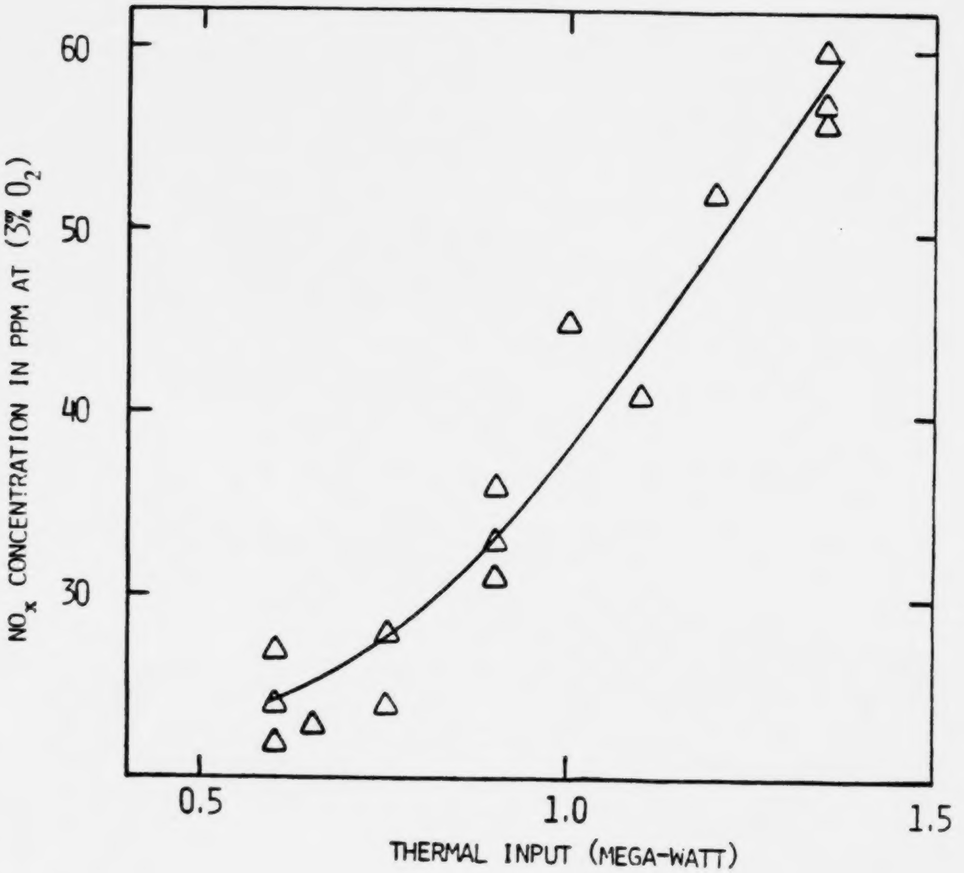

Figure 8. The Effect of Fuel Thermal Input on NO_x Emission from Staged Flames (ϕ = 1.3) (Data obtained in the MIT pilot scale Combustion Research Facility)

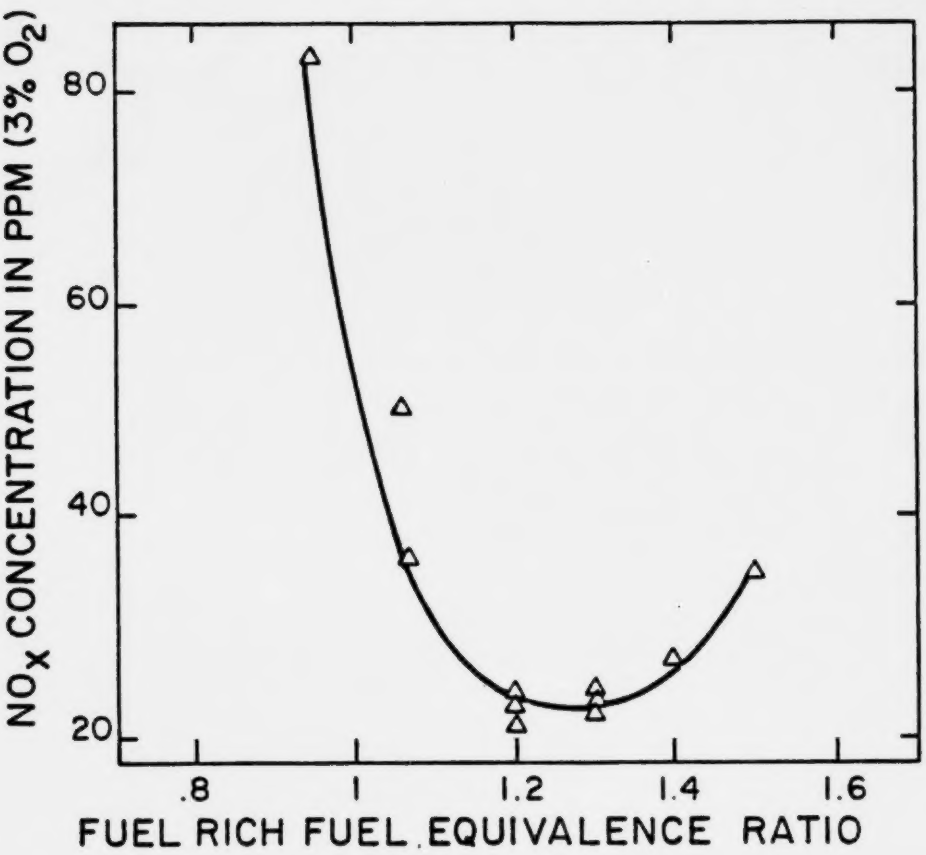

Figure 9. NO_x Emission from Multistage Flames as a Function of the Fuel Equivalence Ratio in the Richest Stage (Data obtained in the MIT pilot scale Combustion Research Facility)

6b-4

NO_x PREDICTION FOR PRACTICAL PULVERIZED COAL REACTORS

L. Douglas Smoot,[1] Scott C. Hill,[2] and Philip J. Smith[3]
Chemical Engineering Department
Brigham Young University
Provo, Utah 84602

ABSTRACT

A model of nitrogen pollutant formation and destruction in pulverized coal reactors is briefly outlined and then evaluated by comparisons of predictions with measurements. The model incorporates effects of turbulence on NO reactions and subsequent predictions show these effects to be important. Model applications show effects of key parameters on NO emissions and illustrate the use of the NO model for interpreting experimental results. The model predicts the observed initial decrease followed by a gradual increase in NO emissions with increased swirl number. The model also predicts the measured increase in NO emissions with increased stoichiometric ratio, but at higher SR values the model underpredicts NO concentrations, partly because of increased thermal NO levels which were not considered. The model also predicts the observed increase in NO with a decrease in particle size and increase in moisture percentage. Results suggest that nitrogen release during devolatilization and gas phase reactions of HCN and oxygen control NO formation, while fuel nitrogen conversion to HCN may be near quantitative and rapid. According to the predictions, NO reduction is dominated by HCN-NO reactions and not by the char-NO reactions. Practical application of the method to pulverized coal reactors is discussed.

INTRODUCTION

Nitrogen pollutants in coal reaction systems have been of concern for several years, and reviews of this subject have been published.[1-4] The prediction of NO formation in turbulent, pulverized-coal systems is very complex because of the large number of reactions often used to describe this process and the turbulent nature of practical systems. Two aspects of the NO reaction process must be addressed in model formulation. The kinetic mechanism itself, and the interactions of the mechanism with the turbulence. Kinetic mechanisms have been postulated to describe NO reactions which involve hundreds of elementary reactions. However, incorporating the effects of the turbulence with a detailed kinetic mechanism is not presently feasible.

The coal combustion model used with the NO model was developed previously[6,7], and is referred to as PCGC-2 (Pulverized Coal Gasification and Combustion:

---

[1] Professor and Dean, Engineering and Technology
[2] Graduate Research Assist., at Los Alamos National Lab., Los Alamos, New Mexico
[3] Assistant Professor

2-Dimensional). Fletcher[8] and Sloan[9] show extensive evaluation of this coal combustion code. This paper provides a brief review of the NO$_x$ model and then summarizes comparisons of the model predictions with the measured effects of key variables. Applications show predicted sensitivity of NO emissions to key parameters and illustrate use of the NO model for interpreting experimental results.

The pollutant species equations are decoupled from the velocity, temperature and major species field equations. The equation set used in the NO model is summarized in Table 1. Fuel nitrogen is assumed to evolve from the coal at a rate proportional to weight loss, and to react instantly to HCN in the gas phase. A specified fraction of the fuel-N released from the coal is assumed to convert to HCN. This percentage relates to both devolatilization and heterogeneous processes. Independent measurements[10,11] in gaseous flames doped with fuel-nitrogen show rapid, near quantitative conversion to HCN. Measurements in coal flames[12] also suggest that fuel nitrogen undergoes significant conversion to HCN during devolatilization, but measurements have not established the precise percent conversion for both coal devolatilization and heterogeneous oxidation. Predictions show that pollutant concentrations are not highly sensitive to small variations of this parameter. Comparisons indicate that assuming quantitative conversion of coal nitrogen to HCN gives best agreement with measured results. However, an 80% conversion value was assumed in most of these comparisons.

The homogeneous rate of HCN decay to NO or N$_2$ includes the effects of turbulent fluctuations to obtain a time-mean reaction rate. The kinetics for these reactions were measured by DeSoete.[13] Heterogeneous reduction of NO is modeled by a slower, (non-fluctuating) rate. The kinetics for this reaction were measured by Levy, et al.[14] Thermal and prompt NO are neglected in these fuel-rich coal flames. The reaction sequence is:

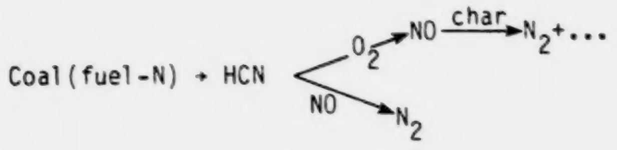

(1)

Global reaction rates are used to describe the kinetic processes. These reaction rates are assumed to be only functions of the local instantaneous stoichiometric ratio at each location in the reactor. This assumption is based on experiments for gas phase systems where the local composition was only a function of the local stoichiometric ratio.[15,16] The model does not require the relationship between the mass fraction and the stoichiometric ratio to be unique for the whole flow field, and thus the reaction times may be different throughout the reactor. The time-mean reaction rates are obtained by assuming that the species mass fractions are linear functions of stoichiometry, and then by integrating the resulting kinetic expressions over the probability density functions for the appropriate mixture fractions. The pollutant concentrations are obtained by solution of the time-averaged species continuity equation, (Eq. 4, Table 1). The NO model is less applicable to fuel-lean systems, since thermal NO is neglected. The NO model is used with a 2-dimensional coal combustion model, but could be adapted to a 3-dimensional code for to staged or multiple-burner systems.

Predictions were made to determine the effects of the turbulence on the NO concentrations. One calculation used only mean values of local temperature and species composition, and thus ignored the effects of the turbulent fluctuations on the pollutant reactions while the second included turbulence-chemistry interaction. The predicted nitrogen oxide concentrations differed by as much as 600% between the two cases.[5]

TABLE 1

EQUATION SET FOR NITROGEN OXIDE MODEL IN TURBULENT, COAL-LADEN SYSTEMS

Description	Equation
1. Rate of Nitrogen Release from the Coal	$\overline{w}_0 = \zeta\, \omega_N\, \overline{S}_p/M_N$
2. Instantaneous Reaction Rate Terms (Constants given in Ref. 13)	$w_1 = \rho A_1 X_{HCN} X_{O_2}^{b} \exp(-E_1/RT)/M_m$ $w_2 = \rho A_2 X_{HCN} X_{NO} \exp(-E_2/RT)/M_m$
3. NO-Char Reduction Reaction (Constants given in Ref. 14)	$\overline{w}_3 = \alpha_p \hat{n}_p A_3 \exp(-E_3/R\hat{T}) A_E \hat{P}_{NO}(\gamma)$
4. Species Continuity for i = NO, HCN	$\overline{\rho}\, \hat{u}(\partial\hat{Y}_i/\partial x) + \widehat{\overline{\rho}v}(\partial\hat{Y}_i/\partial r) - (\partial/\partial x)(\Gamma_Y \partial\hat{Y}_i/\partial x)$ $- (1/r)(\partial/\partial r)(r\hat{\Gamma}_Y \partial\hat{Y}_i/\partial r) = \overline{W}_i$
5. Instantaneous Mass Fractions	$Y_i = \pi_i Y_i^f$
6. Mean Reaction Rate Term by Convolution Over Probability Density Functions	$\overline{w}_i = \overline{\rho}\int_f \int_\eta [w_i(f,\eta)/\rho(f,\eta)]P(f)P(\eta)\,df\,d\eta$
7. Deviation from Fully Reacted Mass Fractions	$\pi_i = (\hat{Y}_i/\hat{Y}_i^f)$
8. Mass Balance for O_2	$\hat{Y}_{O_2} = \hat{Y}_{O_2}^{o} - \hat{Y}_{NO} M_{O_2}/M_{NO}$
9. Overall Mean Reaction Rates for Each Species	$\overline{W}_{NO} = (\overline{w}_1 - \overline{w}_2 - \overline{w}_3)M_{NO}$, $\overline{W}_{HCN} = (\overline{w}_0 - \overline{w}_1 - \overline{w}_2)M_{HCN}$

COMPARISONS WITH OBSERVED TRENDS

Nitrogen Pollutant Data

A review of the literature was made to determine available radial profile and effluent concentrations of nitrogen pollutants in laboratory-scale, pulverized-coal combustors.[5] The review was also used to summarize the observed effects of key variables on nitrogen pollutant concentrations. All the data cases considered were measured in pulverized-coal combustors. Several cases were selected for comparisons with the NO model predictions. The cases used for model comparisons were limited to those which provided the necessary input parameters (e.g., coal characteristics, reactor geometry, air and coal feed rates, etc.), and adequate pollutant measurements for comparisons with predictions. The cases selected for trend comparisons are summarized in Table 2 which shows the source, the case number, and the variable studied. The important input conditions are summarized in Table 3.

Comparisons with Predictions

The NO predictions were compared with the measured effects of selected test variables. Table 4A summarizes results of 24 comparisons where the average absolute difference between predicted and measured NO was less than 12%. Table 4A also shows differences for each variable. The model requires parameters related to the solution technique, coal combustion process, and specific characteristics of the system. The parameters were selected in advance and were not adjusted in an attempt to match predictions with measurements.

Swirl Number. Swirl No. is the axial flux of the inlet secondary stream to angular momentum divided by the product of the axial flux of inlet secondary axial momentum and secondary duct radius and is a measure of the swirling flow intensity. Studies (e.g., 12,17) have shown for subbituminous and bituminous coals that swirling of the incoming air stream which surrounds the coal stream can significantly influence the NO concentrations. Figure 1 compares predicted and measured NO concentrations as a function of swirl number for subbituminous and bituminous coals. The predicted and observed results have a similar shape for both coals, but predicted values are lower at most swirl numbers. For low swirl numbers, NO emissions decreased as swirl number was increased. For high swirl numbers, NO emissions increased as swirl number was increased. The minimum NO emissions occurred at a swirl number of 2.0-3.0, depending on the coal type. However, swirl does not always influence NO_x like in Fig. 1, as discussed subsequently.

These variations in NO emissions with swirl number result principally from differences in the mixing process. The extent of mixing of the coal and air has a significant impact on the volatile nitrogen conversion to NO.[4] Without swirl, ignition was downstream of the inlet region. Lifted flames result in increased NO emissions[18,22,23] and reduction in NO emissions can be partially attributed to flame stabilization at the burner. A delay in ignition allows for increased mixing of coal and oxidizer prior to volatiles combustion. This increases the local oxygen concentration during volatiles combustion, which increases NO formation. The release of coal nitrogen also increases when the flame is detached,[22] probably through changes in the peak temperature. Increased swirl results in more rapid particle heatup from faster mixing with recirculation gases and a change in furnace residence time.[24]

The swirling incoming air results in sufficient mixing to promote early ignition. This stream forms an annulus around the coal stream which creates a fuel-rich central core. Oxidizer from the incoming air is entrained at the outer edge of this core which ignites the volatiles and stabilizes the combustion process near the burner. Heat transfer by radiation from the flame causes nitrogen devolatilization in a fuel-rich environment which favors N_2 formation.

Stoichiometric Ratio. Increased stoichiometric ratio (SR) over the practical range of operation increases NO formation in coal systems[12,18,25] by increasing the oxygen available for reaction with fuel nitrogen. Rees, et al.[18] measured the effects of stoichiometric ratio (0.40-1.15) on NO emissions for a Utah bituminous coal in a laboratory-scale combustor with a parallel, coaxial

TABLE 2

CASES SELECTED FOR TREND COMPARISONS

Reference	Case Number	Key Variable(s)
Rees, Smoot and Hedman[18]	1	Stoichiometric Ratio
Lee, Chen, Pershing, and Heap[19]	2	Particle Size
Harding, Smoot and Hedman[12]	3 and 4	Secondary Swirl
Asay, Smoot and Hedman[17]	5	Secondary Swirl Stoichiometric Ratio Coal Moisture

TABLE 3

PULVERIZED-COAL COMBUSTION DATA CASES COMPARED WITH MODEL PREDICTIONS

	Rees, et al.[18]	Lee, et al.[19]	Harding, et al.[12]		Asay, et al.[17]
	Case 1	Case 2	Case 3	Case 4	Case 5
Reactor Characteristics					
Primary Diameter (m)	0.016	0.051	0.016		0.022
Secondary Diameter (m)	0.054	---	0.084		0.084
Chamber Diameter (m)	0.203	0.152	0.203		0.203
Quarl Angle (degrees)	0	9.4	35		35
Quarl Angle Length (m)	0	0.305	0.040		0.040
Chamber Length (m)	1.524	2.440	1.565		1.565
Secondary Swirl Number	0	0	1.4	3.4	2.0
Heat Loss (%)	10*	50*	10*		10*
Flow Rates					
Primary Flow Rate (kg/s)	0.006	0.007	0.006		0.007
Secondary Flow Rate (kg/s)	0.031	---	0.030		0.019
Primary Velocity (m/s)	30	8	30		20
Secondary Velocity (m/s)	25	---	12		10
Particle Flow Rate (kg/s)	0.004	0.066	0.004		0.003
Inlet Gas Properties					
Primary Temperature (K)	350	640	300		300
Secondary Temperature (K)	580	---	590		590
Pressure (10^4 N/m^2)	8.6	10.1	8.6		8.6
Composition: primary (air)	100.0	100.0	100.0		100.0
(wt, %) secondary (air)	100.0	100.0	100.0		100.0
Coal Properties					
Coal Type	Bituminous	Bituminous	Bituminous		Subbitum.
High Heating Value (MJ/kg)	29.0	29.0	34.1		30.3
Mass Mean Particle Diameter (μm)	49.1	165.0	50.0		50.0
Elemental Composition (dry, wt%):					
C	72.2	73.1	72.5		67.0
H	5.6	5.6	5.5		4.4
O	10.9	11.3	10.5		20.1
N	1.5	1.4	1.4		1.1
S	0.6	0.7	0.5		0.5
Ash	9.2	7.9	9.6		6.9
Moisture (wt. %)	2.5	6.4	2.4		25.0

---

*Estimated due to lack of reported data.

injection of coal and air. Figure 2 shows comparisons of predictions with measured outlet NO concentrations. Asay, et al.[17] also measured the effect of stoichiometric ratio on NO emissions for a high-moisture (25%) subbituminous coal in a laboratory combustor. A swirl number of 1.4 was used, and the SR was varied from 0.57 to 1.17.

For both the swirling and non-swirling diffusion flames, the measured and predicted NO exit values increase with stoichiometric ratio. However, the measured effect of stoichiometric ratio is more dramatic than the predicted effect. At higher SR values, the model underpredicts NO concentrations, probably because the contribution of thermal NO was not included in the model. A lower stoichiometric ratio results in less oxygen available for oxidation of the volatilized fuel nitrogen. Nitrogen is devolatilized into a fuel-rich zone which reduces NO formation and enhances reduction of the NO formed. Particle temperature increases at higher stoichiometric ratios, which in turn causes greater nitrogen devolatilization and increased NO formation.[12,21]

Particle Size. Lee, et al.[19] report the effect of particle size on NO formation for a Utah bituminous coal in a laboratory combustor[26]. Particles in two narrow size distributions were obtained by sieving. These narrow distributions were approximated by discrete particle sizes of 165 μm and 35 μm, respectively. The measurements shown in Fig. 3 indicate that larger particles result in lower NO emissions than smaller particles. This trend was measured at several stoichiometric ratios, but model predictions were only made at SR = 1.0. The NO model predicts the same trend, with similar NO concentrations to that observed.

The effect of particle size on NO emissions results from differences in particle heating and peak temperatures, which subsequently affects the devolatilization rate. Smaller particles heat at a faster rate and attain a higher peak temperature[19,25] which results in a greater extent of coal devolatilization and higher coal burnout. These factors produce more fuel nitrogen which increases NO formation. This is supported by the predicted coal burnout shown in Fig. 3 which indicates that the smaller particles react to a greater extent. In addition, the gases devolatilized from small particles mix and react more rapidly with the surrounding oxidizer than gases do the from large particles[19]. This results in greater oxygen availability and subsequently more NO formation.

Coal Moisture. The effect of coal moisture on NO was reported by Asay, et al.[17] for a high-moisture, subbituminous coal. This coal had an inherent moisture content of 25%, some of which was dried to 4.5% moisture. A swirl number of 1.4 was used with an SR of 0.87. A comparison of measured and predicted NO values for the wet and dried coal is shown in Fig. 4. As the coal moisture content increases, both the predicted and observed NO emissions increase. The effect of coal moisture on NO reactions is attributed to delayed ignition of the wet coal, which results in increased mixing of the coal and oxidizer prior to volatiles combustion. The predicted ignition point was only delayed 5 cm for the high-moisture coal, but this resulted in a higher local oxygen concentration at ignition.

Profiles. The comparisons of NO model predictions were also made with detailed measurements of nitrogen pollutant concentrations from within laboratory combustors. Six sets of profile comparisons have been made and were reported elsewhere.[5,27] These comparisons were summarized in Table 4B. Differences in predicted and measured exit NO concentrations varied from +34% to -25% for the

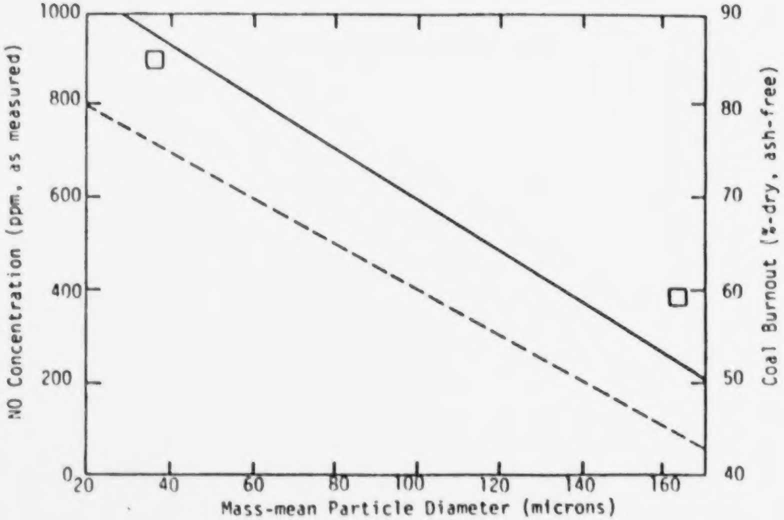

Figure 3. Comparison of predicted (–) and observed[19] (□) effects of coal particle diameter on NO concentration. Predicted effects (--) of coal particle diameter on percentage coal burnout also shown.

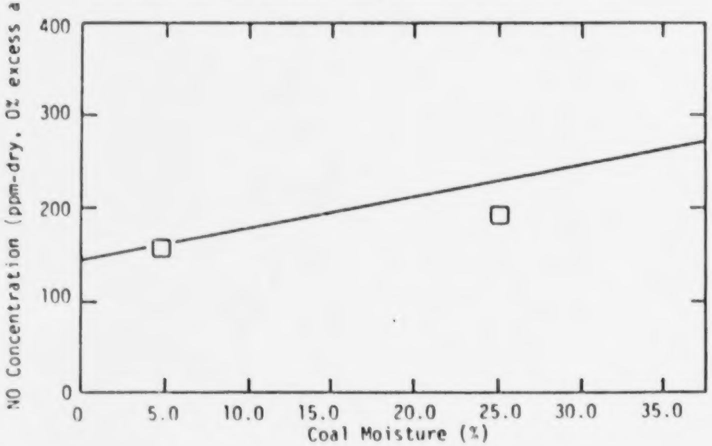

Figure 4. Comparison of predicted (–) and observed[17] (□) effects of coal moisture percentage on NO concentration.

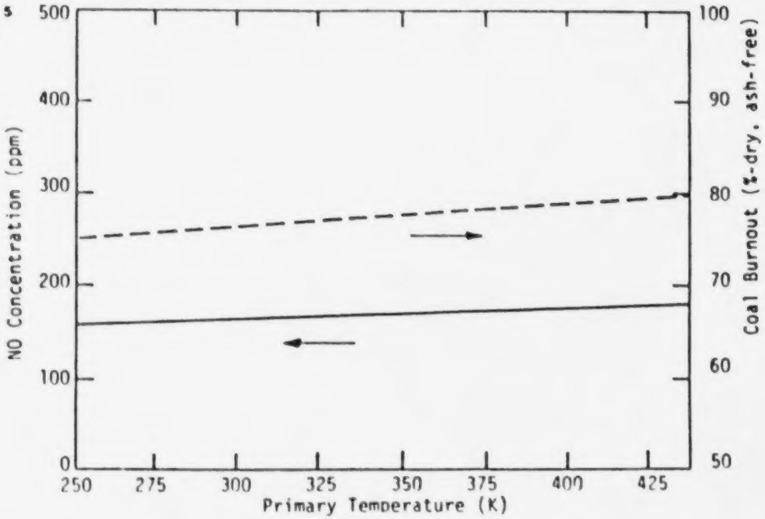

Figure 5. Predicted outlet NO and coal burnout as a function of primary temperature (K).

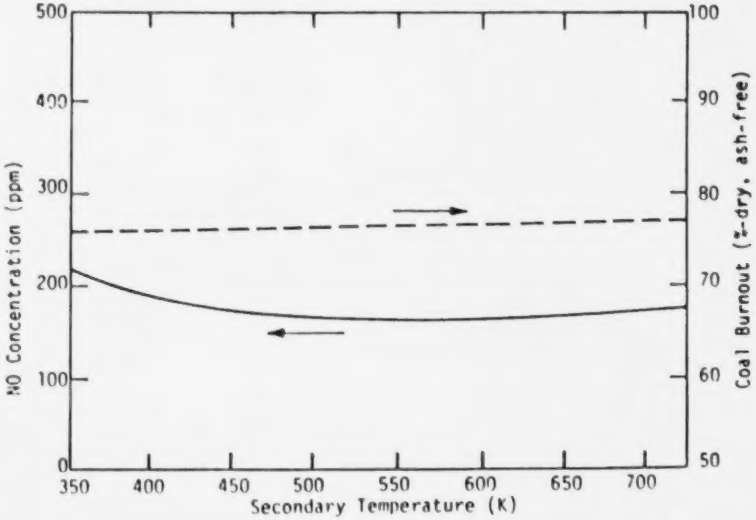

Figure 6. Predicted outlet NO and coal burnout as a function of secondary temperature (K).

TABLE 4

COMPARISONS OF PREDICTED AND MEASURED NO POLLUTANT CONCENTRATIONS

(A) Key Variables	Data Source Ref.	Parameter Range	No. of Cases	Coal Feed Rate (kg/hr)	Flame Type	Average * Difference in Exit NO Values
Swirl Number	12,17	0-10	10	22 & 25	diffusion	+9
Stoichiometric Ratio	17,18	0.5-1.2	10	22	diffusion	-8
Particle Size (μm)	19	40-160	2	25	premixed	+16
Coal Moisture (%)	17	5-25	2	25	diffusion	-12

(B) Local Measurements	Data Source Ref.	Coal Type	Swirl Number	Coal Feed Rate (kg/hr)	Flame Type	Average* Difference in Exit NO Values
Case 1	17	Subbit.	2.0	25	diffusion	+12
Case 2 ($V_p \hat{=} V_s$)	20	Bitum.	0	260	diffusion	-25
Case 3	12	Bitum.	1.4	22	diffusion	+34
Case 4	12	Bitum.	3.4	22	diffusion	+15
Case 5	17	Subbit.	1.4	22	diffusion	+30
Case 6 ($V_p > V_s$)	20	Bitum.	0	440	diffusion	+29

All Thirty Cases	
Average absolute % difference	12%
Average relative % difference	4%

*Positive number indicates measured value is greater than predicted value.

six cases. Also shown are the average absolute and relative percent differences for these cases.

MODEL APPLICATIONS

Sensitivity of NO Emissions to Other Parameters

Predicted effects of several key parameters on NO emissions are noted and applications of the NO model are illustrated. Only parameters related to reactor configuration and operation were considered. The following figures illustrate the predicted effect of various input parameters on NO concentrations and coal burnout. NO emissions are reported on an as-measured basis (no correction for moisture or excess air), and coal burnout is reported on a dry, ash-free basis. It is also important to emphasize the effects of variables discussed herein cannot necessarily be generalized to any combustor or fuel. Simultaneous reductions in NO concentrations and coal burnout result in additional unburned coal. Some methods of NO reduction will not be feasible due to a large decrease in coal burnout. Other effects on furnace operation such as pressure drop, furnace maintenance, and flame characteristics will cause some methods of NO control to be impractical. These aspects were not considered.

Inlet Temperatures. The primary stream generally carries the coal particles into the reactor. Figure 5 shows that predicted NO emissions and coal burnout both increase only slightly as the primary temperature is increased over a small range. The secondary stream temperature is a measure of the preheat of the remaining inlet air required for combustion. Fig. 6 shows that NO emissions gradually decrease and then increase with an increase in secondary temperature. NO emissions are minimum at a secondary temperature of about 550 K. Coal burnout increases only slightly with an increase in secondary temperature. Neither predicted NO emissions nor coal burnout are strong functions of the temperature of the inlet streams. The increase in NO emissions with a decrease in the inlet temperature probably results from a slight delay in ignition of the coal flame.

This predicted trend for NO concentrations is consistent with the trend observed by several investigators. Harding et al.[12] observed a slight decrease in NO emissions with a reduction in secondary temperature from 590 K to 480 K. Harding's conditions were somewhat different from those used for these predictions; however, the observed trend is consistent with the predicted trend. Predicted NO concentrations decrease in this temperature region, and the predicted NO emissions have only a slight dependence on secondary temperature.

Brown, et al.[28] observed that NO emissions increased slightly with secondary temperature. These tests were conducted in a large-scale, staged system designed for front-wall and tangential firing with multiple burners. The secondary temperature was varied from ambient (300 K) to near 1100 K, and the results were reported as a function of first-stage stoichiometry. The effect of secondary temperature on NO emissions varied with first-stage stoichiometric ratio, but in general, NO emissions showed only a weak dependence on secondary temperature.

A higher inlet temperature results in more rapid particle heat-up and a higher final particle temperature. This will influence both the amount of coal devolatilized and the split between the volatiles and the char nitrogen. Rapid particle heat-up also allows more time for coal reaction and the release of fuel nitrogen to the gas phase. This will generally cause both NO formation and coal burnout to increase. However, very little energy (sensible) is contained in the inlet streams relative to the heat of combustion of the coal. A 100 K increase in the primary temperature and a 300 K increase in the secondary temperature both independently resulted in an approximate 60 K increase in the predicted peak temperature. Thus, the changes made in the inlet temperatures resulted in relatively small changes in the predicted peak reactor temperature.

Primary Stream Diameter. For a constant density and mass flowrate, the velocity is inversely proportional to the square of the diameter. For these predictions, the same cross-sectional area of the secondary tube was used to maintain the velocity and mass flowrate of the secondary stream. Figure 7 shows that as the primary diameter is decreased (primary velocity increased), both NO emissions and coal burnout increase. The primary velocity has a dramatic effect on NO emissions and only a slight impact on coal burnout.

Heap, et al.[29] measured the effect of primary velocity on NO emissions for various secondary stream levels. These measurements show that NO emissions can increase or decrease with increased primary velocity depending on the amount of secondary swirl. These tests were conducted in a horizontal, rectangular system, and the average primary velocity was varied from 19-52 m/s. The lowest primary velocity (19 m/s) resulted in the highest NO emissions at all swirl numbers (all higher than the current study). However, at some levels of swirl, the highest primary velocity (52 m/s) resulted in considerably higher NO emissions than the intermediate primary velocity (26 m/s). At these velocities, NO first decreased and then increased with primary velocity as the swirl was increased.

Harding, et al.[12] observed that the primary velocity had only a small impact on NO emissions. These tests were conducted in a laboratory-scale combustor, and the primary velocity was reduced from 30 m/s to 15 m/s. The effect of primary velocity was also shown to be a function of swirl number and stoichiometric ratio, and the effect of primary velocity on NO emissions increased with increasing stoichiometric ratio. Wendt and Pershing[15] observed that NO emissions first decreased and then increased as the primary velocity was increased. These tests were conducted in a laboratory-scale diffusion flame in which the primary velocity was varied from 20-100 m/s by changing the percentage of stoichiometric air in the primary stream. A dramatic increase in NO emissions was observed when the primary velocity caused the flame to lift from the burner. Delayed ignition results in higher NO emission.[19,22,23,28,30]

In this study, the predicted dramatic effect of primary velocity on NO emissions probably resulted mainly from flame detachment from the burner. The primary velocity may also influence nitrogen devolatilization and subsequent NO reactions by changing the particle heating rate.

Secondary Stream Diameter. The secondary stream velocity is inversely proportional to the secondary flow area. Fig. 8 shows that both NO emissions and coal burnout increase slightly as the secondary stream diameter increases (secondary velocity decreases). The predicted trends are opposite and much less dramatic than the predicted effect of primary diameter. In this case, the secondary velocity was varied from 10 m/s to 4 m/s. The difference in the magnitude of change in the respective velocities is probably the cause of smaller differences in NO emissions with variation in secondary diameter. The effect of the secondary diameter on NO emissions is similar to the trend observed by Pershing, et al.[31] in a laboratory-scale diffusion flame with a swirl injector. The secondary velocity was increased from 30 to 60 m/s, and small reductions (approximately 9%) in NO emissions were observed at all swirl levels.

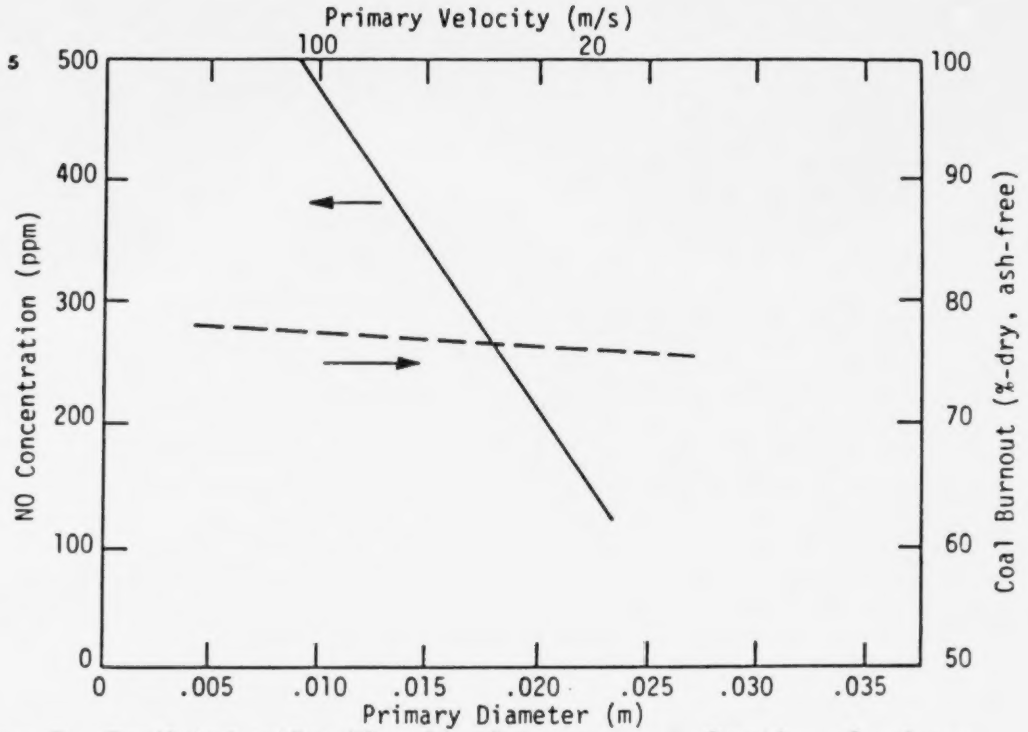

Figure 7. Predicted outlet NO and coal brunout as a function of primary diameter (m).

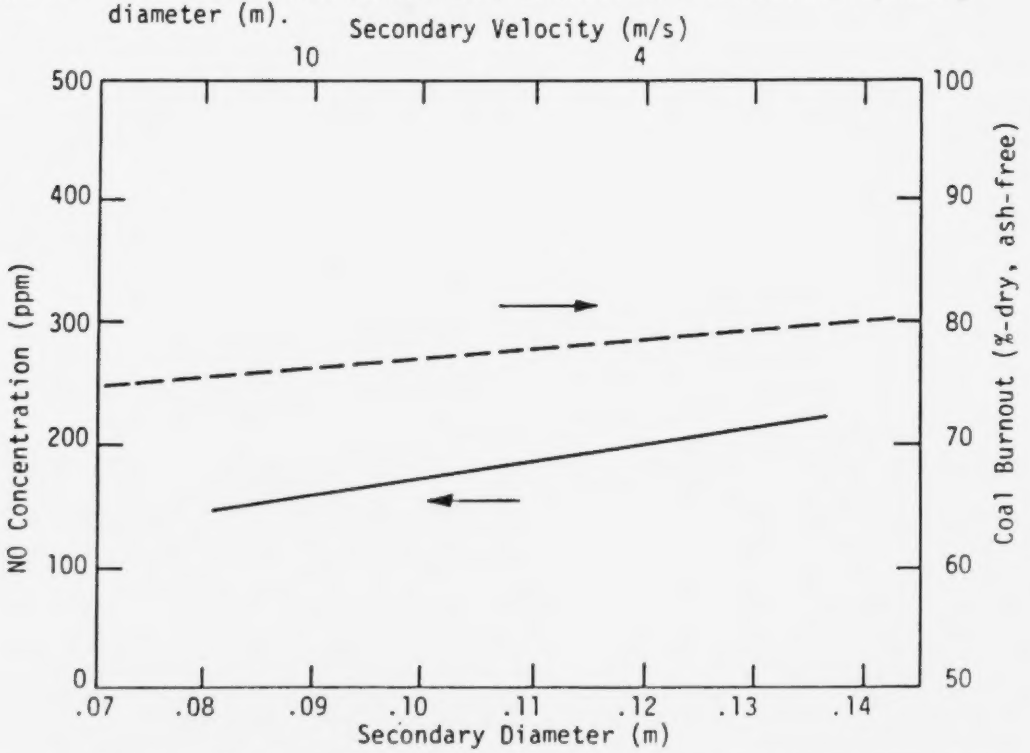

Figure 8. Predicted outlet NO and coal burnout as a function of secondary diameter (m).

Wall Temperature. The wall temperature is dependent on several factors including reactor insulation and accumulation of ash on the walls. Figure 9 shows that both NO emissions and coal burnout increase only slightly with increases in wall temperature. These predicted trends are similar to the predicted effect of primary temperature, and wall temperature probably affects the NO concentration and coal burnout in a similar manner. A study in a laboratory-scale, staged coal combustor showed that the reactor walls did not contribute significantly to NO destruction.[32] This also partially explains the limited influence of wall temperature on NO emissions. Pershing and Wendt[33] observed a similar effect of flame temperature on NO emissions. The flame temperature was varied approximately 220 K by changing the heat capacity and oxygen content of the oxidizer. The change in flame temperature caused an approximate variation of 170 K in the wall temperature, but caused only a slight increase in NO emissions.

Methods of NO_x Reduction

Reactor configuration and operating parameters can have a strong influence on NO reactions. The above predictions were used to select a combination of design and operating parameters to reduce predicted NO emissions. A computation is performed to illustrate the use of the model in selecting operating parameters to minimize NO_x and improve burnout. The key parameters are shown in Table 5. All other model conditions for this case were the same as those used in Case 5 in Table 3.

TABLE 5

KEY SELECTED PARAMETERS TO REDUCTION OF NO EMISSIONS

Key Parameters	Base Case	Low NO_x Case
Primary Temperature, K	300	300
Secondary Temperature, K	590	525
Primary Diameter, cm	2.2	2.5
Secondary Diameter, m	0.094	0.080
Reactor Chamber Diameter, m	0.203	0.400
Reactor Length, m	1.565	3.000
Wall Temperature, K	1000	1000
Reactor heat Loss, %	10	10

A primary temperature of 300 K was maintained, since a lower primary temperature decreased NO emissions only slightly, but also lowered coal burnout. A lower secondary temperature of 525 K was used to reduce predicted NO emissions. Coal burnout was not significantly affected by the secondary temperature over the region considered. A primary velocity of 20 m/s (primary diameter of 0.025 m) was selected since NO emissions were predicted to decrease dramatically with decreased primary velocity. However, a sufficient velocity was maintained to avoid settling of the coal particles. Coal burnout was also predicted to decrease with a decrease in primary velocity which further limited the amount of primary velocity decrease. A secondary diameter of 0.08 m was used since NO emissions were predicted to decrease with an increase in secondary velocity. Coal burnout was also predicted to decrease with an increase in the secondary velocity, and this limited the increase in secondary velocity. A larger chamber diameter of 0.40 m was used since NO emissions were predicted to increase with

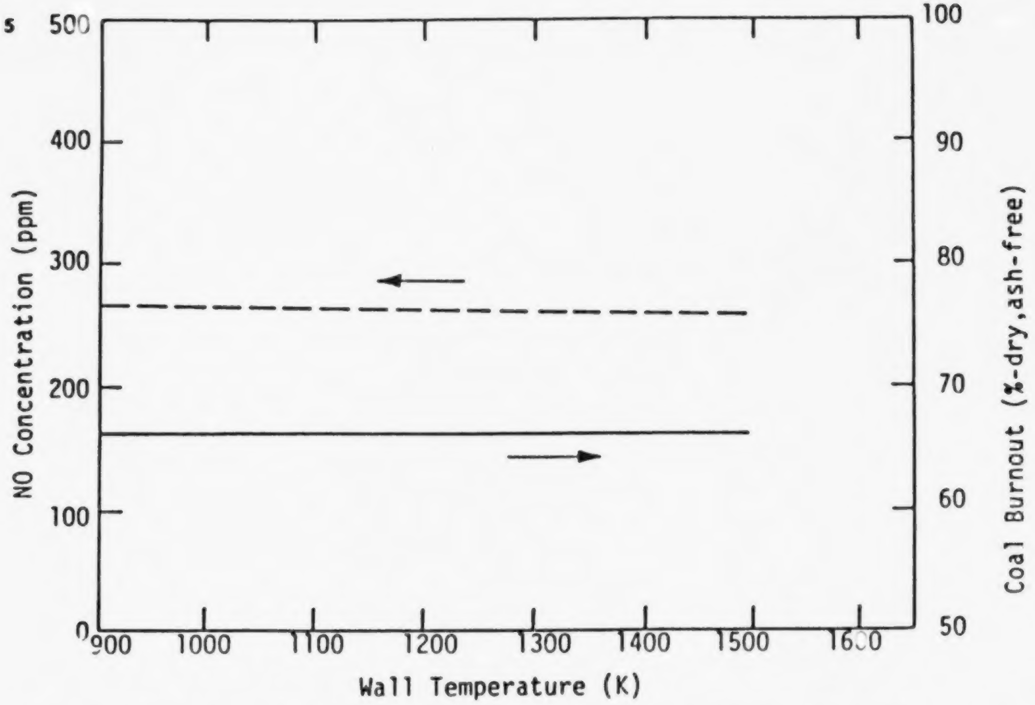

Figure 9. Predicted outlet NO and coal burnout as a function of wall temperature (K).

31. Pershing, D.W., Martin, G.B., and Berkau, E.E., "Influence of Design Variables on the Production of Thermal and Fuel NO_x from Residual Oil and Coal Combustion," AIChE Symposium Series, 71, 19 (1975).

32. Glass, J.W., and Wendt, J.O.L., "Mechanisms Governing the Destruction of Nitrogenous Species During the Fuel Rich Combustion of Pulverized-Coal," Western States Section/Combustion Institute, University of Utah, Salt Lake City, UT (1982).

33. Pershing, D.W., and Wendt, J.O.L., "Relative Contributions of Volatile Nitrogen and Char Nitrogen to NO_x Emissions from Pulverized Coal Flames," Ind. Eng. Chem. Process Des. Dev., 18, 1 (1979).

NOMENCLATURE

Variable	Units	Description
A	$m^2 kg^{-1}$	Char surface are
f		Mixture fraction
M	$kg\ kgmole^{-1}$	Molecular weight
n	m^{-3}	Particle number density
p	-	Probability density function
p	atm	Partial pressure
R	$J\ kgmole^{-1}K^{-1}$	Ideal gas constant
r	m	Radial direction coordinate
S	$kg\ m^{-3}s^{-1}$	Source term
SR	--	Stoichiometric Ratio
T	K	Temperature
u	$m\ s^{-1}$	Axial velocity component
v	$m\ s^{-1}$	Radial velocity component
W	$kg\ m^{-3}\ s^{-1}$	Overall reaction rate for a species
w	$kgmol\ m^{-3}\ s^{-1}$	Individual reaction rate
X	-	Mole fraction
x	m	Axial direction coordinate
Y	-	Mass fraction
α	kg	Particle weight
ω	-	Coal element mass fraction
η	-	Coal gas mixture fraction
π	-	Fractional deviation
ρ	$kg\ m^{-3}$	Density
Γ	$kg\ m^{-1}s^{-1}$	Turbulent diffusivity
ζ	--	% of coal N converted to HCN

Subscripts	Description
E	External
i	Species index
m	Mixture
N	Nitrogen
p	Particles
s	Secondary
Y	Mass fraction
0	Reaction number
1	Reaction number
2	Reaction number
3	Reaction number

Superscripts	Description
b	Order of HCN reaction with respect ot O_2
f	Fully reacted
o	Initial
~	Favre-mean
—	Conventional time-mean

increased chamber diameter. A reactor length of 3.0 m was used since NO emissions were predicted to decrease with increased reactor length, while coal burnout increases with increased residence time in the longer reactor. A wall temperature of 1000 K was maintained since NO emissions were predicted to decrease only slightly with lowered wall temperature. In addition, coal burnout was predicted to increase slightly with decreased wall temperature. A reactor heat loss of 10% was assumed. A high heat loss resulted in lower NO emissions, but this also caused a reduction in coal burnout. Absence of heat loss resulted in both decreased NO emissions and increased coal burnout, but this was not considered a realistic value for practical coal combustors.

Figure 10 shows a comparison of predicted NO contour maps for the base case and the low-NO_x case. NO reactions and concentrations are substantially affected by the conditions shown in Table 5. The peak NO concentrations for both cases show similar values, but the peak values occurred much closer to the reactor inlet in the latter case. Two distinct NO peaks formed in this case, but the base case was characterized by only one NO peak. The integrated NO exit concentrations decreased from 164 to 56 ppm, and coal burnout increased from 76% to 88%. Thus, the conditions in Table 5 resulted in a three-fold reduction of the exit NO levels, while coal burnout was increased by 12%. Even for equal reactor lengths, NO_x is reduced by over a factor of 2. These results demonstrate potential use of the code in development or possible control strategies for reducing NO emissions in coal combustion.

Interpreting Experimental Results

Swirl of the secondary stream is one technique of fuel/air contacting which causes significant changes in NO concentrations. In some cases, increased swirl increases NO emissions.[21,23,28] This probably results from increased mixing of secondary air with volatiles products prior to complete combustion. In other cases, increased swirl initially decreases NO emissions,[12,17] and possible explanations of these observations were discussed previously. Thus, the observed effects of swirl on NO emissions are varied, and indicate that additional parameters influence the NO emissions.

The NO model was used to investigate the swirl level on NO emissions. The conditions were the same (case 5, Table 3) as used to make the predictions shown in Fig. 1, except that the coal stream was assumed to enter at a considerably higher velocity. This case is shown in Fig. 11 and NO emissions first increased and then decreased with increasing swirl number. This is opposite of the trend shown in Fig. 1, but has been observed by several investigators.[21,23,28] The maximum NO emissions occur at a swirl number of approximately 3 (almost the same value where the minimum occurred previously). The differences in the predicted effect of swirl on NO emissions indicate that the relative level of momenta of the swirling air stream and coal stream influence the extent to which these streams mix, and subsequently the amount of NO formed. The differences in NO emissions for the two cases undoubtably result from changes in the mixing pattern caused by interactions of the primary and swirling secondary streams. The relative intensity of the secondary swirl and the primary velocity determines the extent of mixing between the primary and secondary stream.

At low primary velocities, the primary stream initially withstands the swirling secondary flow, and the streams mix only enough to attach the flame to the burner. The secondary stream does not penetrate into the region of combusting volatiles, but forms an annulus around the primary stream. This annulus confines the radial expansion of the primary stream (which contains the fuel) and creates a fuel-rich central core. Thus, the primary stream partially devolatilizes and reacts in a fuel-rich environment, isolated from the oxygen-

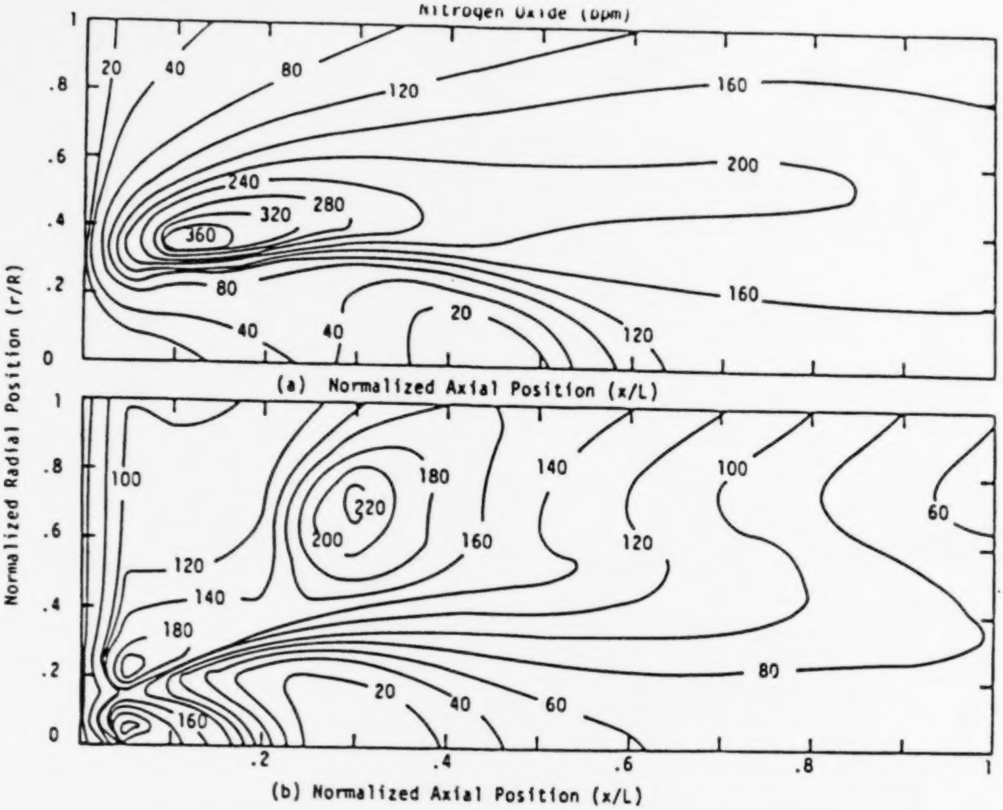

Figure 10. Comparison of predicted NO concentrations for the base case (a) and the case with the conditions used to reduce NO emissions (b).

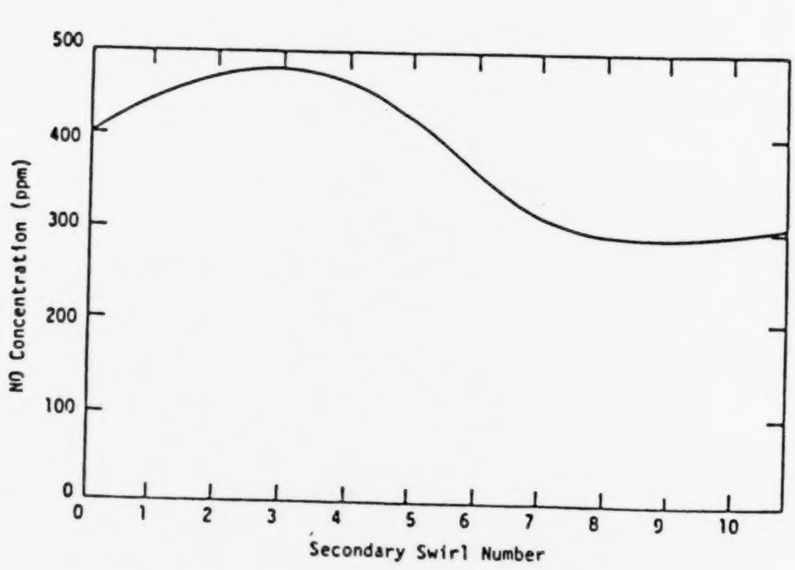

Figure 11. Effect of secondary swirl number on predicted NO concentration for increased primary velocity.

rich secondary stream. As swirl of the secondary stream is increased, the primary stream decays, and mixing of these streams is enhanced. This increases contact of the volatiles and oxidizer, and subsequently increases NO formation.

At higher primary velocities, the primary stream initially withstands the swirling secondary flow, and the high velocity causes the flame to detach from the burner. As swirl of the secondary stream is increased, mixing of the primary and secondary streams gradually increases. At first, the increased mixing increases NO formation. Eventually the flame attaches to the burner, and creates a fuel-rich core similar to that described above. This results in reduced NO formation, and the effect is similar to that shown in Fig. 12. The fuel-rich central core created by the swirling secondary stream tends to decay more rapidly at low primary velocities. This is consistent with the visual observation that in flames with low primary velocities, swirl of the secondary stream dominates flow of the primary stream.[22] Eventual decay of the primary stream results in large bushy flames from early mixing of the coal and oxidizer.

CONCLUSIONS

The agreement of NO model predictions with the observed effects of four key variables indicate that the NO model can give insight into NO_x formation in pulverized coal systems. Agreement was good for comparisons of the effect of swirl for both the subbituminous and bituminous coal flames, and the model predicted the initial decrease followed by a gradual increase in NO emissions as observed with these particular coal flames. In other computations, the use of swirl was shown to mutually increase NO emissions, which has also been observed experimentally for other test conditions. Comparisons of the predicted and measured effect of stoichiometric ratio on NO emissions were reasonable, especially at lower values. At higher values, the model underpredicted NO emissions partially because of the increase in thermal NO levels which is not considered in the model. The model predicts the observed increase in NO emissions with a decrease in particle size and with higher coal moisture content.

Variation of NO emissions to reactor configuration and operating parameters was investigated. Predictions indicate that NO emissions are relatively insensitive to inlet configuration such as primary and secondary diameter. These predictions are generally consistent with trends observed experimentally, but results cannot be generalized to other combustor systems, coals or operating conditions. A computation also illustrated the use of the model in reducing NO_x emission. In this case, a three-fold reduction in NO emissions was achieved (to 56 ppm)while predicted coal burnout increased from 76% to 88%.

ACKNOWLEDGEMENTS

This work was supported by the U.S. Department of Energy, Morgantown Energy Technology Center under contract DE-AC21-80MC14368 with Mr. V. Kothari, Project Officer. The authors also acknowledge the assistance of Lynda Richmond and Dan Gleason in preparing the manuscript and illustrations.

REFERENCES

1. Chen, G.T., Shang, J.Y. and Wen, C.Y., "NO_x Emission from Combustors: A State-of-the-Art Review," DOE Report, DOE/MC/11284-166, Contract No. AM21-79MC11284 (1981).

2. Hayhurst, A.N. and Vince, I.M., "Nitric Oxide Formation from N_2 in Flames: The Importance of 'Prompt' NO," Prog. Energy Combust. Sci., 6, 35 (1980).

3. Wendt, J.O.L., "Fundamental Coal Combustion Mechanisms and Pollutant Formation in Furnaces," Prog. Energy Combust. Sci., 6, 201 (1980).

4. Beér, J.M., Sarofim, A.F. and Lee, Y.Y., "NO Formation and Reduction in Fluidized Bed Combustion of Coal," J. Inst. Energy, 54, 38 (1981).

5. Hill, S.C., "Modeling of Nitrogen Pollutants in Turbulent Pulverized-Coal Flames," Ph.D. Dissertation, Brigham Young University, Provo, UT (1983).

6. Smith, P.J., Hill, S.C. and Smoot, L.D., "Theory for NO Formation in Turbulent Coal Flames," 19th Symposium (International) on Combustion, The Combustion Institute, Pittsburgh, PA, 1263 (1983).

7. Smith, P.J., Fletcher, T.H., and Smoot,l.D., "Two-Dimensional Model for Pulverized Coal Combustion and Gasification," 18th Symposium (International) on Combustion, The Combustion Inst., Pittsburgh, PA, 1285 (1981).

8. Fletcher, T.H., "A Two-Dimensional Model for Coal Gasification and Combustion," PhD Dissertation, Chemical Engineering, Brigham Young University, Provo, UT (1983).

9. Sloan, D.G., "Modeling of Swirl in Turbulent Systems," PhD Dissertation, Chemical Engineering Department, Brigham Young University, Provo, UT (1985).

10. Heap, M.P., Corley, T.L., Kau, C.J., and Tyson, T.J., "The Fate of Fuel Nitrogen--Implications of Combustor Design and Operation," Energy and Environmental Research Corp., Hemisphere Pub. Corp., Washington, D.C. (1978).

11. Takagi, T., Tatsumi, T. and Ogasaward, M., Combustion and Flame, 35, 27 (1979).

12. Harding, N.S., Smoot, L.D. and Hedman, P.O., "Nitrogen Pollutant Formation in a Pulverized Coal Combustor: The Effect of Secondary Stream Swirl," AIChE Journal, 28, 573-580 (1982).

13. DeSoete, G.G., "Overall Reaction Rates of NO and N_2 Formation from Fuel Nitrogen," 15th Symposium (International) on Combustion, The Combustion Institute, Pittsburgh, PA, 1093 (1975).

14. Levy, J.M., Chen, L.K., Sarofim, A.F., and Beér, J.M, "NO/Char Reactions at Pulverized Coal Flame Conditions," 18th Symposium (International) on Combustion, The Combustion Institute, Pittsburgh, PA, 111 (1981).

15. Bilger, R.W., Combustion and Flame, 30, 277 (1978).

16. Fenimore, C.P. and Fraenkel, H.A., Eighteenth Symposium (International) on Combustion, The Combustion Institute, p. 143 (1981).

17. Asay, B.W., Smoot, L.D., and Hedman, P.O., "Mixing Control of NO Formation and Burnout for Pulverized Coals," Comb. Sci. Tech., 35, 15 (1983).

18. Rees, D.P., Smoot, L.D., and Hedman, P.L., "Nitrogen Oxide Formation Inside a Laboratory Pulverized Coal Combustor," 18th Symposium (International) on Combustion, The Combustion Institute, Pittsburgh, PA, 1305 (1981).

19. Lee, J.W., Chen, S.L., Pershing, D.W., and Heap, M.P., "Pollutant Production in Pulverized Coal Flames: The Effect of Coal Characteristics," Western States Section/Combustion Institute, Brigham Young Univ., Provo, UT (1979).

20. Michel, J.B., and Payne, R., "Detailed Measurements of Long Pulverized Coal Flames for the Characterization of Pollutant Formation," IFRF Document No. F-09/a/23, Ijmuiden, Holland (December 1980).

21. Pershing, D.W., and Wendt, J.O.L., "Pulverized Coal Combustion: The Influence of Flame Temperature and Coal Composition on Thermal and Fuel NO_x," 16th Symposium (International) on Combustion, The Combustion Institute, Pittsburgh, PA, 389 (1977).

22. Wendt, J.O.L., and Pershing, D.W., "Physical Mechanisms Governing the Oxidation of Volatile Fuel Nitrogen in Pulverized Coal Flames," Comb. Sci. Tech, 16, 111 (1977).

23. Heap, M.P., Lowes, T.M., and Walmsley, R., "Emission of Nitric Oxide from Large Turbulent Diffusion Flames," 14th Symposium (International) on Combustion, The Combustion Institute, Pittsburgh, PA, 883 (1973).

24. Heap, M.P., Lowes, T.M., and Walmsley, "The Effect of Burner Parameters on Nitric Oxide Formation in Natural Gas and Pulverized Fuel Flames," AFRC/EPA American Flame Days, Chicago, IL (1972).

25. Seeker, W.R., Samuelsen, G.S., Heap, M.P., and Trolinger, J.D., "The Thermal Decomposition of Pulverized-Coal Particles," 18th Symposium (International) on Combustion, The Combustion Institute, Pittsburgh, PA, 1213 (1981).

26. Gershman, R.E., Heap, M.P., and Tyson, T.J., "Design and Scale-Up of Low Emission Burners for Industrial and Utility Boilers," Proceedings of the Second Stationary Source Combustion Symposium, 5, Addendum EPA 600/7-77-073e (July 1977).

27. Hill, S.C., Smoot, L.D., and Smith, P.J., "Prediction of Nitrogen Oxide Formation in Turbulent Coal Flames," 20th Symposium (International) on Combustion, The Combustion Institute, Ann Arbor, MI (1984).

28. Brown, R.A. Mason, H.B., Pershing, D.W. and Wendt, J.O.L., "Investigation of First and Second Stage Variables on Control of NO_x Emissions in a Pulverized Coal Furnace," 83rd National Meeting AIChE, Houston, TX (1977).

29. Heap, M.P., Lowes, T.M., Walmsley, R., and Bartelds, H., "Burner Design Principles for Minimum NO_x Emissions," EPA Coal Combustion Seminar, Research Triangle Park, NC (1973).

30. Wendt, J.O.L., "Process Modifications for NO_x Control in Pulverized Coal Combustion Systems," METC Final Report, University of Arizona, Tuscon, AZ (January 4, 1983).

OPTIMIZED LOW-NO_x PULVERIZED COAL COMBUSTION BY ZONE CONTROL

Ken Okazaki and Kazutomo Ohtake
Toyohashi University of Technology
Department of Energy Engineering
Tempaku-cho, Toyohashi
440 Japan

ABSTRACT

Zone control method is one of the most effective technologies to minimize the NO_x formation in the pulverized coal combustion furnace. In order to get the fundamental and general concept for the optimization of low-NO_x pulverized coal combustion by zone control, first, separated influences of various basic factors affecting NO formation behaviors have been derived by use of a one-dimensional combustion furnace. And next, an optimal condition for zone control method were investigated by the experiments of one-dimensional multi-stage combustion.

These experimental investigations have led to the following important results. The NO formation rate in the early stage of combustion process increases with the oxygen-fuel stoichiometric ratio for large particles and decreases with the particle size, and less effect by the stoichiometric ratio appears for small particles. The conversion ratio from fuel N to NO decreases with the nitrogen content and increases with the stoichiometric ratio especially for high volatile coals, and temperature has little effect on it except for fuel rich condition for high volatile coals. As for the zone control, most effective reduction of NO was attained by setting the reduction zone just after the initial NO formation zone and the oxygen-fuel stoichiometric ratio of 0.8 is preferable for the effective reduction of NO without increases of unburnt materials.

INTRODUCTION

Development of the technologies to attain the high combustion efficiency without deterious pollutant esmissions is one of the keys for modern pulverized coal combustion systems. Complicated phenomena related with thermodynamic, aerodynamic and physicochemical behaviors make the pulverized coal combustion field rather difficult to be analyzed. Among various pollutants from pulverized coal combustion systems, NO_x formation behavior is the most entangled problem between these factors and makes itself difficult to be understood.

Pulverized coal combustion mechanism (1-5) and its NO_x formation process (6-11) have been investigated in some detail, and several recent studies (9-11) have found out some important features of NO_x formation in pulverized coal flames. In spite of those energetic studies, details of combustion and NO_x formation mechanisms of pulverized coal are still not so clear as to give general concepts of low-NO_x emissions for various different burning conditions, burner types and combustor scales.

In this study by use of a one-dimensional laminar flow furnace, first, the most fundamental and general features of NO_x formation in pulverized coal flames are investigated through discriminating between the interacting effects of particle size, nitrogen and volatile matter contents of coal, oxygen-fuel stoichiometric ratio and temperature of NO_x formation. Next, optimization of NO_x reduction in the furnace by zone control method is investigated by setting the reduction and oxidation zones one-dimensionally in the furnace.

Characteristics of NO_x formation discussed in this study can be considered corresponding to that of fuel NO_x even for the use of air as oxidant because almost 90% of total NO_x formed in the pulverized coal flame is due to fuel nitrogen (6).

EXPERIMENTAL SYSTEM AND PROCEDURE

A schematic of the combustion furnace and its flow system is shown in Fig. 1. This combustor is so arranged that phenomena in the furnace change one-dimensionally along the downward flow direction. The mixture of coal dust and air enters into the combustion furnace through a cooling grid, which traps the thermal radiation from the furnace below. The furnace is 2 m in length, 14 cm in inner diameter and constructed with heat insulating porous fire bricks and outer insulating boards. Observation and sampling ports are situated along the flow direction for sampling of gaseous components and particles as shown in Fig. 1. Pt/Pt-Rh 13% thermocouples set inside the protection tubes are equipped for flame temperature measurements. In all experiments, combustion was self-sustained, and the one-dimensionality of flame was confirmed by radial profiles of temperature and concentrations of O_2, HC (total hydrocarbon) and NO at various axial positions.

After heating up the brick of the furnace by a propane-air flame, the pulverized coal-air mixture was fed. Measurements were started after steady state temperature was established. The feeding rate of coal was in the order of 5 kg/h and the residence time was about one second in this furnace. Gas and solid particles were samled out through the sampling ports along the center axis of the furnace with a water-cooled sampling probe equipped with a filter chamber. The solid samples were proximately analyzed through the procedure defined by JIS standard for volatile matter, fixed carbon and ash. The gaseous samples were analyzed using standard continuous instrumentations (chemiluminescent NO, paramagnetic O_2 and FID total hydrocarbon) and a gas chromatograph.

Ultimate and proximate analyses of nine kinds of coals used in these experiments are given in Table 1. Coal A was mainly used and other coals of B - H were used in the case of examining the effects of coal properties. Coal P was used in the experiments of multi-stage combustion.

COMBUSTION HISTORY

The representative profiles of flame temperature, volatile matter content (VM) remained in the burning particles and concentrations of O_2, NO and HC along the center line of the furnace are shown in Fig. 2. The concentrations of HC qualitatively corresponds to that of evolved but unburned volatile matter. The combustion history shown in this figure is explained in detail in our paper (11). NO formation rate is largest in the stage of the largest volatile matter consumption and this corresponds to the fact that NO formed in pulverized coal combustion is mainly due to volatile NO converted from fuel N contained in the volatile matter (6).

NO FORMATION BEHAVIORS IN THE FURNACE

NO formation behaviors in the furnace obtained are shown in Fig. 3 (a and b). In these figures, oxygen consumption ratio ψ is used as abscissa to make clear the separated effect of experimental parameters. The NO concentrations are expressed as those at 0% excess air.

When the particle size is small enough, as shown in Fig. 3a, oxygen-fuel stoichiometric ratio has no significant effects on the NO formation rate in the early stage of combustion process of $\psi < 0.7$, though the final amount of NO increases with the higher stoichiometric ratio. On the other hand, when the particle size is relatively large, as shown in Fig. 3b, the higher stoichiometric ratio makes the NO formation rate larger. These phenomena can be well explained by the theoretical results in Ref. 11, as follows. For small particles, the combustible materials are consumed almost on the particle surface or in the pores of particles and the stoichiometric ratio has an effect only on the number density of particles in the early stage of combustion process. For relatively large particles, on the contrary, a significant effect of stoichiometric ratio appears because the relatively large amount of gas phase reactions take place apart from the particle surface.

Under the same stiochiometric ratio of 1.1, the smaller particles show larger NO formation rate in the early stage of combustion process. This result can be explained by taking the fact into consideration that volatile N in the coal might be bound mainly in the heavy volatile matter with relatively high evaporation temperature (12).

CONVERSION RATIO FROM FUEL N TO NO

Conversion ratio (CR) is defined as the ratio of NO concentration at the exit of the furnace to that of 100% conversion from fuel N. The concentration of thermal NO is relatively small in these experimental conditions (6) and is not counted in this study. The individual effects of various factors on the conversion ratio are systematically and separately derived in this chapter.

Effects of Coal Properties

Conversion ratios to NO were obtained by the experiments for eight kinds of coals of A - H in Table 1 at the same condition of $T_{max} = 1500^{\circ}C$ and $\lambda = 1.2$. Effect of volatile matter content (dry base) on the conversion ratio is shown in Fig. 4. This figure clearly shows that larger volatile matter content makes the conversion ratio to NO larger under the excess oxygen condition except for coal D. The increase of the conversion ratio to NO by the volatile matter could be due to larger conversion from fuel N to gas-phase nitrogen species (for example, NO, HCN, NH_3). However, these coals have different N content as shown in Table 1 and so, Fig. 4 includes not only the effect of volatile matter, but also that of N content. The single effect of N content in the coal on the conversion ratio to NO is shown in Fig. 5. The solid line in this figure is drawn by the Fenimore's equation (13) for the gas fuel NO formation given as

$$[NO]/X = 1 - \exp\{-([NO] + [N])/2X\} \qquad (1)$$

Fig. 5 dramatically shows, including coal D, that the larger the N content, the smaller becomes the conversion ratio and the influence of fuel N is similar as that of the flames of gaseous fuel (13). [N] and X in Eq. (1) mean the NO concentration of 100% conversion from fuel N and the parameter characteristic to the flame, respectively. The value of 1288 ppm for X adopted in Fig. 5 corresponds to that for the fuel rich condition of gas flame (13), and this implies that the conversion of fuel N to NO mainly occurs at the fuel rich zone near the particle surface or in the pores of particles as shown in the theoretical analysis of flame structure (11).

Effects of Stoichiometric Ratio and Temperature

The furnace shown in Fig. 1 was reformed to fit the experimental requirements to a little smaller one and the time interval to the steady state temperature after the change of combustion condition was shortened to about 15 minutes. Propane was fed at a very small rate to stabilize the one-dimensional flame in the furnace. Flame temperature was varied by changing the oxygen content in the oxidant as 23% (air), 26% and 29% by weight. Coal A and E were used in these experiments. Maximum flame temperatures (Tmax) and conversion ratios (CR) to NO under various conditions were measured and, connecting these results, the separated effects of oxygen-fuel stoichiometric ratio and maximum temperature on the conversion ratio could be extracted.

The effect of stoichiometric ratio on conversion ratio is shown in Fig. 6. Conversion ratio increases with the stoichiometric ratio for both coals of A and E, although the dependency is much stronger for coal A. The volatile matter content of coal A is larger than that of coal E, and the ratio of volatile N to total fuel N in the coal can be also considered in this order. So the conversion of fuel N to the gas phase N-species such as NO, HCN and NH_3, the fraction of which largely depends on stiochiometric ratio, especially under the fuel rich conditions, is also larger for coal A. On the other hand, for coal E of lower volatile matter content, the ratio of char N remained in the particle is larger and the rate of char NO formation does not significantly depend on the overall stoichiometric ratio. For the extreme fuel rich condition of $\lambda < 0.8$, the conversion ratio of coal A becomes smaller than that of coal E, and this result is due to the fact that the strong volatile evolution of coal A would suppress the local oxygen availability to form NO and provide a path to HCN and NH_3 (10), and also N_2.

The effect of maximum flame temperature on the conversion ratio to NO is shown in Fig. 7. The conversion ratio slightly increases with the temperature. However, for coal A of high volatile matter content, the large dependency appears under fuel rich conditions. This is due to the decrease of NO fraction in the gas phase N-species and the increase of HCN and NH_3 with the decreasing temperature (14).

Formulation of Conversion Ratio

Based on the experimental results shown in Figs. 6 and 7, the following formula to predict the conversion ratio to NO by the nitrogen and volatile matter contents in the raw coal, stiochiometric ratio and temperature has been obtained by multi-valuable regression algorithm (15),

$$CR = 0.2522 - 0.1755 \cdot N + 0.0005065\ VM^2 \cdot \ln \lambda + 0.0002230 \cdot Tmax \qquad (2)$$

where, VM and N are the volatile matter and nitrogen contents in the raw coal by weight percent and Tmax is the maximum flame temperature by $^{\circ}C$. This formula includes all the effects of VM, N, λ and Tmax on the conversion ratio. The third term in the right-hand side of Eq. (2) represents that the contribution of volatile matter content to the conversion ratio is positive for $\lambda > 1$ and negative for $\lambda < 1$. This expression clearly shows the representative features obtained in Fig. 6 and also agrees well with the results shown in Figs. 4 and 5.

The comparison between measured conversion ratios obtained for eight kinds of coals A - H under various combustion conditions and those calculated by Eq. (2) is shown in Fig. 8. This result implies that Eq. (2) is valid for relatively wide range of nitrogen and volatile matter contents, stoichiometric ratio and temperature.

ONE-DIMENSIONAL MULTI-STAGE COMBUSTION

For the purpose of finding out the optimal zone control of reduction and oxidation zones in the furnace, experiments of one-dimensional multi-stage combustion were performed (16). Injection rings for the injection of propane or oxygen into the furnace were equipped at three positions of L = 0.3 m (No. 1), 0.6 m (No. 2) and 1.2 m (No. 3) below the radiation shielding grid. Initial oxygen-fuel stoichiometric ratio (λ_1) was fixed to be 1.2 in all experiments. Propane was injected from the ports of No. 1 or No. 2 to make the reduction zone in the furnace and effects of this zone on the reduction behaviors of NO were investigated.

Reduction Zone After Initial NO Formation

First, NO reduction behaviors were examined by propane injection at the port of No. 2 and changing the second-stage stoichiometric ratio (λ_2) to be 1.2 (no injection), 1.0, 0.8 and 0.6. The profiles of conversion ratio of fuel N to NO in the furnace are shown in Fig. 9 with flame temperatures, and concentration profiles of O_2, HC and CO are shown in Figs. 10, 11 and 12. From Fig. 9, we can find that this case corresponds to the propane injection just after the initial NO formation process. The final value of CR in the case of no propane injection is 0.396, which agrees very well with the predicted value calculated by Eq. (2). Even in the case of no propane injection, CR slightly decreases after its peak and this is due to the NO reduction by char with existence of CO near char particles. For $\lambda_2 < 1.0$, CR largely decreases after the propane injection and very low value of CR near 0.1 is attained for the case of $\lambda_2 = 0.6$. Figs. 10, 11 and 12 clearly show the existence of stronger reduction zone after propane injection for the lower value of λ_2.

Dependencies of the conversion ratio and concentrations of O_2, CO, HC and CO_2 at the exit of the furnace on the second-stage stoichiometric ratio λ_2 are shown in Fig. 13. The conversion ratio comes to be small as λ_2 decreases and the reduction rate of CR is largest from $\lambda_2 = 1.0$ to 0.8. From $\lambda_2 = 0.8$ to 0.6, the reduction ratio is not so large, which could be explained as that the decrease of CO_2 would supress the further increase of CO and then the increase of reducing effect of this zone.

Reduction Zone During Initial NO Formation

In order to examine the effect of injection position on the NO reduction behaviors, experiments were also performed by propane injection at the former position of No. 1 port (L = 0.3 m). For this case, profiles of conversion ratio and concentrations of O_2, CO and HC in the furnace are shown in Figs. 14, 15, 16 and 17, respectively. From Fig. 14, we can find that the propane is injected during initial NO formation process before its peak. Fig. 18 shows the comparison of final CR and NO reduction ratio between two cases of L = 0.3 m and 0.6 m. Though the peak value of CR in Fig. 14 decreases as λ_2 comes to be smaller, the final conversion ratios are almost the same as those in Fig. 9 for $\lambda_2 = 1.2$, 1.0 and 0.6. On the contrary, the conversion ratio for $\lambda_2 = 0.8$ is higher than that of Fig. 9. This result is considered to be due to relatively weak reducing condition even for $\lambda_2 = 0.8$ by the existence of O_2 during the initial combustion process, which could be supported by the results shown in Figs. 15, 16 and 17.

Oxidation Zone After NO Reduction Zone

Effects of oxygen injection after NO reduction zone are investigated by propane injection at No. 2 port and oxygen injection at No. 3 port (L = 1.2 m). The results for coals P, A and H are shown in Figs. 19, 20 and 21, respectively. These three types of coals have much different properties as shown in Table 1. Coal P has high contents of both volatile matter and nitrogen, coal A is a high volatile and low nitrogen coal and coal H is a low volatile and high nitrogen coal. In each case, the conversion ratio comes to be large again after oxygen injection. Though the final value of conversion ratio for coal P comes up to the level in the case without zone control, the final values of conversion ratio for coals A and H is much smaller than those in the case without zone control. These differences of the effectiveness of zone control, depending on coal properties, are considered to be due to the differences of fuel-nitrogen evolution process along the combustion process by the coal type. The real optimization of zone control for the effective NO reduction in the furnace needs further investigations including the effect of coal properties.

CONCLUSIONS

The following conclusions have been derived on the separated influences of the basic factors on NO formation behaviors and on the NO reduction behaviors by zone control in the one-dimensional pulverized coal combustion.

1) The oxygen-fuel stoichiometric ratio enhances the NO formation rate in the early stage of combustion process for large particles, while the effect is not so significant for small particles. Under the same stoichiometric ratio, NO formation rate is larger for the smaller particles than for the larger, and this implies that volatile N is unevenly bounded to heavy volatile matter.

2) The conversion ratio from fuel N to NO decreases with the N content in the raw coal and is well expressed by Fenimore's equation by adopting an appropriate value of the flame parameter. The conversion ratio increases with the volatile matter content in the raw coal under the excess oxygen condition.

3) The conversion ratio to NO increases with the stoichiometric ratio, and the dependency is much larger for high volatile coals than for low volatile coals. This is due to the fact that the stoichiometric ratio largely affects the fractions of gas phase N-species of NO, HCN and NH_3, especially for high volatile coals.

4) The conversion ratio from fuel N to NO slightly increases with the flame temperature. However, for high volatile coals, the dependency comes to be large under the fuel rich condition. This is due to the decrease of NO fraction in the gas phase N-species with decreasing temperature.

5) The conversion ratio from fuel N to NO in the pure combustion field without turbulent mixing process is well expressed by Eq. (2) as a function of stoichiometric ratio, temperature and contents of nitrogen and volatile matter in the raw coal.

6) Final concentration of NO at the exit of furnace could be largely reduced by zone control of reduction and oxidation zones. The most effective reduction of NO was attained by the fuel injection just after the initial NO formation process and the optimal fuel-oxygen stoichiometric ratio of the reduction zone is likely to be about 0.8.

NOMENCLATURE

CR = conversion ratio from fuel N to NO
dm = mean particle diameter, μm
L = injection point of the furnace, m
T = temperature, $^{\circ}C$
VM = volatile matter content, %
λ = oxygen-fuel stoichiometric ratio
ψ = oxygen consumption ratio

ACKNOWLEDGMENT

The authors would like to express their appreciation to A. Yuki, T. Nishikawa, H. Shishido, S. Watanabe, M. Ono and M. Ohya for their great help in the experiments.

This study was partly supported by the Grant-in-aid for Energy Research of Ministry of Education, Science and Culture of Japan.

REFERENCES

1. Howard, J.B. and Essenhigh, R.H., 11th Symp. (Int.) on Comb., p. 399, (1967).

2. Essenhigh, R.H., Chemistry of Coal Utilization, Second Supplementary Volume (M.A. Elliot, Ed.), Chap.]9, p. 1153, John Wiley & Sons, (1981).

3. Smoot, L.D. and Horton, M.D., Progress of Energy Comb. and Sci., Vol. 3, p. 235, (1977).

4. Timothy, L.D., Sarofim, A.F., and Beer, J.M., 19th Symp. (Int.) on Comb., p. 1123, (1982).

5. Kobayashi, H., Howard, J.B. and Sarofim, A.F., 16th Symp. (Int.) on Comb., p. 411, (1982).

6. Pershing, D.W. and Wendt, J.O.L., I & EC Process Design and Development, Vol. 18, No. 1, (1979).

7. Wendt, J.O.L., Progress of Energy Comb. and Sci., Vol. 6, p. 201, (1980).

8. Pohl, J.L., and Sarofim, A.F., 16th Symp. (Int.) on Comb., p. 491, (1977).

9. Smith, P.J., Hill, S.C., and Smoot, L.D., 19th Symp. (Int.) on Comb., p. 1263, (1982).

10. Chen, S.L., Heap, M.P., Pershing, D.W. and Martin, G.B., 19th Symp. (Int.) on Comb., p. 1271, (1982).

11. Okazaki, K., Shishido, H., Nishikawa, T., and Ohtake, K., 20th Symp. (Int.) on Comb., (1984).

12. Blair, D.W., Wendt, J.O.L., and Bartok, W., 16th Symp. (Int.) on Comb., p. 475, (1977).

13. Flagan, R.C., Galant, S., and Appleton, J.P., Comb. and Flame, Vol. 22, p. 299, (1974).

14. Takagi, T., Tatsumi, T., and Ogasawara, M., Comb. and Flame, Vol. 35, p. 17, (1979).

15. Shishido, H., Okazaki, K., and Ohtake, K., 18th Autumn Meeting of the Society of Chemical Engineers, Japan, p. 92, (1984).

16. Shishido, H., Okazaki, K., and Ohtake, K., 22nd Japan Symp. on Comb., (1984).

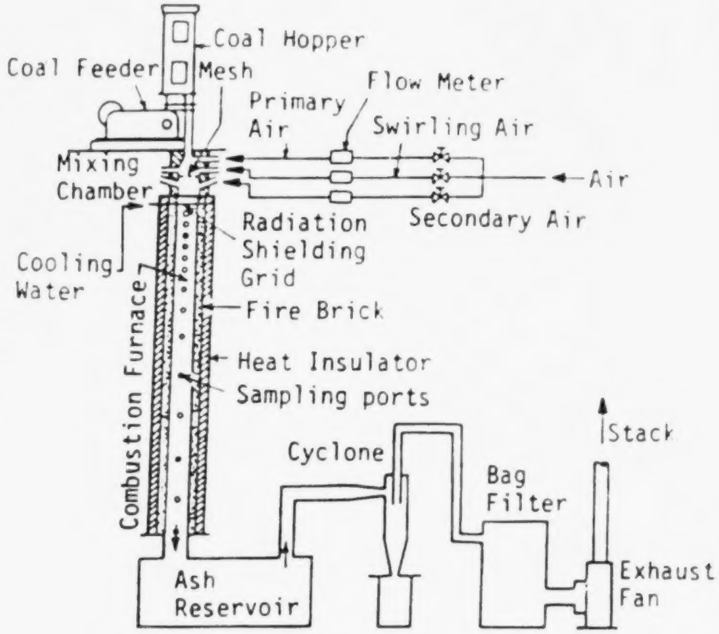

Coal Hopper
Coal Feeder
Mesh
Flow Meter
Primary Air
Swirling Air
Mixing Chamber
Air
Radiation Shielding Grid
Secondary Air
Cooling Water
Fire Brick
Combustion Furnace
Heat Insulator
Sampling ports
Stack
Cyclone
Bag Filter
Ash Reservoir
Exhaust Fan

Figure 1: Experimental Apparatus

: one-dimensional furnace
: furnace length 2 m
: inner diameter of the furnace 14 cm
: coal feed rate 3 - 5 kg/h

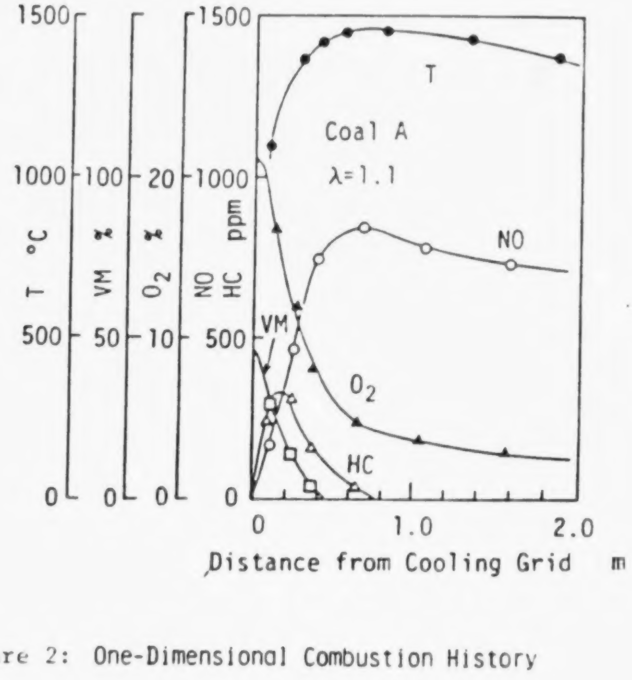

Figure 2: One-Dimensional Combustion History

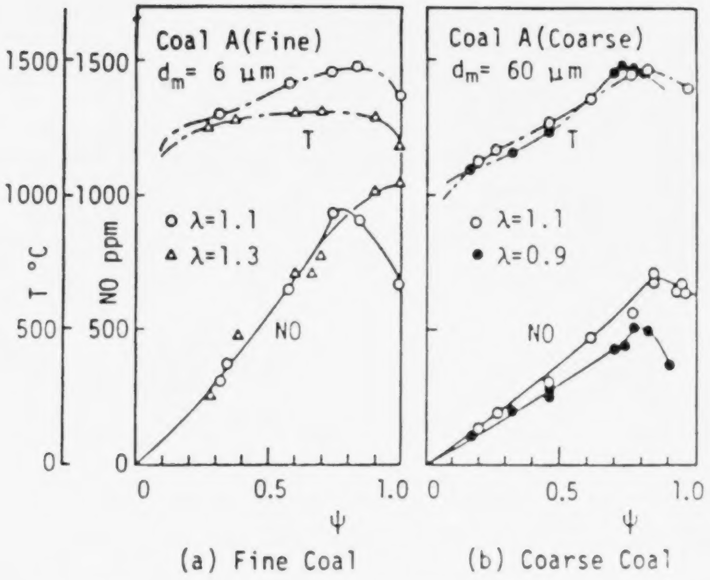

(a) Fine Coal (b) Coarse Coal

Figure 3: NO Formation Behaviors in the Combustion Process (effect of particle size and stoichiometric ratio)

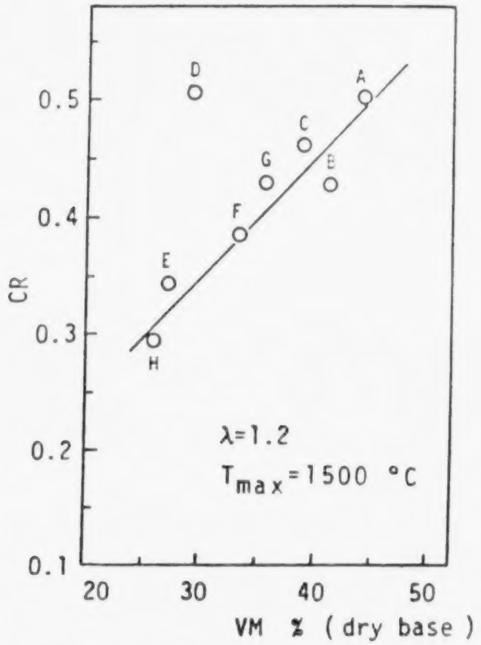

Figure 4: Effect of Volatile Matter Content on the Conversion Ratio from Fuel N to NO

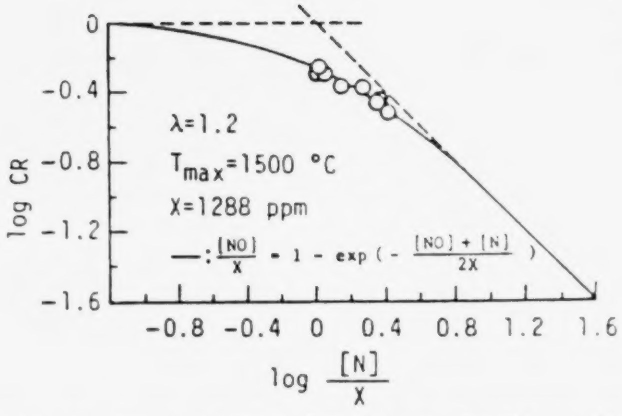

Figure 5: Effect of Nitrogen Content on the Conversion Ratio from Fuel N to NO

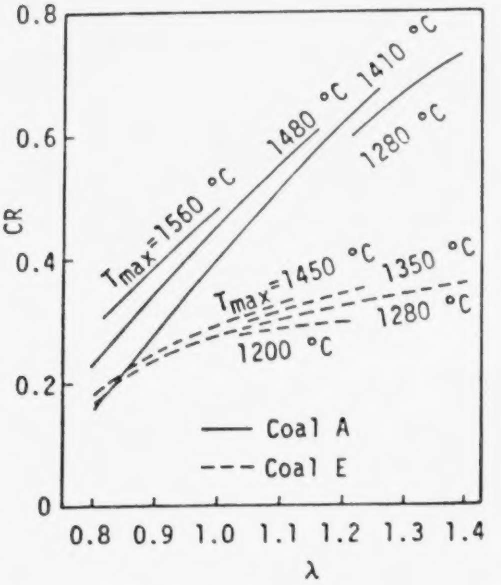

Figure 6: Effect of Oxygen-Fuel Stoichiometric Ratio on the Conversion Ratio from Fuel N to NO

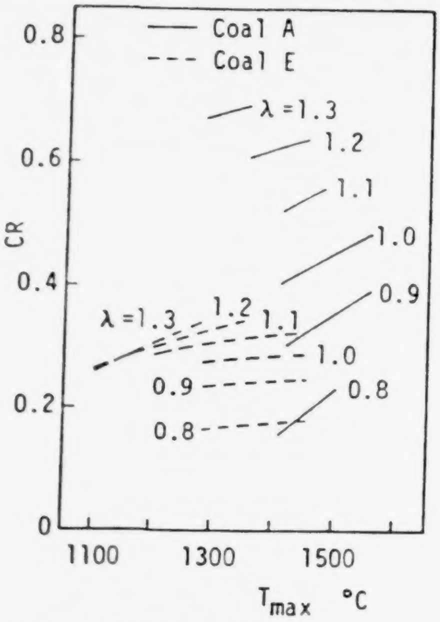

Figure 7: Effect of Maximum Flame Temperature on the Conversion Ratio from Fuel N to NO

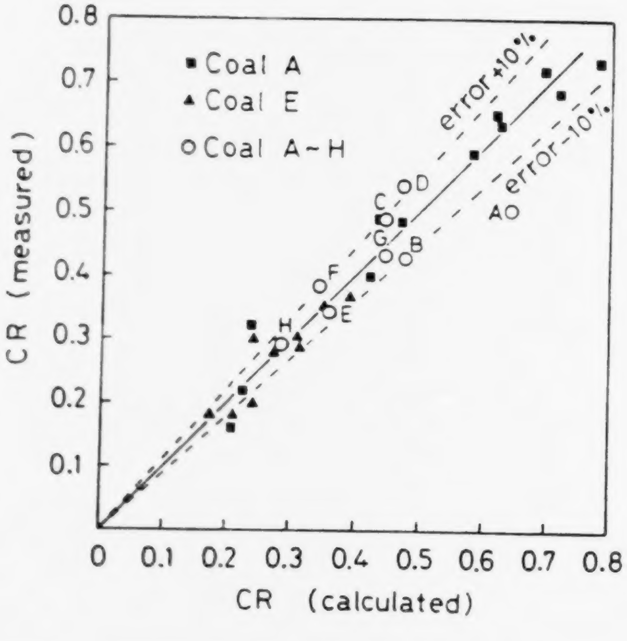

Figure 8: Correlation of Calculated and Measured Conversion Ratios from Fuel N to NO

$$CR = 0.2522 - 0.1755\ N + 0.0005065\ VM^2 \ln \lambda + 0.0002230\ T$$

N, VM : wt% (dry base), T : °C

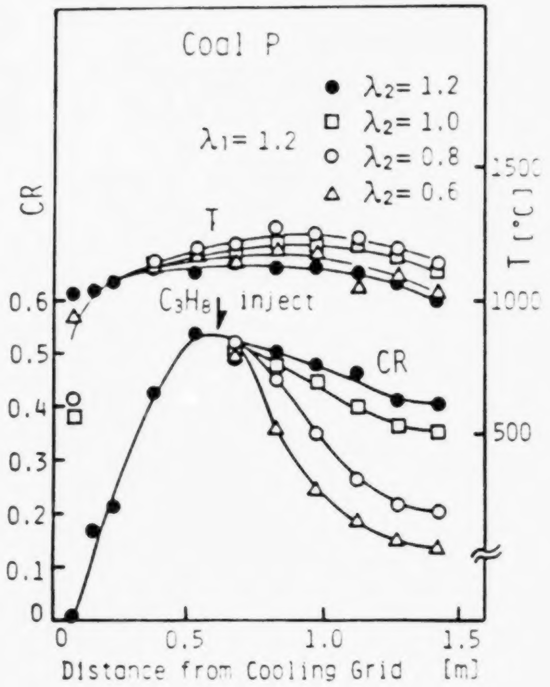

Figure 9: Conversion ratio and temperature in the furnace (reduction zone after initial NO formation process)

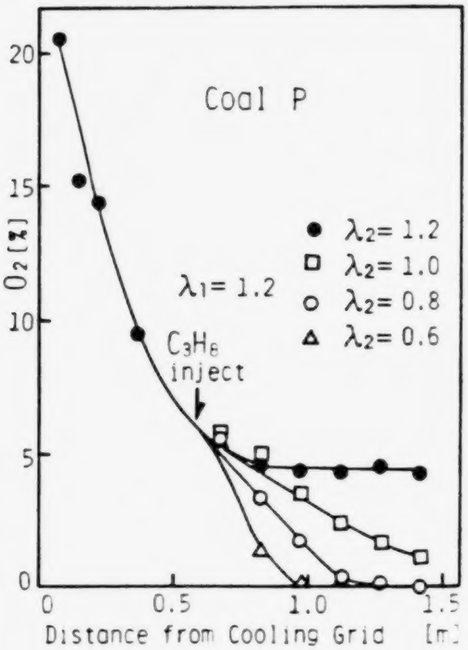

Figure 10: O_2 concentration in the furnace in the case of Fig. 9

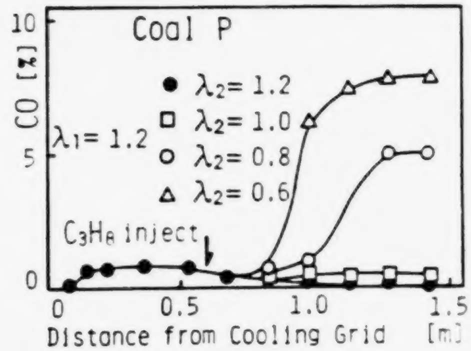

Figure 11: CO concentration in the furnace in the case of Fig. 9

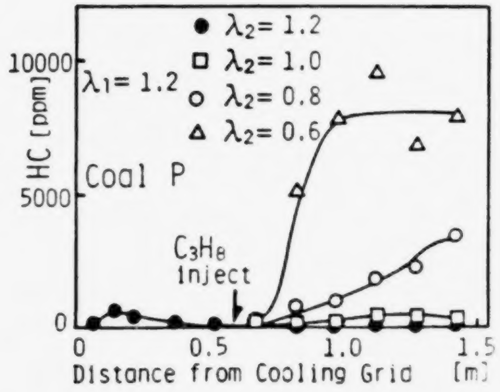

Figure 12: Hydrocarbon concentration in the furnace in the case of Fig. 9

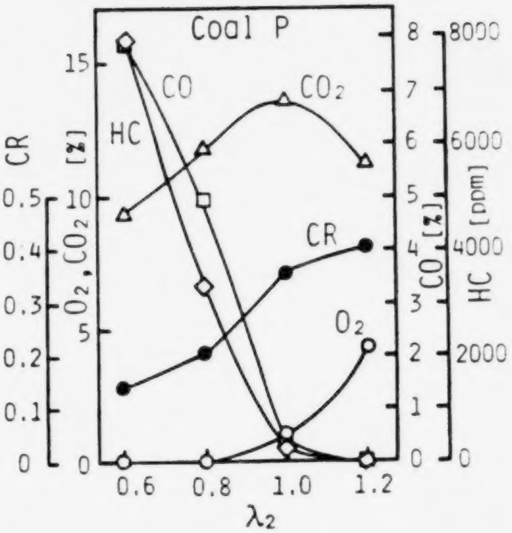

Figure 13: Dependencies of final conversion ratio and concentrations of O_2, CO, CO_2 and HC on the stoichiometric ratio of reduction zone (reduction zone after initial NO formation process)

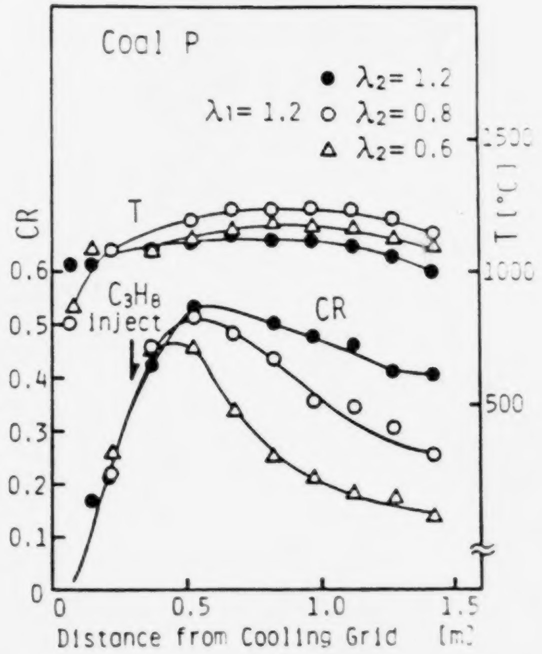

Figure 14: Conversion ratio and temperature in the furnace (reduction zone during NO formation process)

Figure 15: O_2 concentration in the furnace in the case of Fig. 14

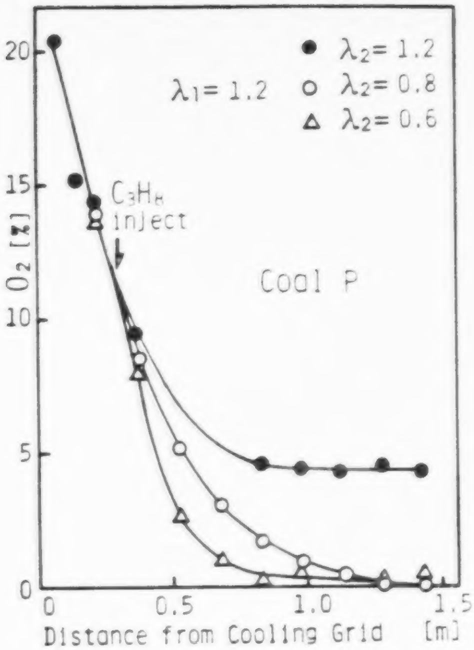

Figure 16: CO concentration in the furnace in the case of Fig. 14

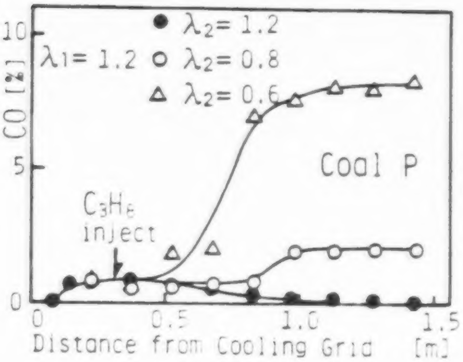

Figure 17: Hydrocarbon concentration in the furnace in the case of Fig. 14

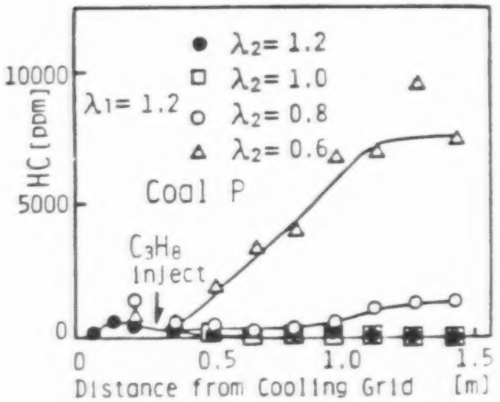

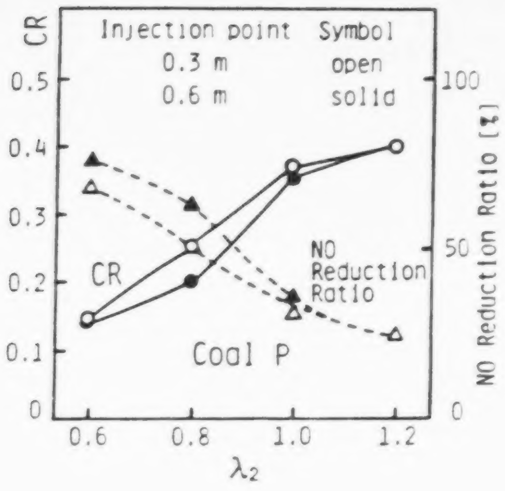

Figure 18: Dependencies of final conversion ratio and NO reduction ratio on the stoichiometric ratio of reduction zone (effect of the position of reduction zone)

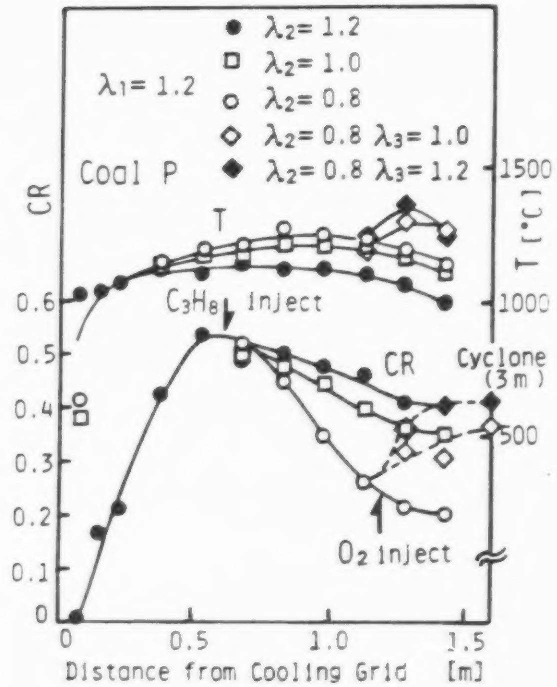

Figure 19: Conversion ratio and temperature in the furnace (effect of oxidation zone after reduction zone, coal P)

Figure 20: Conversion ratio and temperature in the furnace (effect of oxidation zone after reduction zone, coal A)

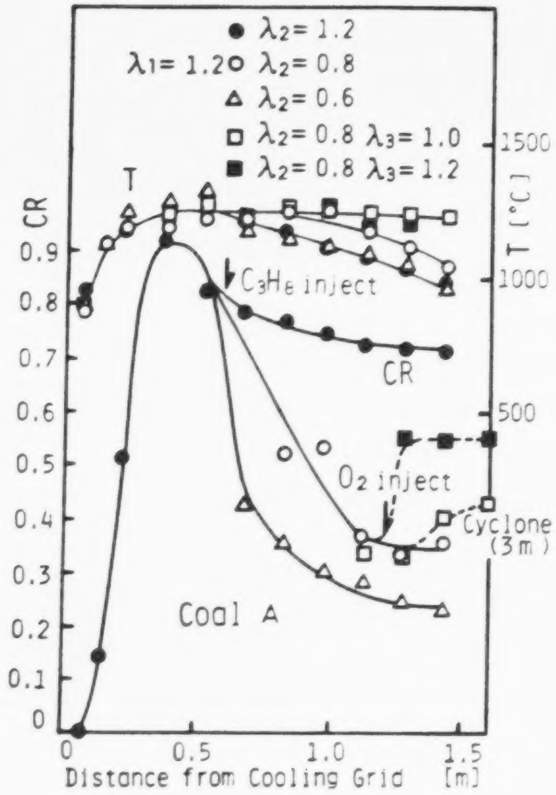

Figure 21: Conversion ratio and temperature in the furnace (effect of oxidation zone after reduction zone, coal H)

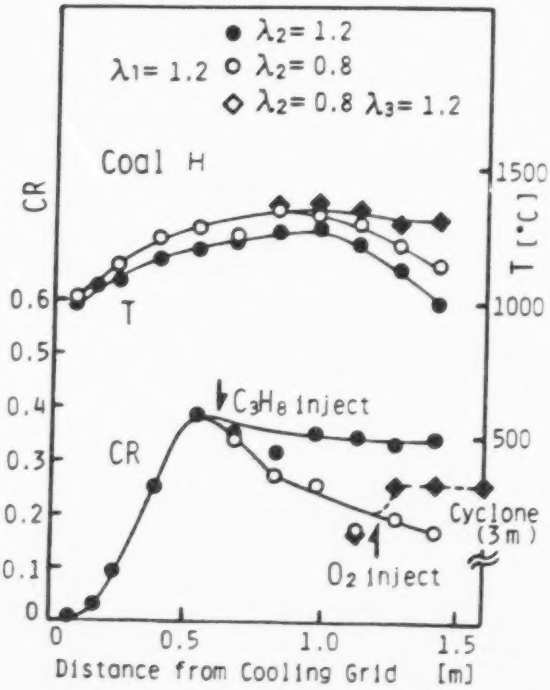

Table 1. Coal Properties

	Coal	Proximate Analysis(%)				Ultimate Analysis(%,dry)				
		M	Ash	VM	FC	C	H	O	N	S
Japan	A	5.5	14.9	42.0	37.6	65.4	5.47	12.5	0.79	0.21
	B	3.2	19.6	40.0	37.2	62.8	5.16	10.6	0.92	0.30
	C	1.4	17.7	38.5	42.4	67.0	5.0	7.4	0.66	2.7
China	D	5.8	7.8	27.8	58.6	77.3	3.98	9.0	0.79	0.70
Australia	E	4.4	10.1	26.1	59.4	73.6	4.08	9.8	1.60	0.35
	F	3.0	10.8	32.5	53.7	73.3	4.53	9.0	1.59	0.51
	G	3.7	8.8	34.3	53.2	75.2	5.04	8.8	1.48	0.38
South Africa	H	2.4	14.8	25.5	57.3	70.5	3.64	6.3	1.64	0.99
North America	P	5.3	9.5	38.6	46.6	71.4	5.3	10.9	1.50	0.74

M : Moisture, VM : Volatile Matter, FC : Fixed Carbon

Session VIIIb: Stationary Engines and Industrial Process Systems

Chairman, Joseph McSorley, EPA

UTILIZATION OF METHANOL AS FUEL FOR A GAS TURBINE COGENERATION PLANT

Dale E. Shore
Gary H. Shiomoto
KVB, Inc.
18006 Skypark Blvd.
Irvine, CA 92714

and

Gerald R. Bemis
California Energy Commission
1516 Ninth Street
Sacramento, CA 95814

ABSTRACT

A field test demonstration of the use of methanol in an industrial-sized gas turbine cogeneration unit was conducted in 1984 at the Central Heating Plant of the University of California at Davis. This program, sponsored by the California Energy Commission, was one of four full-scale demonstrations of the use of clean fuels in mobile and stationary engine applications. These demonstration programs were directed toward the evaluation of clean fuels potentially derived from coal, for meeting California's future energy needs.

A 3,250 kW Allison 501-KB gas turbine, designed originally for either natural gas or distillate fuel oil operation, was converted to methanol and operated for a total of 1036 hours. A methanol storage and handling facility for fueling the engine was designed and built on-site. Engine modifications specific to the utilization of methanol and preliminary test work of the specialized components were performed by the turbine manufacturer. The components were then installed on the engine and the unit was operated on methanol. Emissions and performance data were monitored throughout the test. The relatively low NO_x emissions expected from methanol operation were further reduced by the implementation of water injection via mixing with the methanol prior to supply to the engine. Engine operating problems attributable to methanol were not encountered during the demonstration testing, therefore engine performance was judged satisfactory. However difficulties of methanol pumping compatibility with the engine-driven, high-pressure fuel pump necessitated the use of an off-board centrifugal pump to complete the program.

Note: The use of company tradenames in this document does not constitute an endorsement of their products or services by the authors.

INTRODUCTION

Methanol is a clean fuel which can be synthesized from coal, and has the potential to be used in lieu of current petroleum liquids. Methanol is desirable because of its low pollution emission characteristics, which are in part due to the absence of ash, sulfur and nitrogen in its chemical composition. The clean burning attributes of methanol as a gas turbine fuel were shown previously in a program performed by the Southern California Edison Company (Weir, 1981). The present demonstration program is one of a series conducted for the California Energy Commission's clean coal fuel program, which includes testing of various fuel/engine combinations (Acurex, 1981). The clean coal stationary engine test program was performed to verify methanol as a technically viable gas turbine fuel. The primary objectives of the test were: (1) to demonstrate the safe, efficient and reliable use of methanol fuel in a typical, industrial-sized gas turbine engine over an extended period of time, (2) to document the clean burning, low air pollution emission characteristics of methanol, and (3) to utilize further low NO_x combustion techniques (water injection) to attain the program guideline of 0.1 microgram NO_x per Joule output approximately 40 ppm, dry at 15 percent O_2).

The test program was conducted by KVB, Inc. of Irvine, CA. The host test site was the gas turbine cogeneration facility located at the Central Heating Plant of the University of California at Davis (UCD). The Allison 501-KB engine with a generation capacity of 3,250 kW had originally been designed to operate on distillate oil, but had been recently converted to natural gas operation. The heat recovery boiler was rated at 20,000 lb/hr of saturated steam at 150 psig. Allison Gas Turbine Operations of the General Motors Corporation of Indianapolis, Indiana was contracted to design, fabricate and initially test the engine modifications required for methanol operation, as well as providing technical advice throughout the program. KVB was responsible for the design and fabrication of the methanol fuel forwarding, controls and safety systems, as well as performing the testing operations. The Celanese Chemical Company, Inc. of Dallas, Texas supplied the methanol and was responsible for its delivery to the test site.

RESULTS

Facility and Engine Modifications

The modifications for methanol operation entailed changes to the UCD facility and to the engine. The facility modifications included a new methanol storage facility, a new fuel forwarding system, a water purification and injection system, as well as additional fire detection, vapor detection and safety equipment. The engine modifications, termed the methanol kit, were fabricated by Allison and included a modified high-pressure fuel system. Methanol and natural gas are similarly rated with regard to fire potential and hazard. The UCD engine and facility had been recently converted from distillate oil to natural gas as its primary fuel. In addition to different engine fuel controls and nozzles, the conversion to natural gas required some upgrading of the facility safety systems since gas is more hazardous than distillates. These upgrades included vapor and fire detectors in the engine room, and were similar to those which would have been required for a conversion of distillate fuel to methanol. Improved ventilation of the turbine enclosure was also provided for methanol service. In the event of a methanol leak or fire, these safety systems would initiate an engine shut down. Additional fire detectors were installed at the new storage tank, fuel forwarding and fuel loading stations, and were connected to the existing alarms. An emergency safety shower and eye wash station as well as appropriate warning signs and fire extinguishers were installed.

The methanol storage tank had a capacity of 30,000 gallons and had appropriate connections, fill lines, level indicators or alarms and safety vents. A containment wall of 110 percent tank capacity was constructed around the tank in case of a massive spill or rupture. The tank capacity provided for approximately two days of engine operation at full load, however fuel was delivered daily in order to assure a reserve capacity. Methanol was withdrawn from the tank, pumped, its flow measured with a turbine meter totalizer, filtered, and delivered to the engine high pressure pumping system. The materials of construction were carbon steel up to the fuel forwarding system filters and stainless steel thereafter. The centrifugal pump was constructed of cast iron with a bronze impeller. The seals and gaskets utilized throughout the system were constructed of Buna-N, teflon, nitrile rubber or other methanol compatible materials. Welded connections were preferentially used in the piping system, if possible.

Since water and methanol are miscible, they were premixed at the fuel forwarding skid and then delivered to the engine for implementation of water injection for NO_x control. Tap water was treated with a deionizer system and filtered, prior to mixing with the fuel. The water quality (contaminants) specification was to be at least equal to that of the fuel.

The methanol kit consisted of a modified, engine-driven gear pump, two fuel flow control valves, a flow divider, fuel control solenoids, two fuel manifolds, and modified fuel nozzles (Figure 1). All of the components required a fuel flow capacity approximately 2.2 times that required of distillate fuel oil, plus extra capacity for the water injection (NO_x control). In some cases, standard components were modified, while others were resized or newly constructed.

The engine-driven pump was a two-stage design with a centrifugal boost pump section and two high-pressure gear pump sections. To gain additional flow capacity, the two high-pressure sections were run in parallel (normal distillate fuel operation allows parallel operation for startup and series operation thereafter). The pump design required lubrication by the pumped fluid and used bronze bushings throughout and, therefore, the low lubricating qualities of methanol were of concern. The use of a modified distillate fuel pump was, however, recommended by Allison, after consultation with the pump manufacturer and was based upon the high reliability of the pump, expected low bearing loads and its aviation gasoline (also low lubricity) pumping capability.

A hydromechanical flow control valve of sufficient capacity was not available, therefore two valves in parallel were utilized. These valves were readjusted for the proper startup methanol delivery flow rates and higher flow capacity. The flow divider valve adjusted the pressure to the two sections of the fuel nozzles and was a newly constructed item that was sized for the higher flow rates. The fuel manifolds (teflon hose with stainless steel braid) were the standard distillate fuel parts. The fuel nozzles were modified versions of the standard nozzles. Two separate flow circuits, the pilot and main, were utilized in its design. The pilot section was a high-pressure, low-flow nozzle used primarily during startup, while the main section was a reduced-pressure, high-volume nozzle supplying the majority of fuel at load. The main nozzle was modified to accommodate the higher flow rates of methanol and water. Various fuel flow control solenoids were resized for proper flow rates.

Existing or modified parts were affixed with methanol compatible materials. Viton, a common elastomer in gas turbine fuel systems, was replaced with Buna-N or teflon. Other common materials (aluminum, bronze, steel, etc.) were methanol compatible. Interconnecting tubing among these parts was constructed of stainless steel tubing. With exception of the engine-driven pump and fuel nozzles, most components were assembled on a plate which was attached to the side of the engine.

The modified fuel nozzles were tested in a combustion rig equipped with a 501-KB engine combustor liner for both methanol and methanol/water mixtures. These tests indicated that the nozzles to be utilized in the engine demonstration were adequate with regard to power output, emissions, atomizer performance and fuel burnout, flame heat transfer, combustor liner temperatures, ignition, flame stability (lean blowout limit) and gas outlet temperature pattern or profile. Water injection with up to 30 weight percent water in methanol mixtures was successfully tested at combustor outlet temperatures equal to and higher than those expected for the UCD engine.

In comparison with distillate petroleum fuel oil, the combustor test results of significance were low NO_x emissions, nonexistent smoke emissions, more uniform combustor outlet gas temperatures (potentially higher first stage vane life), and reduced combustor liner metal temperatures with water injection (potentially longer combustor life). In all other respects the methanol performance was adequate for proper engine operation.

The methanol kit was assembled and installed on an 2,500 kW 501-KB engine in the Allison powerhouse. Methanol was supplied from a tanker truck and the engine briefly tested to demonstrate proper engine and component operation. Testing verified startup characteristics, hot restarts, and engine shutdown sequences of the methanol kit. During the startup sequences, good light off, proper engine acceleration and temperature as well as good fuel flow control were attributed to methanol operation. The highest load was limited to 2,440 kW and water injection was not tested. The engine was run for slightly over two hours, including one hour of idle operation. After the successful trial run, the methanol kit was then forwarded to the UCD facility.

The methanol kit was installed on the UCD engine and after some controls adjustments, the engine was started and loaded. After an initial period of operation, problems were encountered in the high-pressure pumping of methanol to the engine combustor section using the engine-driven gear pump. Failures of the pump internals were experienced. These were attributed to the low lubricity of methanol and, possibly, to the added pump loading associated with the water blended into the fuel. Minor modifications to the fuel system were made in order to rectify the problem (Shiomoto, 1985). However, after several unsuccessful attempts and 136 hours of operation using the gear pump, this approach was abandoned.

To complete the test program, a new high-pressure pumping system was required. Allison redesigned and fabricated the fuel system with a high-pressure centrifugal pump to replace the original engine-driven pump. Figure 2 depicts the off-board fuel pump skid, and programmable control valve. This system was designed to duplicate the pressure and flow characteristics of the positive displacement engine-driven fuel system. The flow control valve located on the pump skid tailored the methanol delivery to constant flow with variable pressure, which was necessary for the hydromechanical fuel flow control valves mounted on the engine. One operational problem of the new system was a maximum fuel flow limit (water plus methanol), which was imposed by a combination of the maximum continuous rating of the gas turbine/generator set and the flow limits of the hydromechanical fuel flow control valves. This limited water injection to 0.24 lb H_2O/lb fuel at full load, although higher rates could be attained at lower loads.

Baseline Tests

The engine operability on methanol was found to pose no difficulty to normal engine characteristics. The engine could provide acceptable startups, load changes and control to a steady load. Startups were not attempted with water injection (i.e. with water in the fuel), because the startup fuel flow was manually preset by the hydromechanical flow control valves. The manually controlled water injection was also restricted during load changes, in order to prevent the inadvertent injection of too much water during a drop in load (i.e. reduction of methanol flow). No other engine operability factors were significantly affected by the use of methanol.

Exhaust gas emissions (NO_x, CO, CO_2, and O_2) as well as engine and fuel skid instrumentation were monitored continuously during the demonstration program. Batch sample test measurements were also made for aldehyde and particulate exhaust emissions. Gas turbine exhaust emissions were monitored at the exit of the heat recovery boiler with an extractive, hot line sample system, gas analysis instruments, and an on-line monitor micro-computer system. Approximately every hour, the emissions results were tabulated, recorded, printed, and an instrument calibration performed. Additional engine and fuel system data were gathered and input into the computer to allow calculation of the engine performance parameters. A measurement of steam flow generated from the heat recovery boiler was not available from the plant instrumentation, however, an Allison heat recovery program for the 501-KB engine was utilized to estimate the heat (steam flow) recovered for different operating conditions. The estimated results were indirectly verified with examination of steam flow changes on the central heating plant's main boilers during startups or shutdowns of the cogeneration unit.

A methanol and deionized water analysis is shown in Table 1. The analysis shows the methanol supplied by Celanese to be essentially chemical-grade methanol. Baseline (no water injection) emissions of NO_x, O_2 and CO_2 are shown in Figure 3 for engine operation with methanol and natural gas. The natural gas tests were brief and were conducted to obtain comparative data for the more extensive methanol operation. Comparison operation with distillate oil was not performed. Exhaust gas O_2 concentrations versus generator electrical output were nearly equivalent between the methanol and natural gas. As expected for a gas turbine, the oxygen content decreased with increasing load and higher fuel to air ratio. Similarly, CO_2 content increased with higher load, however a distinct difference is noted between the two fuels. Methanol has a 0.75 to 1.0 percentage point greater CO_2 content at all load settings. Considering that the magnitude of CO_2 in the flue gas was only 2 to 4 percent, this change is significant. The higher CO_2 was the direct result of the difference in combustion chemistry and carbon content of fuels. Compared to natural gas, methanol has a higher carbon content, when compared on an equivalent heat input basis.

Baseline NO_x emissions were significantly altered with the use of methanol fuel. Without water injection, methanol operation resulted in emissions that were approximately one-third of those for comparable natural gas operation. Figure 3 shows the NO_x emissions for methanol to range from 24 to 38 ppm (at 15 percent O_2) for a load range of 50 percent to full load. The rate of change (slope) of NO_x emissions verus load curves show that, in addition to higher emissions, natural gas operation resulted in higher incremental NO_x emission changes with load as compared to methanol. Both natural gas and methanol have been considered relatively clean fuels with regard to NO_x emissions because they contain essentially no fuel-bound nitrogen. Therefore, NO_x emissions for these fuels were the result of high temperature oxidation of nitrogen contained in the combustion air. NO_x increases with engine load due to higher flame temperatures. The magnitude of change is reflected in the turbine inlet temperature (combustor outlet temperature) for the load range. Turbine inlet temperatures for 50 percent, 75 percent and full load were 1450°F, 1560 to 1620°F, and 1760 to 1800°F, respectively. These temperatures do not, however, explain the inherent NO_x emission difference between methanol and natural gas. Peak flame temperatures resulting from methanol combustion is less than traditional gas turbine fuels. For example, the theoretical flame temperatures indicate that methanol burns cooler; methanol = 3490°F, natural gas = 3660°F, and liquid petroleum fuels > 3800°F. These cooler flame temperatures indicate that combustion of methanol will result with less NO_x formation than other fuels.

The NO_x emissions were also calculated on a mass per unit energy output basis (micrograms as NO_2 per Joule output - μg/J) and are presented in Figure 4. Because the unit tested was a cogeneration facility, steam energy generated from the waste heat can be included with the system output. Figure 4 shows data with and without the steam energy heat recovery. With the NO_x presented on an energy output basis, the NO_x emission versus load curves tend to flatten, showing less effect of engine load. However, the natural gas NO_x emissions remain approximately three times higher than methanol. Note that with the steam energy heat recovery plus the electrical energy generated, the program objective of 0.1 μg/J was met for methanol operation for all loads without the use of water injection. NO_x emissions on natural gas were between 0.2 and 0.25 μg/J for the load range.

NO_x mass emissions per energy output evaluated on the basis of electrical energy without the benefit of the waste heat recovery (Figure 4, shaded symbols) was substantially higher than the data with heat recovery, since the steam generation was a substantial portion of the system energy output. In essence, NO_x emissions per energy output were reduced by utilizing cogeneration not because of lower emissions, but due to the higher energy recovery via the waste heat boiler. Emissions for both methanol and natural gas were higher by a factor of approximately three without waste heat recovery. However, the emissions trends remained similar to the previous data with heat recovery.

Combustibles, or incompletely burned fuel products, are generally represented by carbon monoxide (CO). For methanol combustion, aldehydes have also been found to be a significant combustible product. Aldehydes were measured with a wet chemical impinger train and analyzed by the MBTH method (aqueous 3-methyl-2-benzothiazolone hydrazone hydrochloride solution). Figure 5 shows the natural gas and methanol baseline CO and aldehydes emissions as a function of gas turbine load. It is apparent that the CO and aldehydes (analyzed as ppm formaldehyde) emissions were related. Aldehyde emissions were significantly lower than CO emissions for both fuels.

For operation on natural gas, the CO emissions remained at ~ 20 ppm throughout the load range, while aldehydes were relatively constant at a level of ~ 0.2 ppm. At full load, the CO and aldehyde emissions for methanol were similar to natural gas. For methanol, however, the CO and aldehydes emissions increased as load was reduced. The modified (higher flow rate capacity) fuel nozzles may be partially responsible for the increase of combustibles emissions, due to less effective atomization at low flow rates. Additional research, development and optimization of the fuel nozzles and/or combustor liner may be necessary to improve fuel burnout at low loads, if these combustibles emissions are considered to be excessive. However, at the typical high load operation of a gas turbine engine, the combustibles emissions remained low for methanol.

Heat rate for baseline operation with methanol is shown in Figure 6. As expected for a gas turbine engine, the heat rate increased with decreasing load. At high load, the heat rate on methanol was on the order of 14,000 Btu/kWh. The full load heat rate for natural gas was estimated to be approximately 14,300 Btu/kWh, during brief tests.

Power output with methanol was slightly enhanced compared to natural gas. With natural gas, a 1800°F turbine inlet temperature produced 3,020 kW of electrical generation, while the same power output with methanol required a 1760 to 1770°F set point. Raising the temperature setpoint to the engine limit of 1800°F would have raised the electrical generation above that which could be attained with natural gas.

Water Injection Tests

Water injection was only performed with methanol operation as the natural gas installation at the UCD cogeneration facility was not so equipped. As mentioned previously, water injection was performed by premixing water with the methanol at the fuel forwarding skid, prior to the high-pressure fuel system. Water injection will have a large impact upon NO_x emissions, with only small effects upon other emission or engine parameters.

NO_x emission reductions with water injection are shown in Figure 7. At 50 and 75 percent load, NO_x emissions were approximately 10 ppm with a water injection rate of 0.3 lb H_2O/lb fuel, thus representing reductions of 58 and 66 percent, respectively, from their baseline methanol emissions data. The maximum water flow rate for full load operation was limited to 0.24 lb H_2O/lb fuel due to system flow capacity limits, however NO_x emissions were reduced to approximately 14 ppm, or a reduction of 63 percent of the baseline full load emissions. In comparison to data obtained for a natural gas fired turbine using water injection (Weir, 1981), emissions with methanol and water were 70 percent lower. The 10 to 14 ppm emission levels achieved with water injection on methanol represent 80 to 90 percent reductions compared to baseline natural gas NO_x emissions. The three curves of NO_x emission data appear to converge upon one another as water injection rate was increased, thus reducing the load influenced emissions variation noted at baseline. Also, the greatest NO_x reduction effectiveness was for the first increment of water injection, while successive increments of higher water injection rates resulted in less reductions of NO_x.

Higher water injection rates for full load operation was accomplished by slightly reducing the engine output (reducing turbine inlet temperature from 1770 to 1700°F). Two water injection rates were tested; one at the 1770°F maximum injection rate of 0.24 lb H_2O/lb fuel and another at ~ 0.35 lb H_2O/lb fuel. The difference between 1770°F and 1700°F at 0.24 lb H_2O/lb fuel was a load reduction from 3130 kW to 2860 kW and a slight decrease of NO_x emissions. At the high water injection rate, emissions were reduced below 10 ppm. The slightly higher projected full load emissions are indicated by the dashed line in Figure 7. Note that the emissions cited here are on a wet gas basis (corrected to 15 percent O_2 and ISO conditions). Correcting the emissions to a dry basis will raise the ppm levels by ~ 1 ppm at high water injection rates of 0.24 to 0.35 lb H_2O/lb fuel. On a mass emission basis, the high water injection tests for the three loads resulted in NO_x emissions of approximately 0.03 μg/J, when including steam generation output. Without heat recovery, the emissions will be of the order of 0.1 μg/J, with high rates of water injection, for the three loads.

As with the baseline tests, combustibles (CO and aldehydes) emissions trends remained related, but showed only minor effects of water injection (Figure 8). Water injection influenced combustibles emissions only during the low load tests, while emissions at full load were not affected and remained low (20 ppm CO and ~ 0.05 ppm aldehydes). At 50 percent load, CO and aldehydes increased 20 ppm and 1.5 ppm respectively, due to water injection. These changes were low in comparison to the effect of engine load upon combustibles.

Particulate emissions were measured at the full load and maximum water injection (0.24 lb H_2O/lb fuel) test point. EPA Method 5 emissions were below 0.01 lb/10^6 Btu. The filters had very low weight gains and showed no discoloration or obvious material collection. These tests may have also been influenced by a engine lubrication oil leak into the exhaust gas which was discovered subsequent to the demonstration. Some sample probe washes did appear to have an oily residue and therefore may be biased toward higher than normal emissions. Cascade impactor samples were taken to determine particle size distribution, however the low loading of particulates prevented meaningful data, despite an 8 hour sample test.

Water injection showed small, but measurable effects upon engine operation, aside from NO_x emission effects. The engine at the UCD cogeneration facility was controlled by turbine inlet temperature measurement. Injection of water will tend to reduce the mean gas temperature, therefore the engine control system will increase fuel flow to compensate (exclusive of water, i.e. a higher heat input). The trend of higher methanol input with water injection is clearly evident in Figure 9. As a result of the higher fuel flow or heat input, the engine load also increased. Power output increased by 110 kW at 1770°F when water injection was added at a rate of 0.24 lb H_2O/lb fuel.

Despite the gain of power output, a heat rate penalty was the result of water injection. Heat rate increased by approximately 250 Btu/kWh with 0.24 lb H_2O/lb fuel at full load. This phenomenon has been documented in other tests and would be expected for all fuels when utilizing water injection. Similar fuel flow, engine power output and heat rate effects were also seen with data at 50 and 75 percent load.

System Operation and Results of Boroscope Inspections

Aside from the limitation of maximum water injection rate at full load, other operational problems were noted during the test program. These included a flow induced vibration at low engine load and rust deposition in fuel filters. The vibration emanated from the engine-mounted fuel flow control valves and the piping returning excess methanol back to the centrifugal pump. Allison speculated that the vibration resulted from high methanol return flow at low loads which was flashing or cavitating when passing through internal valves in the flow controllers. It was determined that low amounts of water injection (0.5 gpm or 0.075 lb H_2O/lb fuel) was sufficient to eliminate this vibration, therefore, extended low load operation was accomplished in this manner to prevent any damage to fuel system components. In future methanol applications, Allison recommended the use of a centrifugal high-pressure pump, and in lieu of the original methanol kit of the UCD system, a more compatible electronic engine control system. The different control system may circumvent the vibration experienced with the hydromechanical fuel valves.

Rust deposition on the engine-mounted, high-pressure fuel filter was an operational problem which resulted in excessive pressure losses and limited fuel flow rates. This in-line, 10 micron filter required an engine shutdown for dissasembly and cleaning. Ten micron duplex filters located on the fuel forwarding skid did not sufficiently capture rust in the fuel, thereby, leading to deposition on the downstream filter. The upstream fuel forwarding filters were changed to five micron. Despite the better filtration of these filters, the pressure losses gradually increased on the high-pressure 10 micron filter. The rust was found to be originating from the methanol storage tank. Larger capacity, duplex high-pressure filters and a smaller particle size capture for the fuel forwarding filters would be expected to sufficiently reduce the impact of the rust.

Boroscope inspections were performed before, during, and after the methanol demonstration by Allison representatives. These inspections revealed that the cross-over tubes between combustor liners (these allow ignition of one combustor to another) and a reverse flow baffle on the combustor liner were burning or eroding with time. The heat erosion of both areas of the combustor were described as minor and were considered as within serviceable limits for engine operation. The burning of the cross-over tubes was not detrimental to engine operation and is a condition typical for natural gas and liquid fueled engines of this design.

At the end of the methanol test program, the only significant changes were the continued burning of the aforementioned areas. All boroscope inspections showed the turbine blades and vanes to be in good condition, with no notable effects from the methanol. A reddish-brown color on the blades indicated that some of the rust was getting through the two filter sets and a portion had been deposited on the blades. Although no detrimental effect was attributed to the rust coating, it was recommended that improved filtration be used in future applications to remove the rust.

During the last engine inspection following the completion of the test program, an internal engine oil leak (unrelated to methanol operation) was noted. The engine was removed and during the repair disassembly, over-heating damage to the second stage vanes and foreign object damage on the fourth stage blades of the turbine power section was found. By the nature of the damage, Allison determined that the turbine had been subjected to an over temperature condition during a startup, causing typical burning of some of the second stage vanes. Some of the metal thus burned away subsequently damaged the fourth stage blades (foreign object damage). The second stage vanes comprised both a hollow (older) and a solid, more durable (newer) design. Only the older, hollow style vane design was heat damaged. The overtemp condition was severe enough to damage the older less durable design, but not the newer vanes.

The damage was not observable with the equipment utilized for the boroscope inspections. Therefore it could not be determined when the damage had occurred; if it had occurred prior to the demonstration on natural gas, between methanol runs when the turbine was operated on natural gas, or during the demonstration testing. The damage was of a nature which, according to Allison, is not atypical on gas or oil operation. Thus, the damage was not necessarily the result of methanol use, although it could have been. Of significance, was the fact that although the time, fuel, or reason associated with the startup overtemp could not be determined, the latest design second stage vanes were not damaged. Had the engine contained only the newer, solid vane design, no damage to the turbine would have occurred.

ECONOMICS

The capital cost to retrofit the UCD facility to methanol operation totalled \$670,000 and necessarily reflect the developmental nature of the program and the design/fabrication of a one-of-a-kind fuel system. Based on the cost information gathered during the program, the cost to retrofit a similarly sized (3,000 kW) commercial installation would be within a range of \$420,000 to \$770,000. This estimate is variable since the actual costs would be dependent upon the desired quantity of on-site methanol storage, whether the plant had been set up originally for gas or oil firing, and whether the existing design included a water injection system for NO_x control.

For a new installation of similar size, the capital cost difference between a methanol-fueled and a conventional-fueled plant is estimated to be within a range depending upon those aspects mentioned above and upon which conventional fuel is used as the basis of comparison. The difference could be as low as approximately \$18,000, or essentially zero within the estimation accuracy of the present analysis. At the upper end of the range, a new methanol-fueled plant could cost as much as \$500,000 more than a conventional fueled plant.

Based on the UCD experience, the operating and maintenance costs associated with fueling a gas turbine facility are similar to those of a conventional-fueled plant, in terms of operating labor, maintenance labor, and maintenance material costs. However, the overriding impact upon the operating costs of a methanol-fueled plant would be the cost of the fuel itself.

The methanol utilized for the demonstration at UCD was supplied at a delivered price of \$0.60/gallon which is equivalent to $\$9.28/10^6$ Btu (HHV). Natural gas available to the facility during the demonstration ranged in delivered price from \$5.24 to $\$5.40/10^6$ Btu. This difference translates to a daily total fuel cost differential of approximately \$4,000, based upon operating 24 hours per day at baseload (3,000 kW). A fuel cost differential of this magnitude would likely be a detriment in the economics of fueling a gas turbine plant with methanol. However, provided that the demand for methanol increases and the appropriate manufacturing and distribution facilities are expanded, it is reasonable to speculate that the price of methanol may decline. Furthermore, the methanol used at UCD was a chemical grade product. The manufacture of lower purity methanol, suitable for gas turbine fuel, may also be expected to result in reduced fuel costs.

Another very important aspect concerning the cost of methanol as a gas turbine fuel relates to the low air pollutant emissions capability of the fuel. Certain air pollution control agencies require that NO_x emissions from gas turbines be controlled to levels of 25 ppm or less. In order to meet this level of NO_x emission on a natural gas- or distillate oil-fired turbine, water injection and a selective catalytic reduction (SCR) unit would be required. An SCR unit would not be necessary for a methanol-fueled gas turbine. The cost differential between methanol and natural gas or distillate fuel oil may be significantly offset by cost savings resulting from elimination of the SCR requirement.

CONCLUSIONS

The demonstration project showed that a gas turbine plant could be successfully operated on methanol and that extremely low emission levels could be realized. These aspects were proven in spite of the technical difficulties which were experienced. Fortunately, none of the technical problems proved to be insurmountable. The efforts which were required to resolve the problems should be considered as valuable experience and, as such, will contribute measurably to the successful commercial application of methanol as a fuel for gas turbines.

The following specific conclusions can be drawn:

- The technical viability of the use of methanol as gas turbine fuel was demonstrated as a result of 1036 hours of operation of the UCD engine.
- NO_x emissions were within the project goal, even without water injection. NO_x emissions without water injection were 60 percent below emission levels measured on the same engine firing natural gas. NO_x emissions as low as 10 ppm were demonstrated with high rates of water injection.
- Emissions of carbon monoxide and aldehydes for high load operation on methanol were low and similar to levels measured for natural gas operation. At part load, emissions of CO and aldehydes for methanol operation increased and were higher than levels for natural gas.
- Emissions of particulate during methanol operation were negligible and within the accuracy of the measurement techniques.
- The storage and handling system for fueling a gas turbine plant with methanol can be fabricated using conventional engineering practices and commercially available hardware and materials. The proper selection of materials is necessary since methanol is not compatible with some of the elastomers used in a conventional-fuel system.
- The formation and accumulation of rust inside a methanol storage tank can be troublesome with respect to fuel filtering systems. Adequate storage tank precleaning and the proper design of fuel filtration systems will reduce its impact.
- The requirements for assuring safe operation of a methanol-fueled facility are more stringent than those of a petroleum-based liquid-fueled facility but similar to those of a natural gas-fired facility.
- Without major modifications, the use of a gear-type pump designed originally for petroleum-based liquid fuels is inadequate for the high-pressure delivery of methanol in a gas turbine system. A high-pressure centrifugal pump is a satisfactory approach for delivering methanol under high-pressure to a gas turbine combustor.
- Damage to the UCD gas turbine power section was incurred at some time before or during the demonstration on methanol. The damage could have happened during the operation on natural gas or methanol and is, therefore, not necessarily attributable to the use of methanol. The damage was most likely caused by an overtemp condition, which may result from any fuel if the fuel flow rate is not properly controlled during start-up of the turbine.

REFERENCES

Acurex Corporation, "Clean Coal Fuels, Alternate Fuel Strategies for Stationary and Mobile Engines," prepared for California Energy Commission, December 1981.

Shiomoto, G. H. and Shore, D. E. "The Clean Coal Stationary Engine Demonstration Project," prepared for California Energy Commission, May 1985.

Weir, A. , van Klein Smid, A. H. and Danko, E. A., "Test and Evaluation of Methanol in a Gas Turbine System," EPRI AP-1712, February 1981.

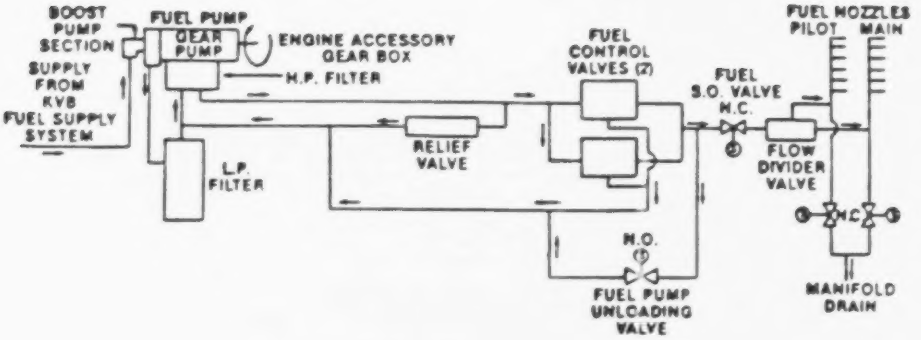
BOOST PUMP SECTION
SUPPLY FROM KVB FUEL SUPPLY SYSTEM
FUEL PUMP
GEAR PUMP
ENGINE ACCESSORY GEAR BOX
H.P. FILTER
L.P. FILTER
RELIEF VALVE
FUEL CONTROL VALVES (2)
FUEL S.O. VALVE N.C.
FLOW DIVIDER VALVE
FUEL NOZZLES
PILOT
MAIN
N.C.
N.O.
FUEL PUMP UNLOADING VALVE
MANIFOLD DRAIN

Figure 1. Methanol fuel system schematic.

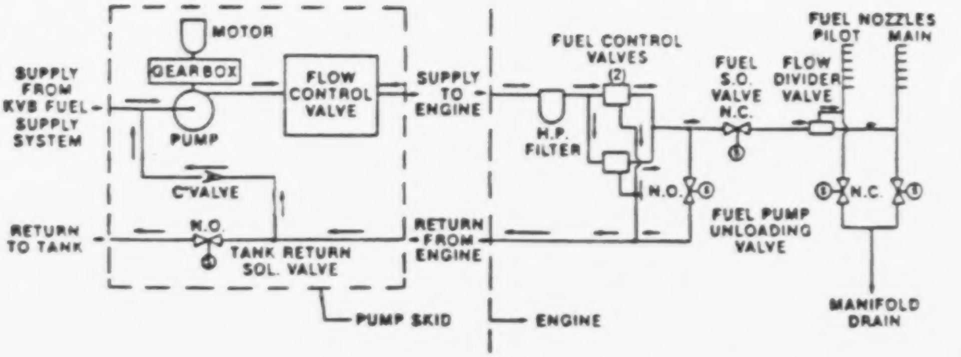
MOTOR
GEARBOX
SUPPLY FROM KVB FUEL SUPPLY SYSTEM
PUMP
FLOW CONTROL VALVE
C VALVE
RETURN TO TANK
N.O.
TANK RETURN SOL. VALVE
PUMP SKID
SUPPLY TO ENGINE
RETURN FROM ENGINE
ENGINE
H.P. FILTER
FUEL CONTROL VALVES (2)
N.O.
FUEL S.O. VALVE N.C.
FLOW DIVIDER VALVE
FUEL NOZZLES
PILOT
MAIN
N.C.
FUEL PUMP UNLOADING VALVE
MANIFOLD DRAIN

Figure 2. Methanol fuel system with off-engine mounted pump skid.

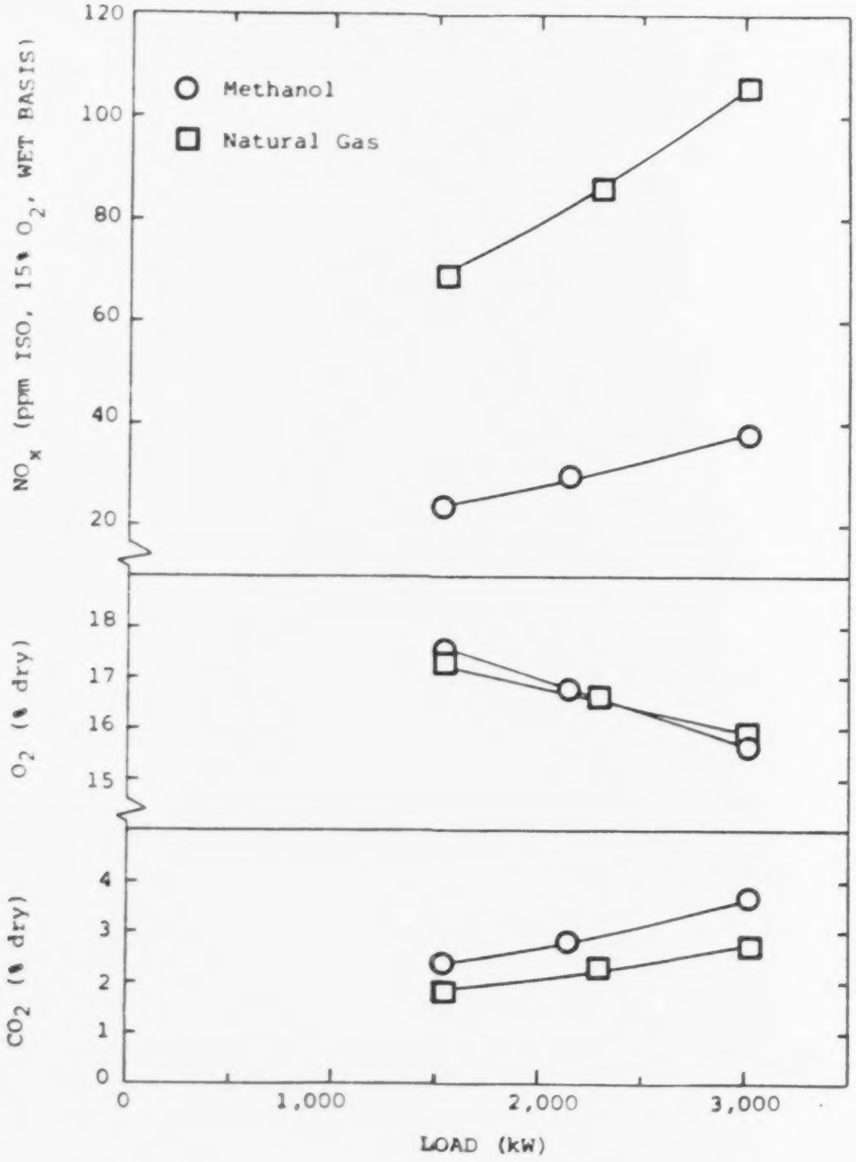

Figure 3. Baseline emissions of NO_x, O_2, and CO_2 for methanol and natural gas operation, no water injection and variable load.

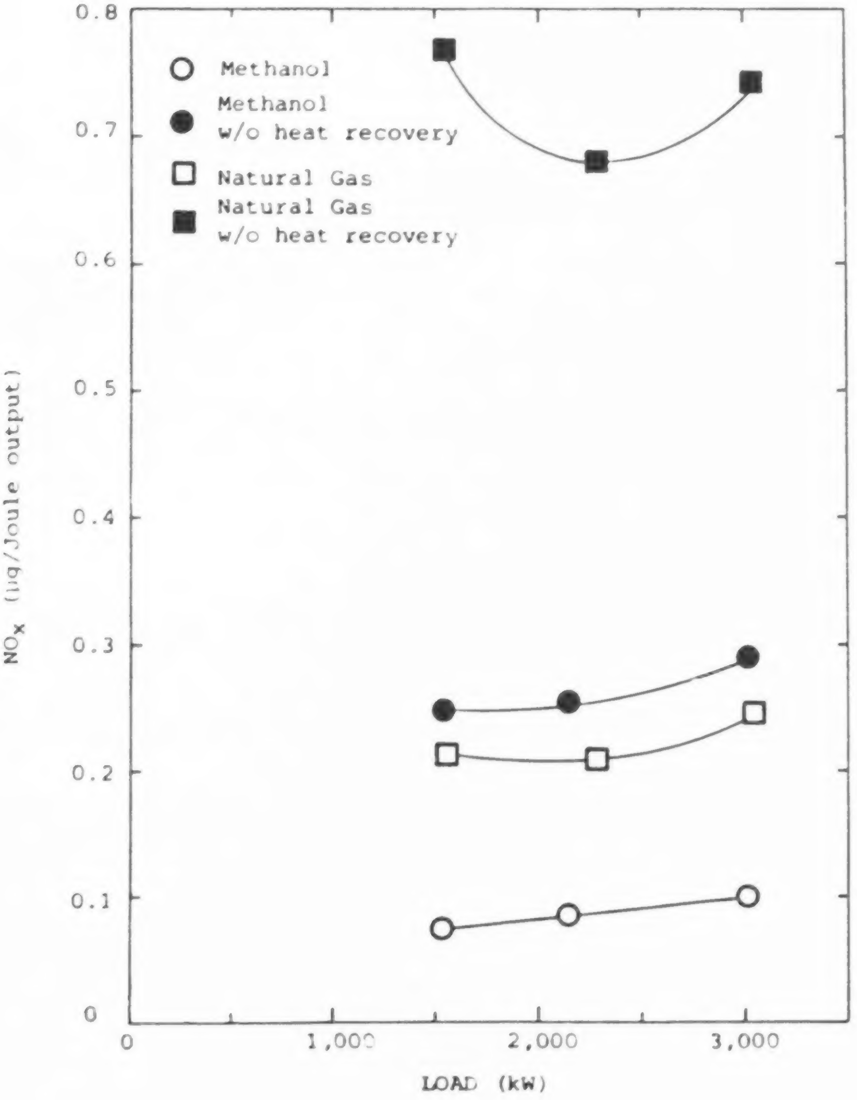

Figure 4. Baseline NO_x emission for methanol and natural gas operation, no water injection and variable load.

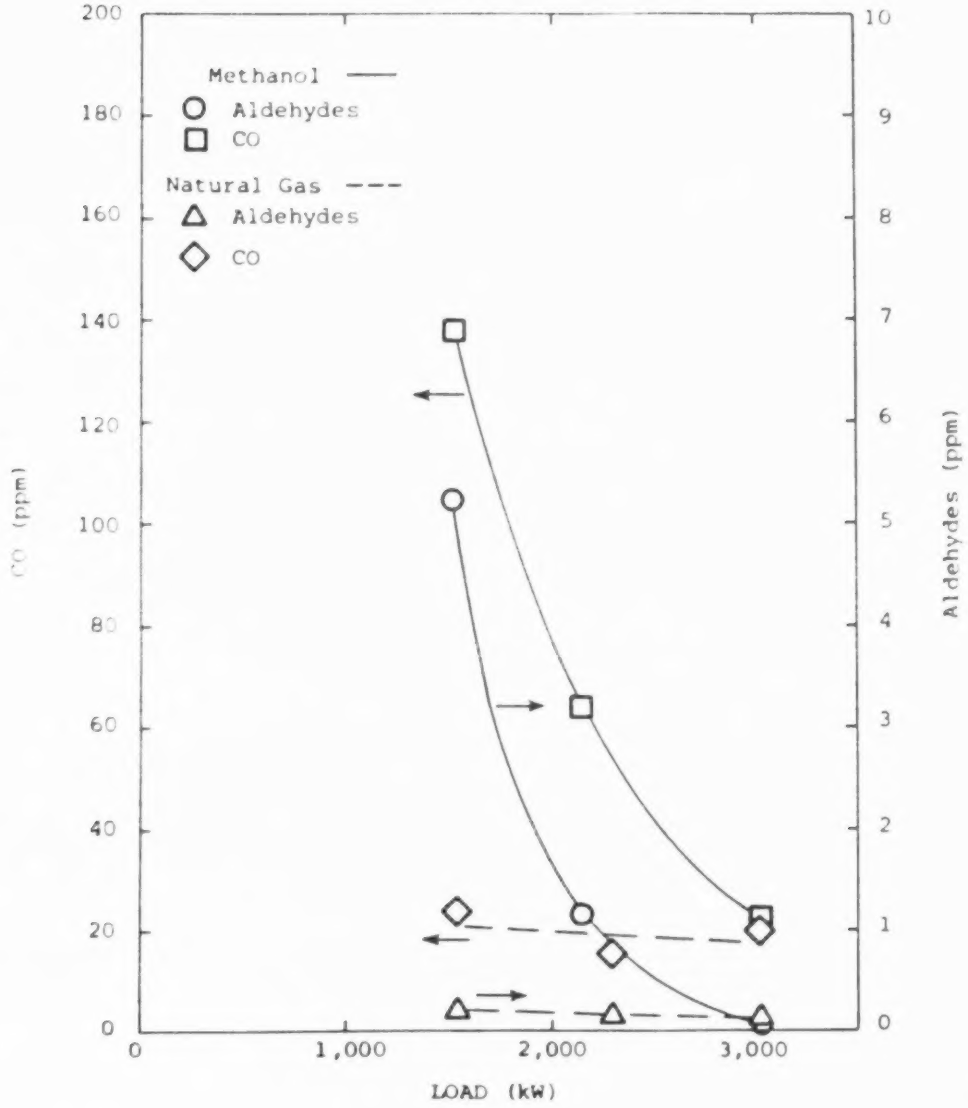

Figure 5. Aldehydes and CO emissions for methanol and natural gas operation, no water injection and variable load.

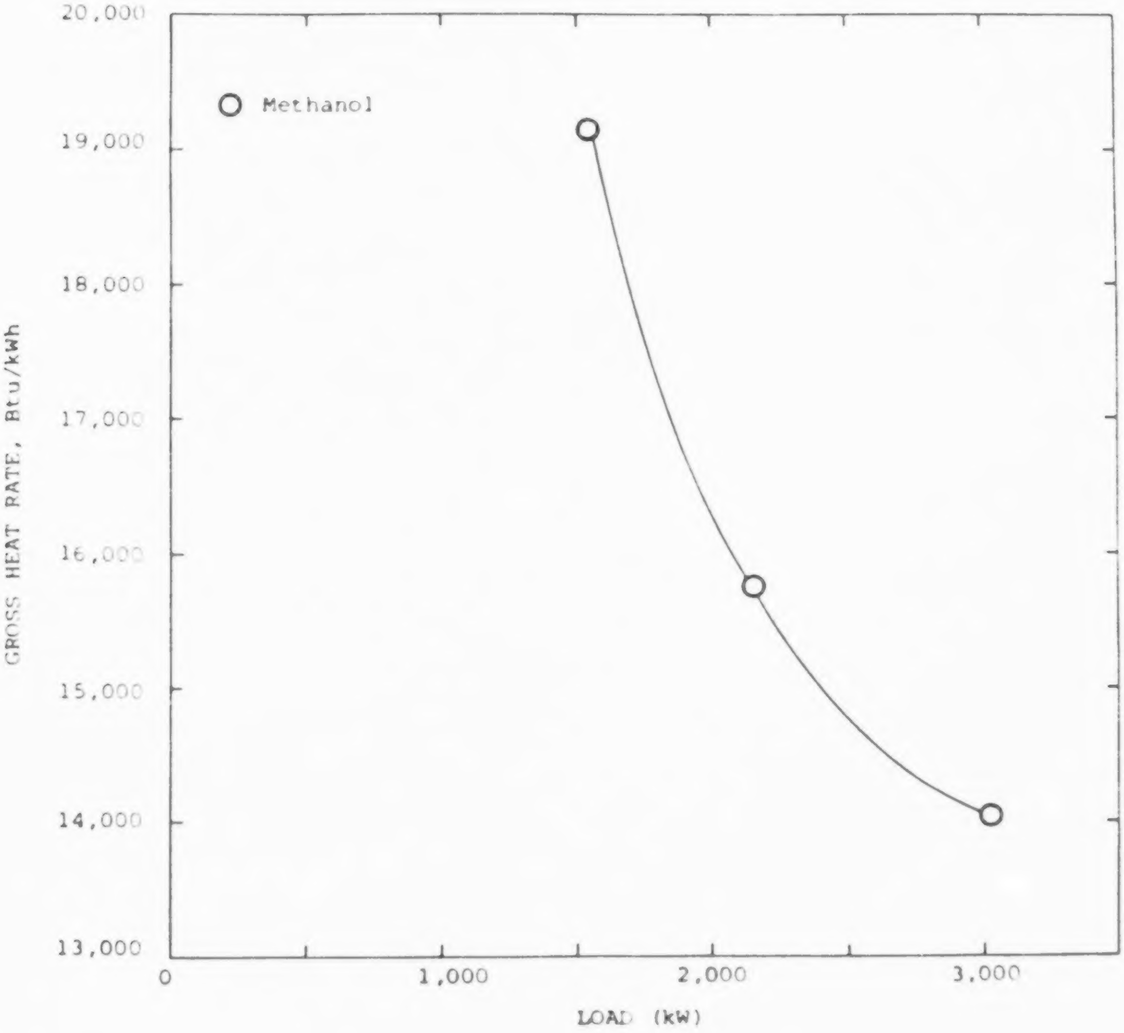

Figure 6. Heat rate for methanol, no water injection and variable load.

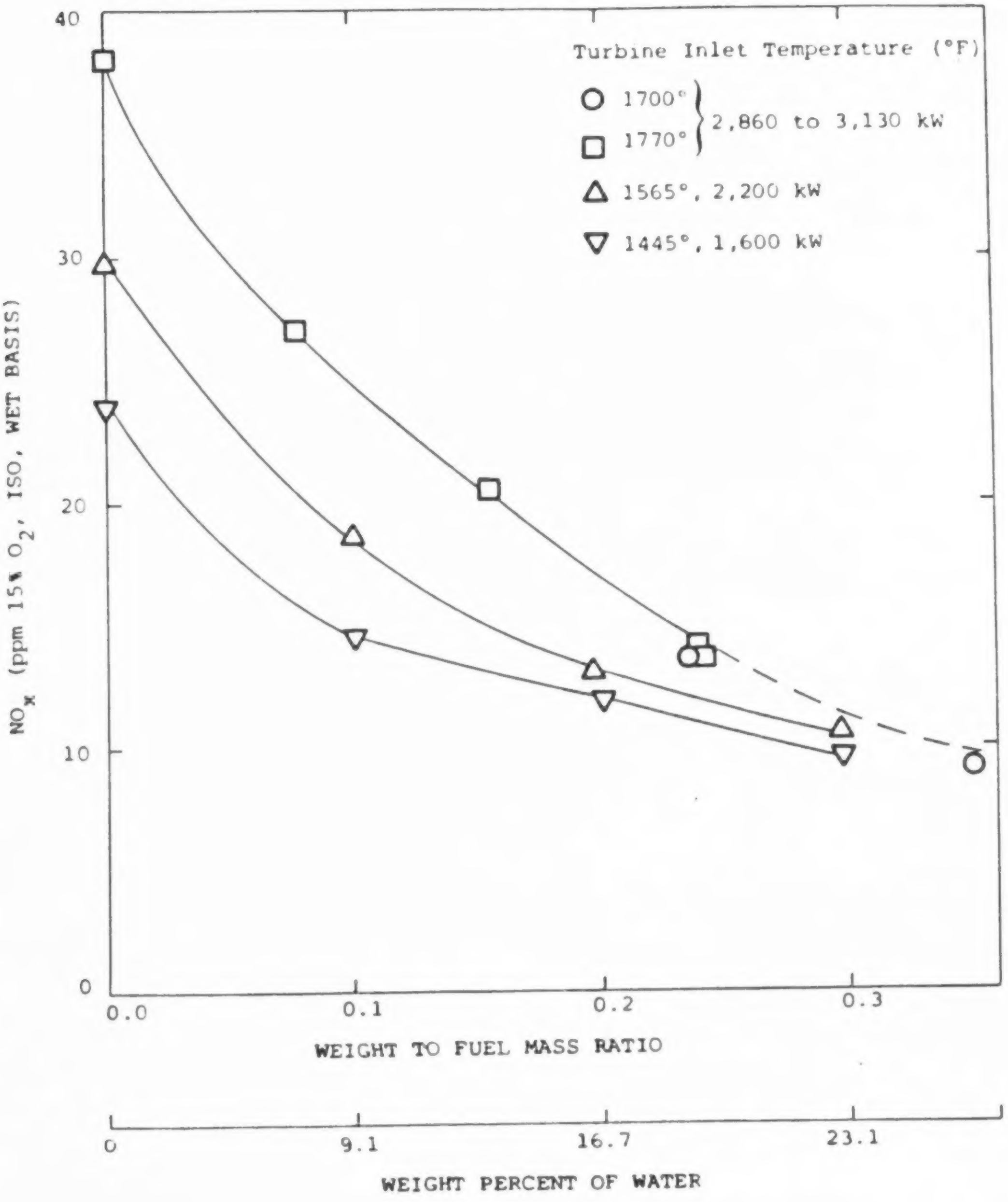

Figure 7. Effect of water injection upon NO$_x$ emissions (ppm) for large injection rate tests.

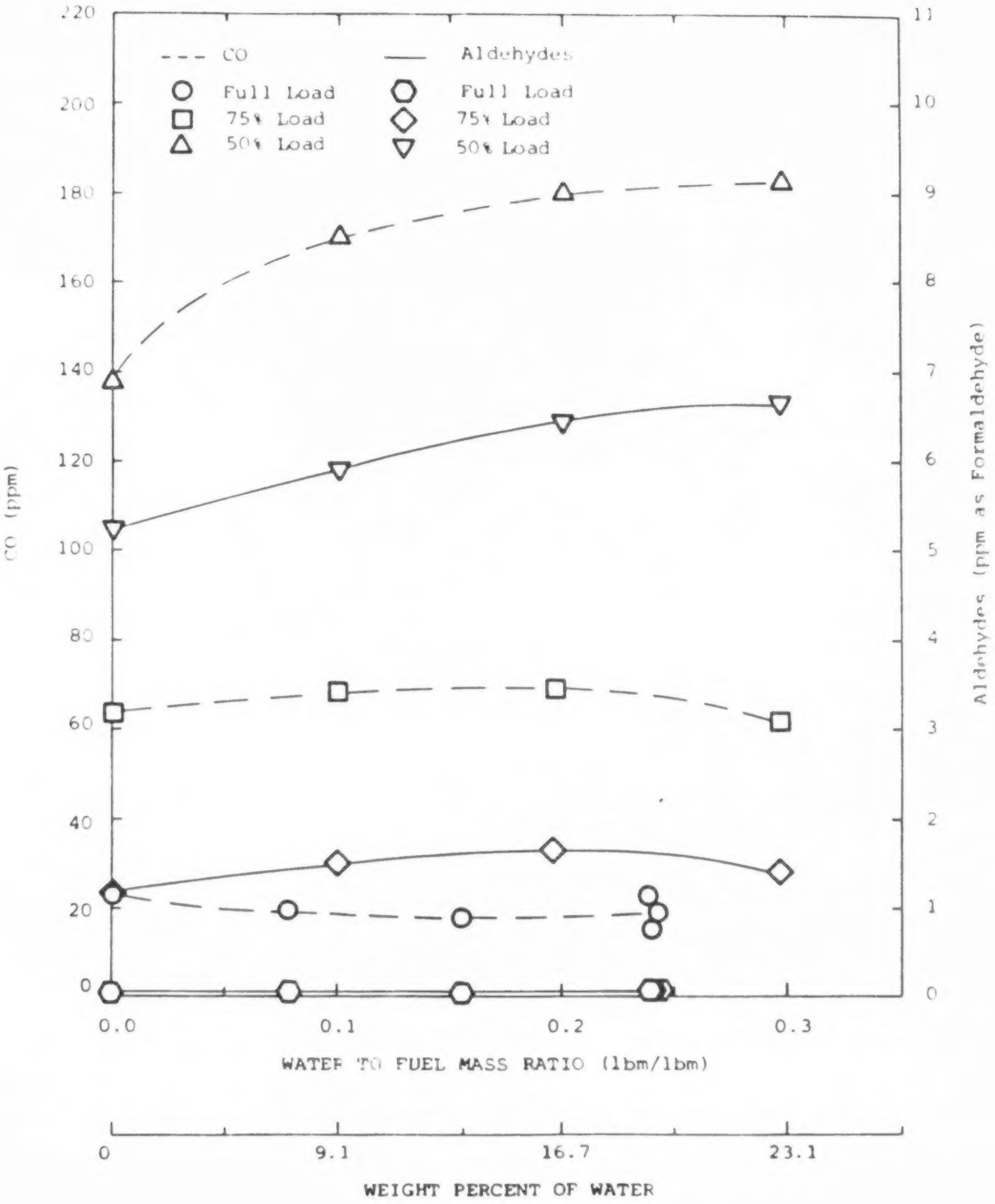

Figure 8. Effect of water injection upon CO and aldehydes emissions.

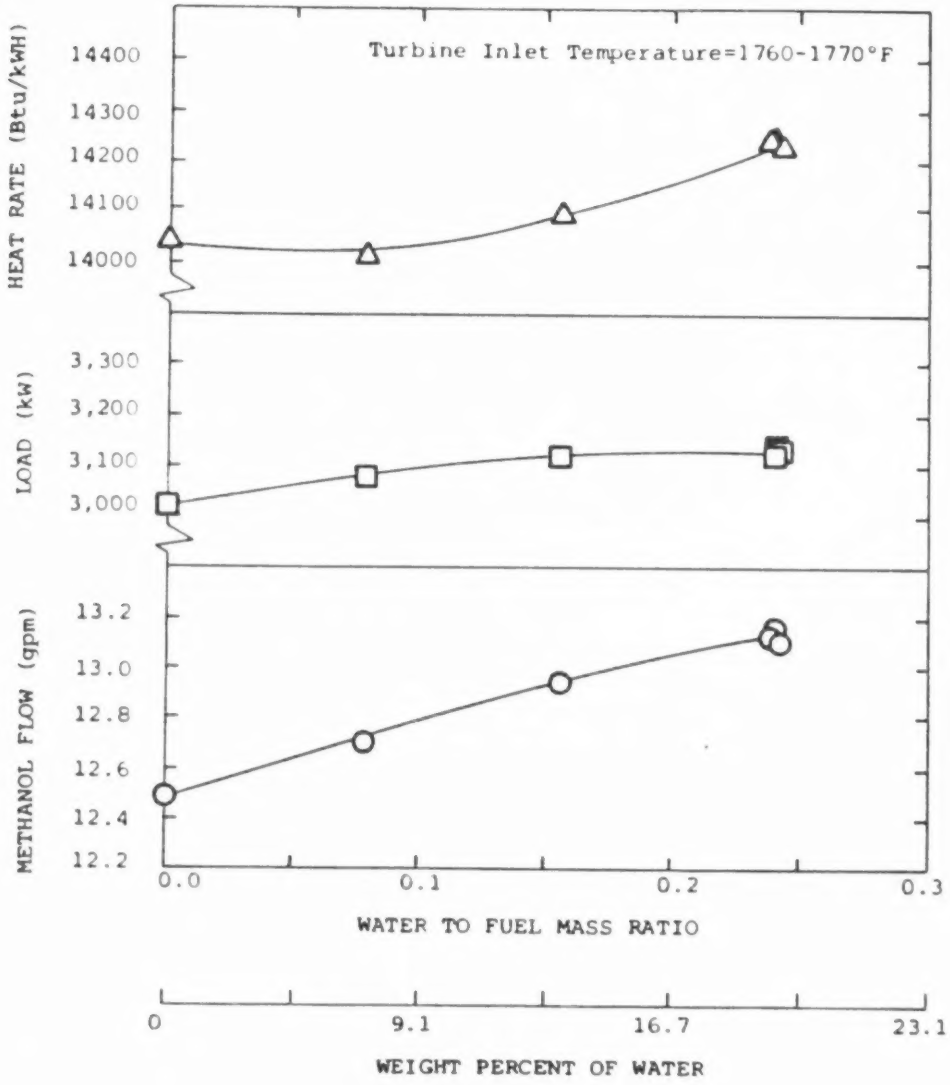

Figure 9. Effect of water injection upon heat rate, load and fuel consumption at full load.

Table 1

METHANOL AND DEIONIZED WATER ANALYSES

METHANOL FUEL ANALYSIS

Ultimate Analysis	
Carbon, %	37.52
Hydrogen, %	12.32
Nitrogen, %	0.0003
Sulfur, %	< 0.001, (ND)
Ash, %	0.00004
Oxygen (by difference), %	50.16
Water Content, ppm	259
Heat of Combustion (Gross, Btu/lb)	9,616

DEIONIZED WATER ANALYSIS

Sodium, ppm	<0.002, (ND)
Silica, ppm	1.3
Total Solids, mg/liter	1.5

ND = Not Detected

Water sample taken upstream of deionizer system filters.

DEVELOPMENT AND FIELD-DEMONSTRATION OF A LOW-NO_x BURNER FOR TEOR STEAMERS

G. England
Y. Kwan
R. Payne
Energy and Environmental Research Corporation
18 Mason
Irvine, CA 92718

ABSTRACT

This paper describes the results obtained in a program to demonstrate in the field a full-scale 16 MW_t prototype low NO_x burner for thermally-enhanced oil recovery (TEOR) steam generators which burn high-nitrogen crude oils. Nitrogen oxide emissions from these TEOR "steamers" have been linked with deteriorating air quality in Kern County, California, and stringent local regulations have been promulgated limiting these emissions to preserve ambient air quality. These regulations can potentially restrict oil production in Kern County.

The burner described in this paper is designed based on a two-stage combustion concept developed from earlier bench-and pilot-scale work. The concept comprises physically-separate zones in which conditions have been optimized to minimize both fuel and thermal NO formation.

The full-scale 16 MW_t commercial prototype burner has been evaluated in a laboratory test furnace and was successfully retrofitted to a field-operating steam generator in Kern County. Results of field test firing heavy crude oil (0.83% N) showed that NO_x emissions below 70 ppm (at 3 percent excess O_2) with low CO and smoke emissions could be achieved with acceptable flame conditions in the steamer radiant section. Detailed emissions characterization also showed that emissions of particulates and organic compounds were well below allowable levels. The burner is currently still operating in the Kern Front oilfield.

INTRODUCTION

A significant fraction of total U.S. oil reserves is recoverable only through the application of enhanced oil recovery processes. Thermally enhanced oil recovery (TEOR) involves injection of low-quality steam into the oil well. This steam is typically produced by combusting crude oil in oil field steam generators ranging from in size from 7-15 MW_t capacity. The crude oils which are fired in these steam generators can be high in nitrogen (0.8-1.0 percent) and sulfur content. Combustion of such fuels leads to high levels of NO_x and SO_x emissions unless preventive measures are taken. ,Approximately one-third of all the steam generators in the United States are located in Kern County, California, where strict state and local regulations limit allowable NO_x emissions from TEOR steam generators.

Regulations in Kern County for new or modified stationary sources (including TEOR steam generators) require that Best Available Control Technology (BACT) or Lowest Achievable Emission Rate (LAER) be applied in order to control the emission of any air contaminant or precurser for which there is a National Ambient Air Quality Standard. NO_x emissions from all steam generators in Kern County are currently limited to 129 ng/J or about 225 ppm, corrected to 3 percent oxygen. Further reductions to 108 and 60 ng/J, about 190 and 105 ppm, may be required if ambient NO_2 concentrations exceed certain trigger levels. Enhanced oil recovery operations are expected to expand in Kern County through 1995. The level of NO_x control required to meet both growth and air quality goals has been difficult to achieve with available technology while maintaining acceptable CO and particulate emissions as well as practical flame conditions within the steam generator.

This paper discusses an EPA-sponsored program which addresses the need for advanced NO_x control technology for oil field steam generators. A full- scale (16 MW_t) burner system has been developed and tested, the concept for which was based on fundamental studies (1). Test results are included for full-scale burner performance in a field-operating steam generator which was retrofitted in the Kern Front oilfield in California.

CONCEPT DEVELOPMENT

Combustion-generated NO_x emissions can be reduced by combustion modification techniques which involve staging the heat release process. Techniques such as flue gas recirculation strive to control NO formed from molecular nitrogen (thermal NO) by suppressing peak flame temperatures and are only partially effective with nitrogen containing fuels (2). NO formation from nitrogen in the fuel (fuel NO) is very sensitive to reactant stoichiometry and can be significantly reduced by initially burning the fuel under fuel-rich conditions. Staged combustion, therefore, involves creating a fuel-rich zone to maximize formation of molecular nitrogen from the nitrogen species (HCN, NH_3, and NO) which are evolved as the liquid fuel decomposes, followed by a fuel lean zone optimized for minimal thermal NO formation. The key parameters controlling NO_x formation during staged combustion were identified in a previous study (3) for liquid fuels ranging from distillate oil to residual oil to alternative coal- and shale-derived oils. The key parameters were first-stage stoichiometry, thermal environment and residence time. NO_x was relatively insensitive to second (burnout) stage parameters. These bench-scale studies showed that under optimum staged conditions, NO_x emissions below 100 ppm were possible and were nearly independent of fuel nitrogen content. The concept was subsequently scaled up and tested at 0.6 and 2.9 MW_t (1,4) to further develop scaling criteria for the full-scale burner design. These pilot-scale tests confirmed that a staged combustion system could be designed and scaled over a 150:1 range which is capable of achieving less than 85 ppm NO (at 3 percent O_2) firing high nitrogen residual oil with low CO and smoke emissions.

Burner Design

Figure 1 illustrates the design of the full-scale commercial prototype burner. Optimization of the fuel-rich and fuel-lean stages is achieved utilizing a physically separate first-stage prechamber. The first-stage chamber is formed by a horizontal cylinder which is refractory lined and recuperatively cooled in order to minimize first-stage heat loss. The exterior of the chamber is also insulated to minimize heat loss to the surroundings. The recuperative design reduces the thermal stresses developed in the lining during transient (startup and shutdown) operation by employing a relatively thin layer of refractory. Substantial primary air preheat (230°C) is developed which enhances fuel vaporization in the ignition zone without increasing the first-stage exit temperature.

A commercial air register, igniter and fuel gun are used. The atomizer is a twin-fluid, internal-mixing design which uses steam as atomizing fluid. The primary throat diameter was scaled up from the pilot-scale burners on the basis of constant velocity. The exit diameter of the chamber is reduced to provide a first-stage exit velocity of approximately 15 m/sec while reducing radiative heat losses from the first stage.

Secondary air is injected at the exit of the chamber through two sets of discrete ports oriented parallel to and normal to the burner axis. The distribution of secondary air between these two sets of ports can be varied to provide control over second-stage mixing. Testing on the bench-scale and small pilot-scale systems had shown that emissions were relatively insensitive to second-stage mixing and excess oxygen level; however at 2.9 MW_t, test results suggested that the influence of these parameters may increase as the scale of the system increases.

A microprocessor-based programable controller serves to control first-stage stoichiometric ratio and second-stage excess oxygen level in order to maintain minimum NO_x emissions. This controller was integrated with the existing pneumatic and flame relay systems of the the host steam generator in the field. Further information on the design of the burner and control system can be found in England et.al. (1).

Full-Scale Evaluation

Full-scale burner performance was characterized in two phases. The initial test phase was conducted in the EER Medium Tunnel test furnace, which is designed to simulate the thermal environment of a typical watertube boiler furnace. The second phase was conducted in a conventional TEOR steam generator located in the Kern County oil fields.

The objectives of the initial series of tests were to cure the refractory lining under controlled conditions firing natural gas, and to optimize burner parameters for emissions and flame shape without risk to field equipment. Shakedown of the mechanical and control systems was dove-tailed into this preliminary test series.

The preliminary emissions testing was conducted firing a residual fuel oil derived from California crude. This residual oil had similar properties to the actual crude oil which was used later in the field evaluation. Nitrogen content of the residual oil was 0.74 percent compared to 0.83 percent for the crude oil. Full-scale burner performance in the test furnace was determined for variations in second stage air injection, load, air register setting, and oil gun configuration. Minimum NO emissions were achieved at first-stage stoichiometic ratio of approximately 0.6 and ranged from approximately 50-58 ppm when firing at 16 MW_t. (All volumetric emission levels throughout this paper are corrected for dilution to 3 percent oxygen). Smoke and CO emissions were essentially insensitive to first-stage stoichiometry and remained at low levels over the range of conditions investigated.

The effect of secondary air injection configuration was also investigated. NO_x emissions increased when secondary air was injected through the radial injection ports. Some degree of control over flame shape could be achieved with the parallel injection ports alone by increasing or decreasing the number of open ports, which changed the secondary air injection velocity. Therefore, the parallel secondary air injection ports were modified to allow on-line control over the secondary air injection velocity and number of ports.

Other parameters which were optimized during the test furnace trials included atomizer pressure and spray angle, primary swirl level and procedures for start up and shut down of the burner. Further information on the test furnace trials is available in England et.al.(5). Upon the completion of these tests, 131 hours of operation had been achieved. The burner was then transported to the host steam generator site in Kern County, California.

FIELD RETROFIT

The retrofit task of the demonstration program involved selecting a host site with an existing steam generator typical of those currently in operation, transportation of the burner to the host site, removal of the existing burner hardware, and installation of prototype burner hardware and controls. TEOR steam generators are relatively simple in construction compared to boilers and utilize a single pass, once-through design. The radiant section is formed by a horizontal refractory-lined steel cylinder with the burner mounted at one end and an exhaust transition leading to a convective economizer section on the other end. Steaming tubes extend axially and are supported near the refractory on tube hangers around the generator's circumference. The entire unit with feedwater pump and controls is normally skid-mounted and shop-assembled and is shipped by rail car or truck to the installation site.

Retrofit installation of the low NO_x burner on the host steamer required replacing the refractory-faced front wall of the radiant section, lengthening the foundation and skid to accommodate the length of the burner, extension of plumbing and electrical wiring and installation of supplementary controls (e.g. programmable controls, additional switches and relays, oxygen probe, etc.). Revised operating procedures to accommodate heatup and cooldown of the refractory lining were also developed. Figure 2 illustrates the installation of the low NO_x burner on the host steamer. The retrofit resulted in an overall extension of the steam generator length by approximately 3.9 meters. Following completion and shakedown of the retrofit, optimization testing was initiated.

FIELD TEST RESULTS

The field testing of the steam generator was accomplished in three phases: 1) optimization; 2) detailed characterization; 3) 30-day evaluation.

Optimization

The purpose of this initial test series was to optimize the burner operating parameters to achieve safe startup and shutdown, acceptable flame characteristics within the steam generator radiant section and to define the operating conditions for minimizing NO, CO and smoke emissions. The steam generator was gradually brought to full load on crude oil. Initial emissions measurements were consistent with the results obtained in the test furnace; however at full load, flame impingement on the walls of the radiant section close to the burner was encountered. The flame shape was much wider and shorter compared to that obtained in the test furnace and this was attributed to the smaller diameter of the steam generator furnace. The initial degree of control over secondary air injection was not sufficient to provide an acceptable flame and other modifications to the burner design were considered. The most promising modifications involved a decrease in the primary chamber exit diameter and/or an increase in the diameter of the parallel secondary air ports. In order to gain a preliminary assessment of the value of these modifications in eliminating flame impingement a brief series of one-fifth scale cold isothermal modeling tests was conducted using an existing flow modeling facility.

Hardware for the one-fifth scale model was geometrically scaled. Secondary air jet velocity was held constant while primary flow rate (and exit velocity) was reduced to maintain the same primary-to-secondary momentum ratio as at full scale. Flow pattern visualization was achieved using plane illumination and injection of bubbles using a commercial neutral-buoyancy bubble generator. Mixing patterns were determined by tracer concentration measurements.

Figure 3 compares the flame and observed flow patterns in the steam generator radiant section under full load conditions to the flow patterns and measured concentration profiles in the one-fifth scale model. Flow patterns in the model and full-scale steamer appeared to be similar and were characterized by a strong external recirculation zone close to the burner exit, rapid expansion of the primary jet toward the wall and a lazy central recirculation zone. The apparent spreading angle of the primary jet boundary was approximately 20 degrees (half angle) and the point of impingement along the wall of the model appeared to correspond to the point of flame impingement observed in the actual steam generator. The concentration profiles also indicated that primary fluid was being very rapidly entrained into the secondary jets and into the external recirculation zone near to the burner as illustrated in Figure 3b. Under these conditions the model appeared to qualitatively simulate the phenomenon observed in the actual steam generator for the baseline configuration.

Figure 4 shows the effect of two modifications on flow patterns observed in the isothermal model. The first modification (4b) involved decreasing the first-stage exit diameter. The diameter reduction increased the primary-to-secondary jet momentum ratio from 0.35 to 0.56. This reduced the apparent spreading angle of the primary jet to approximately 15 degrees and moved the point of impingement on the wall of the model about 50 percent further down stream relative to the baseline case. The intensity of the external recirculation zone was visibly reduced and the central recirculation zone disappeared entirely. Tracer concentration profiles indicated that the entrainment of primary fluid toward the walls close to the burner was significantly reduced without adversely affecting downstream mixing. Figure 4c shows the results of enlarging the secondary air ports, in addition to reducing the primary exit diameter. This combination resulted in a primary-to-secondary jet momentum ratio of 0.99 and the apparent spreading angle of the primary jet was further reduced to approximately 13 degrees. Mixing between the primary and secondary jet was also further delayed although good mixing was still achieved at a distance of approximately equivalent to the mid-point to the steam generator.

The model results suggested that the two modifications considered should each provide a substantial improvement in flame pattern by delaying mixing between the primary and secondary streams, thereby increasing the time available for combustion before quenching on the cool walls of the furnace. The second modification appeared to offer greater assurance for eliminating flame impingement; however there was some concern that complete downstream mixing might be difficult to achieve. It was decided to execute the modification step-wise starting with reduced primary exit diameter. The diameter was reduced by adding an additional ring of refractory brick into the exit of the first-stage chamber and the burner was tested again.

This time no sign of flame impingement was observed. The flame was much narrower than the original flame and was similar in shape to the region in Figure 4b outlined by the 0.6-0.7 iso-concentration profiles. Overall flame length was approximately 5.5 to 6.1 meters. The tail of the flame occasionally licked the steam tubes; however this was considered minor and did not raise concern over tube or refractory life. Since the flame shape produced by the first modification was considered adequate, no further modifications were attempted.

Figure 5 shows NO_x, CO and smoke emissions from the steam generator firing at 15.8 MW_t after optimization of second stage flame shape. Data is shown versus first- stage stoichiometric ratio (SR_1) for two excess oxygen levels. The fuel was Kern Front crude oil (Table 1). Minimum NO_x levels were between 55 and 65 ppm corrected to 3 percent oxygen. CO and smoke emissions were also low at the optimum stoichiometry. However, at SR_1 below the optimum level, smoke was slightly higher at 2 percent excess oxygen than at 3 percent. NO_x and CO emissions appeared to be insensitive to excess oxygen. After defining the optimum operating conditions for the burner/steam generator, the burner control system was programed to maintain these conditions over the full normal operating range. A more detailed emissions characterization was then performed at the optimum full-load operating point which included measurement of particulate mass loading, particulate size distribution, and heavy organic compounds. The accuracy of the continuous gas analyzers for O_2, CO, CO_2, and NO_x was also checked against EPA reference methods.

Detailed Characterization

Particulate emissions were measured by three separate methods: EPA method 5; Source Assessment Sampling System (SASS); and by Anderson cascade impactor. Results from a total of five measurements ranged from approximately 0.023 to 0.046 grams per dry standard cubic meter and averaged 0.034 grams per dry standard cubic meter. Note that condensible particulate is excluded from the standard EPA methods. Total particulate emissions including condensible matter were 0.145 grams per dry standard cubic meter. The Kern County Air Pollution Control District requires condensible matter to be included in total particulate emissions. This is very close to the level expected for quantitative conversion of the ash contained in the fuel. Visual inspection of the particulate catch indicated that carboneceous particulate was not present. Measurement of particulate size distribution using Anderson cascade impactor showed that approximately 65 of the percent particulate was below 1 micron aerodynamic diameter.

The emission of organic compounds was also determined. Total (volatile, semi-volatile and non-volatile) organic compounds emissions were below 0.3 milligrams per dry standard cubic meter. The emission of priority pollutants was between 6 and 14 micrograms per dry standard cubic meter. Although no federal standard has been established for emission of organic species, these levels are considered low for oil-fired sources. The emission of NH_3 and HCN was also low, below 1 ppm.

The thermal efficiency of the host steam generator was determined before and after the commercial prototype burner was retrofitted. Prior to the burner retrofit overall efficiency based on heat loss ranged from 83.6 to 87.8 percent (neglecting unmeasured and radiation losses); and average efficiency was 85.5 percent. Data obtained during the burner tests prior to the 30-day evaluation showed an average efficiency of 86.1 percent. Thus, there is no adverse impact on steam generator efficiency caused by the burner retrofit; in fact operation at lower excess O_2 levels may lead to improved steam generator efficiency.

30-day Evaluation

Following the field optimization tests, the unit was operated under automatic control and a 30-day continuous monitoring test was conducted. Average NO_x emissions were approximately 70 ppm during the test. The results of the 30-day test are given in references 6 and 9.

SCALING AND APPLICATION

Criteria developed in bench-scale and pilot scale tests were applied to the design of the full-scale prototype commercial burner. The key design criteria (6) are:

1. Fuel injection - high quality atomization, pre-mixed fuel/air, and minimal heat extraction.

2. First stage fuel rich zone - Stoichiometric ratio approximately 0.7 to minimize total fixed nitrogen species (TFN) concentration; residence time in excess of 400 milliseconds to allow sufficient TFN decay; control of heat loss to produce a first stage temperature in excess of 1425°C to promote rapid conversion of fuel nitrogen fragments to molecular nitrogen.

3. Second stage air injection - partial quenching to minimize thermal NO formation in the second stage; refractory choke to prevent back-mixing and reduce first-stage heat loss; intermediate to rapid second-stage mixing for minimizing smoke formation and for control of flame shape.

Figure 6 compares minimum NO_x emissions from bench-scale, pilot-scale and full-scale tests versus first-stage residence time. The results represent a 750:1 range in scale. Below approximately 0.6 seconds NO_x emissions increase almost linearly with decreasing residence time. NO_x emissions in the tunnel furnace are slightly higher than the pilot-scale systems. This is due to lower temperatures as a result of higher heat losses from the first stage associated with the smaller scale.

The data indicate that increasing first-stage residence time above 0.6 seconds is only marginally beneficial and may indicate a shift in the controlling mechanisms at very low NO_x levels from first-stage processes to second-stage processes. Although full-scale burner performance indicated that emissions were somewhat sensitive to second-stage parameters (mixing, confinement), this sensitivity is much less severe than typically encountered in conventional combustion systems and the greatest impact of second-stage parameters is on flame shape.

Figure 7 compares NO_x emissions from the prototype burner to field test data (7) for conventional 15 MW steam generator burners and for other current NO_x control technology. Average NO_x emissions from conventional steam generators without NO_x

control range from approximately 230-280 ppm over the range of excess air shown in the figure. The shaded area represents ± one standard deviation from the average and illustrates the range of emissions for variations in fuel and equipment. By comparison, emissions from the prototype low NO_x burner are approximately 65 ppm and insensitive to excess oxygen. This represents a 77 percent reduction over average NO_x emissions at 3 percent excess oxygen without adverse impact on other pollutant emissions. Low NO_x burner data from reference 7 indicates that for these burners, NO_x reduction is mainly a result of operation at reduced excess air levels. More recent low NO_x burner technology (8) has shown that significantly reduced NO_x emissions can be achieved by delayed fuel/air mixing in the steam generator in combination with flue gas recirculation. However, the impact of the resulting flame conditions on furnace integrity has not been fully evaluated and some low excess air conditions can result in high CO and smoke emissions. NO_x reduction by post-flame ammonia injection has produced NO_x emissions levels comparable to those achieved by the prototype commercial burner; however, it is difficult to maintain optimum ammonia injection conditions over extended periods because of changes in heat transfer caused by tube fouling in the convective section. Operation under non-optimum conditions could lead to emission of ammonia and/or higher levels of NO_x.

CONCLUSIONS

The prototype low NO_x burner described in this paper proves the applicability of the general conceptual design criteria developed in bench- and pilot-scale studies. Burners built using this criteria have the capability to achieve NO_x emissions below 100 ppm at 3 percent excess O_2, CO emissions below 50 ppm, low particulate emissions, and flame shape which can be tailored to the individual application.

ACKNOWLEDGMENTS

The work described in this paper was supported under EPA Contract 68-02-3692. The authors wish to express thanks to Chevron USA Inc. for hosting the field demonstration. In particular, the authors wish to thank M. Freiberger, T. Morton, and R. Pogers of Chevron; S. Hill and B. King of Struthers Thermo Flood Corporation; J. Hagan of Peabody Engineering; and S. Eaton of Coen Co. M. Osborne was the U.S. Environmental Protection Agency Project Officer.

DISCLAIMER

"Although the research described in this article has been funded wholly or in part by the United Stated Protection Agency, under contract No. 68-02-3692 to Energy and Environmental Research Corp., it has not been subjected to the agency's required peer and policy review and therefore does not necessarily reflect the views of the Agency and no official encorsement should be inferred".

REFERENCES

1. England, G. C., Heap, M. P., Kwan, Y and Payne, R., "Evaluation and Demonstration of low-NO_x Burner Systems for TEOR Steam Generators." Interim Report EPA Contract 68-02-3692 (February 1983).

   Heap, M. P., et al., "Control of Pollutant Emissions from Oil-Fired Package Boilers." Proceedings of the Stationary Source Combustion Symposium, EPA 600/2-76-152б, NTIS, Springfield, VA (1976).

3. England, G. C., Heap, M. P., Pershing, D. W. and Nihart, R. K., "Mechanisms of NO_x Formation and Control: Alternative and Petroleum-Derived Liquid Fuels." Eighteenth Symposium (International) on Combustion, The Combustion Institute (1981).

4. England, G. C., Heap, M. P., Payne, R., Pershing, D. W., Lanier, W. S., "The Development of Design Criteria for Low NO_x Oil Burners Suitable for Application to TEOR Steamers." Presented at 75th Annual Meeting, Air Pollution Control Association, New Orleans, LA (1982).

5. England, G. C., Kwan, Y., and Payne, R., "Evaluation and Demonstration of Low NO_x Oil Burners Suitable for Application to TEOR steamers: Test Report - Preliminary Evaluation of Commercial Prototype Burner"., EPA Contract 68-02-3692, available NTIS, Springfield, VA (1983).

6. England, G. C., Kwan, Y., and Payne, R., "Evaluation and Demonstration of Low-NO_x Burner Systems for TEOR Steam Generators: Final Report - Field Evaluation of Commercial Prototype Burner", EPA Contract 68-02-3692, available NTIS, Springfield, VA (1984).

7. Nelson, L. P. and Folsom, B. A., "NO_x Emissions From Steam Generators Used in Thermal Enhanced Oil Recovery." Presented at 1981 California Regional Meeting, Society of Petroleum Engineers (1981).

8. Castaldini, C., DeRosier, R., Waterland, L. R., Mason, H. B., "Environmental Assessment of Industrial Process Combustion Equipment Modified for Low-NO_x operation." Proceedings of the 1982 Joint Symposium on Stationary Combustion NO_x Control, Volume 2, EPRI CS-3182 (July 1983).

9. Castaldini, C., Waterland, L, DeRosier, R., Mason, H., "Heavy Oil Low-NO_x Burner Application to an Oil Field Steamer- Emissions Measurements", presented at the 1985 Joint Symposium on Stationary Combustion NO_x Control, Boston (1985)

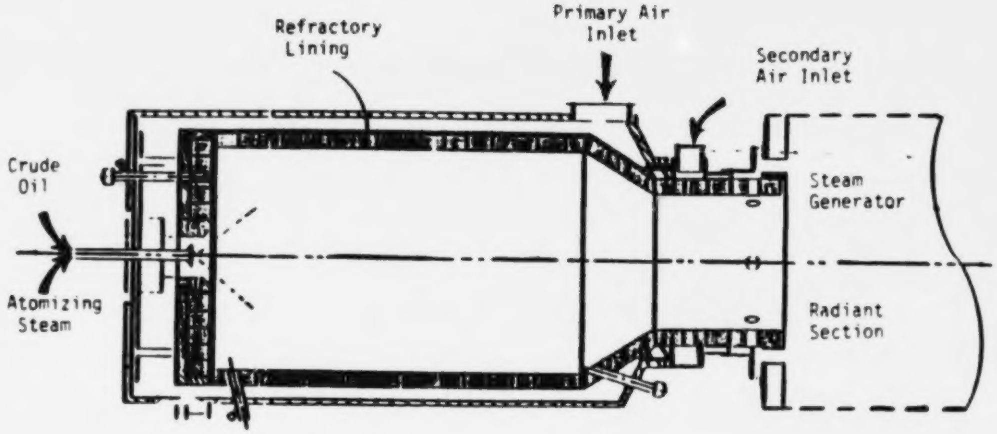
Refractory Lining
Primary Air Inlet
Secondary Air Inlet
Crude Oil
Atomizing Steam
Steam Generator
Radiant Section

Figure 1. Full-scale (16 MW_t) commercial prototype low NO_x burner design for TEOR steam generators.

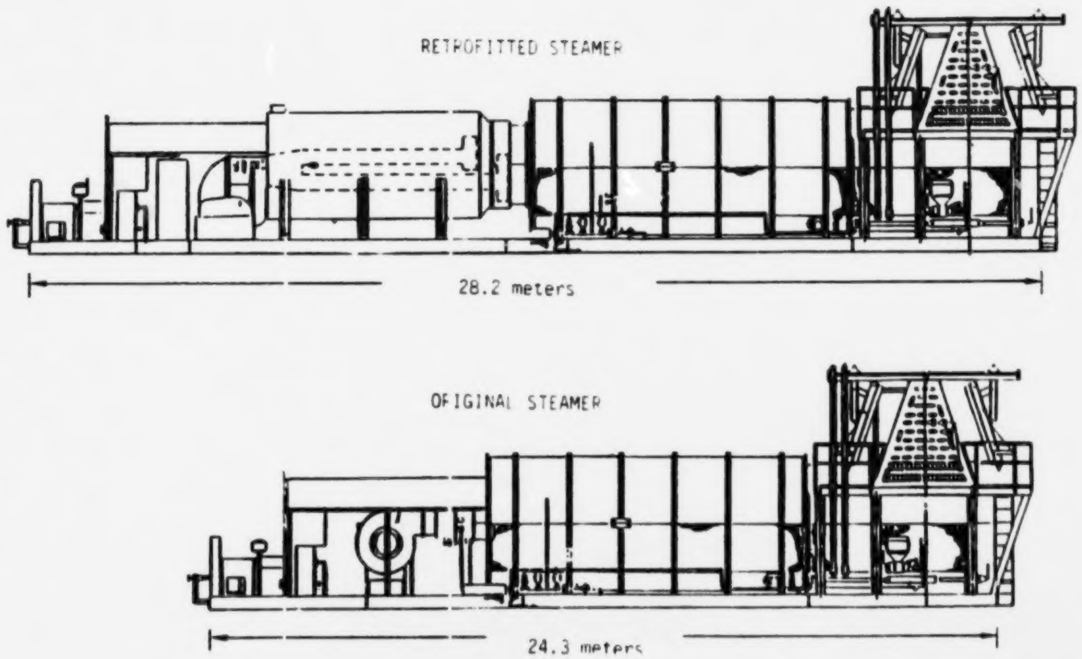
RETROFITTED STEAMER
28.2 meters
ORIGINAL STEAMER
24.3 meters

Figure 2. Retrofit installation of commercial prototype burner on TEOR steam generator.

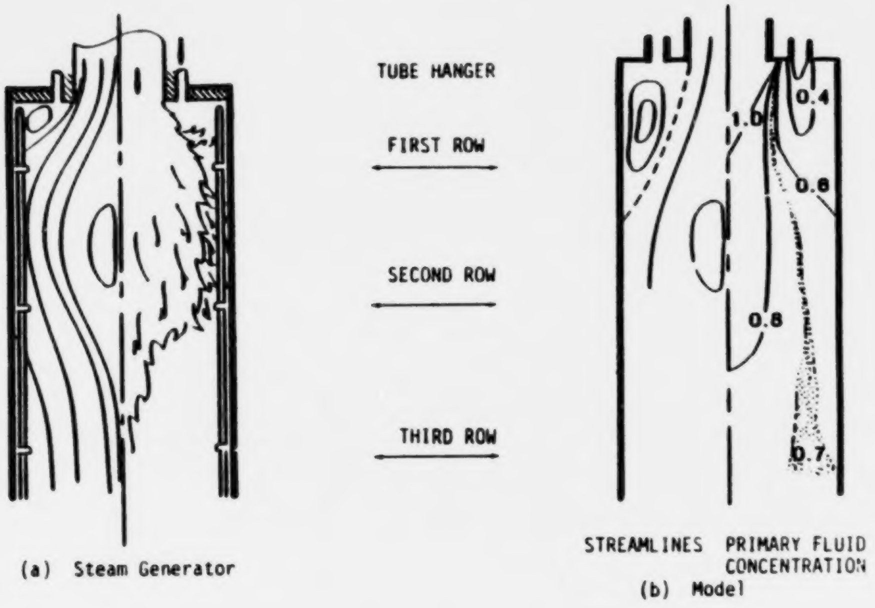
TUBE HANGER
FIRST ROW
SECOND ROW
THIRD ROW
1.0
0.4
0.6
0.8
0.7

(a) Steam Generator

STREAMLINES PRIMARY FLUID CONCENTRATION
(b) Model

Figure 3. Comparison of mixing patterns observed in isothermal model and full scale steam generator.

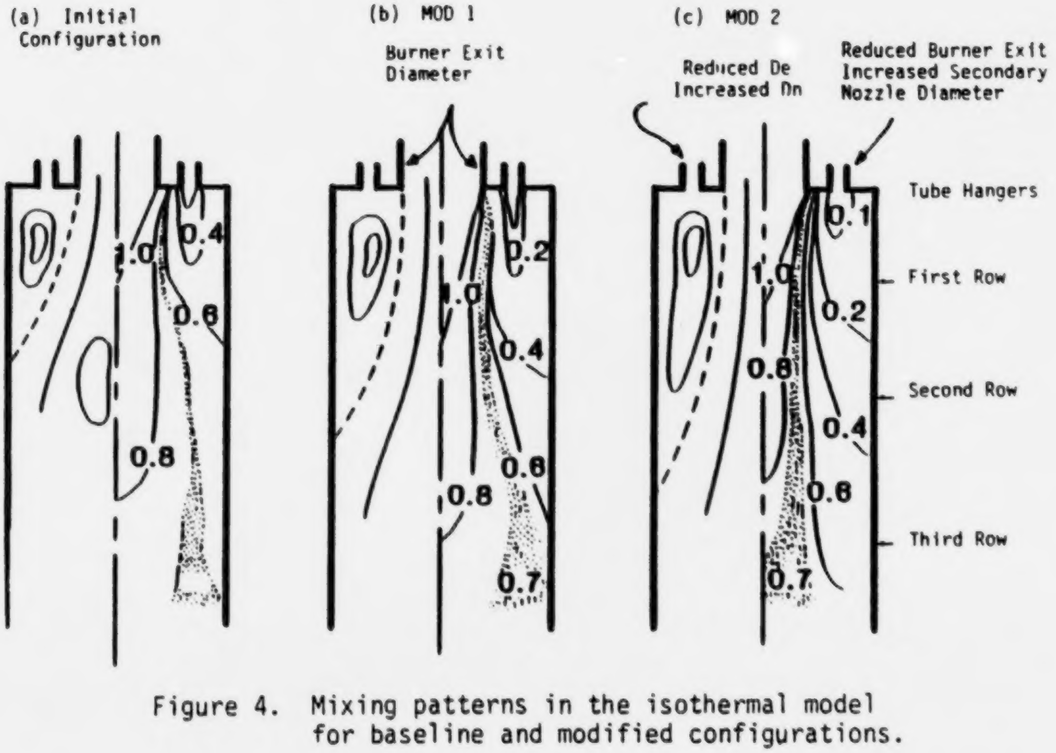
(a) Initial Configuration

(b) MOD 1

(c) MOD 2

Burner Exit Diameter
Reduced De
Increased Dn
Reduced Burner Exit
Increased Secondary
Nozzle Diameter
Tube Hangers
First Row
Second Row
Third Row
1.0
0.4
0.6
0.8
0.7
0.2
0.1

Figure 4. Mixing patterns in the isothermal model for baseline and modified configurations.

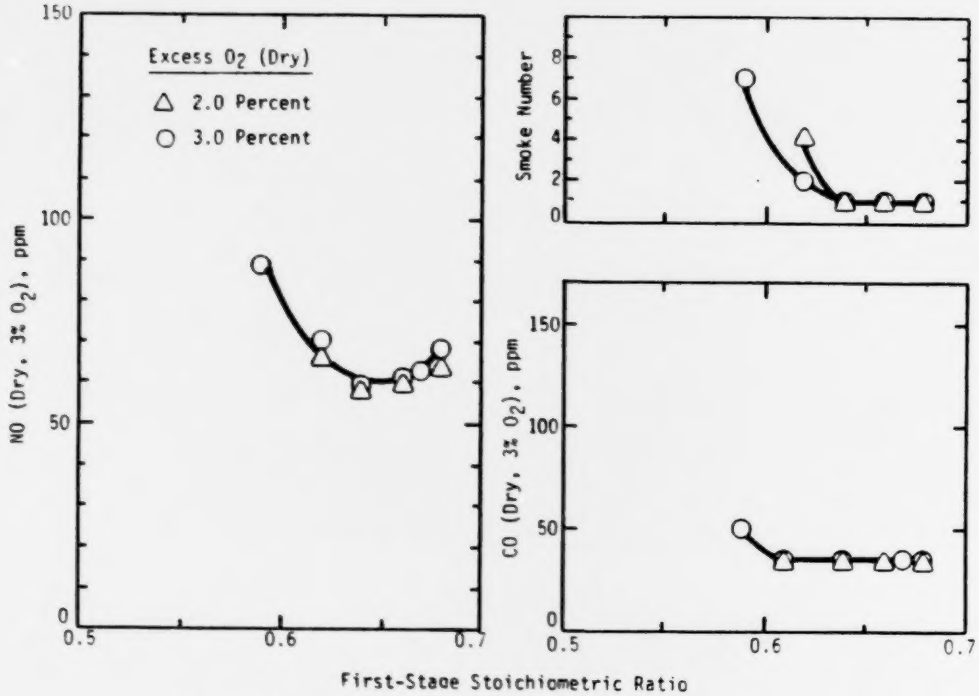

Figure 5. NO_x, CO, and smoke emissions for the modified burner at 15.8 MW_t load.

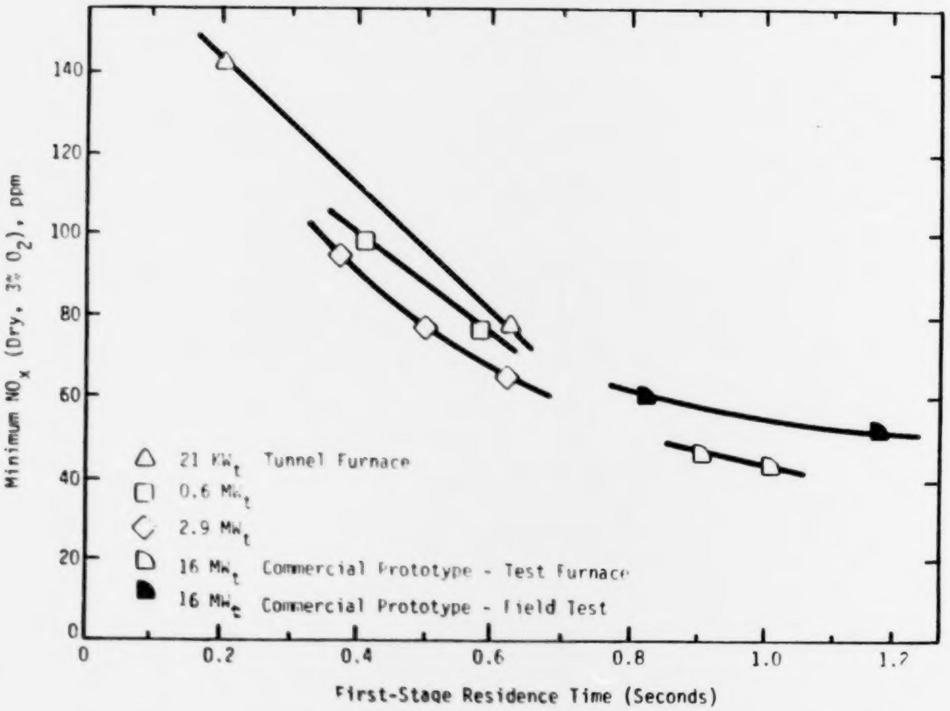

Figure 6. Comparison of low NOx concept performance for bench-scale, pilot-scale, and full-scale systems.

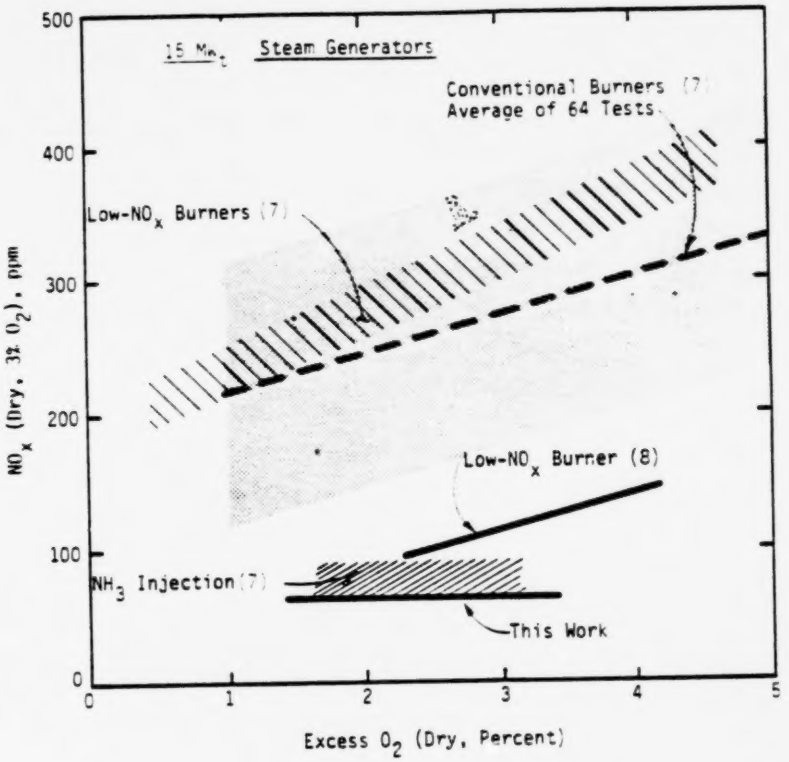

Figure 7. Comparison of prototype burner performance to conventional technology and other low NO_x technology.

Table 1

PROPERTIES OF KERN FRONT CRUDE OIL
AT HOST SITE

Parameter	Value
Ultimate Analysis (Wt%)	
Carbon	85.42
Hydrogen	10.88
Nitrogen	0.83
Sulfur	1.05
Ash	0.03
Oxygen (by difference)	1.79
	100.00
Specific Gravity (@ 15/15° C)	0.978
API Gravity (@ 15°C)	13.2
Viscosity (cp)	
@ 60°C	518
@ 99°C	58
Heat of Combustion	
Gross (kJ/g)	42.6

HEAVY OIL LOW-NO_X BURNER APPLICATION TO AN OIL FIELD STEAMER -- EMISSIONS MEASUREMENTS

C. Castaldini, L. Waterland, R. DeRosier, H. Mason
Acurex Corporation
Energy & Environmental Division
555 Clyde Avenue
Mountain View, California 94039

ABSTRACT

Comprehensive emission measurements and 30-day flue gas monitoring were performed on a 16-MW (55 million Btu/hr) enhanced oil recovery steam generator equipped with the Environmental Protection Agency (EPA) low-NO_x burner firing high-nitrogen crude. The 1-day comprehensive measurements included source assessment sampling system (SASS) quantification of semivolatile organics and 73 trace elements; volatile organic sampling train (VOST) quantitation of volatile organic priority pollutants; EPA Method 5/8 for particulate and SO_x; controlled condensation system (CCS) for SO_x; Andersen impactors for particle size distribution; grab samples for N_2O; and, continuous flue gas monitoring. NO_x emissions during the comprehensive tests averaged 70 ppm at 3 percent O_2, well below the target level of 85 ppm. CO emissions were below 30 ppm and SO_2 averaged about 550 ppm. Solid particulates were emitted at about 27 ng/J (96 mg/dscm); condensible particulates were about half that level. Volatile organics benzene, toluene, and ethylbenzene were measured in the 0.4 to 20 ppb range. Semivolatile organics naphthalene and phenol were detected in the 0.3 ppb range. Subsequent continuous monitoring of flue gas criteria emissions showed NO_x below 80 ppm at 3 percent O_2 with an average of 70 ppm. CO emissions were generally less than 30 ppm.

INTRODUCTION

Over the past 6 years, the EPA has sponsored the development and sequential scale-up of a heavy oil low-NO_x burner employing two-stage combustion. In 1984, a 16-MW (55 million Btu/hr) burner was installed and tested on an enhanced oil recovery steam generator by Energy and Environmental Research Corporation (EERC) under EPA sponsorship. The steamer is owned and operated by Chevron U.S.A. and is located in the Kern Front Oil Field near Bakersfield, California. The goal of the field demonstration was to validate the low NO_x capability and thermal performance of the burner firing high nitrogen (>0.8 percent) Kern County crude. The emission targets for the demonstration were 85 ppm NO_x (3 percent O_2), 45 ppm CO, and acceptable smoke and particulate emissions. The burner development and field demonstration is discussed in a companion paper by EERC at this symposium (1).

Comprehensive emission measurements and 30-day flue gas monitoring of the field demonstration were conducted as part of the EPA-sponsored Combustion Modification Environmental Assessment (CMEA). The CMEA is a field test program aimed at quantifying the effects of NO_x controls and alternate fuels on multimedia emissions and equipment performance. Over the past 5 years, 20 emission and performance characterizations have been made for boilers, furnaces, and engines equipped with conventional and advanced NO_x controls and for boilers firing mixed and waste fuels. One CMEA test particularly relevant to the present program was the emission and performance characterization of an EOR steamer equipped with a Mitsubishi Heavy Industries low-NO_x burner (2).

MEASUREMENT METHODS

The test program encompassed 1-day comprehensive measurements of criteria and other gas species, particulates, trace elements and organics, performed on February 1, 1984, and 30-day monitoring of flue gas criteria pollutants performed from January 21 to February 24, 1984. Table 1 summarizes the sampling and analytical test matrix employed during the comprehensive test program. Fuel samples of the crude oil were collected for proximate, ultimate, and selected trace element analyses. All flue gas emissions were measured at the stack, downstream of the steamer economizer section. Continuous monitors for O_2, CO_2, CO, NO_x, and SO_2 were operated during the comprehensive tests as well as throughout the 30-day continuous emission testing period. Volatile organic species emissions were measured with the volatile organic sampling train (VOST) according to EPA protocol (3). Trace element and less volatile organic compounds were measured using the source assessment sampling system (SASS) per an extended EPA level 1 protocol (4). Particulate and sulfur oxide compounds were measured using combined EPA Method 5/8 and a controlled condensation system (CCS). The size distribution of emitted particulate was determined using an Andersen cascade impactor. Flue gas samples were also collected for analyses of nitrous oxide (N_2O), using gas chromatography with electron capture detection. Certification of the NO_x analyzer readings was performed three times during the 30-day test period using the reference EPA Method 7 protocol.

EOR STEAMER TESTS

Steamer Operation

The EPA/EERC low-NO_x burner employs the staged air combustion concept in which a primary fuel-rich zone is separated from a fuel-lean zone where secondary combustion air is injected. The fuel-rich zone is established in a large refractory lined combustor. Primary combustion air is preheated using a regenerative combustor shell design. Secondary (unpreheated) combustion air is injected radially and axially in the transition zone connecting the combustor to the steamer.

The important operating parameters for the advanced low-NO_x burner are a low first-stage stoichiometric ratio (SR) in the range of 0.60 to 0.65, high combustor temperature of >1,430°C (2,600°F), near the adiabatic flame temperature, and a long first-stage residence time of about 0.6 sec. This combination of long gas residence time and high gas temperature promotes the decay of total fixed nitrogen (TFN) species (HCN and NH_3) to N_2 formed early in the ignition zone from fuel nitrogen under very fuel-rich conditions. Low TFN concentrations at the first-stage exit result in low-fuel NO_x conversion. In the second stage, temperature and fuel/air mixing are important to minimize thermal NO_x while keeping CO, smoke, and particulate in check. Efficient fuel/oil atomization and fuel/air mixing in the ignition zone of the combustor are also beneficial to the decay of TFN in the combustor.

During the 1-day comprehensive emission test program, burner operation was adjusted to achieve emission goals set by the EPA for the field verification program. Table 2 summarizes the burner/steamer operation during this 1-day test. The burner fired Kern County crude with a nitrogen and sulfur content of 1.04 and 1.06 percent, respectively. Total firing rate during this test period averaged approximately

24 l/min (215 bbl/day), corresponding to a heat input rate of nearly 17 MW (57 million Btu/hr). Measurement of primary and secondary airflow indicated a first-stage combustor stoichiometry in the range of 0.61 to 0.65, with an estimated gas residence time of 0.65 sec.

Flue Gas Emissions

Table 3 summarizes gaseous and particulate emissions measured during the comprehensive tests performed on February 1. NO_x emission levels were maintained below 75 ppm as measured, averaging 69 ppm corrected to 3 percent O_2, well below the target of 85 ppm set for the field demonstration program. CO emissions averaged 24 ppm (at 3 percent O_2), again within the 45 ppm program goal. SO_2 emissions measured by continuous monitors were relatively steady at about 565 ppm as measured. Conversion of all fuel sulfur to SO_2 would result in an emission rate of 495 μg/J (643 ppm) compared to the measured level of 435 μg/J (565 ppm).

N_2O levels in the flue gas, at 7 ppm corrected to 3 percent O_2, were about 10 percent of the corresponding NO_x emissions level. This is at the low end of the range exhibited in recent data from several fossil-fuel-fired external combustion sources (5). These other data suggest that N_2O emissions are generally about 20 to 25 percent of the corresponding NO_x level.

Particulate emissions were measured using SASS and EPA Method 5/8 sampling trains. Comparison of the solid particulate catch indicates an emission rate of 7.3 ng/J (26 mg/dscm) based on the SASS results, compared to about 27 ng/J (96 mg/dscm) using the EPA Method 5/8 results. This difference may be attributed in part to the higher sampling temperature of the SASS (230°C) versus the Method 5 (120°C). At higher temperatures, condensible matter which might escape the SASS filter could be caught on the Method 5 filter causing this disparity. Impinger solutions of the EPA Method 5/8 were also analyzed for condensible particulate matter. On the average, the condensed matter accounted for about one-third of the total particulate catch of 40.5 ng/J (146 mg/dscm).

Table 4 summarizes the particulate emission results of the two EPA Method 5/8 sample runs and the corresponding burner/steamer conditions during each test run. As shown, total particulate emissions for both runs were comparable (149 and 142 mg/dscm). This is in the range typical for uncontrolled EOR steamer emissions. However, the split between solid and condensible particulate between the two runs changed significantly. For run 1, only about 43 percent of the Method 5 catch was solid particulate (57 percent condensibles); for run 2, 90 percent was solid particulate (10 percent condensibles). This difference may in part be due to the higher stack temperatures and lower first-stage stoichiometry for run 2.

Table 5 shows results of the Method 8 analyses for the two Method 5/8 runs. For comparison, the average SO_2 continuous monitor reading over each run is also noted. The agreement between the reference method and the SO_2 monitor was within 10 percent for run 1 and 3 percent for run 2. The measured SO_x levels are consistent with total conversion of the fuel sulfur to SO_x (632 ppm at 3 percent O_2).

Table 6 shows results of the controlled condensation (CCS) analysis for two separate measurements made on February 23. By this method, SO_2 emissions were about 600 and 610 ppm as measured, in fairly good agreement with the Method 8 results obtained on February 1. Agreement between the CCS SO_2 measurement and the continuous monitor reading was also good, within 7 percent. However, flue gas SO_3 measured with CCS, at 47 and 51 ppm, was much higher than as measured on February 1 using Method 8. The ratio of SO_3 to total SO_x for the CCS measurements was 7.2 to 7.7 percent. This is well within the range typical for oil-fired sources.

Figure 1 summarizes particle size distribution data obtained in two separate Andersen impactor measurements. The straight line correlation denotes a log-normal distribution. Mean particle size (D_{50}) were 0.056 μm (run 1) and 0.14 μm (run 2); 90 percent of the total particulate was less than 1.4 μm (run 1) and 11 μm (run 2).

Table 7 summarizes the particulate loadings obtained using the Andersen impactors, the SASS train, and EPA Method 5. Interestingly, the Andersen results compare quite well with the SASS measurement. However, both are significantly less than the EPA Method 5 solid (front half) result. The solid particulate collection temperature for each method is also noted in Table 7 (stack temperature for the in-stack Andersen impactors and filter oven temperature for SASS and Method 5). The relatively good agreement between SASS and Andersen particulate load is consistent with the similar high temperatures at which solid particulate is collected in these methods. The high Method 5 solid particulate results suggests that significant quantities of material condense in the temperature range from 120 to 230°C (250 to 450°F), the difference between the Method 5 oven temperature and the stack and SASS oven temperatures.

Organic Emissions

Volatile Organic Emissions. Table 8 summarizes volatile organic species detected in the VOST measurement (three trap pairs were sampled and analyzed, denoted "run" in the table). Only three compounds were detected: benzene, toluene, and ethylbenzene. Flue gas concentrations were 60 μg/dscm (18 ppb) for benzene and less than 4 μg/dscm (1 ppb) for toluene and ethylbenzene, on the average.

Semivolatile Organic Emissions. Total organic emissions were relatively low, about 300 g/dscm, and roughly equally split among the semivolatile (TCO) and nonvolatile (GRAV) boiling point ranges (Table 9). The levels noted reflect the sorbent module extract analysis; the particulate (filter) extract contained negligible organic content. The emissions noted are of the same order of magnitude as emissions measured from recent tests of a steamer equipped with another low-NO_x burner design (the MHI burner (2)). Semivolatile priority pollutants detected were naphthalene, phenol, and dimethylphthalate, all at concentrations well below 10 μg/dscm. The dimethylphthalate noted is most likely a sample contaminant.

IR spectroscopy analysis of the SASS train organic sorbent module extract suggests the presence of aliphatic hydrocarbons and oxygenated hydrocarbons such as aldehydes and/or ketones. A weak spectrum for the blank suggested the presence of small quantities of aliphatic hydrocarbons.

EXTENDED CONTINUOUS EMISSIONS MONITORING

Figures 2 and 3 illustrate the emission trends over the 30-day continuous monitoring test period. The points plotted represent hourly averages of data taken at 5- to 15-minute intervals. Test periods where data gaps appear correspond to unscheduled shutdown of the steamer. The first shutdown occurred during the period of February 12 to February 15; the second from February 16 through 21.

The O_2 and CO_2 traces shown in Figure 2 indicate quite steady operation of the steamer over the entire test period. Flue gas O_2 levels were maintained at about 3 percent. Only during the final day (February 24) did the flue gas O_2 increase to over 4 percent, with a corresponding drop in CO_2 concentration. It is not known whether this increase in O_2 was caused by higher secondary or primary air flow. NO_x emissions, shown in Figure 3, indicate levels generally below 80 ppm, corrected to 3 percent O_2. Average NO_x emissions for the entire test period were about 70 ppm at

3 percent O_2. CO measurements, available only to February 11 due to subsequent instrument malfunction, indicate levels generally below 30 ppm at 3 percent O_2.

ACKNOWLEDGEMENTS

These tests were sponsored by the EPA under contract 68-02-3188. The EPA Project Officers R. E. Hall and J. A. McSorley supported the efforts in all phases of planning, testing, and data reduction. The coordination and logistical support of R. Podgers of Chevron U.S.A., and G. England and Y. Kwan of EERC was essential to the performance of the program and is gratefully acknowledged.

REFERENCES

1. G. England. "Heavy Oil Low-NO_x Burner Application to an Oil Field Steamer -- Development," presented at the 1985 Joint Symposium on Stationary Combustion NO_x Control, Boston, MA, May 6 through 8, 1985.

2. C. Castaldini, et al. Environmental Assessment of an Enhanced Oil Recovery Steam Generator Equipped with a Low-NO_x Burner, Mountain View, CA: Acurex Corporation Report TR-84-161/EE, January 1985.

3. Protocol for the Collection and Analysis of Volatile POHC's Using VOST. EPA-600/8-84-007 (NTIS PB84-170042), March 1984.

4. D. E. Lentzen, et al. "IERL-RTP Procedures Manual: Level 1 Environmental Assessment," 2d ed., EPA-600/7-78-201, (NTIS PB293795), October 1978.

5. L. Waterland, et al. "Environmental Assessment of Industrial Boilers Firing Coal-Liquid Mixtures and Wood," in Proceedings of the 1982 Joint Symposium on Stationary Combustion NO_x Control, Vol. 2, EPRI CS-3182, July 1983.

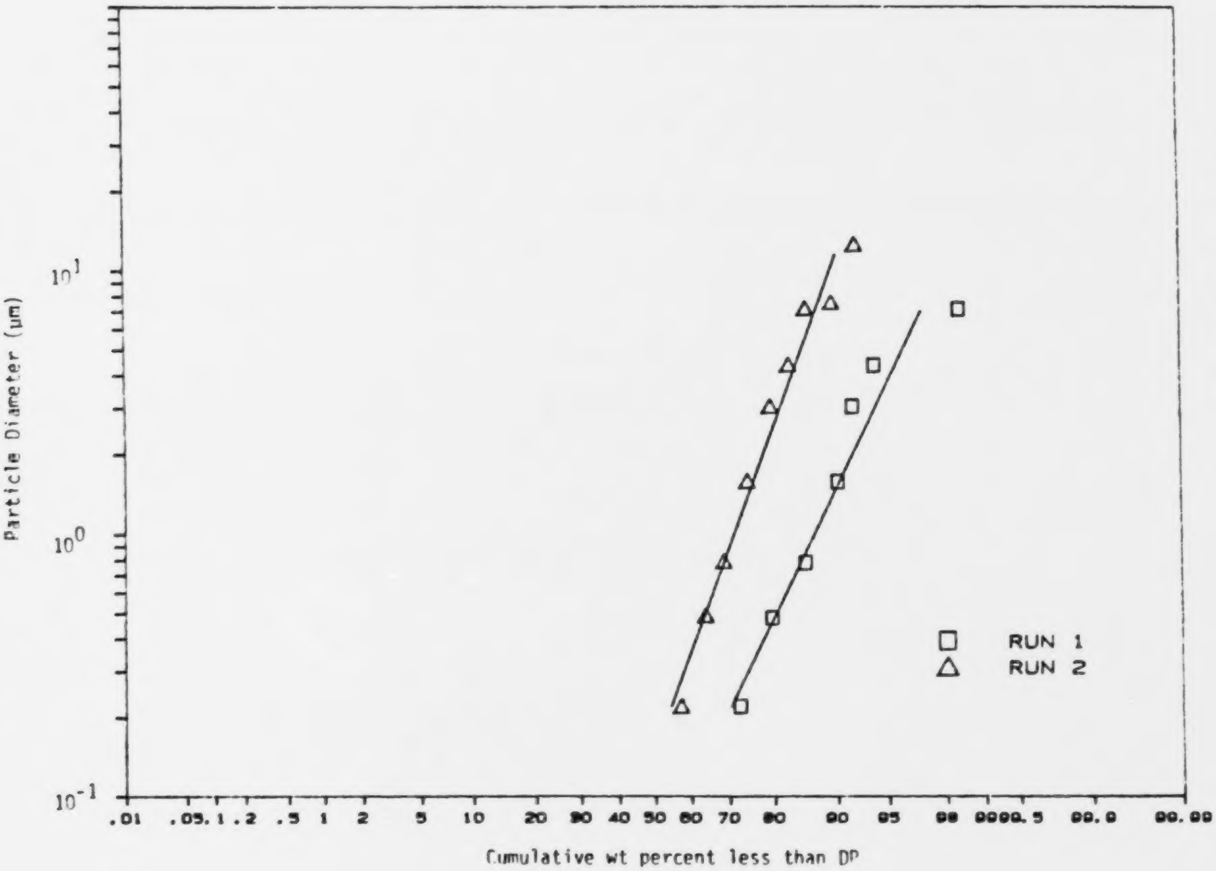

Figure 1. Particle Size Distribution

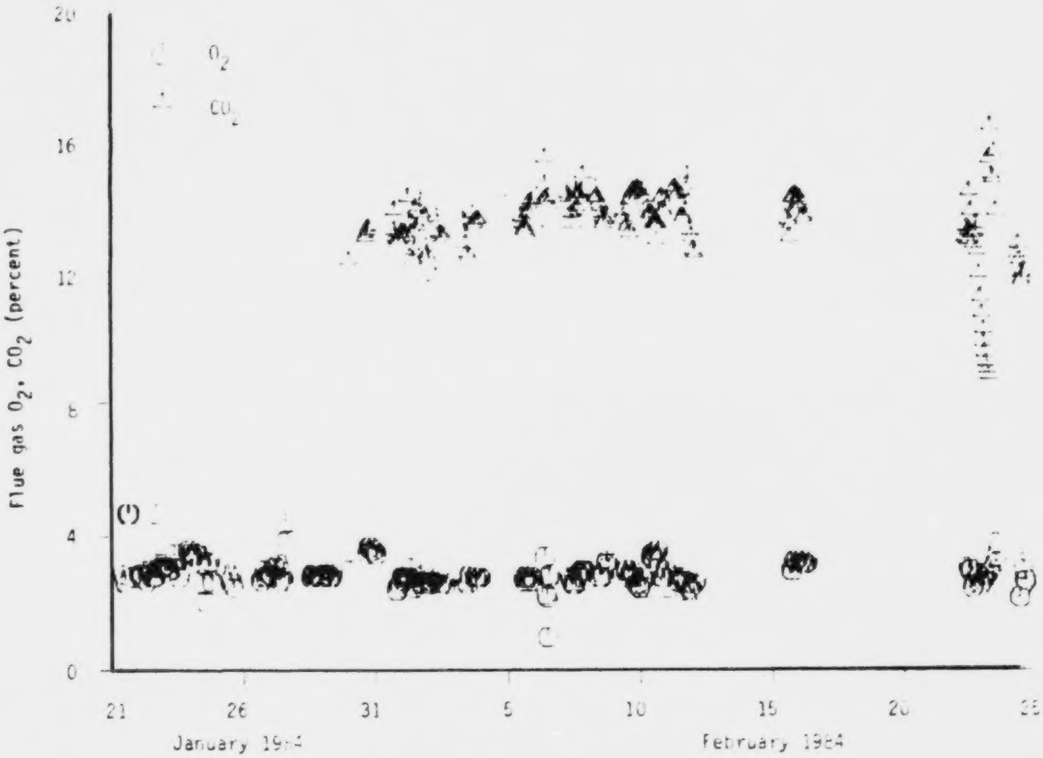

Figure 2. Flue Gas O_2 and CO_2 for the Extended Test Period

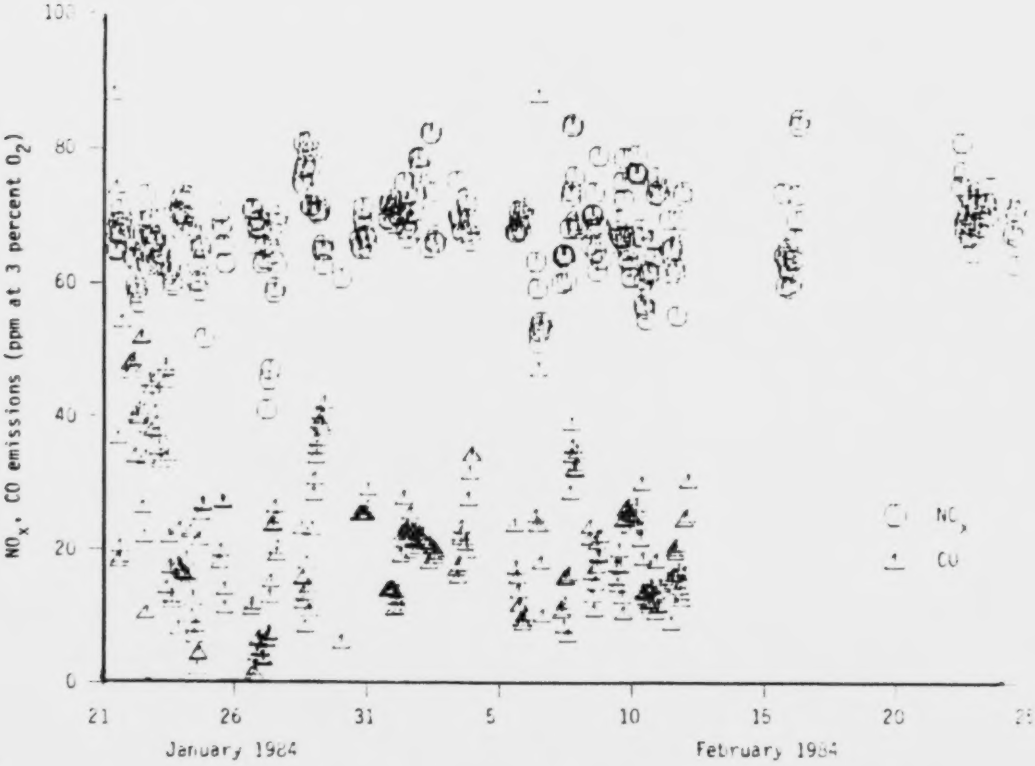

Figure 3. Flue Gas NO_x and CO for the Extended Test Period

Table 1

SAMPLING ANALYSIS TEST MATRIX

Sample/ location	Sampling Protocol	Analysis Protocol
Fuel	Grab sample	Proximate, ultimate, and selected trace elements
Stack	Continuous emission monitors	NO_x, CO, CO_2, O_2, SO_2
	Volatile organic sampling train (VOST)	Volatile organic priority pollutant species by GC/MS (EPA Method 624)
	Source assessment sampling system (SASS)	Selected trace elements, total semi- and nonvolatile organics, semivolatile organic priority pollutant species by GC/MS (EPA Method 625)
	EPA Method 5/8 train	Particulate emissions by EPA Method 5, SO_2, and SO_3 emissions by EPA Method 8
	Controlled condensation system (CCS)	SO_2 and SO_3 by titration
	Andersen impactor sampling system	Gravimetry of nine-stage impactor for particle size distribution
	Grab sample -- multiple sample bombs	N_2O by laboratory GC/ECD
	Grab sample -- multiple sample flasks	NO_x by EPA Method 7

Table 2

STEAMER/BURNER OPERATION

	Range		Average	
Fuel flow, l/min (bbl/day)	23.4 to 24.1	(212 to 218)	23.8	(215)
Heat input, MW (10^6 Btu/hr)	16.4 to 16.8	(55.8 to 57.4)	16.6	(56.6)
Fuel temperature, °C (°F)	129 to 132	(264 to 269)	130	(267)
Feedwater flow, l/min (10^3 bbl/day)	380 to 400	(3.4 to 3.6)	390	(3.5)
Steam pressure, MPa (psig)	7.03 to 9.10	(1,020 to 1,320)	8.41	(1,220)
Steam temperature, °C (°F)	279 to >300	(535 to >570)	--	--
Stack temperature, °C (°F)	232 to 254	(450 to 490)	242	(468)
Burner primary airflow, m^3/s (scfm)	2.71 to 2.87	(5,740 to 6,080)	2.80	(5,940)
Secondary airflow, m^3/s (scfm)	2.38 to 2.95	(5,040 to 6,260)	2.65	(5,630)
First stage stoichiometry	0.61 to 0.65		0.64	
First stage residence time,[b] sec	--		0.65	
Fuel oil analysis, percent weight (dry basis, unless noted)				
Carbon	--		86.2	
Hydrogen	--		11.3	
Sulfur[c]	1.00 to 1.10		1.06	
Nitrogen[c]	1.00 to 1.09		1.04	
Ash	---		0.03	
Moisture[d]	--		0.57	
Oxygen[e]	--		0.4	
Gross heating value, MJ/kg (Btu/lb)	--		42.78	(18,430)
Specific gravity (degrees API) at 60°F	--		12.6	

---

[a] Spans the entire 1-day period of comprehensive testing.

[b] Assumes a combustor temperature of 1,430°C (2,600°F).

[c] Analyses of sulfur and nitrogen were performed in triplicate.

[d] As fired.

[e] By difference.

Table 3

CRITERIA POLLUTANT AND OTHER GAS SPECIES EMISSIONS -- COMPREHENSIVE TESTS

Pollutant	Range		Average
As measured by continuous gas analyzers			
O_2, percent dry	2.3 to 2.8		2.7
CO_2, percent dry	12.2 to 13.7		13.1
CO, ppm dry	21 to 27		24
NO_x, ppm dry	66 to 75		70
SO_2, ppm dry	560 to 579		565
Corrected average gaseous emissions	ppm[a]	ng/J[b]	lb/MBtu[b]
CO	24	8.2	0.019
NO_x[c]	69	39	0.09
SO_2	556	435	1.01
N_2O	7	0.5	0.001
Particulate mass emissions	mg/dscm		
● SASS solids	26	7.3	0.017
● Method 5/8[d]			
-- Solids	96	26.7	0.062
-- Condensible	50	13.8	0.032
-- Total	146	40.5	0.094

---

[a] Corrected to 3 percent O_2.

[b] On a heat input basis.

[c] As NO_2.

[d] Average of two test measurements. Condensible particulate measured, since the Kern County Air Pollution Control District continues to regulate this fraction.

Table 4

FLUE GAS PARTICULATE MEASUREMENT RESULTS

	Run 1		Run 2	
Method 5	(mg/dscm)	(gr/dscf)	(mg/dscm)	(gr/dscf)
Solid (front half)[a]	64	0.028	128	0.056
Condensible (back half)[b]	85	0.037	14	0.006
Total	149	0.065	142	0.062
Burner/steamer operating data:	Range	Average	Range	Average
Fuel flow, l/min (bbl/day)	--	24.1 (219)	--	24.1 (218)
Heat input, MW (10^6 Btu/hr)	--	16.9 (57.7)	--	16.8 (57.4)
Fuel temperature, °C (°F)	129 to 131 (264 to 268)	130 (266)	130 to 131 (266 to 268)	131 (267)
Steam pressure, MPa (psig)	--	7.03 (1,020)	--	9.10 (1,320)
Steam temperature, °C (°F)	--	279 (535)	--	>300 (>570)
Feedwater flow, l/min (10^3 bbl/day)	--	400 (3.6)	--	375 (3.4)
Burner primary air flow, m^3/s (scfm)	167 to 172 (5,900 to 6,080)	170 (6,000)	163 to 172 (5,740 to 6,080)	167 (5,880)
Secondary air flow, m^3/s (scfm)	152 to 158 (5,360 to 5,590	155 (5,460)	153 to 177 (5,390 to 6,260)	170 (6,000)
Combustor stoichiometry[c]	0.62 to 0.64	0.63	0.61 to 0.64	0.62
Stack temperature, °C (°F)	232 to 241 (450 to 466)	236 (456)	244 to 254 (472 to 490)	248 (479)

---

[a] Solid particulate calculated from the filter and probe catches.

[b] Condensible particulate calculated from the impinger solutions; duplicate analyses performed.

[c] Assumes combustor temperature of 1,430°C (2,620°F).

Table 5

SULFUR SPECIES EMISSIONS BY EPA METHOD 5/8[a]

	Run 1	Run 2
Method 8		
SO_2, ppm dry, 3 percent O_2	619	593
SO_3, ppm dry, 3 percent O_2	12.9	4.4
Continuous monitor		
SO_2, ppm dry, 3 percent O_2	557	574
O_2, percent dry	2.7	2.7

---

[a] Tests performed on February 1, 1984.

TABLE 6

SULFUR SPECIES EMISSIONS BY CONTROLLED CONDENSATION[a]

	Run 1	Run 2
Controlled condensation system		
SO_2, ppm dry, as measured	602	611
(ppm dry, 3 percent O_2)	(653)	--[b]
SO_3, ppm dry, as measured	47	51
(ppm dry, 3 percent O_2)	(51)	--[b]
Continuous monitor		
SO_2, ppm dry, as measured	642	--[c]
O_2, percent dry	4.4	--[c]

---

[a] Tests performed on February 23, 1984.

[b] Cannot be calculated, since flue gas O_2 not known.

[c] Monitors inoperative.

Table 7

SUMMARY OF PARTICULATE LOADING MEASUREMENTS

Method		Particulate Load, mg/dscm	Collection Temperature, °C (°F)
Andersen Impactor			
Run 1:	Solid Particulate	30.8	290 (550)[a]
Run 2:	Solid Particulate	38.2	280 (530)[a]
SASS			
	Solid Particulate	26	230 (450)[b]
Method 5			
Run 1:	Solid Particulate	64	120 (250)[b]
	Condensible Particulate	85	
	Total	149	
Run 2:	Solid Particulate	128	120 (250)[b]
	Condensible Particulate	14	
	Total	142	

---

[a] Stack temperature (in-stack impactor train).

[b] Filter oven nominal temperature.

TABLE 8

VOLATILE ORGANIC SPECIES EMISSIONS

Compound	Stack Gas Concentration Run 1 (μg/dscm)	Run 2 (μg/dscm)	Run 3 (μg/dscm)	Average (μg/dscm)	Average (ppb)
Benzene	128	42	9	60	18
Toluene	6.3	1.1	2.3	3.2	0.83
Ethylbenzene	3.2	<1	<1	1.7	0.39

TABLE 9

TOTAL ORGANIC AND SEMIVOLATILE ORGANIC PRIORITY POLLUTANT EMISSIONS

	Emission level[a] (μg/dscm)	Emission level[a] (pg/J)
Total semivolatile organics (C_7 to C_{16}) by TCO	170	50
Total nonvolatile organics (C_{16+}) by gravimetry	130	35
Total organics	300	85
Semivolatile organic priority pollutants[b]:		
Naphthalene	1.4	0.40
Phenol	0.7	0.20
Dimethylphthalate	3.6	1.0
Other priority pollutants	<0.4	<0.1

---

[a] Blank corrected. Levels noted correspond to the sorbent module extract analysis; the filter particulate extract contained negligible organic content.

[b] Average of duplicate analyses.

REDUCTION OF NITRIC OXIDE EMISSIONS ON A FULL-SCALE CEMENT KILN USING PRIMARY AIR VITIATION

S. C. Hunter
R. C. Benson
KVB, Inc.
18006 Skypark Boulevard
Irvine, California 92714

ABSTRACT

KVB has been funded by the U.S. Environmental Protection Agency to conduct research for emission reduction from industrial processes. One phase of this research effort concerns NO reduction from cement kilns. Tests were conducted on a 1100 ton/day long, dry process cement kiln to evaluate the effect of primary air vitiation on NO emissions. Primary air vitiation was accomplished by injecting nitrogen gas into the primary air. As found test results (17 days, 89.75 hours) prior to the nitrogen injection test were used to assess the inherent variability of the cement-making process. The NO emissions averaged about 8 lb NO_2/ton of clinker and varied approximately 30 percent during the as found test series. Lowering kiln exit oxygen from 1.8 percent to 0.7 percent reduced NO by 15-20 percent. Three days of nitrogen injection tests for primary air vitiation were also performed at the test site. Although the testing demonstrated that nitrogen injection will reduce NO, the extent of reduction is extremely variable and is based on the operations and kiln feed at the time. NO mass emissions did decrease 20-30 percent, based on altering the burning zone temperature profile (2550°F - 2490°F) and lowering the primary air O_2 from 21 to 13 percent while maintaining a constant kiln exit oxygen of 1.5 percent. No deterioration of clinker quality was observed.

INTRODUCTION

Although the research described in the paper has been funded primarily by the United States Envronmental Protection Agency through Contract 68-02-3690 to KVB, Inc., it has not been subjected to the Agency's peer review and therefore does not necessarily reflect the views of the Agency and no official endorsement should be inferred.

There is continuing regulatory pressure to reduce emissions of oxides of nitrogen (NOx) from combustion processes. Requirements for NOx reduction from existing sources have been exerted primarily on utility boilers since they are a major emission source, are relatively large individual sources, and are semi-public or public utilities already heavily regulated but in a non-competitive market. New mobile sources have been regulated for several years with allowable emissions decreasing with time. Industrial stationary sources have received less attention but new rules are requiring minimum emissions for new sources, emission tradeoffs for construction or expansion, and, to an increasing extent, emission reductions on existing sources.

The purpose of this paper is to present the results of tests conducted on a full-scale cement kiln to evaluate the feasibility of NOx control by combustion and process modification and the resultant effect on product quality.

REVIEW OF PREVIOUS WORK

The present program is a follow-on study intended to build upon the results of the program reported in Reference 1. The objective of the earlier effort was to determine the effect of burner parameters on near-flame NOx levels for both natural gas and coal fuels. This laboratory effort determined that combustion air preheat, fuel injection velocity, and oxygen content of the primary combustion air stream have first-order effects on NOx levels. These parameters were then selected for implementation on a subscale kiln. Of these three combustion modifications, the effect of carrier (primary) air oxygen concentration on NOx emissions was most significant.

NOx emissions were reduced 37 percent by lowering the carrier gas oxygen to 12.5 percent. While NOx reduction was significant, the subscale clinker quality was not comparable to production clinker, but primary air vitiation did not seem to affect clinker quality substantially from the baseline condition. Acceptable production clinker is approximately 0.5-1.5 percent free lime. The results of the combustion laboratory tests were corroborated by the subscale test results.

Based on these test results, KVB concluded that dilution of the primary air stream with an inert gas offered the highest probability of NOx reduction by combustion modification on a full-scale kiln.

PRESENT APPROACH

The objective of the current program was to implement the results of previous work on a full-scale cement kiln to investigate the effect of combustion modification on product quality.

The test program reported here was conducted at a cement plant in California. The cement company was interested in such a test program because an emission limit goal of 3.1 lb NOx/ton clinker is being considered by the local air quality management district. Data with inert gas injection would be useful input for the decision-making process. Three alternatives were considered for partial inerting of the primary air stream. These alternatives were:

- 600 hp boiler supplying flue gas
- Flue gas recirculation from the kiln stack
- N_2 injection

Alternatives were analyzed for initial and operating costs, operability and flexibility. Nitrogen injection into the primary air stream was the lowest cost alternative for a very short term test. A liquid nitrogen pumper with nitrogen vaporizer was supplied by a local service. The gaseous nitrogen could be supplied at the flow rates needed to achieve an overall primary air/N_2 stream O_2

down to 13 percent. Figure 1 shows a variable-speed cryogenic pump that pushed liquid N_2 to a direct-fired heat exchanger where the nitrogen vaporized and flowed through a metering valve, a shut off gate valve and diffused into a sixteen inch duct.

PROCESS DESCRIPTION

Cement clinker in a long dry kiln is produced in the calcination, sintering, and clinker cooler zones. The raw feed material is charged as a dry pulverized powder into the upper end of the kiln through a feed pipe. The feed passes through a chain section which heats the feed rapidly. The calcination process occurs in the middle third of the kiln. As the calcined feed proceeds towards the lower end of the kiln (burner end), the high temperatures resulting from the coal combustion heat the feed to its sintering temperature. Sintering is the liquefying of the clinker constituents and then cooling to form the four principal cement constituents: dicalcium silicate, tricalcium silicate, tricalcium aluminate and tetracalcium aluminoferrite. The formation of these cement constituents is determined as well as the amount of uncombined (free) lime (0.5-1.5 percent regarded as acceptable) as part of the final product analysis.

KILN SYSTEM DESIGN AND OPERATION

Figure 2 is a schematic of the cement kiln system showing all of the major components. The kiln is a long dry rotary cement kiln 149 m (490 ft) long and 4.1 m (13.5 ft) inside diameter. Two 150 hp motors are required to drive the kiln. The slope of the kiln is 7/16-inch per foot. Maximum kiln speed is 1.33 rpm (90 rph). Kiln rated production is 45 tons of clinker per hour. The thermal input rate is approximately 70.3 MW (240×10^6 Btu/hr). A Southern Utah bituminous coal is normally burned. The kiln is direct fired from a Raymond Model 573 pulverizer rated at 7 tons per hour. A booster fan has been added to increase fuel delivery to 10 tons per hour, uncorrected for moisture loss.

Clinker in the kiln is normally produced at the plant by maintaining a constant fuel rate and varying the kiln speed to hold the burning zone temperature at the desired level. When the burning zone temperature is higher than the desired level, the kiln speed is increased to decrease the front end temperature. If the material temperature and NO rises or falls abruptly, kiln speed step changes are made to counter the rise or fall; the magnitude of the change depending on several factors, including the time rate of change of NO and material temperature.

NO_x EMISSIONS FROM CEMENT KILNS

Cement kiln NO_x emissions depend on a number of factors ranging from fuel and feed nitrogen content to clinker cooler operation and fuel/air splits. Some of the key factors are listed below with a brief discussion of their impacts.

- Burning Zone Temperature
- Fuel/Air Ratio
- Burner Tip Velocity
- Secondary Air Temperature
- Raw Mix Chemistry

- Fuel Nitrogen Content
- Feed Nitrogen Content

The primary/secondary air ratio, primary air/coal burner tip velocity and combustion air preheat temperature have already been previously explored for their importance in NO_x formation (Ref. 1). Secondary air mass flow and temperature in the cooler are primarily a function of the clinker cooler grate speed, clinker bed depth, clinker particle size, clinker rate and flame zone pattern. The amount of secondary air which enters the kiln is controlled by the kiln hood draft. The hood draft is typically maintained at slightly negative pressure (approximately .05-.10 inches water). If excess secondary air is to be trimmed, that air can be vented through cooler chimneys. Adjusting the ID fan damper position (more closed) or opening the vent chimney damper should drop the kiln exit O_2 if all other factors remain constant. The lower kiln O_2 will reduce the NO_x emissions.

NO_x emissions are also significantly affected by feed mix chemistry. Changes in mix chemistry can affect the burnability and formation of the liquid phase in the burning zone.

The fuel and feed nitrogen will in part be converted to nitrogen oxides in the post combustion zone of the kiln. It is expected that the high flame zone temperature necessary for clinkerization results in the vast majority of NO_x formation.

DATA ACQUISITION METHODS

Gaseous emission measurements were made using analytical instruments and equipment contained in a government-furnished mobile instrumentation laboratory. The laboratory is equipped with analytical instruments to continuously measure concentrations of NO, NO_2, CO, CO_2, and O_2. For the as-found, low excess air and nitrogen injection test series, NO was measured with CO, CO_2, and O_2. Measurement of total NOx (NO + NO_2) requires a heated sample line and involves a differential measurement of NO and total NOx, the difference being NO_2. Conditions in the kiln were not sufficiently steady to allow accurate differential determination of NO_2. The gaseous sampling line extracted gas from the exit of the kiln, at the point where raw feed is injected.

An On-line Emissions Monitor Program was written for the Apple II Plus 48K computer to provide automatic digital data acquisition for real time monitoring of emissions data. The computer was programmed to scan every five seconds and print the gaseous emissions data averaged over one, three, five or fifteen minutes. The program provides a continuous visual display of time plots for any two of the gaseous species (e.g., NO, O_2) and records the data printed out on magnetic disk. Strip chart recorders are used to verify the data recorded on magnetic disk and fill in any gaps from the computer, should they occur.

The sampling for oxygen levels in the primary air during the nitrogen injection tests was performed using a portable Teledyne Model 320A oxygen analyzer. The sample port for oxygen measurement was located in the 16-inch diameter burner line approximately 50 ft from the burner tip. During the N_2 tests, carrier gas O_2 was monitored every minute to two minutes.

DATA ANALYSIS METHODS

Daily kiln exit gaseous emissions normally analyzed were NO, CO, CO_2, and O_2. The O_2, CO_2 and CO data are reported on a dry volume basis and the NO data were reported on a dry volume basis corrected to 3 percent O_2. The dry stack gas data were statistically analyzed for the arithmetic mean, sample standard deviation, coefficient of variation and 95 percent confidence level (see nomenclature for definitions).

The volumetric NO concentration was converted to a pounds per ton of clinker basis and reported as NO_2. The plant measurements used for deriving clinker rate are the following:

- Clinker Weigh Belt Scale
- Kiln Feeder Speed (strip chart)
- Kiln Feeder Revolution Counter
- Kiln Speed

Instantaneous clinker rate can also be calculated from a formula for MMBtu per ton clinker based on gaseous emissions data (CO_2, O_2), heating value, ultimate analysis, and ignition loss of the raw feed. Once the MMBtu per ton of clinker is calculated, the fuel rate and heating value are used to calculate the clinker rate. This method was found to be less reliable, compared to using the plant instruments.

AS-FOUND TEST SERIES

Seventeen days of as-found data were collected to assess process variability. Twelve coal samples, 67 clinker samples, 30 raw feed samples, two multiclone dust samples and two combined feed samples (raw feed plus multiclone dust) were collected. A multiclone dust sample was analyzed for particle size and chemical composition.

Table 1 summarizes the daily as-found emissions data on a volumetric and mass basis for Type II feed (15 days) and Type III feed (two days). The as-found emissions (17 days of data, 89.75 hours) averaged 8 pounds NO as NO_2 per ton of clinker.

Figure 3 shows the coefficient of variation for the volumetric NO emissions has been plotted on a daily basis. The coefficient of variation ranges from a low of 14.5 percent to a high of 57.8 percent. The large dispersion from the mean (time weighted average coefficient of variation of 31 percent) shows that daily cement kiln emissions (volume basis) are extremely variable. Figure 4 shows the distribution of emissions factors on a lb NO (as NO_2) per ton of clinker. The distribution shows that approximately 80 percent of the mass emissions data range between 6.5 and 10.5.

Kiln feed samples were analyzed by x-ray fluorescence for oxide content and SO_3. While the feed composition analyses are proprietary and thus not reported, a series of factors and indices used to characterize burnability are reported. The burnability of the kiln feed is the relative ease or difficulty with which the feed is converted into clinker. The average burnability factor of the 37 feed samples was 108.5 with a standard deviation of 2.15 (Type II feed only).

The chemically bound nitrogen in the raw feed was measured for one of the samples. That measurement was 24.9 ± 1.3 ppm. Previous work has indicated that 100 ppm N in a kiln feed is equivalent to about 1.0 pounds NO_2 per ton of clinker if all converted (Ref. 2). Thus, the raw feed nitrogen could conceivably contribute the 0.2-0.3 pounds NO_2 per ton of clinker to the total mass emissions.

The fuel nitrogen content on a weight basis is 1.3-1.5 percent. This fuel bound nitrogen content was consistent based on several sample measurements. The consistency eliminates the fuel nitrogen content as a factor in variable NO emissions.

Clinker analysis results for the as-found clinker samples showed the standard deviation of tricalcium silicate to be approximately 6.6 percent. The variability was traceable to homogenizing silo problems and rock mix difficulties. Figure 5 shows NO versus clinker free lime for the as-found tests. The figure shows considerable scatter, indicating that free lime is affected by factors other than NO alone. Nevertheless, it is apparent that low NO operation tends to increase free lime, a factor that must be considered in any attempt to reduce cement kiln NO emissions.

The main conclusion from the as-found test series was that the wide variation in NO, and the strong correlation of NO with material temperature and difficulty in maintaining stable operation of the kiln render the tasks of controlling NO very difficult. On the other hand, if means can be found to stabilize the process using NO as a key control variable, product quality would be more uniform and the task of controlling NO would be enhanced.

INITIAL NITROGEN INJECTION RESULTS

Evaluation of the primary air vitiation system was based on tests conducted on three separate days. These three testing days were November 15 and November 17, 1983 and April 17-18, 1984. Between the two November tests and the April test, a low excess air test series was conducted.

The objective of the first day of the nitrogen injection tests (November 15) was to shakedown the system to insure that nominal flow rates of up to 0.80 m^3/s (100,000 scfh) would not adversely affect mill operation or burner stability. The mill outlet average oxygen concentration was approximately 17 percent. The objective for the first day of testing was achieved; nitrogen could be injected with no detrimental effect on coal mill operation and no obvious effect on flame stability. The results with regard to the effect of N_2 injection on NO emissions were inconclusive at 17 percent carrier air O_2.

A longer term nitrogen injection test (approximately 3-1/2 hours) at higher N_2 flow rate was performed on November 17th. It was not clear from these tests, whether the NO decreased as a result of nitrogen injection or because the O_2 decreased. Free lime and X-ray diffraction analyses did not indicate any deterioration of product quality during the injection testing.

LOW EXCESS AIR TEST SERIES

Initial tests with short-term nitrogen injection (1-3 hours) indicated that the nitrogen injection caused a reduction in excess air as the result of flow balance changes in the kiln. Therefore prior to proceeding with further nitrogen injection, a 4-day test was conducted to evaluate more closely the effect of excess air on nitric oxide emissions.

Figure 6 summarizes the results, indicating a significant effect of kiln exit O_2 on NO but also showing a strong effect of material temperature. Table 2 shows some of the key mean emissions and operations values for the low excess air test series. Lowered excess air (LEA) decreased NO volumetric and mass emissions by approximately 15-20 percent. The percent reduction was established from a reference baseline of 1050 ppm (corrected to 3 percent O_2) with a kiln exit oxygen of 0.7 percent. The average calculated pounds NO as NO_2 per ton of clinker was 8.07 at reference baseline and 7.02 at low excess air conditions; the resultant reduction was 13.0 percent. The average burning zone temperature, as measured by an optical pyrometer, was 2477°F at reference baseline conditions and 2460°F at LEA conditions. The effect of kiln feed burnability factor on NO emissions was not included in this analysis. Figure 7 shows CO as a function of O_2 for this test series. The curve shows the pronounced effect on CO emissions by lowering the kiln exit O_2 below one percent. Based on this curve, the kiln exit O_2 of 0.7 percent is probably the reasonable low O_2 level for the CO limit.

FINAL NITROGEN INJECTION TEST

The final nitrogen injection test series was performed for approximately eight hours on April 17th and 18th. The objective of this test was to adjust kiln operating conditions during nitrogen injection so that kiln exit O_2 would remain as constant as possible. A constant O_2 would factor out the effect of O_2 which has complicated the data analysis for previous tests.

Figure 8 presents the time plot of lb NO_2/ton of clinker and kiln exit O_2, with the values plotted as three-hour rolling averages to smooth the fluctuations. The objective of holding kiln O_2 constant was not completely met but the O_2 was considerably steadier than in previous tests. The period of N_2 injection is shown on the figure. Lb NO_2/ton of clinker was reduced from about 9.6 lb/ton (21 percent primary air O_2) to about 7.0 lb/ton (13 percent primary air O_2). Table 3 summarizes some of the key emissions and operations data for the nitrogen injection test.

High speed motion pictures were taken of the flame near the tip of the burner at 2,000 frames per second. These films and operator observations indicated a definite lengthening and cooling of the flame. This effect is normal for low NOx operation on other combustion devices, but would require further investigation over a longer time to determine if this effect could be acceptable for clinker quality and kiln life.

Analysis of raw feed and clinker samples indicate that most of the clinker variability could be explained by feed composition variation. Figures 9 and 10 show a time trace of the NO volumetric emissions, material temperature and free lime for the nitrogen injection test series. The free lime content throughout this test series was less than 0.3 percent and alkali content remained less than 0.6 percent. It was concluded that the test did not result in deterioration of clinker quality, but it was apparent that the clinker was being overburned, probably due to the kiln operator's concern for avoiding an upset as the result of the test.

While the percent NO reduction (from baseline to nitrogen injection) was 27 percent, this degree of reduction cannot be attributed entirely to the N_2

injection. Changes in kiln speed, coal flow, material temperature, feed composition, and other variables, in spite of the operator's desire to maintain constant conditions, complicate the data analysis. The data were subject to a statistical time series analysis to attempt to isolate in effects of the important variables.

STATISTICAL ANALYSIS OF PRIMARY AIR VITIATION

After the nitrogen injection test series were completed, the question remained of how much effect does the one percent decrease in mill exit O_2 have on NO emissions, holding all other operational parameters constant. A statistician familiar with systems modeling was retained to consider this question. A summary of his work is discussed below. The first task was to model the behavior of the kiln system operation with a set of simultaneous equations. Six structural equations were devised as model fits for kiln exit NO (ppmV), kiln exit O_2 (percent), rotation speed (rph), material temperature (°F), kiln exit CO (ppmV), and kiln exit CO_2 (percent). The final structural equations both fit and forecast very well for NO, rotation speed and material but only an adequate job for O_2 and CO_2. The final structural equation for NO was modelled with the mill outlet O_2, kiln exit O_2, burnability factor moving average, kiln speed, coal rate and ID damper setting.

Two data sets were derived from the April 17-18 nitrogen injection test series for the purposes of determining the effect of mill outlet O_2 on NO emissions. The data sets are identified as MOD(6)=2 and MOD(6)=4 beginning at 1604 hours and 1606 hours, respectively. MOD(6)=2 has 87 data points with complete observations; however 16 of those data points had to be completed with data from the nearest data neighbor. MOD(6)=4 also has 87 data points with complete observations but 17 of those data points had to be completed with data from the nearest data neighbor.

A summary table of the volumetric NO ppm reduction statistically expected with mill outlet oxygen decrease is reported in Table 4. The reductions are based on partialing out or holding constant certain variables in the NO model. Specifically, for the MOD(6)=2 data subset, if the burning zone temperature, burnability factor, rotation speed and coal rate were held constant, then the effect of raising mill outlet O_2 is estimated to be 51.4 ppm NO (standard error of 9.4 ppm) for each additional percent of O_2 in the experimental range of 12.5 to 21.0 percent O_2. An asymptotic t-test of the null hypothesis that changing mill outlet O_2 under these controlled conditions has no effect on NO indicates that the estimate is significantly different from zero at the 0.0001 level ($P < 0.0001$). Thus, the mill outlet O_2 decrease has a statistically significant effect on NO emissions.

The data show that the NO concentration decrease per one percent decrease in mill outlet oxygen ranges from 16.4 to 76 ppm NO. The two data subsets seem to agree fairly well in the NO concentration decreases. The actual effect depends on what is held constant (by the model) and what is not. No check was made of the linearity between the NO concentration decrease and mill outlet oxygen decrease.

The structural equations do have limitations which should be acknowledged for results interpretation. More variables should be added to the structural equations to improve the system model. In particular, endogeneous variables such as the secondary air temperature, kiln hood pressure and undergrate pressure should be added to the NO model for improved forecasting of perturbations in NO emissions.

Another difficulty with associating a specific NO decrease per one percent decrease in mill outlet oxygen is that the other predictor variables are unlikely to remain constant. If the mill outlet O_2 is decreased from 21 to 13 percent oxygen, operational changes are very likely to occur. Kiln speed changes are made to retain the heat requirements in the burning zone while kiln exit oxygen is expected to decrease. Kiln speed changes will affect the undergrate pressure and consequently the kiln hood pressure.

The interpretation of the results should also be weighed against the ad hoc procedure used to fill in the missing values. For future work any observed time series should consist of sequential data points with no discontinuities.

CONCLUSIONS

- The cement kiln tested had substantial variability in many process parameters which affect NOx emissions. This variability considerably complicated the investigation of the applicability of combustion modifications.
- Stabilizing the process must be an essential part of any attempt to control NOx emissions by combustion or process modifications.
- As-found emissions (17 days of data, 89.75 hours) averaged 8 pounds NO as NO_2 per ton of clinker. The uncertainty of the as-found mean mass emissions data is estimated to be 10 percent.
- Lowered excess air (LEA) decreased NO volumetric and mass emissions by approximately 15-20 percent. The average calculated pounds NO as NO_2 per ton of clinker was 8.07 at reference baseline and 7.02 at low excess air conditions; the resultant reduction was 13.0 percent.
- NO was reduced during short-term nitrogen injection tests, with reductions of the order of 25-30 percent. Because of interacting variables, it was not possible to clearly isolate the effect of nitrogen injection.
- Injection of nitrogen produced a longer, cooler flame; an effect that would require much further investigation, over a longer time, before full-time implementation would be possible.
- Clinker quality remained within the range of normal variability for the kiln tested with no apparent deterioration during low excess air and nitrogen injection tests.
- The test program met the objective of evaluating the effect of combustion modification on product quality, but only on a short-term basis. Longer term tests with improved process stability are required.

REFERENCES

1. W. A. Carter and R. C. Benson, "Application of Combustion Modification Technology for NOx Control to Cement Kilns," Proceedings of the 1982 Joint Symposium on Stationary Combustion NOx Control, Volume 2, EPRI CS-3182, July 1983.

2. E. M. Gartner, "Nitrogenous Emissions From Cement Kiln Feeds," Portland Cement Association Project HM 7140-4330 Report, March 1983.

NOMENCLATURE/EQUATIONS

1. Arithmetic mean ($\bar{x}$): sample average; estimate of population mean, μ.

2. Sample standard deviation (s): dispersion or spread of the data about its mean value ($\bar{x}$)

3. Coefficient of variation (cv): $\frac{s}{\bar{x}} \times 100\%$

4. CI95 or 95 percent confidence interval: probability in percent that the confidence interval for the sample average $\bar{x}$, will include the population mean, μ.

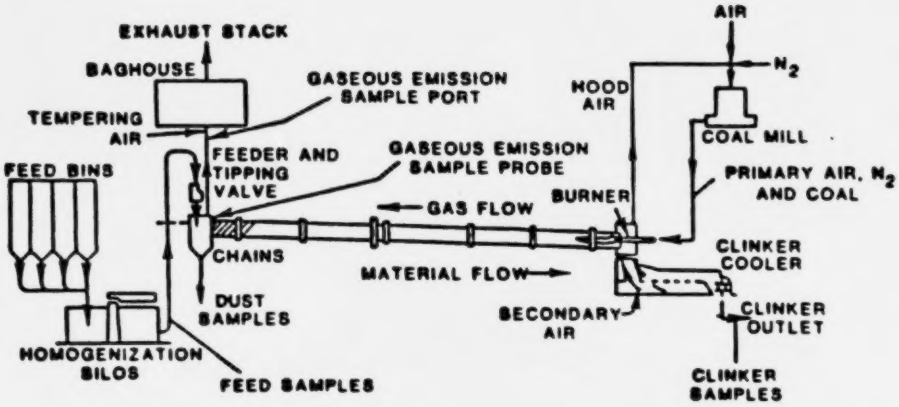
EXHAUST STACK
BAGHOUSE
TEMPERING AIR
GASEOUS EMISSION SAMPLE PORT
FEED BINS
FEEDER AND TIPPING VALVE
GASEOUS EMISSION SAMPLE PROBE
GAS FLOW
CHAINS
MATERIAL FLOW
DUST SAMPLES
HOMOGENIZATION SILOS
FEED SAMPLES
AIR
N_2
HOOD AIR
COAL MILL
PRIMARY AIR, N_2 AND COAL
BURNER
CLINKER COOLER
SECONDARY AIR
CLINKER OUTLET
CLINKER SAMPLES

Figure 1. Schematic of Long Dry Process Test Kiln

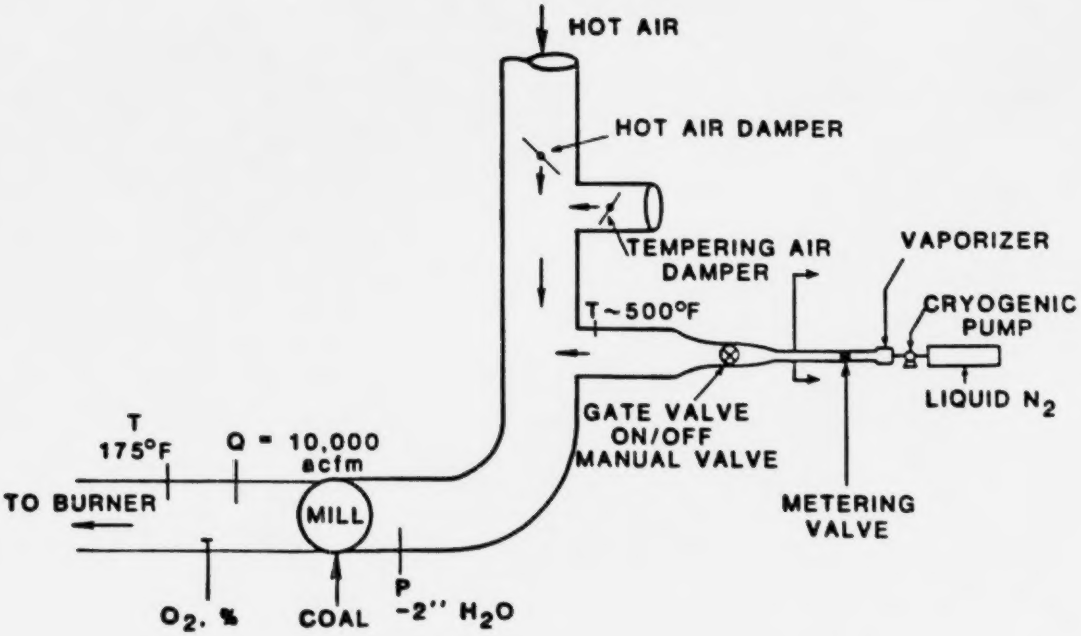
HOT AIR
HOT AIR DAMPER
TEMPERING AIR DAMPER
VAPORIZER
CRYOGENIC PUMP
T~500°F
LIQUID N_2
GATE VALVE ON/OFF MANUAL VALVE
METERING VALVE
T 175°F
Q = 10,000 acfm
TO BURNER
MILL
O_2, %
COAL
P -2" H_2O

Figure 2. Flow and Controls Schematic for Coal Mill Carrier Air

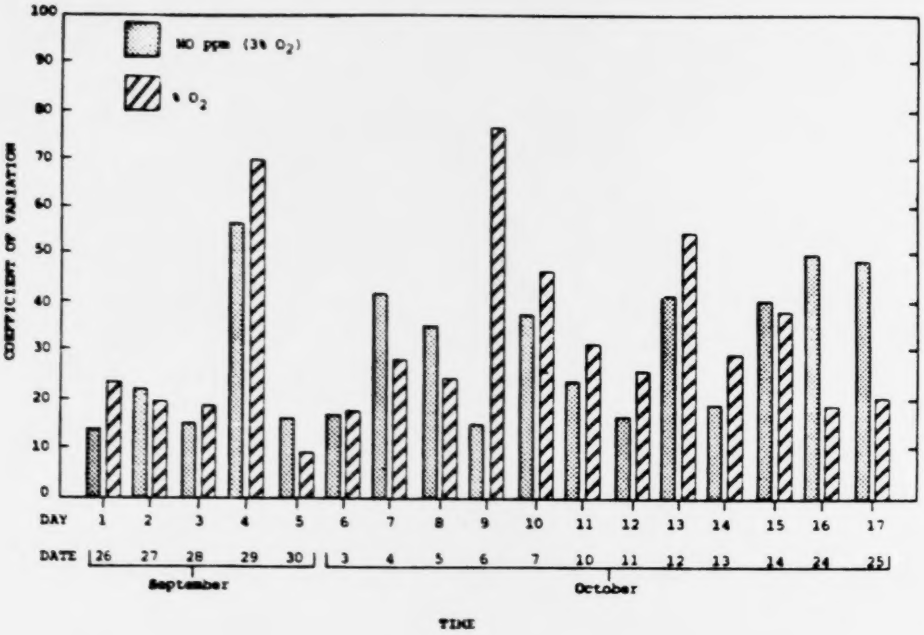

Figure 3. Daily As-Found Coefficient of Variation for NO and O_2 Emissions Data

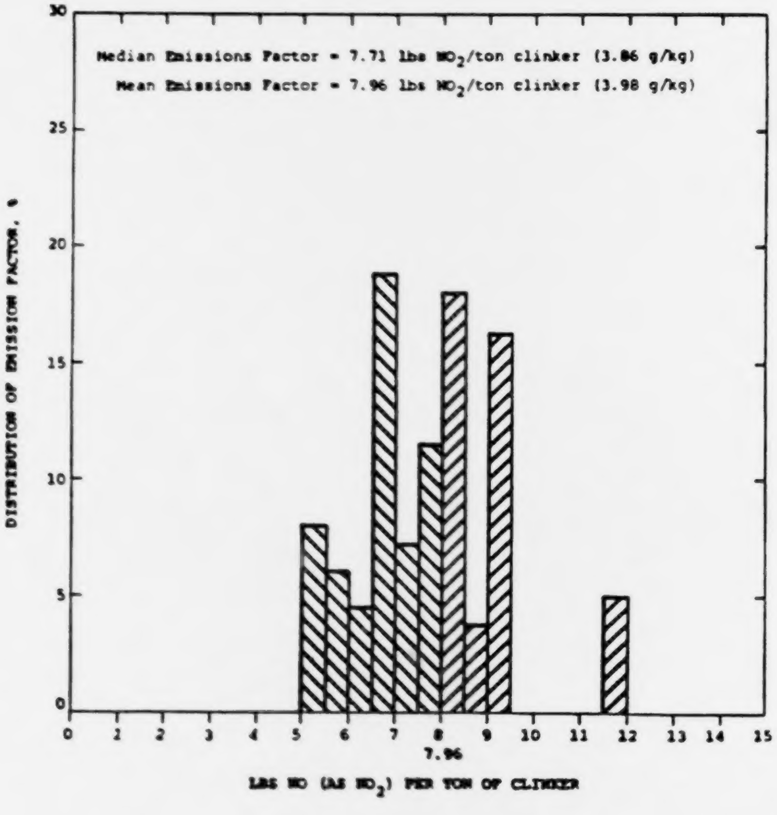

Figure 4. Distribution of Daily As-Found Emission Factor, Lbs NO (as NO_2)/Ton Clinker

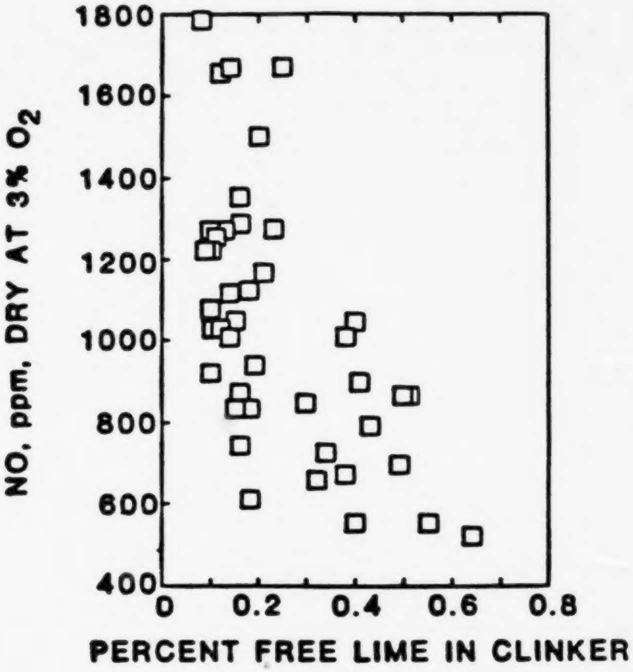

Figure 5. NO Versus Free Lime for As-Found Tests

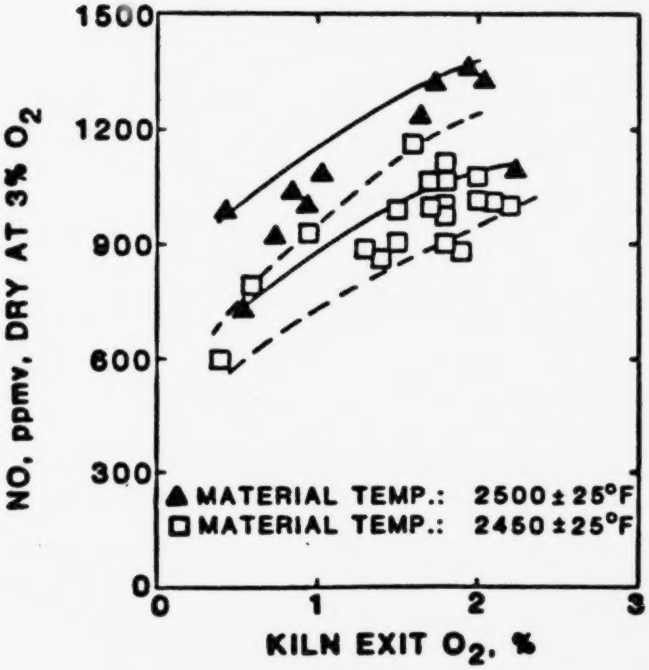

Figure 6. NO Versus O_2 (Material Temperature Range of 2425 - 2525°F)

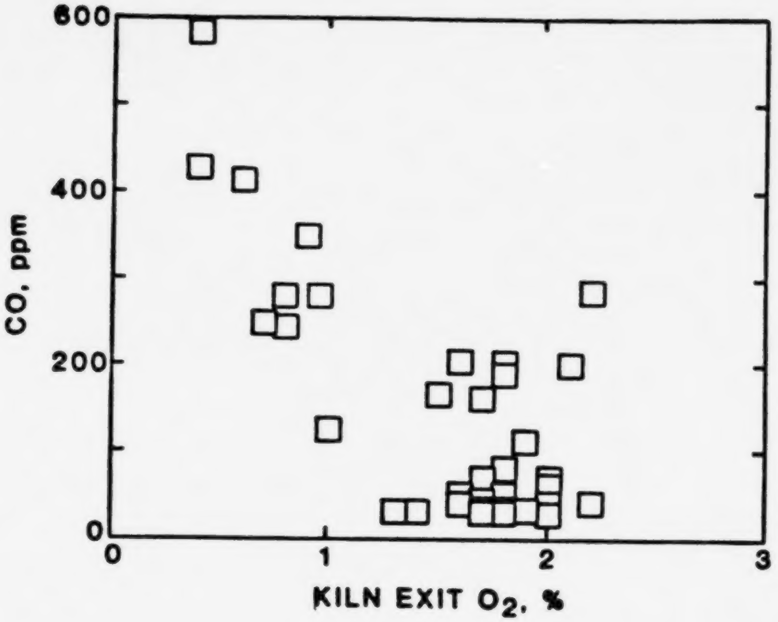

Figure 7. CO Versus O_2

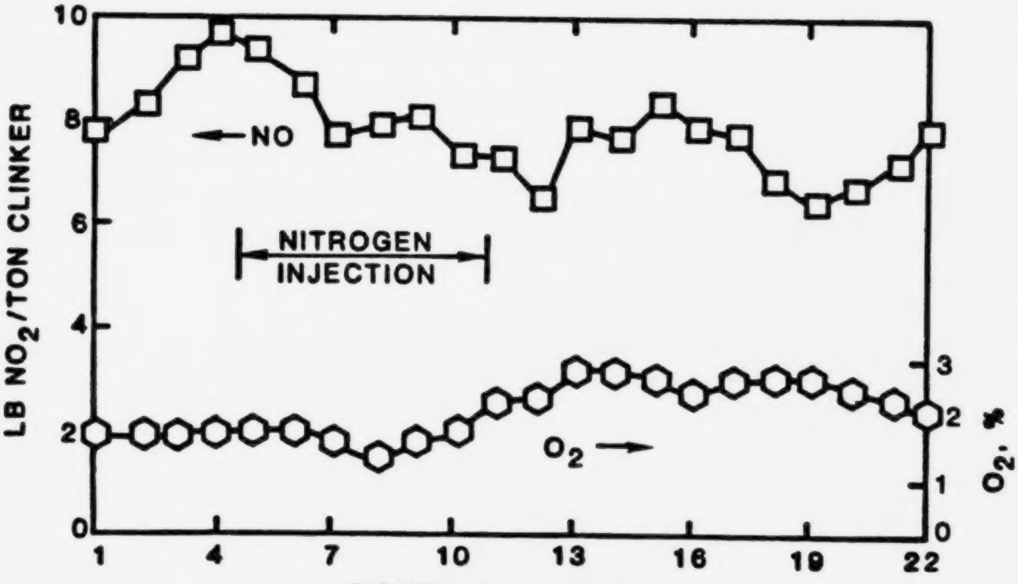

Figure 8. Three-Hour Rolling Average NO and O_2

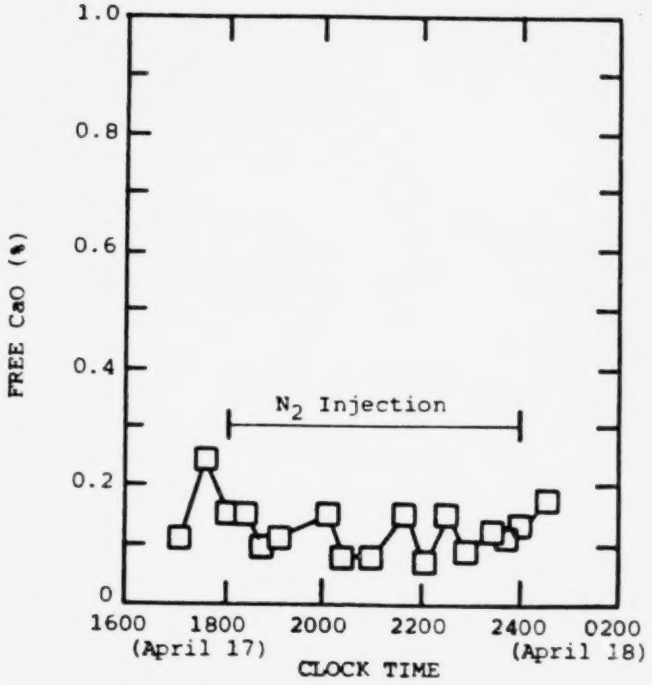

Figure 9. Time Trace of Free Lime for April 17-18, 1984 Nitrogen Injection Test Series

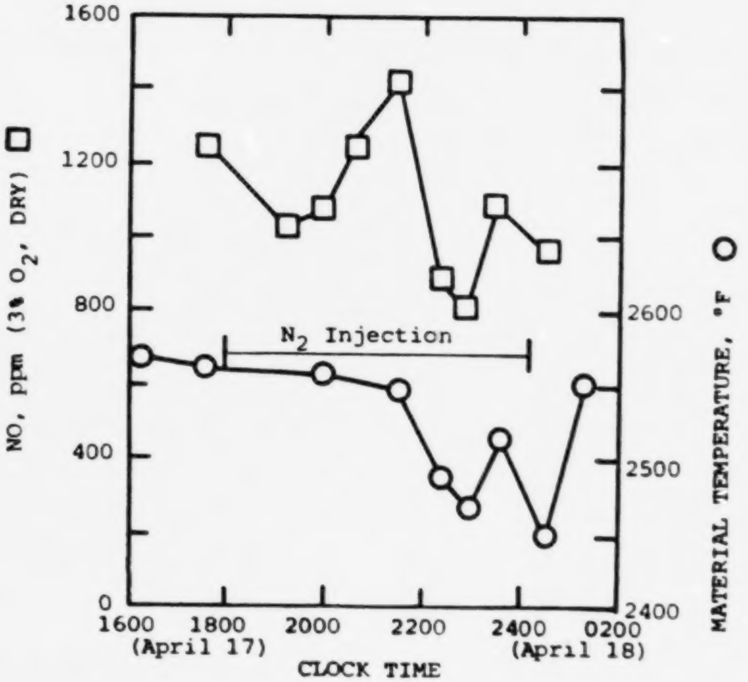

Figure 10. Time Trace of NO and Material Temperature for April 17-18, 1984 Nitrogen Injection Test Series

Table 1

DAILY AS-FOUND VOLUMETRIC AND MASS EMISSIONS

Date	Test Duration		O_2 Vol % Dry		CO_2 Vol % Dry		CO ppmV Dry		NO ppmV Dry ($3\% O_2$)	
1983	Begin	End	Mean	CI95	Mean	CI95	Mean	CI95	Mean	CI95
9/26	1130	1630	2.1	0.3	29.7	1.2	--	--	1510	126
9/27	915	1600	2.0	0.2	28.7	0.6	--	--	1127	148
9/28	845	1600	1.7	0.1	28.8	0.4	--	--	983	65
9/29	845	1530	2.1	0.6	28.3	0.6	--	--	741	181
9/30	900	1530	2.5	0.1	27.9	0.4	--	--	881	59
10/03	845	1230	2.7	0.2	27.3	0.6	--	--	1069	104
10/04	745	1330	2.7	0.4	28.1	0.7	63	39	1096	231
10/05	815	1530	2.0	0.2	28.2	0.6	94	29	1225	162
10/06	745	1045	3.3	1.6	27.7	1.3	65	35	1103	119
10/07	1130	1500	2.9	0.7	28.1	1.1	88	32	860	187
10/10	845	1615	2.7	0.3	27.8	1.1	45	6	963	87
10/11	845	1545	3.4	0.3	27.9	0.6	33	4	974	70
10/12	800	1330	3.5	0.9	28.3	1.1	42	13	977	189
10/13	800	1530	2.0	0.2	30.0	0.7	70	19	906	81
10/14	745	1500	2.0	0.3	29.6	0.6	83	30	658	103
10/24	1000	1500	2.2	0.2	29.5	1.0	90	22	919	206
10/25	1015	1415	2.5	0.3	28.0	0.6	68	19	1021	256

Table 2

LEA TEST SERIES

Baseline: 6.5 Hours of data
26 data points

Lowered Excess Air: 3.25 hours of data
13 data points

	Baseline ($\bar{x}$ ± CI95)	LEA ($\bar{x}$ ± CI95)
Kiln Exit O_2, % Dry	1.82 ± 0.08	0.71 ± 0.23
Kiln Exit CO, ppm	88 ± 30	355 ± 103
Coal Rate, Tons/Hour	9.08 ± 0.04	9.00 ± 0.1
Mat. Temp., 3% O_2	2460 ± 0.04	2477 ± 15
NOm ppmv, 3% O_2	1050 ± 55	880 ± 85
Lbs NO (as NO_2)/Ton Clinkler (Based on Clinker Weigh Scale)	8.07 ± 0.21	7.02 ± 0.07

Table 3

NITROGEN INJECTION TEST SERIES
APRIL 17-18, 1984

Time Test Description	4/17 1503-1700 Hrs. Pre N_2 Inj	$\bar{x}$ ± CI95 4/17 2104-2150 Hrs. N_2 Inj	4/17 2158-2240 Hrs. N_2 Inj	4/18 0008-0054 Hrs. Post N_2 Inj
Mill Exit O_2, % Dry	21.0 ± 0	13.7 ± 0.3	13.1 ± 0.2	21.0 ± 0
Kiln Exit O_2, % Dry	1.4 ± 0.1	2.4 ± 0.3	1.5 ± 0.2	2.4 ± 0.2
Kiln Exit CO, ppmv, Dry	131 ± 51	36 ± 15	47 ± 17	28 ± 2
Coal Rate, Tons/Hr	9.48 ± 0	8.91 ± 0	9.10 ± 0	9.48 ± 0
Clinker Rate, Tons/Hr	52.1	45.6	44.8	43.0
Kiln Speed, rph	72.0 ± 0	63.0 ± 0	61.9 ± 0.5	59.5 ± 1.0
Mat. Temp., °F	2560 ± 4	2556 ± 8	2487 ± 5	2437 ± 11
NO, ppmv, 3% O_2	1464 ± 45	1424 ± 64	877 ± 31	965 ± 22
Lbs NO (As NO_2)/Ton Clinker (based on Kiln Speed)	10.6 ± 0.3	10.9 ± 0.5	7.0 ± 0.3	8.2 ± 0.2

Table 4

STATISTICAL ANALYSIS OF MILL O_2 VARIATION ON KILN NO EMISSIONS

Predictor Variables			[NO](as Measured)/[NO](corrected to 3% O_2)		
Held Constant	Not Held Constant	Data Set	$\frac{\partial[NO]}{\partial[\text{Mill } O_2]}$	Standard Error	P value
Temp, Coal, Rotat, MAA	-	MOD(6)=2	51.4/51.5	9.4/11.8	0.0001/0.0001
Temp, Coal, Rotat, MAA	-	MOD(6)=4	41.0/47.6	8.6/9.4	0.0001/0.0001
Coal, Rotat, MAA	Temp	MOD(6)=2	76.0/71.5	11.2/12.4	0.0001/0.0001
Coal, Rotat MAA	Temp	MOD(6)=4	61.4/65.8	10.8/11.0	0.0001/0.0001
Temp, Coal, Rotat	MAA	MOD(6)=2	33.6/34.5	6.1/7.6	0.0001/0.0001
Temp, Coal Rotat	MAA	MOD(6)=4	36.0/42.6	5.9/6.4	0.0001/0.0001
Temp, Coal MAA	Rotat	MOD(6)=2	53.3/57.1	9.2/11.6	0.0001/0.0001
Temp, Coal MAA	Rotat	MOD(6)=4	42.9/49.0	8.5/9.4	0.0001/0.0001
Temp, Rotat MAA	Coal	MOD(6)=2	19.3/19.4	7.3/8.8	0.0098/0.00306
Temp, Rotat MAA	Coal	MOD(6)=4	20.0/18.9	6.9/7.8	0.0047/0.00175
Temp, Coal Rotat, MAA Damp	-	MOD(6)=2	49.7/42.2	13.7/17.1	0.0006/0.0106
Temp, Coal Rotat, MAA Damp	-	MOD(6)=4	35.7/38.1	12.4/13.5	0.0053/0.0061
Temp, Coal Rotat, MAA Exhaust O_2	-	MOD(6)=2	41.3	11.6	0.0009

Data Sets

MOD(6)=2 4/17 1604 hours starting time; 87 complete observations
MOD(6)=4 4/17 1606 hours starting time; 87 complete observations

Predictor Variables

Temp - material temperature
MAA - burnability factor moving average
Damp - damper setting on the induced draft fan
Coal - coal flow rate
Rotat - kiln rotation speed
Exhaust O_2 - kiln exit oxygen

NO_x CONTROL FOR GLASS-MELTING TANKS

Donald K. Fleming
Institute of Gas Technology

F. Richard Kurzynske
Gas Research Institute

ABSTRACT

The Gas Research Institute (GRI) is undertaking a program to evaluate the factors that influence the production of NO_x in glass-melting tanks. This discussion presents the results to date of the ongoing program, as developed under contract by the Institute of Gas Technology (IGT).

Glass melting is a high-temperature operation, generally employing regenerative furnaces with preheat temperatures for the combustion air of 2000° to 2300°F. Consequently, an uncontrolled glass-melting tank may produce NO_x concentrations of 3000 ppm. Techniques for reducing these emissions are being evaluated in this program. Work effort has advanced through pilot-scale testing and the results from that effort have been correlated to indicate the effects of temperature, excess air utilization, and combustion geometry factors. Staged combustion (both air and fuel) and flue gas recirculation also have been evaluated. Testing is now under way in a commercial furnace to determine scale-up factors for the control parameters.

BACKGROUND

Before presenting the results of this effort, it is helpful to review conventional practices in the high-temperature production of glass. In general, the raw materials — primarily soda ash, limestone, and sand — are chemically reacted to produce soda-lime silicates with evolution of carbon dioxide. The molten glass is maintained at about 2500°F, where it has a viscosity similar to glycerin, for release of the small bubbles of carbon dioxide. In most operations, the heat for this system is provided by natural gas combustion with highly preheated air. A relatively large consumer of natural gas, this industry requires about 250 X 10^{12} Btu/year.

The schematic Figure 1 illustrates the type of furnace that has evolved for glass production. In this figure, the flow of reactants and molten glass is away from the viewer; heat is supplied, primarily by radiation, from the fires over the molten glass. As illustrated, hot air enters the furnace from the left side through a port from the regenerator. Natural gas is fed into the air at a point near the furnace wall and the resulting fire provides the necessary heat energy. Dependent upon the furnace operating characteristics and the type of glass produced, the combustion products leave the furnace through an opposite port at temperatures in the range of 2700° to 3000°F. These hot gases heat the checkerwork within the exhaust regenerator before being discharged through the stack. After approximately 15 to 20 minutes, valves on the combustion air supply, the natural gas, and the ducting to the stack are reversed and the furnace is fired from the alternate side. Contact with the hot checkerwork preheats the combustion air to the temperature range of 2000° to 2300°F before combustion.

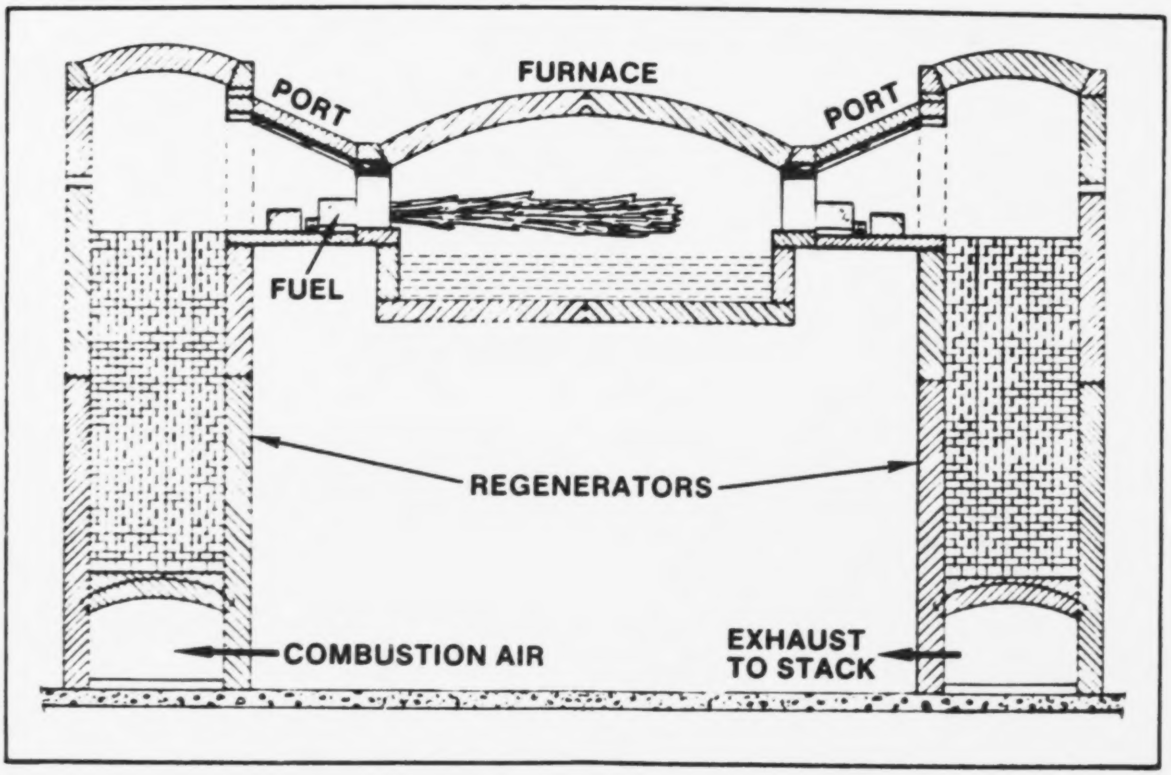

Figure 1. GENERAL CONFIGURATION OF GLASS-MELTING SYSTEM WITH REGENERATIVE AIR PREHEAT

The high-temperature regenerative preheating of air is critical to the efficiency of the process, and to the viability of the industry in remaining competitive with alternative materials. Energy efficiencies approaching 50% may be achieved through regenerative practice; energy demands would be 20 to 35% greater with recuperative air preheat, and more than 2-1/2 times as great if no heat were recovered.

The extreme air preheat, however, is conducive to production of NO_x. Typically, such a glass furnace will produce NO_x concentrations in the range of 1000 to 3000 ppm (corrected to 0% O_2). Regulations are being developed to limit the NO_x production from glass melters; in southern California, a limit of 5.5 pounds of NO_x per ton of glass has been promulgated; that rate of NO_x production is equivalent to 900 to 1000 ppm NO_x (at 0% O_2), dependent upon the efficiency obtained in the specific furnace.

OBJECTIVE

The function of the current program is to evaluate the NO_x production as a function of the furnace operating parameters and to assess the potential for control technologies that might be employed.

INTRODUCTION

In any assessment program, a preferable approach is to always remember the "first principles" involved in the system. Then, by relating observed effects to the first principles, the analysis has a stronger basis and the conclusions reached are more valid.

Unfortunately, in this application — as in most real systems — it is impractical to measure directly the primary, localized controlling variables. A degree of empiricism is required, therefore, to relate the integrated, total system effects to the parameters that are under the control of the experimenter. Nevertheless, one can still relate generally to the first principles for the guidance of the effort.

The general parameters controlling any chemical reaction are:

- Time
- Temperature
- Reactant concentrations

In this effort, the primary chemical reaction of concern is the oxidation of nitrogen to produce NO_x. However, the factors controlling two of the above-listed parameters for NO_x generation are the result of burning of fuel — or oxidation of methane. On the overall systems basis, therefore, one must continually look toward time, temperature, and reactant concentrations for assessment of the overall system, and for the conditions for methane combustion that control the NO_x production.

The thermodynamics of NO_x production have been projected; within a specific furnace of limited residence time, however, the quantity of NO_x produced is strongly rate-limited, or kinetically controlled. Therefore, for evaluation of the effects of various parameters upon NO_x production, the effect of reaction time is extremely important.

A major factor in the kinetic rate expression is the concentration of the reacting materials (in addition to its effect on thermodynamic potential). Thus, the oxygen availability impacts not only thermodynamically but also kinetically.

Because of the kinetic limitations, the rate of NO_x formation is strongly temperature sensitive. Similar to the oxygen availability discussed above, the reaction temperature not only controls the thermodynamics of equilibrium NO_x production, but also the rate of the chemical reaction as it approaches the thermodynamic potential. Also, similar to the oxygen availability, the localized temperatures are not known, but can only be inferred from other data.

A final parameter that is of extreme importance is mixing. A German expression is often quoted, "gemischt ist gebrannt" — which loosely translated means: to mix is to burn. One can write the chemical reactions on paper, but if the reactants are not mixed, the reaction does not occur. In the proposed application, however, mixing is not intense. Rather, long, lazy flames are desired for extended radiance to the load.

The general discussion above indicates the difficulty in interpreting NO_x generation data. Not only are the local temperature and oxygen availability not known, but the reaction times at the localized conditions are also unknown. However, logic can be employed to indicate effects directionally.

Consideration of the ramifications of the fire in a glass melter illustrates these points. Figure 2 is a diagramatic representation of a typical fuel/air inlet geometry on a commercial glass melting system. One measure of the mixing achieved with this geometry would be the vector addition of the mass flows, considering each flow as a linear motion of the center of the mass. A more accurate representation considers the angle of divergence of the gas jet and the cross-sectional area of the air flow. Considering the vertical plane, a locus of points of intersection between the gas and the unburned air results. Examination of the resultant flame would show a situation similar to planned fuel-staging, with low temperature combustion due to dilution and heat transfer from early parts of the flame.

Another consideration in evaluation of the fuel jet is the effect of inspiration of hot furnace gases into the jet, prior to combustion. The effect would result in heating of the gas with subsequent cracking to soot. The combustion of this soot results in a highly luminous flame with good radiance characteristics.

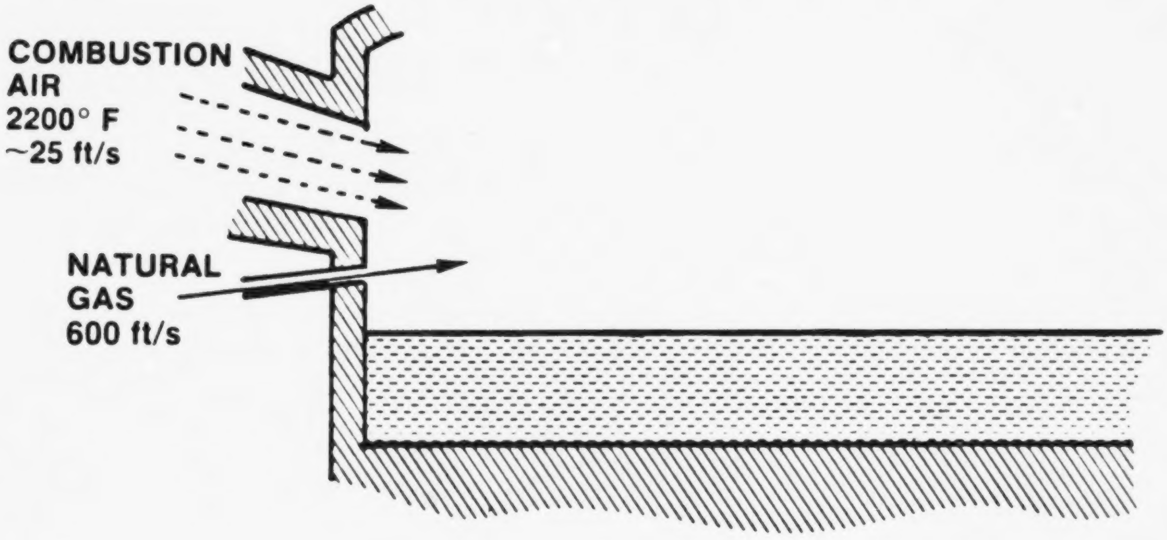

Figure 2. DIAGRAM OF GAS/AIR MIXING SYSTEM

The flame that results from the geometrical configuration shown is relatively long and lazy with good heat-transfer characteristics. It also is a relatively low NO_x configuration. The relatively low temperature of the flame inhibits NO_x production and the high heat-transfer rate reduces the time at extreme temperatures. Both of these effects will tend to reduce the NO_x production.

The preceding discussion illustrates the issues involved in the program and the approach necessary to analyze the data.

TECHNICAL APPROACH

The general approach to the problem was to evaluate the effects of alternative systems over a range of operating variables on a pilot-scale furnace, where excellent instrumentation exists and the system could be controlled; this was followed by testing of a full-scale, commercial furnace to determine scale-up factors. The geometrical mixing factors of port and burner geometry included:

- Overport firing
- Underport firing

- Side-of-port firing
    - 45° injection
    - 90° injection
        - . Effect of port baffle
- Flat floor port
- Inclined floor port.

Each of these mixing configurations was assessed over a range of fuel injection velocities at constant air-preheat temperature and excess air utilization. Earlier work[1] had indicated the effect of air preheat temperature and excess air utilization upon the dependent variables.

In addition to geometrical factors, flue-gas recirculation was assessed, as were both air- and fuel-staged combustion. Technical difficulties precluded the planned assessment of fuel precracking.

In addition to NO_x production, dependent variables included O_2, CO_2, and CO in the exhaust to define excess air utilization and degree of combustion completion. Temperature measurements were taken in the furnace roof and sidewalls, and also in the layer of molten glass in the furnace. Heat transfer through the molten glass to a load in the furnace floor was measured as a function of furnace position. Motion pictures of the flames were taken, in some tests, through a water-cooled periscope to permit visual comparison of the flame characteristics to the data acquired. Furnace surface temperatures were measured and the data were validated by energy balances around the system. Details of the pilot plant furnace and the testing procedure have been presented earlier.[2,3]

PILOT-SCALE RESULTS

Figure 3 presents the effect of air preheat temperature upon the generation of NO_x, as compared to the theoretical production for an adiabatic flame. Of course, the NO_x production does not approach the thermodynamic limits 1) because of kinetic limitations and 2) because the flame does not approach adiabatic temperatures. The burners tested at elevated temperatures resulted in lower relative NO_x production because of the long mixing patterns discussed earlier. In general, higher combustion air preheat increases the NO_x production, as would be expected by the resultant higher combustion temperature and the impact of temperature on both the thermodynamics and kinetics of NO_x production. Reduced operating temperature, however, is not a viable approach to NO_x control because of the severe impact upon furnace efficiency.

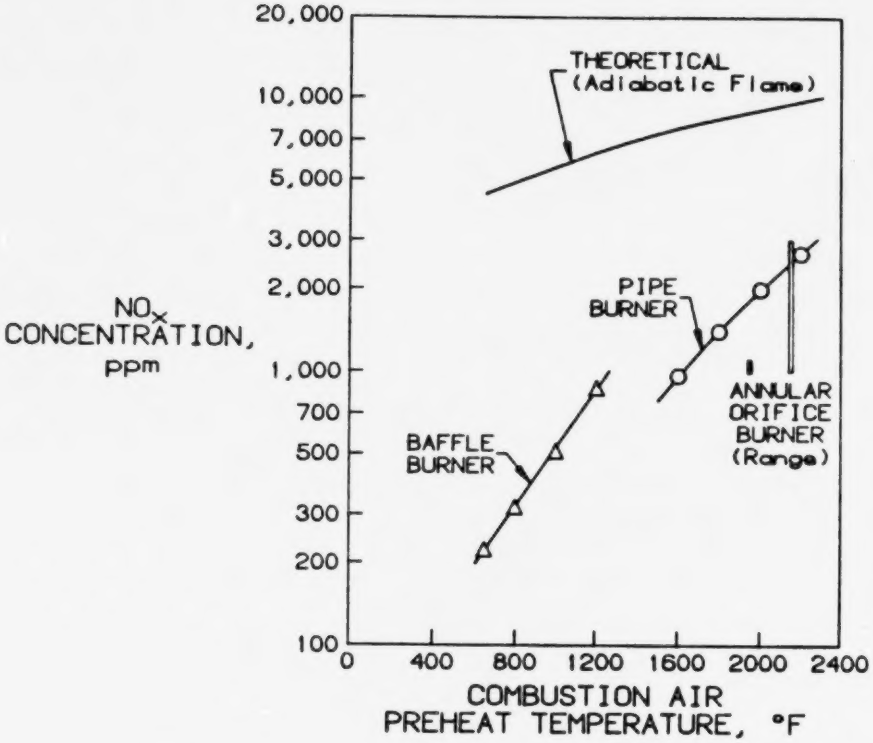

Figure 3. EFFECT OF COMBUSTION AIR PREHEAT ON NO_X PRODUCTION

Figure 4 presents the effect of excess air utilization upon the NO_x production, again with a comparison to the thermodynamic potential for NO_x generation. As expected, reduced excess air improves the NO_x generation, primarily because of the reduced availability of oxygen. At substoichiometric combustion, reduced combustion temperatures also have an effect; this condition also enhances soot production, more radiant flames increasing heat transfer and decreasing time at temperature. Minimization of excess air is a desirable NO_x control technique because this effect also improves furnace efficiency. However, a regenerative furnace is often difficult to operate at low excess air utilization because of regenerator infiltration and reversal valve leakage.

Figure 5 presents the effect of oxygen concentration in the combustion air upon NO_x generation over a range of 10% flue gas recirculation through air enrichment to 27% oxygen. The total excess oxygen is the same in all cases. These data indicate that flue-gas recirculation has little benefit, and oxygen enrichment has a small penalty that might be counteracted by improved production.

Figure 6 presents the effect of fuel/air mixing parameters upon NO_x production and illustrates that a wide range of NO_x may be anticipated, depending upon the furnace

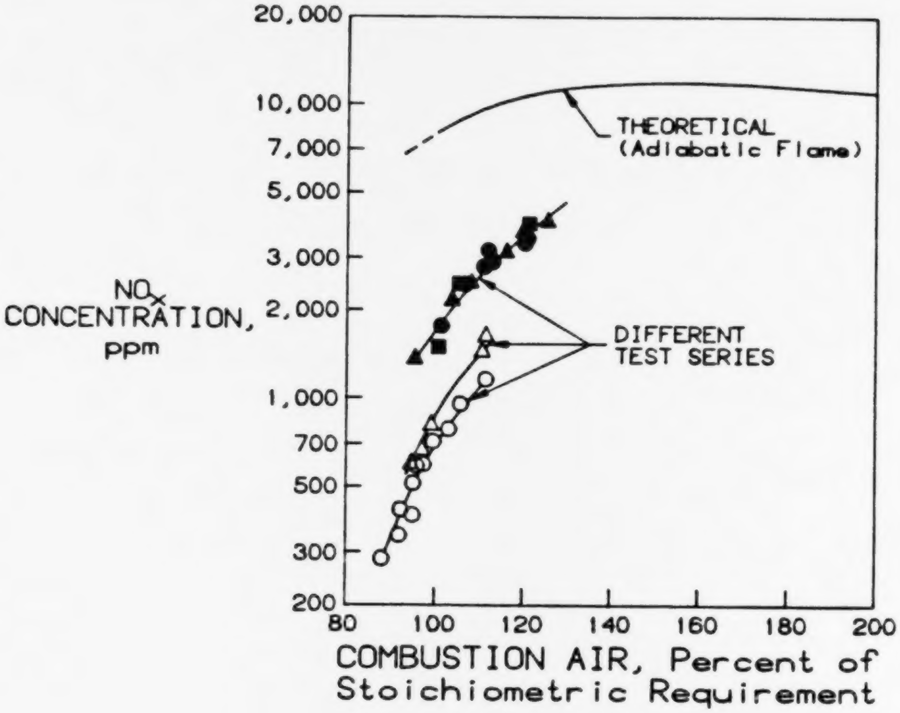

Figure 4. EFFECT OF COMBUSTION AIR ON NO_X PRODUCTION

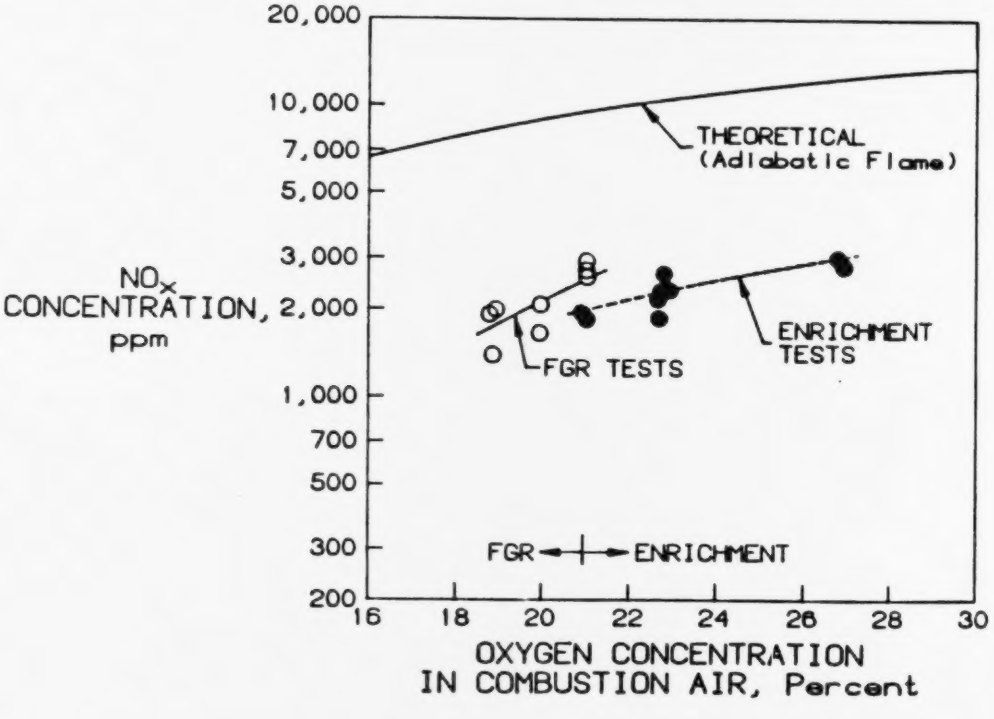

Figure 5. EFFECT OF OXYGEN CONCENTRATION ON NO_X PRODUCTION

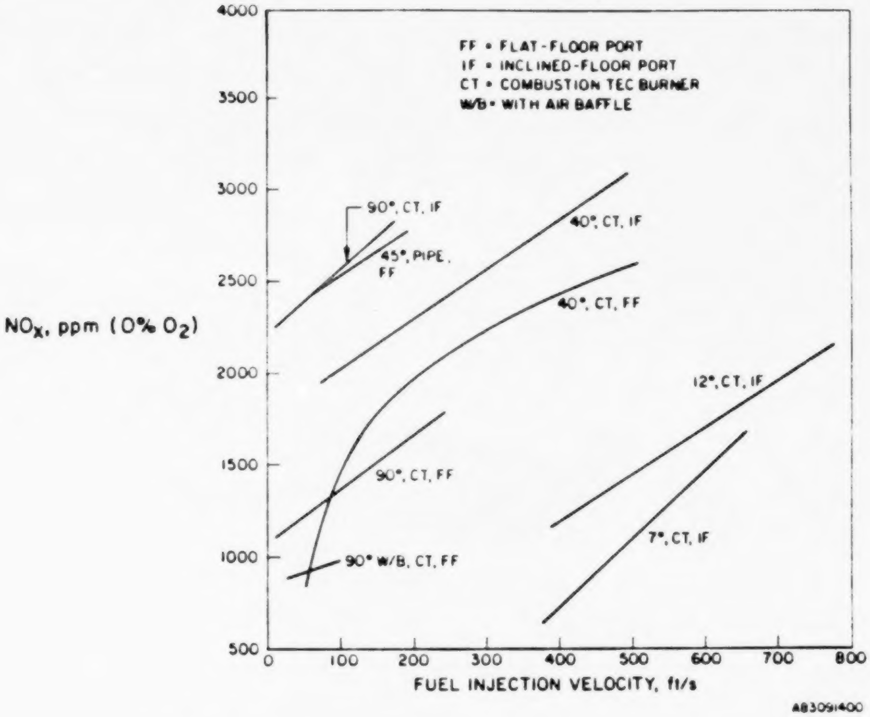

Figure 6. EFFECT OF FUEL-AIR MIXING PARAMETERS ON NO_X GENERATION

geometry employed. In general, higher NO_X production is related to more intense mixing. The longer flames resulting from less intense mixing also provided better heat transfer within the furnace and projected higher furnace efficiency, with the limitation that the flame must remain within the furnace proper and not enter the exhaust port.

Figure 7 illustrates the effects of air staging. For this work, the primary combustion air was adjusted to the stoichiometric ratio indicated in the abscissa of Figure 7, and secondary air was admitted to the furnace downstream of the flame burnout for final oxidation of carbon monoxide at a total excess air utilization of 11%. Although this approach shows excellent NO_X reduction, it suffers from 1) the inefficiencies of admitting cold air to the furnace, and 2) the potential for final burnout and heat release outside of the furnace proper.

Data for fuel staging are not presented. Although this technique was effective in one furnace configuration, it showed little promise in an alternative system and the results, therefore, are inconclusive.

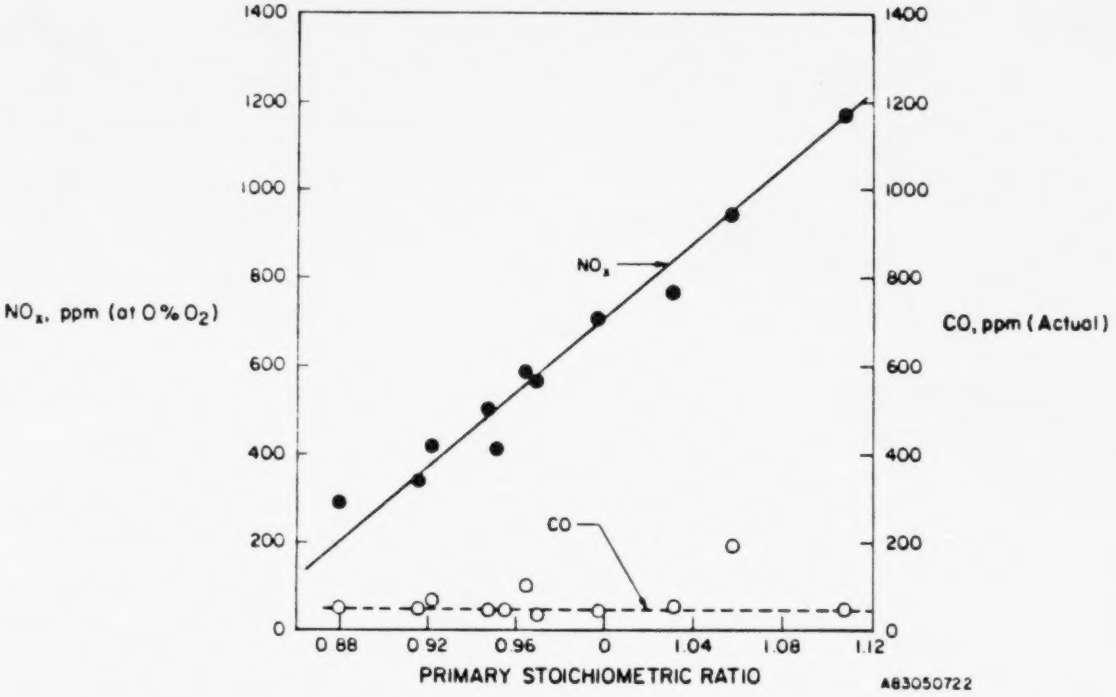

Figure 7. REDUCTION OF NO$_X$ BY COMBUSTION-AIR STAGING

GENERALIZED CORRELATION

During a hiatus in the program, prior to the selection of a full-scale furnace for further testing, the data were reduced to generalized correlations in an in-house R&D program.[4] It was found that the NO$_X$ production (when compared to the amount generated at a reference basis) could be correlated against the major operating parameters. Figure 8 presents the generalized correlation of the pilot-scale data against temperature. This generalized plot includes data at several excess air utilizations and fuel injection velocities reduced to a common basis by referencing to the NO$_X$ production at 2200°F (1205°C) air preheat temperature. Data from full-scale furnaces also show the same relationship. As the preheat-air temperature varies during a furnace cycle, NO$_X$ production also changes; the variation follows the correlation of Figure 8.

Figure 9 illustrates the generalized effect of excess air utilization upon the NO$_X$ production. In this case, the data were referenced to the NO$_X$ production at 3% O$_2$ in the exhaust (15% excess air) and include a range of air preheat temperatures and fuel-injection velocities. This graph should not be extrapolated — at higher excess — air utilizations, the line should curve downward as reduced flame temperatures counteract the effects of greater oxygen availability.

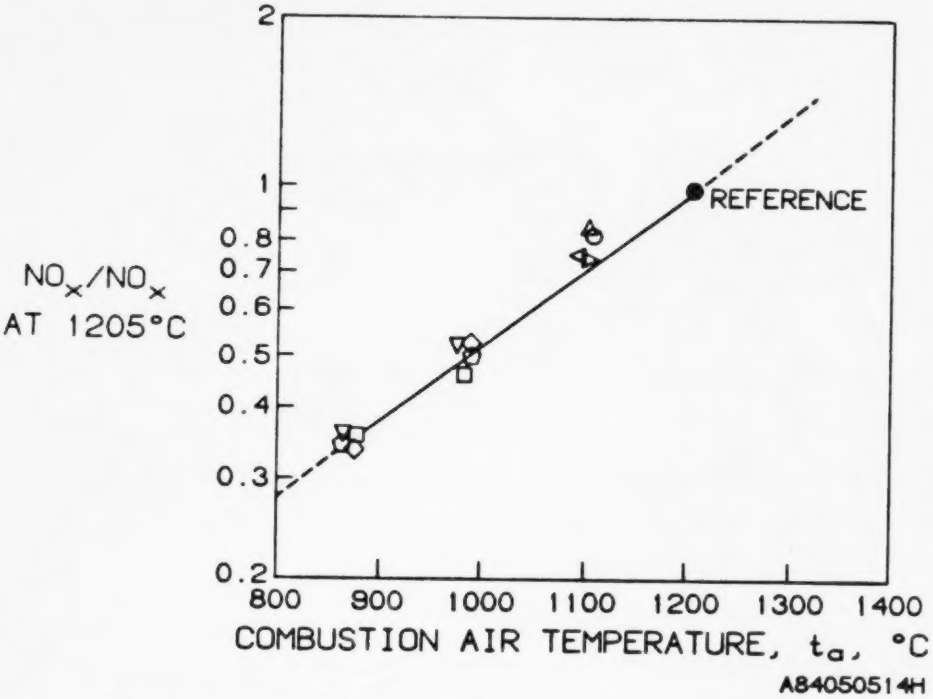

Figure 8. GENERALIZED CORRELATION FOR COMBUSTION AIR

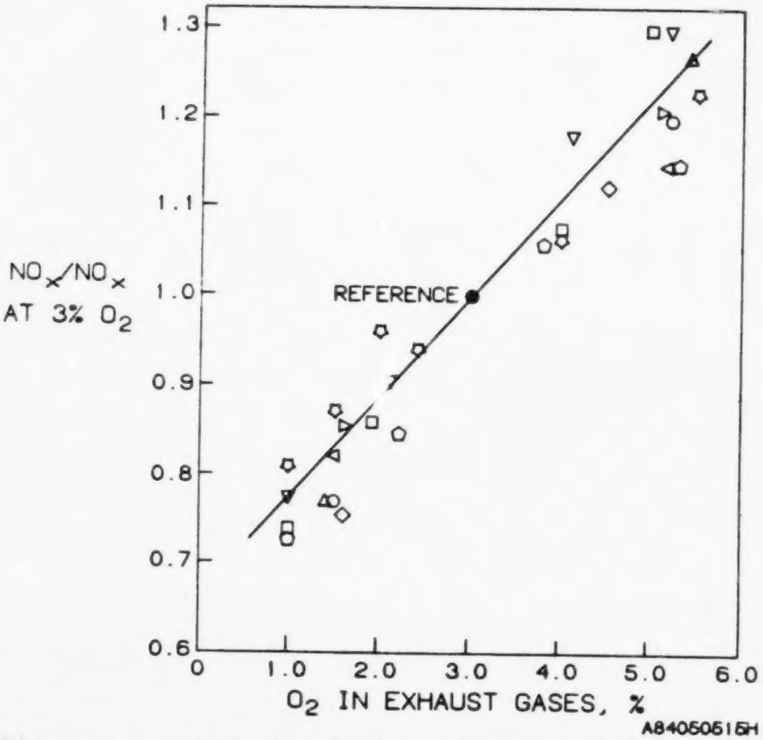

Figure 9. GENERALIZED CORRELATION FOR FUEL/AIR MIXING

Figure 10 provides the generalized correlation for fuel/air mixing parameters, including the data underlying the various lines of Figure 6. The generalized empirical mixing parameter is similar to a vector momentum function, including both air and gas velocities and the angle of incidence of these streams. The two lines generally reflect basically different mixing configurations, and the measured NO_x diverges at lower values of the mixing parameter.

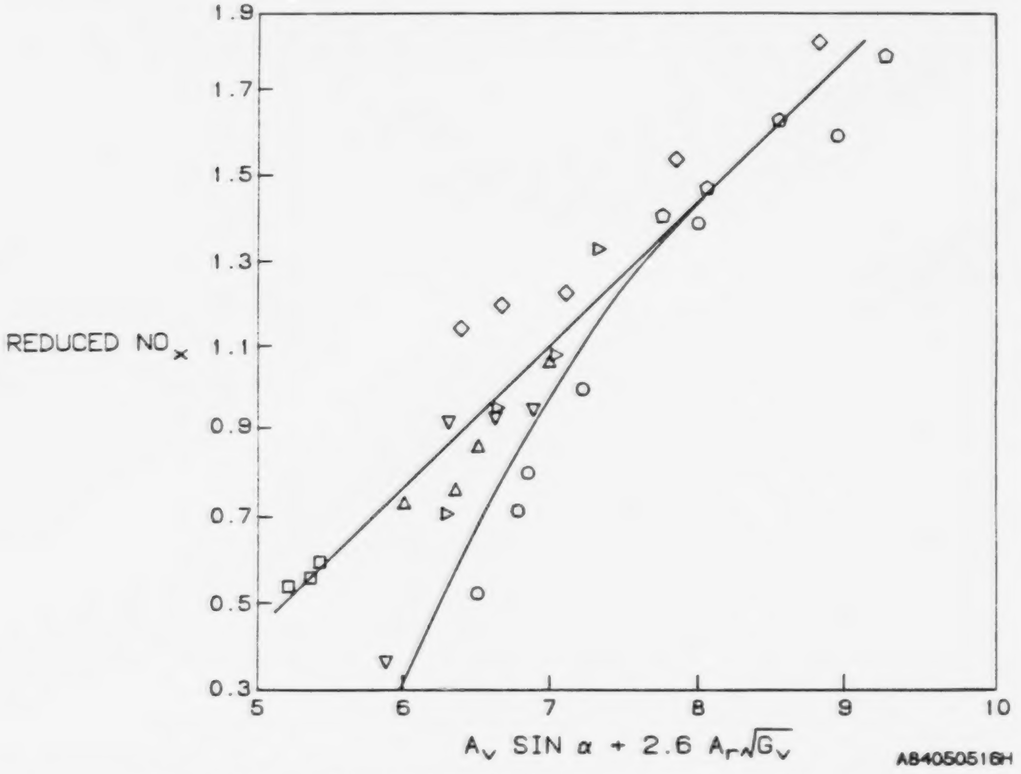

Figure 10. GENERALIZED CORRELATION FOR FUEL/AIR MIXING

CONCLUSIONS — PILOT PLANT EFFORT

The primary conclusions drawn from the pilot plant effort are:

- Decreased fuel/air mixing, with resultant long, lazy flames, tends to reduce NO_x production. This control technique is limited by maintaining the flame within the furnace. With this control technique, heat transfer to the molten glass is increased as the NO_x productions are decreased. This approach appears to have a potential for commercial application.

- Increased combustion air temperature tends to increase the NO_x production. Reduction of combustion air temperature, however, is counterproductive to furnace efficiency.

- Decreased excess-air utilization tends to improve the NO_x production. Simultaneously, furnace efficiency increases because of reduced losses to the stack. Implementation of this control technique may be difficult because of the basic nature of regenerative furnaces. This approach also appears to have a potential for commercial operation.

- Air staging is an effective mechanism for NO_x reduction. Because of the projected loss in furnace efficiency, however, this control technique may not be viable.
- The data on fuel staging were inconclusive. The approach worked well in one furnace configuration but was ineffective in another.
- Flue-gas recirculation appears to be of marginal value.

The above conclusions are based upon pilot-scale testing only. Because of the interdependence of the primary variables in an integrated, full-scale furnace, these conclusions may require modification when applied commercially. Nevertheless, it is anticipated that selective implementation of these control technologies will reduce NO_x emission to the desired range for many commercial glass-melting furnaces without impairing thermal efficiency.

CURRENT PROGRAM STATUS

At the time of this writing, a commercial furnace has been identified for full-scale testing. The purpose of this testing is to acquire data to define scale-up factors relative to results of the pilot-plant performance discussed earlier. Because of the design of the furnace, a relatively wide range of data may be acquired. The work plan has been approved to evaluate:

- Side-of-port firing at a 45° fuel/air mixing angle
- Underport firing
- Fuel injection velocity
- Fuel staging
- Excess-air variation
- Cycle time variation
- System optimization.

Testing of the commercial furnace has commenced.

With the initial testing, several major issues have been resolved. However, complete data acquisition and reduction have not yet been accomplished. The major issues include the following:

- In the underport firing mode, the furnace produces less NO_x than in the side-of-port firing mode. The variation, however, has not yet been quantified.
- The locations for data acquisition have been resolved, with uniformity of temperatures and gas compositions proved by furnace traverses.

The initial testing has also raised several issues that may inhibit data acquisition:

- In the current firing mode, combustion stability is questionable, with significant, periodic variations in exhaust gas O_2 and NO_x concentrations.
- Production job changes are now more frequent than at the time of furnace selection. Steady-state data acquisition may be impaired by the need to change production rate to meet varying product schedules. This effect is interconnected to the length of time required to achieve steady-state conditions because of the thermal inertia of the furnace.
- Heat-transfer measurements within the furnace have been complicated by depositions on the sensors in the high-temperature water-cooled probes and furnace internal temperature measurements have been clouded by the inability to maintain a protective coating on the extreme temperature thermocouples employed.

Other issues that are anticipated include the following:

- Current techniques for glass quality measurements are imprecise. Therefore, it may become difficult to determine, within the time constraints of the program, the impact various NO_x control strategies have upon product quality.
- Variables that could independently be controlled in the pilot plant are interdependent in the integrated, commercial furnace and separation of these variables during data analysis may be difficult. For example, any effect that tends to increase the heat transfer within the furnace will reduce the exhaust gas temperatures and, through the regenerators, reduce the combustion air preheat temperature. Similarly, reduction of the excess air utilized will improve the regenerator effectiveness and increase the combustion air preheat. The separation of the variables as they apply to NO_x control may be difficult.

ACKNOWLEDGMENT

The majority of the work effort reported here was performed under contract to the Gas Research Institute and Southern California Gas Company, with certain effort from outside contracts or IR&D programs. Permission to publish from all sources is gratefully acknowledged.

REFERENCES

1. Abbasi, H. A., Khinkis, M. J., Waibel, R. T. and Boyd, W. D., "Experimental Evaluation of NO_x Control Using a Glass Tank Simulator." Paper presented at the 43rd Conference on Glass Problems, The Ohio State University, Columbus, OH, November 10-11, 1982.

2. Abbasi, H. A., Khinkis, M. J., Fleming, D. K. and Drake, R. A., "Research on Furnace Firing and Process Control of Emissions." Paper presented at the American Ceramic Society 36th Pacific Coast Regional Meeting, San Diego, CA, October 4, 1983.

3. Abbasi, H. A., Khinkis, M. J., and Fleming, D. K. "Evaluation of NO_x Emissions on a Pilot-Scale Furnace." Paper presented at the 44th Annual Conference on Glass Problems, Urbana-Champaign, IL, November 15-16, 1985.

4. Abbasi, H. A., Khinkis, M. J., Fleming, D. K. and Kurzynske, F. R., "Reduced NO_x Emissions from Gas-Fired Glass Melters." Paper presented at the 1984 International Gas Research Conference, Washington, DC, September 10-13, 1984.

19/Paper/RPP

DIESEL ENGINE NO_x CONTROL WITH SCR

J. H. Wasser and R. B. Perry
U. S. Environmental Protection Agency
Air and Energy Engineering Research Laboratory
Research Triangle Park, NC 27711

ABSTRACT

EPA's Air and Energy Engineering Research Laboratory is conducting a long-term test evaluation of a selective catalytic reduction (SCR) system on a stationary diesel engine. The overall goal of this project is to establish the NO_x reduction performance of a diesel SCR unit over a 4000-hour period. This paper reports the interim results obtained during the first 2300 hours of operation. For most of the first half of the test program, NO_x reductions of over 90% were obtained. However, as the 2000-hour point was approached, a drop in NO_x reduction (below 80%) was experienced. Cleaning restored part of the catalyst's original activity, and the test program continued.

INTRODUCTION

The Combustion Research Branch (CRB) of EPA's Air and Energy Engineering Research Laboratory, Research Triangle Park, NC, sponsors contract and in-house programs to investigate emissions from stationary reciprocating internal combustion engines. This paper will describe interim results obtained during the first 2300 hours of a 4000-hour duration test with a full-stream ammonia NO_x reduction catalyst installed in the exhaust system of a diesel engine. The purpose of this in-house test (6 months equivalent operation) program is to assess both the initial and long-term NO_x reduction performance capabilities of a selective catalytic reduction (SCR) system. This test will provide support to EPA Region 9 and Ventura County, California, in carrying out their regulatory responsibilities. Region 9 has provided substantial funding for this research project. Engelhard Industries provided the catalyst and valuable operating information support for this program.

EXPERIMENTAL APPROACH

Baseline emissions characteristics were established for an engine load range from 20 to 165 kW prior to installation of the catalyst. Based on exhaust temperature data from the engine and the manufacturer's specified catalyst operating range (575°F to 825°F; 302°C to 441°C), the engine catalyst test range was defined as between 50 kW and 110 kW. A midpoint at 80 kW was selected for continuous operation of the engine-catalyst system because NO_x emissions are at relatively high levels at that condition (approximately 400 ppm) and particulate emissions had reached a minimum plateau (30 mg/m^3). The catalyst temperatures typically were 785°F (418°C) inlet/715°F (379°C) outlet at 80 kW. The system duty cycle established for the test consists of 24 hours-a-day operation at 80 kW for 5 days a week. Thus, the engine is shut down and restarted once each approximately 100 hours of operation. The catalyst is subject to very high particulate loadings (120 mg/m^3) at each start-up. The test plan consists of varying the ammonia injection rate at selected points in time during the test to confirm the continued NO_x reduction performance of the system. Table 1 outlines the test plan.

EXPERIMENTAL SYSTEM COMPONENTS

The diesel engine used for this study is a 638 in.^{3} (10.5 liter) displacement Caterpillar model D334 rated at 165 kW for continuous electric generation operation. The engine, loadbank, and fuel (No. 2 diesel) were described in detail in previous papers[1,2]. A nominal phosphorus-free lube oil was used to prevent catalyst poisoning. However, analysis indicated some phosphorus is present in the lube oil.

Specific to this study, the Engelhard Torvex® Catalytic Abatement System has been designed to reduce NO_x emissions from a stationary, lean-burn diesel engine. The catalyst is housed in a stainless steel shell consisting of two end cones and a square cross-section center section. Catalyst material used on the monolith is a proprietary formula. Internal aerodynamic design of the system was specific for the particulate-laden exhaust gas normally encountered in a diesel engine.

The ammonia (NH_3) delivery system consists of a 150 lb (68 kg) supply cylinder and regulator, mounted on a scale, a Fischer & Porter Tri-Flat Variable Area Rotometer and/or a Brooks mass flow meter for injection rate measurement, and a 1/4-in. (6.35 mm) stainless steel NH_3 injection nozzle. The injection nozzle has four radially drilled 3/64-in. (1.2 mm) holes 90° apart and located 1/4-in. (6.35 mm) from the nozzle tip. NH_3 injection was initially located at a point 3 ft (0.9 m) from the upstream face of the catalyst. Later in the study (after 2000 hrs), when NO_x performance was reduced, the injection was moved upstream to a point 6.5 ft (1.98 m) from the catalyst to ensure complete mixing.

SAMPLING AND ANALYTICAL SYSTEM

The instruments for criteria pollutants were the same as reported in earlier papers[1,2]. NH_3 was measured with an ion specific electrode method and the Kitagawa tube method. Results of the exhaust gas NH_3 levels were variable, and other methods are being considered for adoption for future testing. Experimental data/calculations were based on mass (weight) of NH_3 injected and NO measured upstream and downstream of the catalyst by a TECO chemiluminescence analyzer.

DATA AND RESULTS

Catalyst NO_x reduction data is presented in Table 2 for engine operation at the 80 kW standard condition. Hydrocarbons were measured with a heated flame ionization instrument. Hydrocarbon concentrations were always less than 10 ppm after the catalyst, less than 20 ppm before the catalyst, and did not change with NH_3 injection levels; thus they were not reported. Carbon monoxide emissions averaged 180 ppm (+/-20 ppm) and did not vary with the NH_3 injection levels. NO_2 levels never exceeded 5 ppm and are not reported.

Catalyst performance is illustrated in Figure 1 for the first 2000 hours of operation. A continual decline in NO reduction with time is evident. By the 2000 hour point, 90% NO reduction could no longer be achieved even with a substantial excess of NH_3. As the 2000 hour point was approached, other evidence of problems in the catalyst was experienced, especially sudden large changes in the pressure drop across the unit. At that point in time, visual inspection of the catalyst became necessary.

On opening the unit, all inside surfaces were found to be coated with a thick deposit of diesel particulate. Many of the passages through the honeycomb were plugged. The interior was cleaned with a vacuum, and pure N_2 cylinder gas was used to blow out the plugging material. Analysis of the material inside the honeycomb indicated that ash from the lubricating oil was a major constituent in addition to unburned carbon. The cleanout operation, including unbolting and rebolting the catalyst housing, required about 4 hours.

The catalyst was repositioned in the exhaust system, and testing was resumed. Figure 2 illustrates the effect of catalyst cleaning on the NO reduction performance of the catalyst. The curve for 2300 hours indicates that a substantial improvement resulted from the physical removal of the accumulated diesel particulate. However, the NH_3 content of the exhaust gas needed to obtain 90% NO reduction is too high (approximately 239 ppm measured; 287 ppm calculated) for NO_x control utilization. Further cleaning of the catalyst will be needed to restore satisfactory operation. At the time this paper was prepared, the catalyst manufacturer was planning recommendations for restoring NO reduction activity.

CONCLUSIONS

- The Engelhard catalyst was successful for over 1000 hours in reducing NO emissions by more than 90% from a diesel engine with low NH_3 excess required.
- Accumulated diesel particulate was responsible for a major portion of the lost catalyst activity. Simple vacuum cleaning and inert gas blowout removal of surface particulate restored a significant amount of activity.
- Further cleaning needs to be attempted for additional improvement.
- If the trace quantity of phosphorus in the lube oil has poisoned the catalytic material itself, the activity will not be restorable.
- Cleaning frequency will be dependent on the engine duty cycle, as start-up operations create the highest levels of particulate production.

REFERENCES

1. Wasser. J.H. Emulsion Fuel and Oxidation Catalyst Technology for Stationary Diesel Engines. In: Proceedings of the 1982 Joint Symposium on Stationary Source Combustion NO_x Control. EPRI No. CS-3182, Vol. 2. July 1983, pp 40-1 to 40-18.

2. Wasser, J. H., and R. M. Statnick. Emission Characteristics of Small Stationary Diesel Engines. In: Proceedings of the Second Stationary Source Combustion Symposium. Vol. V. EPA-600/7-77-073e (NTIS No. PB274897), July 1977. pp 119-141.

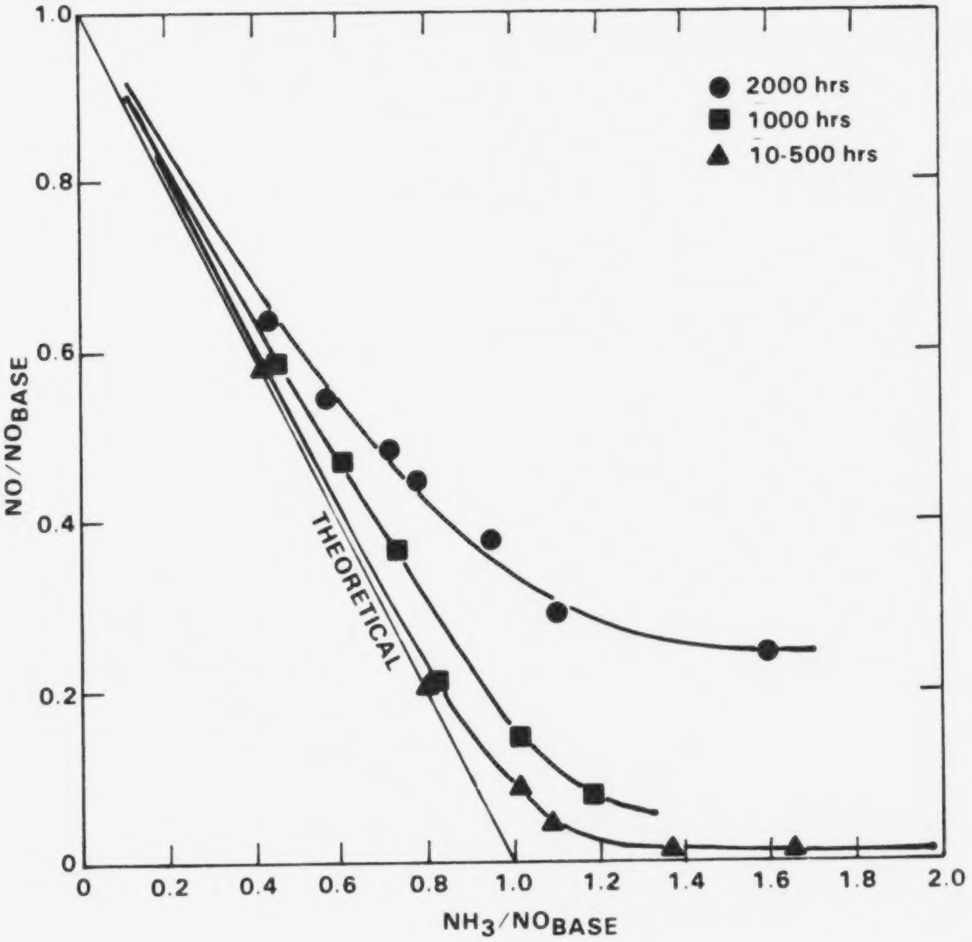

Figure 1. NO Reduction Performance.

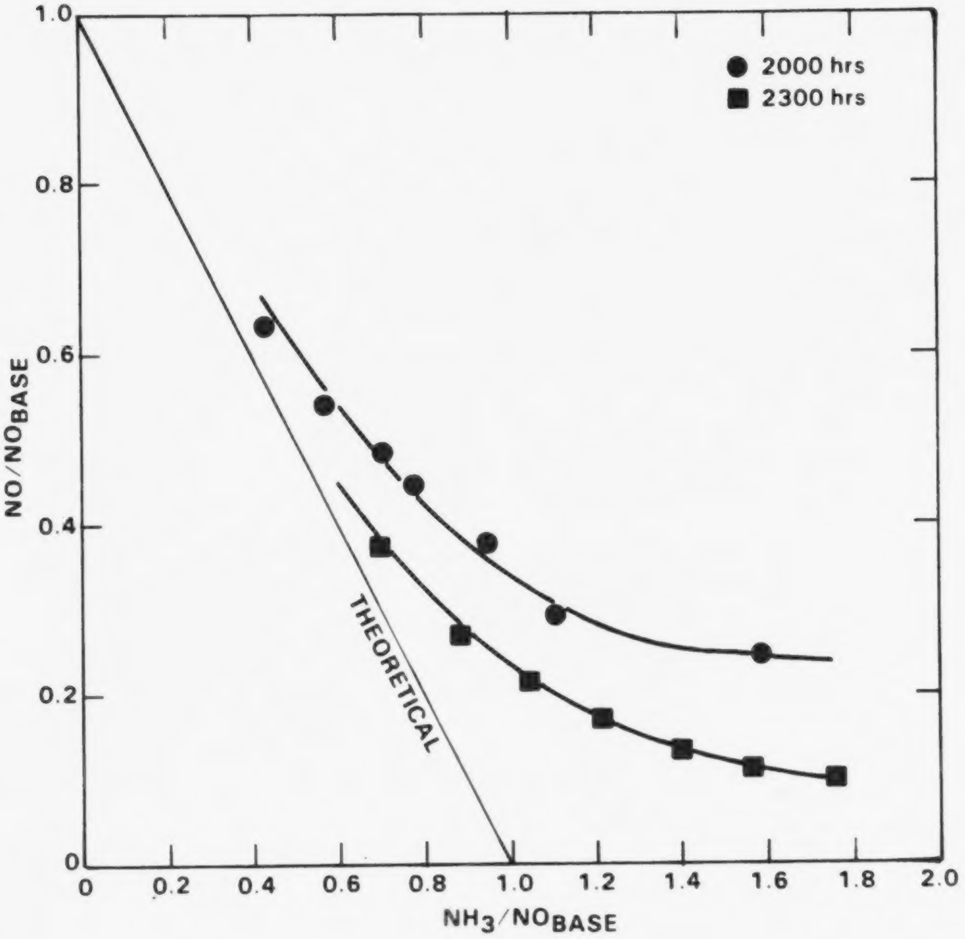

Figure 2. Effect of Catalyst Cleaning.

TABLE 1

EXPERIMENTAL PROGRAM

Experiment Set	Variables	Levels/Range
Baseline	Generator Load	20 to 160 kW
Catalyst @ 80 kW	NH_3/NO_x ratio	0 to 2
	Time	0 to 2300 hrs

TABLE 2

NO_x REDUCTION DATA

Cat. Hours	NO/NO_{BASE}	NH_3/NO_{BASE}	NO, ppm
10-500	1.0	0	433
	0.582	0.41	252
	0.213	0.81	92
	0.089	1.04	38
	0.043	1.09	18.5
	0.0173	1.37	7.5
	0.0173	1.65	7.5
	0.0173	1.98	7.5
1000	1.0	0	350
	0.586	0.45	205
	0.471	0.60	165
	0.371	0.73	130
	0.214	0.81	75
	0.143	0.99	50
	0.077	1.18	27
2000	1.0	0	370
	0.635	0.432	235
	0.541	0.570	200
	0.486	0.708	180
	0.446	0.778	165
	0.378	0.949	140
	0.292	1.114	108
	0.243	1.592	90
2300	1.0	0	384
	0.372	0.70	143
	0.268	0.88	103
	0.216	1.05	83
	0.169	1.22	65
	0.138	1.40	53
	0.117	1.57	45
	0.099	1.75	38

ENVIRONMENTAL ASSESSMENT OF CATALYTIC REDUCTION OF NATURAL-GAS-FIRED ENGINES

C. Castaldini, L. R. Waterland, H. B. Mason
Acurex Corporation
Energy & Environmental Division
555 Clyde Avenue
Mountain View, California 94039

Although the research described in this paper has been funded wholly or in part by the United States Environmental Protection Agency through Contract 68-02-3188 to Acurex Corporation, it has not been subjected to Agency review and therefore does not necessarily reflect the views of the Agency and no official endorsement should be inferred.

ABSTRACT

Field tests were performed on two large-bore, natural-gas-fired reciprocating internal combustion engines, one rich-burn and one lean-burn, equipped with catalytic gas treatment systems for NO_x control. The rich-burn engine was equipped with a nonselective catalytic reduction (NSCR) system in which reducing gases (CO and unburned hydrocarbon) reduce NO to N_2. The lean-burn engine was equipped with a selective catalytic reduction (SCR) system in which NH_3 injected in the engine exhaust gas acts as the reducing agent for NO_x control. The test program for each engine consisted of comprehensive emission measurements for NO_x, CO, unburned hydrocarbon (HC), CO_2, and O_2 by continuous monitors, particulate, cyanide, NH_3, volatile and semivolatile organics, and trace metals at catalyst inlet and outlet locations. In addition, 15-day continuous emission monitoring was performed to record catalyst performance under extended typical engine operation. NO_x reduction by the NSCR system ranged between 54 and 81 percent during comprehensive engine tests but degraded to below 40 percent during the extended monitoring due to changes in engine air/fuel (A/F) ratio. The test engine was not equipped with an A/F controller. HC, CO, and total organic levels decreased across the catalyst, while both cyanide and NH_3 emissions increased. SCR NO_x reduction performance for the lean engine was constant at about 80 percent. The NH_3 concentration at the SCR outlet averaged about 90 ppm.

INTRODUCTION

Reciprocating internal combustion engines represent a major source of NO_x emissions in the California South Coast Air Quality Management District (SCAQMD), with an estimated contribution of 14 percent of the total NO_x from stationary sources in the basin. Due to the continuing nonattainment of both federal and state NO_2 standards, these engines have been the focus of much regulatory attention. On October 26, 1984, SCAQMD Rule 1110.1 was adopted requiring NO_x reductions from existing engines with capacity greater than 37 kW (50 Bhp). This rule calls for the retrofit of rich-burn natural gas engines with NSCR for 80 percent NO_x reduction and lean-burn engines with SCR for 70 percent NO_x reduction. The retrofit schedule extends to the year 1994, with all rich-burn engines with rated power greater than 370 kW (500 Bhp) to be retrofitted by the end of 1985 and 80 percent of lean-burn engines in the size category to be retrofitted by the end of 1987 (1).

The Southern California Gas Company (SoCal) has been involved in the demonstration of NSCR and SCR technologies on reciprocating gas engines for several years. Field tests by SoCal focused on demonstrating feasibility, performance, durability, and impacts on engine operation of commercially available catalyst systems. Early test results have been used by catalyst manufacturers to refine catalytic reactors and control systems for improved performance and durability. Concerns for environmental impacts of catalysts due to cyanide, ammonia, and other emissions were also raised during these tests. In light of these concerns and the potential implications of the widespread engine retrofit program, the EPA's Industrial Environmental Research Laboratory-Research Triangle Park (IERL-RTP) sponsored field tests on two SoCal reciprocating engines retrofitted with catalyst systems: one rich-burn engine equipped with NSCR and one lean-burn engine equipped with SCR. The testing program for each engine consisted of 1-day of comprehensive emission measurements with steady engine operation and a 15-day continuous monitoring period with relatively unrestricted engine operation. This paper summarizes the results of these tests.

MEASUREMENT METHODS

Emission sampling was performed at both catalyst inlet and outlet locations as shown in Figure 1. The sampling protocol used for the comprehensive tests included the following:

- Continuous monitoring for NO/NO_x, NH_3, HC, CO, CO_2, and O_2 (NH_3 for the lean-burn engine only)
- Source assessment sampling system (SASS) for particulate, inorganic trace elements, and semivolatile and nonvolatile organics (trace elements for the rich-burn engine only)
- Volatile organic sampling train (VOST) for volatile organic priority pollutants (for the lean-burn engine only)
- EPA Modified Method 6 for NH_3 and HCN emissions
- Exhaust gas grab sampling for analysis of N_2O with laboratory gas chromatography/electron capture detector (GC/ECD)

SASS samples were analyzed using an extended EPA Level 1 protocol (2). Trace elements were analyzed using spark source mass spectrometry (SSMS) supplemented by atomic absorption spectrometry (AAS) techniques. Semivolatile organics with boiling points between 100° and 300°C (nominally C_7 to C_{16} organics) were analyzed by a total chromatographable organic (TCO) technique. Gravimetry (GRAV) was used to quantitate total nonvolatile organics having boiling points greater than 300°C. In addition, gas chromatography/mass spectrometry (GC/MS) was used to analyze for 58 semivolatile organic priority pollutants, including 16 polynuclear aromatic hydrocarbon (PAH) compounds, according to EPA Method 625. VOST samples were used for analysis of volatile organic priority pollutants in accordance with EPA Method 624. A description of the VOST protocol can be found in Reference 3.

EQUIPMENT EVALUATED

The rich-burn engine tests were performed on a Waukesha 610-kW (818-Bhp) L7042 GU four-stroke naturally aspirated electric generator engine retrofitted with a DuPont PR-5 NSCR catalyst. Table 1 lists engine model specifications. The catalyst is based on a platinum-rhodium formulation with an upper temperature limit of 790°C. Previous tests by SoCal with this catalyst had shown 90 percent NO_x reduction achieved over a narrow A/F range, with A/F sufficiently rich that catalyst inlet CO and HC concentrations exceeded 4,000 and 1,000 ppm, respectively. The engine did not come equipped with a manufacturer-supplied automatic A/F control, nor was one retrofitted for these tests. The NSCR reactor tested in this program had an operating history of 4,000 hours.

The lean-burn engine tests were performed on an Ingersoll-Rand 412 KVS (2,000 Bhp) four-stroke, turbocharged gas compressor engine retrofitted with an Engelhard SCR catalyst system. Table 2 lists engine and compressor specifications. The catalyst is based on a proprietary metal oxide formulation and has an upper temperature limit of 454°C (850°F). Slip stream tests by SoCal using the catalyst had shown the ability of the control system to reduce NO_x by 90 percent, using an NH_3/NO injection rate of 1.0 (molar ratio) at an engine exhaust temperature of about 400°C (750°F).

NSCR RESULTS

1-Day Comprehensive Test

Table 3 summarizes engine operation during the 1-day comprehensive test period. Attempts were made to maintain engine load relatively constant throughout this portion of the program, with A/F ratio set for greater than 80 percent NO_x reduction. This A/F ratio corresponded to near or below stoichiometric conditions of 17.2 on a weight basis. However, generator output varied from 415 to 455 kWe, corresponding to engine load of approximately 450 to 490 kW (600 to 660 Bhp). This caused some variations in the engine exhaust gas composition at the catalyst inlet location. Brake-specific fuel consumption was 12.3 MJ/kWh (8,660 Btu/Bhp-hr), calculated using fuel lower heating value. This represents a loss in fuel efficiency of about 15 percent based on manufacturer specifications for full load operation.

Table 4 summarizes emissions measured at the engine muffler outlet (catalyst inlet) and the catalyst outlet locations. Emissions are presented in milligrams per dry standard cubic meter (mg/dscm), nanograms per joule heat input (ng/J) and in milligrams per horsepower-hour shaft output (mg/Bhp-hr). NO_x emissions were reduced about 70 percent on the average from 770 ng/J (7.8 g/Bhp-hr) to 250 ng/J (2.5 g/Bhp-hr) on a heat input basis. The range in NO_x reduction was from about 50 to 80 percent. This variation was probably caused by the small variations in engine load accompanied by small changes in A/F. As noted above, this engine was not equipped with an automatic A/F controller. Both ammonia and total cyanide increased significantly across the catalyst. Catalyst outlet ammonia levels exceeded inlet levels by over an order of magnitude, 23 to 390 mg/dscm (31 to 490 ppm). Although much lower than ammonia levels, total cyanides showed a much greater percentage increase across the catalyst, from 0.022 to 10 mg/dscm (0.02 to 7.9 ppm). These results are in agreement with previous investigations by SoCal. N_2O emissions were measured during a period of low catalyst activity when both inlet and outlet NO_x levels were about 900 ppm at 15 percent O_2. The measured N_2O concentrations noted represent 2 to 7 percent of the total inlet NO_x and 0.6 to 2 percent of the total outlet NO_x. Previous data collected from external combustion sources has shown N_2O in the range of 15 to 20 percent of total NO_x (4).

Solid particulate emissions showed no noticeable change across the catalyst. In line with a reduction in combustible emissions (HC (as CH_4) and CO), TCO and GRAV organics were also reduced by the catalyst by about 78 and 98 percent, respectively.

Sulfur emissions were the highest of all elements, ranging from 240 to 740 mg/dscm. These emissions translate to a sulfur concentration in the natural gas fuel of about 0.01 to 0.04 percent, corresponding to typical H_2S concentrations. Sodium emissions were the second highest after sulfur. It is possible that sodium salts may have been present in the gas fuel along with sulfur, since natural gas was pumped from underground salt reservoirs. It is also likely that suspended salts (NaCl) may have been present in the intake air. Other trace elements emitted at levels exceeding 25 μg/dscm at either the NSCR system inlet or outlet locations were barium, calcium, chromium, copper, iron, magnesium, manganese, nickel, silicon, silver, tungsten, and zinc. In nearly all cases, the catalyst outlet emissions were higher than inlet emissions, often as much as one order of magnitude or more. This is especially the case for metals such as copper, chromium, iron, magnesium, manganese, nickel, and zinc. Since the lube oil trace element input rates were insufficient to account for either catalyst inlet or outlet emission rates, metallic element emissions may be thought as originating from internal engine parts, the muffler and/or the catalytic reactor.

Table 5 summarizes the PAH and other organic compounds detected by GC/MS analysis of the catalyst inlet and outlet sample extracts. Consistent with the overall reduction in total combustible emissions, these compounds were present at significantly lower concentrations in the catalyst outlet exhaust than in the inlet exhaust. Interestingly, all three-ring fused aromatics were destroyed by passage through the reactor. However, levels of phenol and naphthalene, one- and two-ring aromatics, were increased at the outlet, suggesting that these lower molecular weight aromatics were being formed from higher ring number compounds.

15-Day Continuous Monitoring

The sampling and analysis protocol for this portion of the test program consisted of continuous monitoring of inlet and outlet exhaust gas for O_2, CO_2, CO, NO/NO_x, and HC, with certification of NO_x analyzer readings using EPA Method 7. Since both engine power output and A/F were not restricted to specified ranges, the data obtained can be considered reflective of typical operating practice. Figure 2 summarizes NSCR catalyst inlet and outlet NO_x emission results for the 15-day test period. Each data point in these figures represents an hourly average. Therefore, frequent emission fluctuations are dampened by this hourly average reporting method.

Comprehensive tests were performed on June 7. This test period is indicated in Figure 2 by outlet NO_x levels below 200 ppm (at 15 percent O_2), corresponding to engine A/F levels at or below stoichiometric. Following these tests, the engine assumed a more typical operating condition, which resulted in exhaust O_2 being in the range of 2 to 5 percent. The result of the increase in A/F during the 15-day test period was an increase in inlet NO_x as well as a reduction in catalyst performance. In fact, NO_x reduction by the catalyst generally ranged between 0 and 40 percent. Only once was NO_x reduced by more than 90 percent. This reduction, which occurred during the early hours of June 18, was accompanied by a rapid increase in both CO and HC to levels of 4,000 and 400 ppm (at 15 percent O_2), respectively.

SCR RESULTS

1-Day Comprehensive Test

Table 6 summarizes engine operating characteristics during the comprehensive tests. Engine load was maintained relatively constant, at about 1,270 kW (1,700 hp), throughout this portion of the test program. Brake-specific fuel consumption was estimated at 9.4 MJ/kWh (6,600 Btu/Bhp-hr), based on fuel lower heating value. This is at the low end of representative four-stroke turbocharged engines. The NH_3 injection rate ranged from about 4.4 to 4.9 l/s (565 and 620 scfh), representing NH_3/NO molar ratio of about 1.0. The NH_3 injection rate was controlled by a feedback system which monitored NO_x at the engine outlet and set NH_3 injection rate to maintain appropriate NH_3/NO ratio. The target NO_x reduction for these tests was 80 percent.

Table 7 summarizes emissions measured at the engine muffler outlet (catalyst inlet) and the catalyst outlet locations. Continuously monitored emissions (O_2, CO_2, CO, NO/NO_x and HC) were measured upstream of the NH_3 injection located upstream at the engine muffler. Emissions are presented in mg/dscm, ng/J, and in mg/Bhp-hr.

As shown in Table 7, NO_x emissions were reduced 81 percent on the average from 2,760 ng/J (19.2 g/Bhp-hr) to 513 ng/J (3.57 g/Bhp-hr). NO_x reduction did not vary significantly from this average throughout the test period, indicating relatively constant performance of the catalytic system.

NH_3 emissions measured at the catalyst outlet with an extractive sampling system averaged 39 ng/J (0.27 g/Bhp-hr), corresponding to a volumetric gas concentration of 93 ppm. NH_3 emissions also measured at this location by a continuous monitoring system confirmed these results. Total cyanide increased significantly across the catalyst to a concentration of 2.4 mg/dscm at the catalyst outlet. N_2O levels at the catalyst inlet accounted for about 4 percent of the total NO_x measured. At the catalyst outlet, measured N_2O was 15 percent of the NO_x level. Both TCO and GRAV organics were apparently reduced by the catalyst by about 46 and 82 percent, respectively. This performance coincides with relatively low CO levels that were also measured at the catalyst outlet. Solid particulate emissions were not detectable within the limits of the measurement procedure.

Table 8 summarizes the emissions of volatile and semivolatile organic compounds detected by GC/MS analyses of VOST traps and SASS sorbent extract samples. Volatile organics were measured only at the catalyst outlet. These data show benzene and toluene as the principal compounds, with emission concentrations of about 900 and 250 μg/dscm, respectively, at the catalyst outlet. Other volatiles detected were xylenes, chlorobenzene, and ethylbenzene with concentrations below 100 g/dscm. Naphthalene and 2-nitrophenol were the major semivolatile organics detected at the catalyst inlet. Their concentrations of 8.4 and 5.3 μg/dscm, respectively, were reduced at the outlet to undetectable levels ($\leq$0.4 μg/dscm).

15-Day Continuous Monitoring

The sampling and analysis protocol for this portion of the test program consisted of continuous monitoring of inlet and outlet exhaust gas for O_2, CO_2, CO, NO/NO_x, NH_3, and HC, with certification of NO_x analyzer readings using EPA Method 7. Since both engine power output and NH_3 injection rate were not restricted to specified ranges, the data obtained can be considered reflective of typical operating practice. Figure 3 summarizes SCR catalyst inlet and outlet NO_x emission results. Each data point represents an hourly average. The data indicate relatively steady catalytic NO_x reduction performance, with exhaust O_2 levels at about 11 percent and CO_2 at about 5.5 percent. NO_x levels ranged between 1,200 and 1,600 ppm corrected to 15 percent O_2 at the inlet and about 100 to 400 ppm at 15 percent O_2 at the catalyst outlet location. NO_x reduction efficiency translates to a nearly constant 80 percent throughout the test period. Brief and infrequent periods of reduced or zero NO_x reduction were generally caused by an occasional loss of NH_3 flow or a surge in engine load. Periods of no data are indicative of engine shutdown due to a lubricating system problem. NH_3 emissions at the catalyst outlet, shown in Figure 4, ranged between 0 and typically 150 ppm. These data were obtained by using two NO_x analyzers, one equipped with a molybdenum and one with a heated stainless steel converter, respectively. NH_3 was determined by the difference between the $NO+NO_2+NH_3$ (heated stainless steel converter) and $NO+NO_2$ (molybdenum converter) readouts of the two online instruments. Combustible emissions were 100 to 300 ppm for CO and 750 to 1,250 ppm for HC.

Summary

Emission tests of the rich-burn reciprocating internal combustion engine retrofitted with a NSCR NO_x control system suggest that significant NO_x reduction (>80 percent) cannot be maintained without tight control of A/F within a narrow range. This range spans A/F near or below stoichiometric. The data suggested that corresponding CO and HC engine emissions required for greater than 80 percent NO_x reduction by the catalyst are in excess of 3,000 ppm and 400 ppm at 15 percent O_2, respectively. The extended 15-day continuous monitoring testing indicates the inability of the engine tested to be maintained at the necessary conditions of A/F, CO, and HC to achieve controlled NO_x emissions at or below the regulated level. (The engine had no automatic A/F controller.) The catalyst was found to significantly reduce all combustible emissions, including most PAH. Significant increases in NH_3 and total cyanide emissions were recorded, confirming anticipated and previously discovered trends. Exhaust levels of many inorganic trace elements, primarily metals, also increased across the catalyst.

Emission tests of the lean-burn reciprocating internal combustion engine retrofitted with a SCR NO_x control system suggest that NO_x emission reduction of 80 percent can be maintained with good control on NH_3 injection rate at relatively constant engine load. The catalyst was found to slightly reduce CO emissions, including detected organic compounds. NH_3 breakthrough emissions generally ranged between 0 and 150 ppm corrected to 15 percent O_2. Measurements by wet chemical methods support these levels.

ACKNOWLEDGEMENTS

This work was sponsored by EPA under contract 68-02-3188. Robert E. Hall was the EPA Project Officer. The authors wish to recognize the support and cooperation of SoCal personnel, in particular G. Gardetta, W. Matlock, and E. Harris. The assistance of the Acurex environmental field test crew is also appreciated.

REFERENCES

1. Rules and Regulations, Rule 1110.1, South Coast Air Quality Management District, adopted October 26, 1984.

2. D. E. Lentzen, et al., "IERL-RTP Procedures Manual: Level 1 Environmental Assessment (Second Edition)," EPA-600/7-78-201, NTIS PB 293795, October 1978.

3. E. M. Hansen, "Protocol for the Collection and Analysis of Volatile POHC's Using VOST," EPA-600/8-84-007, NTIS PB 84-170042, March 1984.

4. L. R. Waterland, et al., "Environmental Assessment of Industrial Boilers Firing Coal-Liquid Mixtures and Wood," in Proceedings of the 1982 Joint Symposium of Stationary Combustion NO_x Control, Volume 2, EPA CS-3182, July 1983.

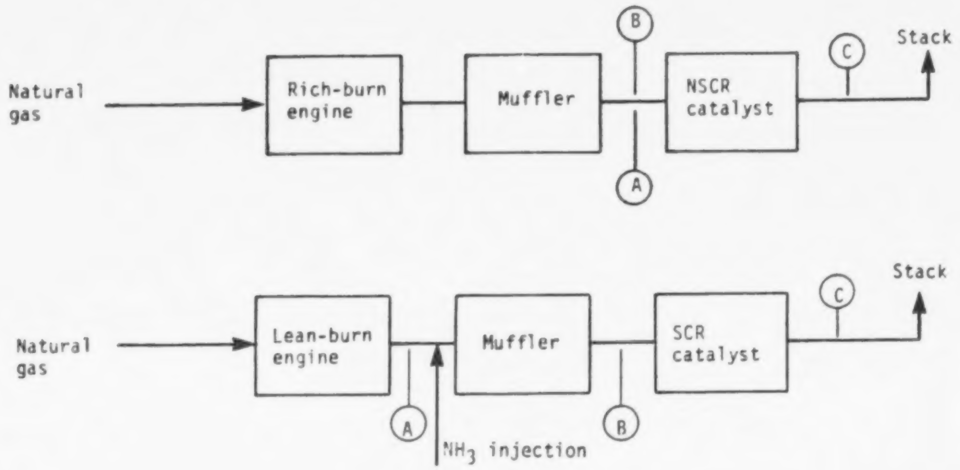
Natural gas
Rich-burn engine
Muffler
B
NSCR catalyst
C
Stack
A
Natural gas
Lean-burn engine
Muffler
SCR catalyst
C
Stack
A
NH_3 injection
B

A -- Catalyst inlet continuous monitoring only
B -- All other sampling at catalyst inlet
C — All sampling at catalyst outlet

Figure 1. Emission Sampling Locations

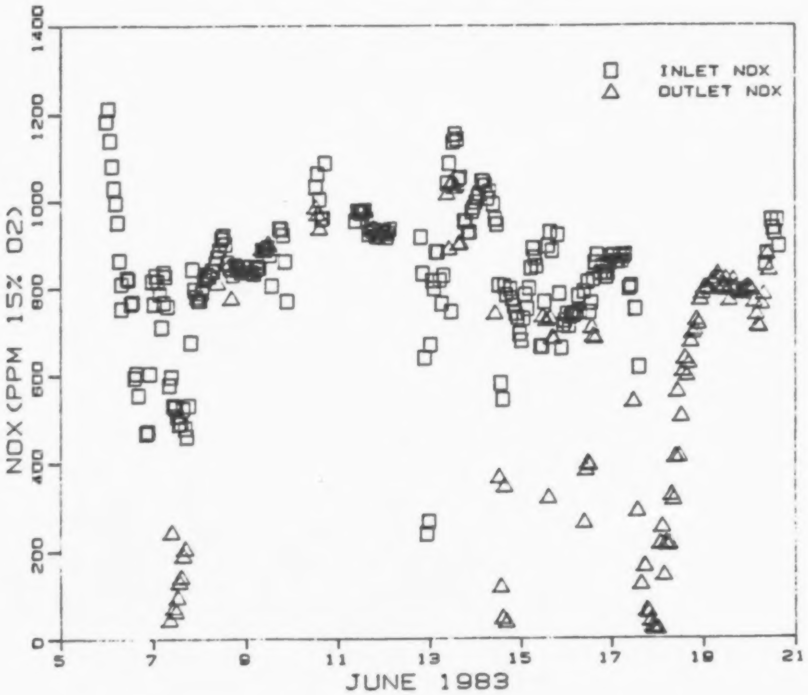

Figure 2. NO_x emissions during the 15-day continuous monitoring period -- rich-burn engine with NSCR system.

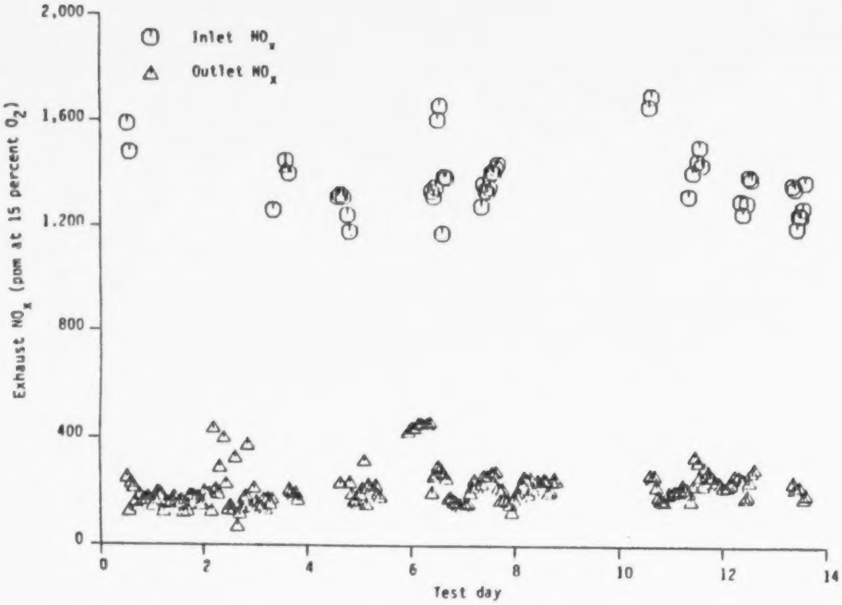

Figure 3. Exhaust NO_x levels for the extended continuous monitoring period -- lean-burn engine with SCR system.

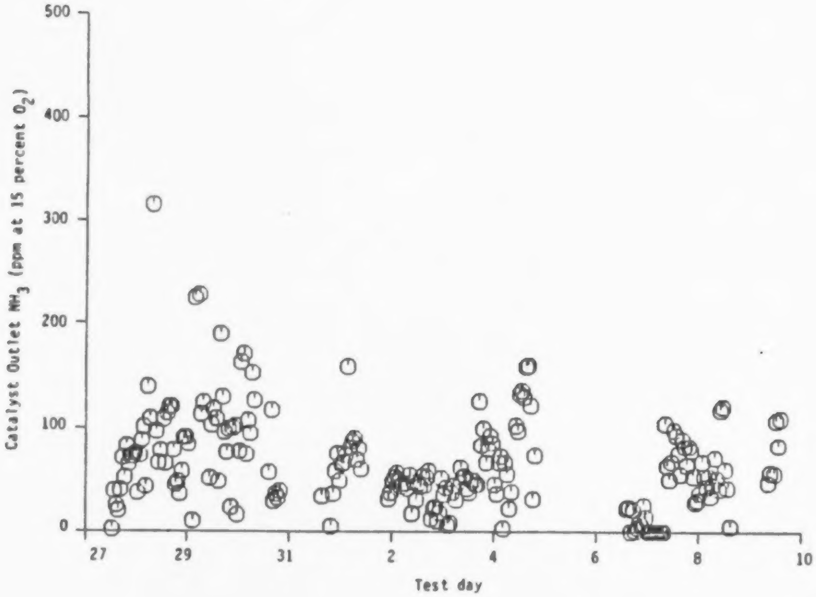

Figure 4. SCR catalyst outlet NH_3 emissions for the extended continuous monitoring period.

Table 1

ENGINE MODEL SPECIFICATIONS*

Manufacturer	Waukesha
Model	L7042 GU
Strokes	4
Air charging	Naturally aspirated
Number of cylinders	V-12
Bore	0.238 m (9.375 in.)
Stroke	0.216 m (8.50 in.)
Displacement/cylinder	9.62 liters (587 in.^{3})
Compression ratio	10:1
BMEP	703 kPa (102 psi)
Bhp/cyl @ rpm	50.7 kW (68 Bhp) @ 900 rpm
Generator output (electrical)	610 kW
BSFC	10,200 kJ/kWh (7,200 Btu/Bhp-hr)
Lubricating oil consumption	70 l/kWh (1.37 gal/Bhp-hr)

---

*Engine operating performance is based on continuous operation ambient conditions of 99.2 kPa (29.38 in. Hg) and 29°C (85°F) and a natural gas fuel (lower heating value) of 33.5 MJ/m^3 (900 Btu/ft^3).

Table 2

ENGINE/COMPRESSOR SPECIFICATION - LEAN BURN

Engine:	
Manufacturer	Ingersoll-Rand
Model	412DT-KVS
Cycle	4-strokes
Air charging	Turbocharged (dual)
Number of cylinders	V-12
Bore	0.387m (15.25 in.)
Stroke	0.487m (18.0 in.)
Displacement/cylinder	44.8 liters (2,735 in.^{3})
Compression ratio	6.5:1
BMEP	1.00 MPa (146 psi)
Bhp/cyl at rpm	125 kW (167 Bhp) at 330 rpm
Compressor:	
Manufacturer	Ingersoll-Rand
Bore (first stage)	0.235m (9.25 in.)
Stroke (first stage)	0.381m (15.2 in.)
Bore (second stage)	0.159m (6.25 in.)
Stroke (second stage)	0.381m (15.2 in.)

Table 3

RICH-BURN ENGINE OPERATION -- COMPREHENSIVE TESTS

Parameter	Range	Average
Ambient		
Dry bulb temperature, °C (°F)	26 to 29 (79 to 85)	29 (84)
Wet bulb temperature, °C (°F)	20 to 22 (68 to 71)	22 (71)
Relative humidity, percent	--	52
Barometric pressure, kPa (in. Hg)	--	96.4 (28.55)
Engine Operation		
Generator output, kW	415 to 455	425
Engine load, kW_t (Bhp)*	448 to 492 (601 to 660)	459 (616)
Fuel flow, m^3/h (scfh)	--	156 (5,569)
Heat input, MW (million Btu/hr)**	--	1.56 (5.33)
Specific fuel consumption, kJ/kWh (Btu/Bhp-hr)**	--	12,300 (8,660)
Air manifold pressure		
• L, kPa (in. Hg vac)	14 to 16 (4.1 to 4.6)	15 (4.4)
• R, kPa (in. Hg vac)	14 to 16 (4.1 to 4.8)	15 (4.5)
Speed, rpm	900 to 910	905
Catalyst inlet temperature, °C (°F)	533 to 536 (991 to 997)	535 (995)
Catalyst outlet temperature, °C (°F)	534 to 561 (994 to 1,042)	552 (1,025)

---

*Horsepower not a measured value -- calculated from generator output times 1.45.

**Based on low heating value.

Table 4

SUMMARY OF EXHAUST GAS EMISSIONS FOR THE RICH-BURN ENGINE, NSCR SYSTEM

Specie	NSCR Catalyst Inlet*			NSCR Catalyst Outlet*			Change in Emission Outlet/Inlet
	mg/dscm	ng/J	mg/Bhp-hr	mg/dscm	ng/J	mg/Bhp-hr	
Criteria and other gaseous pollutants and total organic emissions							
CO	5,350	1,210	1.22×10^4	4,840	1,030	10,400	0.85
HC (as CH_4)	150	34	330	94	20	200	0.61
NO_x (as NO_2)	3,410	770	7,790	1,180	250	2,530	0.32
NH_3	23	5.2	53	390	82	820	16
Total cyanide (as CN^-)	0.022	0.005	0.051	10	2.2	22	440
N_2O**	270	60	600	170	36	360	0.60
Solid particulate	1.3	0.30	3.0	1.3	0.30	3.0	1.0
Total chromatographable organics (C_7 to C_{16})	8.1	1.8	19	1.8	0.40	4.1	0.22
Total GRAV organics (C_{16+})	7.4	1.7	17	0.30	0.055	0.56	0.032
Trace elements							
Barium, Ba	0.049	0.011	0.11	0.064	0.014	0.14	1.3
Calcium, Ca	0.450	0.10	1.1	0.16	0.034	0.34	0.34
Chromium, Cr	0.0007	1.5×10^{-4}	0.0015	0.78	0.17	1.7	1,100
Copper, Cu	0.015	0.0035	0.035	1.2	0.25	2.5	71
Iron, Fe	0.039	0.0090	0.091	0.41	0.088	0.88	9.8
Magnesium, Mg	0.026	0.0059	0.059	0.16	0.033	0.33	5.8
Manganese, Mn	0.0010	2.3×10^{-4}	0.0023	0.032	0.0069	0.069	30
Nickel, Ni	0.0008	1.8×10^{-4}	0.0018	0.69	0.15	1.5	830
Phosphorus, P	0.005	0.0012	0.012	0.03	0.0064	0.064	5.3
Potassium, K	0.17	0.040	0.41	0.36	0.076	0.76	1.9
Silicon, Si	0.12	0.028	0.28	1.4	0.31	3.1	11
Silver, Ag	0.0015	3.4×10^{-4}	0.0034	0.22	0.046	0.46	140
Sodium, Na	150	34	340	160	35	350	1.0
Sulfur, S	240	52	520	740	162	1,600	3.1
Tungsten, W	0.13	0.030	0.30	0.0070	0.0015	0.015	0.05
Zinc, Zn	0.024	0.0055	0.056	0.46	0.089	0.89	16

---

*Average exhaust gas O_2 and CO_2 were 0.1 and 10.2 percent at both inlet and outlet locations.

**N_2O emissions were measured during low catalyst NO_x reduction efficiency following completion of the comprehensive tests. N_2O emissions are averages of two tests during which catalyst inlet and outlet NO_x emissions were about 900 ppm at 15 percent O_2.

Table 5

PAH AND OTHER ORGANICS SPECIES EMISSION SUMMARY (μg/dscm) FOR THE RICH-BURN ENGINE, NSCR SYSTEM

Semivolatile Organics	Inlet	Outlet*
Acenapthene	16.5	<0.4
Acenaphthylene	62.3	1.2
Benz(a)anthracene	5.1	<0.4
Benzofluoranthenes	1.9	<0.4
Bis(2-chloroethyl)ether	2.1	<0.4
Bis(2-ethylhexyl)phthalate	54.9	1.2
Butyl benzyl phthalate	0.7	<0.4
Chrysene	1.9	<0.4
Fluoranthene	0.5	<0.4
Fluorene	17.9	<0.4
Naphthalene	<0.4	28.5
Phenanthrene	40.3	1.4
Phenol	<0.4	1.8
Pyrene	2.2	<0.4

---

*Outlet results are based on the average of replicate analyses.

Table 6

LEAN-BURN ENGINE OPERATION -- COMPREHENSIVE TESTS

Parameter	Range	Average
Ambient		
Dry bulb temperature, °C (°F)	22 to 33 (72 to 92)	29 (84)
Wet bulb temperature, °C (°F)	19 to 21 (67 to 72)	20 (68)
Relative humidity, percent	45 to 55	50
Barometric pressure, kPa (in. Hg)	--	96.2 (28.5)
Engine Operation		
Engine load, kW_t (Bhp)*	--	1270 (1700)
Fuel flow, m^3/h (scfh)	--	327 (11,550)
Heat input, MW (million Btu/hr)**	--	3.29 (11.2)
Specific fuel consumption, kJ/kWh (Btu/Bhp-hr)**	--	9390 (6610)
Air manifold pressure, kPa (psig)	25 to 28 (3.6 to 4.0)	26.5 (3.85)
Air manifold temperature, °C (°F)	68 to 70 (154 to 158)	69 (156)
Engine speed, rpm	320 to 333	325
Exhaust manifold temperature, °C (°F)	380 to 382 (716 to 720)	380 (718)
Catalyst/NH_3 System		
Catalyst inlet temperature, °C (°F)	390 to 400 (740 to 750)	396 (745)
Catalyst outlet temperature, °C (°F)	344 to 382 (652 to 720)	362 (683)
NH_3 flowrate, l/s (scfh)	4.44 to 4.88 (565 to 620)	4.64 (590)
Gas Compressor		
Suction pressure, MPa (psig)	--	4.02 (583)
Interstage pressure, MPa (psig)	--	7.86 (1,140)
Discharge pressure, MPa (psig)	--	18.87 (2,898)
Suction temperature, °C (°F)	26 to 35 (78 to 95)	29 (85)
Interstage temperature, °C (°F)	88 to 93 (180 to 200)	91 (195)
Discharge temperature, °C (°F)	107 to 118 (225 to 245)	113 (235)

---

*Engine load obtained from engine performance curves.

**Heat input based on low heating value (LHV) of natural gas. Specific fuel consumption based on LHV of fuel.

Table 7

SUMMARY OF EXHAUST GAS EMISSIONS FOR THE LEAN-BURN ENGINE, SCR SYSTEM

	SCR Catalyst Inlet*			SCR Catalyst Outlet*			Change in Emissions
Specie	mg/dscm	ng/J	mg/Bhp-hr	mg/dscm	ng/J	mg/Bhp-hr	Outlet/Inlet
NO_x (as NO_2)	4,630	2,760	19,200	860	513	3,570	0.19
CO	287	171	1,190	265	158	1,100	0.92
NH_3**				65	39	270	--
Total cyanide (as CN)	0.007	0.004	0.03	2.4	1.4	10	350
N_2O***	180	108	750	79	79	327	0.73
Total chromatographable organics (C_7 to C_{16})	1.7	1.0	7.0	0.9	0.54	3.7	0.54
Total GRAV organics (C_{16+})	3.2	1.9	13	0.6	0.34	2.4	0.18

---

*Average exhaust gas O_2 and CO_2 were 11.2 and 5.5 percent, respectively, at both catalyst inlet and outlet locations.

**NH_3 emissions at the engine outlet were not measured by wet chemical analysis.

***N_2O emissions were measured after the comprehensive test period. Catalyst inlet and outlet NO_x during these tests were similar to levels measured during the comprehensive tests.

Table 8

VOLATILE AND SEMIVOLATILE ORGANIC EMISSIONS (μg/dscm) FROM THE LEAN-BURN ENGINE, SCR SYSTEM

Compound	Catalyst Inlet	Catalyst Outlet
Volatile organics:*		
Benzene	NA	915
Chlorobenzene		61
Chloroethane		1.8
1,1,dichloroethane		1.5
Ethylbenzene		20
Tetrachloroethane		2.4
Toluene		247
Acetone		17
Total xylenes		85
Semivolatile organics:		
Naphthalene	8.4	0.4
Phenanthrene	0.4	<0.4
2-Nitrophenol	5.3	<0.4
Di-n-butyl phthalate**	3.1	5.5
Bis(2-ethylhexyl)phthalate**	1.9	1.0

Note: NA -- Not available. No measurements for volatile organics performed at the catalyst inlet location.

*Volatile organic emissions measured only at the catalyst outlet. Values presented are blank corrected average of two measurements.

**Suspected contaminants, commonly found in laboratory blanks.

SESSION IXa: OVERVIEW OF FURNACE SORBENT INJECTION SO_2 CONTROL

Chairman, Robert Hangebrauck, EPA

REVIEW OF INTERNATIONAL DEVELOPMENT ACTIVITIES FOR FURNACE SORBENT INJECTION

Dan V. Giovanni
Electric Power Technologies, Inc.
P.O. Box 5560
Berkeley, California 94705

INTRODUCTION

At the 1982 Joint Symposium on Stationary Combustion NOx Control in Dallas, Texas, an entire session was devoted to the discussion of emission control processes based on dry injection of calcium sorbents to meet SO_2 regulations for coal-fired power plants. In November, 1984, EPRI and EPA sponsored the 1st Joint Symposium on Dry SO_2 and Simultaneous SO_2/NOx Control Technologies in San Diego, California. Forty-six papers were presented addressing the latest advances in fundamental research and process design, power plant integration and economic issues, and results from field applications. The scope of technical information discussed at the symposium was a reflection of the significant and widespread developmental activities currently in progress, which involve furnace sorbent injection (FSI) for SO_2 control. This paper attempts to summarize that information by defining the current status of FSI process developments, acknowledging advances in process understanding and design, and identifying yet unresolved technical issues.

TECHNOLOGY HISTORICAL PERSPECTIVE

The concept of furnace sorbent injection originated in the early 1960s as a simple and economic means of meeting anticipated SO_2 removal requirements for new coal-fired power plants. However, trial tests in laboratory furnaces and full scale boilers in the United States, Europe, and Japan generally failed to demonstrate SO_2 removals above 15-40% at practical sorbent-to-sulfur ratios. Removal efficiency was also found to be highly dependent on boiler design and operation, as well as on the type of sorbent and injection system used. Potential adverse effects on boiler performance were also noted (e.g., fouling of furnace heat transfer surfaces and degraded electrostatic precipitator performance). These results, together with the low capital costs projected for wet scrubbers, led to the termination of FSI development in the early 1970s.

There was a resurgence of interest in FSI technology in the mid-1970s due in part to research performed in The Federal Republic of Germany (FRG). That work arose out of a need for incremental SO_2 removal in FRG power plants firing lignitic coal. Experiments at pilot scale showed better results than previous tests in the United States, and triggered multi-year development programs which included testing of bituminous coals. In the same timeframe, the U.S. EPA announced the Limestone Injection Multistage Burner (LIMB) concept for simultaneous SO_2/NOx control. These factors have contributed to widespread renewed interest in FSI technology. Research and development programs underway at EPRI, EPA, DOE, and several other organizations in the United States, Canada, FRG, France, The Netherlands, Sweden, Austria, and Japan span a wide range of laboratory and field test conditions and involve a variety of sorbents, coals, and process methodologies.

PROCESS DESCRIPTION

With furnace sorbent injection, a powdered calcium-based sorbent such as pulverized limestone ($CaCO_3$) or calcium hydroxide (hydrated lime $Ca(OH)_4$) is injected directly into the furnace cavity of a coal-fired boiler, as illustrated in Figure 1. Upon exposure to furnace temperatures, the sorbent rapidly decomposes to form highly reactive lime particle (CaO) which react with SO_2 in suspension to form particles of calcium sulfate ($CaSO_4$). This calcium sulfate, along with any unreacted lime, is then carried out of the furnace by flue gases and collected with flyash in the particulate control device.

The fundamentals of the process are illustrated for limestone in Figure 2. Pulverized $CaCO_3$ particles are injected in the postcombustion product gases of the furnace. Typical gas temperatures may range from 1800 to 2400 F. Upon heating, calcination occurs. CO_2 evolves from the particle and a reactive surface layer of CaO is formed. The particle also undergoes a physical transformation in which specific surface area increases several-fold. At the temperatures of interest the calicination proceeds fairly rapidly such that the particles are typically over 90% calcined in less than one second. The partially calcined particle is also subject to two other chemical/physical mechanisms which occur concurrently -- sulfation and sintering. Sintering by solid diffusion results in the loss of reactive CaO surface. With sufficient time at high temperature (just below the solidus) the atoms move by diffusion and the points of actual contact between particles enlarge so that only one interface forms in the place of the two former surfaces. At temperatures between 1500 and 2200 F, SO_2 will react with CaO to form $CaSO_4$. As shown in Figure 2 for cases with and without significant sintering, the $CaSO_4$ forms a "coating" on the surfaces of the calcined particle.

Calcium utilization is defined to be the molar ratio $CaSO_4$ which is formed to $CaCO_3$ (or $Ca(OH)_2$) in the injected particle. Calcium utilization is typically less than 100% due to the combined effects of incomplete calcination or sulfation. As suggested above, at the temperatures of interest complete calcination is usually achieved within the available time in a typical furnace cavity. Therefore, calcium utilizations <<100% are principally due to incomplete sulfation.

Sulfation may be limited by one or a combination of three mechanisms: (1) pore plugging; (2) solid diffusion; and (3) chemical kinetics. The first two of these mechanisms are also illustrated in Figure 2. The calcined particle may be viewed as a "popcorn-like" structure in which the majority of reactive surface is contained in pores and crevices. As $CaSO_4$ is formed, due to its greater specific volume relative to CaO, it may close-off the entrances to many of the smaller pores. Similarly, $CaSO_4$ may fill the smaller pore volumes. In either case, the migration of SO_2 molecules to the inner particle would be prevented. The solid diffusion limitation may apply for particles whether or not there has been significant sintering. In these instances, reactive SO_2 is encapsulated by $CaSO_4$. For sulfation to continue, SO_2 has to diffuse through this sulfate layer to react with the CaO. The diffusionrate ultimately depends on temperature, SO_2 concentration, and the solid diffusion characteristics of the sulfate layer. The third limiting mechanism for sulfation is chemical kinetics. Not withstanding the forementioned limiting factors, sulfation may not be completed due to kinetic considerations which involve SO_2 concentration, reaction temperature, and time available for the CaO and SO_2 to react.

DEVELOPMENT ACTIVITIES

International development activities have been classified into four groups:

Fundamental: Research at laboratory scale to gain a better understanding of process fundamentals, the behavior of different sorbents, and the mechanisms limiting calcium utilization.

Pilot: Empirical studies on laboratory combustors (typically 0.1 to 1.0 MBtu/hr) for characterization of calicination/sulfation processes and the FSI optimization in terms of calcium utilization.

Industrial: Field applications based directly on pilot studies and incorporating additional emphasis on process integration issues such as large scale sorbent injection/dispersion, fouling and slagging of furnace internals, impact on electrostatic precipitator performance, and solids handling and disposal.

Utility: Full-scale technology demonstrations addressing all aspects of technology scale-up, process integration, emissions compliance, economics, and process reliability.

The are numerous public and private organizations performing work on FSI in each of these categorgies. Based on the information available at the time of the 1st Joint Symposium in San Diego, Table 1 was prepared which provides an indication of the spectrum activites currently in progress.

RESEARCH AND DEVELOPMENT STATUS

Recognizing only the magnitude of developmental activites, one would likely conclude that there have been significant advances in the technology in recent years. Closer examination reveals that whereas there has not been a "breakthrough" of significant consequence, there has been a consolidation of understanding on process fundamentals and technology scale-up.

Among the more important advances regarding FSI, their appears to be a consensus among researchers on the following issues relating to process chemistry.

1. In-furnace calcination occurs in less than 1 second when the sorbent is injected to combustion product gases in the neighborhood of 2000 F.
2. The sulfation rate (calcium utilization) is strongly related to the time/temperature history of the injected sorbent particle.
3. Sintering of CaO particles does occur and will inhibit sulfation.
4. For a given well-mixed combustion system, calcium utilization can be maximized and it is a function of flue gas temperatures at the point of injection and the rate of temperature reduction (quench rate) as the gases pass through the furnace.
5. The sulfation rate (calcium utilization) is proportional to the specific surface area of the calcine (CaO). As shown in Figure 3, which is a compilation of data from the EPRI and EPA pilot scale studies, increasing CaO surface area from 10 to 30 (m^2/g) would result in an increase in calcium utilization from approximately 20 to 35%.

The effectiveness of FSI is typically measured in terms of SO_2 removal as a function of calcium-to-sulfur ratio (Ca/S). The range of experience is illustrated in Figure 4. There are three bands of data represented and each band reflects the range of experience for different injection schemes. The upper two bands are for post flame injection in which the calcination/sulfation processes are decoupled from the primary flame zone. The lower band is for sorbent injection with the fuel. The variation in SO_2 removal for a given Ca/S is attributable to different sorbents (e.g., limestone, dolomite, hydrated lime), injection temperatures, sorbent magnesium content, combustion conditions, quench rates, and uniformity of sorbent-gas mixing. The higher SO_2 removal with post flame injection is likely due to the avoidance of high temperature zones which lead to enhanced sintering and $CaSO_4$ decomposition.

The upper bound of the data bands in Figure 4 represent optimized conditions of sorbent selection, time, temperature, and injection. In Figure 5, SO_2 removal for optimized conditions are presented for different calcium sorbents as a function of Ca/S. This data has been extracted from reports at the 1st Joint Symposium, of bench and pilot scale work. The following general conclusions are apparent:

1. Calcium hydroxide is more effective than calcium carbonate.

2. Dolomitic materials are more effective than non-dolomitic materials.

3. Additives can effectively increase calcium utilization.

4. For all sorbents (without additives) less than 50% of the calicium is utilized at a Ca/S = 1.0.

A generalized research goal common to many programs is to achieve 50% SO_2 removal (or 25% calcium utilization) at a Ca/S less than 2.0, for a "reasonably" cost sorbent. As indicated in Figure 6, this level of performance has been achieved with all sorbents of interest except limestone. Unfortunately, limestone is the least expensive sc bent and despite the favorable performance of the other sorbents they may prove to not be cost effective for full scale applications. Hence, much of the continuing research is directed to increasing calcium utilization with limestone and/or to minimizing the costs associated with the better performing sorbents.

UNRESOLVED TECHNICAL ISSUES

Process Chemistry. Research continues in several interrelated directions in the laboratory addressing issues that may lead to increased calcium utilization. The principal activities involve the following:

1. Mechanisms limiting CaO sulfation. As noted in the discussion on process fundamentals, three distinctly different mechanisms have been identified which may ultimately limit calcium utilization: (1) chemical kinetics; (2) gas diffusion through the solid $CaSO_4$ layer; and (3) loss of available reactive surface area due to sintering, pore plugging, or pore filling. If these mechanisms and their interrelationships were better understood, then perhaps countermeasures could be developed to promote increased sulfation.

2. Role of inherent magnesium. Dolomitic sorbents perform better (higher calicum utilization) than those without inherent magnesium. It has also been verified that magnesium does not react with SO_2 to form magnesium sulfate. Hence, magnesium impurities many favorably effect the gas-solid diffusion or the chemical kinetics. Its role is not presently understood.

3. Role of additives. Limited testing with additives including chromium, sodium, and lithium compounds has shown significant enhancements in calicum utilization for all calcium sorbents. There is evidence that the there may be more than one mechanism by which these additives have an effect. As with magnesium, the role of such additives is not understood.

4. Sulfation of precalcined sorbents. The majority of work has focused on in-furnace calcination and sulfation. The conditions which promote optimum calcination may not be the same for sulfation. In addition, sulfation may interfere with the calicination process and vice versa. Research has been initiated on the independent calcination of sorbents at lower temperature and for longer times (i.e., >> 1 second) to produce CaO material with high specific surface area.

5. Sulfation below 300 F. As currently designed half or more of the calcium is not utilized in the furnace. It may be possible to obtain supplemental SO_2 removal with this material in the low temperature ductwork leading to an electrostatic precipitator or baghouse. At temperatures approaching the water dewpoint of the flue gas the CaO is known to react with SO_2 to form $CaSO_4$. Research has been initiated to ascertain whether this chemistry may be exploited to complement SO_2 removal achieved with FSI.

Process Integration and Scale-up. There are several technical issues involving FSI which cannot be resolved in laboratory combustion facilities. Accordingly, there are a number prototype and demonstration programs at industrial and utility scale involving FSI. These programs will serve three purposes. First, they will demonstrate that SO_2 removals achieved in the laboratory can be successfull scaled to full-size boilers and furnaces. Secondly, they will adress critical issues requiring resolution at larger than laboratory scale. These include: effects of sorbent dispersion and mixing in the upper furnace cavity; load following capability; and effects of non-uniform temperature, velocity, and gaseous composition distributions. Thirdly, the impact on plant operations and performance will be comprehensively evaluated.

In this context, the following issues involving process integration and scale-up have been identified.

1. Control of increased deposition on boiler and air preheater surfaces.

2. Prevention of increased erosion of boiler convective passes due the increased solids loading.

3. Quantification (and mitigation if necessary) of heat flux redistributions that may result in imbalances between differenct zones of boiler circuitry.

4. Control of sorbent mixing/dispersion in large furnace enclosures.

5. Determination of the compatibility of FSI with different combustion systems, including wall-fired, opposed-fired, and corner-fired boilers.

6. Determination of the effectiveness of different sorbents with coals of differring sulfur content and mineral constiuents.

7. Quantification of the impact of FSI upon electrostatic precipitator performance and operation.

8. Evaluation of the effectiveness of alternative means to upgrade ESP performance in light of the consequences of FSI, that is increased solids loading and increased electrical resistivity.

9. Determination of the requirements for solids conveying/storage/disposal into and out of the plant.

10. Clarification of the potential for low temperature heat recovery due to inherent SO_3 removal by FSI.

CONCLUSION

At present, FSI technology is not viewed as a commercial alternative for the control of SO_2 emissions from coal-fired power plants. There are a variety of technical and economic issues which need resolution to improve its commercial attractiveness and bolster industry confidence in the process. Nonetheless, the process has shown significantly improved performance relative to the experiences in the 1960s and 1970s. Furnace sorbent injection does offer the potential for lower cost SO_2 control as compared to conventional flue gas desulfurization processes, and a means for incremental SO_2 control in addition to switching to lower sulfur coal. Accordingly, FSI research and development activity throughout the world is proceeding at a significant pace. There are numerous public and private organizations conducting work on all pertinent technical aspects of the process. The results from this work will form the basis for commercial application, which in most instances will be very site specific.

REFERENCE

Electric Power Research Institute and the U.S. Environmental Protection Agency, Proceedings: First Joint Symposium on Dry SO_2 and Simultaneous SO_2/NOx Control Technologies, EPRI Report No. CS-4178, Volumes 1 and 2, EPRI Project RP2533-3, EPA Contract 68-02-3993, July 1985.

FIGURE 1

FURNACE SORBENT INJECTION

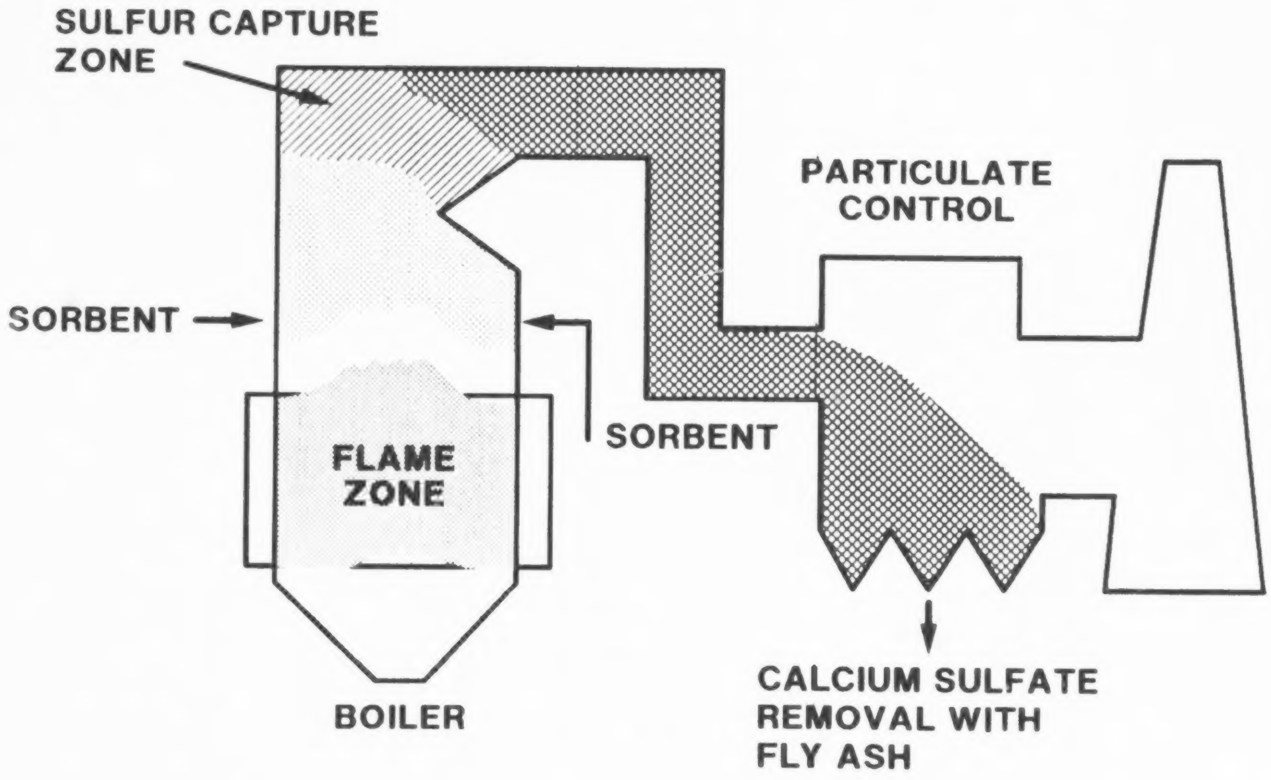
SULFUR CAPTURE ZONE
PARTICULATE CONTROL
SORBENT
SORBENT
FLAME ZONE
BOILER
CALCIUM SULFATE REMOVAL WITH FLY ASH

FIGURE 2

PROCESS FUNDAMENTALS

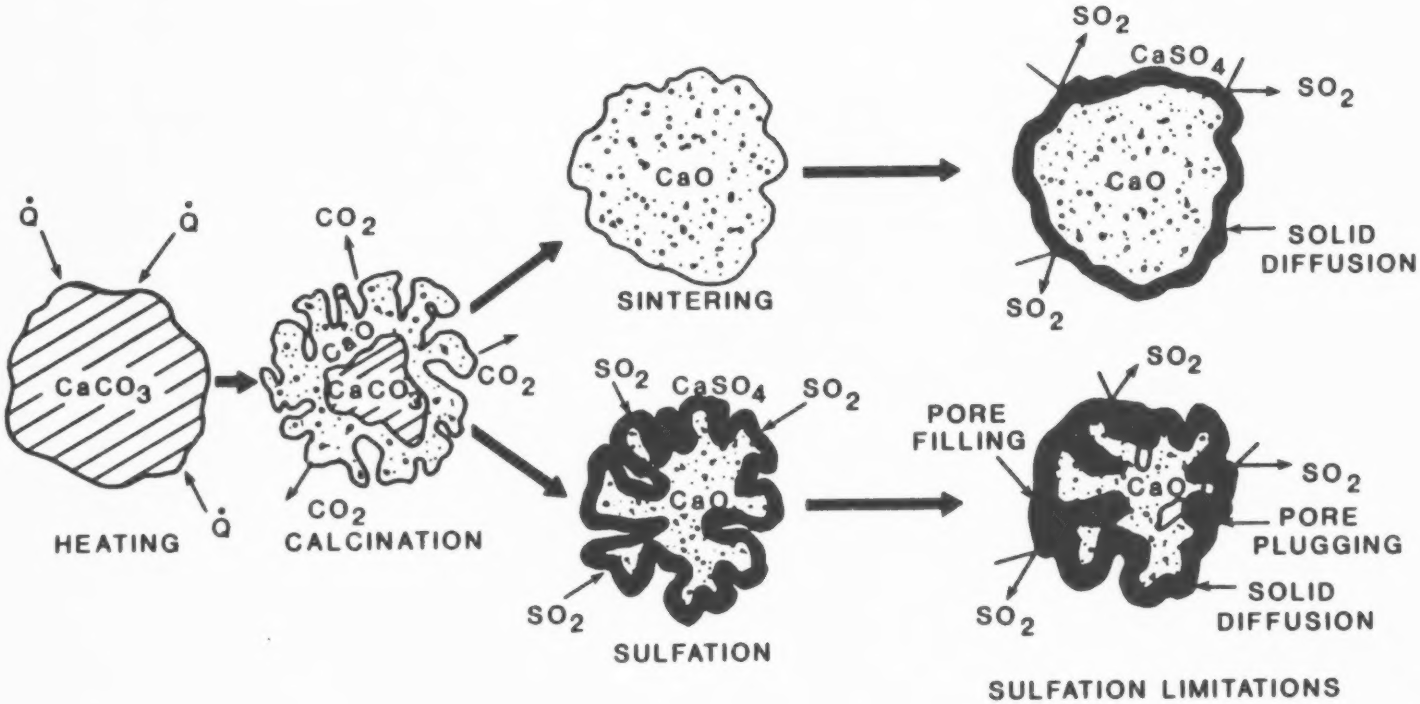
$\dot{Q}$
$\dot{Q}$
$CaCO_3$
$\dot{Q}$
HEATING
CO_2
CaO
$CaCO_3$
CO_2
CO_2
CALCINATION
CaO
SINTERING
SO_2
$CaSO_4$
SO_2
CaO
SO_2
SULFATION
SO_2
$CaSO_4$
SO_2
CaO
SOLID DIFFUSION
SO_2
SO_2
PORE FILLING
CaO
SO_2
PORE PLUGGING
SOLID DIFFUSION
SO_2
SULFATION LIMITATIONS

Fig. 3- EFFECT OF SURFACE AREA ON Ca UTILIZATION

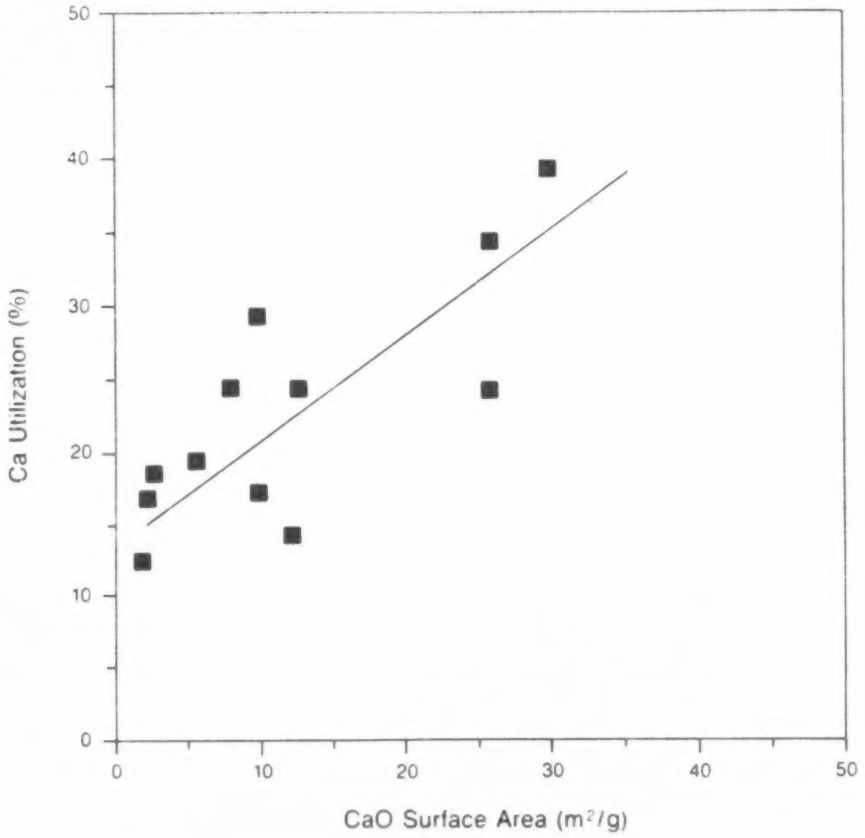

Fig. 4 - FSI SO_2 REMOVAL WITH Ca SORBENTS

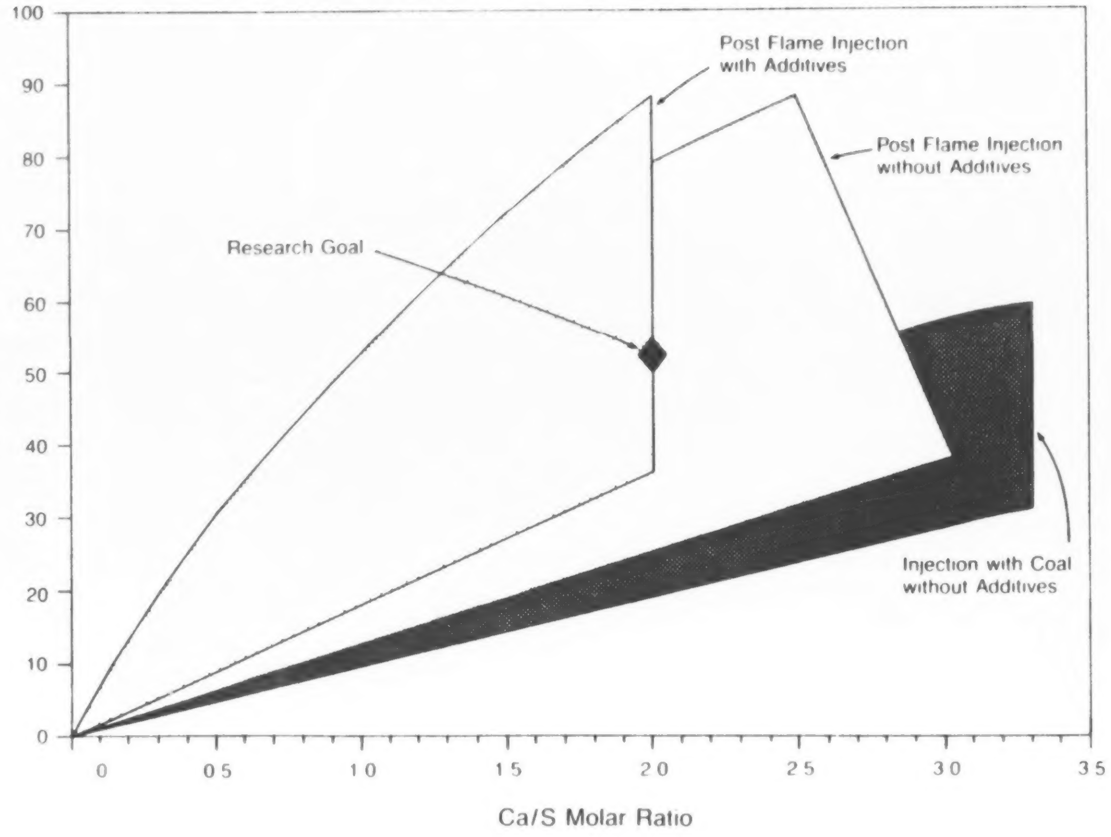

Fig. 5 - FSI SO_2 REMOVAL USING ALTERNATIVE SORBENTS

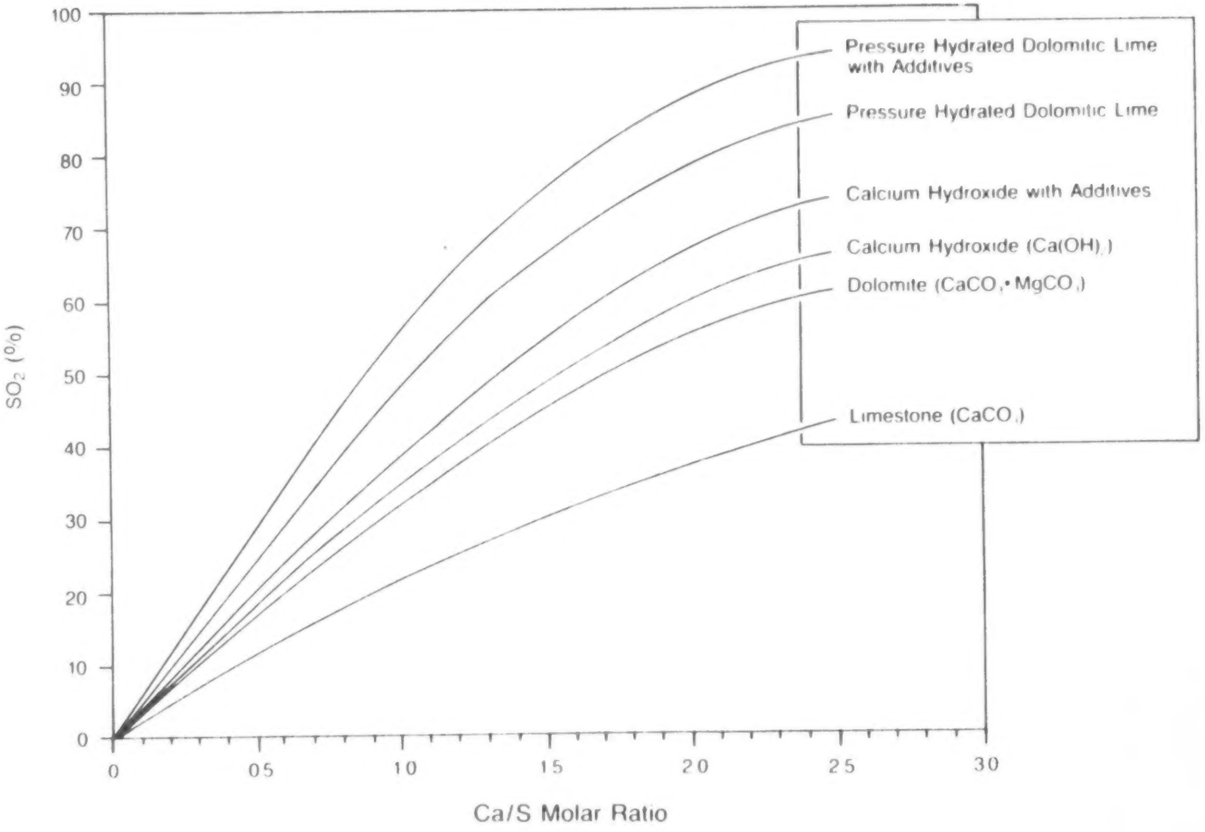

Fig. 6 - APPROXIMATE Ca UTILIZATION @ Ca:S = 2

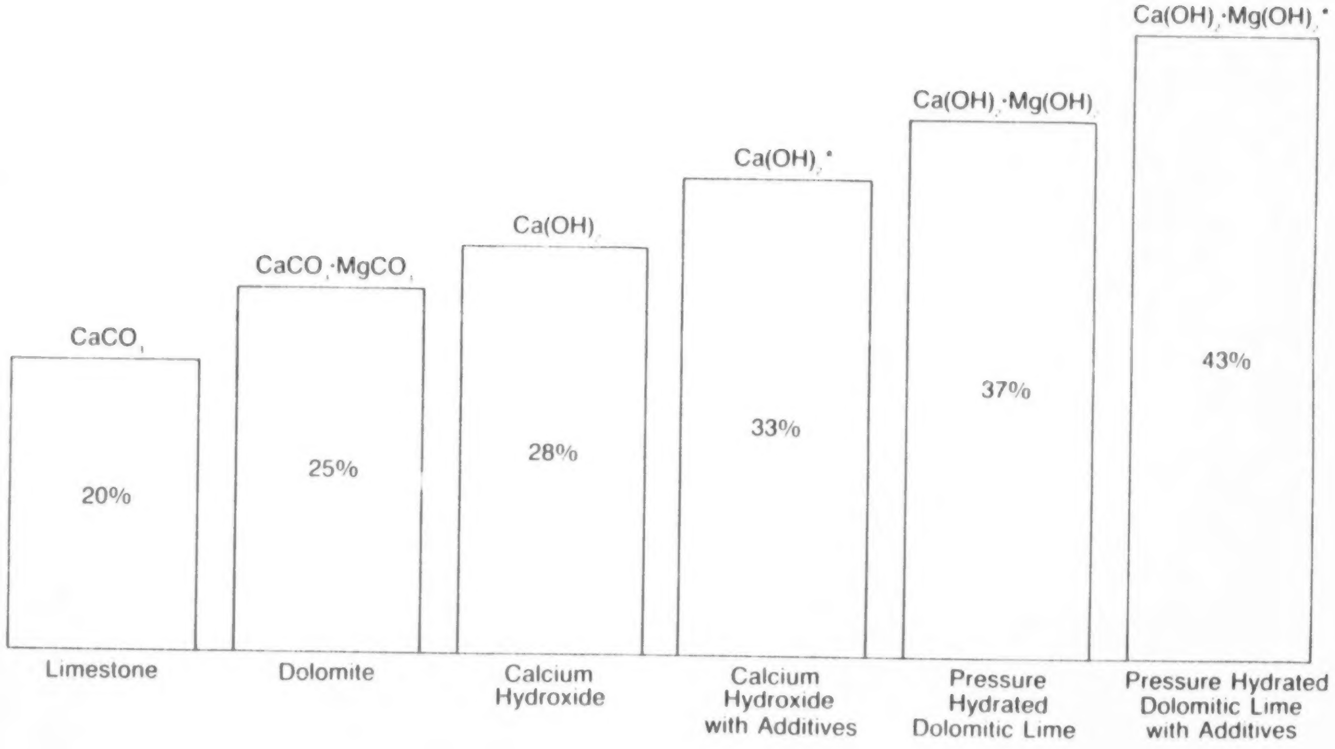

*Additives

TABLE 1

FSI DEVELOPMENT ACTIVITIES

FUNDAMENTAL	PILOT	INDUSTRIAL SCALE	UTILITY SCALE
● Acurex	● Acurex	● Charbonnages de France	▲ Babcock & Wilcox/Ohio Edison
● Battelle Columbus	● Babcock & Wilcox	● CONOCO	▲ Charbonnages de France
● Dravo Lime	● CONOCO	● Energy Environmental Research	▲ Energy Environmental Research
● Energy Environmental Research	● Dravo Lime	● Foster Wheeler	▲ EPRI
● EPRI	● Energy Environmental Research	▲ CANMET	▲ Hamberger Elek
● Fossil Energy Research	● Foster Wheeler	▲ CONOCO	▲ ODK (Austria)
● IFRF	● IFRF	▲ Foster Wheeler	▲ PENELEC/NYSEG
● KVB	● KVB	▲ Research Cottrell	▲ Public Service Indiana
● Northrop Services	● Mitsubishi Heavy Industries	▲ RWE	▲ Radian
● RWE	● RWE	▲ Steinmuller	▲ RWE
● UNDERC	● Southern Research Institute		▲ Saskatchewan Power
● University of Graz	● Steinmuller		▲ Steinmuller
● University of Utah	● UNDERC		▲ U S DOE
● U S EPA - IERL	● U S DOE		■ Babcock & Wilcox
	● U S EPA - IERL		■ Bechtel
	▲ Battelle Columbus		■ Charbonnages de France
	▲ Combustion Engineering		■ Combustion Engineering
	▲ EPRI		■ Foster Wheeler
	▲ RWE		■ Riley Stoker
	▲ Southern Research Institute		■ Sargent Lundy
			■ Southern Company Services
			■ Stearns Catalytic
			■ Stone & Webster
			■ Sweden (Malmo)

● PROCESS CHEMISTRY ▲ PROCESS INTEGRATION ■ DESIGN/ECONOMICS

Technical Status of EPA's LIMB Program

G. Blair Martin and James H. Abbott
Air and Energy Engineering Research Laboratory
U.S Environmental Protection Agency
Research Triangle Park, NC

ABSTRACT

Sulfur oxides (SO_x) and nitrogen oxides (NO_x), two pollutants resulting from the combustion of coal, are believed to be major precursors of acid rain. Limestone Injection Multistage Burners (LIMB) is a potential low cost technology for control of SO_x and NO_x from existing utility and industrial boilers. The LIMB R&D program has provided a detailed understanding of the key processes governing sulfur capture with sorbents. While it appears that limestone alone will not achieve program goals, several other promising sorbents have been identified. Based on the R&D results and cost estimates for use of these sorbents, LIMB shows substantial promise as a SO_x and NO_x control technology for retrofit applications. The ongoing R&D program should resolve the remaining technical questions and provide a basis for widespread private sector commercialization. The purpose of this paper is to provide a summary of the technical status of LIMB related R&D.

INTRODUCTION

The EPA is developing LIMB as a potential low cost control technology for SO_x and NO_x, which are believed to be two of the major precursors of acid precipitation. The LIMB program is structured to provide an understanding of the controlling factors in the process and to establish a basis for private sector commercialization. The purpose of this paper is: 1) to summarize the status of the LIMB program; and 2) to outline planned research and development.

BACKGROUND

Sulfur oxides (SO_x) and nitrogen oxides (NO_x) are two major pollutants resulting from the combustion of fuels. Coal fired utility boilers account for about 70 percent of the SO_x and 20-25 percent of the NO_x emissions in the United States. For the 180,000 MW of coal fired boiler capacity east of the Mississippi River, this amounts to approximately 16 million tons* of SO_2 and 4-5 million tons of NO_x emitted per year. (ref 1) Only about 10 percent of these boilers are subject to NSPS controls for SO_x and NO_x. Therefore to accomplish any significant reduction in SO_x and NO_x requires a retrofit of controls to existing boilers which may have a remaining useful life of from 5 to 30 years. The vast majority of these are wall-fired and tangentially fired boilers.

---

* 1 Ton = 907 kg.

The seriousness of the acid rain problem and the importance of various acid precursor sources are still under debate; however, control of SO_2 from utility boilers is a major element in all proposed strategies. In addition NO_x is increasingly being linked to forest damage mechanisms. Proposed reductions of SO_2 range from 5 to 12 million tons per year, and the issue of an NO_x offset is being debated.

Control Technology Options

The choice of emission control strategies will have a significant effect not only on the ability to achieve any mandated reduction but also on its cost to the nation. The final decision on the technology mix will be based on the availability, specific performance, cost, and overall economic impact on the nation, including socioeconomic factors such as displacement in the work force. Among the control technology options commercially available are coal switching, coal cleaning, and various types of flue gas desulfurization (FGD) systems. In addition, some early analyses indicated that a low capital cost technology would be attractive even at moderate SO_2 removal (e.g., 50 percent control). Although there are several approaches being developed, none of the potential low cost alternatives have been demonstrated. One such rapidly emerging technology is LIMB which is based on injection of sorbents into the boiler for direct capture of SO_2 from the combustion gases.

History of Sorbent Injection

There is a considerable body of background information on sulfur capture by injection of sorbents into a conventional boiler. The information includes the experience in the U.S. with sorbent injection through a number of boilers in the late 1960's and early 1970's, some current experience in Germany on both brown coal boilers and other small-scale experimental facilities, and, finally, EPA testing using the distributed mixing low-NO_x burner with sorbent injection in a pilot-scale facility. A summary of these efforts was presented by the authors at a recent symposium. (ref 2)

Structure of the Program

This background information was used in structuring the LIMB program, which was initiated by the EPA in 1981. LIMB combines sorbent injection for SO_x control with low-NO_x burners for NO_x control. Low-NO_x burners of various designs have been developed by both EPA and private industry and are capable of retrofit applications. SO_x control by sorbent injection is an emerging technology which has been developed by the EPA. The reaction of SO_x with sorbents (i.e., limestone and other alkaline solids) is well known under proper conditions (e.g., wet FGD). LIMB is based on injection of a sorbent directly into the furnace and its subsequent reaction with gas-phase SO_2 to form a dry calcium sulfate. The amount of SO_2 that can be captured is dependent on the type and amount of sorbent, its mixing with combustion gases and fly ash in the furnace, and its thermal history. The relative simplicity of the technology lends itself to a relatively low cost retrofit on a wide variety of systems. The program has been structured to give the best probability of achieving the stated goals of moderate SO_x and NO_x control (50-60 percent) at low cost with applicability to the major portion of the existing boiler population. A secondary objective is to improve the SO_x removal efficiency to 70-90 percent for new sources. To achieve this, work has been concentrated in four major areas, as discussed below.

Generic R&D. The program is centered around generic R&D to provide a complete understanding of the important factors in sulfur capture by sorbents. This work is performed in experimental systems which simulate conditions in a boiler without being subject to hardware constraints. The results to date have shown that sulfur capture is strongly dependent on conditions within the boiler which determine not only the activation of the sorbent but also the resultant reaction with SO_2. This work has shown the necessity for considering sorbents other than limestone (e.g., dolomitic and calcitic hydrates). The generic R&D is currently concentrated in improved sorbent activity for retrofit systems, although it also has application to new systems.

Prototype Testing. The results of the small-scale generic R&D must be scaled up to practical systems. As an intermediate step prior to a demonstration, prototype testing is carried out in large experimental systems. In addition small boilers may be used to provide R&D data on scaleup, operability, and reliability.

Wall-fired Boilers Demonstration. Wall-fired boilers, one of the two major types of boilers, are sold by three manufacturers: Babcock and Wilcox, Foster Wheeler, and Riley Stoker. The wall-fired boiler, which is a major source of SO_2 and NO_x, has been the subject of the initial LIMB development because both the R&D background and large-scale experimental facilities were available. The demonstration program for a representative wall-fired utility boiler was initiated in FY84 and is discussed in more detail below.

Generalization of the Technology. To be widely accepted, a well defined set of criteria for application of LIMB to a wide range of boiler designs, coals, and sorbents is necessary. A limited number of demonstrations alone may not be sufficient for widespread private sector commercialization. A key element of the overall program is to produce the required information and methodologies for applying LIMB R&D to site specific design decisions for any given boiler. This will be accomplished by a combination of modelling techniques and supporting measurements on operating boilers.

STATUS OF THE TECHNOLOGY

A recent EPA/EPRI symposium held in San Diego, California, provided a comprehensive overview of the R&D on LIMB and related dry injection technologies for SO_x and SO_x/NO_x control being performed worldwide. (ref 3)

There was substantial agreement on certain basic aspects of the technology; however, there are a number of technical areas which require further work before the technology can be commercialized. Presentations covered the range from fundamental research to full scale boiler trials. In reviewing the technical data presented, certain categories of R&D were identified and grouped into technical areas. This paper is the EPA's technical summary and interpretation of the presentations and subsequent discussion.

Reaction Mechanisms

There was general agreement that the fuel rich chemistry (reduced sulfur compound) mechanism does not have a major role in sulfur capture under the conditions in pulverized coal fired systems. The reasons for this are not fully understood since the basic kinetics appear favorable. The mechanism for capture of reduced sulfur compounds under fuel rich conditions may be studied further in the context of slagging combustors, where the solids are removed prior to the air addition for oxidation of partial combustion products.

The predominant mechanism for sulfur capture is the fuel lean capture of SO_2 in the upper reaches of the boiler. There was general agreement that SO_2 removal occurred in a temperature window of 1800 to 2100°F (982 to 1149°C) with a possible variance of 200-300°F (111 to 167°C) either high or low. The EPA considers the window to be between 1600 and 2250°F (871 to 1232°C). It should be noted that the effects of residence time within that window were not entirely consistent, but probably within experimental/analytical bounds. In addition some question remains about the order of the reaction with respect to SO_2 as discussed below.

Coal Effects

The majority of the data tended to support the conclusion that the SO_2 capture is relatively independent of fuel sulfur content when it is above about 1% S. At lower sulfur levels the SO_2 capture efficiency tends to decrease due to a reduced gas phase driving force for diffusion. It is believed that a proposed apparent zero order in SO_2 concentration is due to a combination of the chemical kinetic rates and the intraparticle diffusion coefficients.

Sorbents - Performance, and Characterization

Data from EPA, EPRI, and DoE indicated that the reactivity of sorbents was related as follows: 1) dolomitic type sorbents [e.g., $MgCa(CO_3)_2$] are better than calcitic [e.g., $CaCO_3$]; 2) hydrates [e.g., $Ca(OH)_2$] are better than carbonates [e.g., $CaCO_3$] for the same type alkali; 3) limestone [$CaCO_3$] alone is not likely to achieve LIMB performance goals; and 4) the unreactive magnesium (Mg) component of dolomite imposes an additional mass requirement that is not justified by current capture differential over calcitic materials. A number of issues relative to sorbents, which are unresolved at this time and require further work, are discussed below.

For sorbents the key technical and economic issue is the extent of calcium utilization. During the conference the reported range of utilization was from about 10 to 64%, depending on sorbent characteristics, system scale, and operating conditions. Many participants indicated that a calcium to sulfur ratio (Ca/S) of 2 was a likely maximum from the standpoint of solids loading and sorbent economics; however, for certain conditions (e.g., low sulfur coal) a Ca/S = 3 to 4 might be considered. For 50% capture this requires a utilization of 25% at a Ca/S = 2. Mass loading, total sorbent cost, and waste disposal cost all decrease as the utilization increases. The closest thing to unanimity of opinion was that R&D should concentrate on increased utilization with 50% as a suggested goal. While the results reported show promise for improving utilization, further effort is required in three aspects discussed below.

Surface area development and preservation. This is a key to the reactivity of conventional sorbents. There is generally a good correlation between reactivity and surface area for a given class of sorbents, however, differences are observed between investigators when type is changed (e.g., $CaCO_3$ to $CaOH_2$). To date, a limited number of sorbents have been evaluated by any one investigator and, although overlap exists, different investigators have used different sources of similar type sorbents. One problem may be that a larger data base of sorbents characterized in a single facility is required. This should include characterization of activation and deactivation of a wide range of experimental and commercial materials including carbonates, hydrates, and oxides of both calcitic and dolomitic materials. Further investigation of production techniques is also required. Specific points are as follows:

1. Surface area needs to be determined for both the starting material and the sorbent activated under a range of conditions. In addition to surface area more emphasis on pore size distribution should be considered.

2. The kinetics of calcination/dehydration/sintering need to be characterized for high temperature and short time typical of boiler injection of sorbents.

3. The effect of precalcination of limestone to calcium oxide on reaction in the furnace and needs to be examined more thoroughly. Additional process aspects of calcination to produce high surface areas require further work.

4. The effects of hydration conditions on sorbent properties should be emphasized especially for calcitic materials. The effects of initial lime properties on hydrate characteristics and the differences between atmospheric and pressure hydrates must be quantified.

Role of promoters. The use of relatively small quantities of minerals (e.g., sodium compounds) to increase the activity of conventional sorbents for in-furnace SO_2 removal was discussed predominately by EPA inhouse and contract researchers. There was considerable interest in this development; however, a better understanding of several aspects is necessary to assess its applicability to practical systems, including the following:

1. The mechanism of the promotion of reactivity must be established. Current data suggest that different mechanisms may exist for different classes of promoters. The speculations include: modification of ionic diffusion in the particle product layer; fluxing of the surface, leading to faster liquid phase diffusion; stabilization of surface area; and catalysis of SO_2 to SO_3.

2. The optimum conditions for promoter/sorbent contacting must be established. The possibilities include: injection together or separately; injection of the promoter at a higher temperature than the sorbent; avoidance of scavenging of the promoter by fly ash; and incorporation of the promoter in the sorbent at the time of production (e.g., hydration).

3. The interaction of a promoter with the sorbent surface area needs to be understood. The early data with chromium oxide suggested substantial promotion of limestone reactivity and high sorbent utilizations. This occurred even at thermal conditions where measurements of the same sorbent without promoters showed very low surface areas. There are also small scale data that suggest that sodium promoters actually decrease surface area yet increase reactivity. For high surface area sorbents (e.g., hydrates), conditions expected to preserve surface area appear to be beneficial.

4. The role of magnesium in dolomitic sorbents still needs to be established. Its role may be attributable to mechanisms similar to those discussed above, but physical mixtures of $MgCO_3$ and $CaCO_3$ do not show a promotion of SO_2 reactivity.

Sorbent fundamentals. The body of evidence to date does not show a clear relationship between the properties of different starting material (e.g., limestone petrography) and the characteristics (e.g., surface area) of the resultant calcine under comparable conditions. A continuing effort to identify a first principles relationship is necessary. In the absence of such a correlation, a uniform procedure for screening new materials needs to be established.

Injection Technique

There was also general agreement that good mixing of the sorbent with the combustion gases is essential to good SO_2 capture. Most of the investigators concluded that upper furnace injection was superior to injection through the burner; however, there was one important exception discussed later. In addition, there was general agreement that this area needs more attention in the R&D and field application programs.

Any sorbent injection technique must produce rapid and uniform mixing of the sorbent with the combustion gases. Injection through or around the burner is ideal from a mixing standpoint; however, it has the disadvantage of sorbent deactivation due to high temperature and/or ash interactions. Downstream injection solves most of the deactivation problems but requires more attention to injector design location to achieve good mixing and high reactivity. It should be noted that different sorbent types (e.g., high surface area versus promoted materials) may require different injection approaches.

Most of the data presented indicated that injection downstream of the burner gave improved SO_2 capture efficiency. This appeared to be consistent both for small systems, where mixing is not a major constraint, and for larger scale systems [e.g., EPA's large watertube simulator (LWS) firing at 30 MWt] where injection design and sorbent mixing is more of a factor. The exception to this was the Foster Wheeler/Conoco data from a prototype scale experimental facility and an industrial boiler which appeared to show improved capture with a proprietary "inburner" injection scheme using a limestone sorbent. In should be noted that, for a number of burners tested in the LWS, the burner design appeared to have only a minor effect on sulfur capture for sorbent injection at the same location (e.g., with the fuel or the tertiary air). Sorbent type and injection location had larger effects. Further work is planned to evaluate additional burning zone and upper furnace injection configurations; however, the conclusion at this point is that the design of the low NO_x burner is not the critical element in determining the SO_2 capture achieved.

Most boiler applications of sorbent injection appear to be moving toward downstream sorbent injection. There are a number of issues which remain to be solved, including:

1. Injection and mixing systems or approaches must be identified which give satisfactory distribution of the sorbent into the combustion gases at the proper location in the boiler. This must take into account the gas flow and temperature stratifications which occur in practical boilers and provide for mixing over large cross sections.

2. Once the sorbent and carrier fluid are injected, the interaction and subsequent mixing with combustion gases and simultaneous calcination/dehydration of the sorbent must be quantified. Critical loss of sorbent reactivity can occur during this transition period.

3. The thermal impact of the carrier fluid on boiler operation must be assessed. If a significant percentage (i.e., 10-15%) of the boiler gas flow must be used to inject the sorbent, the impact on thermal efficiency will be significant. Techniques must be developed which minimize this effect.

4. The access to the boiler in the desired location may be limited by physical factors, which is a boiler and site specific variable. Techniques must be developed to accommodate design limits identified in process analysis studies.

Impact of Sorbent on Boiler and ESP Operation

As previously mentioned there is a limit on the incremental solids loading which can be passed through the boiler and electrostatic precipitator (ESP). The solids loading governs a number of potential problems including slagging, fouling, erosion, convective pass and air heater plugging, ESP performance, and waste handling and disposal. Many of these subjects were discussed in technical presentations and were a major topic of the panel discussion. Specific topics which must be addressed are:

1. The presence of calcium alone can impact the slagging and fouling tendency of the boiler. Most evidence suggested that deposits during sorbent injection were heavier than conventional ash deposition but were also easier to remove with soot blowers.

2. The effect of sodium (e.g., used as a sorbent promoter) on ash characteristics produced conflicting statements. It is well known that coals (especially lignite and subbituminous) which contain significant amounts of inherent sodium have strong slagging and fouling tendencies. The main boiler effect is in fouling where sodium volatilized during coal combustion subsequently deposits as a liquid layer on convective tube surfaces and promotes accumulation of fly ash deposits. It is also well known that the addition of calcium may beneficially raise ash fusion temperature and decrease fouling tendencies. Data for a sodium containing subbituminous coal shows a reduction in ash bonding strength from 30 (very strong) to 8 (easily removable) by the addition of calcium carbonate. However, there were also concerns that addition of a small amount of sodium as a promoter to a calcium based sorbent will significantly increase slagging and fouling. This apparent inconsistency needs to be resolved.

3. The presentations suggested that furnace heat transfer could be adversely affected in two ways. The most straightforward effect was decreased heat transfer due to deposits on heat transfer surfaces. It also indicated that the deposits could be controlled and heat flux maintained by soot blowing. The second effect is that in a larger boiler (e.g., >300 MWe) the increased solids loading may decrease radiant heat transfer to the water walls and thereby increase exit gas temperature. It should be noted that the European boilers, especially lignite and brown coal fired, for which the data were available have larger furnace volumes than most U.S. boilers of comparable capacity. This may suggest that the effect, if it occurs,

might occur at a larger boiler size in the U.S. Heat transfer measurement and modelling of the Weiher III boiler in Germany (FRG) may provide some insight on this.

4. The increased solids loading, increased ash resistivity, and possible shift in particle size distribution can all impact the performance of the ESP. Since increasing the specific collector area (SCA) of an existing ESP is difficult, other solutions were examined. Bench scale data suggest that the resistivity question can be resolved either with SO_3 conditioning or with humidification of the flue gas. The Conoco presentation suggested that humidification plus pulsed power could restore the performance of a marginal size ESP at the industrial boiler. The EPA program provides for pilot scale ESP testing of these conditioning options alone or in connection with retrofittable hardware (e.g., prechargers). This approach applies existing technology to the solution of LIMB particulate problems and does not involve developing new ESP technology.

5. Finally, the data indicated a near total removal of SO_3 from the flue gas which has two effects. First, it can lower the effective particulate loading in the stack by eliminating the particulate sulfate component. Second, it may allow some cold end heat recovery which would tend to increase system efficiency according to an EPRI analysis.

Waste Disposal

In the past the disposal of waste material has received limited consideration due to the undefined nature of the product from sorbent injection into a boiler. During the conference, major concern was expressed concerning the fate and handling of the unreacted CaO in the waste. A particular concern was the high levels of alkalinity observed during recent tests (e.g., Conoco). In addition solubility of the waste was raised as a problem particularly if sodium compounds were present. Extensive treatment of the waste would adversely affect the economics of the process, if it were required. It should be noted that this is directly related to the efforts to improve sorbent performance, since increased sorbent utilization automatically reduces both the mass of sorbent and the amount of free CaO in the waste.

The LIMB program is considering waste disposal and/or utilization as a part of the engineering analysis activity. Emphasis is being placed on recycle of unreacted sorbent to improve utilization in the boiler and on post collection utilization of the material to achieve a byproduct credit. Preliminary cost analysis indicates that simply eliminating disposal expense, which was assumed to be equivalent to that for fly ash, has significant economic benefits. Additional effort will be devoted to technical and economic aspects of disposal, recycle, and/or utilization of the unreacted CaO.

Economic Analysis

While some preliminary economic analyses have been conducted on LIMB and its comparison to FGD, there are uncertainties which are unavoidable at this stage of development of the technology. The process requirements are not completely defined and, even when they are, site specific factors may play a dominant role in any given application. In addition, many of the R&D issues cited above (e.g., utilization, waste disposal) may have significant positive or negative impacts. For these reasons decision on the future of the technology can not be made based on cost analyses until R&D and several actual boiler applications are completed.

Applicability of LIMB

The extent of applicability of LIMB was raised at the panel discussion. The answer to the question is dependent on both policy and technical questions which are not resolved at this time. It is well known that the extent of control of SO_2 has been debated over a wide range of tonnage (5 to 12 million TPY), and a mandate of FGD for some number of the largest sources has been proposed in at least one bill. It is unknown whether a bubble approach for a system or an individual unit basis will be allowed. The issue of an NO_x offset is not settled. All of these factors will effect the efficiency required for retrofit SO_2 control technology. In addition, it is not known whether a low sulfur coal switching strategy, which is potentially attractive for moderate SO_2 control (i.e., 50%), is a socioeconomically acceptable or logistically possible (e.g., railroad capacity) alternative. Finally, the current rapidly evolving state of development of LIMB does not allow an authoritative evaluation of its practical and economic viability.

Based on current analysis of cost, there are a number of factors which impact the relative cost of LIMB at 50-60% SO_2 control versus FGD at 70-90%. These differences are caused by the fact that LIMB is an operating cost driven technology while FGD is driven more by capital cost. The EPA inhouse computer model indicates that the dominant factors are: 1) sorbent utilization efficiency; 2) sorbent cost; 3) remaining useful boiler life; 4) capacity factor; and 5) coal sulfur content. For constant values of the first two items, LIMB is favored by shorter boiler life (15 years or less); lower boiler load factor (less than 62%); and for lower sulfur coal (less than 2.5%). However, in the final analysis the technical and economic applicability of LIMB can not be definitized until one or more successful demonstrations are completed.

LIMB PROGRAM RESEARCH AND DEVELOPMENT PLANS

This section discusses the R&D plans for each of the four major program areas discussed in the program description above. This R&D covers most of the unresolved issues identified in the discussion of technical status.

Generic R&D

The LIMB program has been based on the fact that a complete understanding of the process is necessary to give the maximum probability of successful commercialization by the private sector. Generic R&D is relatively independent of the hardware-specific constraints of practical boilers and provides information essential for application of LIMB to all boiler designs. This section provides a brief description of the current status, followed by a detailed discussion of plans for FY85 and following years.

Current Status. The R&D has provided an excellent insight on the effects of critical process parameters on SO_2 capture. It has shown how these parameters affect sorbent activation and subsequent sulfur capture as a function of combustion system conditions. It has also provided an understanding of fly ash/sorbent mixture characteristics as related to particulate capture. As a result of these findings, it has been concluded that limestone alone will not achieve the LIMB sulfur capture goals for many units in the U.S. boiler population. However, it has also provided at least two alternate sorbent approaches capable of meeting or substantially exceeding the goal of 50-60 percent capture. These approaches, which are high surface area sorbents and promoters to enhance sorbent activity, are discussed below:

Major Generic R&D Areas. The continuing small-scale R&D needs are divided into three major areas:

1. Inhouse research has identified high surface area sorbents as a key factor in obtaining high efficiency sulfur capture. It has been shown that high surface area can be generated external to the combustion process and/or after injection into the boiler. These materials, which are processed limestone (e.g., hydrates), have shown the potential for sulfur capture in excess of 70 percent. The planned R&D addresses methods for obtaining high surface area sorbents, for optimizing reaction conditions to achieve maximum capture, and for minimizing sorbent costs.

2. Another key factor is the interaction of sorbents with mineral matter which can either enhance or degrade the sorbent reactivity. The most promising results indicate that it may be possible to add small amounts of relatively inexpensive, innocuous promoters (mineral compounds) which will enhance the sorbent activity. Sulfur captures approaching those of high surface area sorbents have been achieved with promoted limestone in limited bench scale experiments. It also appears that promoters can significantly improve the performance of high surface area sorbents (e.g., hydrates). A significant effort is in progress to understand the enhancement mechanisms and to provide the basis for use in practical systems. A similar understanding is necessary for other sorbent/mineral matter interaction which can inhibit sulfur capture and which affect slagging, fouling, and collection characteristics of the particulate.

3. Process analysis has indicated substantial benefits may be derived from recycle of unreacted sorbent and promoters. In addition, utilization of the spent sorbent and fly ash has significant potential economic benefits. The engineering feasibility of these process options for recycle, utilization and/or disposal are being evaluated.

Prototype Testing

Extensive prototype testing of wall-fired boiler low-NO_x burners has been conducted to evaluate sulfur capture potential with injection of conventional sorbents. A substantial data base exists for both NO_x and SO_x control potential of a number of experimental and commercial burners. Any additional work will be in support of site specific decisions for the wall-fired demonstration.

The emphasis has been shifted to tangentially fired prototype systems and to use of improved sorbents, which are identified in generic R&D, for all systems. Tangential prototype work will be initiated in a large-scale experimental facility with a firing system producing a vortex flow field typical of that boiler class. In addition, a cooperative testing R&D program will be conducted on a small boiler (20-40 MW) to evaluate sulfur capture potential, operability, and reliability over short periods with fuel and sorbent flexibility. The prototype work will concentrate on evaluation of optimum sorbents and injection methods to maximize SO_2 capture and on effects of sorbent injection on boiler and particulate control system operability and reliability.

Wall-fired Demonstration

The contract for the wall-fired demonstration was awarded in September 1984, to Babcock & Wilcox Company. LIMB will be installed on a 105 MW single-wall-fired unit at the Edgewater #4 station of Ohio Edison Company. The final site specific design for the installation will be completed in February 1986. Long term testing over a 1 year period will begin in July 1987, and a report documenting the performance evaluation will be completed late in 1988.

Technology Generalization

For ultimate widespread use of the LIMB technology, the R&D results must be integrated with the full-scale boiler demonstration results to provide guidance for commercialization by the private sector. The program includes: 1) process analysis to evaluate applicability and economics for specific systems; and 2) process modelling to provide a methodology useful for site specific designs. The process analysis emphasizes LIMB system options for application to different boiler classes in the population and for minimizing the cost per unit SO_2 removal. The process modelling will provide component models for thermal history, sorbent activation and reaction, injection, and mixing.

SUMMARY

The LIMB R&D program has provided a detailed understanding of the key processes governing sulfur capture with sorbents. While it appears that limestone alone will not achieve program goals, several other promising sorbents have been identified. Based on the R&D results and cost estimates of the use of these sorbents, LIMB shows substantial promise as a SO_x and NO_x control technology for retrofit applications. The ongoing R&D program should resolve the remaining technical questions and provide a basis for widespread private sector commercialization.

REFERENCES

1. Acid Rain and Transported Air Pollutants: Implications for Public Polity (Washington, D.C.: U.S. Congress, Office of Technology Assessment, OTA-O-204, June 1984).

2. G. Blair Martin, J. H. Abbott, "EPA's LIMB R&D Program - Evolution, Status, and Plans." Presented at the EPA/EPRI First Joint Symposium on Dry SO_2 and Simultaneous SO_2/NO_x Control Technologies, San Diego, CA, November 13-15, 1984.

3. Proceedings of the EPA/EPRI First Joint Symposium on Dry SO_2 and Simultaneous SO_2/NO_x Control Technologies, San Diego, CA, November 13-15, 1984. To be published.

9a-3

EPRI'S RESEARCH PROGRAM ON FURNACE SORBENT INJECTION

M. McElroy
Electric Power Research Institute
Coal Combustion Systems Division
3412 Hillview Avenue
Palo Alto, CA 94303

ABSTRACT

The concept of injecting calcium-based alkaline sorbent materials directly into the furnace of coal-fired utility boilers to reduce SO_2 emissions is the subject of major research and development programs in the U.S. and abroad. EPRI is contributing to these efforts by sponsoring an experimental test program to develop an understanding of fundamental process chemistry and optimizing the process for maximum SO_2 removal and calcium utilization. Complementary EPRI projects are addressing engineering system design, economics, and power plant integration issues. These projects will provide the technical basis for designing and operating prototype furnace sorbent injection systems at 50 to 150 MW utility boilers which is the next logical step towards commercialization of the process.

INTRODUCTION

The furnace sorbent injection process is based on the injection of pulverized calcium sorbent materials, such as limestone or hydrated lime, directly into the furnace cavity of a coal-fired boiler. When exposed to furnace temperatures, the sorbent rapidly decomposes to form reactive lime particles, which capture SO_2 in suspension to form particles of calcium sulfate. The flue gases carry this calcium sulfate, along with any unreacted lime, out of the furnace, where the particulate control device collects them with fly ash. In essence, this process attempts to apply to pulverized coal-fired boilers an SO_2 control technique similar in overall chemistry to that used in fluidized-bed boilers.

EPRI is developing this technology because of its potential as a cheaper incremental SO_2 control approach for existing power plants. Evidence shows that the process can reduce SO_2 emissions by 50% or more in utility retrofit applications at significantly lower capital cost than conventional wet flue gas desulfurization systems. If successfully developed, this process would increase utility flexibility for complying with SO_2 control, especially in the event of new legislation regulating SO_2 emissions from older, currently uncontrolled power plants. The lower capacity factors and remaining lives of these plants typically favor a less capital intensive technology. In addition to potential retrofit applications, this process may be integrated with other supplemental controls in the future for an overall SO_2 control capability adequate to meet stricter requirements in new plants.

A number of development issues form the basis for EPRI's furnace sorbent injection R&D projects. SO_2 capture itself is a complex physical and chemical process that is influenced by a variety of factors: sorbent properties, boiler temperatures and residence times, sorbent mixing and dispersion within the furnace, and coal composition. The role that each of these variables plays in determining SO_2 removal must be understood before optimum process designs can be developed for the variety of site-specific utility applications. A major development issue in this regard is identifying an economical means to improve calcium utilization and thereby minimize the quantity of sorbent required. Currently, calcium utilization is relatively low (typically between 15% and 40%) which results in most of the sorbent passing through the boiler unreacted. Increased calcium utilization will further improve the economic advantages of the process since sorbent cost is a major factor effecting the total cost of application. Another issue is the potential impact the process will have on boiler and plant performance and operation which might include fouling, corrosion, slagging, problems of excessive particulate emissions, or increased waste management difficulties. A new unit can be designed to minimize such problems, but in retrofits they may be serious. Improved calcium utilization will minimize these effects.

These issues make the cost of commercial application somewhat uncertain. In addition to EPRI's technical goals, an important objective is to provide realistic cost estimates for utility boiler applications and to refine these estimates as the development efforts proceed.

PROCESS DEVELOPMENT

EPRI and Southern Company Services, Inc. are participating in a project (1) to develop the furnace sorbent injection process. The project consists of pilot scale tests complemented by international information exchanges, fundamental process modeling and bench-scale studies, and a conceptual design for a 50 MW retrofit application. A major task in the project is to understand the mechanisms that control sorbent utilization and to define methods for increasing sorbent reactivity and maximizing SO_2 removal. Therefore, a comprehensive analytic effort to characterize in detail the chemical and physical properties of fuels and raw and reacted sorbents is supporting the bench and pilot-scale experiments. Several prime contractors are providing the broad range of technical capabilities and research facilities required for this effort: Southern Research Institute; KVB, Inc.; Fossil Energy Research Corporation, and the International Flame Research Foundation.

To assess the relative performance of different types of commercial calcium sorbents, extensive pilot testing at scales of 0.5 and 1.0 x 10^6 Btu/h has been completed on 3% sulfur bituminous coal with two varieties of limestone (calcium carbonate), a conventional hydrated lime (calcium hydroxide), and a pressure-hydrated dolomitic lime (calcium and magnesium hydroxides). Limited comparative tests were also performed with dolomite (calcium and magnesium carbonate).

Figure 1 compares the performance of these sorbents in the 1.0 x 10^6 Btu/hr pilot test furnace (2). The SO_2 removals shown are representative of optimum values for each sorbent. For any given sorbent injection rate (as defined by the calcium-to-sulfur molar ratio, Ca/S) there is a considerable variation in SO_2 removal efficiency over the range of sorbent types tested. For example, at Ca/S = 2.0 the SO_2 removals vary from about 30% up to 80%. These removals correspond to calcium utilization efficiencies of 15% to 40%, relatively low compared to the calcium utilizations achieved with conventional flue gas desulfurization. It should also be noted that although increasingly higher

SO_2 removals can be achieved as Ca/S is increased, practical considerations of sorbent costs, boiler deposit rates, particulate emissions, and solid waste disposal will probably dictate a maximum value of Ca/S of between 2 to 3 in most full scale applications.

The hydroxides removed more SO_2 than the carbonates, and for both the hydroxides and carbonates, the dolomitic materials performed best. However, with the dolomitic sorbents, greater SO_2 removal may be offset by their lower calcium content. Because of the presence of inert magnesium in the dolomitic sorbents, the quantity (lb/h) of these sorbents necessary to capture a given amount of SO_2 is about the same as the quantity of non-dolomitic sorbent required to achieve a similar SO_2 removal. Although the magnesium does not itself remove SO_2, its presence appears to enhance calcium use.

The furnace gas temperature at the point of sorbent injection is the most important variable in determining how much of a given sorbent is used. As illustrated in Figure 2, a peak in SO_2 removal is evident for the various sorbents in a narrow temperature range between 1800°F and 2200°F (980°C - 1200°C). At higher temperatures, low SO_2 removal results from the reaction product's instability or the sorbent's rapid deactivation, caused by sintering. At temperatures below 1800°F (980°C), reactions are slower, and incomplete calcination may result in insufficient SO_2 capture in the reaction times available. The optimum temperature would typically occur in a furnace's upper radiant zone and leading convective sections. This makes the section above the flame zone and burner region the preferred injection site in most applications.

Another important parameter in governing SO_2 capture efficiency is the rate of change in flue gas temperature (the cooling or quench rates) after the point of sorbent injection. Tests are in progress to evaluate this effect over a range of quench rates between 100°F/s and 1100°F/s (38°C/s and 590°C/s), a range greater than that encountered in full-scale pulverized coal boilers.

Preliminary results show that SO_2 removal can decline significantly at the highest quench rates, an effect that appears to depend on the sorbent used. This phenomenon, together with the dependence on injection temperature previously noted, may influence sorbent selection for a given boiler. These factors also highlight the need for effective injection system designs that can deliver the sorbent to the proper temperature regions within the furnace and rapidly achieve good mixing with the flue gas in full-scale applications.

Pilot tests have also evaluated the importance of sorbent particle size and surface area of the raw sorbent prior to injection. A range of mean particle sizes from 0.75 to 35 μm in diameter has been examined by testing a wide array of manufactured and naturally occurring carbonate materials as illustrated in Figure 3. Although higher sorbent utilization was observed with smaller particle sizes, the effect was small over the range of commercially practical pulverization, indicating that extraordinary attempts to optimize SO_2 removal by finer sorbent particle production would likely provide a limited return. No clear correlation was found between sorbent utilization and preinjection sorbent surface area, which suggests that this parameter cannot be directly used to indicate sorbent reactivity.

To better understand the processes that occur during calcination and sulfation reactions, gas and solid samples were collected from a pilot-scale furnace when firing natural gas (2). The tests were conducted with natural gas to preclude any reactions with SO_2 and permit collection of sorbent and by-products without interference from fly ash. As a general rule, no significant differences have been observed in sorbent performance with coal or gas other than those attributable to temperature at the injection point. Properties of the sorbent injected into a gas-fired furnace are, therefore, expected to correspond to those with coal in the regions of interest away from the burner zone.

A major finding from these measurements has been the close correlation between calcium utilization and the surface area of the calcine sorbent (i.e., the surface area of the sorbent after calcination in the furnace). The correlation is shown in Figure 4. Sorbents and injection conditions that result in higher calcine surface area remove more SO_2. EPRI has initiated efforts to explore means of promoting higher calcine surface area and reactivity by external pretreatment of the sorbent. One approach involves thermal pretreatment of sorbents prior to furnace injection(3). Preliminary bench scale tests with pressure hydrated lime are inconclusive regarding enhanced SO_2 removal. EPRI is also evaluating the use of chemical promoters to increase the rate of SO_2 absorption on the surface of the sorbent particles.

Although this work is directed specifically toward application in pulverized coal-fired boilers, EPRI has begun a new cofunded project (4) with Babcock & Wilcox Co., Baltimore Gas & Electric Co., and Atlantic Electric Company to assess the applicability of furnace sorbent injection to cyclone boilers. This work will involve tests on a 6 x 10^6 Btu/h experimental furnace that has been equipped with a cyclone burner. Testing will demonstrate SO_2 removal with sorbents injected into the upper cavity of the main furnace (in a similar fashion as envisioned for a pulverized-coal boiler) where high thermal quench rates up to 1500 F/s (800 C/s) may represent a worst case for application. Another objective is to evaluate the impact of the process on convective tube surfaces by measuring fouling build-up rates, deposit cleanability, and heat transfer on a simulated convective tube array. Based on the test results, the engineering feasibility of retrofitting the process to a full-scale cyclone boiler will be assessed.

POWER PLANT INTEGRATION

Several process performance and plant operating issues must ultimately be resolved before widespread application of the technology can be confidently considered. The sorbent utilization and SO_2 removal achieved in the laboratory must be demonstrated at full scale. Assuming that the required residence times exist at favorable temperatures, scale-up should be primarily a matter of achieving proper sorbent distribution and mixing in a large volume. Furnace mixing and disperion models being developed in connection with the furnace sorbent injection development program (1), and in a related NO_x control project(5), will establish design criteria for sorbent injectors that can eventually be applied at specific sites using information on a given furnace's temperature profiles and flow patterns.

Sorbent injection affects power plant operation by increasing the mass of solids passing through the boiler and changing the physical and chemical properties of the ash. These changes can affect furnace conditions, including slagging, fouling, and erosion, and can affect the operation of downstream particulate control and waste-handling equipment. In each case these problems may be more difficult to manage in retrofits than in new units where they could be accounted for from the start.

Early EPRI-sponsored laboratory tests conducted by Combustion Engineering (6) and more recent field trial experiences elsewhere have indicated that fouling, slagging, and erosion of heat transfer surfaces can in most cases be managed by conventional soot blowing, although increased numbers of blowers, careful placement, and modified operation may be required. The potential impacts and countermeasures are site specific, and full verification must await further operating experience at large scale.

To get a preliminary indication of the impacts on particulate control, fly ash size distribution and electrical properties have been measured in conjunction with pilot development testing (1). Results indicate that ash resistivity can increase two to three orders of magnitude during sorbent injection and that the concentration of submicron particles may also increase, depending on the sorbent used. Deterioration in electrostatic precipitator (ESP) performance and increased particulate emissions can be expected unless steps are taken to counteract these effects. Initial attempts to restore electrical resistivity by flue gas SO_3 conditioning suggest that this may be effective where minimal upgrading is required, but further work is required to identify optimum ESP improvement or conditioning systems for a given application.

Solid waste disposal is another area where furnace sorbent injection could require modified power plant design or operation. Increased quantities of solid waste that includes potentially alkaline leachate, exothermic reactions of unreacted lime with water, and the possible cementitious behavior of the waste when wet highlight the need for a detailed assessment of ash transportation, storage, and disposal practice. An evaluation of whether some of these properties might be beneficial for ash utilization is also necessary. Such assessments will be performed in a new project (7) under EPRI's Heat, Waste, and Water Management Program, which will consider the solid waste management of furnace sorbent injection and other emerging SO_2 control technologies.

PROTOTYPE FIELD EVALUATION

EPRI is currently working with government agencies, utility companies, and other interested groups to initiate prototype retrofit and test programs on several 50- to 150-MW coal-fired boilers. The major objectives of these prototype programs are to apply the results of process develoment projects described above to provide generic utility data on process design and performance and to resolve plant impact issues that cannot be fully addressed in the laboratory. Tests on units of this size are considered the next logical step in the development of the technology for commercial application.

EPRI participation in the prototypes and other complementary industry programs will be continued under a new research project (8) that supports testing and engineering design. The first prototype program is scheduled for Public Service Company of Indiana's (PSI) Wabash River generating station in Terre Haute, Indiana, on a 100 MW, wall-fired boiler equipped with an ESP. This site is an ideal test location for this program; the unit is small enough to permit economical evaluation of a number of sorbents, coals, and ESP upgrades, and is still typical of many boilers that would be candidates for retrofit SO_2 controls. In addition, the ESP is relatively small, which provides the opportunity to demonstrate the effectiveness of upgrade approaches in a very challenging and realistic environment. The major participants will include PSI, which will host the tests and provide overall management, the State of Indiana, coal companies, and EPRI. Other utility companies and interested groups, including sorbent suppliers and transportation companies, are also expected to participate. EPRI will be responsible for technical direction and funding for process design, and will also plan, manage, and fund all testing activities. The testing will include a 2-month preretrofit baseline test, scheduled for completion in early 1986, and a 1-1/2 year process optimization and long-term operational test program scheduled to begin in early 1987. The preliminary test plan calls for testing on two coals and two to three sorbents. The testing will include evaluation of SO_2 removal efficiency, boiler impacts, ESP upgrades (humidification, flue gas, SO_3 conditioning, and/or pulse energization), and alternative dry waste handling processes.

At the same time, EPRI is exploring participation in other furnace injection projects, where appropriate, to ensure that operational and other issues of concern to utilities can be fully addressed and that results from our development programs are available and incorporated. Two such projects are the 105-MW demonstration of the limestone injection multistage burner technology (9) planned by EPA and Ohio Edison Company, and the 650 MW trials of furnace sorbent injection (10) scheduled at the Homer City station jointly owned by Pennsylvania Electric Company and New York State Electric & Gas Corporation.

PROCESS ECONOMICS

The capital cost of retrofitting furnace sorbent injection to a coal-fired boiler has been estimated to be between $25/kW and $120/kW. The large range reflects the cost sensitivity to uncertainties associated with the unresolved commercialization issues. Levelized costs, estimated at between 5.0 and 12.0 mills/kWh, are influenced predominately by coal sulfur content and calcium utilization (which determine the quantity of sorbent required), the costs of sorbent, and solid waste disposal costs. The lower value of levelized cost is for burning 2% sulfur coal with minor power plant impacts ("easy" retrofit); the higher value corresponds to a "difficult" retrofit on a 4% sulfur coal.

Substantially lower process costs would be possible if improved sorbent utilization could be achieved at reasonable sorbent costs. Not only would sorbent consumption be less for an equivalent level of SO_2 removal, but smaller material handling requirements and lower solids loading in the boiler and downstream equipment would reduce the plant impacts and their associated costs. For this reason, the current development project emphasizes development of higher reactivity sorbents.

EPRI has recently initiated a new project (11) with Stearns-Catalytic Corporation to update the economic assessment and incorporate results from the latest process development activities. Additional cost estimates for advanced dry injection emission control systems, which combined furnace sorbent injection and other post-furnace dry injection technologies, are also planned.

REFERENCES

1. EPRI Research Project RP2533-1, "Dry Sorbent Emissions Control Process Development." Contractors: Southern Company Services, Southern Research Institute, KVB, Inc., Fossil Energy Research Corporation, others.

2. R. Beittel, et.al., "Studies of Sorbent Calcination and SO_2-Sorbent Reactions in a Pilot-Scale Furnace," in Proceedings: First Joint Symposium on Dry SO_2 and Simultaneous SO_2/NO_x Control Technologies, Volume 1, EPRI Report CS4178, July 1985.

3. L. J. Muzio, et.al., "Flow Reactor Study of Calcination and Sulfation" in Proceedings: First Joint Symposium on Dry SO_2 and Simultaneous SO_2/NO_x Control Technologies, Volume 1, EPRI Report CS4178, July 1985.

4. EPRI Research Project RP2533-5, "SO_2 Reduction by In-Furnace Sorbent Injection in Cyclone-Equipped Coal-Fired Boilers." Contractor: Babcock & Wilcox.

5. EPRI Research Project RP2154-6, "Overfire Air NO_x Control Design and Operating Guidelines." Contractor: KVB, Inc., Dynatech Corporation, Riley Stoker.

6. G. J. Goetz, et.al., "Fireside Consequences of Furnace Limestone Injection for SO_2 Capture" in Proceedings: First Joint Symposium on Dry SO_2 and Simultaneous SO_2/NO_x Control Technologies, Volume 2, EPRI Report CS4178, July 1985. EPRI Research Project RP899-2. Contractor: Combustion Engineering.

7. EPRI Research Project RP2708-1, "Advanced SO_2 Control Waste Management." Contractors: Battelle, Radian, Baker Engineers.

8 EPRI Research Project RP 2786-1, "Testing of Furnace Sorbent Injection for SO_2 Control on a 100 MW Utility Boiler." Contractors to be selected.

9. R. V. Hendriks, "EPA Wall-Fired LIMB Demonstration" in Proceedings: First Joint Symposium on Dry SO_2 and Simultaneous SO_2 $/NO_x$ Control Technologies, Volume 2, EPRI Report CS4178, July 1985.

10. D. W. Carey, et.al. "The Homer city Experience in Developing a LIMB Process for use with Coal Preparation" in Proceedings: First Joint Symposium on Dry SO_2 and Simultaneous SO_2/NO_x Control Technologies," Volume 2, EPRI Report CS4178, July 1985.

11. EPRI Research Project RP2533-4, "Economics of Furnace Sorbent Injection for SO_2 Emission Control." Contractor: Stearns Catalytic Corporation.

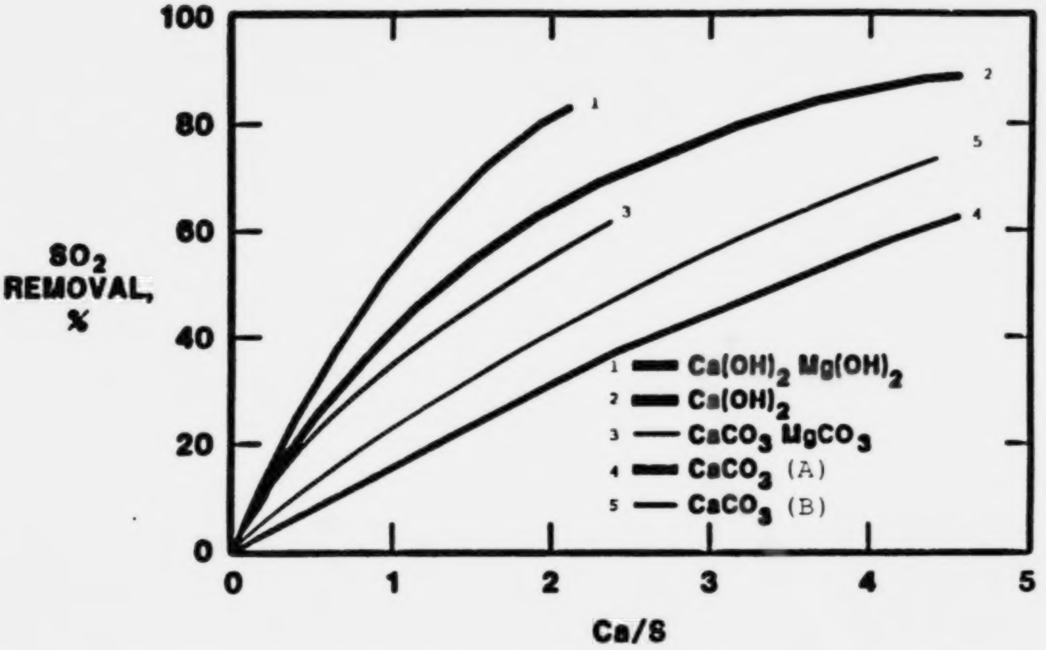

Figure 1. Pilot test data comparing SO_2 removal with four types of calcium sorbent under optimum sorbent injection conditions with 3.0% sulfur bituminous coal. Flue gas temperature at the point of injection was near 2200°F, corresponding to the thermal environment in the upper radiant zone of a coal-fired utility boiler.

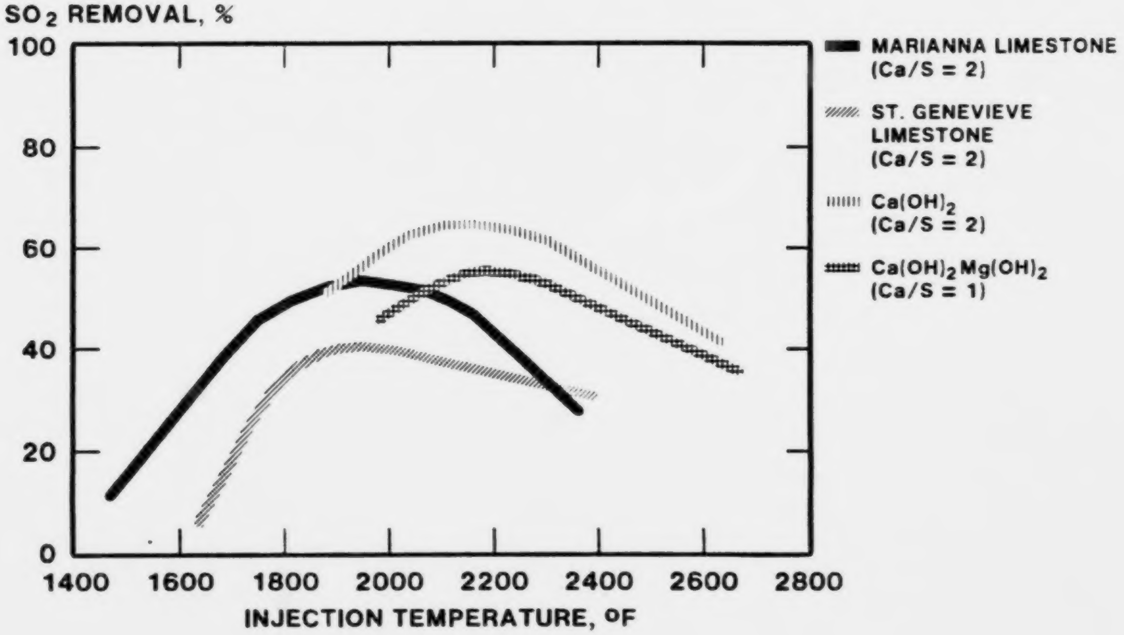

Figure 2. Pilot test data showing the influence of furnace temperature at the point of sorbent injection on SO_2 removal. The rate of temperature change after injection ("quench rate") is also important in determining SO_2 removal.

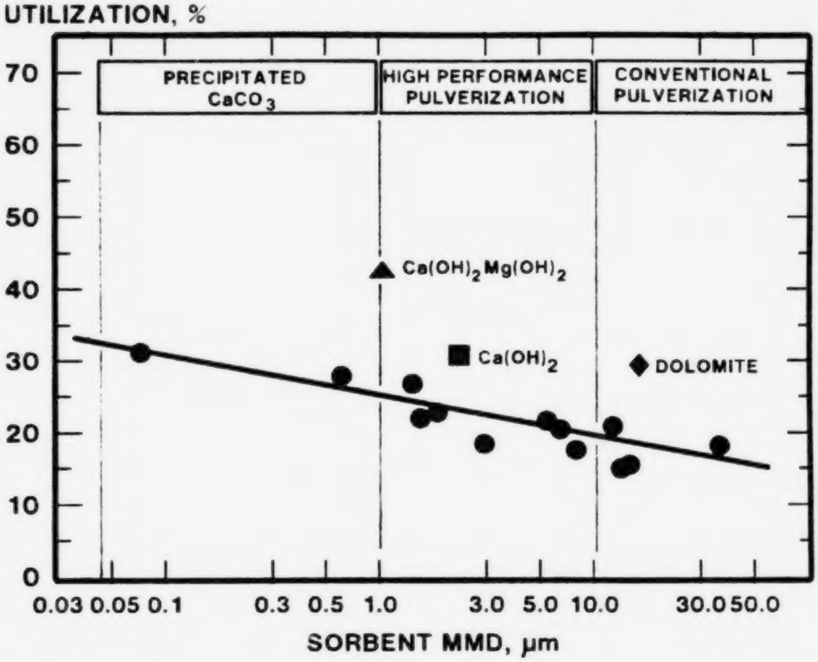

Figure 3. Calcium utilization versus mean particle size for calcium carbonate sorbents (solid circles) at Ca/S = 2. Sorbents were injected at close to optimum temperatures near 2200°F in a pilot scale combustor. Limited data for other sorbents shown indicate higher utilization compared to calcium carbonate at equivalent particle sizes.

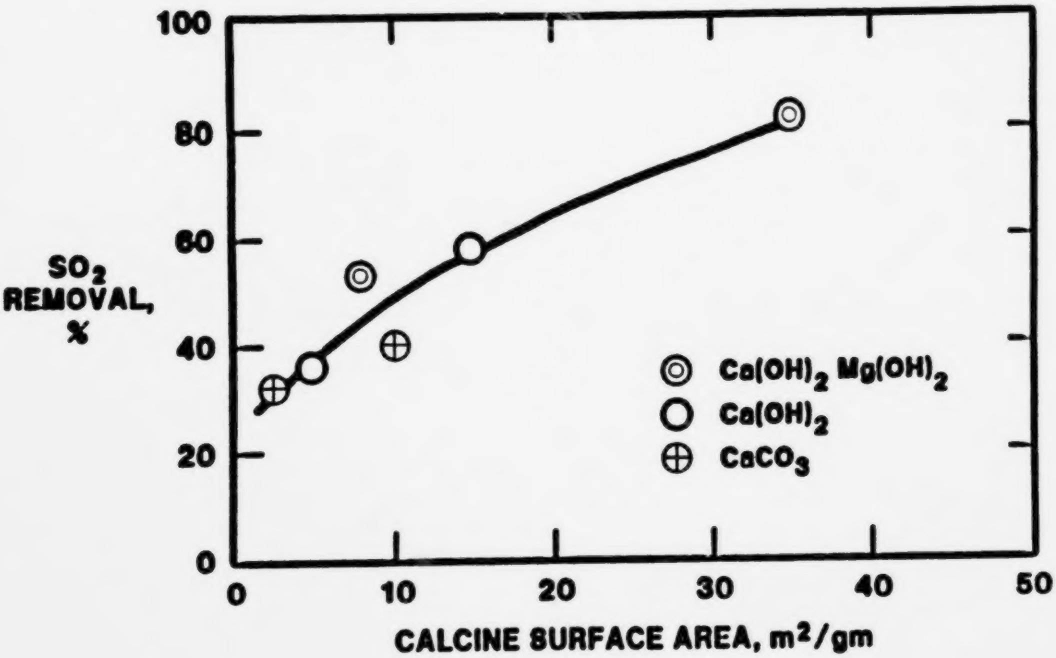

Figure 4. Calcium utilization versus calcine surface area for Ca/S = 2. The variation in surface area for each sorbent was achieved by injection at different locations in the pilot scale combustor: lowest surface area corresponds to burner injection; highest surface area corresponds to injection near optimum temperatures away from the burner zone.

Session IXb: Fuel and Combustion Modifications for Commercial/Industrial Boilers

Chairman, John Wasser, EPA

COMBUSTION MODIFICATION TECHNIQUES FOR COAL-FIRED STOKER BOILERS

G. C. Quartucy
H. J. Buening
R. J. Yang
KVB, Inc.
Engineering and Research Division
18006 Skypark Blvd.
Irvine, CA 92714

ABSTRACT

Combustion modification techniques were applied to full scale coal-fired stoker boilers for the purposes of optimizing boiler operation and reducing emissions. Five full scale stoker boilers of different designs were evaluated. Three of these (two spreader stoker and one vibrating grate stoker boilers) were fitted with flue gas recirculation for the purposes of reducing NO_x emissions and improving boiler efficiency. Test results showed that boiler efficiency improvement and NO_x reduction can be achieved with flue gas recirculation for spreader stoker boilers with intermediate or high minimum excess oxygen levels. Its application at mass-fed stoker boilers, which typically have very short combustion zones, and spreader stoker boilers with very low baseline excess oxygen levels (5 percent or lower) was not successful. NO_x emissions were found to decrease with decreasing excess oxygen levels for spreader stoker boilers, but relatively independent of excess oxygen levels for mass-fed stoker boilers. Overfire air system modifications to enhance jet penetration resulted in significant stack opacity reductions. Particulate emissions were found to be correlatable to the third power of bulk combustion product gas velocity (volumetric throughput rate divided by boiler cross-sectional area). This indicates that reductions in excess air level will result in not only efficiency improvement and NO_x reduction but also significant particulate emissions reductions.

INTRODUCTION

Although the research described in the paper has been funded primarily by the United States Envronmental Protection Agency through Contract 68-02-3166 to KVB, Inc., it has not been subjected to the Agency's peer review and therefore does not necessarily reflect the views of the Agency and no official endorsement should be inferred.

Field tests of five full-scale coal-fired stoker boilers have been made to evaluate the effect of combustion modifications in reducing NO_x emissions and improving boiler thermal efficiency. The combustion modification techniques evaluated included low excess air operation and flue gas recirculation to both the direct-fire air (DFA) and overfire air (OFA). Additional tests were run to evaluate the effectiveness of coal-sorbent pellets in reducing SO_2 emissions.

The results of the initial phase of this test program have been previously reported (Ref. 1). This report summarizes the results of the tests performed on each of the five full-scale boilers.

COAL-FIRED STOKER BOILERS

General Description

Mechanical stokers are designed to feed coal onto, and to remove the ash residue from, a stationary or moving grate in a furnace where coal combustion takes place. Combustion air is fed from underneath the grate through strategically sized and placed passages, called tuyeres, to the coal bed above the grate.

Unlike suspension mode combustion where the fuel is at all times intimately mixed and conveyed by the combustion air, burning coal particles in a stoker furnace are largely stationary except for the movement of the grate. Therefore, the combustion process is often termed "fixed bed combustion." Besides the combustion mode, the distinction between the combustion process in a stoker furnace and that of a suspension-fired furnace lies also in their in-furnace residence times. Mean residence times for fuel particles in a stoker furnace are typically on the order of hours while those under suspension mode combustion are on the order of seconds. As a result, the coal particle sizes in a stoker furnace are in the range of about 2.5 cm (1 inch) while those of pulverized coal are typically around 50 microns.

Combustion

Combustion in coal-fired stoker furnaces takes place in two separate zones. In the fuel bed, coal particles are devolatilized and burn as coal chars where diffusion and chemisorption of oxidants onto the char surfaces, as well as the reactions that lead to the release of carbon monoxide from the char surfaces are the dominant combustion mode. A significant amount of volatile matter is released and burned in the free board immediately above the fuel bed surface where a diffusion flame of gaseous/liquid fuels is the dominant combustion mode. The fuel bed supplies the necessary fuel for the above-bed diffusion flame zone which, in turn, sustains and stabilizes the char combustion in the fuel bed.

Ideally, as air is fed through the grate, a sufficient quantity of oxidant is in contact with all of the coal particles in the fuel bed. If the fuel bed becomes too thick or there are too many fines in the coal supply, adequate contact between air and coal can be disrupted when the air is forced to "channel" through the bed in individual passages. If the fuel bed becomes too thin, certain areas of the grate would offer virtually no flow resistance, allowing much of the air supply to pass through. This could leave the rest of the coal bed burning with inadequate amounts of oxidant.

Overfire Air System

Fuel/air mixing in the free board region of a stoker is inherently poor. Unlike pulverized coal burners, where flow velocity and flame zone aerodynamics can be manipulated by burner design, air flow velocities through the grate are constrained to low values (typically 5 m/sec or less) in order to maintain full fuel bed coverage. Moreover, combustion product gases evolving from the fuel bed generally flow vertically upward, with very little cross-stream mixing. As a result, soot formation in the free board immediately above the fuel bed can become a serious problem. The emission of soot is not only an environmental problem, it can also become the ultimate limiting factor on unit capacity for those stoker boilers not equipped with sophisticated particulate removal devices.

To alleviate these problems, many stoker boiler furnaces are equipped with banks of strategically placed overfire air (OFA) jets. The purposes of these jets are to provide an element of cross stream mixing over the fuel bed as well as to convey more oxidant to reduce soot formation.

The severity of the smoke problem depends on the type of stoker used. For mass fed stokers, coal feed is confined to one end of the furnace. Smoke control by OFA can be effective since the OFA jets only have to cover a limited distance within which the bulk of the coal volatile matter is released. In spreader stokers, the problem can be more severe. Not only is the volatile content of the coal released from the surface of the fuel bed, some of it is released during the flight of coal particles in the spreading process.

Stoker Classifications

Stokers are generally classified by the method of coal feeding and ash removal into four main groups: spreader stokers, traveling grate stokers, vibrating grate stokers, and underfeed stokers.

Spreader Stokers. The spreader stokers are designed to throw coal continuously onto a stationary or moving grate. Ideally, coal is fed uniformly onto the grate and the requirement of air would be the same everywhere on the grate. As a result, combustion air feed is not compartmentized. The coal volatile matter is released either from the coal particles in flight or from the fuel bed surface. A relatively uniform volatile matter combustion zone is established immediately above the fuel bed surface.

In actual practice, the coal is never truly evenly distributed. In fact, experience shows that a spreader stoker operates more smoothly if the coal is distributed more heavily to the rear of the grate so an intense initial combustion zone can be established.

Traveling Grate Stokers. Traveling grate stokers have moving grates in the form of continuous chains, driven by sprockets on a rotating shaft. Coal is fed from a hopper in the front of the grate and the depth of the fuel bed is controlled by an adjustable fuel grate. Since the intensity of combustion is not uniform along the length of the grate, the undergrate windbox is compartmentized to apportion the air feed according to local needs.

Fuel bed combustion stability is maintained by the intense combustion of volatile matter released in the front of the grate. Typically, OFA ports are installed to create high-intensity turbulance in this zone. Many traveling grate furnaces are constructed with a long rear arch, where a strong horizontal element is imparted to the combustion gas flow by furnace geometry and acts to stimulate mixing in the volatile matter combustion zone in the front of the grate.

Vibrating Grate Stokers. Vibrating grate stokers are largely water-cooled. They consist of a grate mounted on a grid of watertubes to provide positive cooling.

The entire structure is supported by a number of flexing plates which provide timely vibration that conveys the coal down the sloped grate. Vibration of the grate tends to keep the bed from forming clinkers, allowing these stokers to burn a wide variety of coals.

Underfeed Stokers. In underfeed stokers, coal is fed into the distillation zone, which is referred to as the retort and pushed upward by the plunger and auxiliary pusher blocks. Air is fed through tuyeres. Raw coal fed into the retort first travels through a gas distillation zone where volatile matter is distilled in the presence of ample air. As a result, the tendency to form soot in the free board is decreased. The distilled coal travels further upward into the coke burning zone where combustion is completed. Eventually, the coal ash travels to the edge of the grate and falls into the ash pit.

OPTIMIZATION OF COAL-FIRED STOKER PERFORMANCE

Coal-fired stoker boilers are a relatively simplistic and reliable means of converting the chemical energy of solid fuels into thermal energy. They do, however, have some unique problems. In this section, the specific problems of coal-fired stoker boilers and the approaches taken to overcome these problems are described.

High Excess Air Requirement

Coal-fired stokers are typically fired with excess air levels far beyond those required for suspension mode combustion. Operation of stoker boilers at 10 percent excess O_2 is rather common. The most harmful effect of high excess air operation is the reduction of boiler efficiency, due to increased dry gas heat losses. Besides the effect of lowered efficiency, the high excess air requirement also tends to limit the maximum furnace capacity.

Causes of the high excess air requirement are several. First, clinker formation can be the result of excess air deficiency. Here, the excess air is a means of bed cooling. For coals with low ash fusion temperatures, massive clinker formation can be caused by the excessively high bed temperatures resulting from combustion with insufficient amounts of excess air. Secondly, high excess air is often required for soot formation suppression. In the free board combustion zone, cross-sectional mixing is poor. Even with OFA jets, smoke can be a problem if adequate excess oxygen is not available. For units with ineffective OFA coverage, high excess air is required to keep the stack opacity in line. Thirdly, distribution and combustion intensity of coal on the grate may not be uniform. Thus, to assure adequate air for combustion in areas with heavy coal coverage, the air supply becomes excessive in areas with light coal coverage. Fourth, under low load conditions, high excess air is needed to enhance combustion stability in a colder furnace. Also, to alleviate the opacity problems at low load, a higher ratio between OFA and DFA is necessary. This also leads to high excess air.

Besides these operational problems, high excess air would also likely lead to higher emissions of nitrogen oxides. The larger quantity of flue gas would also convey a greater amount of particulate matter out of the stack.

Of the problems that lead to the requirement of high excess air, clinker formation is probably the most severe and is likely the ultimate limiting factor on the required excess air level. In most coal-fired stokers, coal distribution and the OFA jet coverage can be improved by more judicial operation.

Flue Gas Recirculation

As described previously, clinker formation in coal-fired stoker boilers is primarily the result of high fuel bed temperatures. To prevent clinker formation, the conventional approach was to increase the amount of UFA so as to provide enough diluents in the fuel bed to prevent high bed temperature. This invariably led to increased stack flue gas losses and reduced boiler efficiency. To alleviate the clinker problems and to improve boiler performance, flue gas recirculation (FGR) was utilized for both the DFA and the OFA.

FGR systems were installed at three full-scale stoker boilers (test sites 1, 2 and 5) and evaluated. Two of these systems contained provisions to recirculate flue gas to the OFA. OFA flue gas recirculation was implemented to evaluate the possibility of replacing a portion of the air by flue gas in the OFA system to reduce further the excess air requirement. A typical stoker flue gas recirculation installation is shown schematically in Figure 1.

OFA Modifications for Smoke Control

Excessive smoke emission is one of the major problems of coal-fired stoker boilers. For spreader stokers, the problem is exacerbated by the fact that volatile matter is released into the free board almost uniformly across the fuel bed. Effective OFA arrangements are often precluded by the limitation of available space for installation. Also, many existing OFA systems are plagued by less-than-effective design in the aspects of jet aerodynamics. A study of jet aerodynamics (Ref. 1) showed that the optimum OFA jet nozzle diameter should be derived from the requirements of effective jet penetration and the minimizing of jet deflection.

The location of the OFA jets is also of critical importance to smoke suppression. Because of the strong bonding of the cyclic molecules that make up soot particles, it is very difficult to oxidize them to CO_2 once they are formed. Thus, it is important to supply as much OFA as possible to the active volatile matter combustion zone to suppress soot formation. OFA jets installed outside the active soot formation zone would have very limited utility.

TEST APPARATUS

Unit Descriptions

Five coal-fired stoker boilers were tested. These included two spreader stoker boilers, two traveling grate stoker boilers, and one vibrating grate stoker boiler. The specifications for these boilers are summarized in Table 1. Table 2 contains the composite analyses of the coal fired at each test site.

Emissions Sampling Instrumentation

Monitoring of the required gaseous and particulate emissions was performed with an EPA-furnished mobile laboratory. The monitoring capabilities are presented in

Table 3. Reference 2 contains a detailed description of the mobile emissions laboratory. Continuous gaseous emissions analyzers provided the capability for measurement of O_2, CO_2, NO_x, SO_2 and CO in the flue gas.

TEST RESULTS AND DISCUSSION

Operation and Efficiency

As mentioned previously, combustion in spreader stokers takes place in two separate zones - the fixed bed combustion zone and the free board volatile matter combustion zone. The major problems associated with these two zones are clinker formation and soot formation, respectively. For all five test sites, the volatile flame above the fuel bed was bright orange in color, indicating a sooty burnout of the volatile matter for all combustion conditions evaluated.

For the Site 1 boiler, an increase in efficiency was recorded as a result of the installation of flue gas recirculation. The gain in efficiency was mainly caused by the decreases in dry gas losses when the minimum excess oxygen level was reduced from 8.0 to 5.0 percent. It was found also that operating adjustments were important in obtaining optimum boiler performance. The operating adjustments included OFA adjustments, and adjustments to the individual coal stoker settings.

Flue gas recirculation was not found to be as successful for test sites 2 and 5. At test site 2, the flue gas recirculation system operated satisfactorily but did not provide an additional gain in thermal efficiency. This is due to the fact that minimum excess oxygen level for satisfactory combustion performance under the baseline conditions (without FGR) was as low as 4 percent. The incorporation of FGR did not result in additional lowering of the minimum oxygen level.

The potential gains in thermal efficiency and improved operation by incorporating the flue gas recirculation system for mass-fed stoker boilers were also evaluated at test site 5, a vibrating grate stoker boiler. Test results showed that the application of FGR was not satisfactory. Unlike spreader stoker boilers where combustion takes place throughout the length of the grate, mass-fed stoker boilers, such as the vibrating grate stoker boiler tested, typically have very short active combustion zones dictated by the location of the furnace arch which limits combustion to the front half of the grate as shown in Figure 2. The addition of flue gas to the direct fired air reduces the concentration of oxygen in the combustion air. This would cause the active combustion zone to lengthen. For spreader stoker boilers, this is of little consequence since the length required for the coal to burn out is much shorter than the total fuel bed length. For mass-fed stoker boilers, however, this effect becomes significant. Not only did it extend the active combustion zone beyond the furnace arch resulting in flame quenching and impingement of flame on the arch, but also combustion at the front portion of the active combustion zone became unstable.

The efficiency data for tests performed on the mass-fed stokers (Sites 3, 4 and 5) are presented in Table 4. During these tests, the efficiency was generally found to increase as the O_2 levels were decreased, provided that the boiler operating parameters were optimized in conjunction with decreasing the O_2 levels. Merely decreasing the excess O_2 levels did not always result in increased efficiency, as the decrease in dry gas losses was at least partially offset by an increase in losses due to carbon carryover. This can be clearly seen in the Site 4 data. At 60 percent load, reducing the O_2 level from 9.2 percent to 7.4 percent resulted in a decrease in operating efficiency. In comparison, a slight efficiency improvement was realized when decreasing the excess air for operation at an 80 percent load. In both cases, the reduction in excess air resulted in a significant increase in refuse combustibles content.

Similar trends are also evident in the Site 3 data, where lowering the O_2 alone provided an efficiency gain of about 2.5 percentage points. When low excess air operation was combined with optimized boiler operation, an efficiency improvement of nearly 5.7 percentage points was realized. The boiler operating parameters optimized included coal bed thickness, grate speed, and undergrate air compartment settings.

Due to the operating problems encountered with the Site 5 flue gas recirculation system, no efficiency data were obtained with the FGR system in service. The data presented in Table 4 show the effect of varying the excess air level for operation wtih FGR.

NO_x Emissions

The Site 1 and Site 2 NO_x emissions are plotted versus stack O_2 in Figures 3 and 4, respectively. The data show that the NO_x emissions levels were influenced primarily by furnace load and O_2 levels. Variations in the amount of overfire air and coal size distribution did not appear to have any significant effect on NO emissions. Figures 3 and 4 show that the O_2 levels played a dominant role in NO_x emissions. Apart from its effect in reducing O_2 levels, FGR did not appear to have any other effect on NO_x reduction. This can be seen in both Figures 3 and 4, which show that for operation at equivalent O_2 levels, NO_x emissions were not affected by the addition of recirculated flue gas. The data also show that furnace load had a significant effect on NO_x emissions.

The Site 3 and Site 4 NO_x emissions are plotted versus boiler exit O_2 in Figures 5 and 6, respectively. The data show that the NO_x emissions for these relatively small (15,900 kg/hr) mass-fed stoker boilers were not affected by either O_2 or load over the range of conditions tested. The absence of load effect on NO_x emissions from these units is most likely due to the relatively low furnace heat release rates and the high oxygen levels over which the tests were conducted. The data also show that the oxygen added above the minimum oxygen levels tested probably did not participate in the NO formation reactions, but acted only as a dilutent.

The Site 5 NO_x emissions are plotted versus boiler exit O_2 in Figure 7. These data show that at fixed load conditions, the NO_x emissions were found to increase with increasing oxygen levels. This effect, which was not seen during the Site 3 or 4 testing, is probably due to the relatively small firebox and corresponding increased volumetric heat release rate of the Site 5 boiler.

Opacity

Figure 8 shows the comparison between the stack opacity readings taken before and after the OFA modifications made to the Site 1 boiler as a function of load. The OFA modifications included increasing the jet nozzle size from 2.5 cm (1 inch) to 5.1 cm (2 inch), the addition of a third row of rear wall jets, flow control to the individual OFA jets as well as flue gas recirculation to the OFA. The data show that the opacity readings were reduced significantly following the OFA modifications. Since the load limit for this test boiler was imposed by opacity regulation, the data presented in Figure 8 also show a potential increase in boiler capacity of 50 percent made possible by the OFA modifications.

Particulate Emissions

Particulate data were obtained isokinetically at both the boiler exit and the stack during the Site 1 and Site 2 testing. The scatter of these data was sizeable, as expected for the data taking process on a full scale boiler where many input conditions can not be precisely controlled.

Even with the data scatter, a general functional relationship of particulate loading for the Site 1 testing can be discerned since an adequate number of data points were taken. Figure 9 is a plot of boiler exit particulate loading as a function of the total furnace throughput rates (combined total of the flow rates of coal, UFA, OFA and recirculated flue gas) or the average combustion gas velocity. From Figure 9, it appears that boiler exit particulate loadings, expressed in kilogram per hour units, can be correlated to the third power of the total throughput rate or the average combustion gas velocity.

Similar to those measured during the testing at Site 1, the Site 2 boiler exit particulate emissions expressed in terms of kilograms per hour were found to be proportional to the total boiler throughput (or average combustion gas velocity) raised to the third power. This relationship is shown in Figure 10, where the boiler exit particulate emissions are plotted versus the boiler average combustion gas velocity The higher relative loading for the Site 2 boiler is most likely due to the extremely high fines content in the coal supply.

Based on these data, it appears that a conclusion can be made that boiler exit particulate loadings from a spreader stoker are determined primarily by furnace throughput rates or the average combustion gas velocity, and not the furnace load.

SO_2 Emissions

SO_2 emissions are primarily dependent upon the fuel sulfur content, assuming complete combustion. The SO_2 emissions measured at Site 1 and Site 3 are plotted versus O_2 in Figure 11 and 12, respectively.

During the Site 1 testing, the measured concentrations of stack SO_2 indicated that the conversion of sulfur in the coal to SO_2 was nominally 82 percent. The measured SO_2 emissions were found to be independent of the excess oxygen levels. As shown in Figure 11, the SO_2 emissions were not affected by flue gas recirculation. The nominal 18 percent retention rate of coal sulfur in ash was higher than the 0-5 percent retention rate typically measured during pulverized coal firing.

During the tests run on the Site 3 boiler using the coal/coal-sorbent pellet mixtures, there was a measured reduction in SO_2 levels of approximately 20 percent as shown in Figure 12. The SO_2 reduction achieved on the subject test boiler appeared to be limited by incomplete combustion of the coal/coal sorbent pellet mixture. The pellets were hard to burn and produced a very smokey fire. The difficulty in burning the pellets is believed to be due to the method in which they were made. Because the pellets are made of tightly packed pulverized coal, they have a lower reactivity than the coal normally fired in the subject test boiler. The low reactivity of the coal-sorbent pellets caused combustion problems similar to those seen in the tests performed on the Site 5 boiler. Again, the flame front extended past the furnace arch toward the rear of the grate, producing unsatisfactory operating conditions. For these reasons, the testing with the coal-sorbent pellets was aborted, thereby providing only a very limited amount of information concerning their performance in the Site 3 boiler.

CONCLUSIONS

Based on the test results presented previously, the following conclusions can be made:

- Boiler efficiency improvements can be achieved with flue gas recirculation for spreader stoker boilers with high or intermediate oxygen levels. The application of flue gas recirculation to mass-fed stoker boilers, which typically have short combustion zones was not successful.

- In the spreader stoker boilers tested, NO_x emissions were dependent on the excess O_2 level and the unit steaming rate (load). The NO_x emissions were not affected by the use of flue gas recirculation.

- In the small mass-fed stokers tested, the NO_x emissions were relatively independent of the excess O_2 level and unit load. This is most likely due to the low design heat release rates of these units.

- Modifications of the overfire air system on a spreader stoker to improve jet penetration resulted in significant reductions in opacity.

- Particulate emissions from spreader stokers were found to correlate to the third power of the bulk combustion product gas velocity. This indicates that reductions in the excess air level can significantly reduce particulate and NO_x emissions, while increasing boiler efficiency.

- The use of coal-sorbent pellets to reduce SO_2 emissions provided reductions on the order of 20 percent. The pellets were not suitable for the subject test boiler, and resulted in several severe operating problems.

REFERENCES

1. Yang, R. J., "Application and Assessment of Combustion Modification Concepts for Full Scale Stoker Coal-Fired Boilers," KVB14-8850-1293, October 1981.
2. Tidona, R. J., et al., "Emissions from Refinery Heaters Equipped with Low-NO_x Burners," EPA-600/7-81-169, October 1981.

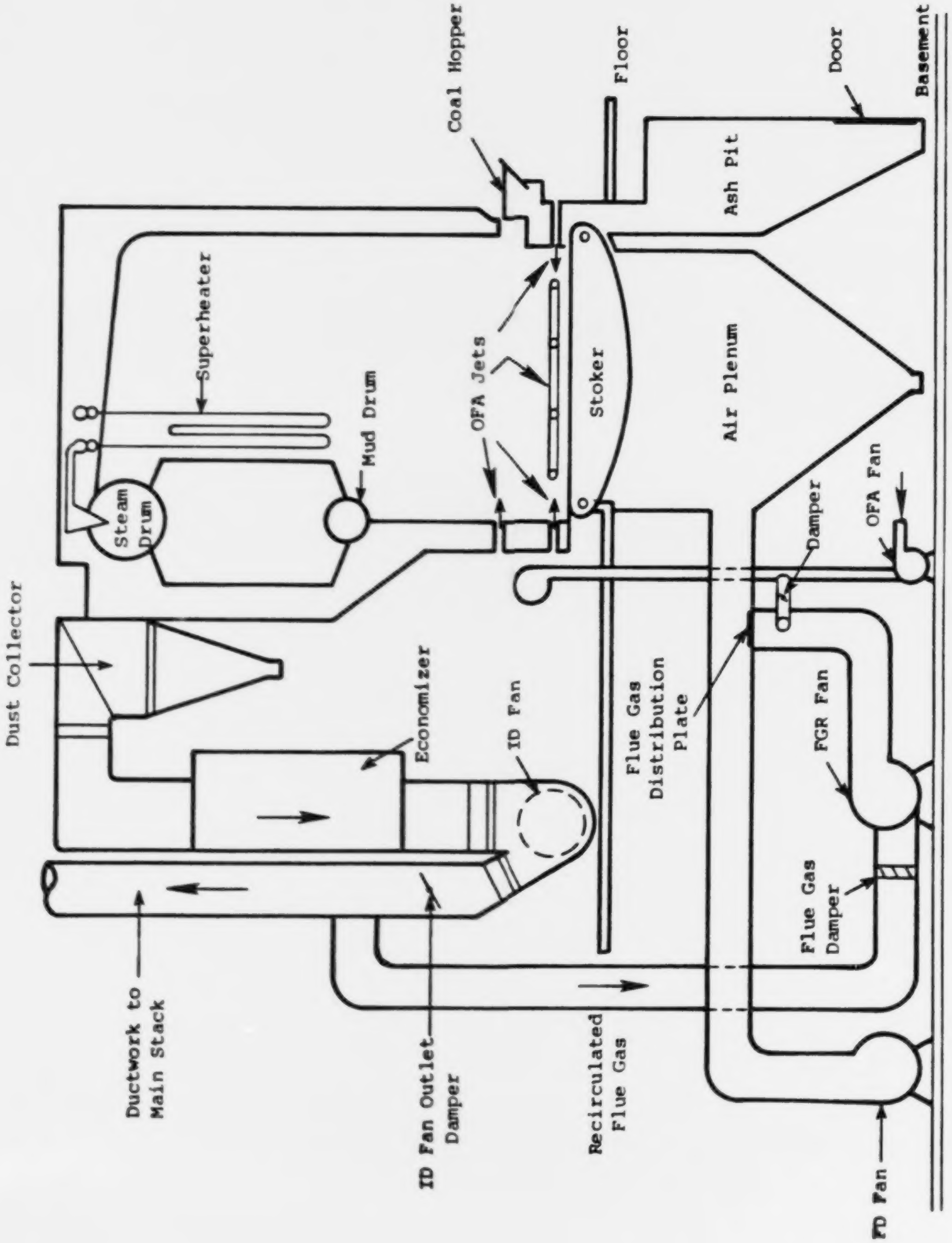

Coal Hopper
Floor
Door
Basement
Ash Pit
Superheater
OFA Jets
Stoker
Air Plenum
Mud Drum
Steam Drum
OFA Fan
Damper
Damper
Dust Collector
Economizer
ID Fan
Flue Gas Distribution Plate
FGR Fan
Flue Gas Damper
Ductwork to Main Stack
ID Fan Outlet Damper
Recirculated Flue Gas
FD Fan

Figure 1. Flue Gas Recirculation System

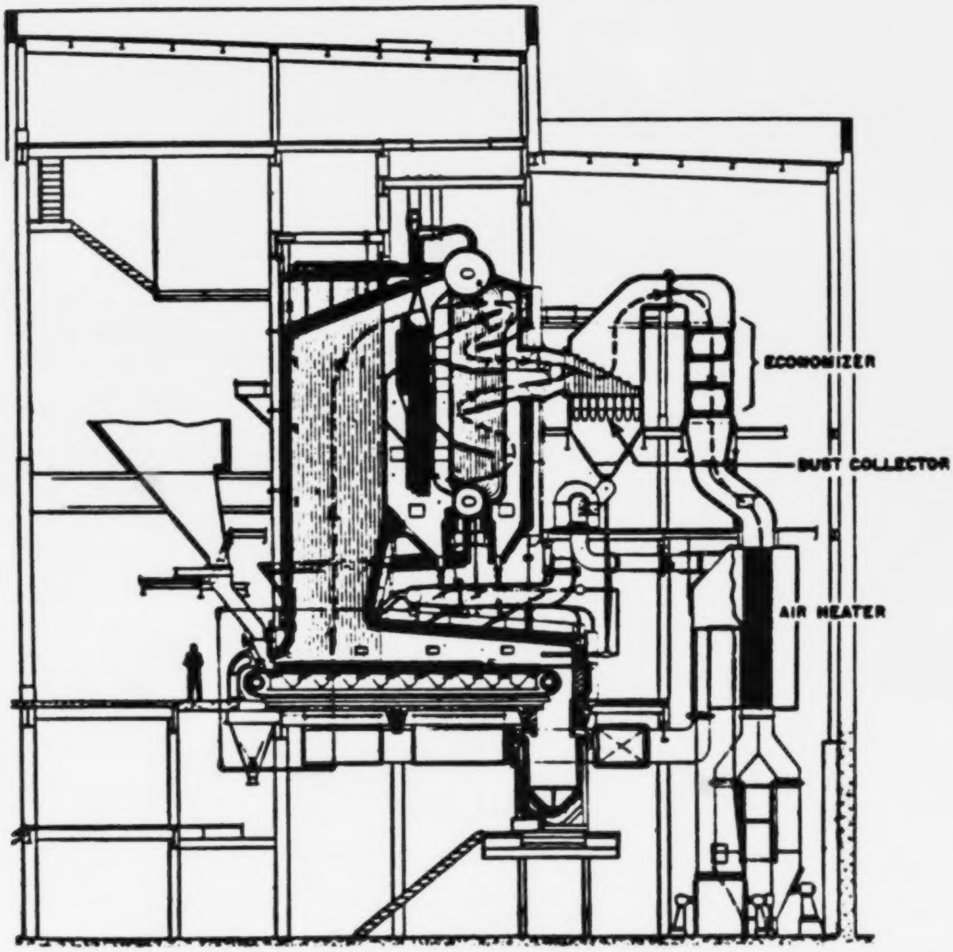
ECONOMIZER
DUST COLLECTOR
AIR HEATER

Figure 2. Side view of typical mass feed stoker showing size of active combustion zone.

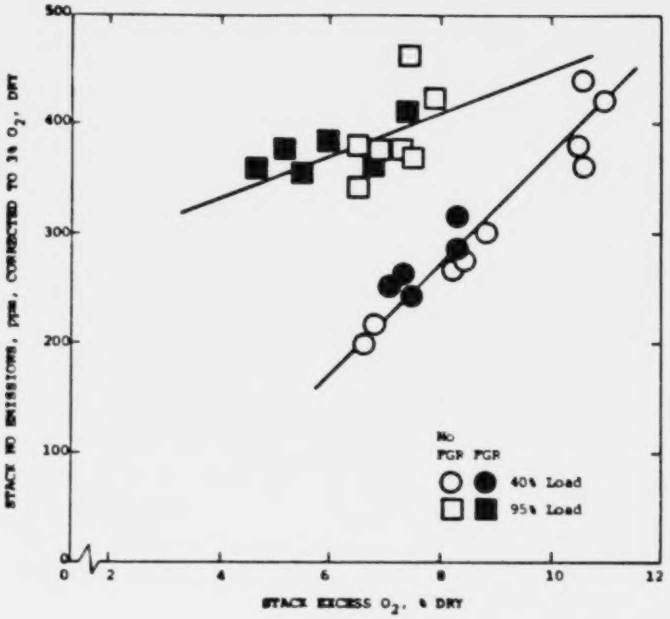

Figure 3. Stack NO emissions versus excess O_2, Site 1.

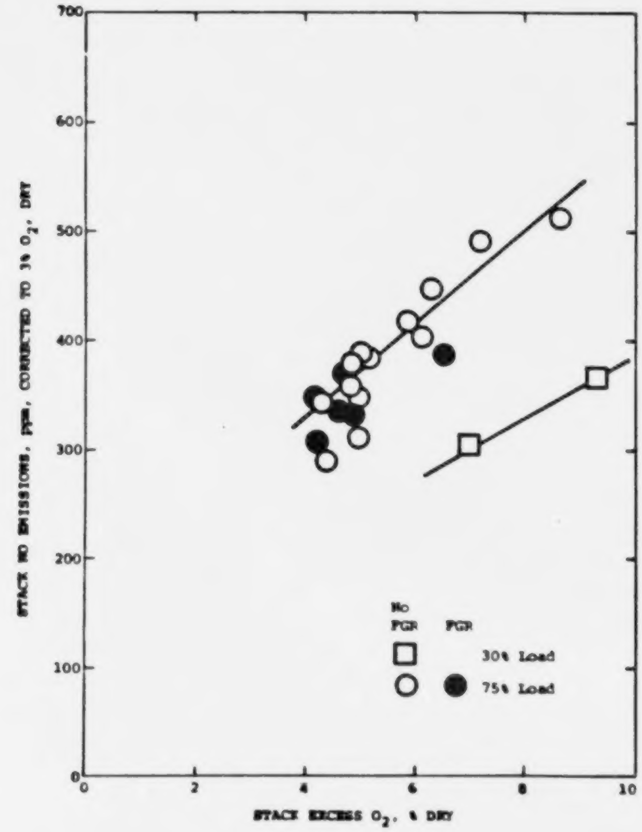

Figure 4. Stack NO emissions versus excess O_2, Site 2.

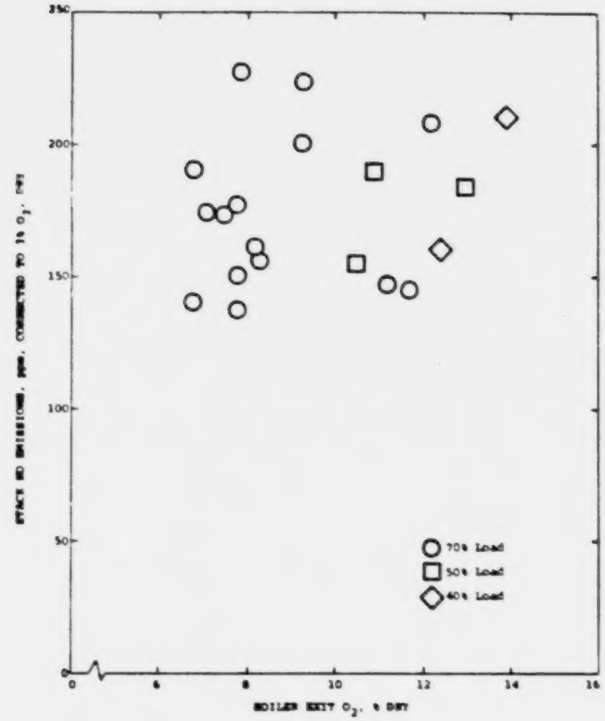

Figure 5. Stack NO emissions versus excess O_2, Site 3.

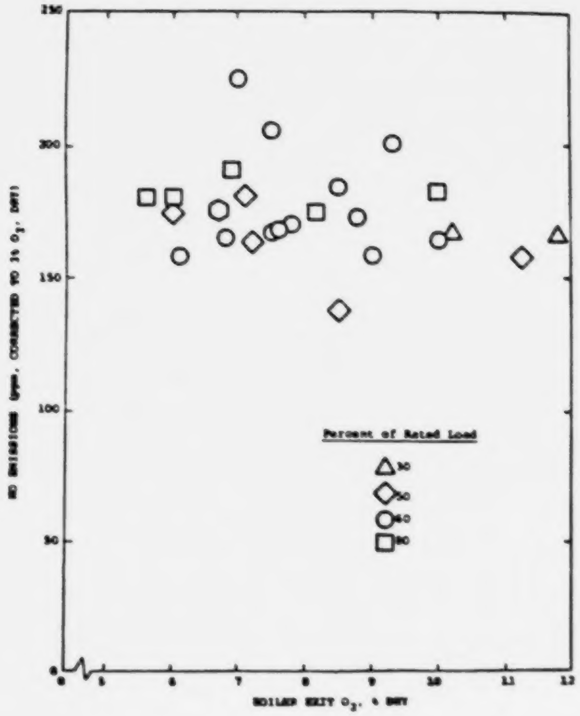

Figure 6. Stack NO emissions versus excess O_2, Site 4.

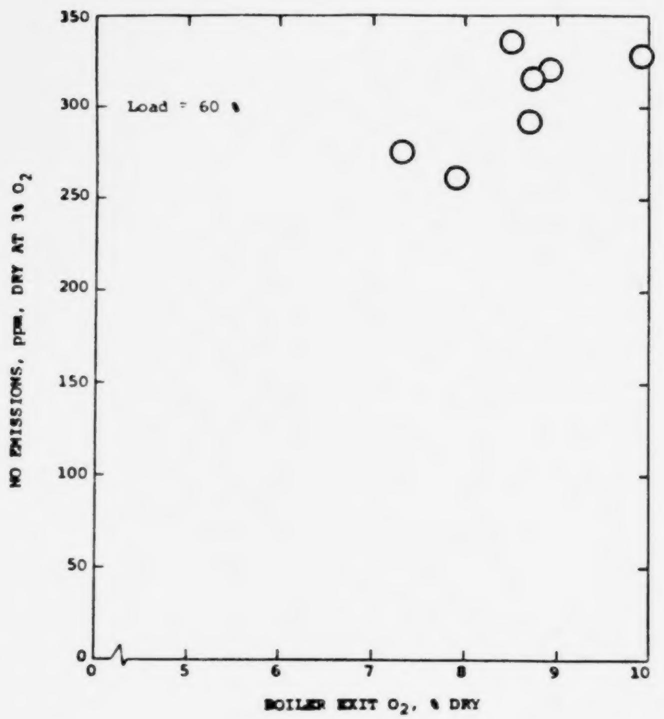

Figure 7. Stack NO emissions versus excess O_2, Site 5.

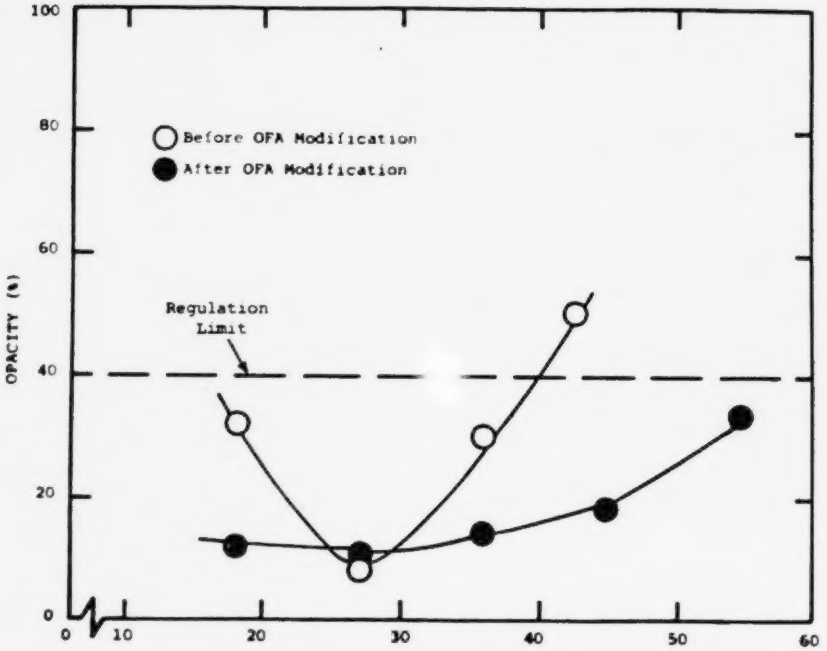

Figure 8. Opacity versus furnace load, Site 1, showing lowest measured opacity point at each load.

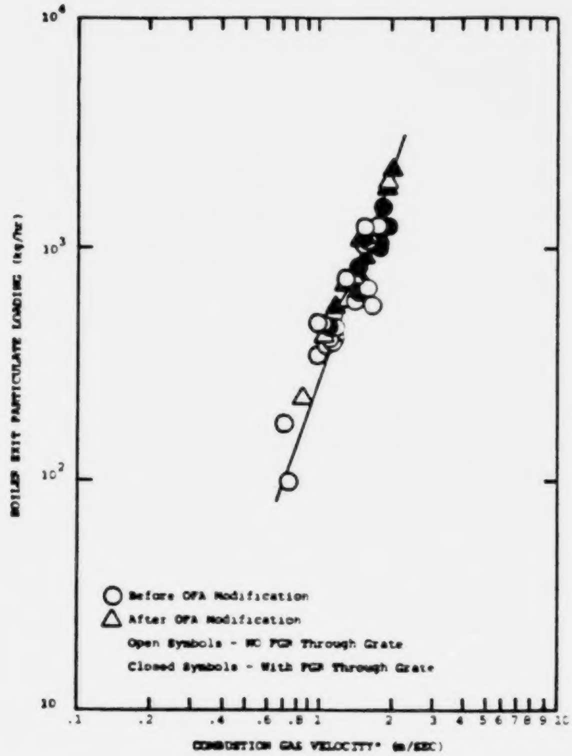

*Near-bed gas phase temperature assumed to be 1540°C

Figure 9. Boiler exit particulate loading versus combustion gas velocity, Site 1.

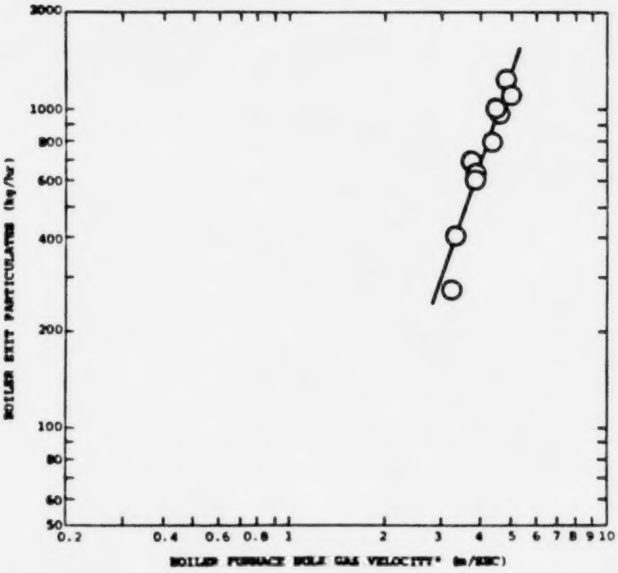

*Near-bed gas phase temperature assumed to be 1540°C

Figure 10. Boiler exit particulate emissions versus furnace bulk gas velocity, Site 2.

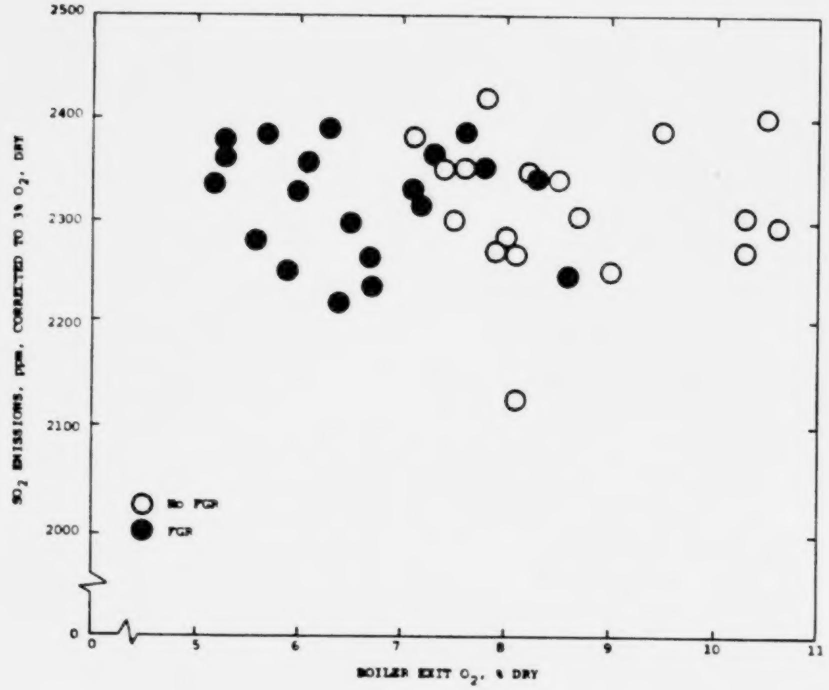

Figure 11. SO_2 emissions versus boiler exit O_2, Site 1.

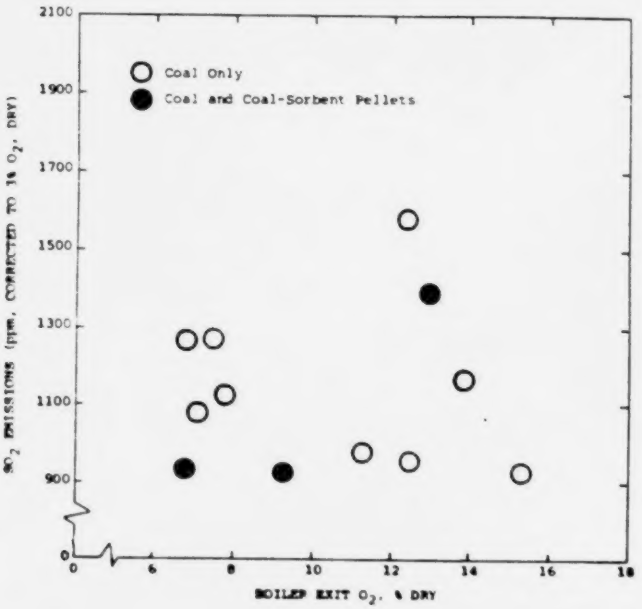

Figure 12. SO_2 emissions versus boiler exit O_2, Site 3.

Table 1

UNIT SPECIFICATIONS

	Site 1	Site 2	Site 3	Site 4	Site 5
Boiler					
Manufacturer	Babcock & Wilcox	Erie City Iron Works	E. Keeler Co.	E. Keeler Co.	E. Keeler Co.
Year Built	1952	1965	1948	1947	1961
Configuration	Multiple Pass	Multiple Pass	Single Pass	Single Pass	Single Pass
Rated Steaming Capacity, kg/hr	45,400	90,800	15,900	15,900	15,900
Design Pressure, kPa	4,805	4,805	1,724	1,724	1,724
Operating Pressure, kPa	4,222	4,481	1,207	1,207	1,207
Steam Temp, °C	382	385	188	188	188
Feedwater Temp, °C	149	149	116	116	116
Operating Air Temp	Ambient	Ambient	Ambient	Ambient	Ambient
Stoker					
Manufacturer	Westinghouse	Detroit Stoker	Coxe Stoker Engrg. Co.	Coxe Stoker Engrg. Co.	Detroit Stoker
Classification	Spreader Stoker	Spreader Stoker	Traveling Grate Stoker	Traveling Grate Stoker	Vibrating Grate Stoker
Effective Length, m	4.94	4.66	4.83	4.83	4.17
Width, m	4.04	6.52	3.26	3.26	2.61
Effective Grate Area, m^2	20.0	36.9	15.8	15.8	10.9
Heating Surfaces					
Furnace Volume, m^3	126	337	49	45	38
Boiler, m^2	131	1,533	409	409	-
Waterwalls, m^2	-	262	55	55	-
Economizer, m^2	483	994	NA	NA	NA
Heat Rate at Design Capacity					
Input to Furnace, MWt	39.3	79.1	13.5	13.5	13.5
Grate Heat Release, kWt/m^2	1,967	2,144	860	860	1,247
Furnace Liberation, kWt/m^3	314	235	280	301	355

Table 2

COAL ANALYSES

	Site 1	Site 2	Site 3	Site 4	Site 5	Coal-Sorbent Pellets
Proximate Analysis (wt %)						
Moisture	7.07	7.53	3.47	6.19	5.95	5.67
Volatile Matter	40.89	37.29	14.99	13.99	17.52	38.89
Fixed Carbon	43.63	45.92	61.81	59.99	61.03	30.13
Ash	8.41	9.27	19.74	19.84	15.50	25.31
Ultimate Analysis (wt %)						
Moisture	7.07	7.53	3.47	6.19	5.95	5.67
Carbon	67.37	66.93	67.81	66.26	69.92	56.54
Hydrogen	4.93	4.80	3.24	3.17	3.78	4.96
Nitrogen	1.34	0.72	1.00	1.06	1.21	1.06
Sulfur	3.27	2.95	1.15	1.03	1.35	2.66
Ash	8.41	9.27	19.74	19.84	15.50	14.33
Oxygen	7.62	7.82	3.55	2.38	2.21	3.78
Calcium	0	0	0	0	0	10.98
Heat of Combustion						
kJ/kg	28,491	28,115	26,918	25,786	28,005	21,373

Table 3

EMISSION MEASUREMENT INSTRUMENTATION

Species	Manufacturer	Measurement Method	Model No.
Oxygen	Teledyne	Polargraphic	326A
Carbon Dioxide	Beckman Instruments	IR Spectrometer	864
Nitrogen Oxides	Thermo Electron Co.	Chemiluminescent	10A
Sulfur Dioxide	DuPont Instruments	UV Spectrometer	400
Carbon Monoxide	Beckman Instruments	IR Spectrometer	865

Table 4

MASS FED STOKER BOILER EFFICIENCY CALCULATIONS

Date 1984	Site	Steam Flow 10^3 lb/hr	Flue Gas Temp., °F	O_2 %	Heat Losses Due to Dry Gas*	 H_2O*	 Refuse Combustibles	Efficiency %	Comments Load	 O_2
10/24	3	23.8	570	11.2	19.08	3.65	4.79	70.88	70%	nominal
10/24	3	25.2	540	8.2	12.48	3.61	8.94	73.36	70%	low
10/26	3	24.9	556	7.1	13.03	3.63	5.19	76.56	70%	low
7/18	4	20.7	581	9.2	15.88	4.03	4.88	73.41	60%	nominal
7/20	4	28.0	620	8.2	14.97	4.06	7.40	71.77	80%	nominal
7/20	4	20.3	562	7.4	12.08	3.97	8.99	73.16	60%	low
7/24	4	28.3	620	6.2	12.33	4.06	9.29	72.51	80%	low
7/27	5	20.5	582	8.7	14.98	4.24	4.44	74.54	60%	nominal
8/01	5	20.8	565	7.3	13.34	4.22	3.73	76.91	60%	low

---

* Units are percent of heat input

EMISSIONS ASSESSMENT OF
COAL-WATER-SLURRY-FIRED INDUSTRIAL BOILERS

L. R. Waterland, R. DeRosier, D. Van Buren, and H. B. Mason
Acurex Corporation
Energy & Environmental Division
555 Clyde Avenue
Mountain View, California 94039

ABSTRACT

This paper describes emission results obtained from field testing of two industrial boilers test-fired with coal-water slurries (CWS). Emission measurements performed included continuous monitoring of flue gas emissions; source assessment sampling system (SASS) sampling of the flue gas, with subsequent laboratory analysis of samples to obtain total flue gas organics in two boiling point ranges, compound category information within these ranges, specific quantitation of the semivolatile organic priority pollutants, and flue gas concentrations of 73 trace elements; EPA Method 5 sampling for particulate; EPA Method 8 sampling for SO_2 and SO_3 emissions; volatile organic sampling train (VOST) testing for volatile organic priority pollutant emissions; gas grab sampling for onsite C_1 to C_6 hydrocarbons emission measurements; gas grab sampling for N_2O emissions measurements; and grab sampling of the CWS fuel and ash streams for inorganic composition determination. Complete emissions measurement results for the two units are presented.

INTRODUCTION

Coal-water slurries have received attention in recent years as an alternative to oil fuels. CWS has the advantage of allowing certain oil-fired boilers to eliminate their oil fuel requirements at modest retrofit cost. Thus, CWS has the potential for application as a near-term technology for conversion of oil-burning facilities to coal firing and thereby offsetting high oil prices and frequently uncertain supply situations. This report presents the results of an emission assessment of a CWS-fired industrial boiler.

In this paper, results of field tests performed on two boilers firing CWS are discussed. The first set of tests (site 1) were performed at the Pittsburgh Energy Technology Center's (PETC) combustion test facility. This facility consists of a 3.0 kg/s steam (24,000 lb/hr) watertube boiler, an air-cooled steam condenser and deaerator, CWS preparation and storage facilities, and pollution control devices. The boiler is a package, two-drum "D"-type watertube originally designed by Nebraska Boiler Company to fire no. 6 fuel oil.

At this facility CWS is prepared by charging a predetermined amount of water to a 6,800 l (1,800 gal) steam-jacketed mix tank with agitator before adding coal through a gravimetric coal feeder. The CWS is then transferred to a 10,600 l (2,800 gal) holding tank with an agitator and recirculation pump. The CWS is pumped to the burner by a Moyno pump. The original burner was modified for abrasive service.

The second boiler tested (site 2) was a Babcock and Wilcox integral furnace, bent tube boiler rated at 7.6 kg steam/s (60,000 lb/hr) at 1.2 MPa (175 psig) located at the Memphis plant of the E.I. du Pont de Nemours & Company. The unit was originally designed to fire distillate oil, process gas, and natural gas, and had been previously modified to accommodate residual fuel oil.

The unit was most recently modified to allow CWS firing under an Electric Power Research Institute (EPRI) CWS demonstration program. The tests reported herein were performed during the 35-day demonstration burn phase of the EPRI project. A CWS formulation prepared by the Atlantic Research Corporation (ARC-Coal) was being fired during the tests performed for this report.

The test protocols and test results for each of these CWS-fired boiler tests are discussed sequentially below.

SITE 1 TEST RESULTS

Boiler Operation

The test program called for flue gas emission measurements with the boiler operating at constant, near-rated capacity with the CWS fuel. Two tests were performed: test 1 with a 60.9 weight percent coal slurry at 14 percent excess air, and test 2 with a 58.9 percent coal slurry at 11 percent excess air. An abbreviated sampling protocol was completed for test 1; test 2 included the complete, planned comprehensive sampling protocol.

Table 1 lists the boiler operating conditions during both tests. With the exception of the fraction of coal in the fuel and the excess air, the boiler was operated at essentially the same conditions for both tests. Table 2 summarizes the fuel compositions for both tests.

Emission Measurements and Results

The sampling and analysis procedures used in this test program conformed to a modified EPA Level 1 protocol (1). All flue gas samples were taken at the boiler outlet, upstream of the unit's particulate control device (baghouse). Emission measurements included:

- Continuous monitoring for O_2, CO_2, NO_x, CO, SO_2, and TUHC
- Source Assessment Sampling System (SASS) for trace elements and organic emissions
- Combined EPA Method 5/8 for particulate and sulfur oxides
- Grab sample for C_1 to C_6 hydrocarbons by gas chromatography (GC)
- Grab sample for N_2O analysis

In addition, samples of the fuel, bottom ash, and baghouse hopper ash were collected for analysis.

The analysis protocol included:

- Analyzing the fuel, ash, and SASS train samples for 73 trace elements using spark source mass spectrometry (SSMS), supplemented by atomic absorption spectrometry (AAS)
- Analyzing the SASS train and ash extract samples for total organic content in two boiling point ranges: 100 to 300°C by total chromatographable organics (TCO) analysis and >300°C by gravimetry (GRAV)
- Analyzing the SASS train and ash extract samples for the 58 semivolatile organic priority pollutants, including many of the PAH compounds of interest from combustion sources
- Performing infrared (IR) spectrometry analysis of organic sample extracts
- Performing liquid chromatography (LC) separation of selected sample extracts with subsequent TCO, GRAV, and IR analyses of LC fractions
- Performing direct insertion probe low resolution mass spectrometry (LRMS) analysis of selected sample extract LC fractions

Bioassay tests were also performed on SASS train and ash samples to estimate their potential toxicity and mutagenicity.

Table 3 summarizes flue gas emissions measured in the test program. Emissions are presented as ng/J heat input and as mg/dscm of flue gas. As a measure of the potential significance of the emissions levels for further analyses, an occuptional exposure guideline for most pollutants is also noted in the table. The occupational exposure guideline noted is either the time-weighted-average Threshold Limit Value (TLV) established by the American Conference of Governmental Industrial Hygienists (2), or the 8-hr time-weighted-averaged exposure limit established by the Occupational Safety and Health Administration (OSHA) (3). These are noted only to aid in ranking the potential significance of the emission levels. In this respect, pollutants emitted at levels several orders of magnitude higher than their occupational exposure guidelines might warrant further consideration, while species emitted at levels significantly lower than their occupational exposure guidelines might be considered of little potential concern. Only elements emitted at levels exceeding their occupational exposure guidelines in these tests are noted in Table 3.

Table 3 shows that several elements were present in the boiler outlet at significant levels. However, flue gas particulate accounts for the major fraction of these elements in the flue gas at this location. Ultimate flue gas discharge concentrations would be significantly reduced after passage through the unit's particulate control device.

The data in Table 3 show that emissions of the vapor phase pollutants NO_x, SO_2, CO, and TUHC were essentially equivalent in both tests performed. However, particulate emissions approximately doubled in test 2. This test was run at slightly lower excess air than test 1: flue gas O_2 of 2.1 percent in test 2 and 2.8 percent in test 1. Also, the CWS in test 2 had slightly more water (less coal) than in test 1. Both of these would be conducive to poorer combustion efficiency. This, in turn, could lead to increased particulate mass emissions as the combustibles losses in the flyash increased. Indeed, the baghouse hopper ash from test 2 was found to contain over 60 percent carbon (dry basis). Unfortunately, no such carbon content data were taken for the test 1 flyash; although, it is interesting that complete emission of all the ash content of the fuel fired would result in particulate emissions of about

3.1 g/dscm. This is just below the measured value in test 1, but less than half that measured in test 2.

The size distribution of test 2 boiler outlet particulate favored coarse particulate as shown in Table 4. Over 60 percent (weight) of the flue gas particulate was greater than 10 μm diameter; almost 70 percent was greater than 3 μm diameter.

Table 3 shows that total organic emissions (C_1 to C_6, TCO, and GRAV) were quite high, at 48 mg/dscm. The nonvolatile (GRAV) boiling point range accounted for most of the organics measured.

Analyses of SASS train and ash extract samples for the semivolatile organic priority pollutant species, a grouping which contains several polynuclear aromatic hydrocarbon compounds, were performed. Results of these analyses are summarized in Table 5. As noted, only naphthalene and several phthalates (which are suspected contaminants) were found in SASS train samples.

The bottom ash extract contained in the greatest number and concentration of the priority pollutants sought. This is consistent with the very high total organic (TCO plus GRAV) content of this sample (8 mg/g). As with the SASS train samples, most of the total organics in the bottom ash (80 percent) was in the nonvolatile (GRAV) boiling point range.

The SASS train organic module extract and the bottom ash extract samples were subjected to liquid column chromatography (LC) separation, with TCO, GRAV, IR, and LRMS analyses of eluted fractions, in an attempt to elucidate the chemical character of the organic material in these samples. These analyses suggested that the flue gas organic consisted largely of oxygenated organics such as carboxylic acids. Oxygenated organics and alkyl aromatics were suggested in the bottom ash extract.

Bioassay tests were performed on the SASS train and ash stream samples. The health effects bioassay tests performed were the Ames mutagenicity assay, and the CHO cytotoxicity assay (4). The results of these assays are summarized in Table 6. The results suggest that the flue gas was of low to moderate toxicity and low mutagenicity. The ash streams were of low to moderate toxicity and nondetectible mutagenicity.

The positive Ames response of the XAD-2 extract is typical of such extracts from SASS tests of combustion sources. Current studies sponsored by EPA's Air and Energy Engineering Research Laboratory are investigating whether such bioassay responses are due to artifact compounds formed when combustion product gas containing NO_x is passed over XAD-2 resin.

SITE 2 TEST RESULTS

Boiler Operation

Table 7 summarizes the boiler operating conditions for the test performed on this unit. As indicated, three of the five available furnaces were fired with the CWS. In addition, about 10 percent of the total heat input to the unit was with natural gas introduced through one burner and through a direct-fired air preheater. Boiler load was slightly greater than 90 percent of rated for the test. Boiler efficiency as calculated by the ASME heat loss method was 72 percent. Table 8 gives the fuel ultimate analysis as reported by the host site for these tests.

Emission Measurements and Results

The sampling and analysis protocol used in this test program was essentially the same as that employed for site 1, with the addition of volatile organic sampling train (VOST) sampling with analysis for the volatile organic priority pollutants. All flue gas sampling was performed in a vertical section of breeching located downstream of the units' induced draft fan, but upstream of the breeching transition section to the stack.

Table 9 summarizes flue gas emissions measured in the test program. Emissions are presented as ng/J heat input and as mg/dscm of flue gas. Again, a measure of the potential significance of the emission levels for further analyses, an occupational exposure guideline for most pollutants is also noted in the table. Only elements emitted at levels exceeding 10 percent of their occupational exposure guideline in these tests are noted in Table 9.

As noted in the table, particulate emissions from this boiler were also quite high at about 4.3 g/dscm. This is not unexpected, however, since the unit had no particulate control device. The emission levels for NO_x, SO_2, SO_3, CO, and N_2O, correspond to 510, 450, 2.6, 285, and 70 ppm corrected to 3 percent O_2, respectively. The NO_x level noted is in the range typical for coal-fired sources. The SO_x (SO_2 and SO_3) levels correspond to what would be expected from this source burning a 1 percent (dry basis) sulfur fuel. The analysis summrized in Table 8 indicates less sulfur in the fuel. However, an independent analysis cited by the host site (5) suggests that the fuel sulfur content could have been above 0.9 percent. The ratio of SO_3 to total SO_x, at 0.6 percent, is lower than the typical 2 to 5 percent range for coal fired sources.

Table 9 notes that several trace elements were emitted at levels significantly higher than their occupational exposure guideline. In fact. two elements were emitted at levels over a factor of 100 times their occupational exposure guideline and another 8 at levels greater than 10 times their guideline. Again, however, this is largely the result of the absence of a particulate control device on the boiler for these tests. In fact, five of the first eight elements noted in the table (aluminum, iron, silicon, sodium, and potassium) are major constituents of the ash fraction of the CWS fuel (5). For further comparison, the criteria pollutants NO_x and SO_2 (in addition to particulates) were also emitted at levels over 100 times their occupational exposure guidelines.

The size distribution of emitted particulate was heavily weighted toward coarse particulate, as noted in Table 10. Over half percent of the emitted particulate mass had a diameter greater than 10 μm; over 50 percent had diameter greater than 3 μm. Combustibles losses in the particulate were quite high as noted in Table 11. Composite particulate had had a carbon content of about 40 percent which, with the hydrogen noted, would give a particulate higher heating value of 13.7 MJ/kg (5,920 Btu/lb).

Table 8 noted that total organic emissions from the unit were about 15.5 mg/dscm, comprised chiefly (over 95 percent) of compounds in the volatile (boiling point less than about 100°C) category. Emissions of both total semivolatile organics (boiling point between 100° and 300°C) were 0.05 mg/dscm; of nonvolatile organics (boiling point greater than 300°) were 0.3 mg/dscm.

Analysis of SASS train samples for the semivolatile organic priority pollutants showed that only naphthalene was present in the flue gas at detectable levels; naphthalene emissions were less than 5 μg/dscm.

Results of VOST testing for volatile organic compounds are summarized in Table 12. The table shows that several chlorinated C_1 and C_2 aliphatic hydrocarbons, chlorobenzene, benzene, and ethylbenzene were emitted at levels in the 1 to 20 μg/dscm range. Such levels of benzene and ethylbenzene are common in combustion source flue gas. The chlorinated compounds also arise whenever chlorine containing fuels are burned. Although not noted in Table 8, an independent host site analysis suggests that the chlorine content of the CWS burned was 0.1 percent.

Bioassay tests were performed on the SASS train organic sorbent module extract and two particulate size fractions. Again, the health effects bioassay tests performed were the Ames mutagenicity assay, and the CHO cytotoxicity assay (4). The results of these assays are summarized in Table 13. The results suggest that the sorbent module extract was of moderate toxicity and mutagenicity and both particulate size fractions were of nondetectable mutagenicity and low toxicity.

ACKNOWLEDGEMENTS

This work was supported by EPA under Contract 68-02-3188. The guidance and support of the EPA Project Officer, Robert E. Hall, is gratefully acknowledged. The authors also wish to recognize the support and cooperation of the several PETC, EPRI, and DuPont personnel who contributed to the success of these test programs.

REFERENCES

1. Lentzen, D. E., et al., "IERL-RTP Procedures Manual: Level 1 Environmental Assessment (Second Edition)," EPA-600/7-78-201, NTIS PB293795, October, 1978.

2. "Threshold Limit Values for Chemical Substances and Physical Agents in the Work Environment with Intended Changes for 1983-84," American Conference of Governmental Industrial Hygienists, Cincinnati, Ohio, 1983.

3. OSHA Safety and Health Standards, 29 CFR Part 1910, Subpart Z.

4. Brusick, D. J., and R. R. Young, "IERL-RTP Procedures Manual: Level 1 Environmental Assessment, Biological Tests," EPA-600/8-81-024, NTIS PB81-228766, October 1981.

5. Perkins, R. P., "Coal-Water Slurry Test in an Industrial Boiler," Final report to the Electric Power Research Institute, EPRI project RP-1875-7, November 1984.

Table 1

BOILER OPERATING CONDITIONS: SITE 1

	Test 1	Test 2
Steam flow, kg/s	3.03	3.03
(lb/hr)	(24,000)	(24,000)
Drum pressure, MPa	1.3	1.3
(psi)	(189)	(189)
Furnace draft, Pa	112	116
(in. H_2O)	(0.47)	(0.466)
Fuel flow, kg/s	0.410	0.39
(lb/min)	(54.2)	(51.8)
Steam temperature, °C	186	188
(°F)	(367)	(371)
Boiler feedwater temperature, °C	101	--*
(°F)	(213)	--*
Combustion air temperature, °C	24	28
(°F)	(76)	(83)
Flue gas temperature, °C furnace exit	272	291
(°F)	(522)	(556)
Excess air, percent**	14	11

---

*Not available

**Calculated from PETC fuel compositon and O_2 concentrations

Table 2

FUEL ANALYSES (PERCENT BY WEIGHT): SITE 1

	Coal (Dry Basis)	CWS (as Fired)		
		Test 1		Test 2
	PETC*	PETC**	This Study*	PETC**
Carbon	82.23	50.08	47.90	48.43
Hydrogen	5.60	3.41	3.34	3.30
Oxygen (by difference)	6.76	4.12	8.56	3.98
Nitrogen	1.60	0.97	1.02	0.94
Sulfur	1.19	0.72	0.80	0.70
Ash	2.62	1.60	1.93	1.54
Additive	--	0.50	--	0.50
Water	--	38.60	36.45	40.6
Higher heating value, kJ/kg	34,459	20,986	21,341	20,296
(Btu/lb)	(14,829)	(9,031)	(9,184)	(8,734)

---

*Measured

**Calculated based on coal ultimate analysis and reported proportion of coal, additive, and water in the CWS formulation

Table 3

SUMMARY OF EXHAUST GAS EMISSIONS*: SITE 1

Compound	Test 1 (ng/J Heat Input)	Test 1 (mg/dscm)	Test 2 (ng/J Heat Input)	Test 2 (mg/dscm)	Occupational Exposure Guideline (mg/dscm)**
SO_2	786	2,580	680	2,480	5
SO_3	0.86	2.8	<0.5	<2	1
NO_x (as NO_2)	136	448	172	624	6
N_2O	18	58	41	148	****
CO	62	202	66	239	55
TUHC (as CH_4)	0.2	0.73	0.53	1.9	****
Solid particulate	1,064	3,485	1,991	7,255	10*****
Total volatile organics (C_1 to C_6)	4.3	14.0	2.5	9.1	****
Total semivolatile organics (TCO)	--***	--	1.6	5.9	****
Total nonvolatile organics (GRAV)	--	--	9.1	33.1	****
Trace Elements					
Iron, Fe	--	--	55	201	1
Phosphorus, P	--	--	3.6	13.2	0.1
Aluminum, Al	--	--	82	297	2
Arsenic, As	--	--	0.3	1.06	0.01******
Silicon, Si	--	--	148	537	10*****
Vanadium, V	--	--	0.46	1.67	0.05
Chromium, Cr	--	--	0.33	1.19	0.05
Beryllium, Be	--	--	0.01	0.045	0.002
Copper, Cu	--	--	0.56	2.03	0.1******
Lead, Pb	--	--	0.23	0.85	0.05******
Barium, Ba	--	--	2	7.95	0.5
Nickel, Ni	--	--	0.37	1.33	0.1
Calcium, Ca	--	--	6.9	25.3	2
Lithium, Li	--	--	0.07	0.27	0.025
Potassium, K	--	--	5.3	19.3	2[g]
Cobalt, Co	--	--	0.17	0.64	0.1
Titanium, Ti	--	--	5.4	20	10*****
Uranium, U	--	--	0.02	0.09	0.05******
Magnesium, Mg	--	--	4.1	15	10

---

*Exhaust O_2 and CO_2 levels averaged 2.76 and 14.9 percent, and 2.08 and 15.7 percent, respectively for the two tests

**Time-weighted-average TLV (2) unless noted

***Double dashes indicate that sample was not obtained; abbreviated test

****No occupational exposure guideline applicable

*****For nuisance particulate

******8-hr time-weighted-OSHA exposure limit (3)

*******Ceiling limit

Table 4

FLUE GAS PARTICULATE SIZE DISTRIBUTION: SITE 1

	Emission Rate		
Particle Size	(g/dscm)	(ng/J)	(Percent of Total)
>10μm	4.34	1,190	63.6
3 to 10μm	0.38	100	5.6
1 to 3μm	1.19	330	17.4
Filter (<1μm)	0.91	250	13.4
Total	6.82	1,870	100.0

Table 5

PAH AND OTHER SEMIVOLATILE ORGANIC PRIORITY POLLUTANT SPECIES DETECTED: SITE 1

	Sample						
	10 + 3 μm Particulate		1μm+ Filter Particulate		XAD + Condensate Extract	Bottom Ash	Baghouse Ash
Species	(mg/kg)	(μg/dscm)	(mg/kg)	(μg/dscm)	(μg/dscm)	(mg/kg)	(mg/kg)
PAH's							
Acenaphthene	--*	--	--	--	--	1	--
Acenaphthylene	--	--	--	--	--	2	--
Anthracene	--	--	--	--	--	1	--
Benz(a)anthracene	--	--	--	--	--	0.4	--
Benzo(j+k)fluoranthenes	--	--	--	--	--	0.4	--
Chrysene	--	--	--	--	--	0.8	--
Fluoranthene	--	--	--	--	--	2	--
Fluorene	--	--	--	--	--	2	--
Naphthalene	0.2	0.9	3.7	7.7	--	42	0.3
Phenanthrene	--	--	--	--	--	11	--
Pyrene	--	--	--	--	--	2	--
Other priority pollutants							
Bis(2-ethylhexyl)phthalate	<0.15	<0.7	3.4	7.2	7.8	84	0.3
Butylbenzylphthalate	<0.07	<0.3	0.2	0.4	2	120	0.08
Diethylphthalate	--	--	0.4	0.8	--	--	0.04
2,4-dimethylphenol	<0.2	<0.9	<0.4	<0.8	<7	5	<0.2
Detection limit	0.05	0.2	0.05	0.1	1.1	0.4	0.04

---

*Double dashes denote less than detection limit noted

Table 6

BIOASSAY RESULTS: SITE 1

Sample	Ames Mutagenicity	CHO Clonal Toxicity
10 + 3 μm particulate	ND	L/M
1 μm + filter particulate	ND	ND/L
XAD-2 + organic module condensate total extract	L	U(L)
Bottom ash	ND	L/M
Baghouse ash	ND	L

Note:
ND -- No detectable mutagenicity/toxicity
L -- Low mutagenicity/toxicity
M -- Moderate mutagenicity/toxicity
U -- Undetermined toxicity. Exact toxicity range could not be determined due to insufficient amount of sample. Test results indicate low toxicity or less.

Table 7

BOILER OPERATING CONDITIONS: SITE 2

Parameter	Range	Average
Steam flow, kg/s (10^3 lb/hr)	6.89 to 7.13 (54.6 to 56.5)	13.1 (55.5)
Steam pressure, MPa (psig)	1.19 to 1.21 (173 to 176)	1.21 (175)
CWS flow, l/s (gpm)*	0.60 to 0.61 (9.5 to 9.7)	0.61 (9.6)
Natural gas flow to burner No. 4, scm/min (10^3 scfh)	1.39 to 1.79 (2.94 to 3.79)	1.48 (3.14)
Natural gas flow to air heater, scm/min (10^3 scfh)	1.58 to 1.76 (3.35 to 3.73)	1.68 (3.55)
Inlet air temperature, °C (°F)	29 to 39 (85 to 102)	36 (96)
Windbox air temperature, °C (°F)	274 to 283 (525 to 542)	279 (535)
Windbox air pressure, kPa (in. WC)	2.79 (11.2)	279 (11.2)
CWS heater temperature, °C (°F)	37 to 38 (98 to 101)	38 (100)
CWS strainer discharge pressure, MPa (psig)	1.35 to 1.38 (196 to 200)	1.37 (198)
Feedwater temperature, °C (°F)	129 (265)	129 (265)
Stack gas temperature, °C (°F)	293 to 304 (559 to 580)	299 (571)
Atomizing air pressure, MPa (psig)		
Burner No. 2	1.41 to 1.42 (204 to 206)	1.42 (206)
Burner No. 3	1.42 to 1.43 (206 to 208)	1.43 (208)
Burner No. 4	1.41 to 1.42 (204 to 206)	1.42 (206)
CWS burner pressure, MPa (psig)		
Burner No. 2	1.13 to 1.16 (164 to 168)	1.14 (166)
Burner No. 3	1.12 to 1.14 (162 to 166)	1.14 (165)
Burner No. 4	1.16 to 1.23 (168 to 179)	1.21 (176)
Furnace pressure, Pa (in. WC)	-77 to -37 (-0.31 to -0.15)	-60 (-0.24)
Excess air (percent)**		45
Boiler efficiency (percent)***		72

---

*Average of two flowmeters installed; one magnetic and one mass

**Calculated from flue gas composition

***Calculated using "ASME test form for abbreviated efficiency test"

Table 8

CWS FUEL COMPOSITION*: SITE 2

Component	Percent by Weight (Dry Basis Unless Noted)
Moisture**	29.7
Solids**	70.3
Carbon	83.3
Hydrogen	5.1
Oxygen***	5.0
Nitrogen	1.4
Sulfur	0.6
Ash	4.6
Higher heating value, MJ/kg (Btu/lb)	34.374 (14,810)

---

*(5), Babcock & Wilcox Analysis
**As fired
***By difference

Table 9

SUMMARY OF FLUE GAS EMISSIONS: SITE 2

Component	Emission Concentration (ng/J Heat Input)	Emission Concentration (mg/dscm)	Occupational Exposure Guideline* (mg/m^3)
Major Constituents			
Particulate	2,510	4,310	10**
SO_2	540	930	5.0
SO_3	3.9	6.7	1.0
NO_x (as NO_2)	440	760	6.0
CO	150	260	55
N_2O	57	98	--***
Total volatile organics (C_1 to C_6)	8.8	15.1	--***
Total semivolatile organics (TCO)	0.03	0.05	—***
Total nonvolatile organics (GRAV)	0.2	0.3	—***
Trace Elements			
Beryllium	0.25	0.43	0.002
Aluminum	160	270	2.0
Iron	47	80	1.0
Chromium	1.3	2.3	0.050
Silicon	225	385	10**
Sodium	28	48	2.0****
Phosphorous	1.1	1.9	0.10
Potassium	16	28	2.0****
Nickel	0.67	1.2	0.10
Lithium	0.15	0.26	0.025
Vanadium	0.26	0.44	0.050
Calcium	7.5	13	2.0
Arsenic	0.032	0.056	0.010*****
Lead	0.097	0.17	0.050*****
Copper	0.19	0.33	0.10*****
Barium	0.74	1.3	0.50
Titanium	9.7	17	10**
Cobalt	0.070	0.12	0.10
Magnesium	4.5	7.7	10
Zinc	0.25	0.43	1.0
Silver	0.0024	0.0041	0.010
Selenium	0.018	0.031	0.20
Bromine	0.063	0.11	0.70
Yttrium	0.082	0.14	1.0

*Time-weighted-average TLV (2) unless noted

**For nuisance particulate

***No occupational exposure guideline applicable

****Ceiling limit

*****8-hr time-weighted-average OSHA exposure limit (3)

Table 10

PARTICLE SIZE DISTRIBUTION: SITE 2

Size Range	Weight Percent of Particulate in Size Range
>10 µm	51.4
3 to 10 µm	40.4
1 to 3 µm	7.8
<1 µm	0.4

Table 11

PARTICULATE CARBON AND HYDROGEN CONTENT: SITE 2

Size Range	Carbon Content (Weight Percent)	Hydrogen Content (Weight Percent)
>3 m (10 µm + 3 µm cyclone catch)	42.67	0.13
<3 m (1 µm + filter catch)	13.13	0.09
Composite	40.19	0.13

Table 12

STACK GAS VOLATILE ORGANIC COMPOUND CONCENTRATIONS: SITE 2

	Stack Gas Concentration**,*** (μg/dscm)						
	Trap set 1			Trap set 3			
Compound*	Tenax Trap	Tenax/ Charcoal Trap	Total	Tenax Trap	Tenax/ Charcoal Trap	Total	Average Total
Chloromethane	0.4	27.6	28	<0.3	12.8	13	21
Vinyl chloride	<0.3	5.2	5.2	<0.3	8.3	8.3	6.8
Chloroethane	<0.3	8.2	8.2	<0.3	12.9	12.9	11
1,2-dichloroethane	0.4	<0.3	0.4	<0.3	<0.3	<0.3	0.4
Benzene	20.9	<0.3	21	25.4	<0.3	25	23
Chlorobenzene	<0.3	<0.3	<0.3	1.5	<0.3	1.5	0.9
Ethylbenzene	<0.3	2.4	2.4	<0.3	1.1	1.1	1.8

---

*Bromomethane, chloroethane, methylene chloride, 1,1-dichloroethylene, 1,1-dichloroethane, t-1,2-dichloroethylene, chloroform, 1,1,1-trichloroethane, carbon tetrachloride, dichlorobromomethane, 1,2-dichloropropane, t-1,3-dichloropropene, trichloroethylene, 2-chloroethyl vinyl ether, bromoform, tetrachloroethylene, 1,1,2,2-tetrachloroethane, toluene, allyl chloride, ethylene oxide, propylene oxide, and 2-nitropropane were also analyzed for and not detected above a detection limit of 0.3 μg/dscm

**Field blank corrected

***Triplicate sets of traps samples; trap set 2 not analyzed

Table 13

BIOASSAY RESULTS

	Bioassay	
Sample	Ames*	CHO**
XAD-2 extract:	M	M
<3 μm particulate (1 μm + filter)	ND	L
>3 μm particulate (3 μm + 10 μm)	ND	L

---

*Mutagenicity test
**Toxicity test
M: Moderate, L: Low,
ND: Nondetectable

DEVELOPMENT OF LOW-NOx COMBUSTION FOR INDUSTRIAL APPLICATION

Tomio Suzuki, Kotaro Morimoto, Keiichi Ohtani, Ryuichi Odawara,
Tatsuo Kohno, Yuichi Matsuda and Mamoru Suyari
Kobe Steel, Ltd.
1-chome, Wakinohama-cho, Chuo-ku, Kobe, Japan

ABSTRACT

Low-NOx emission combustion has been developed for industrial furnaces, boilers, pelletizing kilns, cement plants and gas turbines. More than 350 low-NOx burners of the slow-combustion type for the industrial furnaces have shown a reduction of 30-70% in NOx value and 5-10% in fuel consumption. NOx emission reduction of low-NOx burners for boilers has attained 30-60% in the seventeen boilers of 2-15 tons/hr evaporation. The boiler efficiency of low-NOx burners was higher than that of conventional burners by 2%. The NOx value of low-NOx burners for pelletizing kilns has decreased with an increase in multifuel-firing percentage of coal in coke-oven gas and coal firing. Low-NOx combustion of the Dual Combustion and Denitration (DD) process for a 3600 t/d cement plant has decreased to 110 ppm (10% O_2) in NOx value and 735 kcal/kg-cl in fuel consumption. A new low-NOx combustor of a pre-mixed, prevaporized and fuel-lean type for gas turbines has resulted in an NOx reduction of about 90%.

1. INTRODUCTION

In order to control oxides of nitrogen (NOx) formed during combustion, a number of techniques have been proposed which include flue gas recirculation, non-stoichiometric firing, two-stage combustion, and the use of burners with low NOx emission.[1-7] The application of these techniques to existing industrial furnaces is, however, difficult in practice. A further problem is that the reduction of NOx emission is often regarded as incompatible with efforts to conserve energy. Countermeasures against NOx may result in a drop in flame temperature with a consequent fall in heating efficiency.

Kobe Steel, Ltd. possesses a large number of soaking pits, reheating furnaces, heat treatment furnaces, and melting furnaces and boilers for iron and steel, casting and forging, aluminum and copper, and welding rods in 20 plants. From a standpoint of users of industrial furnaces and boilers, the authors have developed high-efficiency burners which are fully compatible with energy saving and with low NOx emission and are very suitable for application to existing furnaces and boilers.

Kobe Steel, Ltd. has engineering and machinery divisions which sell cement plants, pelletizing plants and gas turbines. The authors have developed low-NOx combustion with energy saving for this combustion equipment.

2. LOW-NOx EMISSION BURNERS FOR FURNACES

2.1 Model E Burner

Slow combustion has been adapted as a heating efficiency measure by suppression of mixing of fuel and air during the initial stages of combustion.

The direction of fuel injection in the model E burner is at an angle to the air stream axis, and the mixing of fuel and air in the primary combustion zone is limited as shown in Fig. 1. Therefore, a local high-temperature region cannot develop. Fuel which is not burned in this zone gradually mixes with air not used in the initial stages and thus combustion is completed. It is therefore possible to obtain uniform combustion. The drop both in the maximum flame temperature and local oxygen partial pressure effectively suppresses thermal NOx and fuel NOx, and thus the NOx value is drastically reduced.

The model E burner is very simple, with the fuel injection inclined to its axis at the tip. Accordingly, costs are low and modification of the burner refractory quarl, for example, is unnecessary. Thus, the design is particularly suitable for application to an existing furnace.

All combustion tests were made in a horizontal, cylindrical wall furnace of dimensions 1000 mm dia. x 4000 mm length. The experiments were conducted under the following standard combustion conditions:

Heat input, 40×10^4 kcal/h
Furnace temperature, 1300°C
Secondary air temperature, 320°C

The performance of the model E burner in the test furnace was assessed by measuring the effects of excess oxygen concentration on NOx emission for three types of fuel (Fig. 2) and of combustion air temperature (Fig. 3). In the first of these tests, the NOx concentration decreased to a value less than half that obtained using a conventional burner. In the second, the NOx level was extremely low and was hardly affected by changes in air temperature. Clearly, these findings are advantageous in practical situations with fluctuating furnace conditions.

2.2 Model EE Burner

The combustion principles of an improved version of the authors' low-NOx burner are shown in Fig. 4. In this burner, combustion air and fuel are injected separately. Thus, mixing of fuel and air is suppressed at the initial stage of combustion, and combustion progresses gently. Consequently, very uniform combustion is obtained, self-recirculation of the flue gas is achieved, and emission of NOx is considerably reduced with a decrease in the quantity of soot produced.

The relation between Bacharach smoke number and NOx emission for various burners is shown in Fig. 5. The smoke number with the model EE burner is about half that obtained from burners with a uniform air stream. The model EE burner is suitable for oxygen-enriched combustion as shown in Fig. 6. The NOx emission of the model EE burner is extremely low and is hardly affected by changes in oxygen percent in the combustion air.

2.3 Heat Transfer Characteristics

In a high-temperature furnace, much of the heat transfer depends on radiation. The representative flame temperature T in combustion systems may be expressed as

$$T_f = \frac{H_L + Q_F + Q_A}{G \cdot C_p} \left[1 - \frac{\eta}{100} \right] \qquad (1)$$

Radiant heat release from the flame is expressed as

$$\eta \propto A_f \sigma \varepsilon_f \{(T_f + 273)^4 - (T_w + 273)^4\} \qquad (2)$$

Fig. 7 shows the relation between radiant heat release and NOx emission when burning heavy oil and kerosine. Generally, the relation between the thermal NOx and the flame temperature can be roughly put in order by Arrhenius's formula if the excess air ratio is fixed. Fig. 7 is the result of calculations according to the following equation.

$$[\mathrm{NOx}]_{th} = 1.45 \times 10^6 \exp\{-E/R(T_f + 273)\} \qquad (3)$$

As explained by Zeldovich[11] and Lavoie,[12] the concentration of thermal NOx is a function of flame temperature, oxygen concentration and residence time, and is particularly affected by flame temperature. Accordingly, as is shown by Equations (1) to (3) and in Fig. 7, a decrease in flame temperature and an increase in the extent of radiant heat release will improve heat transfer and will be effective in suppressing NOx emission. The low-NOx burners described by the authors offer improved heat transfer and energy consumption by increasing flame surface area and flame emissivity through slow combustion.

Temperature distributions in the longitudinal section of the test furnace using the model E burner and a conventional burner are compared in Fig. 8, using butane as fuel. The maximum flame temperature of the low-NOx burner is 82°C lower and the temperature distribution is more uniform. Additionally, NOx emission is reduced to one-fourth of the value obtained using the conventional burner. In the region of the flame, up to an L/D value of 2.6, the low-NOx burner shows a higher value for total radiant heat flux than the conventional burner (Fig. 9). The reason for this higher value, despite the lower flame temperature, is the higher emissivity of the flame due to its greater luminosity.

To confirm this observation, the ratios of the flame emissivities of the low-NOx burner (ε_L) and the conventional burner (ε_C), and of the flame (ε_f) and the gas (ε_g) were determined. For this purpose, a value was first obtained for flame-radiant heat flux (Q_f) by correcting the measured total flux for furnace-wall radiant heat; Q_f may then be calculated from the average flame temperature as follows:

$$Q_f = \varepsilon_f \sigma (T_f + 273)^4 \qquad (4)$$

Gas emissivity can be calculated from Schack's formula[13] and Hottel's correction diagram[14] depending upon the composition of the combustion gas. For practical purposes, calculations may be based upon the emissivities of CO_2 and H_2O, which provide the greater part of the gas radiation.

$$\varepsilon_{CO_2} = \frac{3.5}{4.88} \frac{(pCO_2\ L)^{1/3}}{(T/100)^{1/2}} \qquad (5)$$

$$\varepsilon_{H_2O} = \frac{34.5}{4.88} \frac{(pH_2O\ L)^{0.8}}{(T/100)} \qquad (6)$$

Gas emissivity is corrected as follows:

$$\varepsilon_g = \varepsilon_{CO_2} + \varepsilon_{H_2O} - \Delta\varepsilon \qquad (7)$$

In the flame region, flame emissivity is higher for a low-NOx burner with a value nearly double that of the conventional burner (Fig.10). Gas radiation dominates nearly all the regions ($\varepsilon_f/\varepsilon_g=1$) in the case of the conventional burner, because combustion is completed in the early stage and produces a non-luminous flame. In the case of the low-NOx burner, however, there is a point where the luminous flame radiation occupies about half of the entire radiation ($\varepsilon_f/\varepsilon_g=2$). There is thus a significant contribution from luminous flame radiation in the case of the low-NOx burner.

2.4 Application of Low-NOx Burner in Continuous Reheating Furnaces

The model E burner was used in a butane-burning, continuous, six-zone slab reheating furnace, which was previously equipped with a commercially available, low-NOx burner with an NOx emission of about 120 ppm.

On installation of the model E burner, fuel was injected in a downwards direction in the upper-zone burners and in an upwards direction in the lower-zone burners. This compensated for the drop in temperature of the flame due to the adoption of the new burner by bringing the flame close to the product. With this arrangement, the NOx value was reduced to 40-50 ppm.

Fig. 11 compares the results of calculations of the overall heat absorptivity ϕ_{CG}, derived from measurements of slab temperature when the low-NOx burner and the conventional burner are used. The temperature of the furnace gases above the slab surface rose by about 50-100°C, and their heating property was improved. Owing to the comparatively short flame of the conventional burner, flame-radiant heat transfer by luminous radiation and gas radiation takes place near the burner, and heat absorptivity by the steel is high close to the burner. However, the heat transfer is due solely to gas radiation in the post-flame and is very low. Because the model E burner produces a long, luminous flame which occupies the entire furnace length, the overall heat absorptivity is both high and more uniform with the consequent reduction in fuel costs of about 5%.

The improvement in heating efficiency when using the model E burner may also be demonstrated by data obtained from a 75 tons/hour walking-beam furnace (Table 1). Billet surface temperatures were measured at a point between the furnace discharge and the mill. In this application, the operation of the new burner was optimized to give slow combustion and to promote heat transfer by radiation. Under normal furnace load operation, surface temperatures were raised by about 35°C. Thus, heating efficiency was improved and there was a saving in fuel oil consumption of about 1.5 liter/ton. Emission of NOx was reduced by 30-50%.

2.5 Application of Low-NOx Burner in Soaking Pits

The model E burner was applied to a one-way, top-fired soaking pit using butane as fuel. Before improvement, two-stage combustion using a commercially available, split-flame type, low-NOx burner was giving an NOx emission of 60-100 ppm. The flame was made more uniform by the use of the new burner and NOx concentration dropped to 40-50 ppm. Soaking property data are shown in Table 2. The reduction in fuel costs was about 5%.

NOx values for one heating cycle are shown in Fig. 12. With the conventional burner, NOx emission is extremely high with the formation of a local high-temperature region due to the rapidity of the combustion reaction, which takes place from inside the burner quarl near the burner tip. Emission is also very high in the soaking stage because it is greatly affected by combustion air temperature, furnace temperature and excess air ratio.

On the other hand, with the model E burner, the main combustion reaction takes place inside the furnace and, as a consequence of the long flame, occupies the whole of the interior of the furnace. In this case, the effects of combustion air temperature, etc. are small and thus a significant reduction in NOx emission of 50-75% can be achieved.

Fig. 13 shows a burner design for the coke-oven gas firing of soaking pits. The gas contains 60% H_2 and thus the speed of combustion is high. Radiant heat release from the flame is less because of the low ratio of C/H, and NOx emission from high-temperature gas-fired furnaces is particularly high. When the model E burner was introduced, the combustion air stream was changed from a swirl to an axial stream and velocity of flow was reduced. With these modifications NOx emission decreased substantially and fuel costs were reduced by about 7%.

The detailed results for Model E and EE burners are available elsewhere.[5,3]

3. LOW-NOx EMISSION BURNER FOR BOILERS

Fig. 14 shows the principle of reducing the NOx emission of the low-NOx burner for a boiler. A desired flow pattern having optimum swirl intensity and velocity is formed by a swirler located at the exit position of the air register. Fuel is sprayed to the inner-side region of the outer, hollow, swirling air flow by the positioning of the nozzle tip. The mixing of the fuel and air is controlled to prevent too rapid mixing during the initial period of combustion and contact with the water-cooled wall. Namely, fuel mixes with the primary air of low flow velocity and a portion of the outer swirl flow, and burns first in the fuel-rich state. Next, fuel not burnt up in the fuel-rich zone mixes with the outer swirl flow of high flow velocity and completes burning in the fuel-lean state. Accordingly, this combustion process resembles multistage combustion (two-stage combustion). In the case of strong swirl intensity where there is internal reverse flow, it is expected that there will be self-recirculation of the flue gas. As a result, the maximum flame temperature and local oxygen partial pressure in the initial stage of combustion are dropped. On account of these, thermal NOx and fuel NOx are sufficiently suppressed. Moreover, because the flame is enveloped in the outer swirl flow and combustion is completed without the flame touching the furnace tube nor water tube, generation of soot and CO can be also suppressed. In some cases, improvement in boiler efficiency may be attained as low-oxygen combustion becomes possible, and this is a big advantage of this countermeasure.

Fig. 15 shows the performance of the low-NOx burner in the seventeen flue and smoke tube boilers and water tube boilers of 2-15 tons/hr evaporation. NOx emission is greatly influenced by the nitrogen content of various kinds of fuel and is furthermore changed sharply by boiler type, furnace load, burner type and other operating conditions. This low-NOx burner has a 30-60% reduction of NOx emission, and its reducing effect becomes more remarkable for lighter oil.

4. LOW-NOx EMISSION BURNER FOR PELLETIZING KILNS

Fig. 16 shows the effect of fuel-injection angle on NOx emission in the variable multifuel-firing burner in the experimental furnace. The ratio of coal and coke-oven gas is 1:1 in caloric value. The NOx values are low when pulverized coal is injected at the center and the injection angle of coke-oven gas is zero. The mixing between coke-oven gas and air is delayed at the injection angle of zero, and this results in low flame temperature and low thermal NOx. Furthermore, the oxygen concentration around the coal particles in the flame is low due to consumption by coke-oven gas at first; this suppresses production of fuel NOx from coal.

Fig. 17 shows the effect of O_2 on NOx emission in the variable multifuel-firing burner. The NOx values in multifuel firing of coke-oven gas and coal are lower than those of coke-oven gas or coal combustion. Fig. 18 shows the effect of multifuel-firing percentage on NOx emission in the experimental furnace and the pelletizing kiln as shown in Fig. 19. The NOx values decrease with a decrease in the number of the coal injection holes and an increase of the multifuel-firing percentage of coal. The low-NOx combustion developed in the experimental furnace has the same tendency as the pelletizing kiln.

5. LOW-NOx COMBUSTION FOR CEMENT PLANTS

Kobe Steel, Ltd. (KOBE) and Nihon Cement Co., Ltd., (NIHON) have jointly developed the "DD Process" (Dual Combustion and Denitration Process). In 1976, after completion of the basic research, a 480 t/d plant was installed in the Saiki plant of NIHON, the operating data from which enabled us to develop a commercial plant of the DD process. KOBE has supplied a 3600 t/d NSP utilizing the DD process to the Kamiiso plant of NIHON (Fig. 21).

The DD process is featured by the DD furnace, the precalcining furnace, installed between the fourth-stage cyclones and the rotary kiln. As shown in Fig. 22, the DD furnace can be divided into four zones according to its internal functions.

Fig. 23 shows the temperature distribution in the DD furnace with only the main burners (a) and with both the main and De-NOx burners (b). The highest temperature (900°C) can be seen in the central section (Zone III). However, the temperature distribution in the DD furnace is comparatively uniform and low, since distribution and mixing of the raw material in the furnace is good and there is no specific hot spot with a bright flame. When using De-NOx burners, the temperature of the upper section of Zone I is slightly high, but no specific change of temperature profile can be seen in Zones III and IV. The temperature near the side wall of the furnace is kept between 800°C and 860°C because of the screen formed by the falling raw material. It is observed through analysis of the gas by gas chromatography that about 90% of the fuel is burned in Zones II and III, while the remaining 10% is burned in Zone IV after passing through the orifice. Therefore, these superior combustion characteristics prevent clogging troubles in the succeeding cyclones which are caused by after-burning of unburned gas. Since no material falls down through the throat, and a high-density cloud of raw material is formed in Zone I, the temperature of the kiln exit gas decreases promptly as it enters from the bottom of the DD furnace.

Fig. 24 shows NOx distribution in the DD furnace with and without using De-NOx burners. Fig. 25 shows the distribution of the reducing gas components such as CO, H_2, and CH_4 in the DD furnace with and without using De-NOx burners. A summary of these figures is as follows. When only the main burners are in operation, the NOx level in the exit gas from the fourth-stage cyclones is 190 ppm, which means that NOx is not generated in the DD furnace owing to the fuel burning mechanism at the low temperature atmosphere and that even some NOx in the kiln exit gas is reduced. On the other hand, when both main and De-NOx burners are in operation, more reduction of NOx in the kiln exit gas is carried out and the NOx level at the exit of the fourth-stage cyclones is 110 ppm, which is the result of an approximately 40% reduction of the NOx amount in the kiln exit gas. It can be said that the decomposition of NOx occurs mainly in Zone II when using only the main burners and in Zone I when using the De-NOx burners.

The detailed results for this low-NOx combustion are available elsewhere.[15]

6. LOW NOx COMBUSTOR FOR GAS TURBINES

Fig. 26 shows a new experimental combustor for a gas turbine. Fuel such as kerosine or No.3 oil is sprayed into the premixing and prevaporizing Zone I by a primary pressure atomizer. In this zone, the fuel is mixed with preheated primary air, then it is vaporized. The mixture of fuel and primary air is ignited by a pilot pressure atomizer. The combustion occurs under fuel-lean conditions in the main combustion Zone II. The flame is kept stable by a swirler. The burnt gas is diluted by cooling air in the dilute Zone III to control the velocity distribution and temperature of the gas for a turbine.

Fig. 27 shows the comparison of NOx emission between a new premixed, prevaporized, fuel-lean combustor and a conventional diffusion combustor. The NOx of the conventional combustor is hardly affected by the overall air/fuel ratio. However, the NOx of the new combustor is remarkably decreased with increase of the overall air/fuel ratio. This means that the new combustor shows a uniform combustion and low flame temperature in the main combustion Zone II. This results in the decrease of thermal NOx. The new combustor has a 90% NOx reduction under rated conditions.

7. CONCLUSION

Kobe Steel, Ltd. has developed low-NOx combustion for industrial furnaces, boilers, pelletizing kilns, cement plants and gas turbines. This low-NOx combustion has been successfully applied to many furnaces, boilers and plants. The most important features of experience gained in their application are as follows:

(1) Low-NOx emission burner for industrial furnaces

(a) NOx emission values (at 11% excess O_2 as standard) of more than 350 burners for various fuels are typically

butane, 30-50 ppm
C-heavy oil, 45-60 ppm
coke-oven gas, 45-60 ppm
kerosine, 30-50 ppm

(b) The burners increase flame radiation and optimize temperature distribution in the furnace. Fuel consumption in burners used in soaking pits and reheating furnaces shows a reduction of 5-10%.

(2) Low-NOx emission burner for boilers

NOx emission reduction of 30-60% has been attained in the seventeen boilers of 2-15 tons/hr evaporation. The boiler efficiency of the low-NOx burner is higher than that of the conventional burner by 2%.

(3) Low-NOx emission burner for pelletizing kilns

NOx values decrease with a decrease in the number of coal injection holes and an increase of the multifuel-firing percentage of coal in coke-oven gas and coal firing.

(4) Low-NOx combustion for cement plants

NOx value in the kiln exit gas in a 3600 t/d full-scale commercial plant has decreased to 110 ppm (10% O_2) by using De-NOx burners in the Dual Combustion and Denitration process. Heat consumption is 735 kcal/kg-cl for a clinker production of 3060 t/d.

(5) Low-NOx combustor for gas turbines

The new experimental combustor of a premixed, prevaporized and fuel-lean type has a 90% NOx reduction under rated conditions.

NOMENCLATURE

T_f	flame temperature, °C
H_L	lower calorific value of fuel, kcal/kg
Q_F	sensible heat of fuel, kcal/kg
Q_A	sensible heat of combustion air, kcal/kg
G	combustion exhaust (flue) gas quantity, kg/kg of fuel
C_p	specific heat at constant pressure of combustion gas (flue gas), kcal/°C kg
[illegible]	radiant heat release from flame, %
A_f	flame surface area, m^2
σ	Stefan-Boltzmann constant=4.88×10^{-8} $kcal/m^2hK^4$
T_w	temperature of furnace or heated object, °C
ε_f	flame emissivity
ε_{CO_2}	emissivity of carbon dioxide
ε_{H_2O}	emissivity of steam
$\Delta\varepsilon$	correction term
ε_g	gas emissivity
pCO_2	equilibrium partial pressure of carbon dioxide, atm
pH_2O	equilibrium partial pressure of steam, atm
L	gas effective thickness, m
T	gas temperature, k
$[NOx]_{th}$	thermal NOx concentration, ppm
E	activation energy, 34.6 kcal/mol
R	gas constant

REFERENCES

1. B.P. Breen, et al. 13th Symposium (International) on Combustion, The Combustion Institute, 1971, p. 391.
2. D. Barnhard and E. Diehl. Control of nitrogen oxides in boiler flue gases by two-stage combustion, APCA, June 1959.
3. K. Yamagishi et al. 15th Symposium (International) on Combustion, The Combustion Institute, 1974, p. 1157.
4. D.W. Turner et al. Influence of combustion modification and fuel nitrogen content on nitrogen oxides emissions from fuel oil combustion, Presented at 64th Annual AIChE Meeting, San Francisco, November 1971.
5. T. Takagi et al. Evaluation of various factors affecting nitric oxide formation and effectiveness of some emission control system, Fuel, 53, 4, 1974, p. 114.
6. J.P. Tomany et al. A survey of nitrogen oxides control technology and the development of a low NOx emissions combustor, Trans ASME, Ser A, 93, 3, 1971, p. 293.
7. T. Suzuki and K. Morimoto. Development of low NOx air register for boiler, J. Jap. Boiler Assoc., 173, 1979, p. 34.
8. T. Suzuki et al. Heat transfer characteristics and practical applications of high efficiency, low NOx emission burners, J. Inst. Energy, 55, 1982, p. 216.
9. T. Suzuki et al. Development of high efficiency burners with low NOx emission, J. Inst. Energy, 55, 1982, p. 212.
10. T. Suzuki and K. Morimoto. NOx emission characteristics from kerosine and heavy fuel oil in high temperature furnaces, IFRF Doc. No. F29/1a/7, 1978.
11. Ya. B. Zeldovich. Acta Physicochim, USSR, 21, 1946, p. 577.
12. G.A. Lavoie. Combustion and Flame, 15, 1970, p. 97.
13. A. Schack. Arch Eisenhuttenwesen, 1939, p. 241.
14. H.C. Hottel and R.B. Egbert. Trans AIChE, 38, 1942, p. 531.
15. K. Ohno et al. 38th Cement Manufacturing Technical Symposium Reports, 1981 ,p. 46.

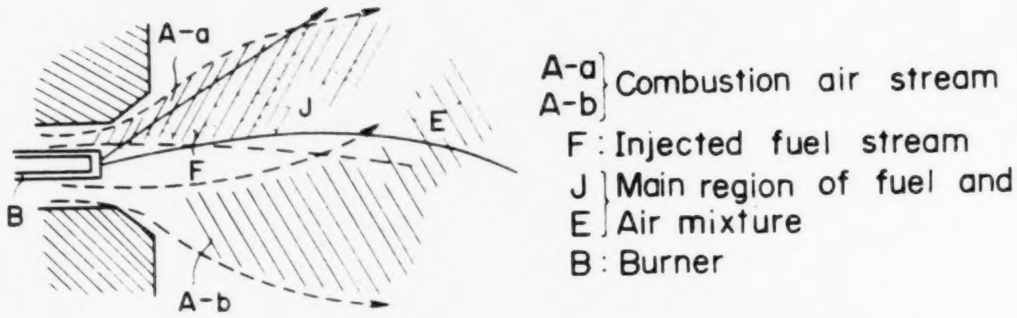

A-a
J
E
F
B
A-b
A-a
A-b
Combustion air stream
F : Injected fuel stream
J
E
Main region of fuel and
Air mixture
B : Burner

Fig. 1 Principle of combustion of model E low-NOx burner

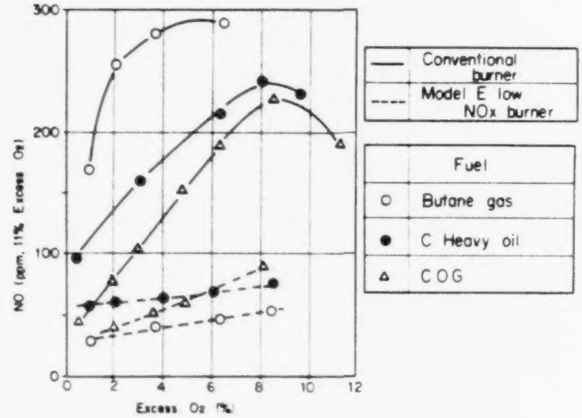

Fig. 2 Effect of excess O_2 on NOx emission (30° burner quarl)

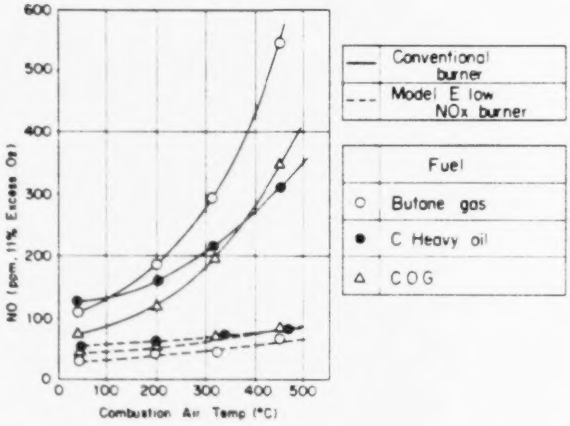

Fig. 3 Effect of combustion air temperature on NOx emission
(30° burner quarl)

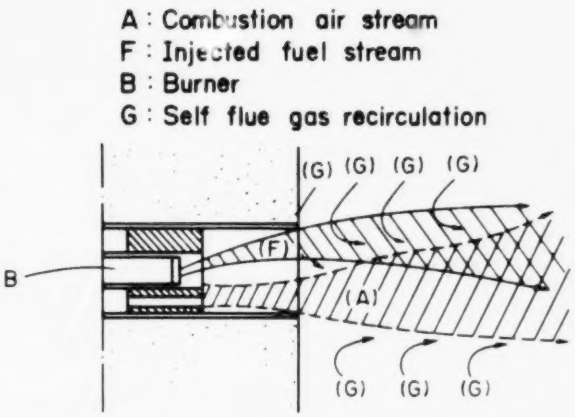
A : Combustion air stream
F : Injected fuel stream
B : Burner
G : Self flue gas recirculation
(G)
(F)
(A)
B

Fig. 4 Principle of combustion of model EE low-NOx burner

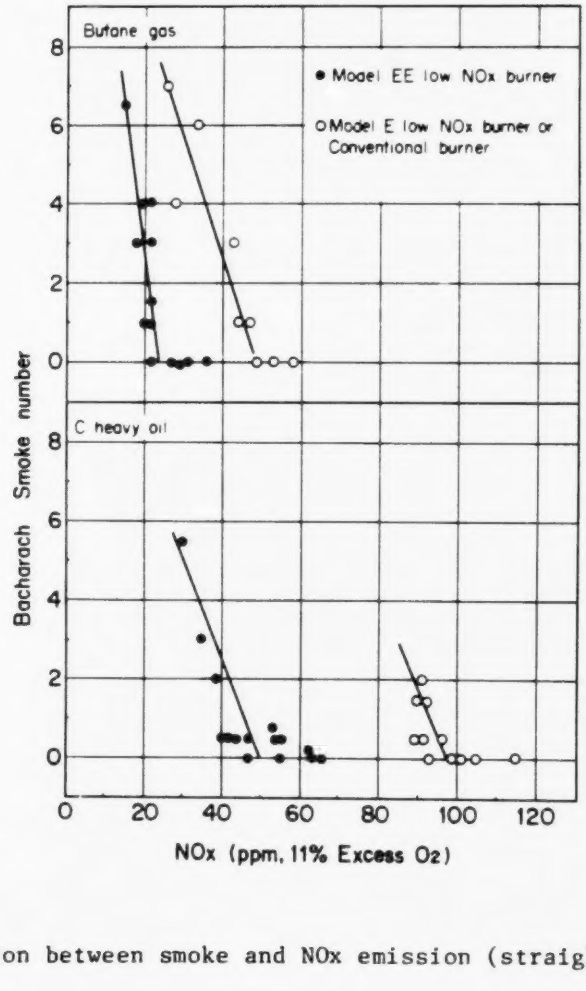

Fig. 5 Relation between smoke and NOx emission (straight burner quarl)

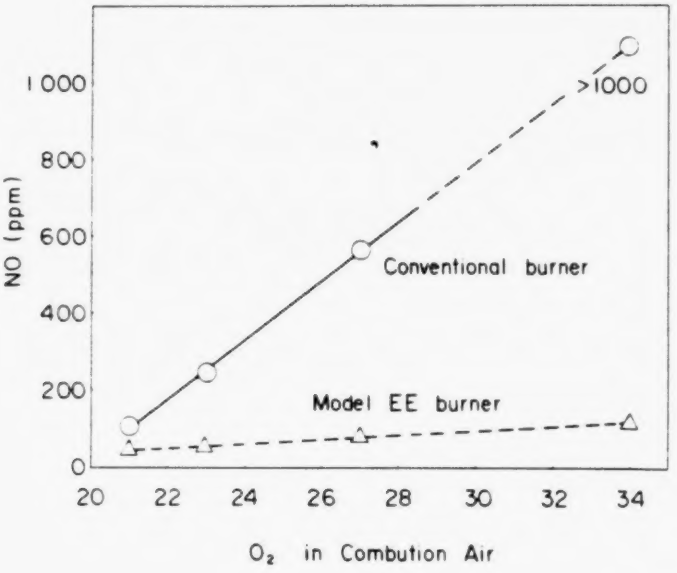

Fig. 6 Effect of oxygen enrichment on NOx emission

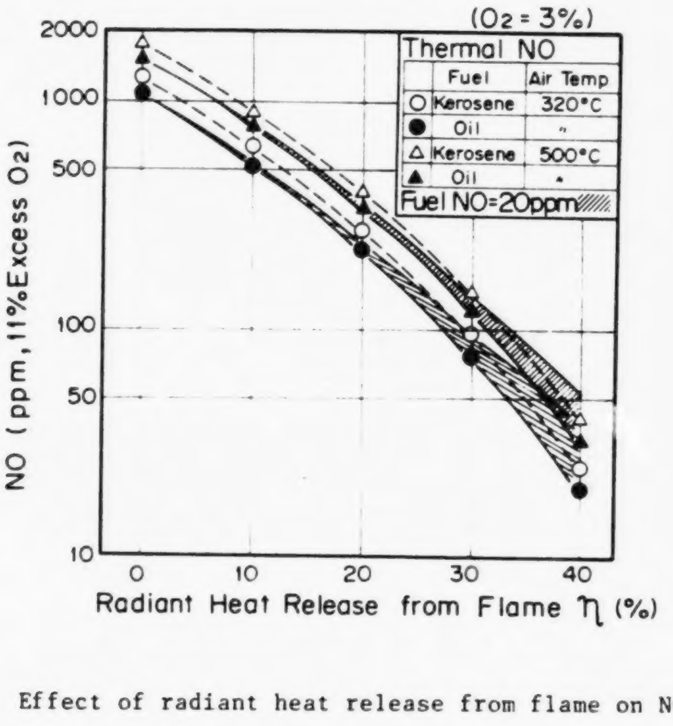

Fig. 7 Effect of radiant heat release from flame on NOx emission

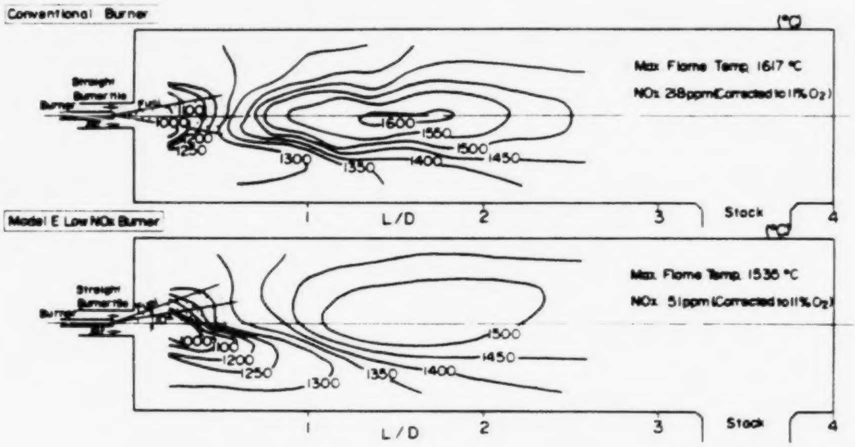
Conventional Burner
(°C)
Max Flame Temp. 1617 °C
NOx 218ppm(Corrected to 11% O2)
Straight
Burner tile
Burner
1600
1550
1500
1450
1400
1350
1300
1250
1200
1000
1100
1
L/D
2
3
Stock
4
Model E Low NOx Burner
(°C)
Max Flame Temp. 1536 °C
NOx 51ppm (Corrected to 11% O2)
Straight
Burner tile
Burner
1500
1450
1400
1350
1300
1250
1200
1100
1000
1
L/D
2
3
Stock
4

Fig. 8 Isotherms in combustion furnace

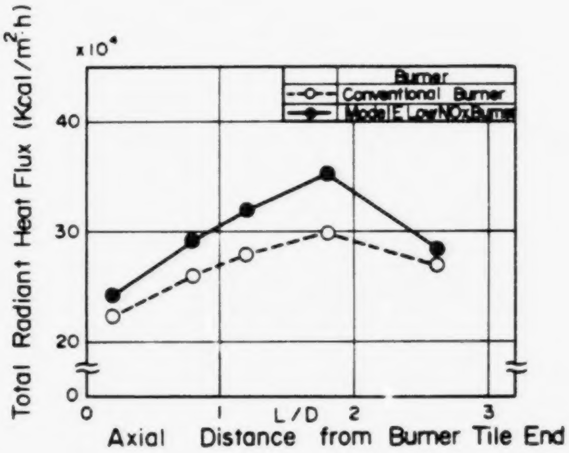

Fig. 9 Distribution of total radiant heat flux

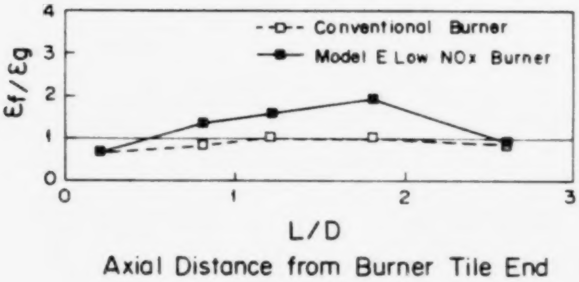

Fig.10 Relation between flame emissivity and burners

Table 1 Billet temperature raising characteristics in reheating furnace (heating capacity 75 tons/h)

		Ordinary combustion method		Slow combustion method	
Low load operation	Experimental time (min)	180		180	
	C-heavy oil consumption (l) (Preheating zone, upper heating zone)	800		794	
	Average temperature of billet surface (°C) Difference (°C)	Surface pyrometer 918.3	Optical pyrometer 901.8	Surface pyrometer 922.3 - 4.5	Optical pyrometer 908.8 - 7.0
Usual load operation	Experimental time (min)	105		105	
	C-heavy oil consumption (l) (Preheating zone, upper heating zone)	919		918	
	Average temperature of billet surface (°C) Difference (°C)	Surface pyrometer 981.2	Optical pyrometer 951.1	Surface pyrometer 1017.9 - 36.7	Optical pyrometer 984.4 - 33.3

Table 2 Soaking property of steel ingot

(10 hours after start of temperature raising)

Measuring position	Temp difference (°C)	
	Model E low NO$_x$ burner	Conventional burner
Top and bottom of ingot A	41	60
Top and bottom of ingot C	52	70
Wall side and inner side of ingot B	2	21
Top of ingot A and bottom of ingot C	90	120

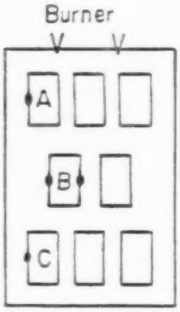

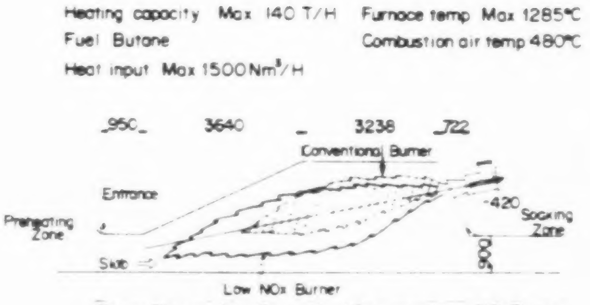
Heating capacity Max 140 T/H
Furnace temp Max 1285°C
Fuel Butane
Combustion air temp 480°C
Heat input Max 1500 Nm³/H
950
3640
3238
722
Conventional Burner
Entrance
Preheating Zone
420
Soaking Zone
900
Slab
Low NOx Burner

Flame Shapes of the Conventional Burner and Low NOx Burner

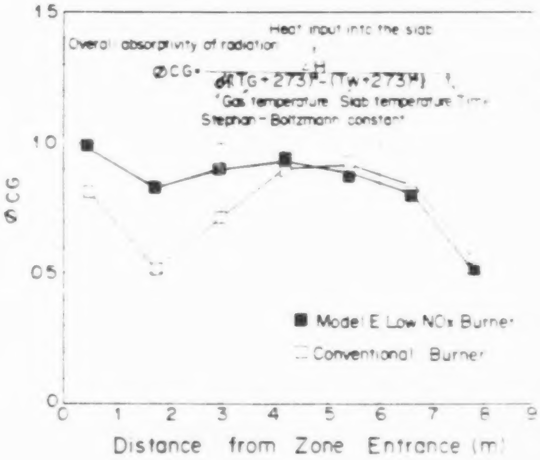

Fig.11 Overall absorptivity of radiation in upper heating zone in a continuous reheating furnace

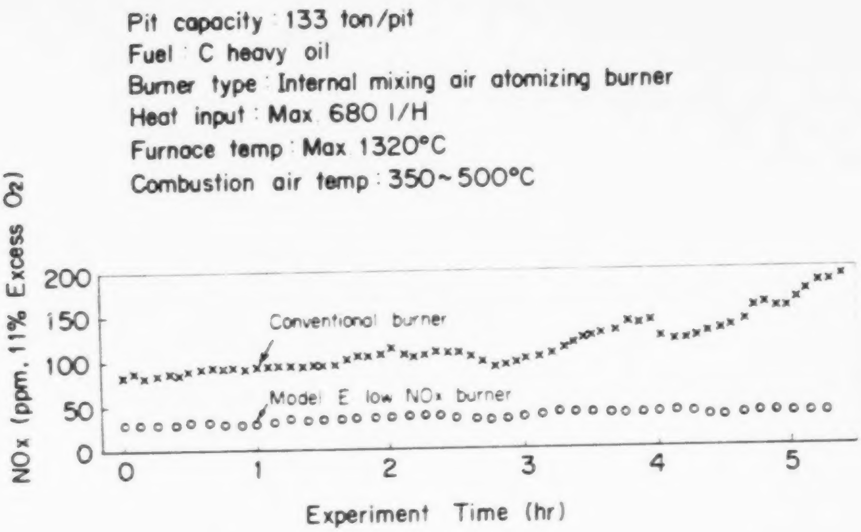

Fig.12 Comparison of NOx emission of heavy-oil firing in a top one-way soaking pit.

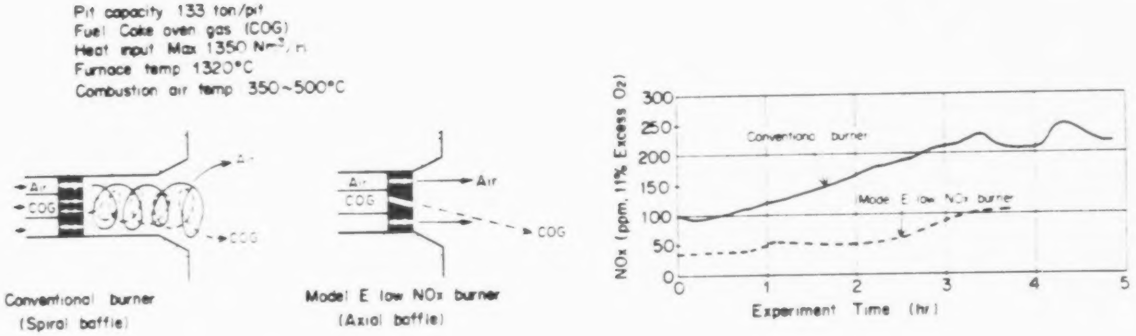

Fig.13 Comparison of NOx emission of coke-oven gas firing in a top one-way soaking pit.

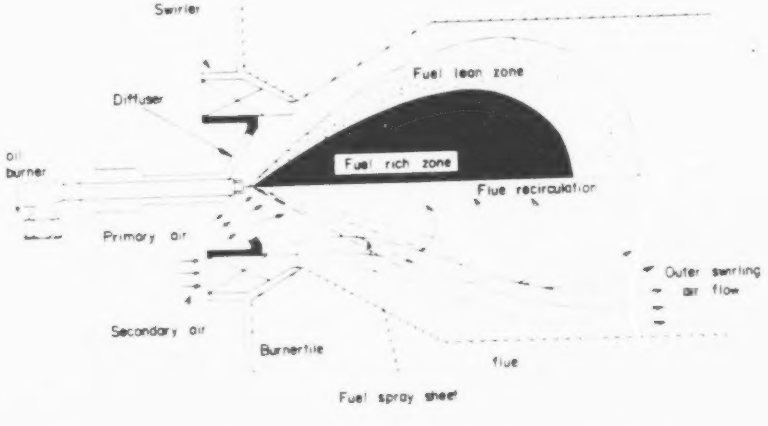
Swirler
Diffuser
Oil burner
Fuel lean zone
Fuel rich zone
Flue recirculation
Primary air
Outer swirling air flow
Secondary air
Burnertile
flue
Fuel spray sheet

Fig.14 Principle of reducing NOx emission of low-NOx burner for boilers

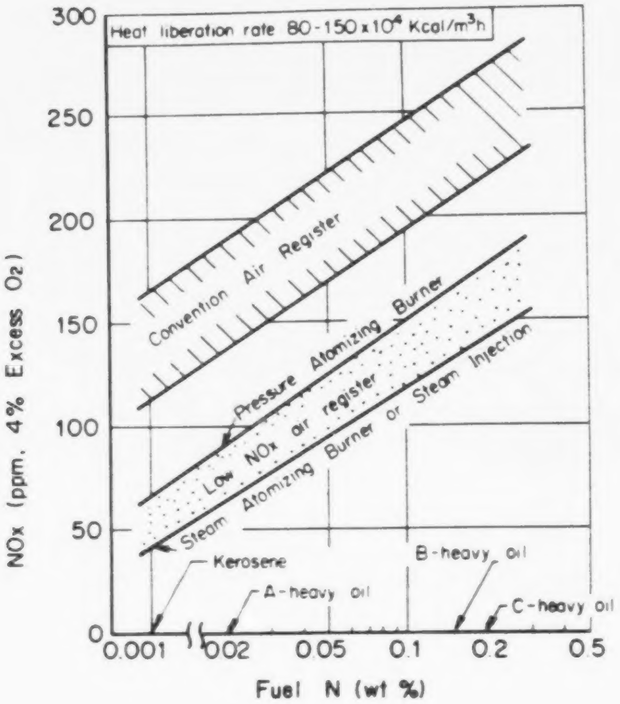

Fig.15 Performance of low-NOx burner for boilers

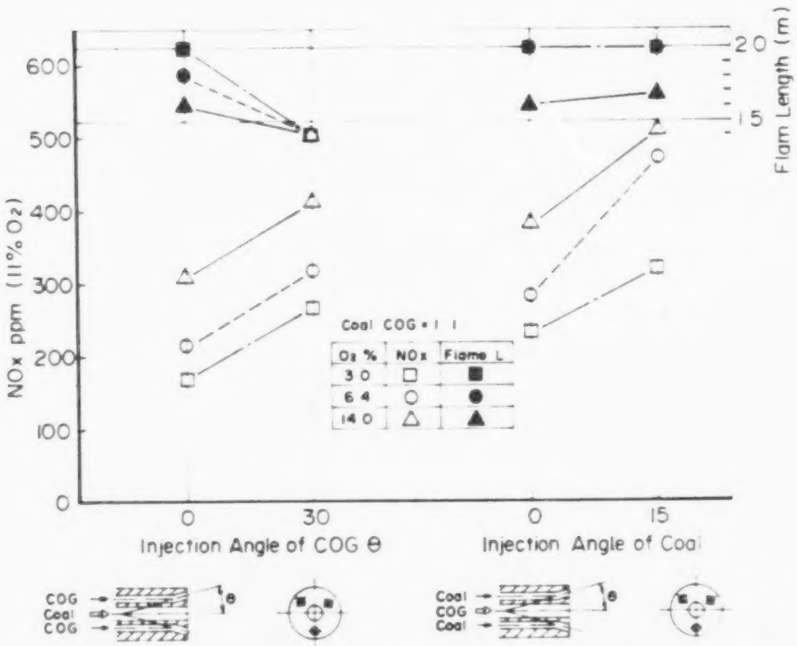

Fig.16 Effect of fuel-injection angle on NOx emission in coal and coke-oven gas firing

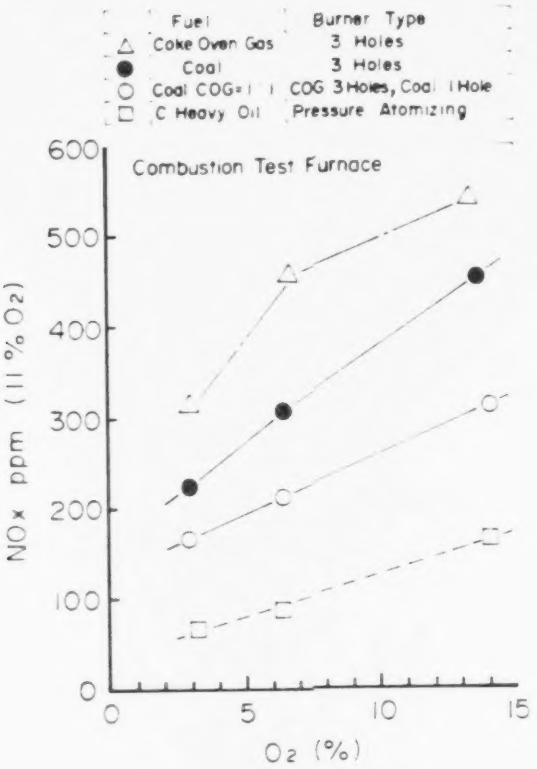

Fig.17 Effect of O_2 on NOx emission in multifuel firing

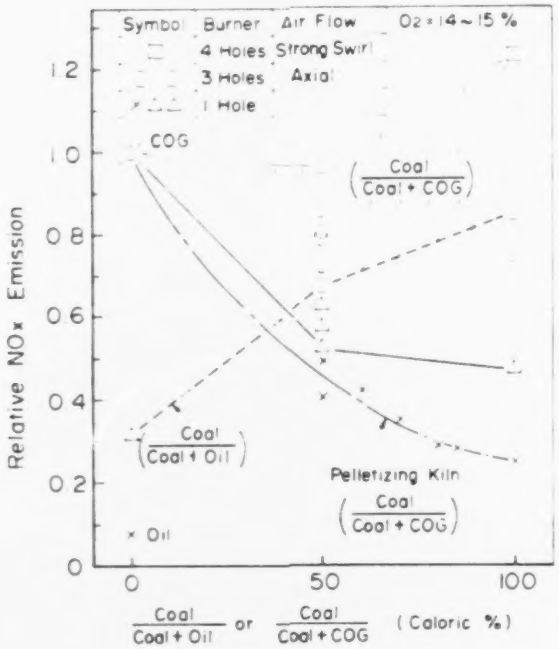

Fig.18 Effect of multifuel-firing percentage on NOx emission in experimental furnace and pelletizing kiln

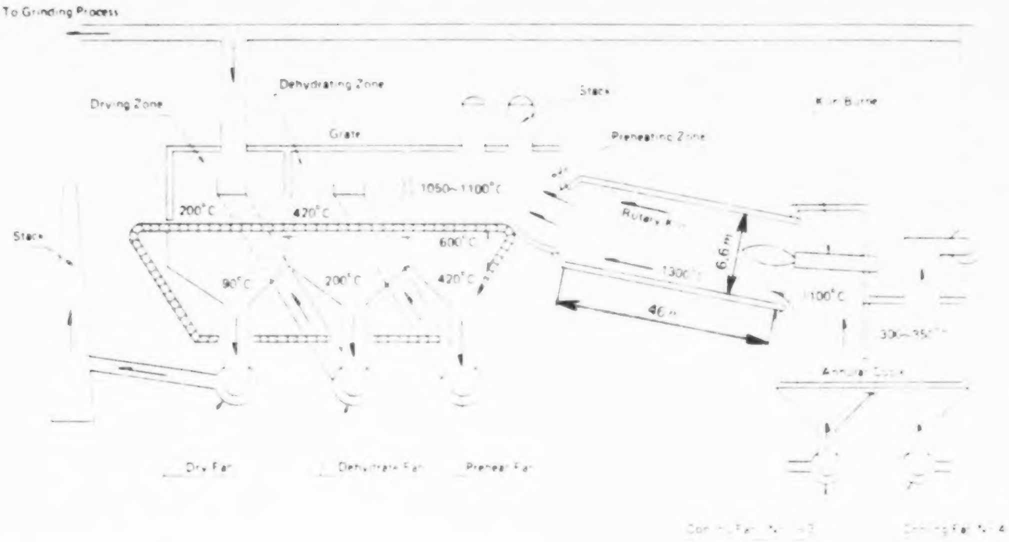
To Grinding Process
Dehydrating Zone
Drying Zone
Stack
Kiln Burner
Grate
Preheating Zone
1050~1100°C
200°C
420°C
Stack
600°C
Rotary Kiln
6.6m
90°C
200°C
420°C
1300°C
46m
1100°C
300~350°C
Annular Cooler
Dry Fan
Dehydrate Fan
Preheat Fan
Cooling Fan No.1~3
Cooling Fan No.4

Fig.19 Outline of pelletizing plant

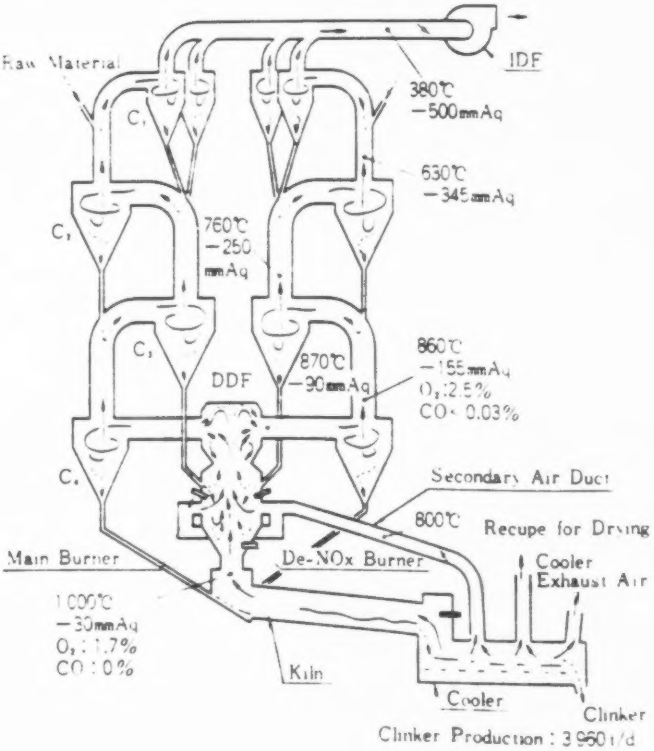
Raw Material
IDF
C_1
380℃
−500mmAq
630℃
−345mmAq
C_2
760℃
−250
mmAq
C_3
860℃
−155mmAq
O_2:2.5%
CO< 0.03%
DDF
870℃
−90mmAq
C_4
Secondary Air Duct
800℃
Recupe for Drying
Main Burner
De-NOx Burner
Cooler
Exhaust Air
1,000℃
−30mmAq
O_2: 1.7%
CO : 0%
Kiln
Cooler
Clinker
Clinker Production : 3,960 t/d

Fig.20 Outline of cement plant

Fig.21 General view of DD process

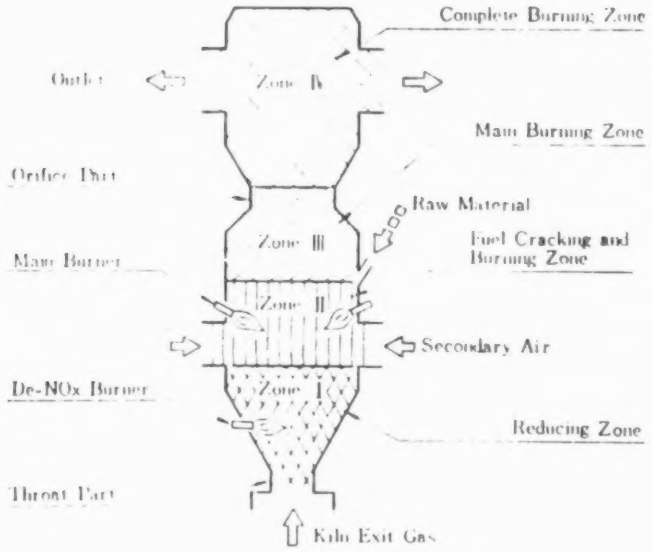
Complete Burning Zone
Outlet
Zone IV
Main Burning Zone
Orifice Duct
Raw Material
Zone III
Fuel Cracking and Burning Zone
Main Burner
Zone II
Secondary Air
De-NOx Burner
Zone I
Reducing Zone
Throat Part
Kiln Exit Gas

Fig.22 Various zones and their functions in DD furnace

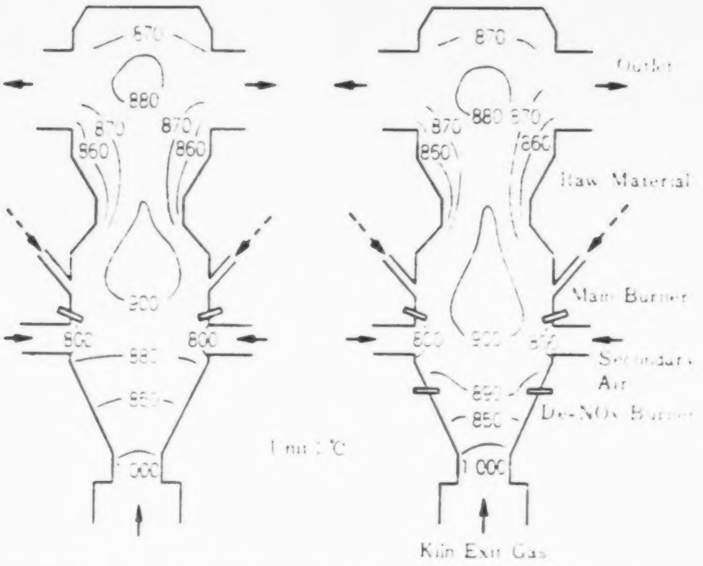
870
880
870
860
900
800
880
850
1 000
Unit : °C
Outlet
Raw Material
Main Burner
Secondary Air
De-NOx Burner
Kiln Exit Gas

a) With Main Burner Only b) With Main and De-NOx Burner

Fig.23 Temperature distribution in DD furnace

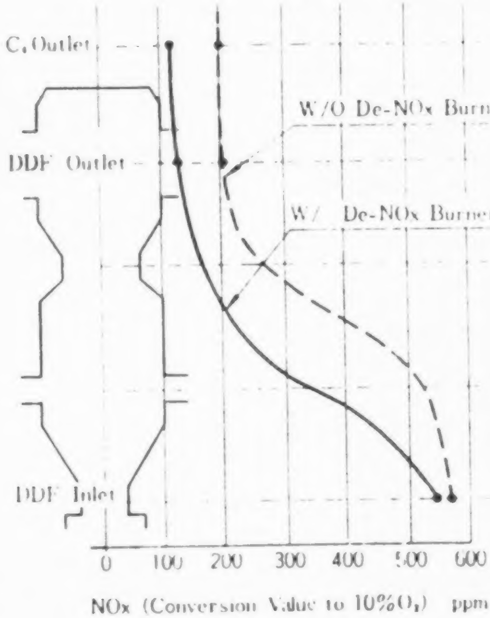

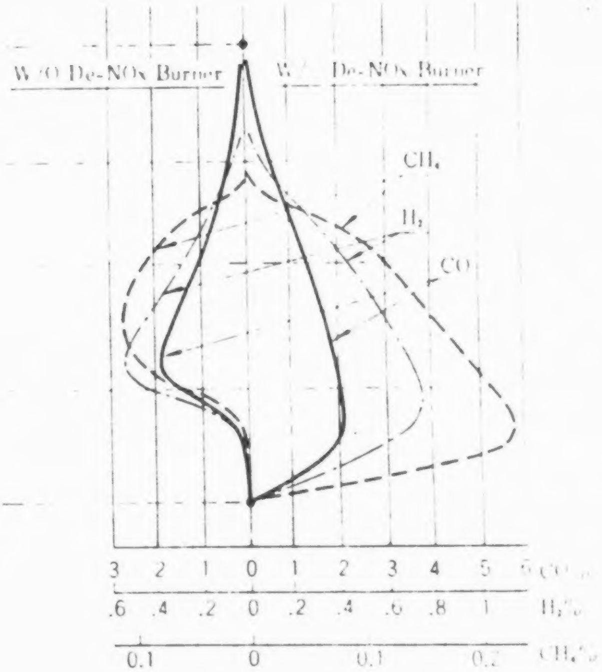

Fig.24 NOx distribution in DD furnace

Fig.25 Distribution of reducing gas components in DD furnace

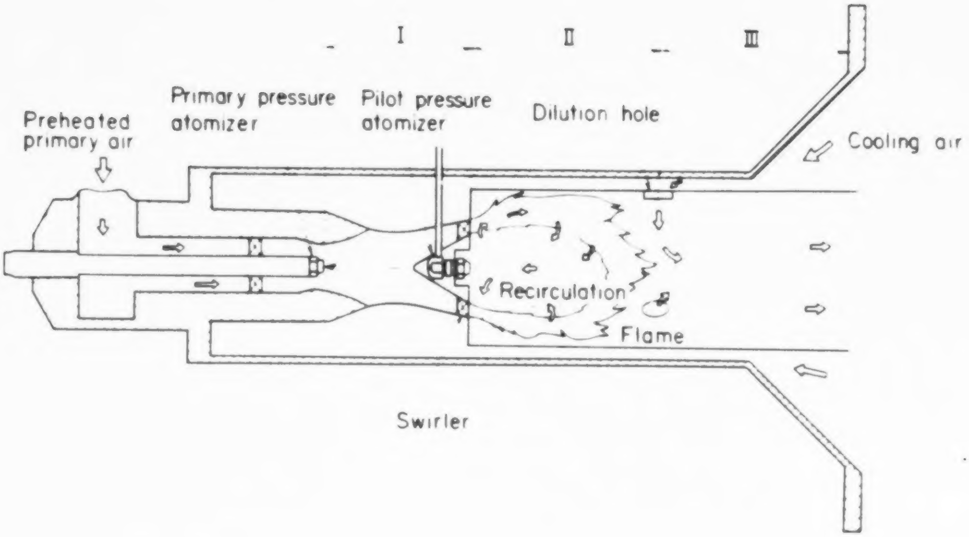
I
II
III
Preheated primary air
Primary pressure atomizer
Pilot pressure atomizer
Dilution hole
Cooling air
Recirculation
Flame
Swirler

Fig.26 New experimental combustor for gas turbine

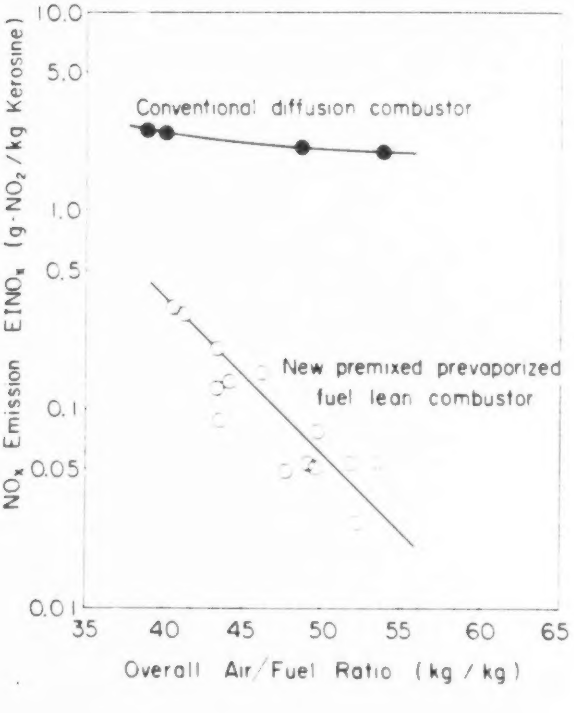

Fig.27 Comparison of NOx emission between new experimental combustor and conventional combustor

EMISSIONS ASSESSMENT OF COFIRING COAL AND WASTE PLASTIC IN A COMMERCIAL BOILER

L. R. Waterland, R. DeRosier, H. I. Lips, and H. B. Mason
Acurex Corporation
Energy & Environmental Division
555 Clyde Avenue
Mountain View, California 94039

ABSTRACT

This paper describes emission results obtained from field testing of a stoker-fired commercial boiler firing a coal/waste plastic mixture. The two tests were performed; one with the unit firing its typical coal fuel (test 1) and one with shredded waste polyethylene terphthalate (PET) beverage bottles added to the coal to about 16 percenty by weight in the mixed fuel (test 2). NO_x, total unburned hydrocarbon (TUHC), and solid particulate emissions were relatively unchanged for the two tests as was the emitted particle size distribution. Sulfur oxides emissions decreased with the coal/PET fuel in keeping with its lowered sulfur content; average CO emissions were also decreased. Flue gas emissions of most trace elements were comparable for both tests, as were the trace element compositions of corresponding ash streams. However, lead emissions were significantly increased for test 2. This increase reflects the increased lead content of the mixed coal/PET fuel. The cyclone hopper ash for the coal/PET test had consistently lowered leachable trace element and anion content than that for the coal fuel test. Total flue gas organic emissions were comparable for both tests, although levels of several semivolatile priority pollutants were higher for test 2.

INTRODUCTION

Some states, Vermont included, are now requiring deposits on beverage containers as a means of controlling litter and encouraging recycling and reuse as containers . The popular plastic beverage containers cannot be reused as containers. One means of reclaiming these is to use them as a fuel supplement in an energy recovery operation. In one such project, the use of waste PET bottles is being evaluated as a fuel supplement in a commercial boiler at a quarry and stone-cutting plant in Barre, Vermont. Past efforts have indicated that under proper operating conditions PET is a clean-burning, high-heating-value fuel with no apparent environmental problems associated with its use as a solid fuel supplement. The tests described in this paper were performed to confirm that this is the case by performing a comprehensive evaluation of the emissions and ash discharge compositions from the boiler burning its typical coal fuel and a coal/PET mixture.

The boiler tested was a coal-fired firetube unit with an underfeed stoker. The unit was rated at 0.6 kg/s steam at 100 kPa (4,640 lb/hr at 15 psig). Nominal full load coal feedrate was 180 kg/hr (400 lb/hr). The boiler was equipped with a cyclone collector for particulate emissions control.

TEST RESULTS

Boiler Operation

The test program called for flue gas emission measurements and ash discharge stream sampling with the boiler operating at constant, near-rated capacity with both fuels. Two tests were performed: test 1 with the unit firing its typical coal fuel, and test 2 with a coal/PET mixture containing about 16 percent by weight shredded PET beverage bottles.

Table 1 summarizes the boiler operating conditions and the fuel ultimate analysis for both tests. As indicated, test 2 was run at approximately the same coal feedrate as test 1 (110 kg/hr); however the test 2 fuel mixture contained about 20 kg/hr of added waste PET. Consequently heat input and boiler load were slightly higher for test 2. Boiler efficiency, calculated by the ASME heat loss method, was unchanged at about 79 percent.

Emission Measurements and Results

The sampling and analysis procedures used in this test program conformed to an extended EPA Level 1 protocol (1). All flue gas sampling was performed in the unit's stack, downstream of the cyclone collector, except for the continuous flue gas analyzers which were operated both at the stack and at the boiler exit. Emission measurements included:

- Continuous monitoring for O_2, CO_2, NO_x, CO, and TUHC
- Source assessment sampling system (SASS) for trace elements and semi- and nonvolatile organic emissions
- Volatile organic sampling train (VOST) for volatile organic emissions (test 2 only)
- Combined EPA Method 5/8 for particulate and sulfur oxides
- HCl train sampling
- Grab samples for N_2O analysis

In addition, samples of the fuel, bottom ash, and cyclone hopper ash were collected for analysis. The analysis protocol included:

- Performing proximate, ultimate, and heating value analyses of fuel samples, and ultimate analyses of bottom and cyclone hopper ash samples
- Analyzing the fuel, ash, ash aqueous leachates, and SASS train samples for 73 trace elements using spark source mass spectrometry (SSMS), supplemented by atomic absorption spectrometry (AAS)
- Analyzing ash aqueous leachates for selected anions using ion chromatography
- Analyzing VOST traps for the volatile organic priority pollutants
- Analyzing ash sample organic extracts for total nonvolatile organic content by gravimetry (GRAV)

- Analyzing the SASS train organic extract samples for total organic content in two boiling point ranges: 100° to 300°C by total chromatographable organics (TCO) analysis and >300°C by GRAV

- Analyzing the SASS train extract samples for the 58 semivolatile organic priority pollutant species, including many of the polynuclear aromatic hydrocarbon (PAH) compounds

- Performing infrared (IR) spectrometry analysis of organic sample extracts

- Performing liquid chromatography (LC) separation of selected sample extracts with subsequent TCO, GRAV, and IR analyses of eluted LC fractions

Bioassay tests were also performed on SASS train and ash samples to estimate their potential toxicity and mutagenicity.

Table 2 summarizes flue gas emissions measured in the test program. Emissions are presented as ng/J heat input and as mg/dscm of flue gas. As a measure of the potential significance of the emissions levels for further analyses, an occupational exposure guideline for most pollutants is also noted in the table. The occupational exposure guideline noted is either the time-weighted-average Threshold Limit Value (TLV) established by the American Conference of Governmental Industrial Hygienists (2), or the 8-hr time-weighted-averaged exposure limit established by the Occupational Safety and Health Administration (OSHA) (3). These are noted only to aid in ranking the potential significance of the emission levels. In this respect, pollutants emitted at levels several orders of magnitude higher than their occupational exposure guidelines might warrant further consideration, while species emitted at levels significantly lower than their occupational exposure guidelines might be considered of low potential concern. Only elements emitted at levels exceeding 10 percent of their occupational exposure guidelines in these tests are noted in Table 2.

Table 2 shows that flue gas concentrations of chromium, sodium, nickel, iron, lead, and cobalt were significantly higher for test 2 than for test 1. The test 2 flue gas levels for all these except cobalt were also greater than their respective occupational exposure guidelines. The high levels of all these except lead are thought to be artifacts of the sampling method employed, combined with some form of flue gas sample contamination with a corrosive compound. The SASS train sample accounting for the largest fraction of these elements in test 2 was the first impinger solution. This sample generally contains insignificant quantities of all but the most volatile elements (e.g., mercury). Indeed this was the case for test 1, and for most other elements in test 2. However, this sample had very high concentrations of the elements noted (except lead) as well as chlorine, fluorine, and sulfur. The fact that most of the elements noted are components of stainless steel (i.e., chromium, nickel, iron, and cobalt) suggests that some corrosive compound (e.g., sodium chloride, fluoride, and/or sulfate) was introduced into the SASS train for test 2, leading to artifically high apparent chromium, sodium, nickel, iron, and cobalt emissions.

The higher lead emissions for test 2, noted in Table 2, are thought to be actual increases. The coal/PET fuel had significantly higher lead content (28 ppm) than did the coal itself (3 ppm). The source of the added lead is indeed the waste PET. Unfortunately, the trace element emission levels noted in Table 2 for test 2 are based on an estimated 1 to 3 μm SASS train particulate emission rate and the assumption that the 1 to 3 μm particulate had the same composition as the less than 1 μm particulate (the 1 to 3 μm SASS particulate sample for test 2 was destroyed in transit from the field to the laboratory). Consequently, the significance of the increased lead emission levels cited deserves further study.

Emission levels of the other elements noted in Table 2 were quite comparable between the two tests. In fact, the trace element content of all SASS train samples (except the impinger solution and lead in the fine particulate noted above), the bottom ash, and the cyclone hopper ash were quite comparable for both tests.

The data in Table 2 show that boiler emissions of NO_x, solid particulate, and total semivolatile and nonvolatile organics were relatively unchanged with the addition of the PET to the boiler fuel. Stack concentrations of SO_2 and SO_3 were decreased, in keeping with the lower sulfur content of the coal/PET fuel (the apparently small difference noted in Table 2 is amplified considerably when corrected in each instance to a common flue gas O_2 level, e.g., 3 percent). CO emissions were decreased with the coal/PET fuel as well.

The HCl emission level noted in the table for test 2 corresponds to almost three times the amount which would be expected from the chlorine content of the fuel. The above discussion regarding the possible introduction of inorganic chloride into the SASS train suggests that perhaps extraneous chloride was introduced into the HCl train as well. This train measures total vapor phase (at stack temperature) inorganic chloride, not strictly HCl.

Further analysis of the SASS train organic sorbent module extract via LC fractionation and IR spectroscopy of both the total extract and the eluted LC fractions suggests that the organic emissions for both tests were roughly 25 to 35 percent aliphatic hydrocarbons, 40 percent less polar oxygenated hydrocarbons, and 25 to 35 percent more polar oxygenates.

Table 3 summarizes the organic priority pollutant emission results obtained. Emission levels of the semivolatile compounds detected were significantly increased with the coal/PET fuel, despite the fact that total semivolatile organic emissions were relatively unchanged. The phthalates noted in the table could be sample contaminants. Phthalates are common contaminants in SASS train samples at levels comparable to those noted in Table 3. However, the fact that levels detected in the test 2 samples were generally significantly higher than those in the test 1 samples, and that phthalates are expected to be found in PET, suggest that these compounds may actually have been present in the test 2 flue gas.

Table 3 also notes that several chlorinated C_1 and C_2 aliphatic hydrocarbons, chlorobenzene, toluene, and ethylbenzene were emitted during test 2 at levels ranging from <1 to about 24 μg/dscm. The levels of the aromatic hydrocarbons noted (toluene and ethylbenzene) are in the range typically encountered in VOST tests of combustion sources. The source of the chlorinated compounds is not clear, although these compounds do arise whenever chlorine, even inorganic chloride, is introduced into a combustion process. It is interesting that these compounds were detected in the test 2 flue gas, the same test with apparent chloride introduction into the SASS train, and unaccountably high (perhaps again due to extraneous flue gas chloride) chloride emissions measured with the HCl train.

Table 4 summarizes the results of the nonvolatile (GRAV) organic analyses of the bottom ash and cyclone hopper ash extracts. For test 1 only the cyclone hopper ash contained measurable levels of nonvolatile organics. For test 2, the organic content of the bottom ash increased, although that of the cyclone hopper ash was about half that for test 1.

Infrared spectra of bottom ash extracts suggests that only aliphatic hydrocarbons were present in these. Analyses of cyclone ash extracts via LC fractionation and IR spectrocopy suggests that these contain 30 to 40 percent aliphatic hydrocarbons, 15 to 20 percent less than polar oxygenated hydrocarbons such as aldehydes and ethers, 40 to 55 percent more polar oxygenates such as carboxylic acids, alcohols, and ketones.

Table 5 summarizes the concentrations of the priority pollutant trace metals in aqueous leachates of the ash stream samples prepared according to Level 1 guidelines (1). As a measure of the potential significance of these concentrations for further analyses, the water quality criterion (4) for each element is noted in the table. Again, these are noted only to aid in ranking the potential significance of the leachable element levels noted. Only elements having at least one leachate concentration greater than its water quality criterion are noted.

The data in Table 5 show that the cyclone ash leachates for both tests contained considerably higher levels of the inorganic priority pollutants than did the bottom ash leachates. The test 2 bottom ash leachate contained slightly higher levels of most of the elements noted. However, the cyclone ash leachate for test 2 contained significantly lower levels of all the elements noted (with the possible exception of mercury). This suggests that the addition of waste PET to the boiler's fuel may have had the beneficial effect of decreasing leachable toxic trace element discharges in the cyclone hopper ash stream.

Table 6 summarizes the leachable anion content of the ash stream aqueous leachates. As for the inorganic priority pollutants, the anion levels in cyclone ash leachates are significantly higher than those of bottom ash leachates. However, no consistent trend in composition between corresponding ash leachates for the two tests is apparent. Interestingly, the chloride and sulfate concentrations in the test 2 ash stream leachates are slightly lower than those from test 1. One might expect that if a corrosive component were present in the test 2 combustion gas, as implicated by the results of the SASS, HCl, and VOST analyses discussed above, evidence of this component would appear in the ash leachates, especially the cyclone ash leachate. An alternative explanation would be that the component was present in the vapor phase at the cyclone temperature, although this seems unlikely.

Bioassay tests were performed on the SASS train organic sorbent module extract and the ash stream samples. The health effects bioassay tests performed were the Ames mutagenicity assay, and the CHO cytotoxicity assay (5). The results of these assays are summarized in Table 7. The results suggest that the flue gas was of moderate to high toxicity and mutagenicity for both tests. The cyclone hopper ash had nondetectable toxicity for both tests. However, this sample's mutagenicity apparently decreased from borderline moderate/high in test 1 to borderline low/moderate for test 2. This observation is consistent with the decreased leachable arsenic and beryllium contents noted in Table 5, and confirm that the addition of waste PET to the unit's fuel may have had the beneficial effect of decreasing the potential environmental hazard posed by this discharge.

The positive Ames responses for the sorbent module extracts noted above are typical for such extracts from SASS tests of combustion sources. Current studies are investigating whether such bioassay responses are due to artifact compounds formed when combustion product gas containing NO_x is passed over XAD-2 resin.

ACKNOWLEDGEMENTS

This work was supported by EPA under Contract 68-02-3188. The guidance and support of the EPA Project Officer, Robert E. Hall, is gratefully acknowledged. The authors also wish to recognize the support and cooperation of the several State of Vermont and Rock of Ages Corporation personnel who contributed to the test program.

REFERENCES

1. D. E. Lentzen, et al., "IERL-RTP Procedures Manual: Level 1 Environmental Assessment (Second Edition)," EPA-600/7-78-201, NTIS PB293795, October 1978.

2. "Threshold Limit Values for Chemical Substances and Physical Agents in the Work Environment with Intended Changes for 1983-84," American Conference of Governmental Industrial Hygienists, Cincinnati, Ohio, 1983.

3. OSHA Safety and Health Standards, 29 CFR 1910, Subpart Z.

4. 45 FR 79318, November 28, 1980.

5. D. J. Brusick, and R. R. Young, "IERL-RTP Procedures Manual: Level 1 Environmental Assessment, Biological Tests," EPA-600/8-81-024, NTIS PB 81-228766, October 1981.

Table 1

SUMMARY OF BOILER OPERATION AND FUEL ANALYSES

	Test 1 (Coal Fuel)	Test 2 (Coal/PET Fuel)
Boiler operation (over the SASS sampling period)		
Steam load, kg/s (10^3 lb/hr)	0.38 (3.0)	0.42 (3.3)
Steam pressure, kPa (psig)	17 (2.5)	21 (3.0)
Feedwater inlet temperature, °C (°F)	12 (54)	13 (55)
Stack temperature, °C (°F)	146 (295)	165 (329)
Firebox temperature, °C (°F)	768 (1,415)	882 (1,620)
Fuel feedrate, kg/hr (lb/hr)	110 (240)	130 (285)
Excess air, percent	47	77
Boiler efficiency, percent	79.3	79.1
Fuel ultimate analysis (percent by weight as fired)		
Carbon	69.5	71.4
Hydrogen	5.2	5.5
Sulfur	1.0	0.6
Nitrogen	1.5	1.4
Oxygen[a]	11.4	11.7
Ash	8.5	6.8
Moisture	2.7	2.4
Chloride	0.2	0.2
Higher heating value, kJ/kg (Btu/lb)	31,212 (13,450)	31,270 (13,479)
PET, weight percent	0	16.4

---

[a] By difference.

Table 2

SUMMARY OF FLUE GAS EMISSIONS[a]

Component	Test 1 (Coal Fuel)		Test 2 (Coal/PET Fuel)		Occupational Exposure Guideline (mg/m^3)[b]
	(ng/J heat input)	(mg/dscm)	(ng/J heat input)	(mg/dscm)	
Major constituents:					
NO_x (as NO_2)	176	270	165	280	6.0
SO_2	800	1,210	690	1,160	5.0
SO_3	4.6	7.0	3.4	5.7	1.0
CO	69	105	38	64	55
HCl	--[c]	--[c]	206	347	7.0[d]
Solid particulate	35	54	41	69	10[e]
Total semivolatile organics (TCO)	0.049	0.075	0.071	0.12	--[f]
Total nonvolatile organics (GRAV)	0.575	0.875	0.641	1.08	--[f]
Trace Elements:					
Chromium, Cr	0.0065	0.010	3.03	5.17	0.05
Sodium, Na	0.42	0.65	63	107	2.0[d]
Nickel, Ni	0.017	0.027	2.23	3.81	0.10
Iron, Fe	2.05	3.18	16.2	27.6	1.0
Lead, Pb	0.020	0.030	0.65	1.10	0.050[g]
Phosphorus, P	1.39	2.15	0.79	1.35	0.10
Arsenic, As	0.011	0.017	0.029	0.049	0.010
Aluminum, Al	1.38	2.15	1.43	2.45	2.0
Lithium, Li	>0.017	>0.026	>0.081	>0.014	0.025
Calcium, Ca	1.24	1.93	0.28	0.49	2.0
Beryllium, Be	0.00063	0.00097	0.00093	0.0016	0.002
Silicon, Si	>1.52	>2.36	3.00	5.12	10[e]
Potassium, K	0.59	0.91	0.57	0.97	2.0[d]
Cobalt, Co	0.0019	0.003	0.024	0.041	0.10
Cadmium, Cd	0.0016	0.0025	0.010	0.018	0.05[d]
Vanadium, V	0.011	0.018	0.0073	0.012	0.050
Copper, Cu	0.020	0.032	0.021	0.035	0.10[g]
Platinum, Pt	--[h]	--[h]	0.00031	0.00052	0.002
Silver, Ag	0.0017	0.0026	0.0010	0.0018	0.010
Selenium, Se	0.0068	0.010	0.024	0.041	0.20
Barium, Ba	0.036	0.056	0.012	0.021	0.50

---

[a] Flue gas O_2 and CO_2 averaged 7.0 and 12.0 percent (dry) for test 1 and 5.2 and 12.9 percent for test 2.

[b] Time-weighted average TLV (2) unless noted.

[c] HCl sampled for test 2 only.

[d] Ceiling limit.

[e] For nuisance particulate.

[f] No occupational exposure guideline applicable.

[g] 8-hr time-weighted-average OSHA exposure limit (3).

[h] Less than the method detection limit.

Table 3

SUMMARY OF ORGANIC PRIORITY POLLUTANT EMISSIONS

Compound	Emission Concentration (μg/dscm) Test 1 (Coal Fuel)	Emission Concentration (μg/dscm) Test 2 (Coal/PET Fuel)
Volatile organic priority pollutants:	--[a]	
Chloromethane		1.0
Chloroform		4.5
1,2-Dichloroethane		2.0
Trichloroethylene		24
Tetrachloroethylene		2.5
Toluene		14
Chlorobenzene		7.5
Ethylbenzene		0.7
Semivolatile organic priority pollutants:		
Naphthalene	2.2	16
Phenanthrene	<0.4	3.0
Fluoranthene	<0.4	2.2
Phenol	<0.4	20
Bis(2-ethylhexyl)phthalate	4.4	4.2
Diethyl phthalate	<0.4	6.0
Di-n-butyl phthalate	<0.4	0.4

---

[a] Volatiles sampled for test 2 only.

Table 4

ASH STREAM TOTAL ORGANIC CONTENT (mg/kg ash)

Sample	Total Nonvolatile Organics by Gravimetry Test 1 (Coal Fuel)	Total Nonvolatile Organics by Gravimetry Test 2 (Coal/PET Fuel)
Bottom ash	<80	220
Cyclone hopper ash	1,100	500

Table 5

PRIORITY POLLUTANTS IN ASH LEACHATES AT CONCENTRATIONS EXCEEDING THEIR WATER QUALITY CRITERIA

Element	Bottom Ash Leachate Concentration (μg/l) Test 1 (Coal)	Bottom Ash Leachate Concentration (μg/l) Test 2 (Coal/PET)	Cyclone Hopper Ash Leachate Concentration (μg/l) Test 1 (Coal)	Cyclone Hopper Ash Leachate Concentration (μg/l) Test 2 (Coal/PET)	Water Quality Criterion (mg/l)[a]
Arsenic	0.030	0.010	4.1	0.20	2.2×10^{-5}[b]
Beryllium	<0.001	<0.002	0.32	0.070	3.7×10^{-5}[b]
Nickel	0.01	0.02	4.0	0.80	0.0134
Selenium	0.10	0.10	0.80	0.20	0.010
Chromium	0.02	0.06	3.7	1.0	0.050
Cadmium	<0.001	0.004	0.17	0.10	0.010
Thallium	<0.001	<0.002	0.21	0.09	0.013
Mercury	0.002	<0.001	<0.001	<0.001	1.44×10^{-4}
Lead	<0.004	0.009	0.27	0.10	0.050
Barium	0.06	0.30	2.1	0.05	1.0
Antimony	<0.004	0.20	0.15	0.05	0.146

---

[a] (4)

[b] Water quality criterion based on cancer risk; level noted corresponds to increased lifetime risk of 10^{-5}.

Table 6

ASH STREAM LEACHABLE ANION ANALYSIS RESULTS

Anions	Concentration (mg/l) Test 1 (Coal Fuel) Bottom Ash Leachate	Concentration (mg/l) Test 1 (Coal Fuel) Cyclone Hopper Ash Leachate	Concentration (mg/l) Test 2 (Coal/PET Fuel) Bottom Ash Leachate	Concentration (mg/l) Test 2 (Coal/PET Fuel) Cyclone Hopper Ash Leachate
Chloride	2.6	300	1.3	180
Fluoride	0.25	0.46	0.10	1.8
Nitrate	<1.0	<10	<1.0	<10
Nitrite	<1.0	<10	<1.0	<10
Phosphate	<1.0	<10	<1.0	<10
Sulfate	300	29,000	220	12,000
Sulfite	20	5,000	20	5,000

Table 7

BIOASSAY RESULTS

Test	Sample	Bioassay Response[a] Ames Mutagenicity	 CHO Clonal Toxicity
1 (coal)	XAD-2 extract	H	M
	Bottom ash	ND	ND
	Cyclone hopper ash	M/H	ND
2 (coal/PET)	XAD-2 extract	M	H/M
	Bottom ash	ND	ND
	Cyclone hopper ash	L/M	ND

---

[a] ND -- Nondetectable mutagenicity/toxicity
L -- Low mutagenicity/toxicity
M -- Moderate mutagenicity/toxicity
H -- High mutagenicity/toxicity

A LOW-NO_x BURNER FOR GAS-FIRED FIRETUBE BOILERS

John P. Kesselring and Wayne V. Krill
Alzeta Corporation
2343 Calle Del Mundo
Santa Clara, California 95054-1008

ABSTRACT

A field evaluation program has been conducted under sponsorship of the Gas Research Institute to evaluate the durability of the fiber burner in gas-fired firetube boilers. The fiber burner is a radiant surface burner that typically operates with NO_x emissions of 15 ppm, CO emissions of 20 ppm, and essentially no hydrocarbons. Under this program, four firetube boilers ranging in size from 245 kW (25 hp) to 960 kW (100 hp) were retrofit with the fiber burner and operated for up to 24 months. Tests of the burners installed at these sites show a one to two percentage point increase in efficiency, 80 percent reduction in NO_x, and up to 80 percent reduction in CO. In addition, the ability of the burner to allow increased boiler loads has been demonstrated, and flame noise has been virtually eliminated.

INTRODUCTION

The Pyrocore® fiber burner for firetube boiler applications has been evaluated in field testing and is rapidly approaching commercialization. Burner development and field evaluation have been supported over the previous 3 years by the Gas Research Institute. This paper describes the boiler performance results from these tests, continuing the earlier development of the burner concept reported at the 1983 International Gas Research Conference in London (1).

The Alzeta gas-fired ceramic fiber burner is a premixed, power burner that uses a radiant ceramic surface as the heat source rather than a conventional suspended flame. As shown in Figure 1, the burner consists of a porous layer of ceramic fibers through which premixed gaseous fuel and air are passed and ignited on the outer surface. The surface glows flamelessly and uniformly at about 1,270K (1,800^{o}F). It operates at very low excess air and pressure drop, turns on and off instantly, is noiseless, and is not susceptible to thermal shock.

Major advantages of the burner are its very low NO_x emissions -- 15 ppm -- and the enhanced efficiency of the radiant section of the heat exchanger. The low NO_x level is due to the low combustion temperature which suppresses thermal NO_x formation. Enhanced radiation promotes greater heat transfer in the system's radiant section and results in lower stack gas temperatures. In firetube boilers, a one to two percentage point increase in boiler efficiency is typical.

The burner operates at a nominal heat release rate per unit area of burner surface of 315 kW/m^2 (100,000 Btu/hr-ft^2). Because the heat input is based on surface area, the burner is easily scalable. Burners ranging in size from 4.4 kW

(15,000 Btu/hr) up to 290 kW (10^6 Btu/hr) are made using the same type of support structure and forming techniques. Also, the burner can be made in a variety of geometric shapes, notably flat plates and cylinders. This versatility makes the burner appropriate for a variety of industrial uses.

The advantages of the fiber burner in firetube boilers were first proven in laboratory tests of a 245-kW (25-hp) low-pressure steam boiler sponsored by the U.S. Environmental Protection Agency. A one-piece burner was constructed and operated for over 1,300 hours. During the test, NO_x emissions were reduced by 80 percent with CO and HC emissions of the same levels as those from the conventional burner. In addition, excess air levels were reduced, resulting in a 1- to 2-percent boiler efficiency increase. Overfiring to 120 percent of rated load was also found possible without detrimental effects to boiler tube weldments.

These advantages are important in firetube boilers where 40 percent of the gas used in the U.S. industrial sector is consumed. In small- and medium-sized boilers used for industrial process and space heating, gas is the preferred fuel. The ability of the fiber burner to enhance natural gas's low pollutant and noise emissions and allow more efficient production of steam are of wide interest in the industrial market.

In initial concept tests, the single-piece burner design and the inherent 2-to-1 turndown ratio of the burner surface firing rate limited the boiler low fire rate to 50 percent of capacity. In addition, due to its large size and tight spacing within the combustion chamber, the single-piece burner presented some problems in installation as a retrofit system. Therefore, a segmented burner was devised as the solution to size and turndown problems. These refinements provided the basis of the field evaluation phase of the program.

OBJECTIVES

The objective of the burner field evaluation was to implement the required design changes to the burner and demonstrate durability in field service. An assessment of user acceptance and analysis of burner cost versus benefits are being performed to accelerate commercialization. These objectives have been met by Alzeta and its subcontractor, York-Shipley, Incorporated, by retrofitting fiber burners in four industrial boilers at different sites and testing the system performance for varying periods at each site. Thermal and emissions performance goals are at least a 1-percent thermal efficiency increase and less than 20 ppm NO on the retrofit boilers, and retrofit performance has been compared to baseline performance as measured with the conventional gas burner in place. Satisfactory burner durability, as evidenced by no change in thermal or emissions performance over the test period, is an additional goal. The plan for achieving these goals and the field test results are discussed in the following two sections.

TEST PLAN

The project was organized into five technical tasks, including:

1. Site selection

2. Burner design and fabrication

3. Site preparation

4. Installation

5. Field testing

Field boiler tests were planned for four locations within the United States: (1) West Coast, near Alzeta, (2) York-Shipley boiler test bay in York, Pennsylvania, (3) an industrial site near York-Shipley, and (4) Eastern Ohio, a unique potential market area due to the prevalence of Ohio Special boiler designs. Selection criteria to be satisfied by each host site included: (1) normally gas-fired boiler, (2) size range from 245 to 980 kW, and (3) adequate room for burner retrofit. Columbia Gas Systems personnel, particularly from Columbia Gas of Pennsylvania, provided instrumentation and site information for the industrial site near York-Shipley in Pennsylvania, and East Ohio Gas Company located the site and provided instrumentation for the Eastern Ohio field test.

All test sites were selected during the first 8 months of the project. The locations and boiler uses are listed in Table 1. All units are normally gas fired; sites 2, 3, and 4 also maintain capabilities for backup oil firing. Tests have been conducted at each of the sites. In addition, burner testing has been ongoing in the Alzeta laboratory to evaluate system design concepts developed during the project.

Since each field boiler had unique demands for process steam, burner data were obtained under various operating conditions and load schedules. At each site, data were taken on the boiler in the as-found condition and following optimization of burner O_2 levels for the conventional burner, and additional data were obtained at periodic intervals of the test duration of the fiber burner. Data generally included the input gas and/or feedwater rates, appropriate temperatures and pressures, and stack O_2 and CO levels. NO_x measurements were also made at Sites 3 and 4 as well as at the Alzeta lab. CO_2 and hydrocarbon emissions have been monitored at Alzeta.

BURNER DESIGN AND LABORATORY TESTING

Most firetube boiler installations have insufficient room at the burner and backwall ends of the boiler for insertion of a single-piece burner. These space limitations and the handling difficulties or larger burners required that the fiber burner be segmented. The shorter burner sections are thus sequentially inserted into the firetube until the burner is assembled to its total length.

Since burner segmenting represented a significant departure from one-piece burner design (requiring interfaces between burner sections), a prototype 245-kW segmented burner was designed and tested at Alzeta to evaluate the performance and durability of the concept prior to design of the field units.

Testing the burner allowed refinements to be made prior to construction of the burners for the 392-kW, two 588-kW, and 980-kW test sites. A second 245-kW burner of similar design to these units was also constructed and tested at Alzeta.

Initial testing of the prototype showed the need for a higher pressure combustion air blower to overcome pressure drop through the burner flow passages. The refined second design reduced burner pressure drop, allowing use of blowers similar in size to those used on conventional burners of the same firing rate. The 245-kW version of the field test burner is shown in Figure 2.

Testing of the laboratory 245-kW burner included performance measurements over ranges of excess air and boiler load, investigation of obtaining lower boiler loads by staging the operation of the burner segments, and durability evaluation to 500 hours of operation. Since more complete data could be obtained in laboratory testing, these results are described below.

NO, CO, and HC emissions for firing of one to four burner segments were obtained over a boiler load range of 12 to 125 percent. The four-segment data are shown in Figure 3. The data show:

- NO increases with load (i.e., burner surface temperature)
- HC was generally below 20 ppm
- CO was also below 20 ppm, except at low loads for the 1, 2, and 3 segment firing where surface firing rates approach the low capabilities of the burner material.

The resulting boiler efficiency is shown as a function of load in Figure 4, reaching 88 percent efficiency at 12 percent load.

Tests were also conducted to evaluate compatibility of the burner with existing control systems. On/off, high/low, and full modulation burner controls have all been qualified in the laboratory and were subsequently implemented in the field installation.

The successful emissions and efficiency performance of the laboratory burner provided confidence in the four-segment field site burner design. The listed program goals were left to be evaluated during the field tests described next.

FIELD INSTALLATION AND TEST RESULTS

At each of the four burner field sites initial preparations were made to the system to provide the necessary instrumentation and to determine available equipment and gas pressure. These activities allowed characterization of emissions and efficiency of each boiler with the conventional burner in place. Following retrofit of the burner, comparative emissions and efficiency measurements were made to evaluate the fiber burner effects on system operation. Each retrofit presented some unique demands and results, and the activities at each of the sites are described below in the order in which installations were performed.

York-Shipley Boiler Test Bay

The York-Shipley test bay is used for checkout of each assembled boiler prior to shipment. The test area contains utilities and available instrumentation for testing of newly manufactured boilers. The 588-kW (60-hp) boiler used in this project was new off the assembly line, set up with a modulating control system, and equipped with the required instrumentation.

The 588-kW boiler exhibited similar CO emissions to those of the 245 kW-boiler (both with conventional burners) at Alzeta. In general, 10 percent excess air represents the lower operating limit to maintain CO emissions below 20 ppm.

The 588-kW fiber burner was designed to accept the existing blower and burner controls. Required changes to the system included installation of a new pilot, switchover of flame controls from infrared to ultraviolet sensing,and removal of the boiler target ring. Additional viewports were also added to the boiler rear door. Completion of the retrofit required approximately 8 hours.

Following installation, tests were run under similar conditions to those for the conventional burner. Only limited CO data were obtained due to unavailability of instrumentation at York-Shipley. A comparison of boiler efficiency with the two burners is shown in Figure 5. Fiber burner data are shown primarily at 10 and 20 percent excess air. The fiber burner results in about a 0.5-percent increase in efficiency over that of the relatively efficient new conventional burner-equipped system. Figure 5 also shows the results of varying segment operation, reaching loads as low as 20 percent of rating.

Following installation in April 1983, the York-Shipley boiler was operated during two shifts per day, 5 days per week to accumulate test hours. At approximately 1,000 hours of operation in September 1983, significant reductions in maximum achievable load were encountered. Inspection of the burner flow passages showed large amounts of dust ingested from the test bay atmosphere. As maximum load approached 39 percent, the burner was removed from the boiler and returned to Alzeta. Combustion air filters for the blower were subsequently implemented as standard burner equipment at other test sites.

Vandenberg Air Force Base

The 392-kW (40-hp) test boiler at Vandenberg AFB is located in a dining room facility, providing low-pressure steam for cooking and cleaning. The boiler is in service with low load factors over much of the year and with a seasonally higher demand during the summer months to support ROTC activities. The boiler operates in an on/off mode (fixed firing rate) to maintain steam pressure of 10 to 13 psig, cycling several times each hour. This site therefore represented a good opportunity to test the burner's durability in cyclic operation.

Site preparation included installation of a gas meter at the boiler inlet to determine firing rate and to record total gas usage. With the conventional burner, the system was found to be operating at 62 percent of rated load. This operating condition was fixed by the blower air shutter which was frozen in a partially open position. Efficiency was measured as 81 percent with the fixed 55 percent excess air. The somewhat lower efficiency than had been achieved in prior 245-kW and 588-kW boiler testing is probably a result of the age of the unit (installed in 1966). CO emissions were relatively high at 240 ppm (corrected to 0 percent O_2).

Installation of the fiber burner was complicated by the age of the boiler, requiring modifications to the refractory and freeing of rusted and seized components. Retrofit was completed within 8 hours, and the burner was easily interfaced with the on/off control system.

Tests of the fiber burner produced a boiler efficiency increase at approximately 2 percent, comparable to prior 245 kW and 588 kW results. Excess air was set at approximately 15 percent, and CO ranged from 4 to 37 ppm (at 0 percent O_2).

The system has performed well for over 2 years, accumulating nearly 3,800 hours of use through the first 2 years of operation. Also, the burner has achieved approximately 60,000 cycles. Tests will continue through the 1985 summer use period.

Peter Paul Cadbury

The three boilers in the Peter Paul Cadbury plant in York, Pennsylvania supply process steam for the production of York Peppermint Patties and steam for space heating. Burner installation in July 1983, occurred during a period of low demand and directly followed a scheduled annual boiler inspection. Since total steam demand reaches available capacity during peak usage, overfire capabilities were of interest at the site. The fiber burner allowed 20-percent additional capacity while maintaining internal boiler gas-side temperatures at acceptable levels. The conventional burner was controlled by a high/low firing combination.

Site preparation was supported by Columbia Gas System Service Companies through the loan of two gas meters for the retrofit No. 2 588-kW (60-hp) boiler and its companion No. 1 boiler. A NO_x meter was also loaned during initial testing of the fiber burner. The No. 2 boiler was fitted with a feedwater meter by Alzeta.

The boiler was tested with the conventional burner both prior to and following the annual inspection. Prior to inspection, the boiler was found to be operating rich over most of the load range. Data was taken between the low and high points of 35 and 100 percent of rated load by manual movement of the modulating linkage. Since operation was rich, CO emissions always exceeded 2,000 ppm. Adjustments to the fuel-air ratio were also made at each load to provide data at 20 percent excess air. At the adjusted conditions, CO ranged from 85 to 400 ppm (at 0 percent O_2). The boiler efficiency was 83 percent at full load and about 2 percent less efficient that the new York-Shipley boiler.

Fiber burner installation at Peter Paul was somewhat more complex than at previous sites. Since the maximum achievable load on the York-Shipley boiler had been 98 percent, a higher pressure blower was required at Peter Paul to achieve overfire with the fiber burner. In addition, Peter Paul is located in an older area of the Columbia Gas system where available gas pressure is limited to 7 to 10 in. w.c. -- marginal for achieving the desired load. For these reasons, a sealed blower was installed for simultaneously compressing the mixed gas and air. Significant control wiring modifications were also required.

The data obtained for the Peter Paul boiler with the fiber burner have shown 0.5- to 1-percent increases in efficiency over that of the conventional burner. Significant reductions in CO were achieved from conventional burner levels of 85 to 400 ppm. With the fiber burner, CO ranged from 5 to 40 ppm over the rated load range. Limited measurements of NO_x varied from 8 to 20 ppm for the fiber burner.

In February 1984, following 7 months of operation, damage to the burner occurred in an incident apparently related to gas pressure fluctuations. Since a lower pressure drop, 2 to 1 modulation burner design was now available, a second burner was installed at Peter Paul in July, 1984. This burner ran successfully until January, 1985, when an incident very similar to the February, 1984 one occurred, again damaging the burner. A replacement burner and an improved control system were installed in April, 1985.

Hall Chemical Company

Hall Chemical Company in Wickliffe, Ohio, uses process steam in the manufacture of various metallic salts. The 980-kW (100-hp) Ohio Special boiler is an overfired 686-kW (70-hp) design, eliminating the need for a licensed operator under Ohio regulation. The burner operates in a high/low mode with the set point selected manually by plant personnel. Four other boilers exist at the plant. The site was prepared with the installation of gas and feedwater meters by East Ohio Gas Company personnel. East Ohio Gas has also supported data taking and arranged for NO_x measurements to be made by an independent contractor.

In an initial visit to Hall, data taken on the conventional burner showed the two load points to be 39 and 81 percent of rated load. Data were taken between these settings and up to 90 percent load (limited by maximum blower air shutter opening) by manual movement of the linkage. Prior to fiber burner installation, additional data at selected values of excess air were taken. The latter data are reported in comparison to fiber burner results. CO emissions were 40 to 110 ppm, and NO_x emissions were approximately 75 ppm at these adjusted conditions.

Fiber burner installation utilized the same blower and control system as for the conventional burner. Again, flame controls were modified to accept an ultraviolet flame sensor. Retrofit was completed within 8 hours. The Hall boiler and two sections of the fiber burner are shown in Figure 6.

Figure 7 shows conventional and fiber burner boiler efficiencies. Boiler efficiency was taken at three values of excess air for the conventional burner firing over its possible load range. Loads above 80 percent with the conventional burner were obtained only intermittently, as an instability developed in the flame at that load. Fiber burner data were taken primarily at 10 and 20 percent excess air at high and low loads, showing a nominal 1 percent increase in efficiency. CO and NO_x emissions were reduced by the fiber burner to 35 ppm and 15 ppm, respectively.

Three different burners were operated at Hall Chemical for 3,450, 2,500, and 1,500 hours, respectively. The first burner was operated with unfiltered combustion air and eventually became subject to severe load reduction capability, as was experienced at York-Shipley. The latter two burners both experienced a manufacturing inconsistency that resulted in shortened life of the fiber layer; this problem has now been solved.

CONCLUSIONS

A summary of the retrofit results to date at the four field test sites and the Alzeta laboratory is shown in Table 2, including the approximate number of operating hours. Improvements in efficiency of about 1 percent have been typical, meeting the goal of the program. Reductions in CO have been most significant in older boilers, and NO_x reductions to below 20 ppm were consistently achieved. In addition to the verification of these performance parameters, acceptable durability of burner design features and materials has been demonstrated and compatibility with a variety of existing ultraviolet-based control systems has been shown. User interest in the quiet operation, low emissions, and ability to overfire standard boilers by 20 percent above rated capacity has been high.

Calculations show that for each percentage point increase in boiler efficiency (typical for current installations) per 980 kW (100 hp), the gas savings are approximately $1,100 per year. At current projected production costs for burners of 980-kW size, payback would occur in 2 to 3 years. These early estimates show potential for commercialization of the burner concept.

The field test results indicate the need for longer duration operation and material evaluation to achieve the 5- to 10-year burner lifetime required in most industrial uses. Extension to larger boilers represents the next logical step. These systems will require more complex controls and the potential for distillate oil firing as an alternate fuel. These activities are proceeding as the burner approaches commercialization.

REFERENCES

1. R. Schreiber, W. Krill, J. Kesselring, R. Vogt, and M. Lukasiewicz. Industrial Applications of the Radiant Ceramic Fiber Burner, Alzeta Corporation, Mountain View, CA: IGRC/D06-83, 1983 International Gas Research Conference, June 13-16, 1983.

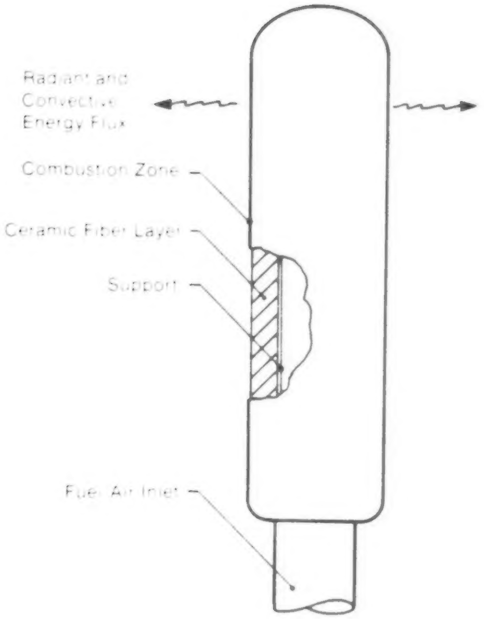
Radiant and
Convective
Energy Flux
Combustion Zone
Ceramic Fiber Layer
Support
Fuel Air Inlet

Figure 1. Ceramic Fiber Burner

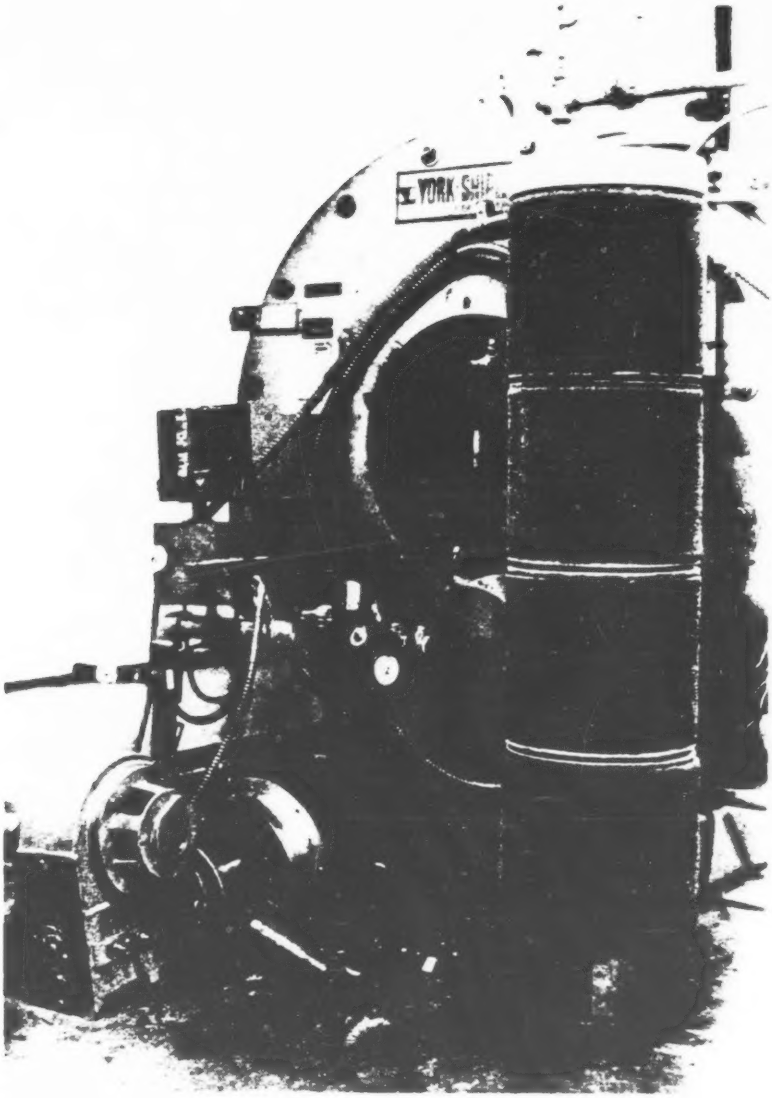

Figure 2. Four-Segment 245-kW Fiber Burner

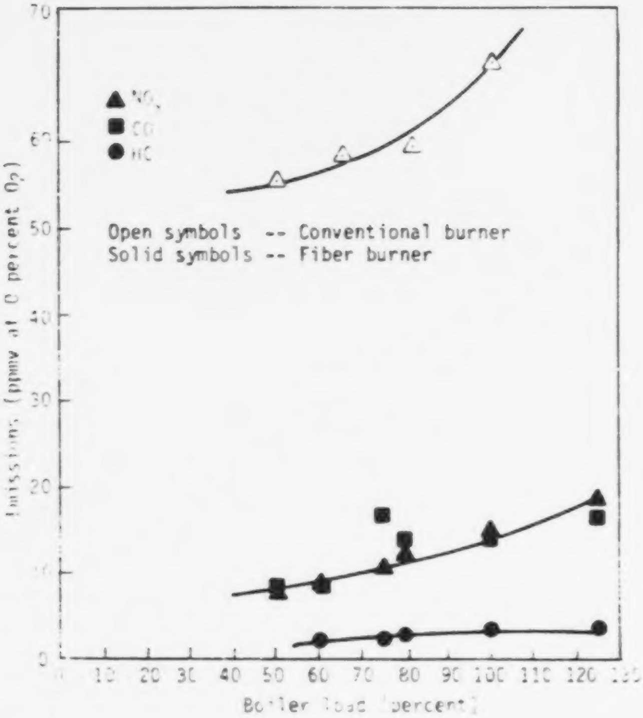

Figure 3. Four-Segment 245-kW Burner Emissions

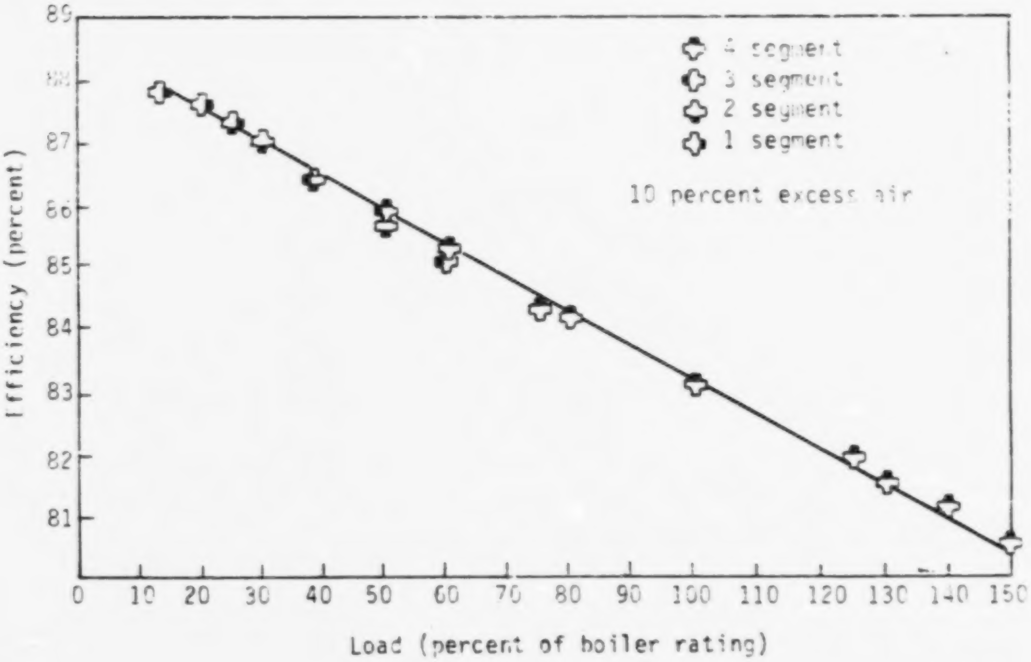

Figure 4. 245-kW Boiler Efficiency With Four-Segment Fiber

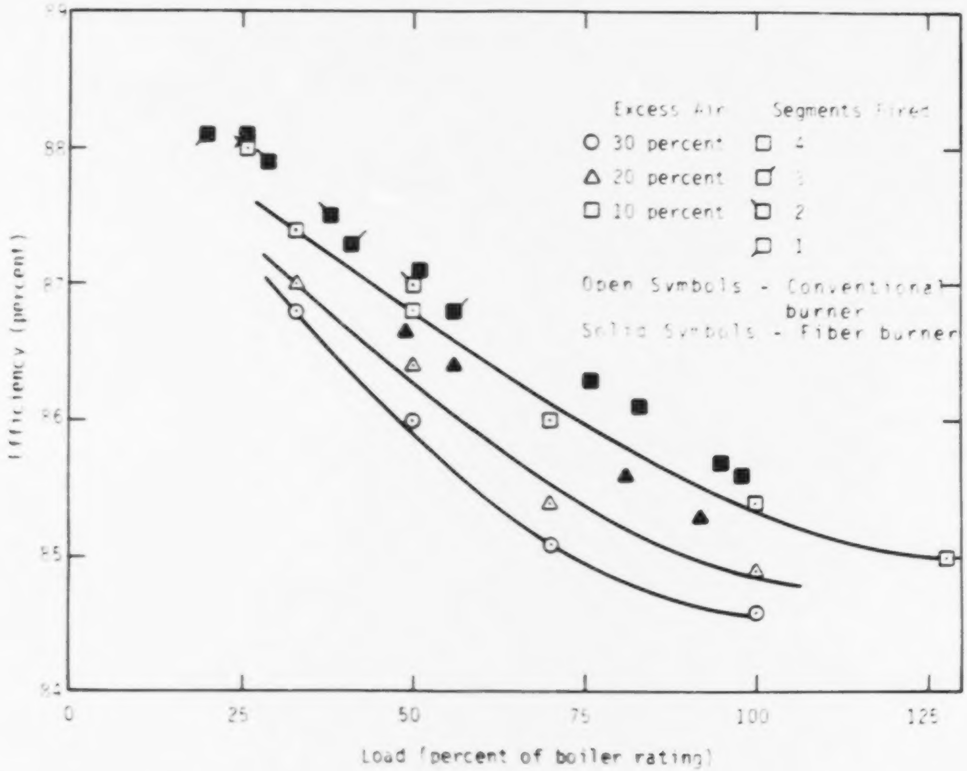

Figure 5. York-Shipley 588-kW Boiler Efficiency with Fiber Burner

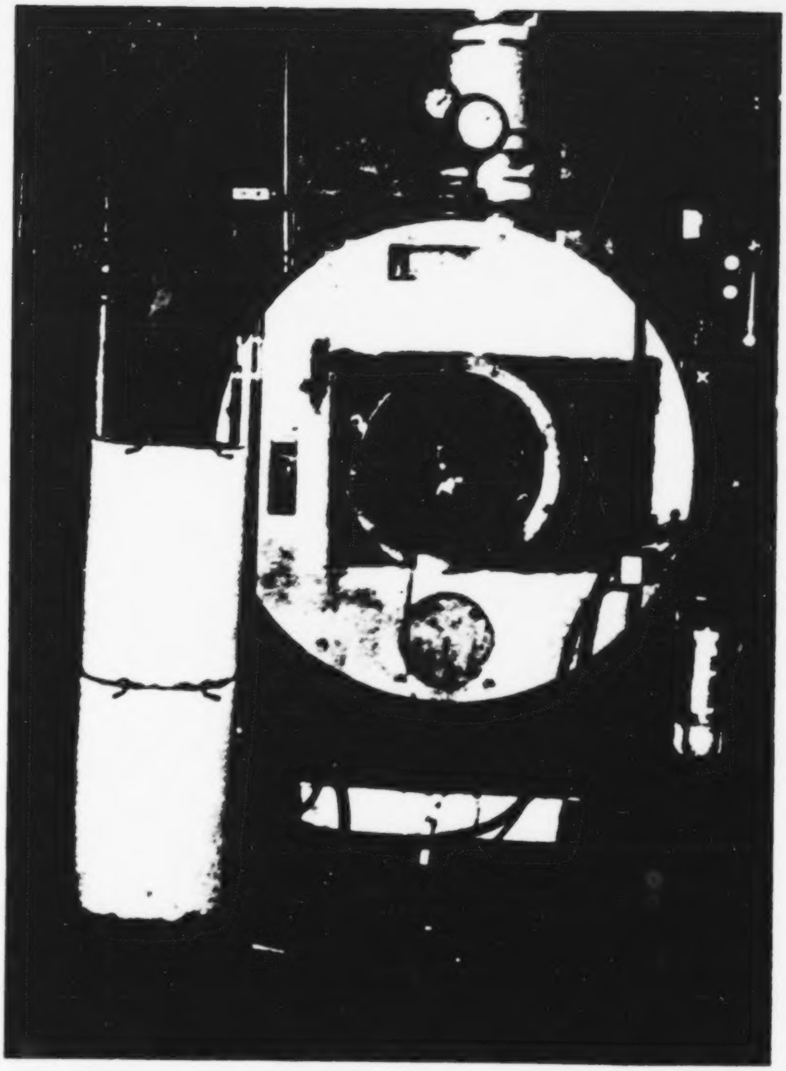

Figure 6. Hall Chemical Company 980-kW Ohio Special and Fiber Burner

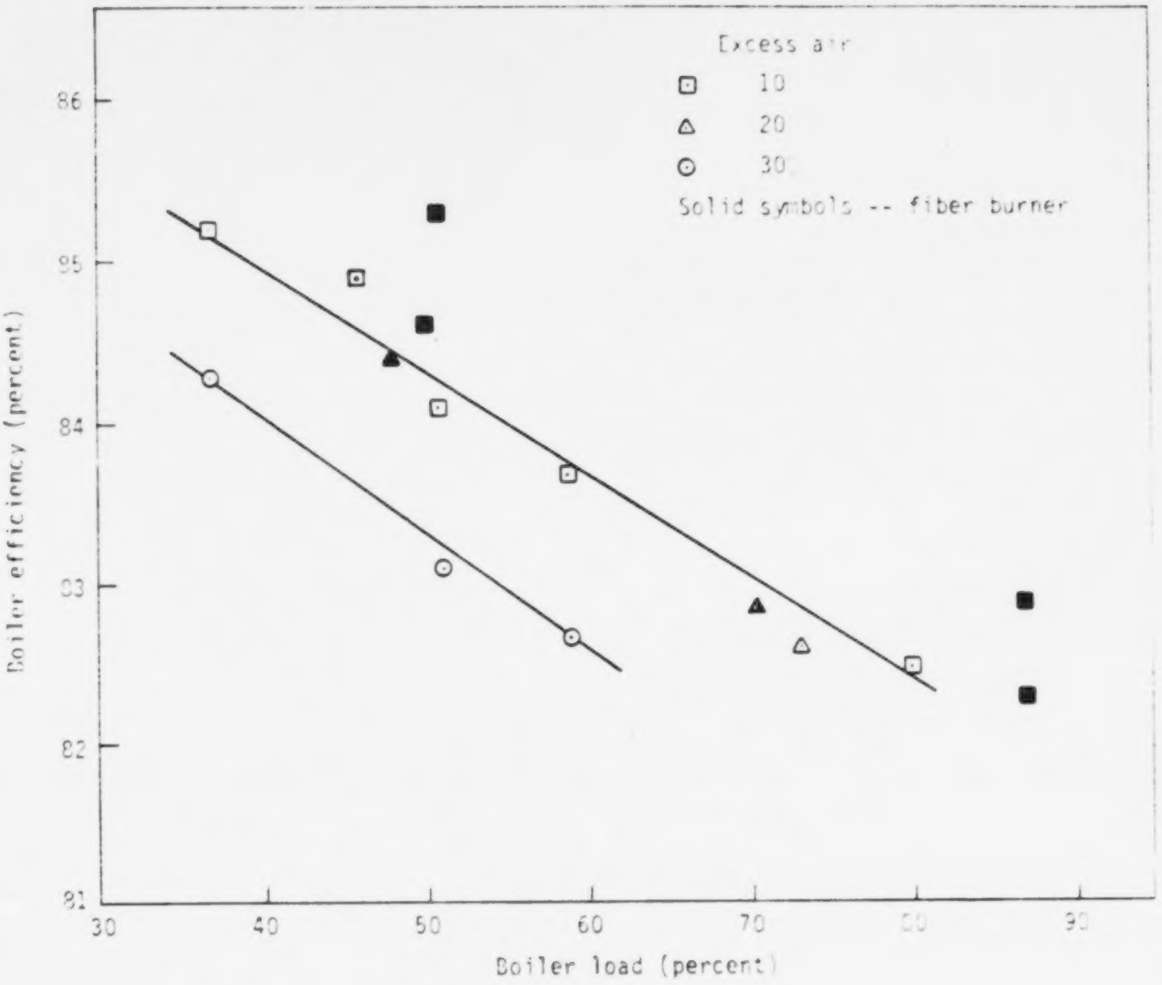

Figure 7. 980-kW Ohio Special Boiler Efficiency Comparison

Table 1

SELECTED BURNER TEST SITES

Site	Boiler	Boiler Use
1. York-Shipley test bay York, PA	588-kW high-pressure steam	Test bay setup. 2:1 burner modulation.
2. Vandenberg Air Force Base Lompoc, CA	392-kW low-pressure steam	Mess hall cooking and cleaning. Cycles on and off at full load (no burner modulation).
3. Peter Paul Cadbury York, PA	588-kW high-pressure steam	Process steam. 2:1 burner modulation.
4. The Hall Chemical Co. Wickliffe, OH	980-kW Ohio Special high-pressure steam	Process steam. Set up for high/low firing. Extra capacity available.

Table 2

FIELD TEST FIRETUBE BOILER COMPARISON*

Site	Boiler Size (kW)	Burner Type	Excess Air (%)	CO (ppm)	NO (ppm)	HC (ppm)	Boiler Eff. (%)	Hours of Operation
Alzeta Laboratory	245	Conventional	16	11	57	0	82.8	NA
		Fiber	10	10	10	10	83.3	500**
York-Shipley Boiler Test Bay York, PA	588	Conventional	15	10	--	--	85.0	NA
		Fiber	10	10	--	--	85.8	2,000
Vandenberg AFB California	392	Conventional	55	240	--	--	81.0	NA
		Fiber	10	0	--	--	82.3	3,800
Peter Paul Cadbury York, PA	588	Conventional	20	400	--	--	83.2	NA
		Fiber	7	35	20	--	84.0	3,450 2,500
Hall Chemical Company Wickliffe, OH	980 Ohio Special	Conventional	7	1,000	80	--	82.7	NA
		Fiber	13	35	18	--	83.7	3,450 2,500 1,500

*All results at high fire conditions, emissions corrected to 0% O_2.
**On segmented burner.

Appendix A.

LIST OF ATTENDEES
1985 JOINT SYMPOSIUM ON STATIONARY COMBUSTION NO_x CONTROL
MAY 6-9, 1985, BOSTON, MASSACHUSETTS

Pentti J. Aalto
Pequod Associates
129 South Street
Boston, MA 02114
(617) 542-8567

Duane Abbott
Stauffer Chemical Co.
2000 Michigan Street
Hammond, IN 46320
(219) 932-7651

Jerry Ackerman
Babcock & Wilcox
1562 Beeson Street
Alliance, OH 44601
(216) 821-9110

Michael Acree
Babcock & Wilcox
20 S. Van Buren
Barberton, OH 44203
(216) 860-1699

Bialecki Adolph
U.S. Naval Civil Engineering Lab.
Code L71
Port Hueneme, CA 93043
(805) 982-4116

Rui Afonso
Dynatech R/D Co.
99 Erie Street
Cambridge, MA 02139
(617) 868-8050

Per-Olof Alfredsson
Flakt AB
Box 81 001
S-104 81
Stockholm, SWEDEN
(08) 714 40 00

Charles D. Allen
Arizona Public Service Company
P.O. Box 21666
Phoenix, AZ 85036
(602) 271-7442

Shankar Ananthakrishna
NM EID/Air Quality Bureau
P.O. Box 968
725 St. Michael's Drive
Santa Fe, NM 87504-0968
(505) 984-0020 x357

Robert Andel
United Illuminating Company
80 Temple Street
New Haven, CT 06506
(203) 787-7811

David K. Anderson
Combustion Engineering, Inc.
1000 Prospect Hill Road
Windsor, CN 06095
(203) 688-1911, x4812

Mark W. Anderson
Kerr-McGee Corporation
P.O. Box 25861
Oklahoma City, OK 73125
(405) 270-2528

Hiroshi Aoki
Ishikawajima Harima Heavy Industries
30-13, 5-Chome, Toyo, Kotoku
Tokyo, 135 JAPAN
03-699-2682

Yasuo Arai
Electric Power Development Co.
3412 Hillview Avenue
P.O. Box 10412
Palo Alto, CA 94303
(415) 855-2278

Peter Asmuth
Stadtwerke Duesseldorf AG
Postfach 11 36
4000 Duesseldorf
WEST GERMANY

Robert G. Augur
Northeast Utilities
P.O. Box 270
Hartford, CT 06141-0270
(203) 665-5475

Robert Ballew
Department of Environmental Protection
Air Quality Control
Bay Building - AMHI
Augusta, ME 04333

Amiram Barilan
Prototech Company
70 Jaconnet Street
Newton Highlands, MA 02161
(617) 965-2720

Arthur H. F. Barlow
C-E Power Systems
2102 Business Center Drive, #206
Irvine, CA 92715
(714) 955-1711

Joe Barsin
Babcock & Wilcox
205 Van Buren Avenue
Barberton, OH 44203
(216) 860-1552

David F. Bartz
Dynatech R/D Co.
99 Erie Street
Cambridge, MA 02139
(617) 868-8050

Sushil K. Batra
Thermo Electron Corporation
P.O. Box 459
45 First Avenue
Waltham, MA 02254
(617) 890-8700 x304

Sandra A. Beaton
U.S. Environmental Protection Agency
60 Westview Street
Lexington, MA 02173
(617) 861-6700 x249

Janos Beer
Massachusetts Institute of Technology
Department of Chemical Engineering
Room 66-552
77 Massachusetts Avenue
Cambridge, MA 02139

Thomas W. Beggs
JACA Corporation
550 Pinetown Road
Ft. Washington, PA 19034
(215) 643-5466

Angelo Benanti
ENEL
via G. B. Martini, 3
Rome, ITALY
(06) 85091

Linda M. Benson
Riley Stoker Corporation
9 Neponset Street
Worcester, MA 01606
(617) 852-7100

Mogens Berg
ELKRAFT Power Co., Ltd.
5, Lautruphoj
2750 Ballerup, DENMARK
2 660022

Niklas Berge
Studsvik Energiteknik AB
S-61182 Nykoping
SWEDEN
(46) 155-80000

Robert D. Bessette
Old Ben Coal Company
333 West Vine Street
Lexington, KY 40507
(606) 231-6429

Ananda Bhat
Pennsylvania Electric Company
1001 Broad Street
Johnstown, PA 15907
(814) 533-8560

Bhuwan Bhushan
Babcock & Wilcox Co.
20 S. Van Buren Avenue
Barberton, OH 44203
(216) 860-2631

Gary Bisonett
Pacific Gas & Electric
77 Beale Street, Room 3035
San Francisco, CA 94106
(415) 972-6950

John W. Bjerklie
Consolidated Natural Gas
Service Co., Inc.
11001 Cedar Avenue, Room 300
Cleveland, OH 44106
(216) 421-2715

A. Michael Blaney
Thermo Electron Instruments
108 South Street
Hopkinton, MA 01748
(617) 435-5321

John C. Bonacci
Englehard Corporation
2655 U.S. Route 22
Union, NJ 07083
(201) 964-2714

John C. Bonacci
Englehard Corporation
2655 U.S. Route 22
Union, NJ 07083
(201) 964-2714

J. D. Bornemann
Royal Schelde
P.O. Box 16
4380AA Vlissingen
THE NETHERLANDS

Steve Bortz
KVB, Inc.
18006 Skypark Boulevard
Irvine, CA 92714
(714) 250-6314

Don Boyd
Flakt, Inc.
P.O. Box 87
Knoxville, TN 37901
(615) 693-7550

Edwin J. Brailey, Jr.
New England Power Service Co.
25 Research Drive
Westboro, MA 01582
(617) 449-2374

Willem T. Broer
N. V. Nederlandse Gasvnie
P.O. Box 19
9700 MA Groningen
THE NETHERLANDS

Kenneth R. Brookes
NEI International Combustion, Ltd.
Sinfin Lane
Derby, ENGLAND DE2 9GJ
0332 760223

W. J. D. Brooks
Central Electricity Generating Board
(G.D.C.D.)
Barnett Way
Barnwood
Gloucester, GL4 7RS
UNITED KINGDOM

Richard A. Brown
Acurex Corporation
485 Clyde Avenue
Mountain View, CA 94043
(415) 964-3200

W. Brown
Central Electricity Generating Board

C. Philipp Brundrett
W. R. Grace
Davison Chemical Division
P.O. Box 2117
Baltimore, MD 21203
(301) 659-9192

Edward Bullinger
Potomac Electric Power Co.
1900 Pennsylvania Avenue, NW
Washington, DC 20068
(202) 872-2370

Yorgi Bunyoz
Flakt Denmark A/S
Meterbuen 33
2740 Skovlunde, DENMARK
(02) 914411

Nigel Burdett
Central Electricity Generating Board
Marchwood Engineering Laboratories
Marchwood, Hampshire
UNITED KINGDOM
0703-865711 x344

Douglas Burnham
Babcock & Wilcox Co.
20 S. Van Buren Avenue
Barberton, OH 44203
(216) 860-6794

David Burre
Frito-Lay, Inc.
P.O. Box 47250
Dallas, TX 75247
(214) 689-1595

Robert C. Carr
Electric Power Research Institute
3412 Hillview Avenue
Palo Alto, CA 94304
(415) 855-2422

Douglas Carter
U.S. Department of Energy
Washington, DC 20585
(202) 252-9684

Frederick R. Casiello
Peabody Engineering Corporation
39 Maple Tree Avenue
Stamford, CT 06906-0331
(203) 327-7000

Carlo Castaldini
Acurex Corporation
555 Clyde Avenue
Mountain View, CA 94039
(415) 964-3200

John Chandler
Department of Environmental Protection
Air Quality Control
Ray Building - AMHI
Augusta, ME 04333

Julius Chang
National Center for Atmospheric Research
P.O. Box 3000
Boulder, CO 80307-3000

Albert Burton
Fuel Tech
83 Taylor Place
Stamford, CT 06902
(203) 359-1320

Charles F. Carlin, Jr.
Northeast Utilities
P.O. Box 270
Hartford, CT 06141
(203) 665-3737

Roy Carlson
National Energy Administration
S-117 87 Stockholm, SWEDEN
(08) 744-91-36

James Chen
Englehard Corporation
Menlo Park, NJ 08817
(201) 321-5229

Fred M. Childs
Chas. T. Main
Prudential Center
Boston, MA 02199
(617) 262-3200

Stanley Chin
U.S. Environmental Protection Agency
JFK Federal Building (APC-2311)
Boston, MA 02203
(617) 223-4879

Schiao-Feng Chou
Babcock & Wilcox
Alliance Research Center
1562 Beeson Street
Alliance, OH 44601
(216) 821-9110 x615

Roger Christman
Christman & Associates
11708 Bowman Green Drive
Reston, VA 22090
(703) 435-3219

Woo Chung
Los Angeles Dept. of Water & Power
111 N. Hope Street, Room 604
Los Angeles, CA 90051
(213) 481-4726

Ed Cichanowicz
Electric Power Research Institute
3412 Hillview Avenue
Palo Alto, CA 94304
(415) 855-2374

Paul L. Cioffi
Babcock & Wilcox
20 S. Van Buren Avenue
Barberton, OH 44203

Matt Clark
Babcock & Wilcox
20 S. Van Buren
P.O. Box 351
Barberton, OH 44203
(216) 860-2667

Robert Clark
San Diego Gas & Electric Co.
4600 Carlsbad Boulevard
Carlsbad, CA 92008
(619) 438-2371

Kevin Cleary
California Air Resources Board
1102 Q Street
Sacramento, CA 95814
(916) 322-8269

Mitchell Cohen
Combustion Engineering, Inc.
1000 Prospect Hill Road
Windsor, CT 06095
(203) 688-1911, ext 2482

Richard Cohen
New York Power Authority
10 Columbus Circle
New York, NY 10019
(212) 397-7795

Robert J. Collette
Combustion Engineering, Inc.
1000 Prospect Hill Road
Windsor, CT 06095-0500
(203) 285-5687

Robert Connearney
C. T. Main, Inc.
101 Huntington Avenue
Boston, MA 02199
(617) 262-3200

Peter Costanza
New Jersey Dept. of Environmental
  Protection
CN-027
Trenton, NJ 08625
(609) 984-0495

T. E. Cottrell
Central Electricity Generating Board

David A. Cowdrick
Tampa Electric Co.
P.O. Box 111
Tampa, FL 33601
(813) 228-4111

Richard Coyne
Chas. T. Main
Prudential Center
Boston, MA 02199
(617) 262-3200

William Cress
Allegheny Power Service Corporation
800 Cabin Hill Drive
Greensburg, PA 15601
(412) 838-6721

Edward P. Crockett
American Petroleum Institute
1220 L Street, NW
Washington, DC 20005
(202) 682-8318

Peter Dacey
Coal Research
International Energy Agency
14/15 Lower Grosvenor Place
London SW1W OEX
ENGLAND

James Damon
Stearns Catalytic Corporation
4500 Cherry Creek Drive
Denver, CO 80222
(303) 692-2458

C. Bruce Damrell
Boston Edison Co.
800 Boylston Street
Boston, MA 02199

Dan Danbeck
Public Service Commission of Wisconsin
P.O. Box 7854
Madison, WI 53707
(608) 266-2655

Shirley Darrah
Geo-Centers, Inc.
320 Needham Street
Newton Upper Falls, MA 02194
(617) 964-7070

Lawrence Davidson
Stone & Webster
245 Summer Street
Boston, MA 02107
(617) 589-2381

Lawrence Decker
Dynatech R/D Co.
Cambridge, MA 02139
(617) 868-8050

Craig T. Derbidge
Electric Power Research Institute
3412 Hillview Avenue
Palo Alto, CA 94304
(415) 855-2427

David Dixon
Department of Environmental Protection
Air Quality Control
Ray Building - AMHI
Augusta, ME 04333

William H. Dow
Boston Edison Co.
800 Boylston Street
Boston, MA 02199
(617) 424-3228

Brian Doyle
Consulting Engineer
Oscawana Lake Road
Putnam Valley, NY 10579
(914) 528-0137

Sam N. Duran
Texaco U.S.A.
P.O. Box 10269
Bakersfield, CA 93389
(805) 832-4010

Owen W. Dykema
Rockwell International
Rocketdyne Division
8900 DeSoto Avenue
Canoga Park, CA 91307
(818) 700-3977

Sherman Eaton
Coen Company
1510 Rollins Road
Burlingame, CA 94010
(415) 697-0440

James Edwards
Alloy Surfaces Co.
100 Locke Road
Wilmington, DE 19809
(302) 762-8900

Andrea Egense
TRW
One Space Park
127/1360
Redondo Beach, CA 90278
(213) 517-7349

Goran Eklund
Studsvik Energiteknik AB
61182 Nykoping
SWEDEN
(46) 155-80 000

William Ellison
Ellison Consultants
4966 Tall Oaks Drive
Monrovia, MD 21770
(301) 865-5302

Glenn England
Energy & Environmental Research Corp.
18 Mason
Irvine, CA 92718
(714) 859-8851

Robert Erdmann
Coen Company, Inc.
1510 Rollins Road
Burlingame, CA 94010
(415) 697-0440

Michael Esche
Saarberg-Holter Umwelttechnik GmbH
HafenstraBe 6
6600 Saarbrucken
WEST GERMANY
(681) 32104-06

David Eskinazi
Electric Power Research Institute
3412 Hillview Avenue
Palo Alto, CA 94304
(415) 855-2918

William W. Farmer
Georgia Power Company
P.O. Box 4545, 333 Bldg. (18th Floor)
Atlanta, GA 30306
(404) 526-7194

Hamid Farzan
Babcock & Wilcox Co.
1562 Beeson Street
Alliance, OH 44601
(216) 821-9110 x385

Edwin L. Field
Arthur D. Little, Inc.
20 Acorn Park
Cambridge, MA 02140
(617) 864-5770

A. R. Fischer
Houston Lighting & Power Company
12301 Kurland Drive
Houston, TX 77034
(713) 481-7602

Woody Fiveland
Babcock & Wilcox
1562 Beeson Street
Alliance, OH 44001

Donald K. Fleming
Institute of Gas Technology
4201 W. 36th Street
Chicago, IL 60632
(312) 890-6431

Tim Flora
Ohio Edison
Edgewater Plant
200 Oberlin Avenue
Lorain, OH 44052
(216) 244-1991, ext 218

G. Foley
Central Electricity Generating Board

Mark R. Ford
General Electric Co.
1100 Western Avenue, M/C 464X1
Lynn, MA 01910
(617) 594-5793

Kuniyoshi Fujiyama
Electric Power Development Co., Ltd.
8-2, Marunouchi, 1-Chome
Chiyoda-ku, Tokyo 100
JAPAN
(03) 212-2211 x3351

Rosemary Furfey
Dept. of Environmental Quality
Engineering
Division of Air Quality Control
1 Winter Street
Boston, MA 02108
(617) 292-5762

Wendy M. Gabers
Corning Glass Works
Main Plant 8-5-1
Corning, NY 14831
(607) 974-7175

N. Geoffrey Galluzzo
Black & Veatch, Engineers-Architects
P.O. Box 8405
Kansas City, MO 64114
(913) 967-2834

Michael Gambburg
Coen Company, Inc.
1510 Rollins Road
Burlingame, CA 94010
(415) 697-0440

Richard E. Gannon
AVCO Everett Research Laboratory
2385 Revere Beach Parkway
Everett, MA 02149
(617) 381-4630

Paul W. Garbo
Paul W. Garbo Consultant
48 Lester Avenue
Freeport, NY 11520
(516) 378-0393

James S. Geier
Colorado Department of Health
4210 E. 11th Avenue
Denver, CO 80220
(303) 331-8576

Carl R. Gerber
U.S. Environmental Protection Agency
Office of Research and Development
Washington, DC 20460

Gerald Gilbert
Dynatech Corporation
99 Erie Street
Cambridge, MA 02139
(617) 868-8050

Dan V. Giovanni
Electric Power Technologies
P.O. Box 5560
Berkeley, CA 94705
(415) 653-6422

Robert F. Goecker
Marcona Ocean Industries, Ltd.
700 West Hillsboro Boulevard
Building 3, Suite 205
Deerfield Beach, FL 33441-1898
(201) 826-2202

R. Mark Golightley
Ohio Edison
76 South Main Street
Akron, OH 44308
(216) 384-4943

Robert Grace
Combustion Engineering, Inc.
1000 Prospect Hill Road
Windsor, CT 06095-0500
(203) 285-5292

Jack Greene
U.S. Environmental Protection Agency
AEERL/RTP
Research Triangle Park, NC 27711

Robert T. Greene
Central & South West Services
2121 San Jacinto Street, Suite 2300
Dallas, TX 75266
(214) 754-1368

Roberto Grimaldi
ENEL-DCO
Via G. B. Martini, 3
00197 Roma, ITALY

Paul Grogan
Dept. of Environmental Quality
Engineering
Air Quality Control
1 Winter Street, 8th Floor
Boston, MA 02108
(617) 292-5594

Vir Gupta
I.E.P.A.-D.A.P.C.
2200 Churchill Road
Springfield, IL 62706
(217) 782-2113

Jon E. Haebig
U.S. Environmental Protection Agency
AEERL/RTP
Research Triangle Park, NC 27711

John W. Hagley
Pennsylvania Power & Light Co.
Two N. Ninth Street
Allentown, PA 18101
(215) 770-5159

Robert E. Hall
U.S. Environmental Protection Agency
Combustion Research Branch
(MD-65)
Research Triangle Park, NC 27711
(919) 541-2477

Finn Hals
AVCO Everett Research Laboratory
2385 Revere Beach Parkway
Everett, MA 02149
(617) 381-4527

Robert P. Hangebrauck
U.S. Environmental Protection Agency
AEERL/RTP
Research Triangle Park, NC 27711

Douglas Harckham
Airoil Flaregas Limited
Horton Road, West Drayton
Middx UB7 8B9
UNITED KINGDOM
0895-444031

Don Hardesty
Sandia National Labs
Combustion Research Division
Livermore, CA 94550
(415) 422-2321

Franz Hastik
Siemens Aktiengesellschaft Oesterreich
Siemensstrasse 88-92
A-1210 Vienna, AUSTRIA

Arthur Hausberger
United Catalysts, Inc.
P.O. Box 32370
Louisville, KY 40232
(502) 637-9751

John Haws
Salt River Project
Coronado Generating Station
P.O. Box 1018
St. Johns, AZ 85936
(602) 337-4131

Wolfgang Heer
Universitat Karlsruhe
IIP Hertzstrasse 16
D-7500 Karlsruhe
WEST GERMANY
07211608-4417

Klaus Hein
Rheinisch-Westfalisches
Elektrizitaswerk
Kruppstr. 5
4300 Essen 1
WEST GERMANY
02271/584-2234

Malcolm Hepworth
Amax Research and Development, Inc.
5950 McIntyre Street
Golden, CO 80403
(303) 279-7636

Bo Herrlander
Flakt Industri AB
S-35187 VAXJO
SWEDEN
0470 87623

J. W. Holden
Salt River Project
Box 52025
Phoenix, AZ 85072-2025
(602) 236-5900

William Holewinski
Wisconsin Power & Light Company
222 W. Washington Avenue
Madison, WI 53593
(608) 252-3343

John Edward Hopper
HM. Industrial Air Pollution
Inspectorate
HSE Intercity House, Mitchell Lane
Victoria St, Bristol
ENGLAND B5A 5AN
0272-290681

Hann S. Huang
Argonne National Laboratories
9700 South Cass Avenue
Argonne, IL 60439
(312) 972-3125

S. C. Hunter
KVB, Inc.
P.O. Box 19518
Irvine, CA 92714
(714) 250-6280

Boyd E. Hurst
Exxon Research and Engineering Co.
P.O. Box 101
Florham, NJ 07932
(201) 765-6917

H. Ikebe
Ishikawajima-Harima Heavy Ind.
IHI Tokyo Office
Tokyo Genboku Kaikan 30-13
5-Chome, Toyo Koto-Ku
Tokyo, 135, JAPAN

Reda S. Iskandar
Corning Glass Works
MP-08-05-1
Corning, NY 14831
(607) 974-7306

Daniel Itse
Riley Stoker Corporation
9 Neponset Street
P.O. Box 547
Worcester, MA 01606
(617) 792-4800

Keijo Jaanu
Ekono Oy, Helsinki, Finland
POX 27, 00131
Helsinki 13, FINLAND
(90) 46911

Kurt Jakobson
U.S. Environmental Protection Agency
401 M Street, SW
Washington, DC 20460
(202) 382-2583

Betty K. Jensen
Public Service Electric & Gas Co.
P.O. Box 570, MC 16A
Newark, NJ 07101
(201) 430-6633

Stephen A. Johnson
Physical Sciences, Inc.
P.O. Box 3100, Research Park
Andover, MA 01810
(617) 475-9030

Gary D. Jones
Radian Corporation
P.O. Box 13000
Research Triangle Park, NC 27709
(919) 541-9100

Masahito Kawashima
NGK Insulators, Ltd.
767 Third Avenue
New York, NY 10017
(212) 758-6020

Helmut Keinhorst
Vicepresident des Umweltbundesamtes
Bismarckplatz 1
D-1000 Berlin 33
030-8903256/257

Edward J. Kenney
Arthur D. Little, Inc.
20 Acorn Park
Cambridge, MA 02140
(617) 864-5770, ext 3314

Stephen E. Kerho
KVB
18006 Skypark Boulevard
Irvine, CA 92714

Harold A. Kerry
Southern California Edison Co.
2244 Walnut Grove Avenue
Rosemead, CA 91770
(818) 302-1890

John P. Kesselring
Alzeta Corporation
500 Clyde Avenue
Mountain View, CA 94043
(415) 965-8282

John Kiff
Joy Manufacturing Co.
4565 Colorado Boulevard
Los Angeles, CA 90039
(818) 240-2300

Lawrence P. King
Babcock & Wilcox
1562 Beeson Street
Alliance, OH 44601
(216) 821-9110

Harold M. Kitching
Northeast Power Service Co.
25 Research Drive
Westboro, MA 01582
(617) 366-9011, ext. 3014

William Kohanik
Public Service Electric & Gas Company
P.O. Box 570
80 Park Plaza, 15A
Newark, NJ 07101
(201) 430-7551

Jaroslaw Konieczny
Technische Universitat Wien
Getreidemarkt 9
A-1060 Wien
(0222) 5601-4720

David Kopta
Utah Bureau of Air Quality
2870 Connor Street
Salt Lake City, UT 84109
(801) 278-2276

Paul J. Koziar
WIS DNR
Box 7921
Madison, WI 53707
(608) 266-7790

Martin Kozlak
Combustion Engineering, Inc.
1000 Prospect Hill Road
Windsor, CT 06095
(203) 688-1911, x2492

Gunther H. Kraus
American M.A.N. Corporation
50 Broadway, 18th Floor
New York, NY 10004
(212) 509-4545

James Kraynak
Norton Company
P.O. Box 350
Akron, OH 44309
(216) 673-5860

F. Richard Kurzynske
Gas Research Institute
8600 W. Bryn Mawr
Chicago, IL 60631
(312) 399-8203

Michael Lambert
194 Hillside Street
Boston, MA 02120

John W. Larson
Riley Stoker Corporation
P.O. Box 547
Worcester, MA 01613
(617) 792-4801

Peter Larsson
Porzellanfabrik Frauendhal
A-8523 Frauental
AUSTRIA
3462/2000

Albert LaRue
Babcock & Wilcox
20 S. Van Buren
Barberton, OH 44203
(216) 860-1493

Dorothy Lau
Ontario Hydro
700 University Avenue, H10E3
Toronto, Ontario
CANADA
(416) 592-7306

Neal Lebo
Gilbert/Commonwealth, Inc.
P.O. Box 1498
Reading, PA 19603
(215) 775-2600

Jean Pierre LeCalvez
Cerchar
BP19 62 Mazingarbe, FRANCE
21729233

Peter Larsson
Porzellanfabrik Frauendhal
A-8523 Frauental
AUSTRIA
3462/2000

Albert LaRue
Babcock & Wilcox
20 S. Van Buren
Barberton, OH 44203
(216) 860-1493

Dorothy Lau
Ontario Hydro
700 University Avenue, H10E3
Toronto, Ontario
CANADA
(416) 592-7306

Neal Lebo
Gilbert/Commonwealth, Inc.
P.O. Box 1498
Reading, PA 19603
(215) 775-2600

Jean Pierre LeCalvez
Cerchar
BP19 62 Mazingarbe, FRANCE
21729233

George Lee
Energy & Resources Canada
555 Booth Street
Ottawa, Ontario, CANADA
(613) 996-4570 x186

Ron Lenzer
Babcock & Wilcox
20 S. Van Buren Avenue
P.O. Box 351
Barberton, OH 44203
(216) 860-6779

Seymour Levy
Northeast Utilities Service Company
P.O. Box 1928
Hartford, CT 06144-1928
(203) 721-2427

Robert Lewis
Combustion Engineering, Inc.
1000 Prospect Hill Road
Windsor, CT 06095-0500
(203) 285-5968

Anita D. Liang
Babcock & Wilcox
1562 Beeson Street
Alliance, OH 44601
(216) 821-9110

Charles Lim
Norton Company
P.O. Box 350
Akron, OH 44309
(216) 673-5860

Mark Linsberg
Dayton Power and Light Company
P.O. Box 468
Aberdeen, OH 45101
(513) 549-2641

Robert Lisauskas
Riley Stoker Corporation
9 Neponset Street
P.O. Box 547
Worcester, MA 01606
(617) 792-4800

George Losel
Kraftwerk Union
Hammerbacherstr. 12+14
Postfach 3220
8520 Erlangen, WEST GERMANY
46144182

Michael Lukasiewicz
Gas Research Institute
8600 W. Bryn Mawr Avenue
Chicago, IL 60631
(312) 399-8315

Richard R. Lunt
United Engineers & Constructors, Inc.
30 South 17th Street
P.O. Box 8223
Philadelphia, PA 19101
(215) 422-3595

Christa M. Mahar
Pequod Associates, Inc.
129 South Street
Boston, MA 02111
(617) 542-8567

Michael Maher
DEQE/DAQC
5 Commonwealth Avenue
Woburn, MA 01801
(617) 935-2160

Jason Makansi
Power Magazine
1221 Avenue of the Americas
New York City, NY 10020
(212) 512-4239

John L. Marion
Combustion Engineering, Inc.
1000 Prospect Hill Road
Windsor, CT 06095
(203) 688-1911

Lewis Maroti
Dynatech R/D Co.
99 Erie Street
Cambridge, MA 02139
(617) 868-8050

Gregory Martel
Northeast Utilities
1866 River Road
Middletown, CT 06457
(203) 346-9639 x375

G. Blair Martin
U.S. Environmental Protection Agency
AEERL/RTP
Research Triangle Park, NC 27711

John Martin
Stone & Webster Engineering Corp.
245 Summer Street
Boston, MA 02107
(617) 589-8868

John Martinez
Radian Corporation
P.O. Box 13000, Progress Center
Research Triangle Park, NC 27709
(919) 541-9100 x305

Howard Mason
Acurex Corporation
485 Clyde Avenue
Mountain View, CA 94043
(415) 964-3200

Scott Mason
State of Maine
Station 127
Augusta, ME 04333
(207) 289-2437

Ted Masters
United Catalysts Inc.
P.O. Box 32370
Louisville, KY 40232
(502) 637-9751

John Maulbetsch
Electric Power Research Institute
3412 Hillview Avenue
Palo Alto, CA 94304
(415) 855-2438

James D. Maxwell
Tennessee Valley Authority
501 Chemical Engineering Building
Muscle Shoals, AL 35661
(205) 386-2814

Mallory May
Gifford-Hill & Company, Inc.
P.O. Box 47127
Dallas, TX 75247
(214) 258-7175

Michael W. McElroy
Electric Power Research Institute
3412 Hillview Avenue
Palo Alto, CA 94304
(415) 855-2471

Dennis McGarry
Owens Corning
Technical Center
Granville, OH 43023
(614) 587-7337

Claire McHale
Riley Stoker Corporation
9 Neponset Street
P.O. Box 547
Worcester, MA 01606
(617) 792-4800

Joseph A. McSorley
U.S. Environmental Protection Agency
AEERL/RTP
Research Triangle Park, NC 27711

Lee Meinders
Martin-Marietta Basic Product
399 N. Park Avenue
Easton, CT 06612
(203) 268-6239

Romuald Michalek
Englehard Corporation
70 Wood Avenue, South
Iselin, NJ 08830
(201) 321-5342

Alain Milhau
Agency for the Quality of the Air
Tour Gan-Cedex 13
92082 Paris La Defense 2
FRANCE
(1) 776.44.21

Kenneth Mitkowski
Northeast Utilities
P.O. Box 270
Hartford, CT 06141-0270
(203) 665-3957

Shigehiro Miyamae
Ishikawajima Harima Heavy Industries
30-13, 5-Chome, Toyo, Kotoku
Tokyo, 135 JAPAN
03-699-2682

Nino M. Molino
New England Power Service Co.
25 Research Drive
Westboro, MA 01582
(617) 366-9011

Ralph Mongeon
Riley Stoker Corporation
9 Neponset Street
Worcester, MA 01606
(617) 792-4811

Hukam C. Mongia
General Motors Corporation
Allison Gas Turbine Division
P.O. Box 420
Indianapolis, IN 46206-0420
(317) 242-5945

Keith A. Moore
Rockwell International
6633 Canoga Avenue
Canoga Park, CA 91304
(818) 700-4016

Shigeki Morita
Babcock Hitachi, Ltd.
6-9 Takaramachi Kure
Hiroshima, JAPAN
0823-21-1161

Dominick J. Mormile
Con Edison of New York
4 Irving Place
New York, NY 10003
(212) 460-6275

William Morton
Keeler/Dorr-Oliver
238 West Street
Williamsport, PA 17701
(717) 326-3361

Albert Moussa
A. D. Little, Inc.
20 Acorn Park
Cambridge, MA 02140
(617) 864-5770, x5483

Barbara Muenzen
Orange and Rockland Utilities, Inc.
One Blue Hill Plaza
Pearl River, NY 10965
(914) 577-2579

Jim Mulholland
U.S. Environmental Protection Agency
AEERL/RTP
Research Triangle Park, NC 27711
(919) 541-7663

Nobuaki Murakami
Mitsubishi Heavy Industries, Ltd.
Nagasaki Technical Institute
1-1, Akunoura-Machi
Nagasaki City, 850-91
JAPAN
0958-61-2111 x7061

Michael J. Murphy
New England Power Co.
25 Research Drive
Westboro, MA 01851
(617) 366-4011

John P. Mustonen
Stone & Webster Engineering Corp.
245 Summer Street
Boston, MA 02107
(617) 589-8626

Larry Muzio
Fossil Energy Research Corporation
29541 Vista Plaza
Laguna Niguel, CA 92677
(714) 836-1070

Richard B. Myers
Pacific Gas & Electric
77 Beale Street, Room 2535
San Francisco, CA 94106
(415) 972-1575

Ippei Nakayama
Mitsubishi Corporation
6-3, Marunouchi, 2-Chome
Chiyoda-ku
Tokyo, JAPAN

Mehdi Namazian
Acurex Corporation
555 Clyde Avenue
Mountain View, CA 94039
(415) 964-3200

Teruo Namiki
Mitsubishi Heavy Industries, Inc.
Power Systems Headquarters
Shin-Tamachi, Bldg. 34-6
Shiba, 5-Chome
Minato-ku, Tokyo
JAPAN
03-455-5711 x5409

Paul S. Natanson
Exxon Research and Engineering Company
P.O. Box 101 (Building 102)
Florham Park, NJ 07932
(201) 765-1594

Thomas Natario
DEQE/DAQC
5 Commonwealth Avenue
Woburn, MA 01801
(617) 925-2160

Joseph T. Newman
Bechtel Group, Inc.
P.O. Box 3965
San Francisco, CA 94119
(415) 768-1943

Dana Nicoll
Central Mass. Air Pollution
  Control Dist.
75 Grove Street
Worcester, MA 01605
(617) 792-7653

Alex Nicols
Santa Fe Energy Company
10737 Shoemaker Avenue
Santa Fe Springs, CA 90670
(213) 944-0311

Per Nielsen
Danish Boiler Owners Association
Copenhagen, DENMARK 2860

R. Niesh
Central Electricity Generating Board

K. Nishikawa
Mitsubishi Heavy Industries
6-3 Marunouchi, 2-Chome
Chiyoda-ku,
Tokyo 100, JAPAN
210-2121

John Norris
Southern California Edison Co.
2244 Walnut Grove
Rosemead, CA 91770
(818) 302-4955

John Norris
Southern California Edison Co.
2244 Walnut Grove
Rosemead, CA 91770
(818) 302-4955

Ken Nowak
Fuel Tech
61 Taylor Reed Place
Stamford, CT 06906
(203) 359-1320

Peter Nutcher
Process Combustion Corporation
P.O. Box 12866
Pittsburgh, PA 15241
(412) 257-2080

William J. Oberjohn
Babcock & Wilcox
1562 Beeson Street
Alliance, OH 44601

George R. Offen
Electric Power Research Institute
3412 Hillview Avenue
Palo Alto, CA 94304
(415) 855-8942

Ken Okazaki
Toyohashi University of Technology
Department of Energy Enginering
Toyohashi, 440 JAPAN

N. Okigami
Hitachi Zosen Corporation
Technical Research Institute
1180, Amarube-Shimo
Maizuru City, Kyoto-Pref, 625
JAPAN
0773-63-1000

Lars Olsson
Flakt, Inc.
146-148 Sound Beach Avenue
Old Greenwich, CT 06870
(203) 637-5401

Hayes Orender
Babcock & Wilcox
20 S. Van Buren Avenue
Barberton, OH 44203
(216) 860-2584

Henry H. Osborn
C-E Air Preheater
Andover Road
Wellsville, NY 14895
(716) 593-2700 x661

Michael Osborne
U.S. Environmental Protection Agency
AEERL/RTP
Research Triangle Park, NC 27711
(919) 541-4113

Ronald G. Ostendorf
Procter & Gamble
7162 Reading Road
Cincinnati, OH 45222
(513) 763-4457

Delbert M. Ottmers, Jr.
Radian Corporation
8501 Mo-Pac Blvd.
P.O. Box 9948
Austin, TX 78766
(512) 454-4797

Brad J. Overmoe
Energy & Environmental Research Corp.
8001 Irvine Boulevard
Santa Ana, CA 92705
(714) 552-1803

Joseph H. Oxley
Battelle-Columbus Laboratories
505 King Avenue
Columbus, OH 43201
(614) 424-7885

Tom Parks
DEQE/DAQC
5 Commonwealth Avenue
Woburn, MA 01801
(617) 935-2160

Roy Payne
Energy & Evironmental Research Corp.
18 Mason
Irvine, CA 92718
(714) 859-8851

David W. Pearsall
Combustion Engineering, Inc.
1000 Prospect Hill Road
Windsor, CT 06905
(203) 688-1911

Luciano Pelloni
BBC Brown Boveri
CH-5401 Baden
SWITZERLAND
(050) 756885

Craig Penterson
Riley Stoker Corporation
9 Neponset Street
Worcester, MA 01606
(617) 852-7100

Daniel H. Pepoon
Clean Air Engineering, Inc.
207 North Woodwork Lane
Palatine, IL 60067
(312) 991-3300

Michael Perlsweig
U.S. Department of Energy
FE-23
Washington, DC 20545
(301) 353-4399

Ellen Petrill
Electric Power Research Institute
3412 Hillview Avenue
Palo Alto, CA 94304

Stanley J. Piekos
Riley Stoker Corporation
9 Neponset Street
Worcester, MA 01606
(617) 852-7100

Wade Ponder
U.S. Environmental Protection Agency
AEERL (MD-60)
Research Triangle Park, NC 27711
(919) 541-2821

William Powers
Naval Energy & Environmental Support
  Activity
Port Hueneme, CA 93043
(805) 982-4758

Michael Pratt
New Jersey Dept. of Environmental
  Protection
1259 Route 46
Parsippany, NJ 02054
(201) 299-7560

Jay Ratafia-Brown
Science Applications International
1710 Goodridge Drive
P.O. Box 1303
McLean, VA 22102
(703) 448-6343

Jim Reese
Energy & Environmental Research Corp.
18 Mason
Irvine, CA 92718
(714) 899-8851

Klaus-Dieter Rennert
L & C Steinmuller GmbH
Fabrikstr. 1, 5270 Gummersbach 1
FEDERAL REPUBLIC OF GERMANY
(0049) 2261 85-2-897

Otto Rentz
Institut for Industrial Production
Herzstrabe 16
7500 Karlsruhe 21
WEST GERMANY

Michael J. Rini
Combustion Engineering, Inc.
1000 Prospect Hill Road
Windsor, CT 06095
(203) 228-3479

Robert Rio
DEQE/DAQC
5 Commonwealth Avenue
Woburn, MA 01801
(617) 935-2160

Chris P. Robie
Stearns Catalytic Corp.
P.O. Box 5888
Denver, CO 80217
(303) 692-3193

Larry W. Rodgers
Babcock & Wilcox
Alliance Research Center
1562 Beeson Street
Alliance, OH 44601
(216) 821-4110

Ron Rogers
Flakt, Inc.
P.O. Box 87
Knoxville, TN 37901
(615) 693-7550

Erik Rosenberg
Elkraft Power Company Ltd.
5, Lautruphoej
2750 Ballerup, DENMARK
(2) 66 00 22

Ann Ruebush
Chevron Research Co.
576 Standard Avenue
Richmond, CA 94802
(415) 620-3708

Wayne Rugenstein
The Detroit Edison Company
6100 W. Warren, Rm. H139
Detroit, MI 48210
(313) 897-1346

Ashok Sachdev
Atomic Energy of Canada, Ltd.
Whik Shell Nuclear Research
Pinawa, Manitoba ROE 1L0
CANADA
(204) 753-2311, x2438

Norman Samish
Shell Development Co.
P.O. Box 1380
Houston, TX 77001
(713) 493-7944

Henry Sanematsu
Los Angeles Department of
Water & Power
111 N. Hope Street
Los Angeles, CA 90012
(213) 481-4906

A. Sarofim
Massachusetts Institute of Technolog
Department of Chemical Engineering
Room 66-466
77 Massachusetts Avenue
Cambridge, MA 02139
(617) 253-4566

Jacob J. Scheffer
Boston Edison Co.
800 Boylston Street
Boston, MA 02199
(617) 424-2319

H. N. Schenck
Fuel Tech
12 Stanton Road
Darien, CT 06820
(203) 359-1320

Edmund Schindler
Foster Wheeler
110 S. Orange Avenue
Livingston, NJ 07089
(201) 533-2707

Herbert Schuster
Deutsche Babcock Werke AG
Duisburgerstrasse 375
D-4200 Oberhausen
WEST GERMANY
(0208) 833-2853

Ralph L. Scott
U.S. Department of Energy
METC
P.O. Box 880
Collins Ferry Road
Morgantown, WV 26505
(304) 291-4323

James G. Seebold
Chevron Corporation
555 Market Street
San Francisco, CA 94105-2870
(415) 894-2484

Takashi Segawa
IHI
c/o Foster Wheeler Energy Corp.
110 S. Orange Avenue
Livingston, NJ 07039
(201) 533-2236

Nancy L. Seidman
Northeast States for Coordinated
Use Management
607 Boylston Street
Boston, MA 02116
(617) 437-9007

Utpal Sengupta
Fluor Engineers, Inc.
200 West Monroe Street
Chicago, IL 60606
(312) 368-3821

Joan Serra
Physical Sciences, Inc.
Dascomb Research Park
P.O. Box 3100
Andover, MA 01810
(617) 475-9030 x536

Dale E. Shore
KVB, Inc.
P.O.Box 19518
Irvine, CA 92714
(714) 250-6225

G. Gary Simpson
Westinghouse Idaho Nuclear Company
P.O. Box 4000
Idaho Falls, ID 83403
(208) 526-0036

H.P.A. Singh
Pacific Lighting Energy Systems
6055 E. Washington Blvd., Ste. 822
Commerce, CA 90040
(213) 725-1139

Walter Smit
Plains Electric G&T Corp., Inc.
P.O. Box 6551
Albuquerque, NM 87197
(505) 884-1881

Kenneth Smith
The Ontario Ministry of the
Environment
880 Bay Street, 4th Floor
Toronto, Ontario
CANADA M5S 1Z8
(416) 965-5776

Lowell L. Smith
Energy Technology Consultants, Inc.
2091 Business Center Drive, #100
Irvine, CA 92715
(714) 833-2523

L. Douglas Smoot
Brigham Young University
270 Clyde Building
Provo, UT 84602
(801) 378-4327

Robert Snodgrass
Riley Stoker Corporation
9 Neponset Street
P.O. Box 547
Worcester, MA 01606
(617) 792-4800

William Snyder
Union Carbide Corporation
Old Saw Mill River Road
Tarrytown, NY 10591
(914) 789-5374

Todd Sommer
Pyro Engineering
P.O. Box 19009
Akron, OH 44319
(216) 682-4007

Donald Squires
Dept. of Environmental Quality
Engineering
Air Quality Control
1 Winter Street, 8th Floor
Boston, MA 02108
(617) 292-5594

Robert Statnick
Conoco
4000 Brownsville Road
Pittsburgh, PA 15228
(412) 854-6758

George C. Stegmann
Consolidated Edison of New York
4 Irving Place
New York, NY 10003
(212) 460-2754

Sidney Stone
The Cleveland Electric
Illuminating Co.
P.O. Box 5000, Room 810-A
Cleveland, OH 44101
(216) 622-9800, x3256

Joseph P. Strakey
U.S. Department of Energy
Pittsburgh Energy Technology Center
P.O. Box 10940
Pittsburgh, PA 15236
(412) 833-7255

Ivor J. Stuart-Sheppard
Ontario Hydro
700 University Avenue
Toronto, Ontario
CANADA M5G 1X6

Keith Summons
Ontario Hydro
700 University Avenue
Toronto, Ontario
CANADA M5G 1X6
(416) 592-5935

Kohei Suyama
Mitsubishi Heavy Industries, Ltd.
Nagasaki Shipyard and Engine Work
1-1, Akunoura-Machi
Nagasaki City, 850-91
JAPAN
0958-61-2111

Mamoru Suyari
Kobe Steel, Ltd.
1-Chome, Wakinohama-cho
Chuo-ku, Kobe, JAPAN
078-251-1551

Tomio Suzuki
Kobe Steel, Ltd.
1-Chome, Wakinohama-cho
Chuo-ku, Kobe, JAPAN
078-251-1551, x3474

J. Derek Teare
Massachusetts Institute of Technology
MIT E40-479
Cambridge, MA 02139
(617) 253-4241

Donald P. Teixeira
Pacific Gas and Electric Co.
3400 Crow Canyon Road
San Ramon, CA 94583
(415) 820-2000 x479

Gunnar Tejle
ASEA STAL AB
Fack S-581-01 Linkoping
SWEDEN
(013) 12-94-00

Jack T. Thompson
Tennessee Valley Authority
705 Edney Building
Chattanooga, TN 37401
(615) 751-2774

Richard E. Thompson
Fossil Energy Research Corporation
29541 Vista Plaza Drive
Laguna Niguel, CA 92677
(714) 836-1070

Larry S. Trowsdale
Kerr-McGee Chemical Corp.
P.O. Box 367
Trona, CA 93562
(619) 372-4311 x2299

Joel Vatsky
Foster Wheeler Energy Corporation
9 Peach Tree Hill Road
Livingston, NJ 07039
(201) 533-2105

John M. Vaught
General Motors Corporation
Allison Gas Turbine Division
P.O. Box 420
Indianapolis, IN 46206-0420
(317) 242-4680

Stephen Vayda
Pyropower Corporation
5120 Shoreham Place
San Diego, CA 92122
(619) 458-3055

Gary R. Veerkamp
Pacific Gas and Electric Co.
77 Beale Street, Room 2533
San Francisco, CA 94106
(415) 972-1576

Y. Veurink
Stork Boilers
P.O. Box 20, Hengelo
THE NETHERLANDS
074-454321, x3370

Richard Waibel
John Zink Company
4401 S. Peoria
P.O. Box 702220
Tulsa, OK 74170
(918) 747-1371

John H. Wasser
U.S. Environmental Protection Agency
AEERL/RTP
MD-65
Research Triangle Park, NC 27711
(919) 541-2476

Keiri Watanabe
Mitsubishi Heavy Industries, Ltd.
5-1, Marunouchi
2-Chome, Chiyoda-Ku
Tokyo 100, JAPAN
(03) 212-3111

Larry Waterland
Acurex Corporation
485 Clyde Avenue
Mountain View, CA 94043
(415) 964-3200

Allan Watson
Lotepro
1140 Avenue of the Americas
New York, NY 10036
(212) 575-7878

James E. Watson
North American Manufacturing Co.
4455 E. 71st Street
Cleveland, OH 44105
(216) 271-6000

Greg F. Weber
University of North Dakota
Energy Research Center
Box 8213, University Station
Grand Forks, ND 58202
(701) 777-5222

Christopher P. Wedig
Stone & Webster
245 Summer Street
Boston, MA 02107
(617) 589-5737

Jost Wendt
University of Arizona
Department of Chemical Engineering
Tucson, AZ 85721

George Weth
U.S. Department of Energy
Washington, DC 20545
(301) 353-2804

Alex Weir, Jr.
Southern California Edison Co.
2244 Walnut Grove Avenue
Rosemead, CA 91770
(818) 302-2785

Ronald J. Willey
Northeastern University
342SN
360 Huntington Avenue
Boston, MA 02115
(617) 437-3962

Jimmie L. Williams
Corning Glass Works
SP-DV-19
Corning, NY 14831
(607) 974-3220

David Winkler
Johnson Matthey
436 Devon Park Drive
Wayne, PA 19087
(215) 341-8519

John K. Winkler
Dept. of Environmental Quality
Engineering
Lakeville Hospital
Lakeville, MA 02346
(617) 947-1231, x680

Joop Witkamp
N.V. K.E.M.A.
Utrechtseweg 310
6812 AR Arnhem, HOLLAND
085-563625

Robert A. Wolff
Robert A. Wolff Consultants
RFD 1 Box 630
Bristol, NH 03222
(603) 744-5817

Ronald H. Wolk
Electric Power Research Institute
3412 Hillview Avenue
Palo Alto, CA 94304

James F. Wood
Babcock & Wilcox Co.
P.O. Box 351
Barberton, OH 44203
(216) 753-4511

Robert J. Yang
KVB, Inc.
18006 Skypark Boulevard
Irvine, CA 92714
(714) 250-6268

Jin S. Yoo
ARCO Petroleum Products Company
400 E. Sibley Blvd.
Harvey, IL 60426
(312) 333-3000 x573

Bunyoz Yorg
Flakt Denmark A/S
Meterbuen 33
Skovlunde, DENMARK
01-914411

Bert Zauderer
Coal Tech Corp.
P.O. Box 154
Merion, PA 19066
(215) 667-0442

Emil Zisek
Reichhelm, Inc.
P.O. Box 5037
Westport, CT 06811
(203) 838-7478